Molecular Recognition and Component Selection in Supramolecular Gels

William Edwards

PhD

University of York

Department of Chemistry

June 2013

Abstract

This thesis will cover aspects of molecular recognition and component selection in supramolecular gels. In the first section a bola-shape alkene appended organogelator is tested for its response to a number of cations. The gelator was found to undergo a gel-sol transition upon addition of Li^+ and Ag^+ and not when either Na^+ or K^+ was added. The response to Li^+ was caused by the higher charge density of the ion compared to the other group I metals, allowing it to disrupt the intermolecular hydrogen bonding between the gelator molecules. The response to Ag^+ was shown to be due to an interaction between this ion and the alkene groups of the gelator. This demonstrated that the silver(I)-alkene interaction can be utilised in the gel phase.

The second part of this thesis will investigate the formation of multi-component gels based on 1:1 complexes formed between a lysine based, carboxylic acid bearing dendron and a monoamine. The forces underpinning gelation as well as the effect of changing the solvent and changing the amine used are all investigated. This section then explores component selection, where a number of possible amines are added to a starting mixture but the dendron will form a gel with predominately one of the amines in preference to the others. The amines that are not incorporated into the network were easily viewed by NMR spectroscopy. A number of different amines were tested which all formed gels of different thermal stabilities with the dendron and also had different pKa values. Both of these factors were shown to be important in driving the preferential selection of a certain amine as they described the amines ability to form a complex with the dendron (pKa) and assemble as part of a gel network (thermal stability).

The thesis then describes the effect of using chiral amines, enantiomers of which form complexes with the chiral dendron which are diastereomeric. The effect of using different enantiomers of an amine was studied and found to dramatically alter the structure of the gelator network and the behaviour of the gel formed. These effects could be tuned by mixing different amounts of each enantiomer into the sample. As the gels formed with different enantiomers had different thermal stabilities they were able to be used in a number of experiments to test for component selection. These did indeed show this effect to be taking place, with the enantiomer which formed the most stable gel preferentially incorporated into the gelator network.

The final section of this thesis reverses the concept in the previous section and investigates the effect of changing the chirality of the lysine based dendron when mixing it with non-chiral amines, or a single enantiomer of a chiral amine. When mixed with non-chiral amines, as expected, changing the chirality of the dendron changed the structure of the gelator network and the properties of the gel formed and this could be tuned by mixing different amounts of the dendron enantiomers. Unexpectedly, this resulted in more thermally stable gels being formed with the racemic mixtures rather than their enantiopure equivalents, a very rare occurrence. When chiral amines were used the results were very similar to the previous section, with different enantiomers of the dendron changing the nano-scale structure of the network and the properties of the gels formed. Again this effect could be tuned by using different amounts of the dendron enantiomers to form the gel. Finally these systems were also tested to see if they could exhibit component selection but this study was inconclusive, partly down to the disruptive effect excess dendron had on the gel network formed.

Contents

Lists of Tables, Figures and Schemes

Tables

Figures

Schemes

Acknowledgments

I would like to thank Prof. David Smith for giving me the opportunity to conduct this research. I would also like to thank the EPSRC and University of York for funding as well as Dr Victor Chechik for his imput into this work. I would also like to thank all the academic and technical staff who have helped me with various techniques, they are: John Harrington (FEG-SEM), Meg Stark (FEG-SEM/TEM), Dr Andrew Leech (CD), Heather Fish and Amanda Dixon (NMR), Dr Carl Heaton (MS), Dr Stephen Cowling (DSC), and Prof. Ian Hamley and Ashkan Dehsorkhi (SAXS/WAXS).

All the people I have worked with in the Smith group, particularly Dr Cécile Lagadec, have shaped my time here and the work in this thesis, Dr Bart Nelissen, Amanda Dixon, Dr Anna Barnard, Dr Dan Welsh, Dr Michelle Smith, Stephen Bromfield, Tunde Okesola, Rex Chang, Dan Cornwell and Buthaina Albanyan have, in varying degrees, taught me many new things and kept me entertained in the lab, something for which I am grateful. I would also like to thank the many project students I have worked with, although their work is not contained within this thesis it has been invaluable in determining which projects to pursue further.

Finally, I would also like to thank Naomi for taking my mind away from chemistry and my family for supporting me throughout my time at university.

Declaration

I declare that this work is entirely my own except where acknowledged. Some of the work included in Chapter 2 has previously been published in W. Edwards and D. K. Smith, *Chem. Commun.*, 2012, **48**, 2767-2769, and some of the work in Chapter 3 has previously been published in W. Edwards and D. K. Smith, *J. Am. Chem. Soc.*, 2013, **135**, 5911-5920.

William Edwards

Chapter 1

Introduction

Chapter 1 – Introduction

1.1. Introduction to Supramolecular Gels

1.1.1. Supramolecular Chemistry

Supramolecular chemistry is the study of non-covalent interactions between different species and has been termed "chemistry beyond the molecule".[1-5] These non-covalent interactions include ionic interactions (100-350 kJ mol^{-1}), hydrogen bonding (4-60 kJ mol^{-1}), dipole-dipole forces (5-50 kJ mol^{-1}), π-π interactions (5-20 kJ mol^{-1}), van der Waals forces (<5 kJ mol^{-1}) and the hydrophobic effect.[6] The existence of interactions between molecules had been known for many years, but in the first half of the twentieth century non-covalent forces and structures formed by them – for example micelles[7] and biomolecules such as DNA[8] – were studied and understood in more detail. In the second half of the twentieth century the work of Cram,[9] Lehn[10] and Pedersen,[11] producing pre-designed molecules (such as **1** and **2**, Figure 1.1.) that selectively bound certain cations via non-covalent bonding pioneered the development of supramolecular chemistry, along with host-guest chemistry[12-15] and molecular recognition[16, 17] and earned them a Nobel Prize in 1987. Although these concepts were not entirely new, it was the increased sophistication and control of these approaches that furthered understanding and possibility for supramolecular chemistry.

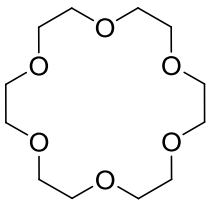

1

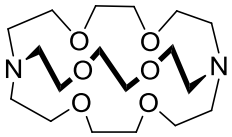

2

Figure 1.1. Crown ether (**1**) and cryptand (**2**), examples of cation binding molecules.

One of the most exciting concepts to arrive with the development of supramolecular chemistry was molecular self-assembly.[18-25] Self-assembly occurs when molecules – if suitably designed and under the right conditions – spontaneously organise into more complex structures held together by non-covalent forces.[26] This opened the possibility of generating complex structures from smaller, more readily synthesisable molecules, or even combining this approach with covalent bond forming chemistry.[4, 27] As the forces underpinning this assembly

are non-covalent and therefore reversible, so the formation of these structures is also reversible (or switchable). This reversibility leads to an amount of error checking, ensuring that hopefully the most thermodynamically stable product is formed with minimal formation of side-products. The ability to use self-assembly to produce nano-scale structures from molecular species ("bottom-up" synthesis) has led to its exploitation in a range of nanotechnology applications.[18, 28-30] One of the most facinating aspects of supramolecular chemistry and self-assembly is that although the individual interactions are relatively weak, harnessing many of them provides very strong bonding in supramolecular structures[31] and can even lead to the formation of macroscopic materials.

1.1.2. Supramolecular Gels

Despite being known and studied since at least the nineteenth century,[32-34] gels have been notoriously hard to define.[35, 36] They are generally recognised by their appearance to the naked eye as a soft solid that exhibits no macroscopic flow – having a jelly-like appearance. Gels consist of two components, gelator molecules and solvent. The gelator molecules most commonly form a fibrous 3D network and the solvent becomes immobilised between the fibres due to capillary forces – stopping bulk flow. The network formed by the gelator molecules is solid-like and dispersed through the solvent, the diameter of the fibres is normally on the nanometre scale which makes gels a colloidal state of matter.

Gelators have found use in a number of everyday applications including food, hygiene and cosmetic products. The gelators used in these products are usually chemically bonded polymers as they are relatively chemically inert, stable and after years of use in such products have been proven to be safe and reliable.[37, 38] These gels are often termed chemical gels and the polymers in the gel can be crosslinked by specific non-covalent interactions, microcrystalline regions between different polymers or chain entanglement.[38] The same qualities that make these polymer gels so suitable for some applications (stability, chemical inertness) can make them less suitable for others, specifically where a responsive or "smart" material is needed.

As well as these chemical gels – made from chemical polymers in solvent – there are also supramolecular gels.[39, 40] These are made from low mass gelator molecules, which self-assemble to form the fibrous network which immobilises the solvent and induces gelation. Often only a few weight percent of the gelator is required to fully immobilise the solvent. As these gelators are small molecules they allow us to probe how molecular structure of the

gelator controls the nano-scale assemblies they form and how this in turn controls the properties of the gel formed. As they are held together by non-covalent interactions they tend to be more responsive (or "smart") than their chemical gel counterparts and more readily synthesisable. This ease of synthesis and ability to better characterise a small molecule than a polymer should mean that it is easier to incorporate functionality into the gelator, and to monitor how changes in structure to the gelator molecule control gel properties – leading to more tuneable materials.[41-43] The fact they are formed by self-assembly of small molecules into nanoscale architectures which then support gelation mean their development will lead to new opportunities in the broader field of nanotechnology, with the potential to create nanoscale objects in a "bottom-up" fashion in the gel phase, as well as the opportunity to form interesting and potentially useful soft materials.

All of the gels studied in this thesis are supramolecular gels. Two of their most important features are their ability to respond to stimuli – most commonly their reversible formation – and the fact that functionality can be (relatively) easily built into these systems. As a result both of these abilities will be the subject of further review in this introduction. However first it is important to look at the formation of supramolecular gels, common families of molecules that are reported as low molecular weight gelators and the role played by the main component – the solvent.

1.1.3. Formation of Supramolecular Gels

The formation of supramolecular gelator networks from small gelator molecules is still relatively poorly understood. One of the most enlightening studies on this subject was published by Aggeli *et al.* and describes the assembly of two eleven-residue oligopeptides, one of which was capable of inducing gelation in water.[44] It was found that the peptides first formed single, twisted helical tapes (supramolecular polymers), the helicity of twist of the tape originating from the L chirality of the oligopeptides. These tapes then paired up to form twisted ribbons which were able to further assemble to form fibrils. The final step documented was the formation of thicker fibres from aggregation of these fibrils (steps a-f Figure 1.2.). The formation of each step in this hierarchical process is dependent on the difference between the free energy cost of reorganising the previous structure and the free energy benefit of forming the next structure. This was shown to be dependent on a number of factors relating to the structure of the gelator molecule and its solubility. Factors such as; interactions between different gelator molecules (tape formation), strength of interaction between different faces of

the tapes (ribbon formation) – which could also be driven by hydrophobicity of the tapes, and the strength of interactions between ribbons (fibril and fibre formation). The chirality of the molecule was shown to be crucial, giving the structures their preferential twist. This ensured that for any structure to increase its width there was an energy cost in rearranging its twist to further aggregate. At a certain point this is not compensated by the benefit of aggregation, so the chirality of the molecule leads to twisted structures, which controls their growth to finite widths. This model shows gelation is a hierarchical process that is influenced by a number of sometimes competing forces that are determined by the structure of the gelator molecule and its relationship with the solvent.

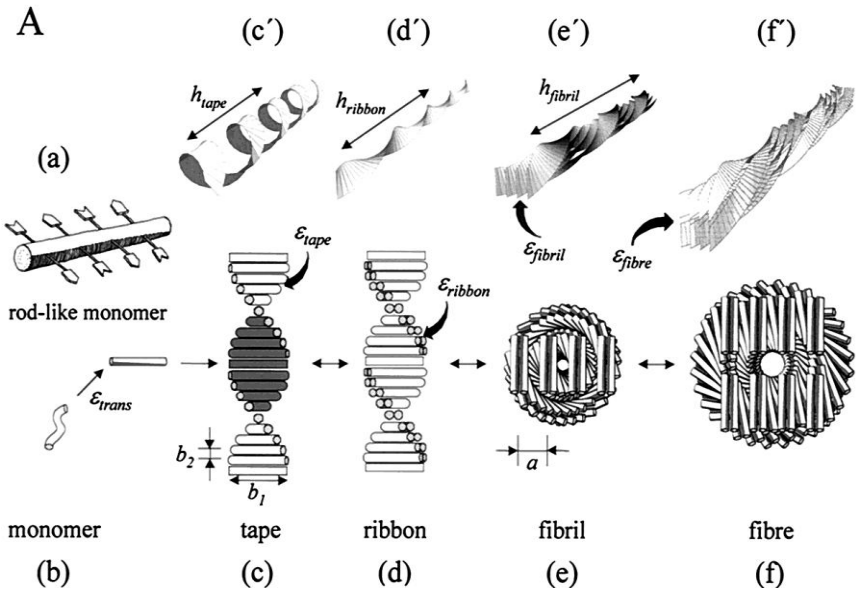

Figure 1.2. Proposed hierarchical assembly of oligopeptide in aqueous solution. Adapted from reference[44]

As shown by Aggeli *et al.* the first step in assembly of low weight gelators is the formation of tapes – otherwise known as supramolecular polymers. The formation of supramolecular polymers has been reviewed by Meijer and co-workers and they describe the two main models of supramolecular polymerisation.[45, 46] The first is isodesmic supramolecular polymerisation where the association constant of every step of chain growth is equivalent, the affinity of a free monomer for the polymer is unaffected by its length.

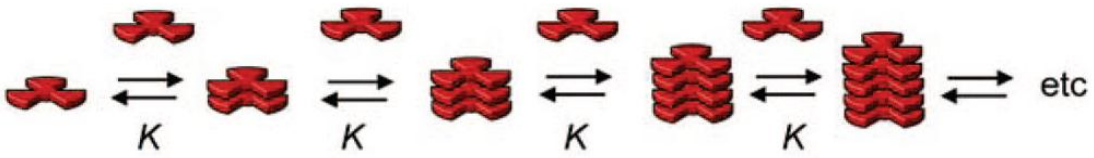

Figure 1.3. Schematic of isodesmic growth of a supramolecular polymer. Adapted from reference[45]

The other major type of supramolecular polymerisation is cooperative growth. Cooperative supramolecular polymerisation occurs when a monomer is more likely to form an intermolecular interaction with the polymer (above a certain length) than another monomer. This can be caused by a number of effects including electronic or structural modifications to a polymer of a certain critical size, less entropy being lost when a more organised polymer binds a monomer than when two monomers bind, or due to increasing hydrophobic effect. Cooperative supramolecular polymerisation can often be described by two association constants, one K_n to describe the slower nucleation period and another, K_e to describe the more favourable elongation period (K_n / K_e < 1).

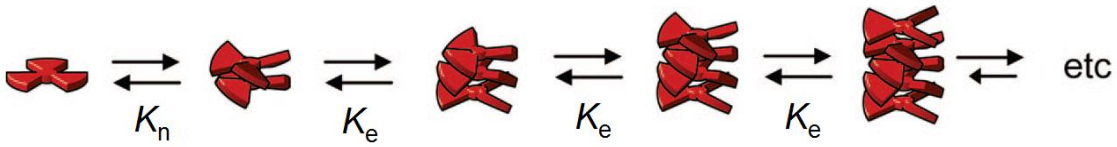

Figure 1.4. Schematic of cooperative growth of a supramolecular polymer. Adapted from reference[45]

Most of the research into gelators indicates that before the sol-gel transition, growth of supramolecular polymers occurs via a cooperative process.[47-53] Smith, Escuder, Miravet and co-workers have published a study of peptide based gelators which assemble due to intermolecular hydrogen bonding between amide and carbamate groups.[54] In this study they found that the cooperativity of the assembly was influenced by the structure of the gelator and that this in turn affected the stability of the gel formed, the more cooperative assemblies forming the more stable gels. Similarly a recent study by Sánchez and co-workers studied the assembly of oligo-(phenylene ethynylene)-based tricarboxamides and found that with increasing solvent polarity, the assembly became less cooperative until in chloroform isodesmic assembly was observed.[55] In agreement with the previous comments, cooperative assembly led to stable gels whilst isodesmic assembly in chloroform did not induce gelation.

What these treatments do not fully describe is the connections between fibres formed from supramolecular polymers which are needed to create a gel supporting network – this aspect of gel formation is very poorly understood.[39, 56, 57] A number of different types of connections between fibres have been proposed including attractive interactions between fibres at cross-link points, sections of different polymers that twist or bundle together, or the branching of growing fibres leading to an interlinked network. Raghavan and Douglas suggest that chain entanglement could lead to gelation, explaining why such a diverse range of molecules can induce gelation, however this has not been shown experimentally.[57]

1.1.4. Relationship to Crystallisation

The most common method of making gels is to heat an amount of solvent to fully solubilise a gelator which is insoluble or partially soluble at room temperature. This supersaturated solution is then allowed to cool and as it does so, the gel forms. This process of gel fibres aggregating to form a solid-like network out of solution has an obvious parallel with crystallisation, as does the way gelator molecules must pack together to form gel fibres, held together by directional intermolecular interactions.[43] It has been suggested that gelation and crystallisation are in fact competing processes with ordered assembly of molecules in one dimension leading to gel fibres and ordered assembly in three dimensions leading to crystallisation.[43, 58, 59] As such, slight changes to molecular structure can cause one pathway to be favoured over another, albeit, unpredictably.[60, 61] To highlight the link between crystallisation and gelation there have been a number of gel to crystal transitions reported in the literature[58, 62-66] and the crystal structures of gelators have been used to rationalise the gelation ability, or lack thereof, of a molecule.[43, 67, 68] However, the crystal structure of a gelator is not necessarily a reliable representation of the packing of molecules in gelator fibres and any structural information found using this technique should be considered with this in mind.[61] To further demonstrate the importance of changes to molecular packing of gelators, Weiss and co-workers have reported a reversible opaque gel-clear gel transition upon heating, due to slight changes in molecular packing of the gelator expelling solvent previously included in the gel fibres.[69] All of this work demonstrates how important molecular packing is in gel fibres, how very small changes to gelators can change their molecular packing – which in turn produces dramatic changes in materials properties – and that understanding or even observing the packing of gelators in the gel phase is still very problematic and in many cases unattainable.

1.1.5. Influence of Solvent

Many different types of solvent have been reported to have been gelated, not just organic solvents[70, 71] and aqueous solutions[72] but also ionic liquids,[73-75] liquid crystals[76] and even supercritical CO_2.[77, 78] The solvent in a gel can be removed, if the network collapses a xerogel is formed, if the network remains self-supporting and the space previously occupied by solvent is filled by gas (air), an aerogel is formed.[79, 80] Given its relationship with, and similarity to crystallisation, the dependence of the gelation ability of a molecule on its solubility is not surprising. It is often observed that if a proposed gelator is readily soluble in a solvent, it will form a solution and if it is too insoluble it forms a precipitate. Gelation only occurs somewhere between these two points, when there is the correct solubility balance. The gelator needs to be solvophobic enough to aggregate but solvophilic enough for the fibres formed to remain dispersed and not aggregate further and form a precipitate.[41, 54] This perhaps explains the dominance of amphiphiles in the field of hydrogelators.[72] Exploring this balance of solubility using a range of solubility and dissolution parameters is an active field of research and is covered in more detail in Chapter 3. Despite the choice of solvent appearing quite restrictive there are many examples of gelator that can gel different classes of solvent. One such example has been reported by Minakuchi *et al.* who demonstrated that a series of peptide based amphiphilic gelators (an example of which, **3**, is shown in Figure 1.5.) were able to immobilise aqueous solutions, organic solvent and ionic liquids, requiring only 0.5-2 wt% in most cases, regardless of solvent class.[75]

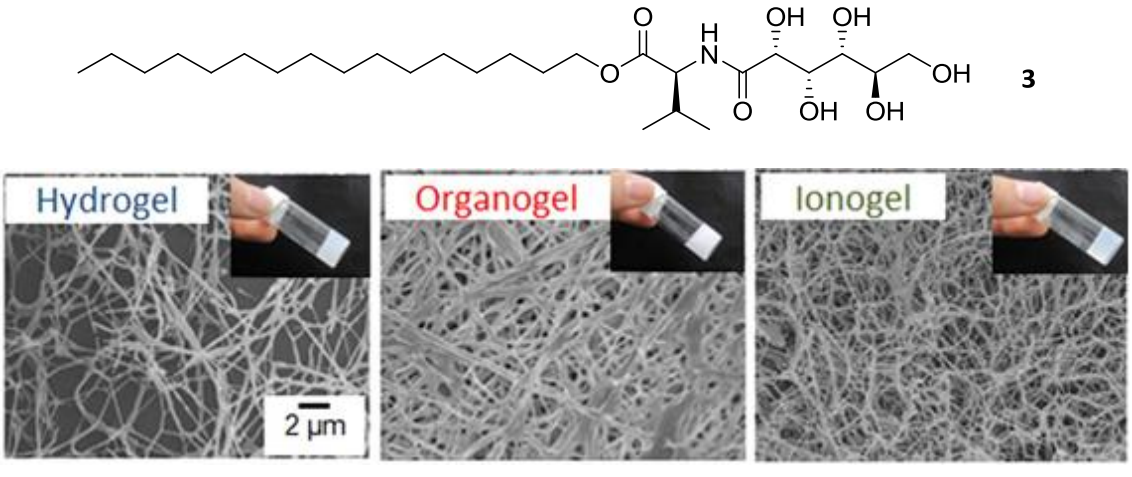

Figure 1.5. Peptide based amphiphilic gelator and its ability to gelate different classes of solvents. Scale bar 2 µm. Adapted from reference[75]

There have also been a number of studies to elucidate exactly how solvent molecules interact with the gelator network. Yemloul *et al.* have shown using measurement of the toluene T_1 longitudinal relaxation time that roughly 40% of the toluene in a specific organogel sample was in close contact with the gel fibres, leading the authors to conclude that this amount of solvent was embedded within the fibres.[81] Using a similar experiment Tritt-Goc and co-workers studied a toluene gel formed by a sugar based gelator and found that only 3% of the solvent is closely interacting with the gelator fibres.[82, 83] The fact that these experiments were carried out on different samples and using different methodologies may account for the large discrepancy in these results.

The intercalation of solvent molecules into gel fibres was studied by Jeong *et al*.[84] They found that gels formed from an organogelator with two long alkyl chains in alcoholic solvents had different circular dichroism spectra and decreased thermal stability as longer alcohols were used as the solvent (from methanol to octanol). This was found to be caused by mutual attraction between alkyl chains of the gelator and alcohol solvent, driving the larger alcohols to intercalate into the gelator fibres. This disrupted the gelator assembly and lowered thermal stability of the gels (Figure 1.6.). A number of other studies have been published investigating the effect of solvent size or flexibility on self-assembly,[85-88] it has even been proposed that the role of solvent in the formation of supramolecular aggregates could be as important as the role of water in protein folding.[89]

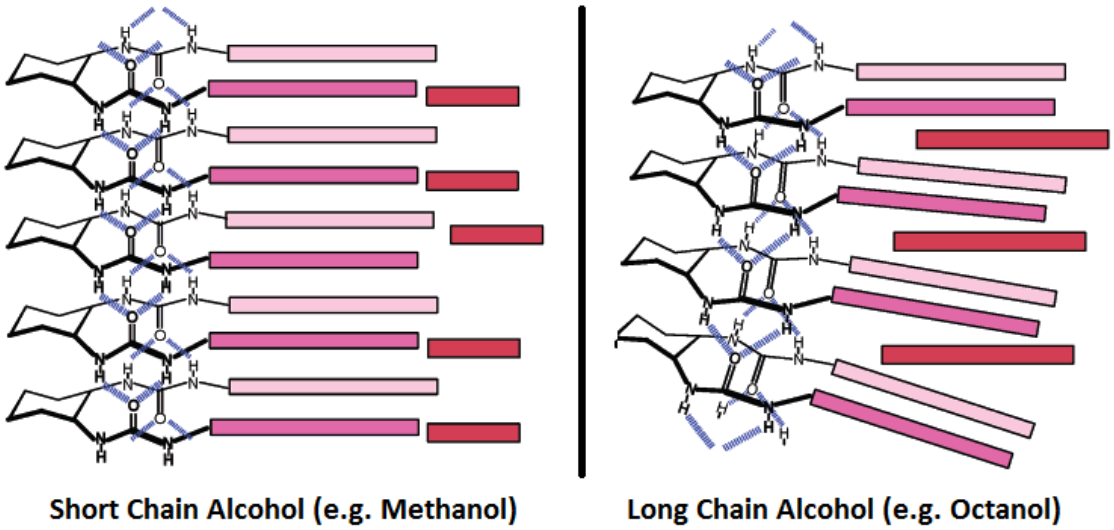

Figure 1.6. Packing of bisurea gelators appended with alkyl chains (pink and lilac) in alcoholic solvents (red). Adapted from reference[84]

1.1.6. Types of Gelator Molecules

Discovery of a new type of gelator is often a serendipitous event, with attempts to rationally design new low mass gelators proving very difficult.[41-43] Part of the problem is the diversity of molecules that are capable of inducing gelation. As already discussed, gelator molecules generally need to have strong intermolecular interactions in one direction that allow the molecular recognition that encourages tape/fibre formation.[90] They must also have an unusual solubility profile, neither being too soluble (resulting in a solution), nor too insoluble (resulting in a precipitate/crystal formation). This balance can often be seen in one molecule, for example, demonstrated by the use of amphiphilic molecules as hydrogelators – the fibres form as a kind of phase separation with hydrophilic groups on the outside, interacting with solvent and the hydrophobic part inside the fibre where the aqueous solvent can be excluded.[72]

Some of the simplest organogelators are the *trans*-1,2-diaminohexane based gelators such as **4** (Figure 1.7.) reported principally by the groups of Hanabusa[91] and van Esch.[92-96] These gelators commonly contain amide or urea groups which form intermolecular hydrogen bonds and provide a driving force for gel formation. These gelators also commonly have alkyl chains which pack favourably due to van der Waals forces.[96] Similar to these bis amides and ureas are a number of peptide based bisamides and ureas (**5**, Figure 1.7.) which were first reported by Hanabusa and form via the same combination of hydrogen bonding and van der Waals forces.[97-99] There is also a large interest in Fmoc-protected peptide gelators (such as **6**, Figure 1.7.) which can commonly form hydrogels as a result of hydrogen bonding between peptide bonds and π-π interactions between the aromatic Fmoc groups.[100-102]

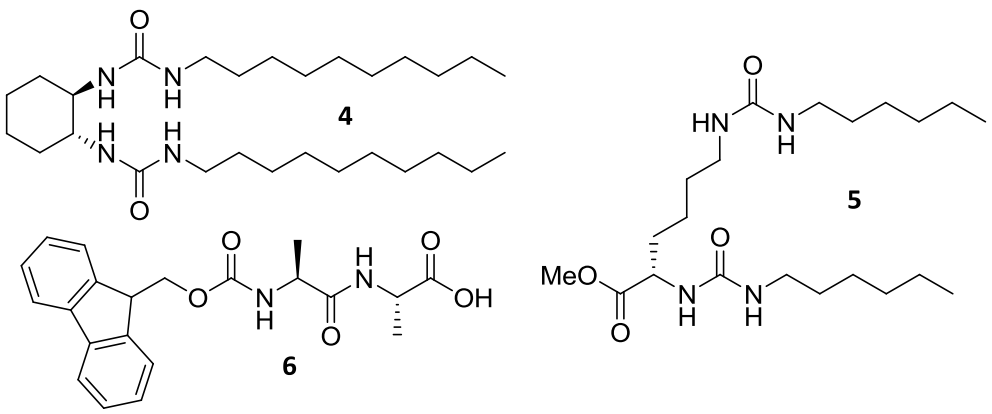

Figure 1.7. Examples of common types of supramolecular gelators, either simple bis urea or peptide based gelators.

This combination of hydrogen bonds and π-π interactions have been utilised in another class of gelators which are based on a benzene-1,3,5-tricarboxamide core (**7**, Figure 1.8.).[103] These gelator molecules have been reported by a number of researchers, most notably Meijer[86, 89] and have been shown to be capable of immobilising both organic or aqueous solvents, depending on the pendant groups.[104] Another important classes of gelators are oligo-(*p*-phenylenevinylene) (**8**, Figure 1.8.) which rely on π-π interactions to assemble into gelator networks.[105] There are also other gelators which are based on biological molecule including a range of steroid based gelators[106, 107] and sugar based gelators[108, 109] (**9** and **10**, Figure 1.8.).

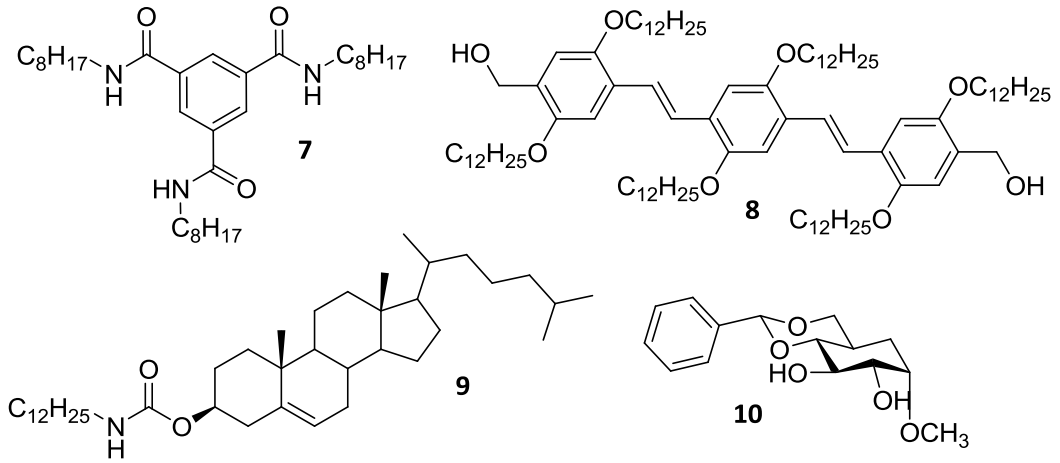

Figure 1.8. Examples of common types of supramolecular gelators. Two types of aromatic cored gelators, steroidal gelator and sugar appended gelator.

All of these well known classes of gelators follow the basic principles of having directional intermolecular interactions, as well as different parts of the molecules being differently soluble in the gelated solvents. However, Abdallah and Weiss have reported how long unbranched alkanes (with between 24 to 36 methylene groups) are able to immobilise organic solvents, including shorter chain alkanes (heptane to hexadecane).[110] These ultra-simple gelators were shown to be highly effective despite breaking the apparent empirical rules of gelator design.

1.1.7. Triggers for Gel Formation and Destruction

As described in section 1.1.4., the process of forming a gel is similar to that of crystallisation. As such, most gels are formed by simply heading a precipitate of gelator in solvent until the gelator is solubilised, then allowing the solution to cool over time, during which the gel will form and the sample "set". However, whilst this is by far the most common method of forming a gel it can be impractical for a number of applications, as is the use of ultrasound, another

common method of inducing gelation.[111-114] An increase in temperature is also the most common method of causing gel disassembly. As the temperature increases, the entropy gain of having a gelator molecule free in solution rather than in the organised gel fibres becomes more important. Eventually a temperature will be reached where this entropy term will outweigh the enthalpic benefit of the intermolecular interactions between the gelator molecules and at this point the gel network will disband. The thermal stability of a gel is a commonly measured property and the temperature of gel-sol transition is termed the T_{gel}. Due to changes in temperature or sonication being impractical stimuli in many applications, other triggers have been used to induce gelation or destroy a gel, often with the gelator being specifically designed to respond to this signal. As this responsiveness is one of the most important properties of supramolecular gelators some examples of important triggers are highlighted below.

One of the most exciting possibilities is to be able to induce gelation instantaneously when mixing gelator and solvent. This type of gelation is commonly proposed as a method of reducing the environmental impact of oil spills, with an organogelator capable of instantly gelating crude oil in the presence of sea water limiting the spread of pollutant and aiding recovery of the oil.[115, 116] This approach has been used by John and co-workers to produce a system that used open-chain sugar based gelators (the most successful of which, mannitol based **11**, is shown in Figure 1.9.) to immobilise food and fuel oils in the presence of an aqueous phase.[117] This could be conducted at room temperature by using a carrier solvent (ethanol) that solubilises the gelator and can be used to introduce it to the system. When added to the biphasic mixture of oil and water, the ethanol partitions into the aqueous phase and the gelator into the organic phase, inducing gelation. The process was found to be very robust with the nature of the aqueous phase (acidic, neutral, basic, saturated with NaCl or $CaCl_2$) not affecting gelation. The authors also demonstrated that the gelated oil could be recovered almost quantitatively – on a small scale at least – by removing the water and distilling the oil at above the T_{gel} of the gel. This process also recovered the gelator which remained unaffected and could then be reused. A similar system also using ethanol as a carrier solvent has been reported by Banerjee and co-workers, in this instance using a phenylglycine based amphiphilic gelator.[118]

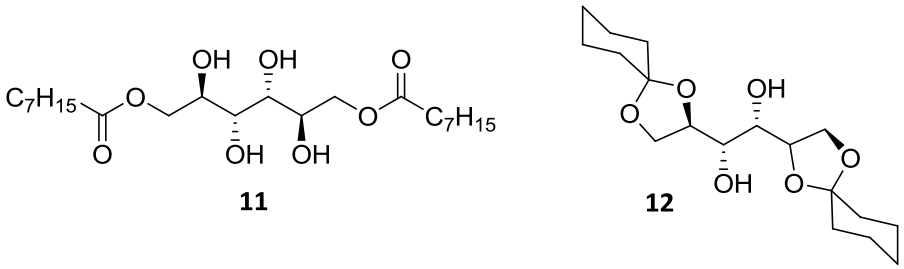

Figure 1.9. Mannitol based gelators which selectively gel oils in the presence of water when introduced via a carrier solvent.

Also hoping to remediate oil spillages, Prathap and Sureshan have reported another mannitol based gelator capable of immobilising oils in the presence of water (**12**, Figure 1.9).[119] In this experiment, the authors argue that the use of a carrier solvent that partitions into the aqueous phase is an unnecessary additional pollutant and propose using a warmed solution of gelator in organic solvent – so the carrier solvent is also gelled. In this report, a warm solution of gelator (in diesel) was sprayed on to a thin layer of diesel on an excess volume of water. The diesel "spill" was gelled even when being agitated by a mechanical shaker and was robust enough to be removed by forceps. The diesel and gelator could be recovered by distillation with 92% recovery of diesel.

A different approach to inducing gelation upon mixing under mild conditions is to synthesise the gelator *in situ*. Suzuki and co-workers have reported the elegant study of the *in situ* synthesis of bis- and tris-urea gelators (**13**-**19** in Figure 1.10.) by simple mixing of the amine and isocyanate starting materials, which are each soluble in the solvent gelated by the urea products.[97, 120] The bis- and tri- ureas produced can also be prepared in advance and when tested conventionally (with a heat-cool cycle) were shown to be good gelators of a range of organic solvents. When the same gelators were formed *in situ*, in most cases the gels produced were very similar to the conventional gels. However in the case of **17** and **18**, the *in situ* gelators were able to induce gelation in acetone, whereas the conventional (prepared in advance) gelators were not. This paper not only showed the ease of synthesis of *in situ* gelators but how, as their formation is different, they may be a way to access different gel materials.

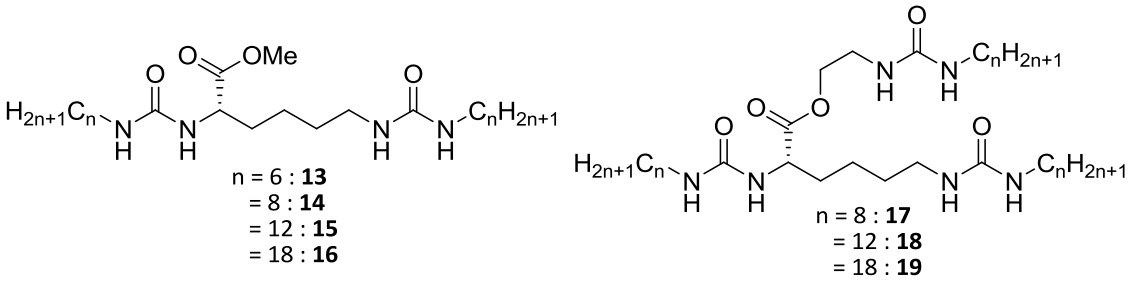

Figure 1.10. Bis- and tris-urea gelators that were shown to be effective organogelators when synthesised *in situ*.

Another method of inducing instantaneous gelation under mild conditions is to use so-called multi-component gelators, which are covered in more detail in Section 1.2. In these systems, the "gelator" is not just one molecule but at least two different species that interact non-covalently. Suzuki and co-workers have also utilised this approach to produce an organogel which can form instantaneously upon mixing amine terminated, lysine based molecule **20** (Figure 1.11) with a range of organic acids.[121] In general the acid with the longest alkyl chain tested (stearic acid) was the most effective for gel formation in a range of organic solvents and oils. Interestingly, the gelation ability of this complex was superior to that of the analogue single component gelator, where the acid-amine interaction was replaced with an amide bond. Dastidar and co-workers have also reported instantaneous gelation using an acid amine complex but in most instances this example requires a small amount of co-solvent to dissolve the different starting materials and a short period of sonication for the gel to form.[122, 123]

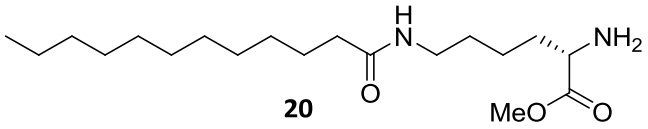

Figure 1.11. Molecule that is mixed with organic acids by Suzuki and co-workers to induce instant gelation on organic solvents and oils at room temperature.

Perhaps again highlighting the relationship between gelation and crystallisation are examples of gelation being induced by addition of a solvent in which the gelator is poorly soluble (an anti-solvent) to a solution of the gelator in a good solvent. This of course changes the solubility balance between molecule and surrounding solvent and induces the gelator to form the solid-like gelator network. Liu and co-workers have reported a molecule (**21**, Figure 1.12.) which forms hexagonal organic nanotubes which can underpin gelation.[124] This occurs when

molecule **21** is dissolved in a good solvent such as DMSO, THF, DMF or chloroform and an anti-solvent such as an alkane solvent or water is added, the gel forms instantaneously upon mixing of the solvents. Varying the solvents used changed the inner diameter of the tubes from 50-500 nm. A range of guest molecules could be incorporated into the tubes by solubilising them in the anti-solvent before it is added to the solution of gelator. The authors indeed show that a range of biological and dye molecules were successfully incorporated into the tubular gel network. A more simple form of anti-solvent induced gelation was reported by Steed and co-workers who formed gels by dissolving a gelator in methanol or DMSO and then adding water to form the gel.[125]

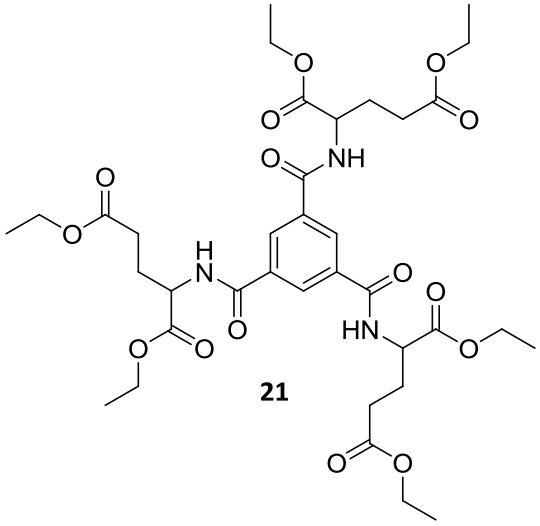

21

Figure 1.12. Gelator that forms organic nanotube based gels upon addition of anti-solvent.

As well as these methods of trying to instantaneously induce gelation by mixing gelator and solvent, there is a lot of interest in stimuli responsive gels. These are gels where the assembly/ disassembly of the gelator network can be controlled by specific stimuli and is a key approach to generate functional materials from supramolecular gels.[126] Controlled pH changes have proven to be a very useful method of inducing reversible gel formation/destruction. One example which illustrates the control pH change can have on gelation is reported by Ulijn and co-workers.[127] In this report the authors formed gels by adding insoluble Fmoc-protected dipeptides (**22**-**27**, Figure 1.13.) to pure water, the pH was increased by addition of concentrated NaOH solution and the precipitates became clear solutions as the carboxylic acid of the gelators was deprotonated. Following this treatment by dropwise addition of concentrated HCl solution resulted in the formation of clear gels.

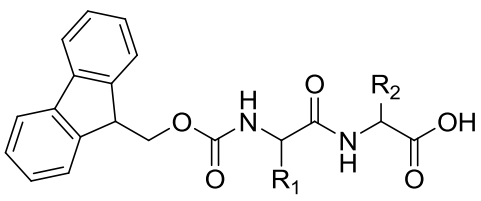

R_1 = H, R_2 = H : **22**
R_1 = CH_3, R_2 = H : **23**
R_1 = CH_3, R_2 = CH_3 : **24**
R_1 = $CH_2CH(CH_3)_2$, R_2 = H : **25**
R_1 = CH_2Ph, R_2 = H : **26**
R_1 = CH_2Ph, R_2 = CH_2Ph : **27**

Figure 1.13. Fmoc protected dipeptide gelators which are solubilised and subsequently gelate due to controlled changes in pH.

Despite this method of inducing gelation via modulation of pH change being a common technique for preparing Fmoc-peptide gels it can lead to inhomogeneous samples if gelation occurs faster than diffusion of the acid through the gelator solution. For this reason, Adams *et al.* developed a system using glucono-δ-lactone (**28**), which is hydrolysed in water to form gluconic acid (**29**) (Figure 1.14.) to induce gelation in a number of Fmoc dipeptide gels (including **25** and **26**).[128] The benefit of using glucono-δ-lactone over HCl is that its rate of diffusion through the sample is much faster than its hydrolysis and therefore gelation. This leads to a constant rate of gelation throughout the sample which produces gels with greater homogeneity. The authors demonstrated that in their case, neither glucono-δ-lactone nor the hydrolysis product gluconic acid were incorporated into the gel network and remained mobile in solution.

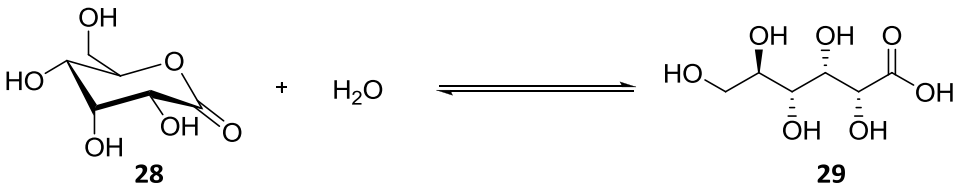

28 **29**

Figure 1.14. Hydrolysis of glucono-δ-lactone to form gluconic acid.

Enzymes have also been used to induce gelation in hydrogelators.[129, 130] Xu and co-workers reported using alkaline phosphatase, an enzyme that removes phosphate groups under alkaline conditions, to trigger hydrogelation of Fmoc-protected peptide gelators.[131] An example of this was the conversion of phosphate appended pro-gelator **30** to gelator **31** (Figure 1.15.). Pro-gelator **30** was dissolved in phosphate buffer (pH = 9.6) with one equivalent of Na_2CO_3. To this solution, alkaline phosphatase was added and the sample was incubated at 37°C for 30 minutes, after which time an opaque gel was formed. In related work, the same group demonstrated that using a similar process with acid phosphatase to induce gelation,

inhibitors of that enzyme could be screened, its effectiveness being judged by whether the easily observed sol-gel transition occurred and if so, at what concentration of inhibitor.[132]

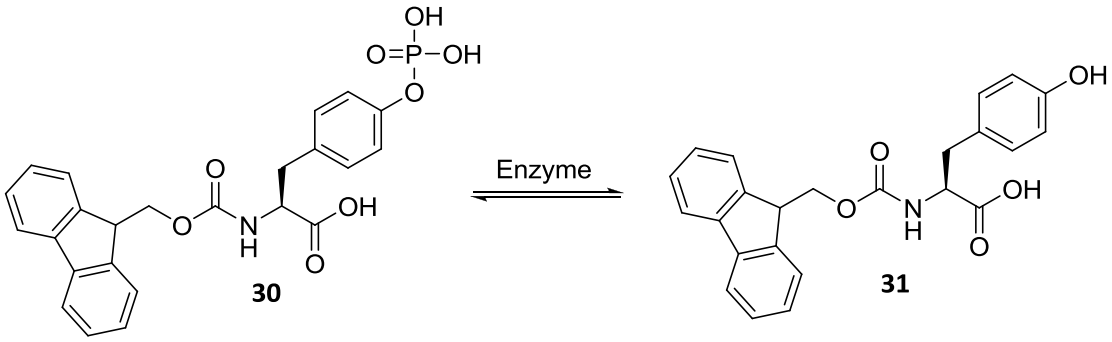

Figure 1.15. Removal of phosphate group of pro-gelator **30** to form gelator **31**.

Sáez *et al.* have reported an organogelator (**32**, Figure 1.16.) that selectively collapsed in response to the presence of catechol, a response not observed with a range of structurally similar compounds.[133] A number of experiments were conducted with analogues of gelator **32** which found a combination of hydrogen bonding and π-π stacking between gelator **32** and catechol were responsible for the destruction of the gel. This is one example of the selective destruction of a gel by a chemical species binding to the gelator molecule, something investigated in more detail in Chapter 2 of this thesis.

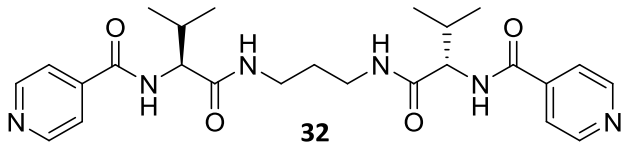

Figure 1.16. Catechol responsive organogelator.

Light has also been used to trigger a reversible gel-sol transition.[134-136] For instance Shinkai and co-workers reported azo-appended cholesterol gelator **33** (Figure 1.17.). The gel formed from this gelator in butanol was converted to a solution if irradiated with UV light (330-380 nm), as this caused roughly 38% of the gelator to isomerise to the *cis* form – which was unable to support a gel.[137] This solution, if irradiated with visible light (>460 nm), would again form a gel as this led to the *cis* form of gelator **33** to isomerise to the gel supporting *trans* form. This process was shown to be repeatable over a number of cycles.

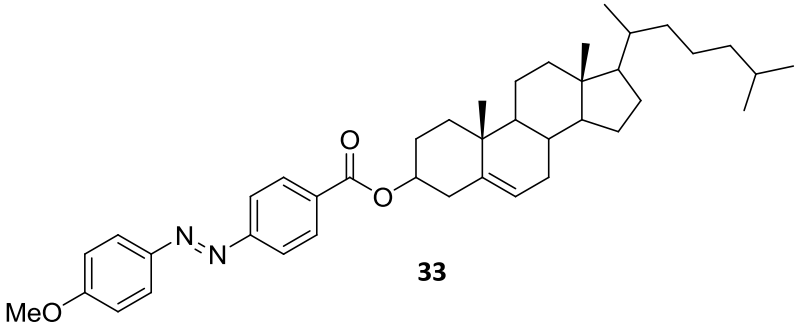

33

Figure 1.17. Light responsive azo-appended gelator.

Of course gelators do not only have to be responsive to only one stimulus. Many of the examples of gelators in this section which respond to unusual triggers will also assemble/disassemble with changes in temperature for instance and a number of examples of extremely responsive gelators which respond to multiple stimuli have been published.[126, 138, 139] All of these examples demonstrate one of the main properties of supramolecular gels – their formation is reversible, often over many cycles and sometimes due to a very specific stimulus.

1.1.8. Functional Gels

Aside from learning fundamental lessons about molecular self-assembly and how materials can be generated from small molecules, one of the largest driving forces for continuing research into supramolecular gels is the fact that they could be used in a range of advanced and high-tech applications.[140-143] The use of supramolecular gelators to contain oil spills has already been discussed. Some other potential applications of supramolecular gels will be highlighted here to illustrate the potential they have to produce useful, high value materials.

The first application of supramolecular gels discussed here is their potential use as catalytic reaction media.[144, 145] Ecuder, Miravet and co-workers have done a lot of work in this field[146, 147] and have reported the use of an L-proline based amphiphilic hydrogelator (**34**, Figure 1.18.) to catalyse an enantioselective aldol reaction with reagents in an organic phase.[148] The authors first formed hydrogels using gelator **34**, on to which a toluene solution of both reagents was added. When left at 5°C for 24 hours the product of the aldol reaction was obtained in quantitative yield and at 88% ee. It was shown by NMR experiments that even at 30°C no gelator was visible in the aqueous phase of the gel, so this was not the cause of the catalytic activity. Neither was there any present in the toluene phase, so neither was this the catalytic species. Therefore, the authors conclude that the catalytic species must be **34** in the gel fibres and that the hydrophobicity of the interior of the fibres provided by the stacking alkyl chains

allows the reagents of the aldol reaction to come into contact with the catalytic L-proline residues of the gelator. When the reaction was conducted at higher temperatures, the yield remained unchanged, but the selectivity of the reaction dropped considerably (18% ee at 25°C). The authors attribute the higher selectivity at lower temperatures to the increased rigidity of the gel and restricted movement of reagents at lower temperature. It was shown that the gel was recyclable, either being reused after the organic phase was decanted or being destroyed, washed and reformed using a change in temperature or pH to assemble/disassemble the gel. To further illustrate how the assembly of molecules into gelator fibres can alter function, the same authors published a study on a bola-L-proline gelator which was observed, when assembled, to exhibit a large enhancement of basicity.[149]

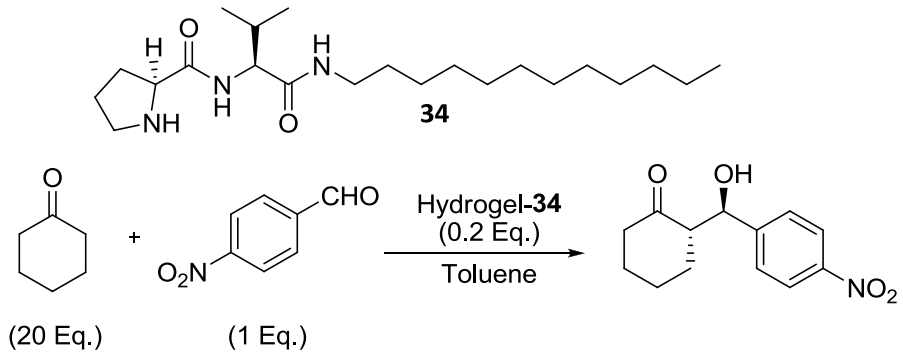

Figure 1.18. Catalytic hydrogelator **34** and the aldol reaction used to test its catalytic activity.

Another potential application of supramolecular gels is using them to create nanostructured covalent materials. As seen in section 1.1.3 the formation of these gels is a hierarchical process with the molecules forming nanometer scale objects (tapes to fibres) of defined dimensions and architecture. If these can be covalently trapped[150] or transcribed into inorganic structures[151] this could be a very efficient route for the "bottom-up" synthesis of nanostructured materials. It may also lead to the production of more robust macroscopic materials with the same functionality as the supramolecular gels used to form them. The covalent trapping of supramolecular gels has been attempted via a number of different routes. Smith and co-workers have used Grubbs catalyst to perform alkene metathesis on assembled alkene appended gelators.[152, 153] In one report, this group reported that alkene appended bis urea **35** (Figure 1.19.) was heated and dissolved in toluene, then allowed to cool to room temperature slowly (0.5°C min^{-1}). It formed a gel underpinned by a fibrous network.[154] This network could be covalently fixed by pipetting 20 mol% Grubbs catalyst (2nd generation) onto the gel and allowing it to diffuse through the sample over 24 hours. When an equivalent

sample of gelator was heated and cooled rapidly – by leaving on the lab bench after heating – the sample formed a viscous solution rather than a gel. Field emission gun scanning electron microscopy (FEG-SEM) showed the sample consisted mainly of hollow spheres. These could be covalently fixed using the same methodology as that used for the gel sample. After this treatment, FEG-SEM showed that the spheres had been smoothened by the covalent cross-linking but were still present. This demonstrates the use of a simple supramolecular gelator to produce different robust, nanostructured materials using a simple methodology. Other approaches to covalently trapping self-assembled gel networks include the use of click chemistry as reported by Díaz *et al.*[155, 156] and the use of UV light to initiate the photopolymerisation of diacetylene units as reported by the groups of Kim,[157] Weiss[158] and Stupp.[159]

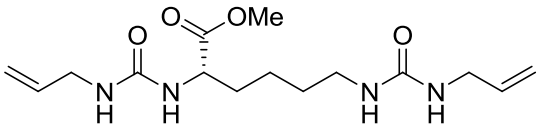

35

Figure 1.19. Alkene appended bis-urea organogelator which has been covalently fixed to produce morphologically different materials.

The final use of supramolecular gels highlighted here is in biological systems.[160-162] The two main applications in this field are either as scaffolds for cell growth (hydrogels)[163-165] or materials for drug delivery (hydrogels or organogels).[166, 167] The ability of a supramolecular gelator to be a good drug delivery agent will of course depend on its toxicity and other biological factors but from a materials point of view, often the most important two features are functionality and responsiveness. An example which illustrates this well was published by Vemula *et al.*[168] In this study the authors synthesised a number of gelators, of which the most interesting were bola amphiphilic gelators **36** and **37** (Figure 1.20.). These molecules both contain the pain and fever reducing drug acetaminophen (paracetamol) as part of their structure. Both of these molecules were shown to effectively form hydrogels which could be destroyed over time by addition of lipolase which cleaves the ester bond linking the drug moiety to the rest of the molecule. It was clearly shown by the authors that this system provided controlled release of acetaminophen. The system was then improved by incorporating hydrophobic model drug curcumin to the gel, adding it during gel formulation. The hydrophobic nature of this molecule means it sits within the hydrophobic parts of the gel fibres, and does not leach out into the surrounding aqueous solution. However, when lipolase

was added the gel was destroyed and both acetaminophen and curcumin are released into solution – vitally this process occurs slowly, avoiding burst release. The authors tested the toxicity of their pro-drug compounds using mesenchymal stem cells, it was shown that cell viability, proliferation and differentiation was unaffected by the presence of the pro-drug gelators. This example shows how the principle of building functionality into the readily synthesisable gelator molecules – in this case incorporating a drug molecule – and ensuring the gel is responsive to a certain stimulus – an enzyme – can produce highly advanced and potentially useful materials.

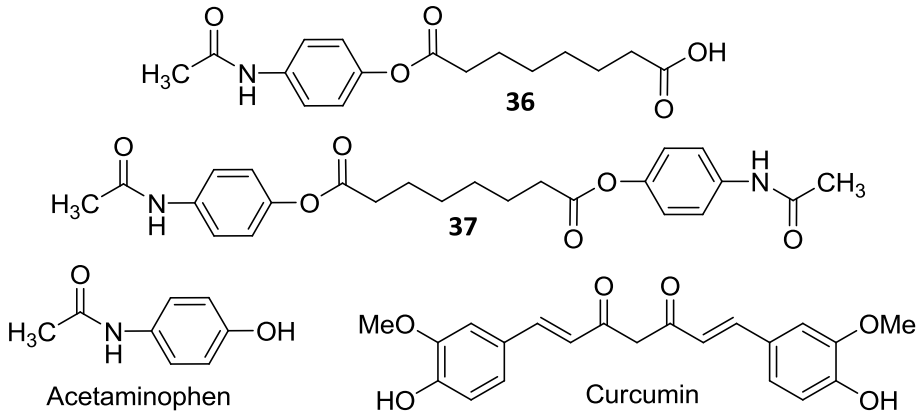

Figure 1.20. Pro-drug gelators synthesised by Vemula *et al.* and structure of acetaminophen and curcumin.

There are of course many other proposed applications for supramolecular gels including molecular electronics,[169-173] light harvesting,[174] a number of sensory gels,[133, 175, 176] and even a proposed use in optics.[177] However a full discussion of these is beyond the scope of this introduction. In summary however, these reports illustrate how the fundamental lessons learned in the study of supramolecular gels can, even if not directly, led to the development of functional, useful materials in real world applications.

1.2. Multi-Component Gels

In many of the examples highlighted so far, a gel has been formed by a single molecule and solvent. Indeed this is how many gels are formed, but there are also numerous examples of so-called multi-component gelators[178, 179] and they represent a large and increasingly important class of soft material. In a recent review by Buerkle and Rowan[178] the field of multi-component gelators was broken into three broad sub-sections. The first of these are gels which form when multiple species – none of which are gelators in their own right – are mixed and induce gelation in a solvent. The second class is mixed gelator gels, where known gelators are mixed together to create materials with new properties. The third class is where addition of a non-gelling component can alter the properties of the gel. These divisions are sensible and are broadly kept intact in this overview of multi-component gelators.

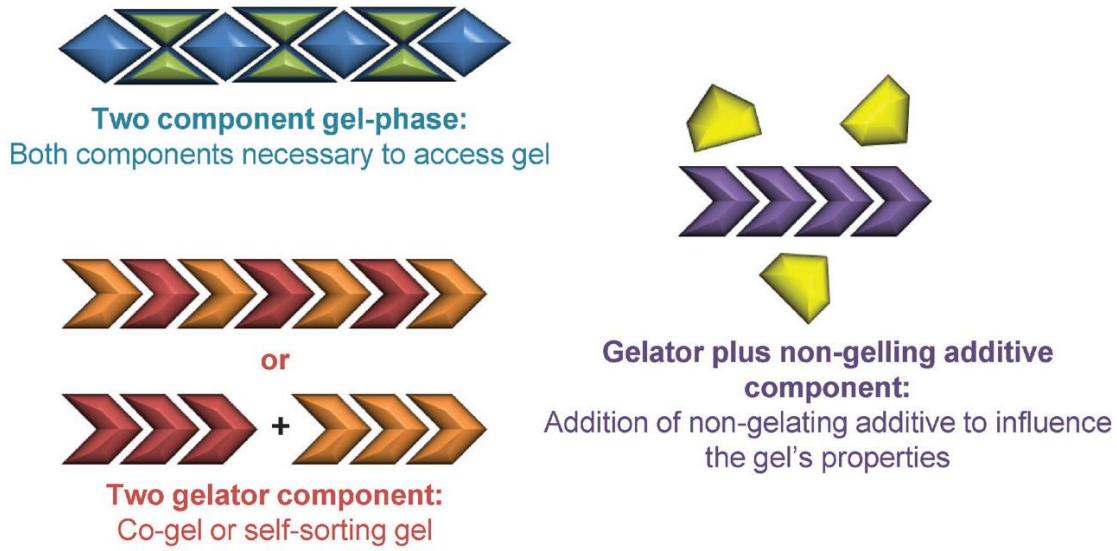

Figure 1.21. Different types of multi-component gels as defined by Buerkle and Rowan. Adapted from reference[178]

The main reason research is conducted into multi-component gels is to discover soft materials with a more diverse range of properties than is currently known and to be able to tune these properties with greater control. It is envisaged that increased tunability of supramolecular gels will allow factors such as gel strength, stability, nanostructure or any other property inherent in a particular gel to be controlled by simple mixing of different gelator molecules. This is desirable, as the design of supramolecular, low weight gelators with specific properties is a field which is still in its infancy.[41-43] The possibility of creating functional soft materials by

mixing a known gelator with a co-assembling functional molecule – the adding of functionality to materials essentially from the "bottle" – is an enticing possibility driving research into multi-component gels. The first broad sub-section highlighted here are gels in which multiple-components are required for gelation, as these systems are most relevant to the work reported in this thesis.

1.2.1. Multiple-Components Required for Gelation

The first example of a gel which required two molecules to form the gel network was reported by Hanabusa and co-workers in 1993 (Figure 1.22.).[180] These molecules were triaminopyrimidine based **38** and barbituric acid based **39**. Each molecule has two hydrogen bonding "faces", **38** having donor-acceptor-donor ability and barbituric acid based **39** having acceptor-donor-acceptor ability. This led to complimentary hydrogen bonding between each unit, and as each has two hydrogen bonding "faces" two-dimensional tapes were formed. These tapes were the supramolecular polymers that were shown to underpin gel formation in a range of organic solvents. Yagai, Kitamura and co-workers produced a family of similar multi-component gels which showed increasing gelation ability with two donor-acceptor-donor melamine based units being covalently liked and mixed with acceptor-donor-acceptor type cyanurates or barbiturates.[181] The stability of the gels formed by these mixtures was increased further by introducing covalently cross-linked cyanuric acid units.

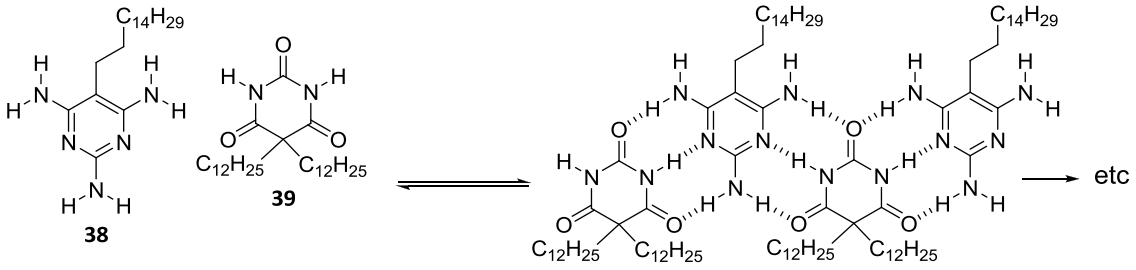

Figure 1.22. Two-dimensional tapes formed by complimentary hydrogen bonding molecules reported by Hanabusa and co-workers.

The Nandi group have reported a two-component hydrogel based on 3:1 complexes of riboflavin (**40**, also known as vitamin B2) and melamine (**41**) (Figure 1.23.).[182, 183] In these gels the photoluminescence of the riboflavin molecules was dramatically increased. The authors propose that this is due to two factors; firstly that the hydrogen bonding sites of the riboflavin are now "blocked" by melamine, which reduces its ability to hydrogen bond with water, reducing quenching of the photoluminescence. The authors also postulated that the

complexes are protected from dynamic quenching when they form part of the extended gelator network. The gel could not be formed in a basic medium, which the authors attributed to deprotonation of the imide proton of the riboflavin, destroying the complementary hydrogen bonding arrays.

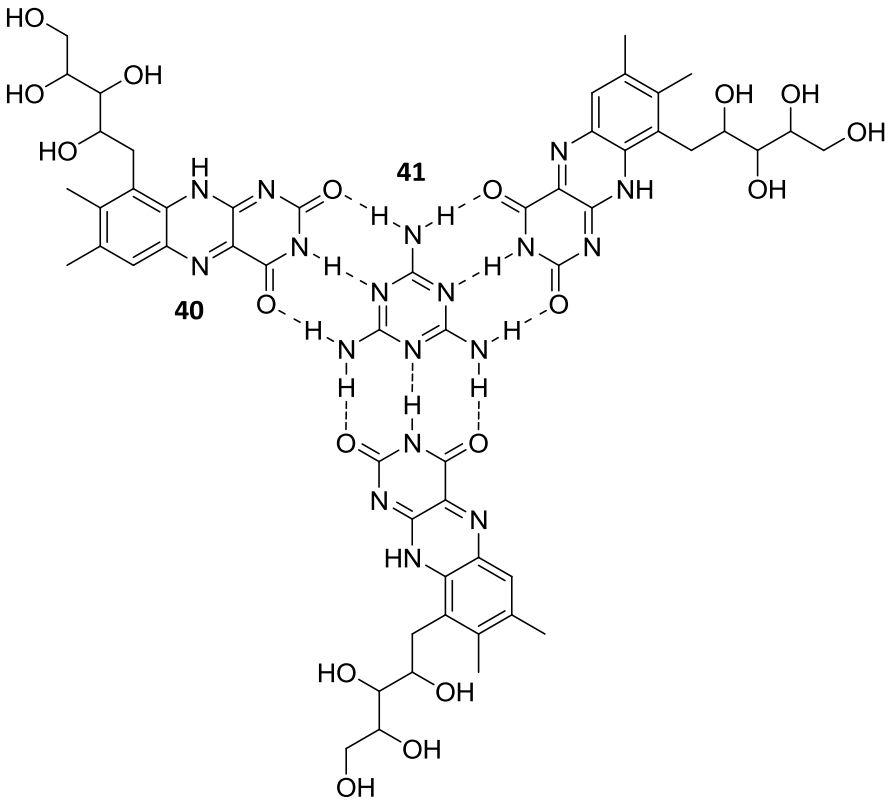

Figure 1.23. The 3:1 complex of riboflavin to melamine reported by the Nandi group that forms gels in water.

Another example of a multi-component gel formed from complementary hydrogen bonding arrays was reported by the Shinkai group. They took similar molecules to those previously used by Hanabusa and appended a cholesterol to each of them (**42** and **43**) (Figure 1.24.).[184] Cholesterol based gelators are well known and widely reported in the literature.[106, 107] In this example, it was seen that slow cooling, which resulted in neat, complementary hydrogen bonding between each molecule, led to molecular tapes that were likely to precipitate out of solution. Conversely, more rapid cooling which led to irregular hydrogen bonding between molecules better caused gel formation. In most studies of molecular recognition, this would be considered a faulty process but in this case it led to more irregular fibres which were less prone to precipitation and had free hydrogen bonding sites which allowed the fibres to cross-

link, here leading to a more stable gel. Subsequently another example of a two-component gelator was reported by this group, this time based on a barbital based guest binding to a host molecule which wraps around it, forming a more familiar host-guest complex.[185]

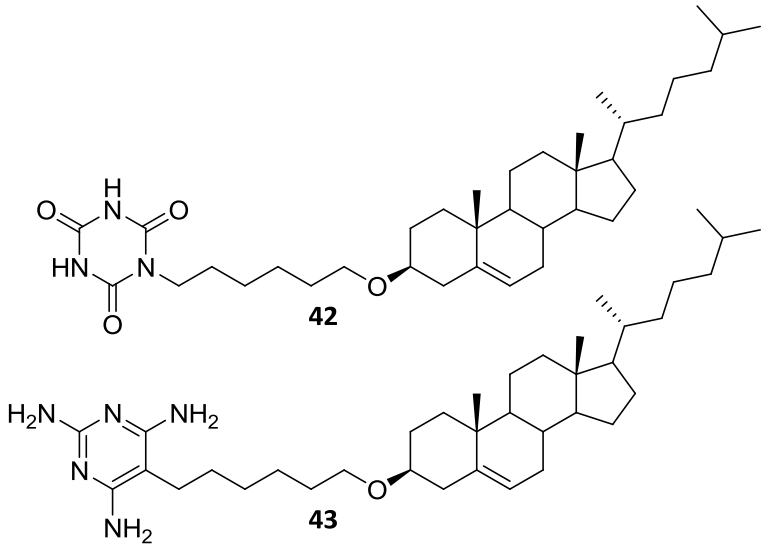

Figure 1.24. Molecules used by the Shinkai group to form two-component organogels.

As well as these examples of multi-component gels that are formed with complementary hydrogen bonding arrays, many multi-component gels are based on an acid-base interaction. Bhattacharya and co-workers have investigated a wide range of different acid and amine mixtures and their ability to form hydrogels.[186, 187] Generally, they found that more hydrophobic acids were more effective for inducing gelation, and that whilst diamines led to the formation of weakly-interacting nanotubes – which led to weak gels, oligomeric amines led to the formation of highly cross-linked fibrous networks which resulted in stronger gels. Furthermore, it was found that the rheological properties of the gel could be changed by changing the ratio of acid to amine. Suzuki and Hanabusa have also reported an amino acid based acid-base two-component oragnogelator.[121, 188] Similarly to the work by Bhattacharya they found that the properties of the gel could be readily tuned by judicious choice of acid and base components. Dastidar and co-workers have reported another example of acid-base based two-component gelators.[189, 190] One study examined the gelation ability of cyclobutane-1,1-dicarboxylic acid when mixed with imidazolium derivatives in nitrobenzene (Figure 1.25.). It was found that even slight structural changes to the imidazole would result in no gelation being observed and that having a free carboxylic acid in the complex was vital, as hydrogen bonding between these free acids greatly strengthened the gel formed.

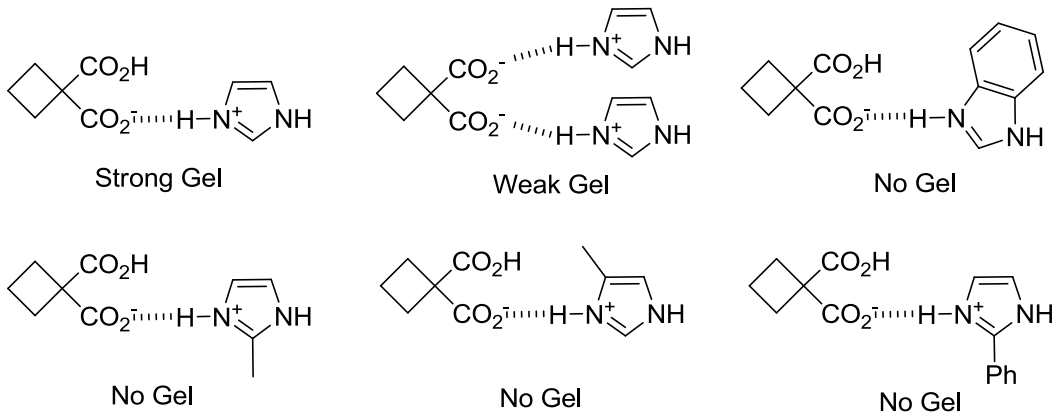

Figure 1.25. Two component mixtures formed by Dastidar and co-workers and their gelation abilities in nitrobenzene.

Nam, Lee and Hong have reported a number of acid-base two-component gelators.[191, 192] In one of these studies they reported the formation of gels between diamine aromatic cores (**44** and **45**) and carboxylic acid bearing, amide containing aromatic amphiphiles (**46** and **47**) (Figure 1.26.). Again the properties of the gels formed could be tailored by simply mixing different acid and base components. When **45** and **47** were used, electron microscopy revealed not only a fibrous network which underpinned gelation but also the presence of microtubes. These microtubes could be separated by diluting and vigorously stirring the gel. Furthermore it was found that the solvent used to form the gel had an effect on the type of microtubes formed, with cyclohexane and decalin producing tubes of different shape and thickness, however the tubes produced in the decalin gel could not be isolated.

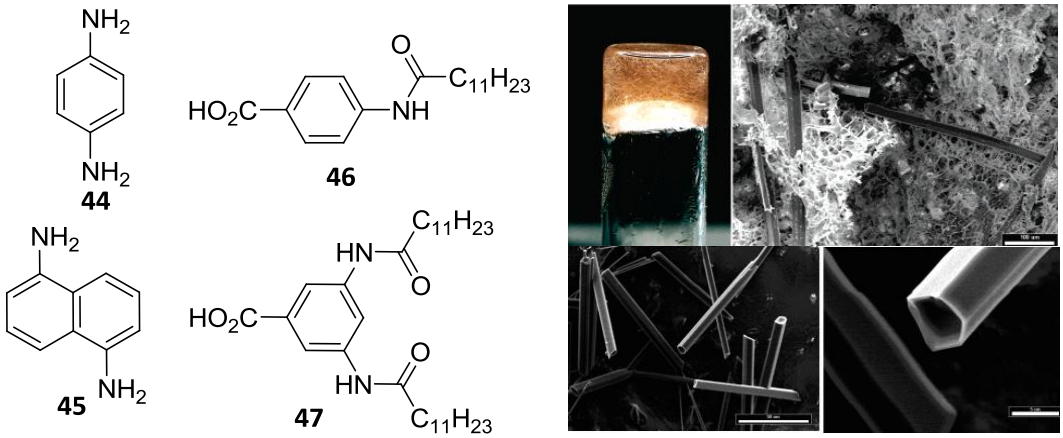

Figure 1.26. Compounds used to form two-component gels by Hong and co-workers. SEM images of Top – gel formed by **45** and **47** in cyclohexane (2:1 ratio, 20 mM concentration of diamine), Scale bar = 100 µm and Bottom – microtubes recovered from gel sample. Scale bars 50 µm (left) and 5 µm (right). Adapted from reference[191]

An example of a simple aromatic acid / alkyl amine two component gelator has been reported by Shinkai and co-workers.[193] This study found that a mixture of anthracene-9-carboxylic acid (**48**) and dodecylamine (**49**) (Figure 1.27.) formed a stable gel in cyclohexane. It was observed that when the gel was irradiated with UV light the anthracene moieties underwent dimerisation and as a result the gel was destroyed. The dimerisation could be reversed by heating at 30°C in darkness, but this led to formation of a precipitate, not gel formation. The gel could be reformed however, by heating to the solvent boiling point and then cooling to 15°C. As such, the gel network had a dual stimuli-responsive behaviour, being destroyed by UV irradiation and being reformed by increased temperature.

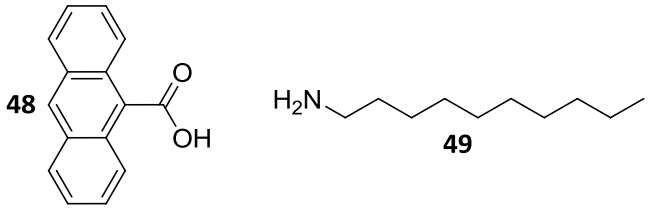

Figure 1.27. Compounds that form two-component gel reported by Shinkai and co-workers.

The Smith group has produced a series of acid-amine organogelators based on acid bearing lysine dendrons and aliphatic diamines, an example of which is shown in Figure 1.28 (**50** and **51**).[194-196] A series of investigations have revealed the effect of changing the ratio of dendron to

amine,[197, 198] varying the length of the amine spacer[199] and dendritic generation on gel formation.[200] In one study a comparison between these two-component gelators and equivalent covalently linked one component gelators was made.[201] It was found that upon covalent fixing of the dendron to the diamine, the thermal stability of the gels was generally increased, as was predicted, most likely due to the extra intermolecular hydrogen bonding amide group produced by the new covalent linkage. Not only was it demonstrated that the effect of varying chain length and dendron generation were different in each system but the transcription of chirality from molecular level to nanoscale aggregates (as evidenced by circular dichroism) was greatly reduced in the covalently linked molecules. This was rationalised as being due to the fact the acid-base two-component gelator had dendron head groups that were freer to arrange themselves according to chiral preference, whilst the covalently tethered head groups were less able to do so.

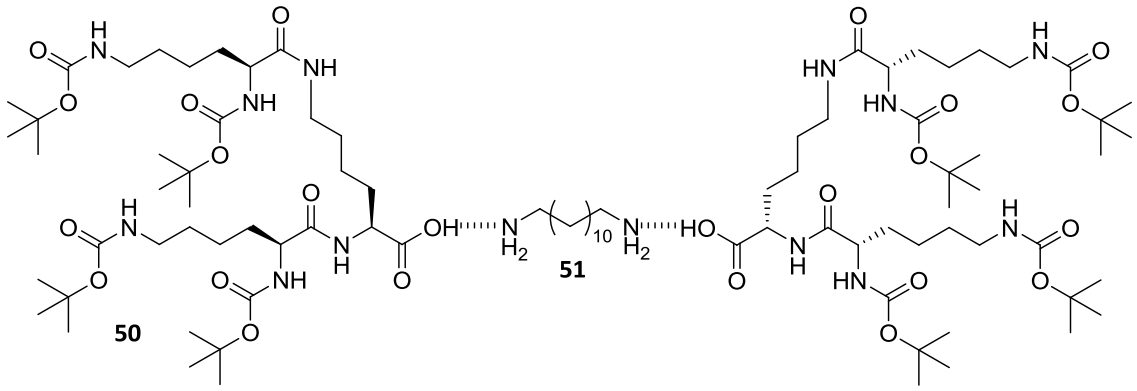

Figure 1.28. Two-component dendron / diamine gelator complex and one component equivalent reported by Smith group.

There have also been a number of multi-component gelators reported which utilise the donor-acceptor interaction.[202-208] The first example of such a gel was reported by the group of Maitra who reported that certain bile acids functionalised with aromatic groups (for example **52**) could form organogels when mixed in 1:1 stoichiometry with electron poor trinitrofluorenone (TNF) (Figure 1.29.).[209] The temperature dependence of the charge transfer UV band (and gelation) was clearly demonstrated. A later follow-up paper documented how a range of simpler alkyl chain appended pyrene molecules could gel organic solvents with or without TNF, depending on the length of alkyl chain and nature of linking group between the alkyl chain and the aromatic ring as this determined the strength of intermolecular hydrogen bonding.[210]

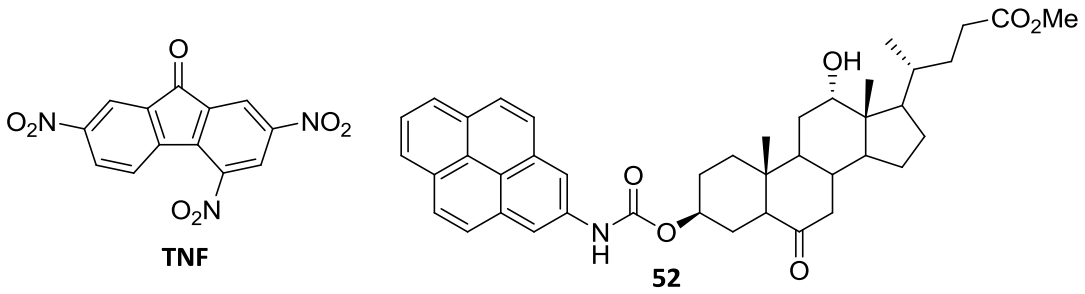

Figure 1.29. Example of molecules used by Maitra in first example of donor-acceptor multi-component gel.

Smith and co-workers have also reported a two-component charge transfer based gel (Figure 1.30.).[66] This system also used TNF but this time mixed in a 2:1 ratio with a dipyrene functionalised lysine (**53**). This mixture was shown to form a red (typical of a charge transfer band) gel in a non-polar solvent mixture of 90:10 styrene to divinylbenzene. Fascinatingly, if left to stand for 24 hours, the homogenous gel slowly converted into an inhomogeneous precipitate. This showed the gel was metastable and would convert from gel to crystalline solid over time. This change was further evidenced under scanning electron microscopy (SEM) which showed the sample after aging contained micro-crystalline aggregates of gelator fibres. A similar gel-crystal transition was seen in a two-component gelator by Tang and co-workers.[211]

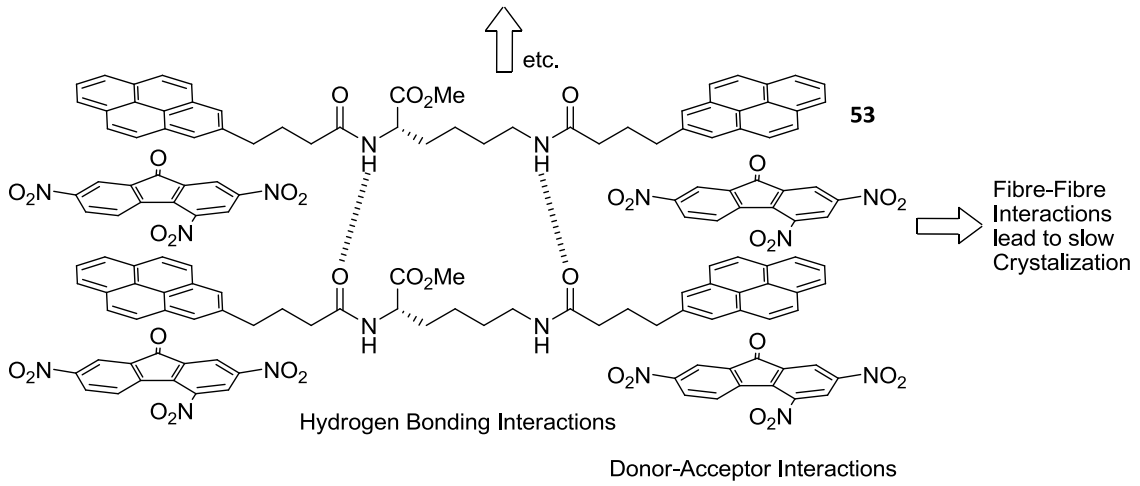

Figure 1.30. Two-component gel reported by Smith and co-workers, showing how aggregation of fibres leads to precipitation.

McPherson and co-workers have reported a series of gels formed from 1:1 mixtures of the surfactant sodium bis(2-ethylhexyl)sulfosuccinate (AOT) and different phenol molecules (Figure 1.31.).[212-215] These were shown to be formed of stacked phenol molecules which were stabilised in non-polar solvents by the surfactant. The phenol and AOT molecules interacted via hydrogen bonding interactions. These gels were seen to revert to a solution upon an increase in temperature or when exposed to the atmosphere and allowed to absorb trace amounts of moisture, which led to the formation of mono-disperse reverse micelles. The AOT surfactant has also been used to form two-component organogels with a bile acid sodium salt as reported by Raghavan and co-workers.[216]

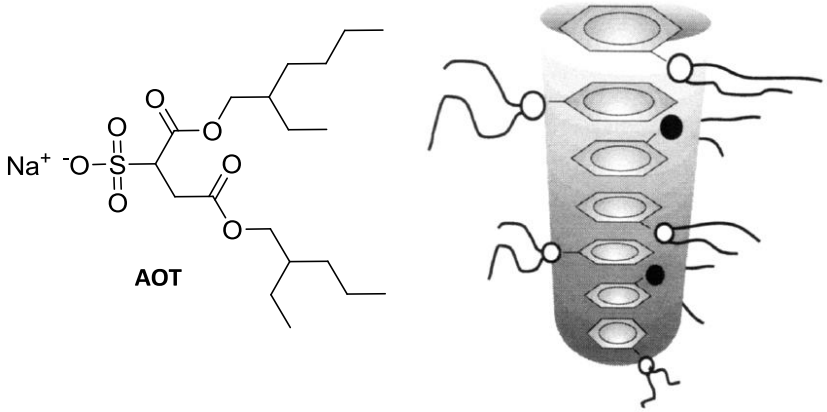

Figure 1.31. Surfactant salt AOT and self-assembled fibrils formed by 1:1 mixture of AOT and phenol in organic solvent.

A very interesting example of multi-component hydrogelators comes from the group of Osakada.[217] This report describes the formation of pseudorotaxanes from amphiphilic salt "rods" and cyclodextrins (Figure 1.32.). When only the amphiphile is present in solution it forms micelles, but micelle formation is stopped when one cyclodextrin sits around the amphiphile to form the [2]pseudorotaxane. As more cyclodextrin is added and the [3]pseudorotaxane is formed which is able to assemble into supramolecular polymers via interactions between the cationic pyridyl and the electron rich C_6H_3-3,5-$(OMe)_2$ moieties of different pseudorotaxanes and these polymers led to formation of a gel network. Furthermore, it was shown that this gelator was highly responsive to a number of chemical stimuli such as NaCl or urea that were introduced and were able to disrupt the intermolecular interactions that underpinned gel formation. This gel is based on a well known host-guest interaction – a hydrophobic moiety being encapsulated by a cyclodextrin in an aqueous environment.

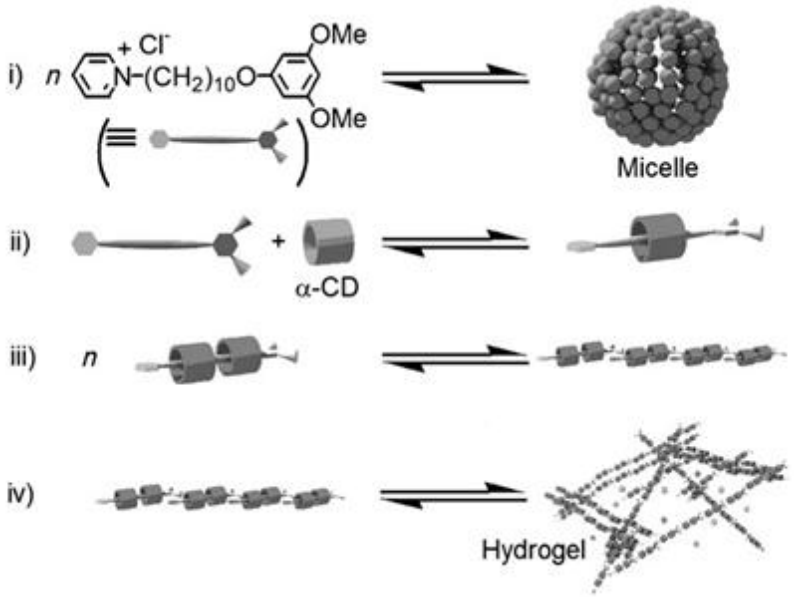

Figure 1.32. Formation of hydrogel from pseudorotaxane of charged amphiphile and cyclodextrin as reported by Osakada and co-workers. Adapted from reference[217]

Another interesting example of a multi-component hydrogel based on controlled host-guest interactions has been reported by Danjo, Yamaguchi and co-workers (Figure 1.33.).[218] They were able to form a gel from a 1:1 mixture of D_3 symmetric tris(spiroborate)cyclophane (**54**) and Ir(2,2':6':2''-terpyridine)$_2$(PF_6)$_3$ (**55**). The cyclophane acts as a twin bowl which is able to half-bind one of the large Ir complexes on each face; this allows a 1:1 mixture of each component to form a supramolecular polymer. When this mixture is formed in *N,N,N',N',N'',N''*-hexamethylphosphoric triamide a gel can be produced when the sample is heated above its LCST (estimated to be 78.5 °C), the gel then returns to a sol when allowed to cool to ambient temperature. This is an unusual example of formation of an organogel upon heating rather than cooling – it is universally considered that such gelation events are driven by entropy rather than enthalpy.

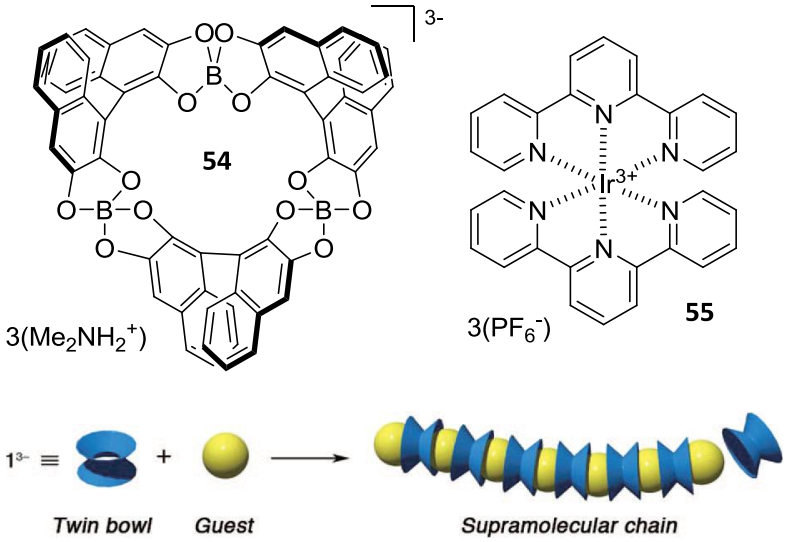

Figure 1.33. Tris(spiroborate)cyclophane twin bowl and Ir complex guest reported by Danjo, Yamaguchi and co-workers and schematic showing formation of supramolecular chains. Adapted from reference[218]

This example is very similar to another class of multi-component gelator where one of the components essential for gelation is a metal ion. These systems are commonly called metallogels.[219, 220] As many of these types of gel are covered in Chapter 2 as part of the section on silver(I) containing gels, only a couple of key examples will be highlighted here. The first comes from the Besseling and Marcelis groups, who designed a dumbbell shaped ligand with a 2,6-pyridinedicarboxylic acid moiety at each end (**56**) (Figure 1.34.).[221, 222] This group can bind to a range of metal cations, leading this molecule to form supramolecular polymers. These are capable of underpinning gelation when mixed with ions such as La^{3+} and Nd^{3+} in aqueous solution. The coordination polymers that formed consisted of rings with a 2:2 ratio of M^{3+} to ligand which are then connected by another ligand. The network could be broken down by the addition of Zn^{2+} ions as their inability to coordinate three ligands disrupted the gel network.

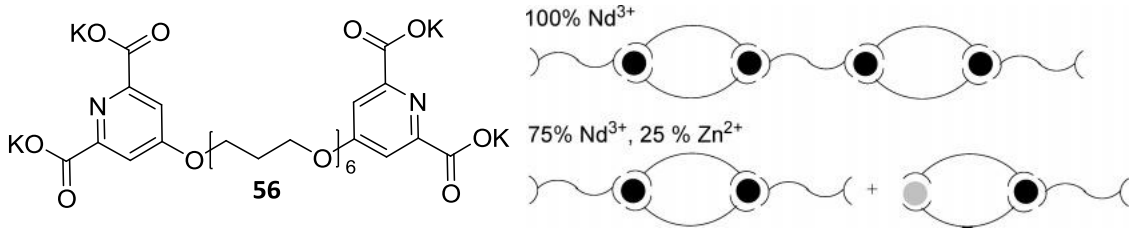

Figure 1.34. 2,6-Pyridinedicarboxylic acid based ligand and the coordination polymers it forms with Nd^{3+} and disrupted polymer caused by addition of Zn^{2+}. Adapted from reference[222]

The second example of a multi-component metallogel comes from the Rowan group.[223, 224] They reported another dumbbell shaped ligand, this time appended with 2,6-bis(N-methyl-benzimidazolyl)pyridine moieties (**57**) and their formation of gelation supporting coordination polymers with Zn^{2+}. Not only were these gels were shown to be responsive to a range of stimuli but they were shown to be formed by the aggregation of semi-crystalline globular particles of the coordination polymer. A consequence of this was that a gel formed by slow cooling could be sonicated, causing destruction of the gel, but also causing the globular particles in solution to become smaller. When the sample was removed from the sonication bath, these smaller particles could form an even more densely packed network and resulted in the formation of an even stronger gel.

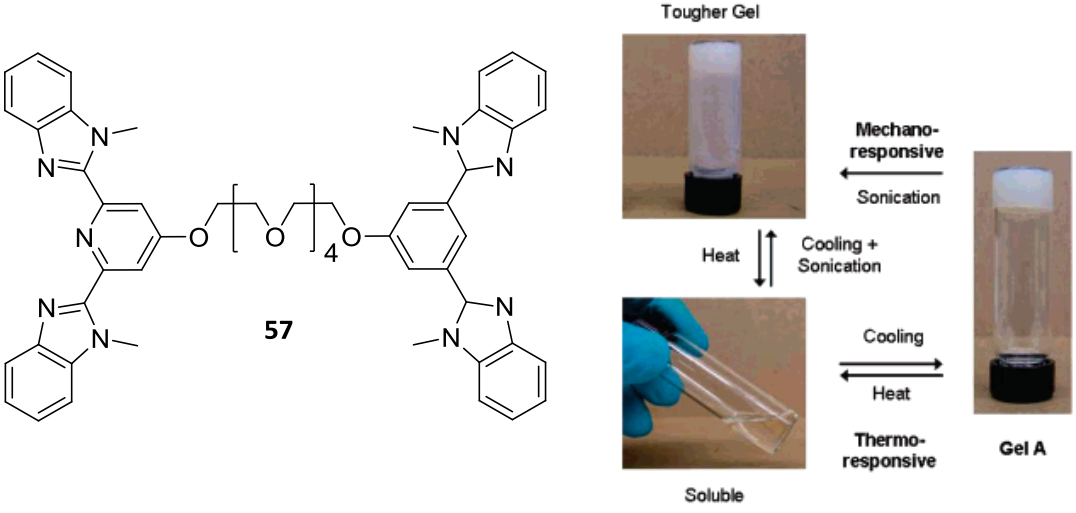

Figure 1.35. Ligand used by Rowan and co-workers to produce metallogel and the response of these gels to heating and sonication. Adapted from reference[223]

There are also a number of more unusual examples of multi-component gelators where mixing the components leds to gelation. One of these was reported by Wang, Kong, Yang and co-

workers.[225] It was envisaged by the authors that a hydrophilic phosphorylated, Fmoc protected tyrosine (**58**) would be converted to more hydrophobic Fmoc-tyrosine-OMe (**59**) by reaction with a phosphatase enzyme[131] (Figure 1.36.) and that this hydrophobic molecule would be able to induce gelation in PBS buffer. When conversion of this molecule was attempted with a high concentration of the enzyme a precipitate formed. Gelation was only observed when low concentrations of the enzyme were used. This is because in this instance not all of the initial starting material was dephosphorylated so co-assembled fibres of starting material (**58**) and product (**59**) resulted. These co-assemblies had a better balance of hydrophobic and hydrophilic character and allowed the formation of a gelator network, rather than a precipitate.

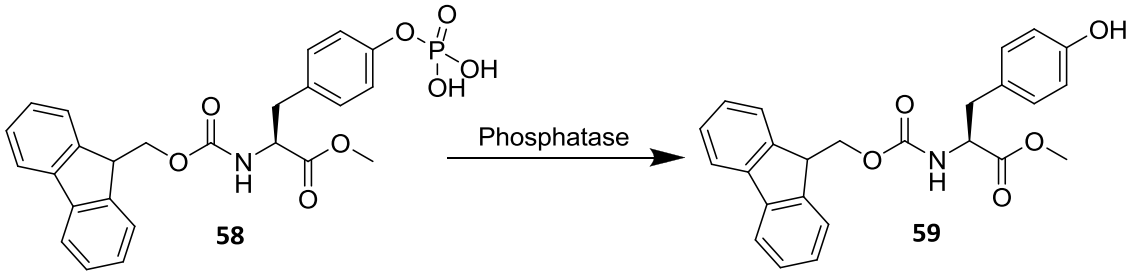

Figure 1.36. Hydrophilic starting material and more hydrophobic dephosphorylated product obtained after reaction with phosphatase.

A second unusual example of a multi-component gel comes from the group of van Esch.[226] They mixed a bisaldehyde (**60**) with a number of bisamines which resulted – through reversible covalent imine bonds – in the formation of polymeric type species, which were able to form vesicles in solution (Figure 1.37.). It was observed that these vesicles could coagulate, likely due to reversible covalent interactions between them, to form a network capable of inducing gelation. This could occur – in some instances – upon simple mixing. Despite the gelating species actually being a mixture of covalent oligomers/polymers/macrocycles the reversible nature of these covalent bonds and the formation of the gel from mixing small molecule building blocks mean it is worth considering here, despite not strictly being a gelator network actually made up of non-covalently linked small molecules. The reversible nature of this gel was demonstrated by it undergoing a gel-sol transition when heated to ca. 65°C.

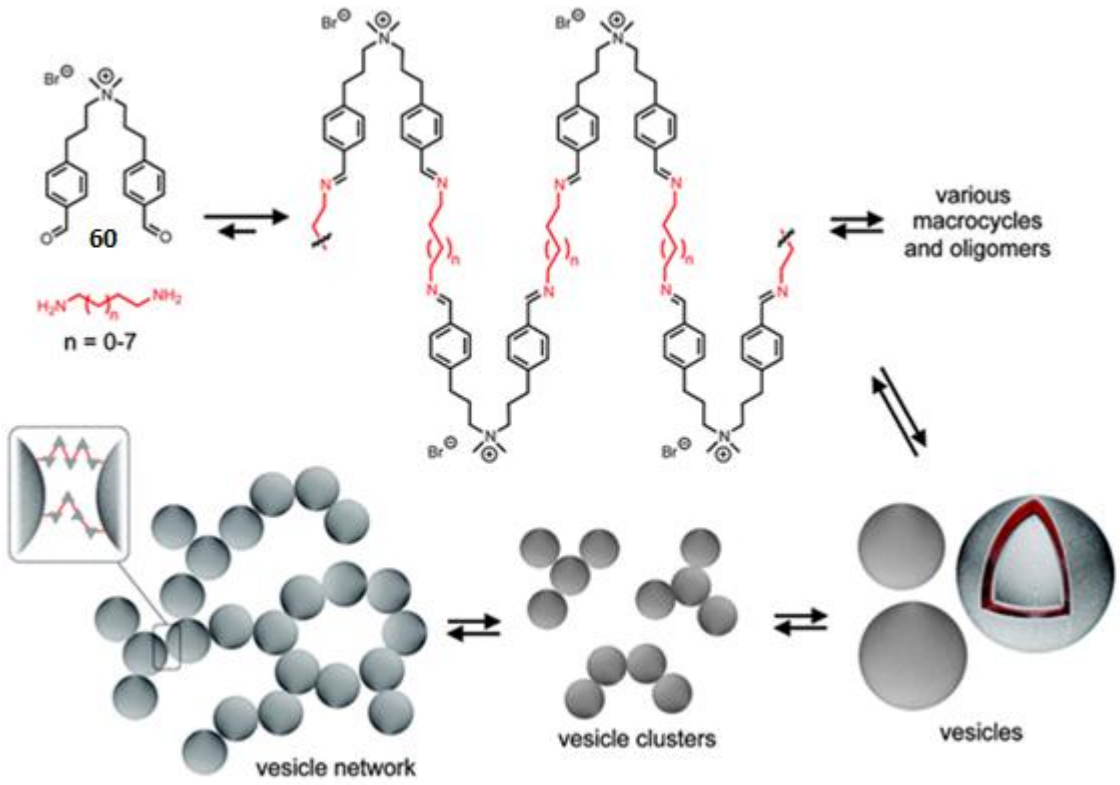

Figure 1.37. Formation of multi-component gel starting with formation of polyimine oligomers and macrocylcles, followed by further assembly to crosslinked vesicular network. Adapted from reference[226]

Another example of a multi-component gel which may not comfortably fit into the standard definition of a supramolecular gel (i.e. being made of discreet small molecules held together by non-covalent forces) was reported by Aida and Mynar.[227] In this report clay nanosheets (CNSs) were suspended in water, followed by addition of sodium polyacrylate (ASAP). This polymer is able to wrap around the edges of the CNSs and causes them to disentangle and become homogenously dispersed due to charge repulsion between anionic polymers. This was followed by addition of a guanidine appended, dumbbell shaped dendritic binder which binds to the faces of different CNSs and cross-links them, forming a sample spanning gelator network (Figure 1.38.). Gelation could still be achieved without the polymer, but was less effective as the CNSs were agglomerated and less available for binding with the dendritic molecule. The resultant gel was shown to be remarkably strong, self-healing and the solvent could be exchanged from water to THF with the gel retaining its macroscopic structure.

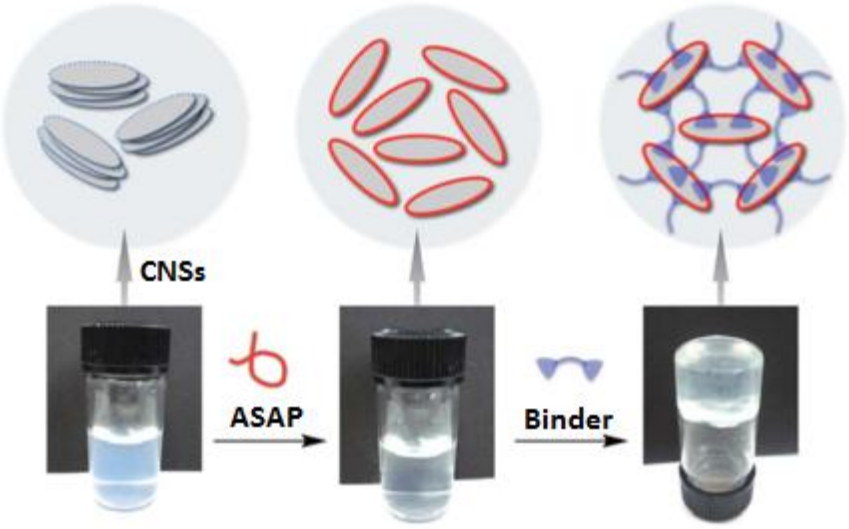

Figure 1.38. Formation of gel reported by Aida, Mynar and co-workers. Aggregated CNSs are suspended in solution. Addition of ASAP causes charge repulsion between individual CNSs and this results is disaggregation. Addition of dumbbell shaped dendritic binder cross-links individual CNSs causing formation of gelating network. Adapted from reference[227]

These selected examples have highlighted many different approaches to creating gels by mixing different non-gelling components. In many instances, this has allowed the properties of the gel to be far more tuneable, or in some way enhanced, either by changing which molecules are mixed together or changing the ratio of one to another.

The idea of forming gels from mixtures of different species provides the possibility of investigating component selection. This occurs when a library of potential gel forming species are mixed, and some are selectively incorporated into the gel network over the others. This concept is very strongly linked to that of dynamic combinatorial chemistry,[4, 228-230] where a library of compounds, all in equilibrium, can interconvert. This process is under thermodynamic control and involves the formation of either non-covalent or more commonly reversible covalent bonds. Component selection has been investigated in a range of supramolecular assemblies[231-237] but there are still very few examples in supramolecular gels.

The first such example was only published in 2005 by Lehn and co-workers.[238, 239] They investigated the formation of hydrogels formed from stacks of guanine quartets (G-quartets). These are formed by complementary hydrogen bonding between four guanine derivatives templated around a metal cation. The report started by demonstrating that a hydrazide appended guanine derivative (**61**) could form hydrogels and that when mixed with different

aldehydes, the resulting acylhydrazones could form either precipitates, solutions or stronger gels. This was taken adavantage of by mixing **61** with another hydrazide (**62**) which showed no hydrogelation ability whatsoever and with two aldehydes (**63** and **64**) – only one of which (**63**) reacted with **61** to form a gelating acylhydrazone (**65**). Therefore acylhyradzone **65** – which was formed from **61** and **62 –** was the only gelating acylhydrazone. It was clearly shown that at 25°C **65** was preferentially formed as it was stabilised due to its ability to induce gelation (Figure 1.39.). This also led to the formation of **68** which is made from the remaining components. At 80°C there was no gelation and each possible acylhydrozone (**65**-**68**) was present in equal amounts (ca. 25% of each). This was the first example of gelation driven component selection and had been achieved using reversible covalent bond formation to form the gelator, stabilised by hydrogen bonding and π-π interactions within the gel fibre assembly.

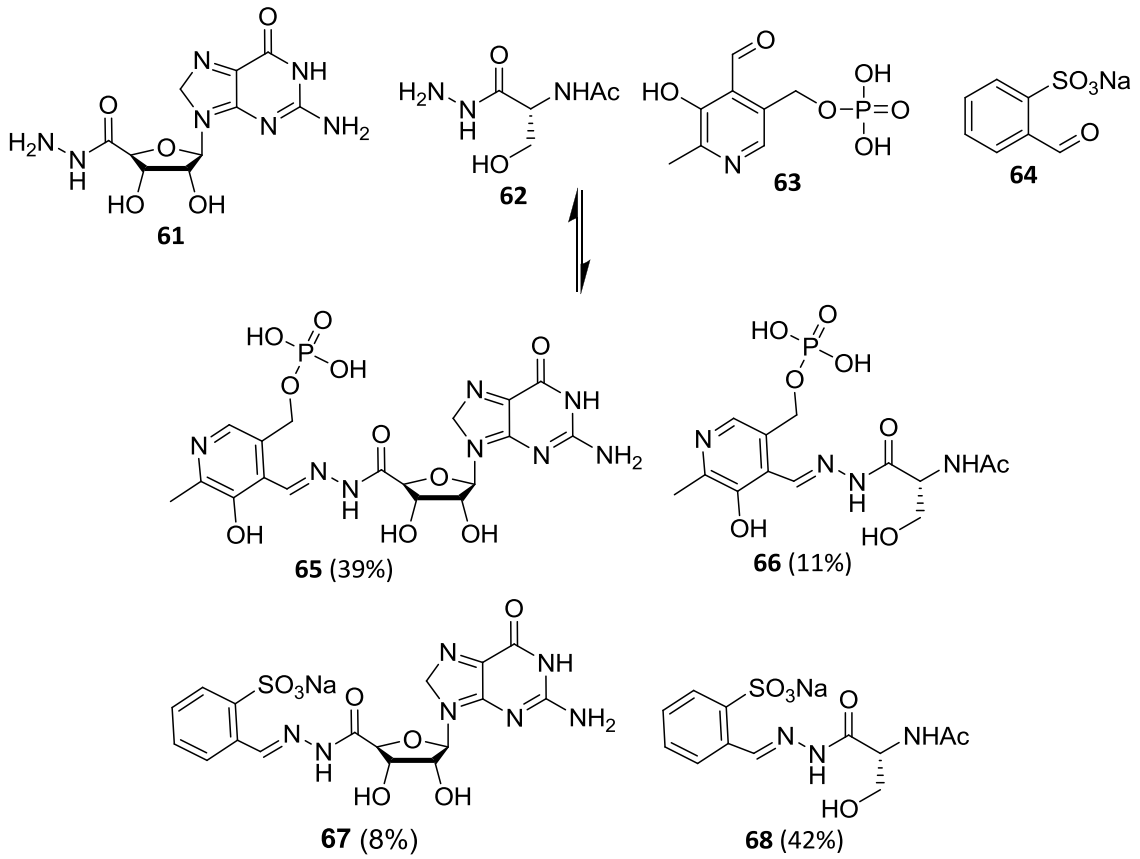

Figure 1.39. Component selection using gelation as a driving force as demonstrated by Lehn and co-workers.

The Li group have published another report on gelation driven component selection which also involves formation of reversible covalent bonds, in this case imines.[240] They found that an amine appended cholesterol molecule (**69**) was unable to induce gelation in a range of organic

solvents, however when mixed with certain aldehydes (**70**-**72**) an imine was formed which could induce gelation in alcohols (Figure 1.40.). When a simpler – but more reactive – non-cholesterol based amine (**73**) was used, none of the imines formed with the same aldehydes were able to induce gelation. Three-component mixtures containing equal amounts of both amines and one aldehyde were then tested. In these mixtures the aldehyde effectively had a choice of which amine to form an imine with, one of which was more reactive (**73**) and one which allowed the product imine to form stable gels (**69**). In solvents where gelation was supported, the cholesterol appended amine preferentially reacted to give the product imine capable of forming a gel network. In solvents where gelation was not supported, the more reactive non-cholesterol amine reacted preferentially. In solvents forming partial gels, the bias for either was minimal. This was another clear example of gelation driven component selection.

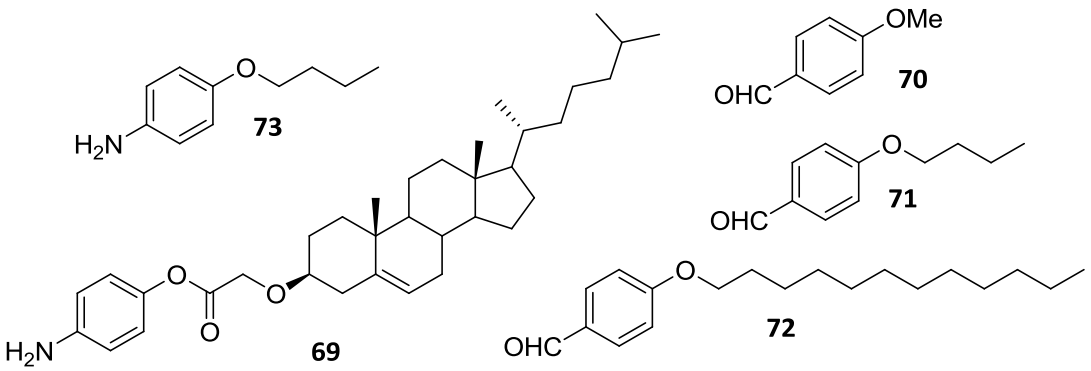

Figure 1.40. A selection of amines and aldehydes used by Li and co-workers to demonstrate gelation driven component selection.

Ulijn and co-workers have reported another example of a dynamic library of compounds that will preferentially form one product which can self-assemble more favourably.[241, 242] In this report the gelating species were the product of an amide formation reaction between an Fmoc-protected amino acid and a methyl ester protected amino acid, catalysed by an enzyme. The fact the enzyme also catalyses the reverse reaction – hydrolysis – creates a dynamic library of compounds. It was shown that an Fmoc-Thr (**74**) could react with either Phe-OMe (**75**) or Leu-OMe (**76**) (Figure 1.41.) to produce either Fmoc-ThrPhe-OMe or Fmoc-ThrLeu-OMe in 96% and 84% yield respectively. When **74**, **75** and **76** were mixed together in a competition experiment, the yields of each potential product change to ca. 82% and 14% respectively. This suggested to the authors that the Fmoc-ThrPhe-OMe product was able to self-assemble more effectively. Another experiment confirmed that this process was driven by competing

equilibria, when to form Fmoc-ThrLeu-OMe an equivalent of Phe-OMe was added and the yields of the two possible products changed to those observed in the previous competition experiment.

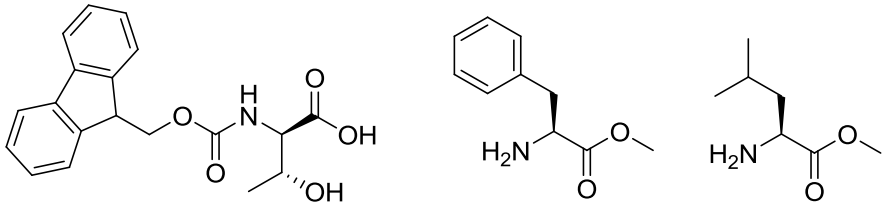

74 **75** **76**

Figure 1.41. Protected amino acids used in component selection experiments under enzyme catalysed dymanic conditions as reported by Ulijn and co-workers.

The Smith group have also reported gelation driven component selection in a gel formed from an acid appended lysine based dendron (**51**) and aromatic diamines (**77**-**79**) which are positional isomers of one another (Figure 1.42.).[243] In this case however the components interact non-covalently rather than through reversible covalent bond formation. When the dendron is mixed with each different amine the resultant sample is different. When **77** is used the sample remains a solution, when **78** is used a partial gel is formed and when **79** is used a strong gel is formed. It was clearly shown by ^{1}H NMR that when an equal amount of dendron and each diamine (a 1:1:1:1 ratio) is mixed a gel is formed and the vast majority of amine incorporated into the network is **79**, which forms the acid-base complex best able to self-assemble.

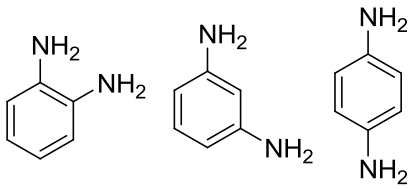

77 **78** **79**

Figure 1.42. Amines used in component selection experiment by Smith and co-workers.

More recently the Smith group has published another example of gelation driven component selection, this time based – like Lehn's work – on the formation of reversible covalent acylhydrazone bonds.[244] In this report gels were formed by the products of acylhydrozone formation between commercially available building blocks; lauric hydrazide and a range of

aldehydes (**80**-**84**) (Figure 1.43.). The best gel forming aldehyde was **80** (undecanal). When lauric hydrazide was added to a 1:1:1:1 mixture of **80**-**83,** it preferentially reacted and formed a gel with **80**. This was due to both the superior reactivity of **80** and the fact that this product acylhydrazone could form a stable gel, whilst the other possible products could not. A more subtle difference in aldehyde was also used to induce component selection when to a 1:0.5:0.5 mixture of hydrazide, **80** and **84** (below the minimum gelation concentration of the hydrazide or either acylhydrozone) excess **80** was added. This induced the formation of a gel like material and indicated that the better aldehyde for gelation (**80**) could displace **84** in the acylhydrazones with gelation providing the driving force for the adaptive behaviour.

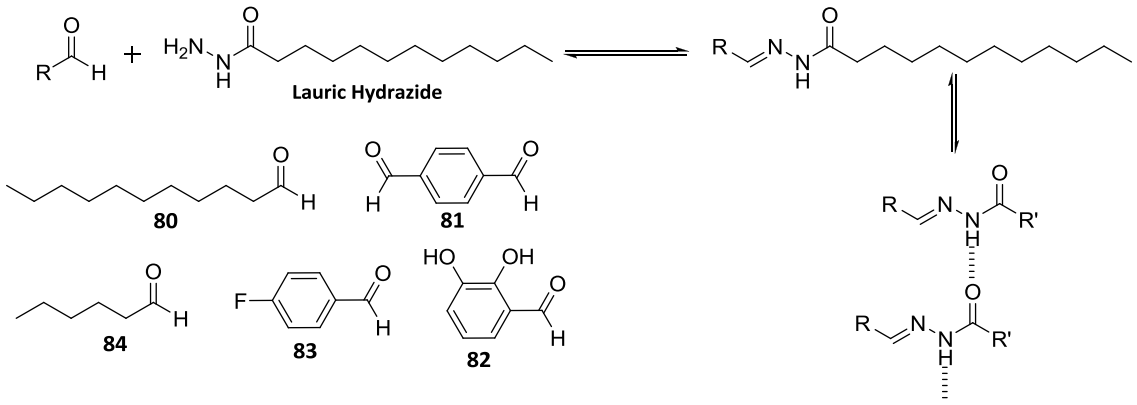

Figure 1.43. Lauric hydrazide and range of aldehydes used to demonstrate component selection in acyl hydrozone gels as reported by Smith and co-workers.

These examples have shown forming gels from multiple components can in fact be a driving force for component selection. Most of the gels involve the formation of gelator molecules from the initial components added via reversible covalent bond formation, with only one example presented by Smith and co-workers using a true non-covalent multi-component gelator.

1.2.2. Mixing Gelators

As well as gels formed from the mixing of different components which individually have no gelating ability, there have also been many studies on the effect of mixing different known gelators. These are sometimes called composite gels and the main principle behind this work is that the properties of the resultant materials will be highly tuneable, with the chemist being able to access gels that show either properties of both different gelators, a mixture of each – dependent on the ratio of each used – or in some cases completely different behaviour to that

shown by each gelator individually. In basic terms, the mixing of different gelators can have two extreme results. Either the gelators will both assemble into the same network – so called co-assembly – or they will each form individual and non-interacting networks – so called self-sorting. Both of these effects have been investigated in other supramolecular assemblies and are often known by the terms social and narcissistic self-sorting.[245, 246] Of course between these two extremes gelators can also form partially self-sorted networks, or separate fibres which interact at the network level.

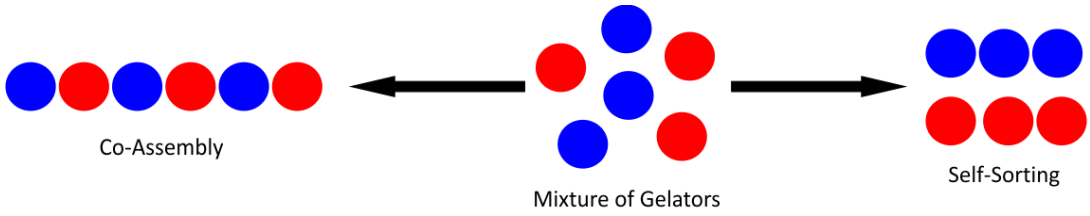

Figure 1.44. Diagram showing the extremes of co-assembly and self-sorting.

One of the first eaxmples of a co-assembled gel comes from the groups of Shinkai and Reinhoudt who formed gels two similar glucose based gelators (Figure 1.45.).[247] Each molecule is a gelator in its own right but a 1:1 mixture of both led to gels with a much higher thermal stability in certain solvents. In this instance the mixed system produced a colour change upon gelation from colourless to yellow, which was found to be due to a charge transfer band between the two-gelators. This indicated that the mixed system forms a donor-acceptor complex between the gelator with an electron poor aromatic ring (**85**) and the gelator with an electron rich aromatic ring (**86**). Interestingly, gels formed by each gelator in diphenylether showed a flat tape morphology by TEM but the mixed gel showed a twisted tape morphology (Figure 1.45.), indicating that the co-assembly changed the way molecular chirality was transcribed into the nanoscale fibres. Pakulski and co-workers have also iventigated creating tunable behaviour in gels by mixing two sugar based gelators.[248]

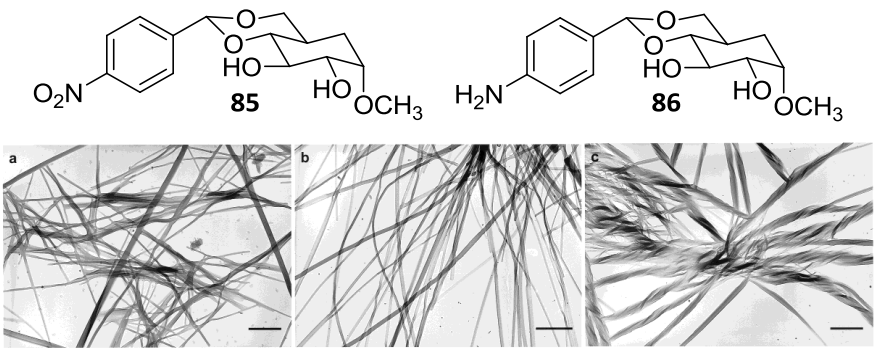

Figure 1.45. Sugar based donor-acceptor gelators. TEM images of xerogels of A) **85**, B) **86**, and C) **85** and **86**. All dried from diphenylether gels, Scale bars = 1 μm. Adapted from reference[247]

Escuder, Miravet and co-workers have investigated the effects of mixing a series of amidocarbamate organogelators (**87**-**91**) (Figure 1.46.).[249] Their initial finding was that when these bola-type molecules have different length alkyl spacers at their core their gelation ability is changed. The study then went on to describe the effect of mixing these different gelators on gel formation. What they surprisingly found was that the mixtures of compounds were far more effective gelators than each individual molecule, even when the largest and smallest of the gelators (**87** and **91**) were mixed it still improved their gelation ability as measured by the minimum concentration needed to form a gel. Not only was this found to be the case for a binary mixture of gelators but also a tertiary mixture, with three different gelators (**87**, **89** and **91**) providing an even more potent gelating mix. The same effect was also seen in a family of novel tetraamido gelators (**92**-**96**). The gelation of mixed biscarbamate systems has been studied by Sundararajan and co-workers.[250]

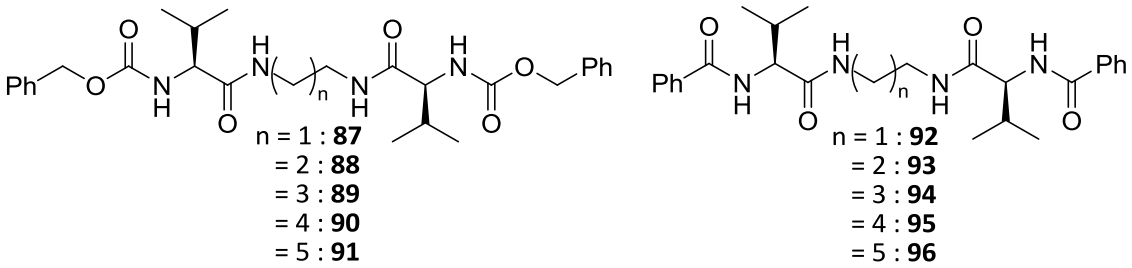

Figure 1.46. Amidocarbamate and tetraamido gelators studied by Escuder, Miravet and co-workers.

Suzuki and Hanabusa have investigated the effect of mixing a lysine based bisamide organogelator (**97**) with its own alkali metal salt derivatives (**98**-**100**) (Figure 1.47.).[251] The

carboxylic acid compound is a capable organogelator but is insoluble in water. The alkali metal salt carboxylate derivatives are completely soluble in water and actually perform as superior organogelators to the original carboxylic acid compound. Mixtures of the carboxylic acid and carboxylate compounds however, were able to gelate water and a range of other aqueous solutions. This was due to the fact that carboxylate salts individually formed micelles that were incapable of inducing gelation but a mixture of carboxylate and carboxylic acid resulted in a different hydrogen bonding arrangement, which resulted in fibre formation to become more favoured, leading to gel formation. The authors also state that mixing the more hydrophobic carboxylic acid and the more hydrophilic carboxylate compounds produced mixtures with the right solubility balance to induce gelation, an excellent example of a how mixing gelators can modulate the properties of the gel. The mixing of bisurea gelators has also been investigated – separately – by Steed[68] and Bouteiller.[252, 253]

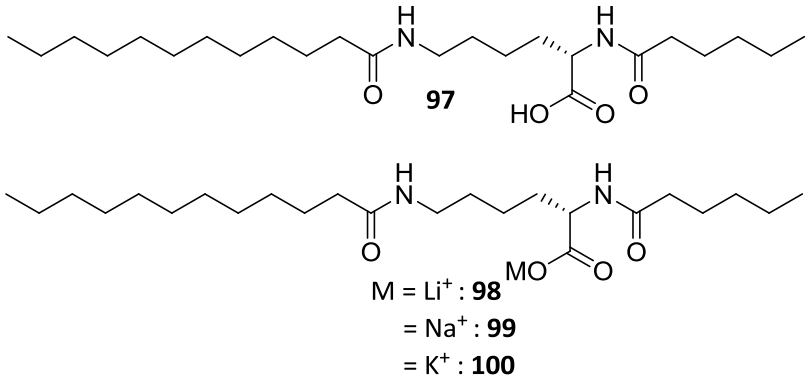

Figure 1.47. Carboxylic acid and carboxylate gelators mixed by Suzuki, Hanabusa and co-workers to induce gelation in aqueous solution.

Stupp and co-workers have probed the effect of mixing synthetic polypeptide gelators as a method of modulating fluorescence for the production of bio sensor gels (Figure 1.48.).[254] They first synthesised a fluorescent peptide gelator (**101**) that, when assembled, exhibited quenching of its own fluorescent unit due to close aggregation of these aromatic groups. When the assemblies of this molecule were "diluted" by addition of a co-assembling non-fluorescent peptide (**102**) the quenching was removed and an increase in the intensity of fluorescent emission was observed. This was utilised as a biosensor by co-assembling the fluorescent peptide with a heparin binding one (**103**). The fluorescent peptide emitted at a similar wavelength to the absorption of fluorescein tagged heparin so fluorescence resonance energy transfer (FRET) could be used to monitor binding of the biological macromolecule to

the dispersed gel fibres under confocal microscopy. The co-assembly of different peptide based gelators has also been observed by Nilsson and co-workers who observed that a stronger hydrogel could be formed from a mixture of PEG functionalised and non-PEG functionalised gelators, as this mixing modulates the solubility profile of the co-assemblies.[255]

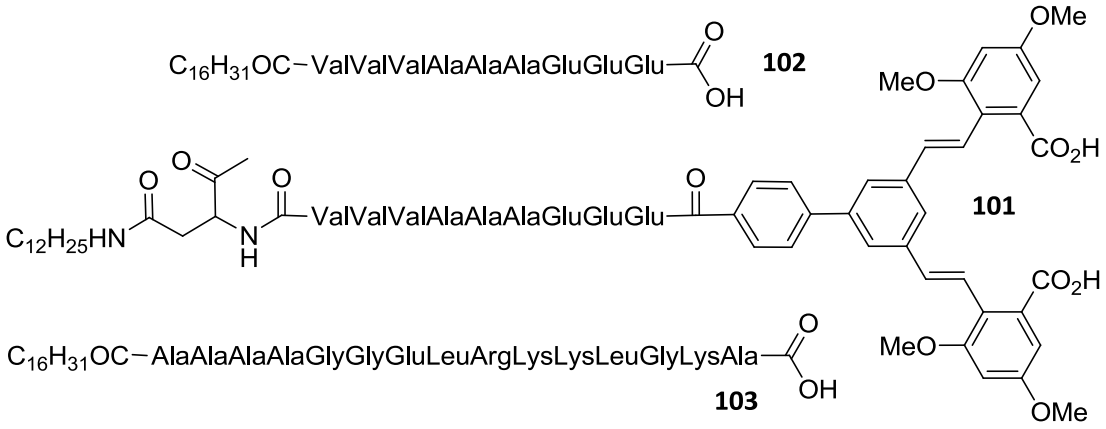

Figure 1.48. Structure of peptide hydrogelators produced by Stupp and co-workers.

Recently, a large study by Maitra, Guerzo, Desvergne and co-workers has investigated the effect of forming composite gels with mixtures of perfluorinated bile acid derivatives (**104**-**111**) and a dialkyl functionalised anthracene (**112**) (Figure 1.49.).[256] This study was most interesting because it probed the co-gelation of two structurally different gelators which had no obvious mutual interactions. It was shown during this study that mixing of two components does form a co-assembled gel and that in a few cases the co-gel was more thermally stable than the gels formed form either component individually, even if this was solvent dependant. A co-assembly in DMSO was able to impose a chiral environment on the non-chiral anthracene derivative so that it produced a circular dichroism spectrum via its close aggregation with a chiral bile acid derivative. Interestingly the authors also found that when analysing the aerogels, both gelators adopted a similar mode of molecular packing, which was very similar to that observed in the composite gel. This led the authors to postulate that molecules which individually pack with similar symmetry and cell parameters are capable of forming co-assemblies, even if their molecular structures are very different.

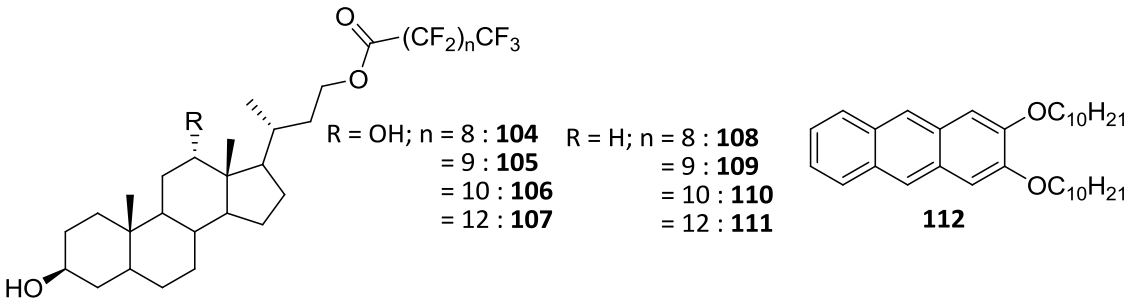

Figure 1.49. Bile acid derivatised and anthracene based gelators shown to co-assemble.

Hamachi and co-workers have investigated the pH response of a hydrogel formed from co-assembly of a known hydrogelator (**113**) and a carboxylic acid bearing molecule (**114**) (Figure 1.50.).[257, 258] Both molecules formed co-assemblies that were capable of gelating water, ideally at a 1:1 ratio. When the pH of this gel was reduced by exposure to HCl vapour, the gel network was seen to shrink to roughly half its original volume. This change could be reversed (by addition of buffer) and this process repeated at least 6 times. The shrinkage was due to the carboxylic acid bearing molecule becoming re-protonated at lower pH causing the negative charge of the carboxylate groups to be neutralised and the network to become far more closely packed. Based on this the authors proposed a model of co-assembling known gelators with “additive commander” molecules that were not gelators in their own right but could co-assemble with gelators and add some functional / responsive property to the gel network. The authors further demonstrated that shrinking of the gel could be used to release hydrophilic B vitamins but was less successful at releasing hydrophobic flavone derivatives which stayed localised in the hydrophobic parts of the gelator network.

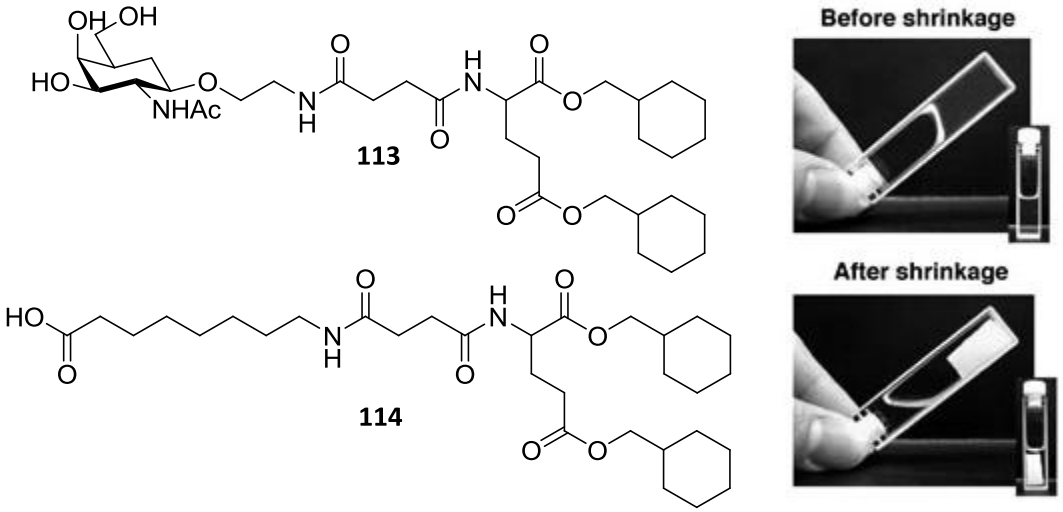

Figure 1.50. Hydrogelator and co-assembling carboxylic acid additive used by Hamachi and co-workers to produce a pH responsive shrinking gel (shown on right). Adapted from reference[257]

The idea of adding a functional molecule to co-assemble with a known gelator has been exploited by Díaz and co-workers.[259] In this work, the authors formed gels with a known hydrogelator based on cystine with amounts of structurally related alkene functionalised molecules added. Multi-valent thiol functionalised molecules and a photoinitiator were also added and irradiation with UV led to thiol-ene coupling between the alkene functionalised molecules and the thiol crosslinkers (Figure 1.51.). This led the previously very weak gel to become a highly robust, crosslinked network, which was able to undergo far harsher treatment, such as sterilisation. The report also investigated how the crosslinking affected drug diffusion from the gel, demonstrating that as expected, more heavily crosslinked samples had slower diffusion kinetics.

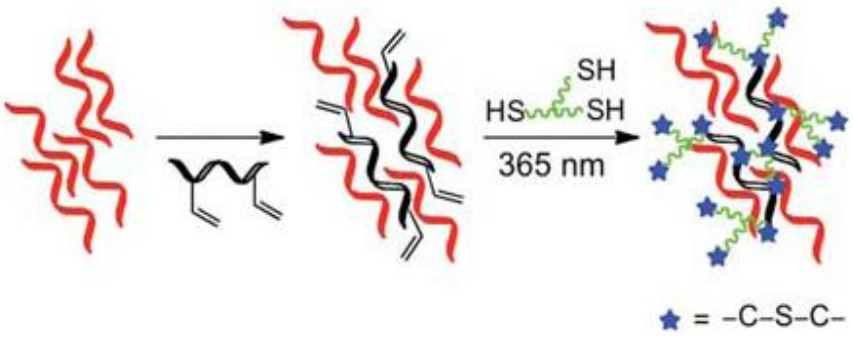

Figure 1.51. Overview showing gelator (in red) being co-assembled with structurally related alkene functionalised molecule. Addition of thiol cross-linker and UV irradiation led to thiol-ene cross-linking. Adapted from reference[259]

The previous two examples do not involve the mixing of two gelating species but use co-assembly to produce a far more functional gel than the gelator can form alone. For this reason, they have been included in these highlights of co-assembled gels. The other main type of composite gel is those which self-sort. Self-sorting of assembling molecules has been observed in a range of supramolecular structures[260-265] but there are still relatively few examples of self-sorting gels.

Smith and co-workers published a comprehensive article on their investigations into the self-sorting (or not) of a family of dumbbell shaped dendritic lysine based gelators.[266] Through a series of experiments, it was shown that mixing dendritic head groups of different chirality or different generation, i.e. size, could cause self-sorting of the gelators. In contrast to this, it was seen that changing the length of the linker between head groups did not induce self-sorting of the gelators and resulted in co-assembly. This showed that changes to the dendritic group, where the intramolecular hydrogen bonding groups are located could control molecular recognition between different gelator molecules. Changes to the linker, with no control over hydrogen bonding and therefore molecular recognition could not induce self-sorting. The same group then went on to investigate self-sorting in a different family of lysine based gelators.[152, 267] In this study, it was seem that two similar gelators with either peripheral Boc groups (**115**) or hydrocarbon chains (**116**) were able to self-sort into two different gelator networks when mixed in 9:1 styrene to divinylbenzene, even providing a striking FEG-SEM image of the two separate networks (Figure 1.52.). Furthermore it was shown that alkene functionalised gelator (**116**) could be post-polymerised by addition of Grubbs catalyst and the network of the Boc protected gelator (**115**) then removed by washing. The same group has also recently published

a study of self-sorting between two well known gelators; dibenzylidene sorbitol and a pyridine appended cholesterol gelator previously reported by Shinkai.[268]

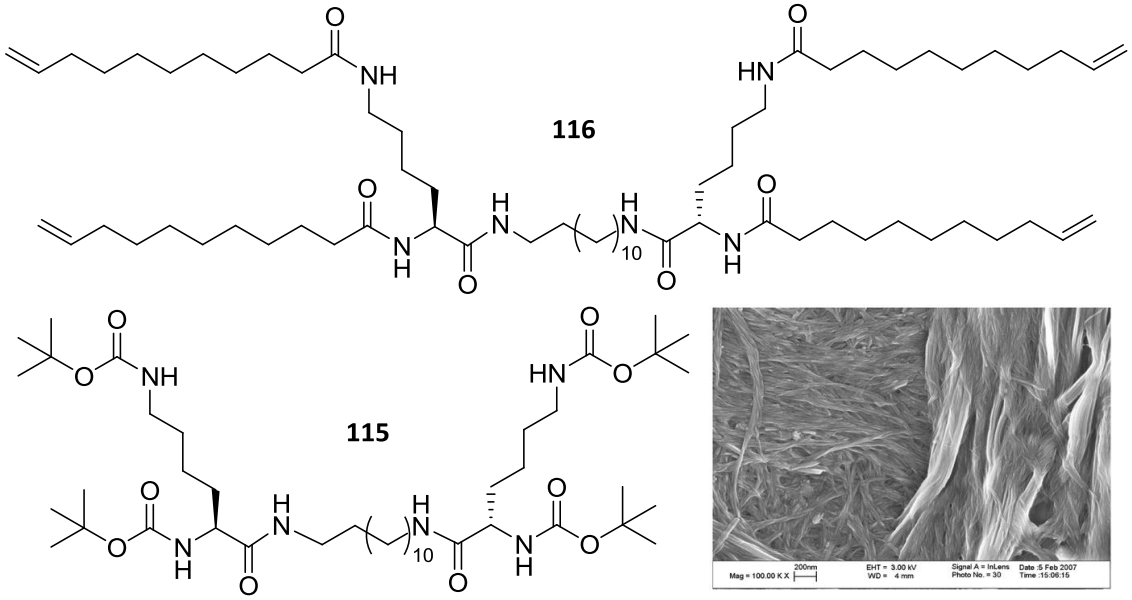

Figure 1.52. Self-sorting gelators studied by Smith and co-workers and FEG-SEM image showing separate networks formed in the mixed sample. Scale bar = 200 nm, dried from 9:1 styrene to divinylbenzene solvent. Adapted from reference [152]

The Shinkai group has reported another instance of self-sorting gel.[269] In this report the authors took two known organogelators, one a p-type semiconductor (**117**) and the other an n-type semiconductor (**118**) (Figure 1.53.). When a mixture of both gelators formed a gel it was shown to be self-sorted, which the authors attributed to the different number of hydrogen bonding sites on each gelator. Gelator **117**, with four hydrogen bonding sites, was shown to have an aggregation constant (K_{agg}) two orders of magnitude higher than **118**, causing self-recognition of this molecule to be highly favoured. The materials produced were interesting as the junctions between the p-type and n-type gelator fibres became p-n junctions – where current can flow in only one direction – due to a charge transfer interaction (Figure 1.53.). In the final section of the paper a photo-induced current was indeed generated using a drop cast film of a self-sorted gel. Ghosh and Das have also reported a self-sorting mixture of donor and acceptor gelators based on a mismatch of hydrogen bonding sites between the two different molecules.[270]

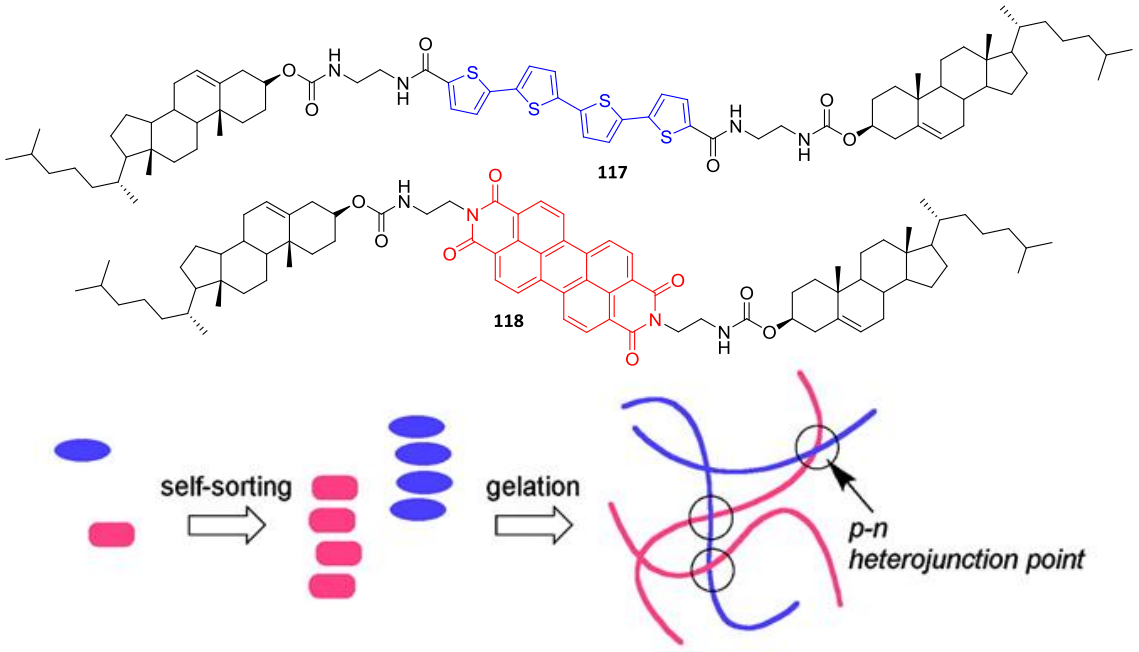

Figure 1.53. P-type and n-type gelators used by Shinkai and co-workers to produce self-sorted, p-n junction containing mixed gel. Adapted from reference[269]

Adams and co-workers have reported an example of self-sorting gelators which self-sort due to one network being formed before the other.[271] This study used two naphthyl appended dipepide gelators (**119** and **120**, Figure 1.54.) which each assembled into gelator networks when the pH of the sample drops below the apparent pKa value of each gelator (5.9 for **119** and 5.1 for **120**). Using the diffusion and hydrolysis of glucono-δ-lactone through the sample to induce a slow lowering of pH led to **119** (higher pka) forming a gelator network before **120**, which only as the pH dropped further became protonated and started to assemble. The authors were able to demonstrate that the resulting gel was indeed composed of two separate networks identical to the ones the gelators formed individually.

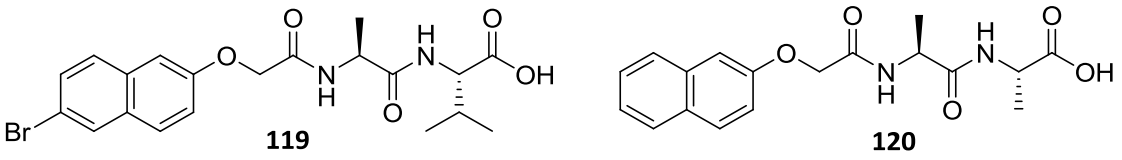

Figure 1.54. Self-sorting gelators reported by Adams and co-workers.

Another example of the self-sorting of gelator networks has been reported by Velázquez and Luque. Interestingly in this example it was proposed that whilst each network formed separately, both interacted on the nanometer level which resulted in a synergistic effect on gel

stability.[272] Van Esch and co-workers have added another twist to the field of self sorting gelators by orthogonally assembling both a gelator and a surfactant to produce inter-penetrating networks of surfactant vesicles and fibrous gelator network.[273]

1.2.3. Additives to Gelator Network

The last major family of multi-component gels are samples where a species is not incorporated into the gelator network itself but none the less has an effect on the gel properties. This is the least relevant section to the work covered in this thesis and as such only a few key examples will be covered. The first such example comes from the group of Liu who found that mixing molecules **121** and **122** in a 56:44 ratio (10 wt% total concentration) in diisooctylphthalate solvent produced an opaque paste, which when viewed under an electron microscope revealed a sample of needle-like crystals (Figure 1.55).[274] However when a very small amount (0.004 wt%) of an ethylene/vinyl acetate copolymer was added a strong gel was formed under the same conditions. The authors proposed a model of gelation whereby the polymer adsorbed to the growing end of the needle crystals causing imperfect crystal growth and a branching point to from. Many such events took place during the cooling of the sample to produce a highly branched network of fibres that supported gelation. The concentration of polymer added was found to control the mesh size of the gel network formed. The same authors published further studies of the effect non-gelating additives – in this case surfactants – can have on gelation,[275, 276] as have the Rowan group.[277]

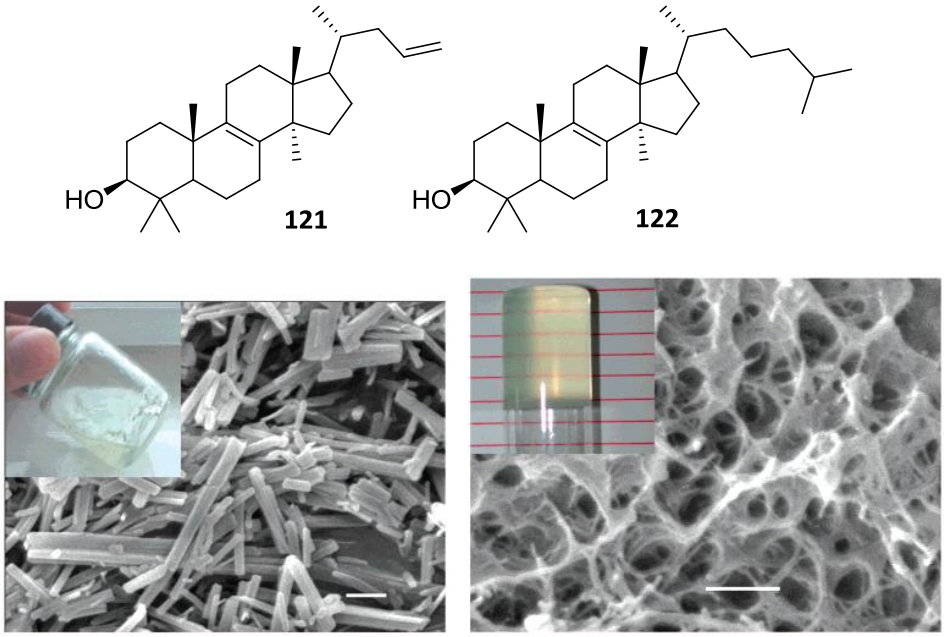

Figure 1.55. Structures of **121** and **122**. Images are: Left – a 10 wt% mixture of **121** to **122** (56:44) and Right – the same mixture but with 0.004 wt% ethylene/vinyl acetate co-polymer added. Scale bar = 1 µm. Both dried from diisooctylphthalate solvent. Adapted from reference[274]

These reports of multi-component gels show that mixing different species in the gel phase can result in previously unattainable tunability of the gel properties or the discovery of novel attributes in a gel. This can be achieved by mixing known gelators, mixing compounds that individually do not form gels or by adding compounds that are not required for gelation but can co-assemble and add almost "bottled" functionality to a gel phase material. Many of these concepts have been extended further to crucial supramolecular subjects such as self-sorting and component selection and the few examples of gels that exhibit these effects will aid our understanding of these processes and most likely led to the generation of more novel, functional materials.

1.3. Chirality in Gels

1.3.1. Influence of Chirality

Chirality is a very important influence in many molecular recognition processes[278] and in the control of secondary structure of macromolecules.[279] A very neat example of this is the homochirality of amino acids in the animal and plant kingdoms (L) and in bacterial life (D).[280, 281] In these life forms, the secondary and tertiary structure of proteins is controlled in part by the chirality of the amino acid residues in the polypeptide chain. In many enzyme-catalysed reactions, a substrate of "wrong" chirality will not be able to react due to steric clashes caused by this change in chirality. The ability to utilise this type of chiral control in man-made macromolecules and materials is very important[279] and supramolecular gels are no exception.[282] Research into chirality in supramolecular gels is closely related to chirality in supramolecular polymers – as this is often the first step in gel formation – and this research is in turn heavily influenced by chiral effects in chemically bonded polymers. As such, this review of the influence of chirality in supramolecular gels will begin with a brief outline of key work in both of these two related fields, beginning with the study of chirality in chemical polymers.

1.3.2. Chirality in Polymers

This section will specifically focus on work from the group of Green as this is commonly cited as a major influence on those studying chirality in supramolecular systems. In 1989, Green and co-workers published a paper reporting what they described as the "sergeants and soldiers experiment" where a small amount of chiral monomer was incorporated into a largely non-chiral polymer, resulting in disproportionately large optical activity.[283] This effect had been previously observed in polymers but this paper not only coined the term "sergeants and soldiers" but also proposed the mechanism by which this is achieved. The basic polymer used in this study was poly(n-hexyl isocyanate) (Figure 1.56.) which was known to exist in a helical conformation with long stretches of M or P helix separated by energetically unfavoured helix reversal points.[284] As the polymer contained no chiral centres there were equal amounts of M and P helix and overall the secondary structure of the achiral polymer was racemic. However, the authors found a non-linear response in $[\alpha]_D$ with increasing levels of incorporation of chiral monomer into the polymers. The authors proposed that this was achieved because incorporation of chiral sergeants biased a section of helical polymer to either M or P, depending on the stereochemistry of that chiral monomer. As helix reversal points were so

infrequent, this bias would affect a large number of achiral monomers. Through this mechanism, a small number of chiral "sergeant" monomers can induce certain chirality on a large number of achiral "soldier" monomers.

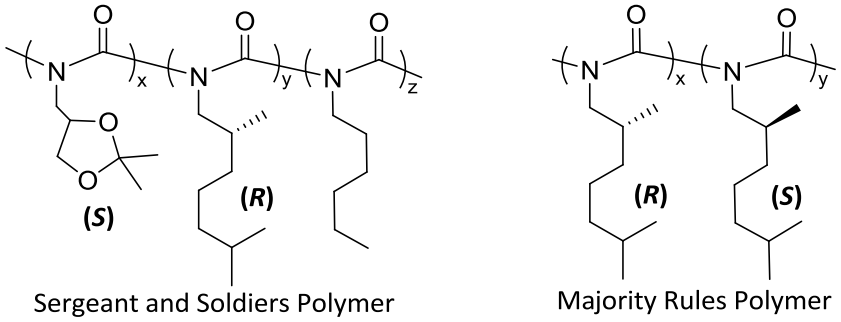

Sergeant and Soldiers Polymer Majority Rules Polymer

Figure 1.56. Different polymers used by Green and co-workers to investigate the effect of chirality on polymer conformation.

In 1995 another paper from Green and co-workers reported that incorporation of a slight enantiomeric excess or *R* or *S* monomer in poly(2,6-dimethylheptyl isocyanate) (Figure 1.56.) could also produce an unusually large change in optical rotation or circular dichroism spectrum.[285] The authors proposed that this was due to the energy cost of having a chiral monomer as part of the polymer chain with the "wrong" helical preference being far less than the energy cost of a helix reversal point. This results in many monomers sitting in helices of the "wrong" handedness rather than the helix screw sense changing. The energy cost of incorporating each enantiomer of monomer into a helix of the wrong type means that a slight majority of one enantiomer makes it more favourable for the helix to be in this monomer's preferred conformation. The authors describe this as the "Majority Rules" effect, where the majority monomer will enforce its preferred conformation on the whole polymer. They also point to its potential application in supramolecular polymers.

Green, Selinger and co-workers have also combined the two concepts described above and reported an effect in polymers of a slight imbalance of chiral monomers which are also highly diluted by achiral monomer.[286] Much like in the "sergeant and soldiers", the high helix reversal penalties cause the amplification of chirality along large segments of polymer chain.[287] The dependence of the amplification of chirality on the high energy barrier of helix reversal has been demonstrated by the dependence of all of these effects on temperature, the amplification of helical handedness decreasing with increasing temperature as helix reversal points become more common.[288]

1.3.3. Chirality in Supramolecular Polymers

Heavily influenced by the work of Green; Meijer and co-workers have produced a large body of work on chiral effects in supramolecular polymers.[289, 290] In 1997, this group published the first report of a supramolecular polymer which showed induced amplification of chirality, obeying the "sergeant and solders" principle.[291] This paper studied mixtures of disc-shaped molecules **123** and **124** which were able to assemble in alkane solvents (Figure 1.57.). The overall measured chirality of the sample had a nonlinear dependence on the amount of **123** added with a very small amount producing a large increase in the strength of the observed circular dichroism spectrum. It was found that a single molecule of chiral **123** (sergeant) was able to induce helicity on roughly eighty non-chiral molecules of **124** (soldiers). As this was a dynamic supramolecular polymer not a chemically bonded one, this amplification of chirality could occur upon sample addition of **123** to a sample of **124**. The same group have demonstrated that a range of different assembling molecules can show this effect in organic solvents[292, 293] or in aqueous solution.[294, 295]

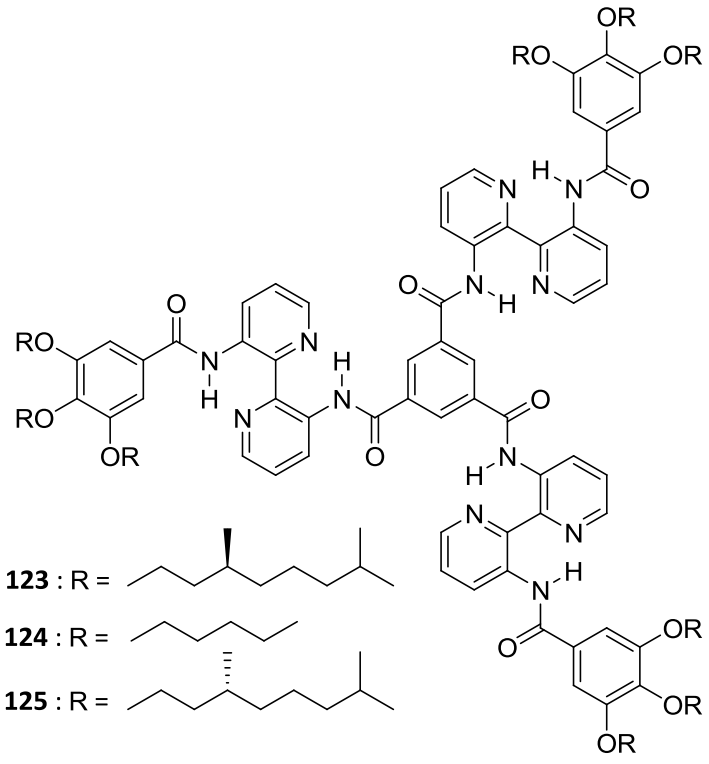

Figure 1.57. Molecules used by Meijer and co-workers to probe chiral assembly.

This group has also demonstrated the first example of the "majority rules" effect occurring in supramolecular systems.[296] This study again used C_3-symmetrical disc shaped molecules, in this case enantiomers **123** and **125** (Figure 1.57.). It was shown that net helicity of the sample had a non-linear dependence on the enantiomeric excess of the sample (Figure 1.58.), with a relatively low excess of either enantiomer producing a sample with the same overall helicity as an equivalent sample of that enantiomer alone. Again it was seen that the mismatch penalty of accommodating a molecule in a helix of the wrong handedness was far less than the energy penalty of reversing the direction of the helix.

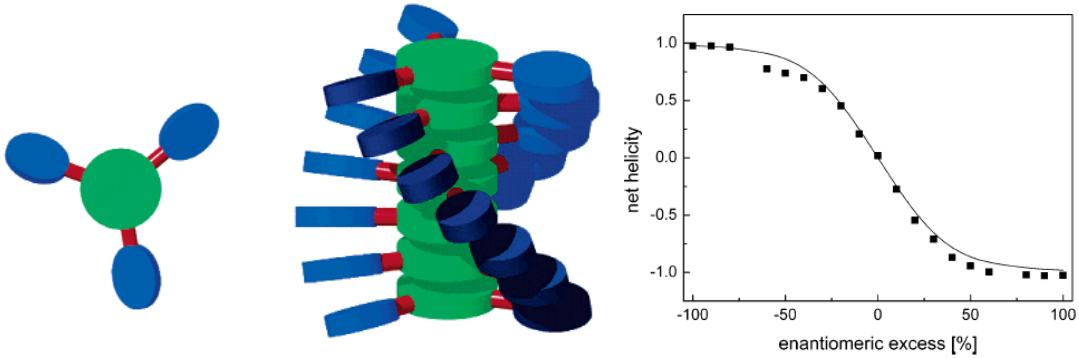

Figure 1.58. Model of aggregation of disc shaped molecules reported by Meijer and co-workers and a graph showing the change in net helicity of the sample with changing enantiomeric excess. Adapted from reference[296]

A number of papers have been published by the same group with collaborators documenting supramolecular polymers made with a range of achiral or chiral molecules which obey both the "sergeant and soldiers" and "majority rules" effects.[297-299] Their research into chirality in supramolecular polymers has also led to reports of chiral induction through the bonding of chiral acids to racemic stacks of an achiral molecule,[300] deracemisation of a racemic mixture of molecules using a chiral "super sergeant" and the introduction of chirality into a molecule,[301] and subsequently a helical polymer, by hydrogen/deuterium substitution.[302]

The same group have also investigated similar effects in porphyrin-based systems[303] and have even managed to demonstrate a "chiral memory" effect where the chiral sergeant is removed but its helical sense is still enforced on the achiral monomers.[304] In this report, achiral Cu porphyrins were co-assembled with chiral (*S*) Zn porphyrins and led to the amplification of helicity in the co-aggregates known as the "sergeant and soldiers" effect. Addition of the base quinidine (QND) led to selective ligation of the chiral Zn porphyrins which caused them to

depolymerise. Despite the supramolecular polymers now consisting of almost entirely achiral Cu porphyrins, the circular dichroism spectrum of the sample was largely unchanged, so the helicity of the aggregates was still the same as that enforced by the now removed chiral porphyrins. Heating this sample to above its elongation temperature (T_e) led to complete disassembly of the polymers and a loss of net helicity upon cooling, as there is very little chiral "sergeant" to direct helix direction. However heating to just below the T_e followed by cooling led to partial regain of helicity as small sections of helical polymer were not fully disassembled and could direct the assembly of the other monomers upon cooling, acting as chiral seeds.

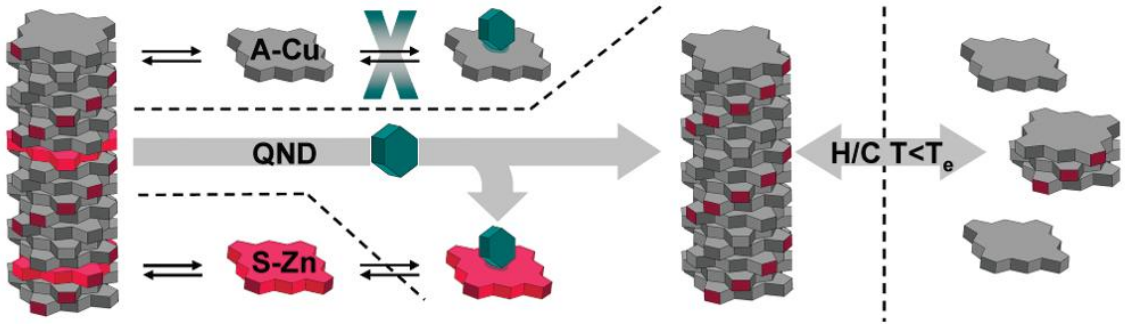

Figure 1.59. Co-assembly of porphyrins into helical co-assemblies and subsequent removal of chiral porphyrin by ligation with based QND. If polymers produced are heated to below their elongation temperature, cooling will reform templated helical polymer. Adapted from reference[304]

Of course many other groups have also made vital contributions to this field.[305-316] A fascinating example of this work was reported by Fenniri and co-workers.[317] They studied the assembly of a self-complementary hydrogen bonding, crown ether functionalised molecule (**126**). In methanol solution, this molecule first assembled into hexameric rosettes which were able to stack and form nanotubes. Preferential helicity could be induced on these nanotubes by the introduction of a zwitterionic chiral amino acid, which bound into the crown ether moiety of **126**. Both the chirality and structure of the amino acid determining the direction and extent of net helicity imposed on nanotubes in the sample.

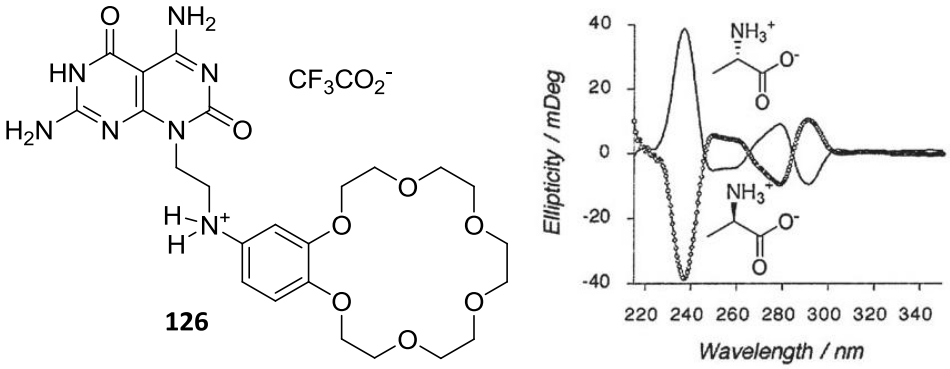

Figure 1.60. The crown ether functionalised molecule used by Fenniri and co-workers and the nanotubes it was shown to form in methanol. Also the circular dichroism spectra produce after addition of excess **D** or **L**-alanine. Adapted from reference[317]

1.3.4. Chirality in Supramolecular Gels

That chirality can influence the formation and assembly of gelators has been known for many years. In 1965, Tachibana and Kambara reported that the lithium salt of 12-hydroxystearic acid – still one of the most widely used gelators – would form fibrous twists of opposite handedness depending on whether the D or L form was used.[318] They also reported that a racemic mixture of the two formed flat tapes, with no helical twists being observed. Despite this early beginning, the effect of chirality on gelators is still poorly understood and frequently produces unpredictable and fascinating results in the study of supramolecular gels.[282] The chirality of a gelator, as Tachiban and Kambara oberved, will control how it assembles into nanoscale objects such as helical tapes and this, in turn, will control the materials properties of the gel formed. A recent report from Dey and co-workers which compared the gelation ability of a series of chiral gelators with their non-chiral counterparts illustrates well the effect chirality can have on gelation.[319]

Enantiomeric gelators will of course have equal gelation ability but the gels produced will have opposite chirality when analysed by techniques such as circular dichroism or electron microscopy. Often a racemic mixture of chiral gelator is inferior in gelation ability to an enantiopure equivalent.[320-324] An example of this was reported by Kim, Zentel and co-workers who tested each enantiomer of a simple chiral urea against the racemic mixture and found the racemic mixture to be able to gel fewer solvents and requiring a higher concentration to induce gelation in solvents it could gel.[325] They also tested a non-chiral analogue of this molecule and found this to be an even worse gelator than the racemic mixture. An example of

the effect of mixing chiral gelators has also been reported by the Smith group.[326] This report concerned changing the chirality of dendritic head group **50** which formed a gelator when mixed with diamine **51**. When the D lysine based and L lysine based dendrons were mixed the nanoscale morphology of the gels as evidenced by electron microscopy and circular dichroism changed with the changing ratio of enantiomers. The thermal stability of the gels was highest for the enantiopure samples and decreased with increasing amount of the other enantiomer.

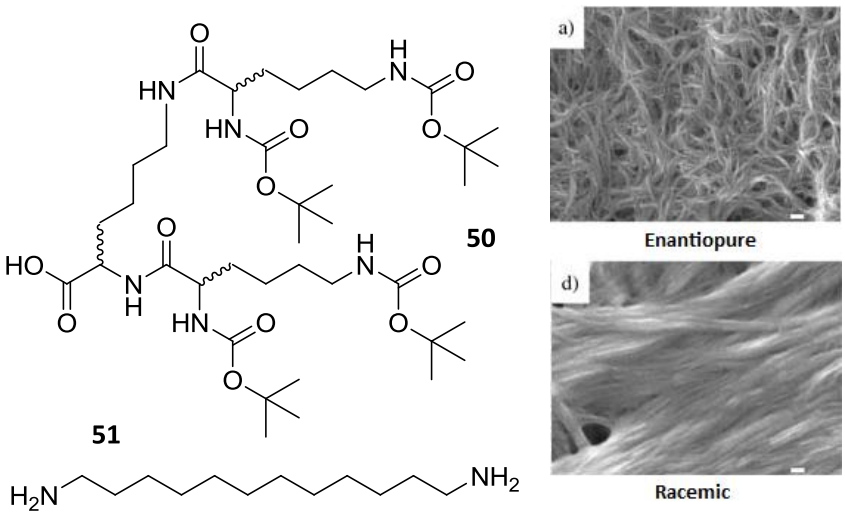

Figure 1.61. Chiral dendron and diamine used to induce gelation by Smith and co-workers. FEG-SEM images of enantiopure gel ([**51**] = 5 mM, [**L,L,L-50**] = 10 mM) and racemic gel ([**51**] = 5 mM, [**L,L,L-50**]= 5 mM, [**D,D,D-50**] = 5 mM). Scale bar = 100 nm, all dried from toluene gels. Adapted from reference[326]

There are some more unusual examples of racemic gels that are better gelators than their enantiopure equivalents. Many of these examples have been published by the Žinić group.[327] They found that the racemic version of bis(amino alcohol)oxalamide gelator **5** was a far more effective gelator than the (*S*,*S*) enantiomer alone (the meso compound (*R*,*S*) however showed no gelation ability) (Figure 1.62.).[328] The authors rationalised this by proposing a different packing method for the enantiopure and racemic gels. The enantiopure and racemic gelators formed bilayer type ribbons which then aggregated with each other. Crucially they hypothesised that in the racemic gel, each enantiomer formed separate bilayer tapes and that these then interacted preferentially with tapes of the opposite chirality, this favourable heterochiral tape-tape interaction increased the gelation ability of the racemic mixture. The same group have also reported that the racemic mixture of a number of bisamide gelators can occasionally be more effective than their enantiopure equivalents.[329, 330]

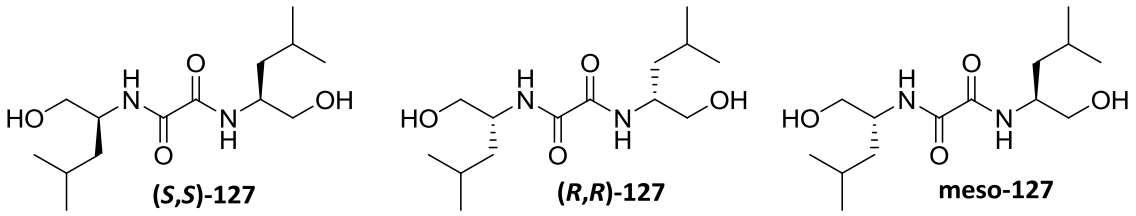

Figure 1.62. Bis(amino alcohol)oxalamide molecules used by Žinić and co-workers to probe chirality in gelation.

The same group reported another interesting example of a mixed chiral system.[331] They reported that mixing (*S*,*S*)-**128** with either (*S*,*S*), (*R*,*R*) or racemic **127** produced gels with very different gelation efficiencies. Surprisingly the mixture of (*S*,*S*)-**128** and (*S*,*S*)-**127** was a far more effective gelation mixture than either component individually, requiring a lower concentration to induce gelation and forming more thermally stable gels (Figure 1.63.). This was not observed for the mixtures with (*R*,*R*) or racemic **5** and was termed a "synergistic gelation effect" by the authors. It was proposed that this was due to a similar packing effect as put forward in their other studies – that each gelator formed separated tapes which then interacted more favourably in a hetero-sense rather than a homo-sense.

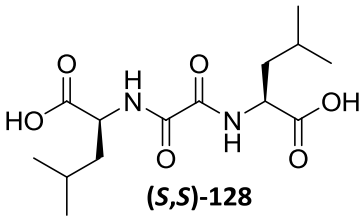

Figure 1.63. Carboxylic acid functionalised oxalamide gelator and thermal stability of gels formed by mixing it with (*S*,*S*)-**127** in xylene.

Friggeri, van Esch and co-workers have probed the gelation ability of mixtures of diastereomeric C_3-symmetrical disc shaped molecules. They found that racemic mixtures of a gelator molecule and diastereomeric mixtures of a gelator and non-gelator both increased gelation ability and gel stability.[332] It was shown that this occurred because different gelators co-assembled in the same fibres. Schneider and co-workers have recently reported that self-assembling racemic polypeptide gelators are superior to their enantiopure equivalents.[333] The authors reported that they were unsure as to whether the enantiomers were interacting on a molecular level (co-assembling), or whether favourable interactions between enantiomeric assemblies caused the increased gelation ability (as proposed by Žinić for his gelators). An

unusual example of chirality in gels was reported by Lazzaroni, De Feyter, Amabilino and co-workers who described a series of porphyrin gelators which generally showed decreased gelation ability with decreasing molecular chirality, with the achiral analogue being the equally most effective gelator.[334]

Chiral gels can also exhibit the same amplification of chirality that has been observed in supramolecular polymers. Ishi-i and co-workers reported chiral induction in a sample that exhibited the "sergeant and soldiers" effect.[335] Chiral induction could be achieved by mixing a small amount of their chiral sergeant (a C_3-symmetrical triazine cored gelator) with a similar achiral alkene functionalised molecule. What was noticeable about this example is that Grubbs catalyst was added and covalently fixed the helical fibres (Figure 1.64.). The chiral sergeant could then be removed but its preferred chirality remained transcribed onto the aggregates.[336] Haino and co-workers have also used similar C_3-symmetrical aromatic-cored molecules to demonstrate chiral induction in organogels.[337]

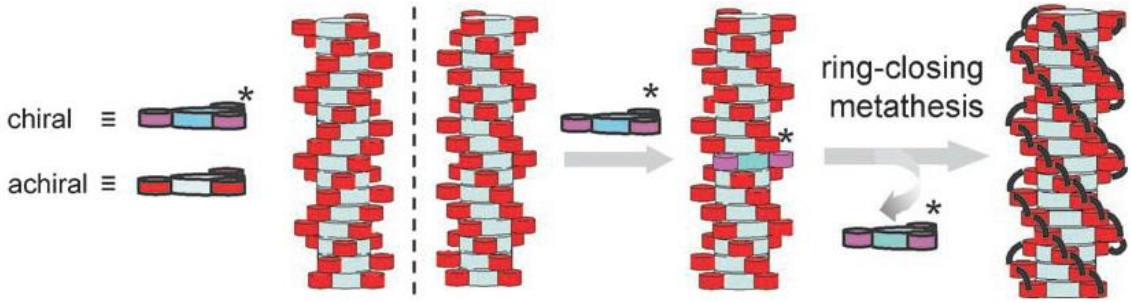

Figure 1.64. Process used by Ishi-i and co-workers to induce and covalently fix preferred chiral preference on an achiral molecule. Adapted from reference[335]

Aida and co-workers synthesised a chiral amphiphilic, aromatic-cored gelator **129** (Figure 1.65.).[338] It was reported that each enantiomer formed chiral nanotubes of opposite helicity. When both enantiomers were mixed at different ratios there was a clear "majority rules" effect where the major enantiomer enforced its preferential handedness on the chiral nanotubes formed Mixing the enantiomers also reduced the thermal stability of the nanotubes.

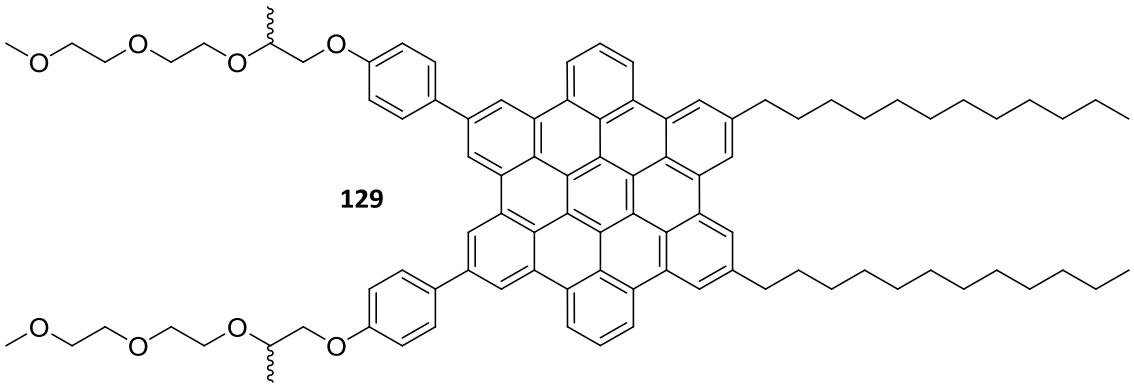

Figure 1.65. Chiral gelator reported by Aida and co-workers.

Yagai and co-workers have demonstrated the "majority rules" effect in a stacks formed from chiral multi-component gelators.[339] This gel was formed by a 3:1 mixture of chiral perylene bisimide based **130** and cyanuric acid. It was reported that both enantiomers of **130** were mixed with cyanuric acid in methanol and chloroform, the solvent was removed and the mixture redissolved in methylcyclohexane. Using this process the amplification of the helicity of the fibres produced according to the preference of the major enantiomer of **130** was observed. The method of mixing was shown to be very important as other methods of sample preparation did not result in amplification of chirality. When an achiral analogue was synthesised the "sergeant and soldiers" effect was not observed.

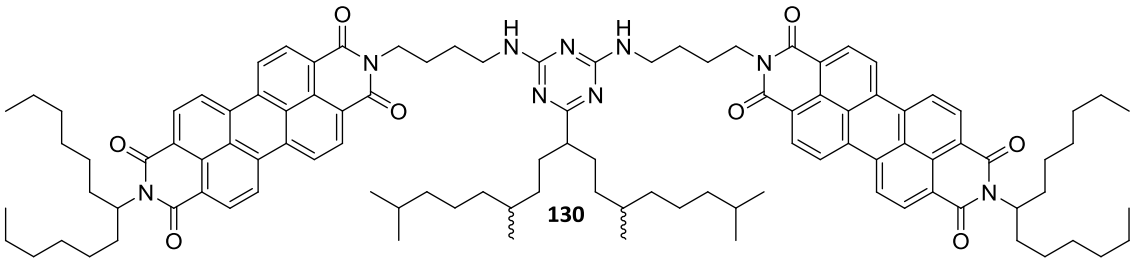

Figure 1.66. Chiral perylene bisamide based ligand synthesised by Yagai and co-workers.

Other examples of chiral induction with gelators have been presented by Maitra,[340] and Yang and Sun.[341] A different example of this type of induction has been reported by Ajayaghosh and co-workers.[342, 343] They synthesised a chiral and an achiral version of an oligo(*p*-phenyleneethynylene) molecule (**131** and **132**, Figure 1.67.). The achiral variant will assemble in decane to form vesicles, whilst the chiral molecule shows no aggregation under the same conditions. However, when both of the molecules are mixed they co-assemble to form helical nanotubes which are capable of supporting gelation. This was shown to be the case even when

the chiral molecule was added to pre-formed vesicles in solution, this shows the dynamic nature of the assemblies. In these co-assemblies, the chirality of the chiral molecule is transferred to the nanoscale aggregates, an example of the induced amplification of chirality in the co-assembly leading to a vesicle to helical tube transformation.

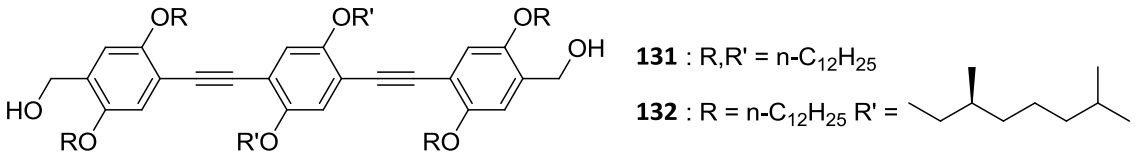

Figure 1.67. Chiral and achiral oligo(p-phenyleneethynylene) molecules reported by Ajayaghosh and co-workers.

Amplification of chirality in the gel phase does not have to be reliant upon a coassembly between chiral and achiral analogues of a gelator molecule. A chiral molecule that is neither a gelator, nor a co-assembling analogue of the gelator can be added and induce chirality on the self-assembled network. An example of this approach is reported by Li and co-workers. They report the synthesis of a series of achiral foldamer organogelators (**133**-**138**) which are seen to assemble into helical tubes which form the network that supports the gel (Figure 1.68.).[344] An amount of alkylated glucose molecule (**139**) was added to the assembled foldamers. This led to the formation of hydrogen bonded columns of glucose derivatives in the centre of the tubes which caused the foldamer molecules to exhibit an induced circular dichroism spectrum. The spectrum recorded could be reversed by using D rather than L glucose. It was also seen that this addition of alkylated glucose to the foldamers increased their gelation ability.

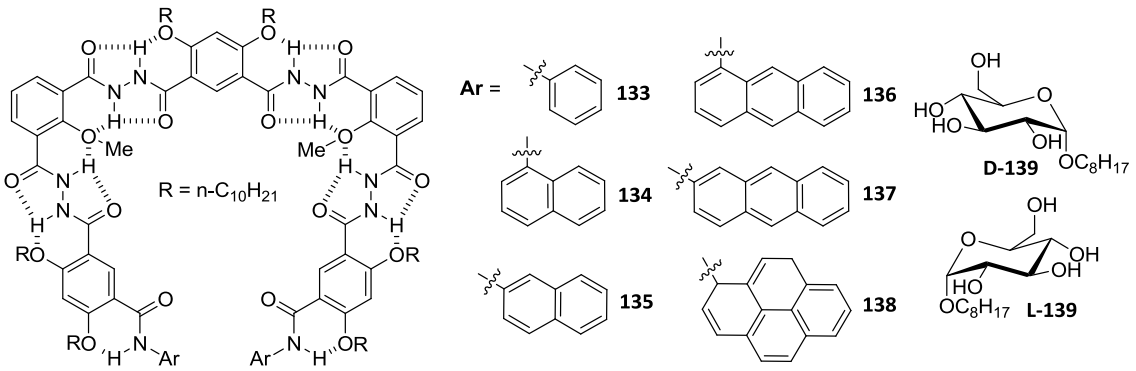

Figure 1.68. Foldamers and alkylated glucose molecules synthesised by Li and co-workers.

Shinkai and co-workers have reported an oligothiophene cored, crown ether appended achiral organogelator (**140**) (Figure 1.69.).[345] They observed that when chiral bisammonium salt (**141**) was added to the gel formed by a heat-cool cycle, gelator **140** exhibited an induced CD signal, the sign of which was dependant on which enantiomer of **141** was added. The gel showed increasing CD signal until 1 equivalent of **141** was added after which point excess guest disrupted the assembly and reduced the observed signal. Interestingly, addition of guest caused improved thixotropic behaviour in the gel, but after mechanical stress had been applied, the gel that was reformed no longer showed an induced CD signal. This gel could be destroyed by heating and allowed to cool, after which the induced CD signal would reappear. The authors proposed that this gel was a chiral memory switching system, where cycles of different treatment could determine whether molecular chiral information was expressed in the material or not.

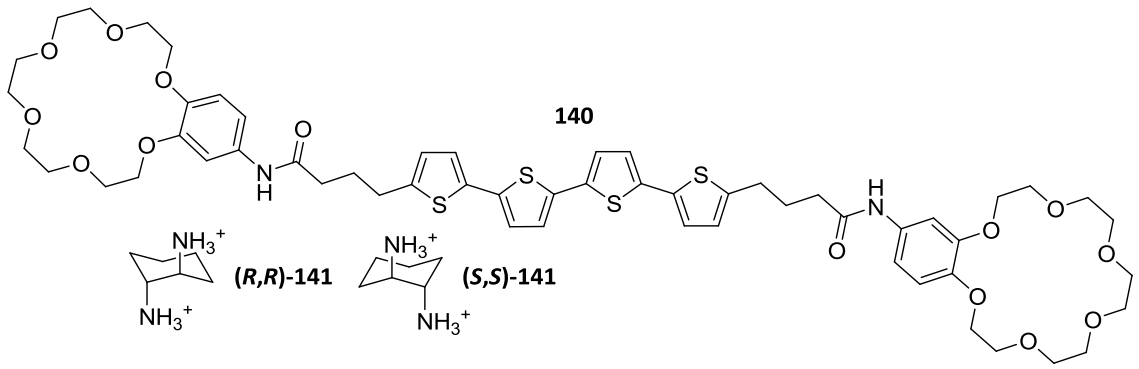

Figure 1.69. Oligothiophene cored gelator reported by Shinkai and co-workers and chiral guest molecules which can induce chirality in the supramolecular gel.

Liu and co-workers have reported an example of addition of achiral metal salts to a chiral gelator inducing a helical twist in previously non-twisted flat tapes.[346] The amphiphilic L-glutamide based gelator (**142**) (Figure 1.70.) was shown to form gels in DMSO which when dried and viewed by SEM showed a thick nano-fibrous morphology. Upon addition of Cu^{2+} delicate helical tapes where formed, leading to a more stable gel. A similar effect was observed with many other cations, the identity of the cation changing the pitch of the helices formed. Modelling studies combined with X-ray diffraction measurements showed the gelator alone formed a bilayer structure. Cation binding to the acid of the gelator meant that they were no longer involved in hydrogen bonding and this led to the formation of helical structures, the chirality of the gelator being transcribed to the nanoscopic assemblies. Ihara and co-workers have also investigated the effect of adding metal salts on the chirality of

glutamide based gelators.[347] Liu has also published a similar study showing that addition of bipyridine ligands to glutamic acid based gelators can cause a similar effect, producing delicate chiral twists from a previously poorly defined fibrous network.[348]

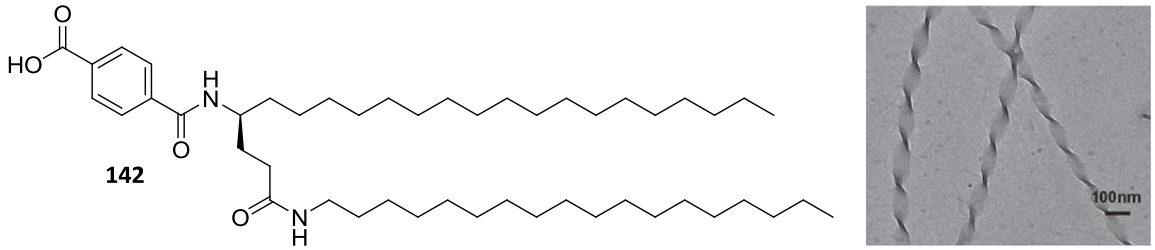

Figure 1.70. Amphiphilic acid appended gelator and SEM image fibres of gelator and Cu^{2+} dried from DMSO gel. Scale bar = 100 nm. Adapted from references[346]

All of the examples highlighted so far have involved some degree of co-assembly between different chiral molecules, or chiral and achiral species. There are examples however of mixtures which can self-sort due to the different chirality of each molecule. Messmore, Sukerkar and Stupp have demonstrated self-sorting based on chirality of dendron rodcoil gelators (**143**) in acetonitrile (Figure 1.71.). Assembled, enantiopure samples of each enantiomer showed equal and opposite CD spectra and when viewed under atomic force microscopy (AFM) showed helical nanostructures of opposite handedness. A racemic mixture of **143** showed no CD signal – as expected – but when viewed under AFM showed identical nanostructures to those viewed in the enantiopure samples. Crucially, helices of both handedness were observed in the sample, demonstrating self-sorting had most likely occurred.[349]

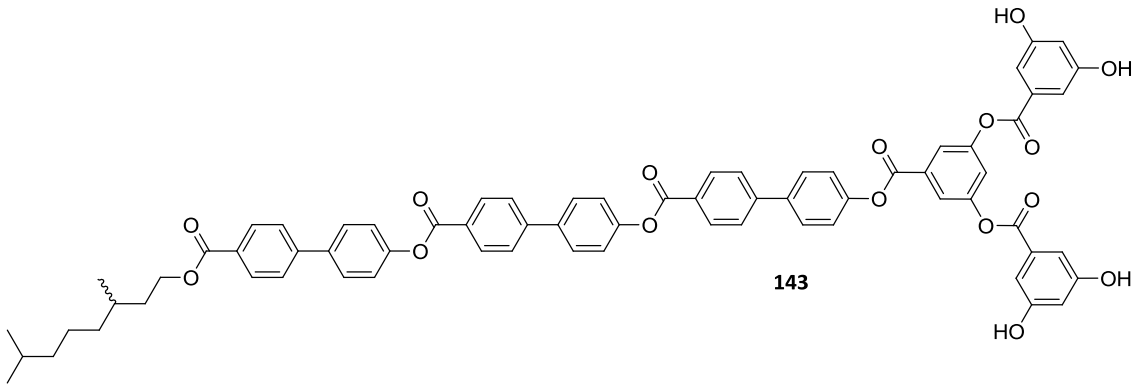

Figure 1.71. Chiral dendron rodcoil synthesised and studied by Stupp and co-workers.

Banerjee and co-workers have demonstrated chiraly driven self-sorting in chiral two-component gelators.[350] The gelators are formed from matching enantiomers of Fmoc-glutamic acid and lysine. The L enantiomers of both amino acids forms one gelator which assembles into left handed fibres as viewed by AFM, and the D enantiomers form the other enantiomeric gelating complex which assembles into right handed fibres. When a racemic mixture of all four chiral components was mixed, separate left and right handed helical fibres are visible in the same sample (Figure 1.72.). Other examples of chirally self-sorting gels have been produced by Cicchi, Pescitelli and co-workers[351] and also by Smith and co-workers.[266]

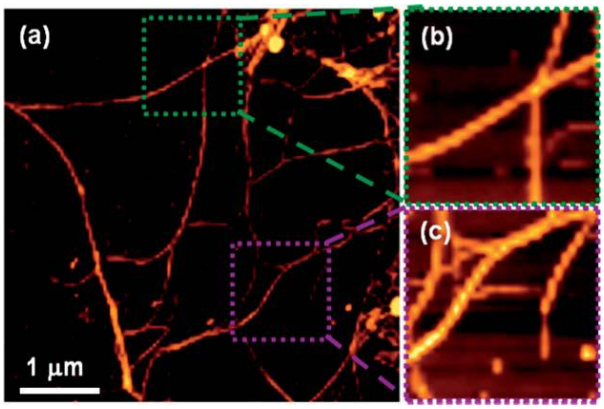

Figure 1.72. AFM image of self-sorted racemic mixture of gelators. A) Image of racemic sample. B) Close up of right handed helical fibre. C) Close up of left handed helical fibre. Scale bar = 1 µm. Adapted from reference[350]

As well as the self-recognition that occurs in self-sorting gels, chiral gels have been reported that are able to selectively respond to other chiral species, chiral recognition proving an important process in a number of fields.[278] An example of this chiral recognition occurring in the gel phase has been published by Tu and co-workers who showed that a Pt pincer-cholesterol complex (**144**) was an effective gelator of organic solvents (Figure 1.73.). It was also capable of visually discriminating between (*R*) and (*S*)-BINAP within a certain concentration range. Addition of (*S*)-BINAP followed by a heat-cool cycle led to the formation of a new gel which, when viewed under SEM, showed additional crystalline rods as well as the familiar gel network. On addition of (*R*)-BINAP followed by a heat-cool cycle no new gel was formed, i.e. the gel had demonstrated enantioselective destruction for the BINAP ligands.[352]

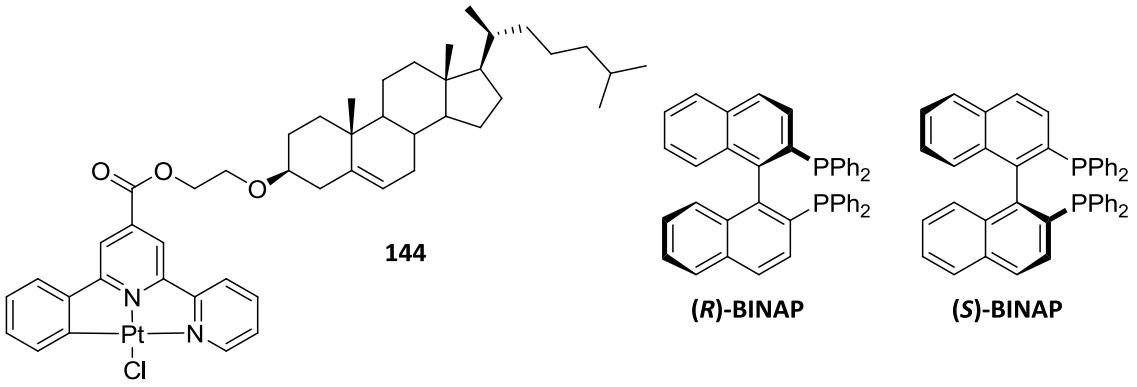

Figure 1.73. Pt pincer-cholesterol complex organogelator reported by Tu and co-workers and (*R*) and (*S*) BINAP which created different responses in the gel.

Yu, Pu and co-workers have reported another metallogel, this time a BINOL-terpyridine-Cu(II) complex (**145**) which was able to gelate organic solvents upon sonication (Figure 1.74.).[353] Furthermore the authors reported that the gel collapsed upon addition of 0.1 Eq (*S*)-phenylglycinol followed by sonication, whereas the same treatment with (*R*)-phenylglycinol still resulted in a gel. It was found that twice as much of the (*R*) enantiomer was required to destroy the gel, demonstrating again enantioselective collapsing of a gel. Both phenylglycinol enantiomers could react with **145** to displace the Cu(II) ion but the reaction between **145** and (*S*)-phenylglycinol was more favourable resulting in this enantiomer being the more potent trigger for gel destruction.

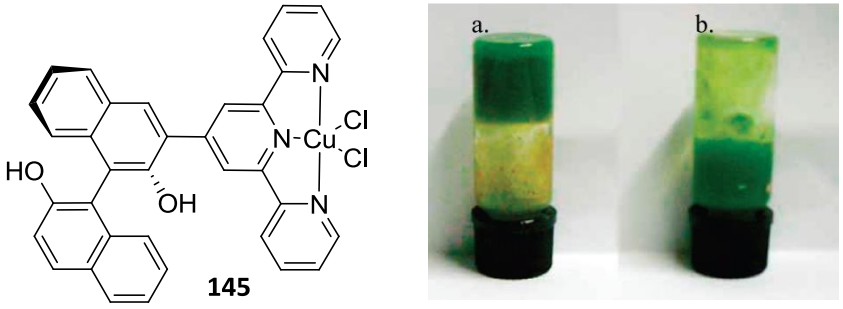

Figure 1.74. BINOL-terpyridine-Cu(II) complex gelator and A – Gel after addition of (*R*)-phenylglycinol and B – Collapsed gel after addition of (*S*)-phenylglycinol. Both chloroform. Adapted from reference[353]

A fascinating example of chiral recognition in the gel phase has been published by Xu and co-workers.[354] This group synthesised both enantiomers of Fmoc-Ala-Ala which are both hydrogelators and tested their response to the antibiotic vancomycin (Van). The D-Ala-D-Ala

sequence is known to bind to Van but the L-Ala-L-Ala is known to not bind to Van. This meant that addition of only 0.01 Eq. of Van to the Fmoc-D-Ala-D-Ala hydrogel led to ca. 40% of the water in the hydrogel being released, 0.1 Eq. led to the gel becoming a milky precipitate and finally 1.0 eq. led to a clear solution being formed. Addition of even 1.0 eq. of Van to the Fmoc-L-Ala-L-Ala gel had no effect. The reason for this is that when mixed with Fmoc-D-Ala-D-Ala, Van binds to most of the hydrogen bonding sites and sterically blocks aggregation with other gelator molecules (Figure 1.75.), whilst with the L enantiomer, this binding does not take place. Liu, Zhang and co-workers have published another report of a gel being able to discriminate between enantiomers of another biologically derived molecule, in this case D/L-tartaric acid.[355]

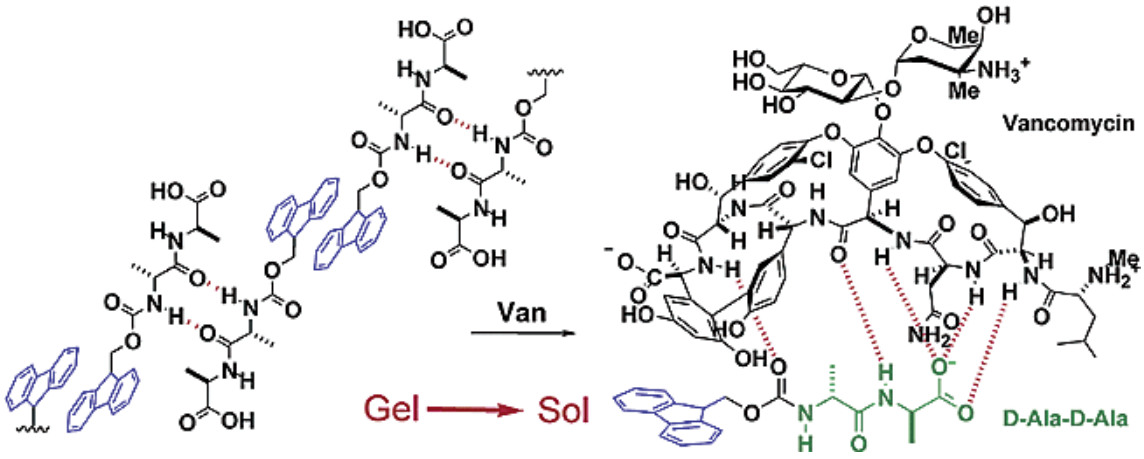

Figure 1.75. Schematic of Fmoc-D-Ala-D-Ala gel collapse caused by addition of vancomycin (Van). Adapted from references[354]

Van Esch, Feringa and co-workers have reported a fascinating system where the interplay of molecular and supramolecular chirality can control the stereochemistry of a photocyclisation reaction and allows metastable materials to be formed.[356] Gelator **146**, a chiral dithienylethene cored molecule appended with (*R*)-phenylethyl amides was synthesised and shown to form fibres with P helicity which supported gelation following a heat-cool cycle in non-polar organic solvents such as toluene. When this gel was irradiated with 313 nm light, **146** underwent a cyclisation reaction to form **147** (Figure 1.76.). Interestingly when formed in this way (from the gel phase), **147** was formed in a diastereomeric excess (de) of 96% (major diastereomer has (*R*,*R*) stereocenters newly formed at the core), but when a solution of **146** was irradiated, the **147** formed had 0% de. This showed that the P form of **146** preferentially aggregated, leading to the (*R*,*R*) diastereomer of **147** which is formed from this arrangement. The **147** gel formed by this process is however metastable, with the (*R*,*R*) diastereomer of **147** preferentially

aggregating into fibres of M helicity – which also support gelation - if heated to form a solution and allowed to cool. This gel can then undergo the reverse photoreaction if irradiated with light at 420 nm. This leads to the formation of **146** but the stereochemistry of the gel is retained, so the new gel of **146** has fibres of M helicity. As shown at the first step, **146** would rather aggregate into fibres of P helicity and will do so again if heated to a solution and allowed to cool.

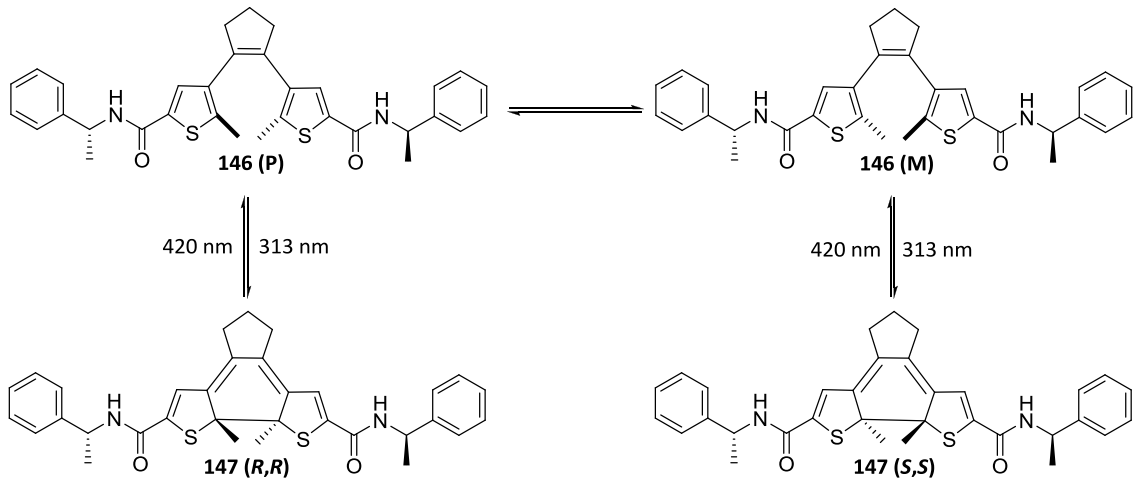

Figure 1.76. Different conformers of **146** and the diastereomers of **147** that result from photocyclisation of each.

This process therefore leads to the formation of four different gels based on **146** or **147** with either P or M helicity. First the gel of **146** with P helicity is formed by heating it to form a solution and allowing to cool. Then irradiation with light at 313 nm led to formation of a gel of **147** with 96% de, mostly (*R*,*R*) core due to P helicity of previous gel, which is retained through the photochemical process. This gel is metastable and can be heated to a solution and allowed to cool to form the favoured **147** (*R*,*R*) gel with M helicity. Irradiation of this gel with 420 nm light will cause the formation of **146**, again the stereochemistry of the previous gel is retained so it is the M form of **146** that is produced. As this is also a metastable gel heating to a solution and allowing to cool will form the favoured P form of this molecule and gel fibres of P helicity. This of course was the starting gel and the whole process can be repeated many times without degradation of the system. This process is summarised in Figure 1.77.

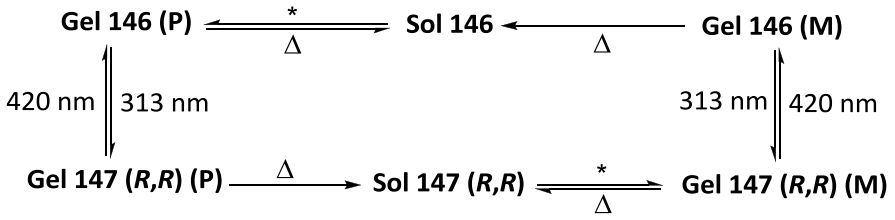

Figure 1.77. Summary of switchable system developed by Feringa and van Esch.

The same groups published a further report on a similar system which utilised a "sergeant and soldiers" type mixing of chiral and achiral photoresponsive molecules to control the stereochemistry of photocyclisation reactions.[357] In related work, Shinkai and co-workers have managed to use the chirality of a two-component gelator to control the stereochemistry of the photodimerisation of the anthracene moiety of the gelator[358, 359] and Shimizu and co-workers have demonstrated that the reversible photodimerisation of a gelator can lead to helix formation from previously nonhelical fibres.[360]

A gel can be chiral even if the gelator is not. One example of this was reported by Okano *et al* using charged oligomeric hydrogelator **148**.[361, 362] When a gel was formed with this gelator via a standard heat-cool cycle it showed no CD signal. However, when the hot solution was stirred as it cooled, the resultant gel would demonstrate a CD signal, the sign of which was dependant on the direction of stirring (positive CD for counter clockwise (CCW), negative for clockwise (CW)). This effect could also be demonstrated repeatedly on the native gel as it had thixotropic behaviour (Figure 1.78.). When achiral fluorescent dye Rhodamine B was added to the sample it was influenced by the chiral environment and demonstrated not only a CD signal but also circularly polarised fluorescence due to the stir-induced chirality of the gel network.

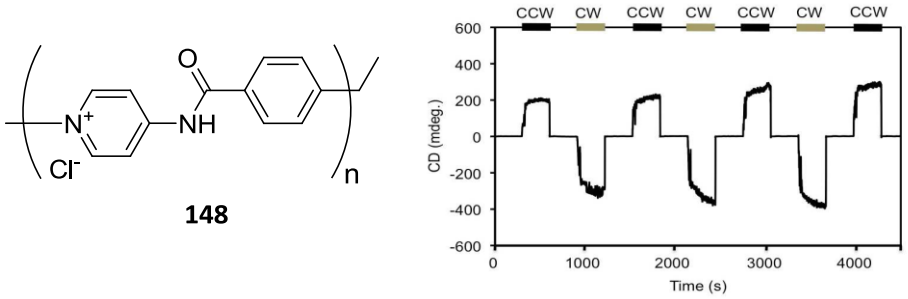

Figure 1.78. Oligomeric gelator **148** and thioxotropic behaviour of hydrogel after counter clockwise (CCW) or clockwise (CW) stirring monitored by CD. Adapted from reference[361]

A macroscopically chiral gel can be produced from an achiral gelator even without an obvious source of chirality. In most cases – as already seen in much of the work highlighted here – an achiral molecule will assemble in to helices of different handedness and overall the sample will be racemic. Normally the initial formation of a helix of a certain handedness, will template the formation of more helices of this handedness, this will happen many times with a roughly equal number for either direction. However, if formation has very few of these initial events it is easy to get an imbalance in the number of P and M helices, this imbalance is then amplified as these initial objects template further assembly. This effect is known as "chiral symmetry breaking" and has been observed for supramolecular assemblies[363-366] and in one instance, reported by the group of You, in the gel phase.[367] In this study, two curved ligands could each assemble with a stoichiometric amount of silver(I) salt to form helical supramolecular polymers. These could aggregate to form a network capable of supporting gelation in a range of organic solvents (Figure 1.79.). When the gels were analysed by CD, strong signals were observed, despite all components being achiral. Crucially, the sign of the CD signal could be either positive or negative, with each spectrum being observed a roughly equal number of times for different samples. This is different to what is sometimes reported as symmetry breaking where a small amount of chiral dopant is added,[368, 369] or vortex flow used, as in the previous example.[370]

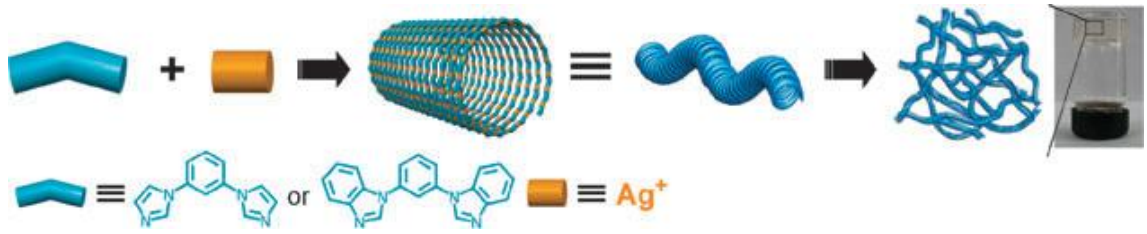

Figure 1.79. Chiral gel formation form mixture of curved ligands and silver(I) ions. Adapted from reference[367]

1.3.5. Solvent Chirality

So far the chirality of the gelator has been discussed but solvent chirality can also be very important. Induction of chirality from solvent has been observed on molecules in solution,[371] on the conformation of polymers[372, 373] and on the conformation of supramolecular polymers.[374-379] Kogiso and co-workers have demonstrated a very interesting report of gelation being dependant on a matching between gelator chirality and solvent chirality.[380] This report is based on chiral aspartame based gelator **149** and the ability of each enantiomer to gelate

either (*R*) or (*S*)-propylene carbonate (PC). It was observed that the L gelator was able to gelate (*R*)-PC but not (*S*)-PC and the D gelator was able to gelate (*S*)-PC and not (*R*)-PC. Further analysis showed the mode of aggregation, so that at the concentration measured, only the "right" combinations of chirality formed a continuous fibrous network capable of supporting gelation. A similar study conducted by Würthner and co-workers showed that the chirality of limonene solvent used could control the handedness of helices formed by an achiral gelator.[381]

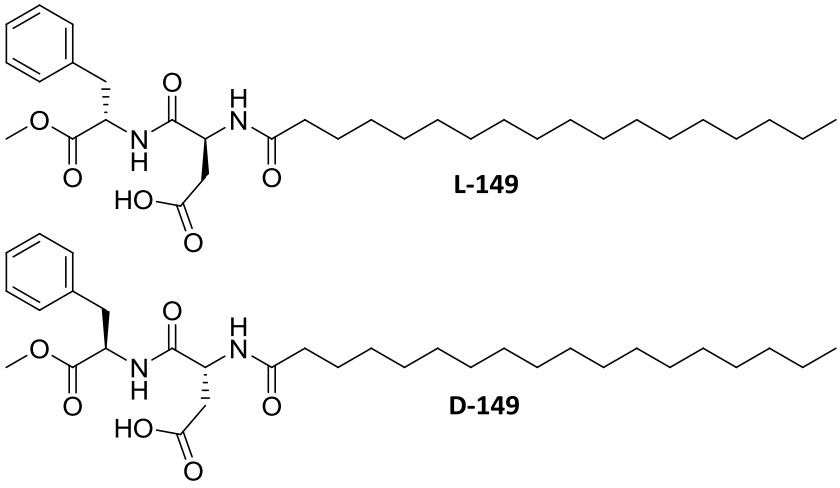

Figure 1.80. Aspartame based gelator that can only gel a chiral solvent when the chiral match is correct.

The work highlighted here demonstrates that clearly, chirality has a vital role to play in the assembly of molecules and consequently on the gel phase. Chirality has been shown to be able to control the properties of a gel that is formed and effects such as chiral amplification and the increase of gelation ability upon mixing of gelators with different chirality have been observed. The chirality of self-assembled gels have been used to control self-sorting, chiral recognition and reactions that occur in the gel phase. This collection of highlighted work demonstrates how important it is to understand the effect of chirality on gel materials and to be able to control and tune these effects.

1.4. Project Aims

This project will investigate the response of supramolecular gels to the introduction of new species. The first part will investigate the destruction of gels formed from a lysine based organogelator upon the introduction of certain cations. The experiments conducted will determine which of the cations tested will trigger the gel-sol transition and also discover the reasons behind the ability of the gel to discriminate between the different cations. One of the interactions investigated will be the silver(I)-alkene interaction which has until now not been used in a gel. Probing how this kind of molecular recognition works is vital if stimuli responsive gels are to be used in future to create useful materials.

The focus of this project will then move to multi-component gelators. First, novel gelation mixtures formed from a known lysine based dendron and different monoamines will be characterised. The forces underpinning gelation and the influence of different solvents are to be investigated, as will the effect of using different amines on the gels that were formed. Then the effect of component selection will be investigated. If the dendron is challenged with a number of different amines with which it can form a gel, will one be preferentially included in the gelator network over the others and if a pre-formed gel is challenged with a new amine, can this be incorporated at the expense of the amine used to form the gel.

The next part of the project will look at the effect of chirality on these multi-component systems. How the chirality of different amines dictates the properties of the gels formed will be investigated, as will can the type of component selection studied in the previous section be repeated using amines of opposite chirality. The final part of this investigation will reverse these experiments, using enantiomeric lysine dendrons to tune the properties of the gels formed and again investigate whether component selection can be driven by chirality.

Overall the project will examine molecular recognition in supramolecular gels, whether this is based on the gel responding to certain cations due to specific intermolecular forces or certain components being selectively incorporated into the gelator network over others due to a difference in structure or chirality. The driving forces behind all of these effects will be examined with the aim of providing a basis for further investigation into these systems and the generation of more useful functional materials.

Chapter 2

Silver(I) Responsive Gels

Chapter 2 – Silver(I) Responsive Gels

2.1. Introduction

2.1.1. Silver(I) Containing Gels

The silver(I) cation is being increasingly used in gelation systems. For instance there are many examples of gels that are formed from coordination polymers which contain Ag^+. An early example came from the group of Shinkai and investigated the ability of a series of pyridine appended cholesterol molecules, one of which (**150**, Figure 2.1.) formed a fibrous network and induced gelation in organic solvents upon addition of AgOTf.[382]

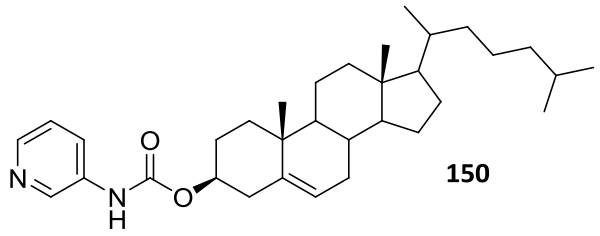

150

Figure 2.1. Pyridine appended cholesterol based molecule that was shown to be able form a gel in organic solvents upon addition of AgOTf.

Lee and co-workers have described a pyridine appended molecule (**151**, Figure 2.2.) that complexes $AgBF_4$ and then forms a hydrogel.[383] The coordination polymers generated aggregates into helical bundles, these bundles then entangle and cause immobilisation of the solvent. Gelation was found to be sensitive to addition of other anions. Upon addition of $Bu_4N^+F^-$ to the gel, the strength of the Ag^+-F^- interaction causes decomplexation of the silver(I) cations from the coordination polymer leading to destruction of the gel network, and a free flowing solution was formed. Upon addition of $Bu_4N^+C_2F_5CO_2^-$, the conformation of the supramolecular polymer changed from a helical *cis*-like arrangement to a linear *trans*-like arrangement. The long helical bundles become much shorter ribbons, which could no longer underpin gelation. Both these changes were found to be reversible upon addition of more $AgBF_4$ (Figure 2.2.). The same group have also observed how changing anion size in these supramolecular polymers changes the supramolecular structure that were formed, with $CF_3SO_3^-$ producing a columnar arrangement which could induce gelation in polar solvents.[384]

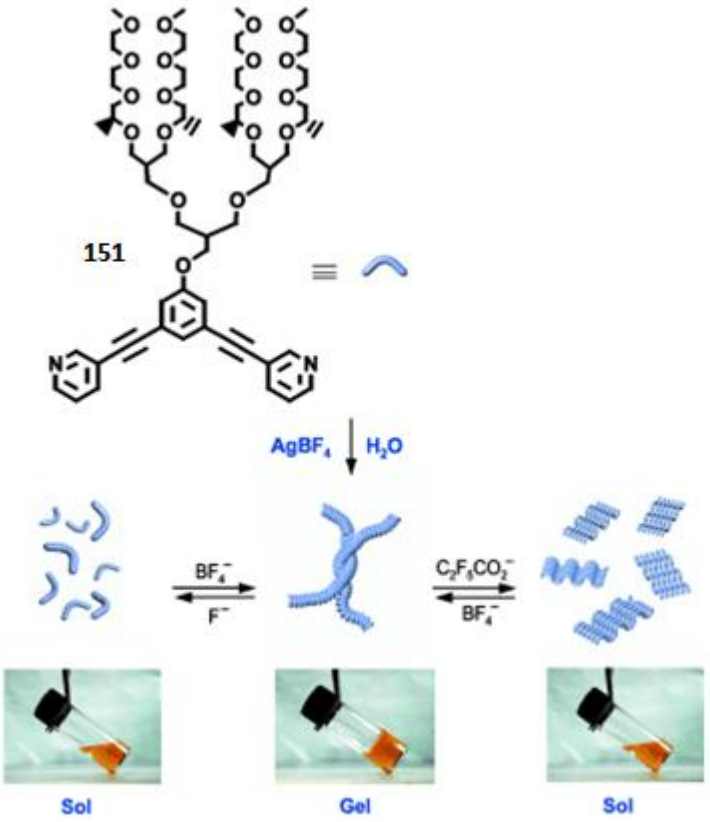

Figure 2.2. Molecule used by Lee's group to produce coordination polymers with Ag^+ and the effect of addition of different cations. Adapted from reference[383]

The groups of Bian and Gao have reported an example of a binaphthylbisbipyridine-based ligand (**152**) which, when mixed with Ag^+, is capable of forming nanotubular helices (Figure 2.3.).[385] These formed long coordination polymers which assembled into an entangled fibrous network, capable of gelating acetonitrile. A range of cations were used and were shown to control both the stability of the gel and the morphology of the coordination polymers that are formed. Perhaps more interesting is a follow-up paper by the same authors which details the results of testing the racemate of this ligand and shows that this initially results in the formation of heterochiral metallocycles containing two ligands and two silver(I) cations which was still able to assemble and induce gelation.[386]

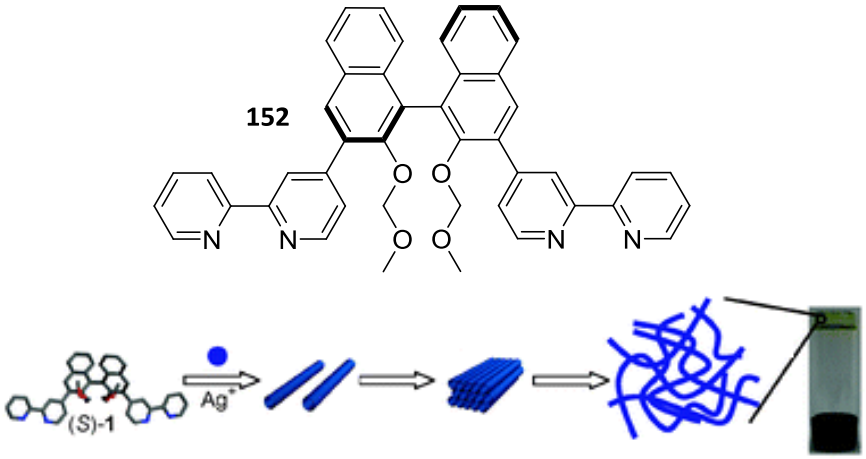

Figure 2.3. Binaphthylbisbipyridine-based ligand synthesised by Bian, Gao and co-workers and its proposed method of assembly to form a gel network with Ag^+. Adapted from reference[385]

The groups of Hardie[387] and Steed[388] have – separately – also been investigating supramolecular gels formed from coordination polymers containing silver(I) cations. The most interesting example of this has been the work of Steed and co-workers, who found that if a gel formed with a bis-urea ligand (**153**) which is appended with pyridine groups was mixed with $AgBF_4$ and left exposed to light, silver nanoparticles would form within the gel sample (Figure 2.4.).[389] The rate of formation of the nanoparticles could be increased if the gels were irradiated with UV light (365 nm) or retarded if the samples were kept in the dark. Similarly the Das group has used a tryptophan based hydrogelator to form polydisperse silver nanoparticles under mild conditions.[390]

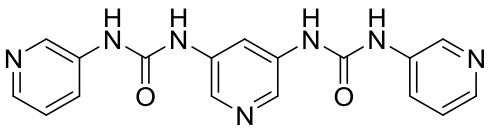

153

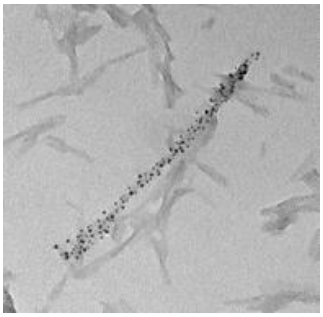

Figure 2.4. Ligand synthesised by Steed and co-workers and TEM image of silver nanoparticles formed on gelator fibre. Adapted from reference[389]

Related to this system is a report by Park and co-workers who synthesised a pyridine appended ligand (**154**) which formed a 2:1 complex with Ag^+. This was able to assemble into a

fibrous network that is able to form a gel in 1,2-dichloroethane (Figure 2.5.).[391] This gel is strongly fluorescent due to aggregation-induced enhanced emission and can be turned back to a non-fluorescent solution upon addition of tetrabutylammonium fluoride which, due to the strong Ag^{+}-F^{-} interaction, removed the silver(I) from the gelator complexes. Importantly, if drop-cast films formed from this complex were exposed to UV light (365 nm, 15 minutes) silver nanoparticle formation was observed and the surface plasmon resonance of the nanoparticles caused the previously blue emission from the film to become yellow.

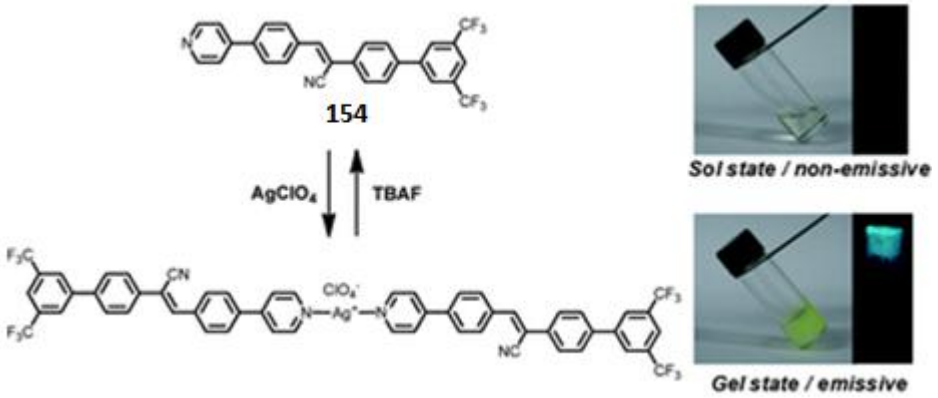

Figure 2.5. Ligand and gelating complex used by Park and co-workers and fluorescence of the gel state. Adapted from reference[391]

The Jiang group have shown that a gel formed from a glutathione (GSH) and Ag^{+} coordination polymer can be turned back to a solution by addition of iodide.[392] This was shown to be a highly selective transition with a number of other anions tested (F^{-}, Cl^{-}, Br^{-} and $H_2PO_4^{-}$) not triggering this transition due to their weaker interaction with Ag^{+}. Related to this is a report by Nandi and co-workers who formed a hydrogel with a 2:1 mixture of Ag^{+} to melamine (Figure 2.6.).[393] The gel was responsive to changes in pH, with high pH (9.2) causing the gel to break and a white precipitate of AgOH to form. At low pH (<4.0) the gel network was disrupted as the nitrogens on the ring of melamine become protonated and were no longer available to complex the Ag^{+} ions. The gel was also responsive to the addition of some anions (Cl^{-}, Br^{-} and I^{-}) but addition of more Ag^{+} caused to gel to reform. Initial work indicated that this gel was able to adsorb certain anionic dyes from "waste" water although the reason behind the selective uptake of anionic dyes was not determined.

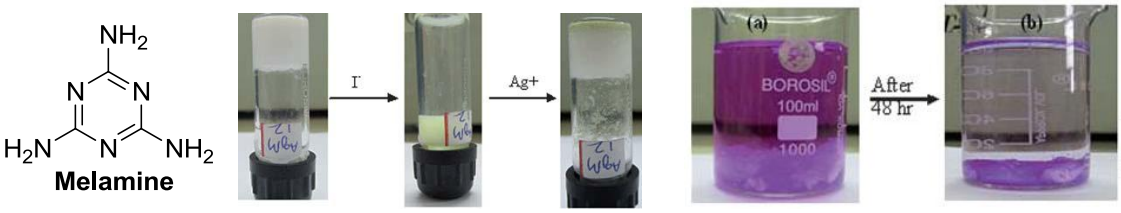

Figure 2.6. Structure of melamine with response of 2:1 Ag^+ to melamine gel to addition of I^- and then further Ag^+. Also showing the uptake of rose Bengal dye from solution. Adapted from reference[393]

Another innovative use of silver(I) coordination polymer gels has been reported by Tang and co-workers (Figure 2.7.).[394] This group used a C_3 symmetrical, pyridine terminated ligand (**155**) to form a metallogel with $AgNO_3$ in polar solvents. The gel could be formed with cross-linking monomer *N*,*N*'-methylenebisacrylamide (MBA) and initiator benzoyl peroxide (BPO) present and these compounds had no impact on the assembly of the gel network. It was found that thermally initiated polymerisation of the MBA could be achieved, and due to interaction between the bisamide containing MBA and the silver(I) cations in the formed gel fibres, the polymers formed were templated by the fibrous network. It was shown that the coordination polymer gel network could be removed by treatment with ammonia leaving templated, hollow, polymeric nanotubes.

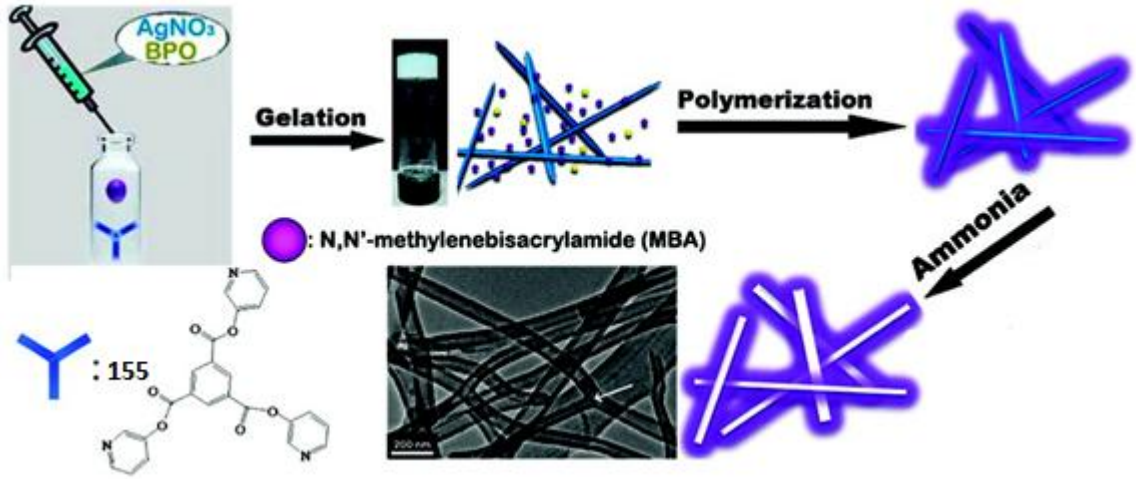

Figure 2.7. Process used by Tang and co-workers to produce polymer nanotubes templated by silver(I) containing metallogel. Adapted from reference[394]

Wu and co-workers reported an organogel underpinned by ligand (**156**) forming a 2:1 complex with a silver(I) cation (Figure 2.8.).[395] These complexes stack via hydrogen bonding interactions between the ligands, and form fibrils which assemble further to form the gel network. The gel was found to be sensitive to the addition of KI solution, becoming a solution with a precipitate of AgI. If the precipitate is filtered off and more $Ag^{+}CF_3SO_3^{-}$ added the gel is reformed. The gel was also found to be sensitive to hydrogen sulfide gas. Again if the precipitate (Ag_2S) was filtered off and more silver(I) salt added, the gel was reformed. This is an excellent example of a multi-responsive, reversible, metalloorganic gel.

Figure 2.8. Silver(I)-ligand complex formed by Wu and co-workers and its ability to undergo reversible gel-sol transitions upon addition of chemical stimuli. Adapted from reference[395]

The Thompson group have reported a highly responsive cyclodextrin based gelator (**157**), Figure 2.9.).[396] Their gelator was responsive to a number of metal ions including silver(I), which bound to the amine group of the gelator, disrupting hydrogen bonding and causing electrostatic repulsion between gelator molecules. The gel could be reformed with addition of KI which removed the Ag^{+} ions from solution as an AgI precipitate. The gels were also found to be pH sensitive due to the protonatable / deprotonatable amine and hydroxyl groups. This example is contrasting to the others described so far in this introduction as it reports a pre-existing gel that is responsive to addition of Ag^{+}, not a gel which requires the coordination of silver(I) cations to a ligand in order for it to form.

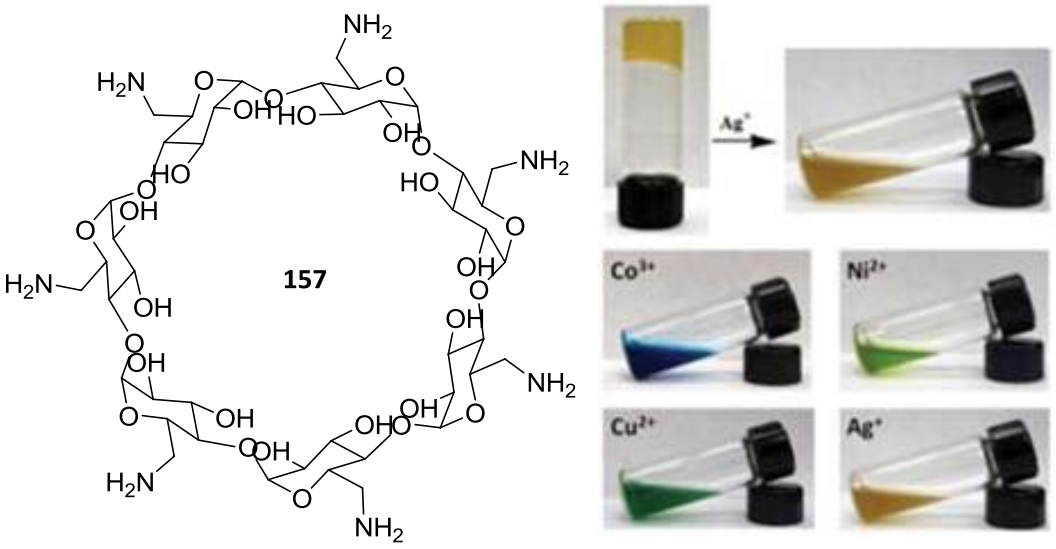

Figure 2.9. Cyclodextrin based gelator used by Thompson and co-workers to demonstrate gel collapse in response to Ag^+ addition. Also shows response to other metal cations. Adapted from reference[396]

All of the reports of silver(I) containing gels recorded so-far are based on an N-Ag^+ interaction, with pyridine groups being by far the most common way to build Ag^+ binding functionality into a molecule. Indeed, nitrogen atoms contained in heterocyclic systems are the most common type of ligand for forming Ag^+ containing coordination polymers.[397]

2.1.2. The Silver(I)-Alkene Interaction

Alongside the use of nitrogen heterocycles to form coordination complexes with Ag^+, the Ag^+-alkene interaction can also be used. This interaction is surprisingly strong (*ca.* 140 kJ mol^{-1})[398] and has been known and written about for decades[399, 400] but, outside of the synthesis of discrete organometallic complexes, its use in supramolecular chemistry or non-covalent synthesis is yet to be fully exploited. One problem is that these compounds are commonly unstable.[400] Ag^+-alkene interactions are, however, widely used in other applications, most notably these include chromatography[401] and Ag^+ is used as, or as part of NMR shift reagents for alkenes,[402-405] making NMR a very useful technique with which to study these complexes.

Beyond discrete metalloorganic coordination compounds, use of the Ag^+-alkene interaction as a useful supramolecular interaction has been limited to solid state coordination polymers. Steel and co-workers have produced a number of silver(I)-alkene complexes and propose their use as a "supramolecular synthon".[406] For instance, Steel's group uses (*R*)-limonene as a bridging ligand between silver(I) cations to form a one dimensional coordination polymer

which was then characterised by X-ray crystallography.[407] In another example, three isomers of divinylbenzene were used to create either discrete metalloorganic complexes or, extended coordination polymers, depending on the silver(I) salt used (Figure 2.10.). Again these structures were characterised by X-ray crystallography.[408]

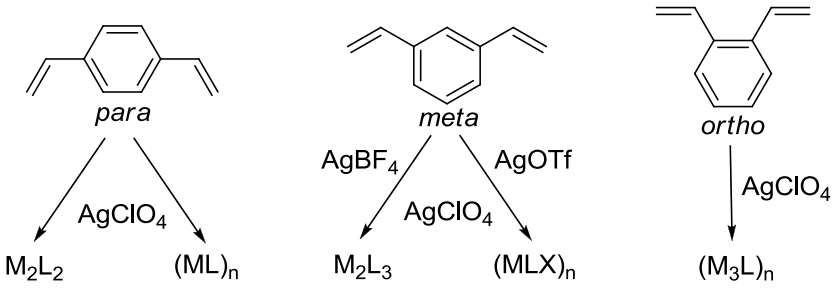

Figure 2.10. Products formed by Steel and co-workers using divinylbenzene ligand and silver(I) containing salts. Adapted from reference[408]

The closest example to seeing the Ag^+-alkene interaction in the gel phase is a report by the group of Yam which demonstrated that a series of alkynylrhenium(I) tricarbonyl diimine complexes could form a complex with Ag^+ utilising an Ag^+-alkyne interaction.[409] which could further assemble to form a thermally reversible gel.

The aim of this work was to demonstrate that the Ag^+-alkene interaction could be utilised in the gel phase. Whether the binding of Ag^+ and alkene in a gel could occur and whether this, in turn, would cause gel destruction was investigated. Other cations should be unable to interact with the alkene – providing a significant advantage over the use of Ag^+-N interactions. This would be achieved by taking a known gelator and testing its response to certain chemical stimuli, including a silver(I) salt.

2.2. Results and Discussion

2.2.1. Response to Cations

Gelator **G1-ene** had previously been investigated for its ability to undergo intermolecular alkene metathesis in the gel phase[152] and its ability to form co-gels with another gelator.[267] As such it was synthesised in good yield (overall yield 56%) according to previously published methodology, shown in Scheme 2.1.

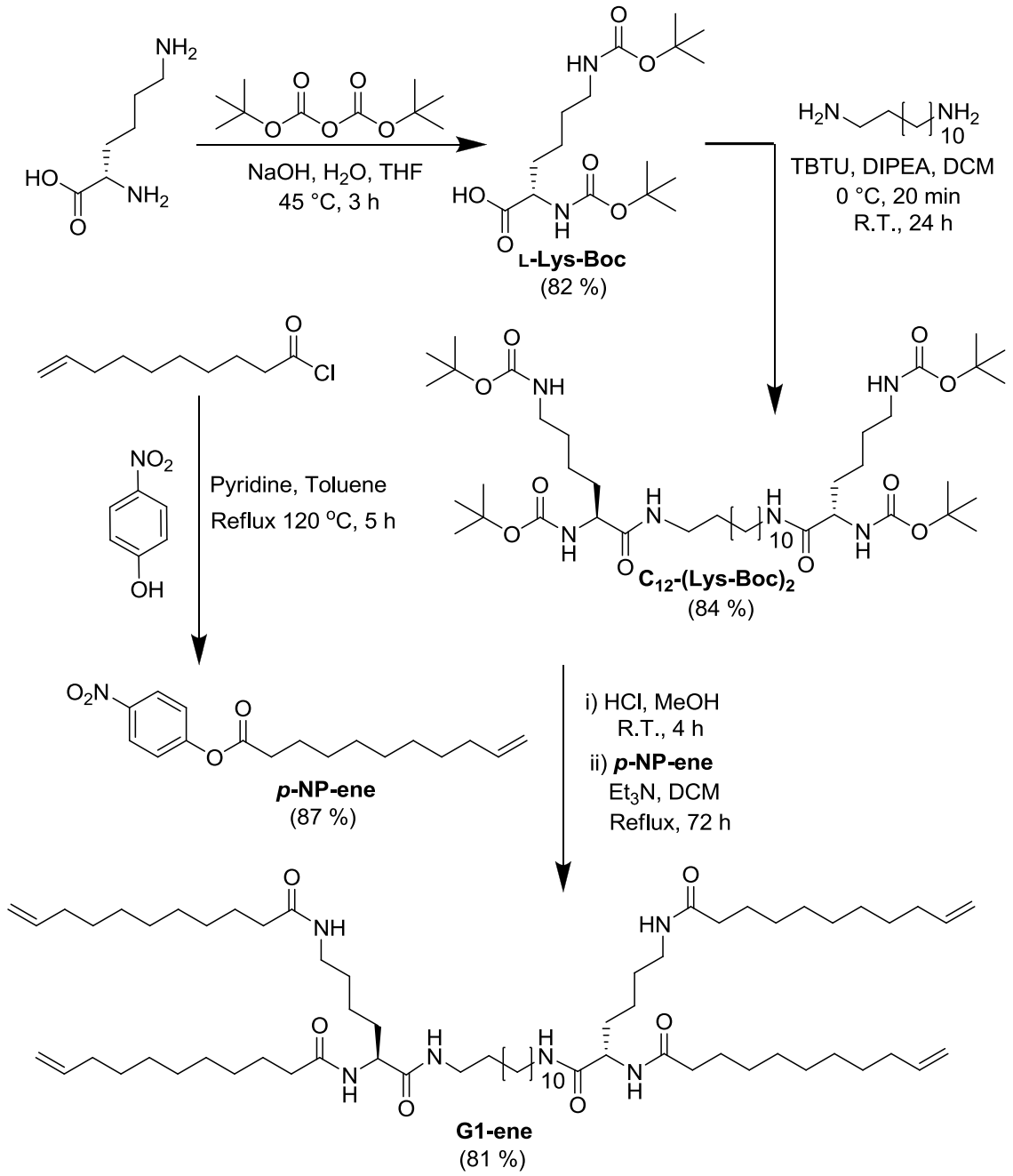

Scheme 2.1. Synthesis of **G1-ene**

The synthesis began with the conversion of the amine groups of L-Lysine to *t*-butylcarbamate (Boc) groups to form **L-Lys-Boc**. These molecules were then coupled to either end of 1,12-diaminododecane using the common peptide coupling reagent TBTU to produce compound **C_{12}(Lys-Boc)$_2$**. The Boc groups were then removed using HCl gas in methanol and the resulting amines reacted with active ester ***p*-NP-ene** to produce **G1-ene**. Compound **G1-ene** is a strong gelator of organic solvents and contains only two very simple types of functional group;

secondary amides and terminal alkenes. The minimum gelation concentration (MGC) of **G1-ene** required to form a gel in EtOAc was 0.64 mM. The gels formed were opaque and showed a fibrous morphology when the xerogels (dried gels) were viewed under FEG-SEM (Figure 2.11.).

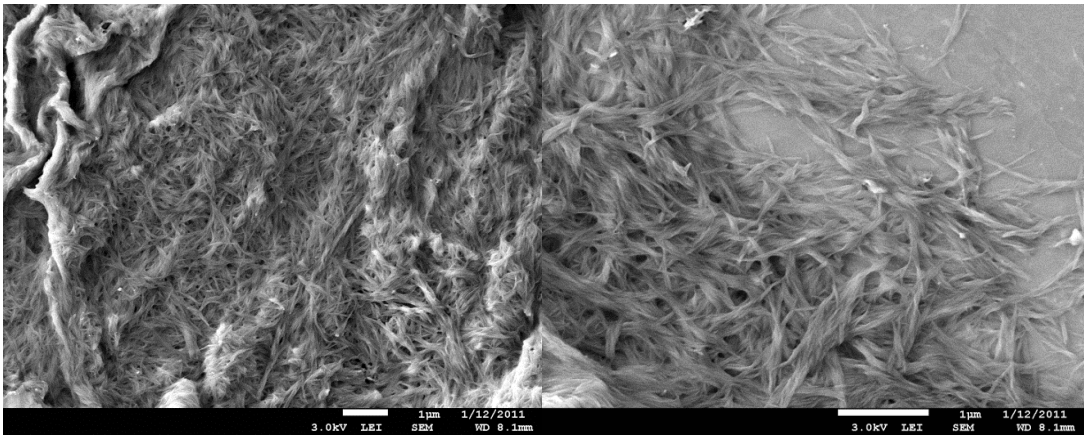

Figure 2.11. FEG-SEM image of xerogel produced from 10 mM gel of **G1-ene** in EtOAc. Scale bars = 1 µm (left) and 2 µm (right).

Cation responsive gels[219] have proven to be an important class of "smart" materials,[142] especially when the response of the gel phase occurs selectively in the presence of some cations and not others. There are few reports of Ag^+ responsive gels[383-386, 388, 392, 395, 396, 411] and no previous report uses an alkene as the Ag^+ binding site. It was hypothesised that Ag^+ would interact with the alkene groups of **G1-ene** and trigger a response. Furthermore, the response of the **G1-ene** gel to group I metal ions may be different to any response to silver(I), due to their predicted lack of interaction with the peripheral alkene groups. This would therefore demonstrate cation selectivity using simple functional groups. The response of **G1-ene** gels to different cations was investigated.

The cations investigated were Ag^+, Li^+, Na^+ and K^+. The salts containing these cations were $AgSbF_6$, $LiPF_6$, $NaPF_6$, $KSbF_6$, all of which have large non-coordinating anions which should not interfere with the gel network. These anions also aided the solubility of the salts in organic solvent; all of these salts were soluble in EtOAc.

To test the response of **G1-ene** gels to metal salts, 10 mM gels were formed by sonicating a known mass of **G1-ene** in EtOAc (0.5 mL), then heating the sample until a homogeneous clear solution was formed, before allowing it to cool – and set – overnight. Then a known amount of each salt was dissolved in more EtOAc (0.5 mL) and gently pipetted on top of the gel (without

disturbing the surface). Any changes to the gels were then recorded. It is important to note that addition of EtOAc in the absence of metal salts caused no change to the gel.

The addition of $AgSbF_6$ had the most noticeable effect on the gel. Within minutes this metal salt caused breakdown of the gel as it diffused through the sample from top to bottom. Small amounts of $AgSbF_6$ only triggered a gel-sol transition at the top of the gel, and it took ca. 30 equivalents to guarantee total gel-sol transition throughout the sample.

The presence of $LiPF_6$ also produced a response when added to the **G1-ene** gels. Like $AgSbF_6$ the $LiPF_6$ salt triggered a gel-sol transition as it diffused through the gel, with a small amount of salt only triggering the gel-sol transition at the top of the sample. It took 10 equivalents of $LiPF_6$ to guarantee total gel destruction, less than the 30 needed for $AgSbF_6$, but the response took much longer, occurring over hours rather than minutes.

Neither $NaPF_6$ nor $KSbF_6$ elicited a response from the gel, even when 30 equivalents of each were added. This demonstrates a selective cation response from these **G1-ene** gels. This also proves that the anion is playing no role in the gel-sol transitions as both the PF_6^- and SbF_6^- anions are in salts that do and do not elicit a response from the gel. The results of the cation responses are illustrated in Figure 2.12.

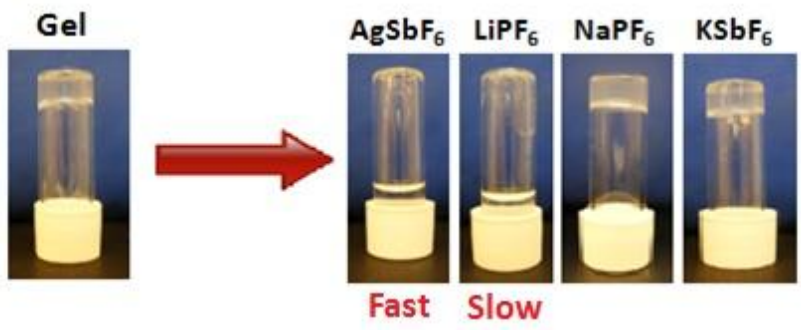

Figure 2.12. Pictures of **G1-ene** gels response to metal salts.

2.2.2. ATR-FTIR of Xerogels

To gain some insight into which functional groups of **G1-ene** were involved in this selective response, Attenuated Total Reflection – Fourier Transform Infra-Red (ATR-FTIR) spectroscopy was used. Gels of **G1-ene** were made and treated with the salts as previously described. These samples were then dried under vacuum to produce xerogels which were analysed as solids by ATR-FTIR and compared to the spectrum of an untreated **G1-ene** xerogel.

In the spectrum of untreated **G1-ene** xerogel, bands at 993 and 910 cm^{-1} were assigned as alkene bends. Bands at 1633 and 1535 cm^{-1} were assigned as the carbonyl and amide II stretches respectively. The spectrum of the $AgSbF_6$ treated xerogel shows the carbonyl stretch shifted from 1633 to 1628 cm^{-1} and the amide II shifted from 1535 to 1547 cm^{-1}. This weakening of the C=O bond and strengthening of the C=N bond (amide II) was assigned to an Ag^+-amide interaction. More interestingly, the alkene bands at 993 and 910 cm^{-1} had disappeared and been replaced by a single band at 949 cm^{-1} (Figure 2.13). This is likely due to the Ag^+-alkene interaction.[412] The large new peak at 656 cm^{-1} is due to the SbF_6^- ion (Sb-F stretch).

The spectrum of the $LiPF_6$ treated xerogel showed a similar shift in carbonyl and amide II bands from 1633 to 1629 cm^{-1} and from 1535 to 1547 cm^{-1} respectively. However, the spectrum showed no change to the alkene bends compared with the untreated **G1-ene** xerogel. This indicates that $LiPF_6$ interacts with the carbonyl groups but not the alkene. The xerogel treated with $NaPF_6$ has carbonyl and amide II bands shifted to 1629 and 1538 cm^{-1} respectively, a smaller shift compared to untreated **G1-ene** than caused by $AgSbF_6$ or $LiPF_6$. This shows a weaker interaction between the amide and Na^+. The $KSbF_6$ treated xerogel showed no significant differences in the ATR-FTIR spectrum to untreated **G1-ene**. All spectra are shown in Appendix A.

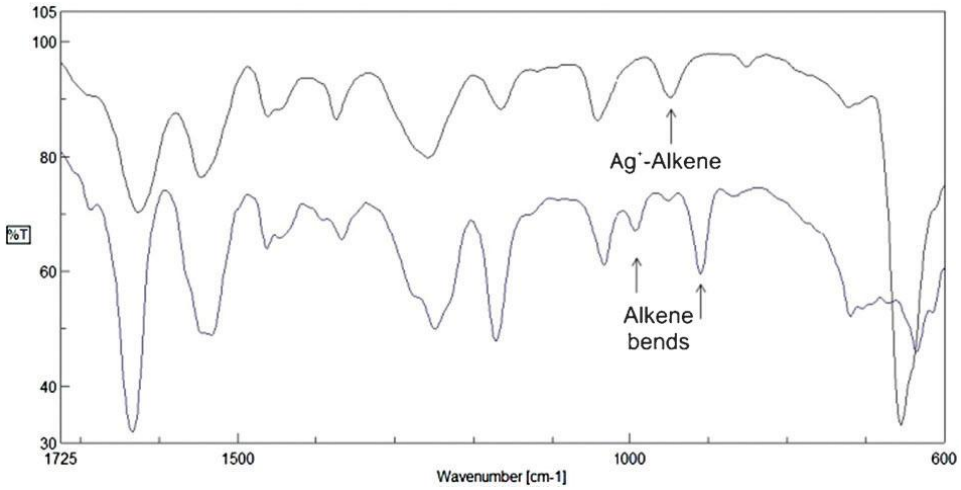

Figure 2.13. ATR-FTIR spectra from **G1-ene** xerogel (bottom) and **G1-ene**/$AgSbF_6$ xerogel (top)

In conclusion the ATR-FTIR analysis shows that Ag^+ has a strong interaction with both the amide and alkene groups of **G1-ene**. Li^+ binds to the amide but not the alkene, Na^+ binds

weakly to the amide and leaves the alkene unperturbed and K^+ has no noticeable interaction with either group.

2.2.3. NMR Experiments

To gain further insight into metal binding to **G1-ene**, NMR spectrometry was used. However, compound **G1-ene** was poorly soluble in many solvents, and was only able to form gels or precipitates in EtOAc – both of which are "invisible" to solution phase NMR. A small molecule analogue of **G1-ene** was therefore synthesised in the hope that it would be more soluble, allowing us to determine how a molecule with the same functional groups as **G1-ene** interacts with the cations. Compound **C_4-Lys-ene** was synthesised by protecting an L-lysine with a methyl ester group, then taking this protected amino acid and coupling two unsaturated acids to the amine groups using TBTU. The methyl ester of this compound was then removed to unmask the carboxylic acid. Finally, this acid was coupled to butylamine, again using TBTU (Scheme 2.2). Unfortunately however, compound **C_4-Lys-ene** was not soluble in EtOAc.

For this reason, even smaller analogue compounds **A-ene**, **A-ane** were synthesised and used alongside commercially available **Octene** (Scheme 2.3.). These compounds contain amide and alkene, amide alone and alkene alone respectively. This would allow us to study the effect of the different functional groups on cation binding.

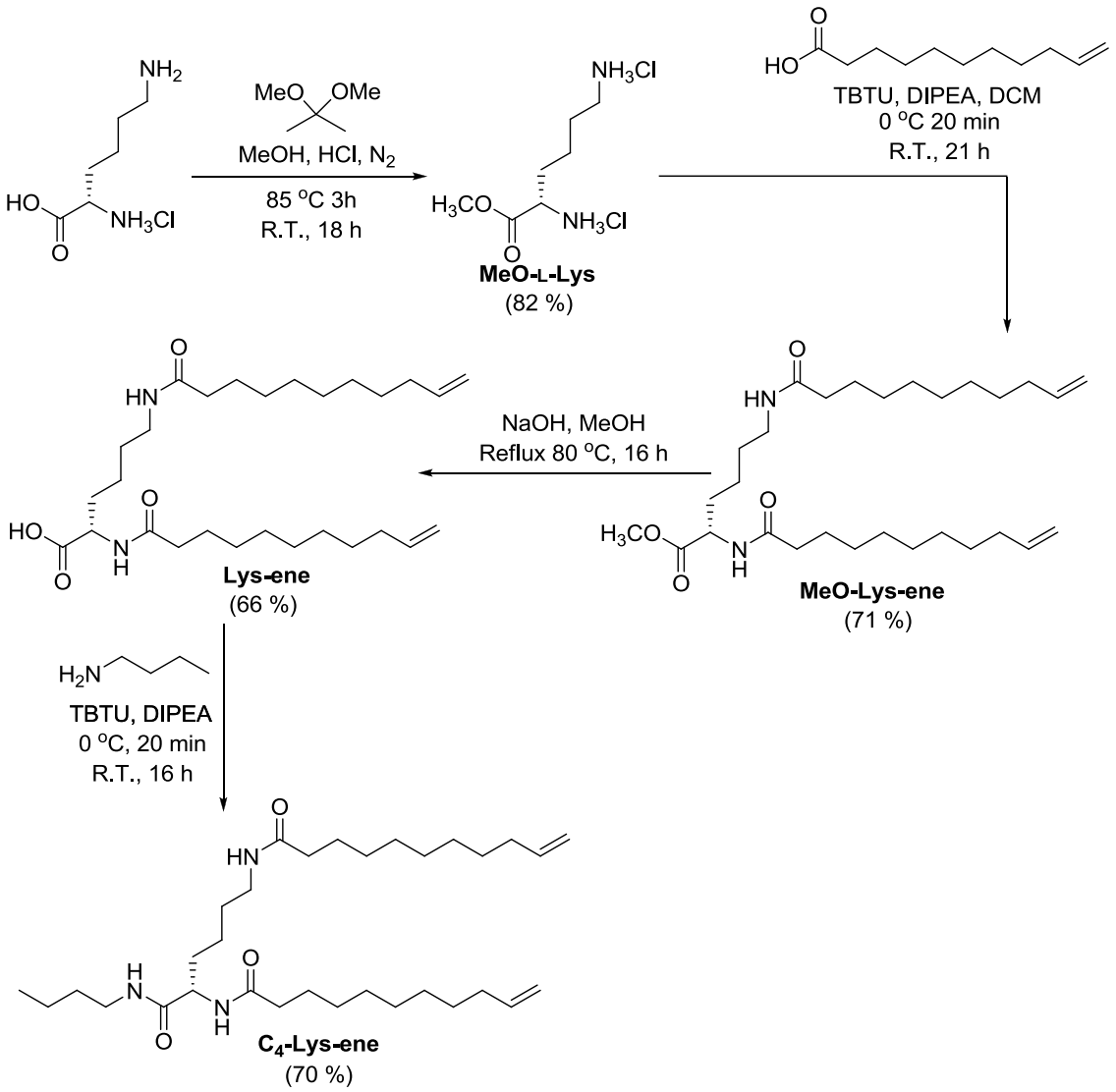

Scheme 2.2. Synthesis of compound **C_4-Lys-ene**.

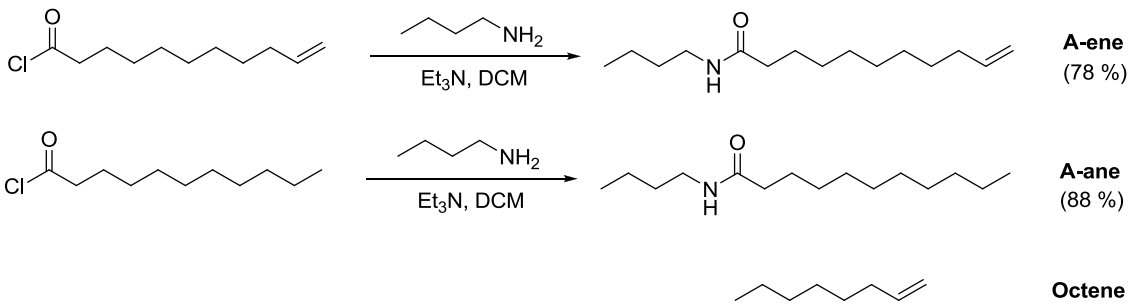

Scheme 2.3. Synthesis and structure of **A-ene**, **A-ane** and **Octene**.

Due to the poor availability and very high cost of deuterated EtOAc, the experiment was conducted using non-deuterated solvent, so ^{13}C NMR spectra were recorded. This provided the added benefit of showing directly the effect of cation binding on the amide carbonyl. In an initial experiment, two molar equivalents of each salt were added to a 50 mM solution of **A-ene** in EtOAc. The resulting change in chemical shift of the amide carbonyl and the terminal carbon of the alkene are shown in Figure 2.14. The presence of Ag^+ caused a significant perturbation in the resonances of both amide and alkene functional groups, indicating the Ag^+ ion binds to both in solution. The upfield shift in the alkene resonance has previously been observed in Ag^+-alkene complexes.[404, 405] The addition of Li^+ also caused a change in chemical shift of the amide group which was, in this case, accompanied by peak broadening. This likely indicates that the kinetics of Li^+-amide binding are slow on the NMR timescale. However, addition of Li^+ led to no perturbation in the shift of the alkene signal, so has no interaction with this group. Neither Na^+ nor K^+ ions had a significant effect on the ^{13}C NMR spectrum of **A-ene**, demonstrating that neither ion interacts strongly with this molecule.

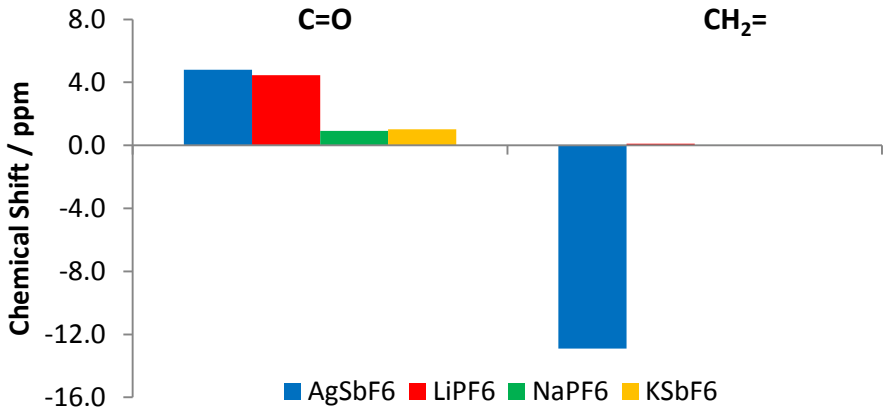

Figure 2.14. Change in chemical shift for amide and alkene of **A-ene** upon addition of two equivalents of each salt.

Both Ag^+ and Li^+ caused gel destruction and both bind strongly to the amide carbonyl. The NMR experiment suggested that complexation of a cation to the amide carbonyl was responsible for gel breakdown. This is a sensible hypothesis as the gel network is underpinned by intermolecular hydrogen bonding between the amide groups of **G1-ene** molecules. To test this hypothesis **G1-ane** was synthesised following the process shown in Scheme 2.4. The synthesis of **G1-ane** was identical to that of **G1-ene**, except that the active ester (***p*-NP-ane**) used did not have an alkene group terminating the alkyl chain. Therefore **G1-ane** was identical

to **G1-ene** except that it lacks peripheral alkenes. If gels of **G1-ane** behaved in the same way to the presence of ions as **G1-ene** gels, this would confirm that the alkene was not required to respond to Ag^+. When gels of **G1-ane** were tested for cation response it was found that they were still responsive to Li^+ and still unresponsive to Na^+ and K^+, just like gels of **G1-ene**. However, they were now completely unresponsive to Ag^+.

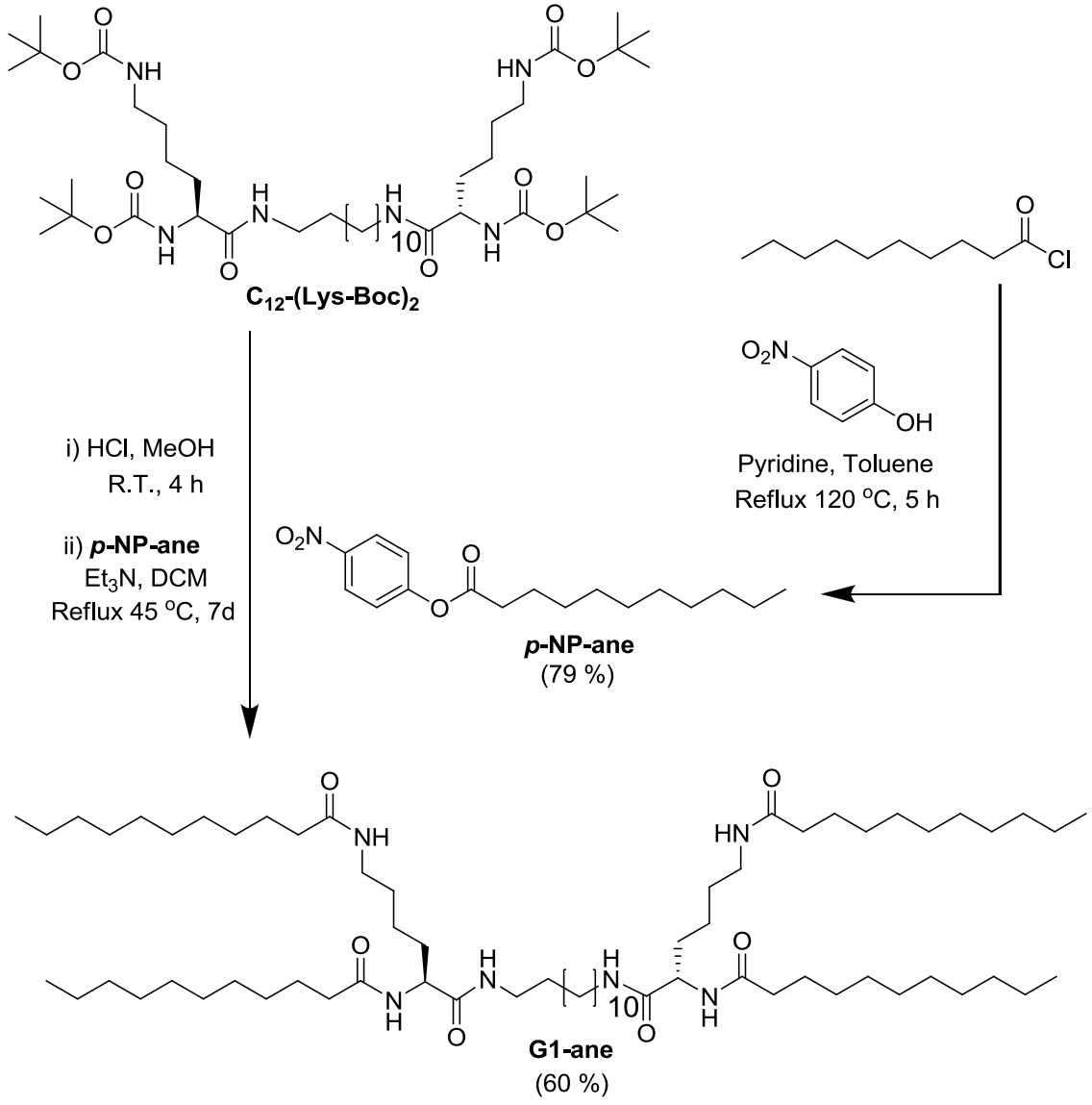

Scheme 2.4. Synthesis of **G1-ane**.

Whether Ag^+ binding to the amide influences binding at the alkene, or vice versa, was investigated using further ^{13}C NMR experiments. The binding of $AgSbF_6$ to the three small molecule analogues - **A-ene**, **A-ane** and **Octene** - was measured. This would show the influence

of binding to either group on the other, i.e. how binding to alkene changes without the amide and vice versa.

Firstly, a Job plot analysis with each compound was undertaken. The plots for the CH_2 and C=O of **A-ene** are shown in Figure 2.15 and the plots for the CH_2 of **Octene** and the C=O of **A-ane** are shown in Figure 2.16. The CH_2 plots of both **A-ene** and **Octene** show predominately 1:1 binding (with a small contribution from 1:2 M:L). The plots following the amide resonance of **1-ene** or **1-ane** were more complex indicative of a mix of 1:4, 1:3, 1:2 and 1:1 stoichiometries.

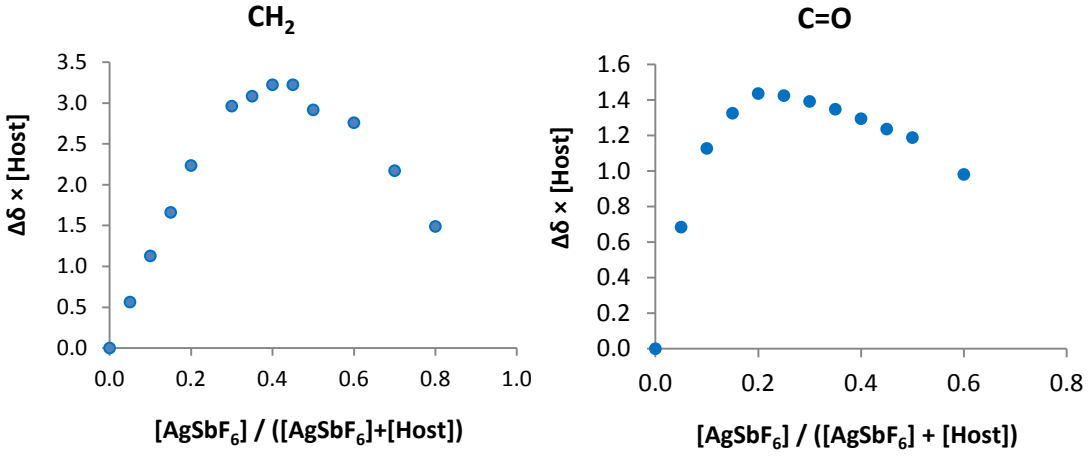

Figure 2.15. Job plot analysis of **CH_2** and **C=O** of **A-ene** with $AgSbF_6$.

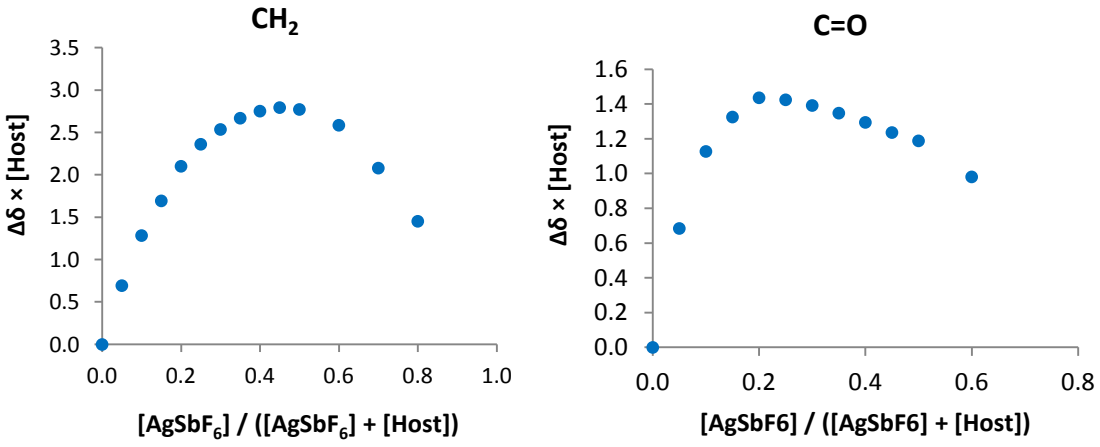

Figure 2.16. Job plot analysis of **CH_2** of **Octene** and **C=O** of **A-ane** with $AgSbF_6$.

Titrations were then carried out with each compound. The chemical shift of the alkene resonances upon addition of $AgSbF_6$ has been plotted in Figure 2.17. and the resulting binding

curves have had stability constants fitted with WinEQNMR2[413] using a 1:1 stoichiometry. The *log*K values produced were 1.8 for **A-ene** and 1.4 for **Octene** (both 15% error). The plot showing a comparison of the measured change in chemical shift upon addition of $AgSbF_6$ and the change predicted using the calculated *log*K value for the CH_2 of **A-ene** is presented in Figure 2.18. and shows a very good fit between the two. We can conclude from this that the presence of the amide group in **A-ene** has only a very small effect on the interaction between the alkene group and Ag^+ ion as the *log*K values for Ag^+-alkene binding are very similar in each case.

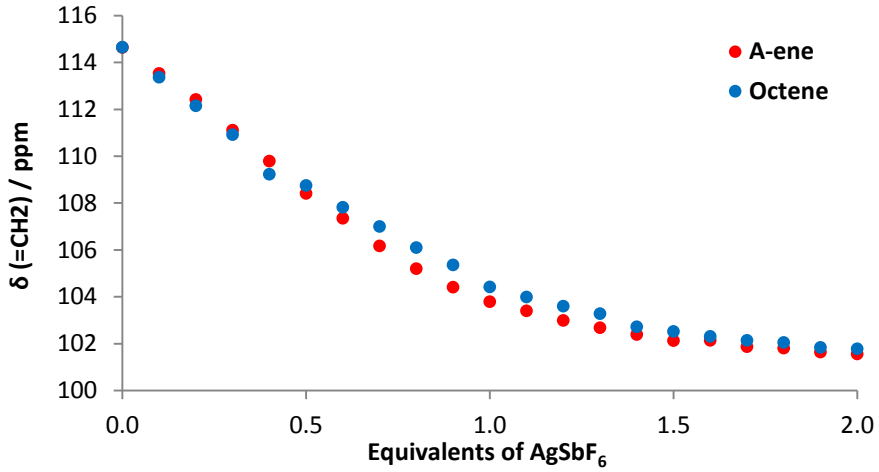

Figure 2.17. Shift in alkene CH_2 with increasing amounts of $AgSbF_6$.

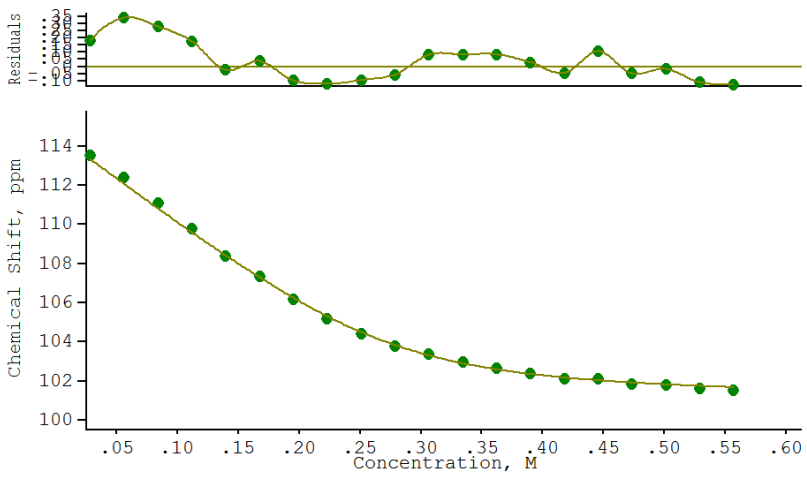

Figure 2.18. Plot showing measured shift of alkene CH_2 group of **A-ene** with increasing amount of $AgSbF_6$ (points) Compared to theoretical data using calculated binding constant (line). Plot above shows residual error for each point.

Stability constants for the binding of an amide to Ag^+ could not be fitted reliably due to the ill-defined stoichiometry of the complexes. However, when the binding curves for the amides of **A-ene** and **A-ane** are compared they are seen to be very similar (Figure 2.19.). This shows a very similar interaction between each amide and $AgSbF_6$. Compound **A-ene** reaches saturation slightly more slowly than compound **A-ane**, which might indicate that Ag^+ to alkene binding occurs before the ion interacts with the amide in the solution phase.

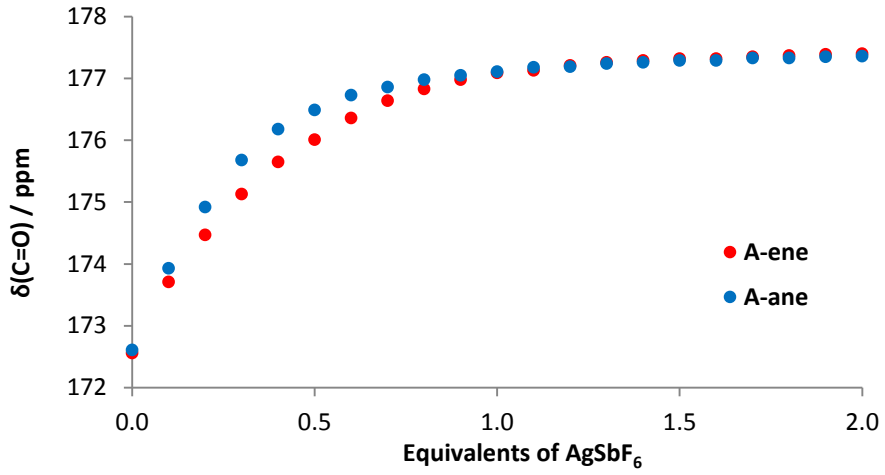

Figure 2.19. Shift in amide C=O with increasing amounts of $AgSbF_6$.

The data suggests that simultaneous binding to the amide and alkene of **A-ene** occurs. When describing the binding of **A-ene** to Ag^+ the evidence shows that:

i) The primary binding site of Ag^+ is the alkene (ca. 1:1 binding) as in **Octene**

ii) An ill-defined number of amides can subsequently bind weakly to the alkene bound Ag^+

In the gel phase, it is clear from the different responses of **G1-ene** and **G1-ane** to $AgSbF_6$ that the Ag^+-alkene interaction is the primary driving force behind the rapid sensory response to this cation. The response of the **G1-ene** gel to Ag^+ ions may be caused by repulsive electrostatic interactions between Ag^+ ions bound to the alkenes of **G1-ene** molecules in the gel fibres. However it cannot be ruled out that the Ag^+ ions first interact with the alkenes, which disrupts packing of molecules in the gel fibres and exposes the amide groups, which can then be bound by the same Ag^+ ions. As the hydrogen bonding between amides underpins the gel network, this would also undermine the structure of the gel. The rapid response of **G1-ene** gels to the Ag^+ ions is likely due to the alkene groups being present on the periphery of the gel

fibres. The slow response to Li^+ is likely because the amide groups it exclusively interacts with will be more inaccessible inside the gel fibres. The selective response shown to Li^+ but not to Na^+ or K^+ by gels of **G1-ene** is likely due to the fact that the smaller and more charge dense Li^+ can get to and perturb the amides in the gel fibres sufficiently to undermine fibrous network. It is likely that Na^+ nor K^+ were either too large, or not charge dense enough to significantly disrupt the amide-amide interactions in the network.

A final ^{13}C NMR experiment was used to test the mechanism of cation induced breakdown. The NMR of the EtOAc gel of **G1-ene** was taken (Figure 2.20.). As expected, the gelator peaks are so broad they are not visible and only solvent peaks are seen. When either $AgSbF_6$ of $LiPF_6$ was added to the gel, the gelator peaks became visible as the gelator became more mobile as the gel was broken down. Crucially, the chemical shifts closely resemble the shifts of **A-ene** when it is binding Ag^+ or Li^+, including the distinctive upfield shift of the alkene resonances when a complex with Ag^+ is formed. This proves that the cations complex to **G1-ene** in the proposed manner, which induces the gel-sol transition.

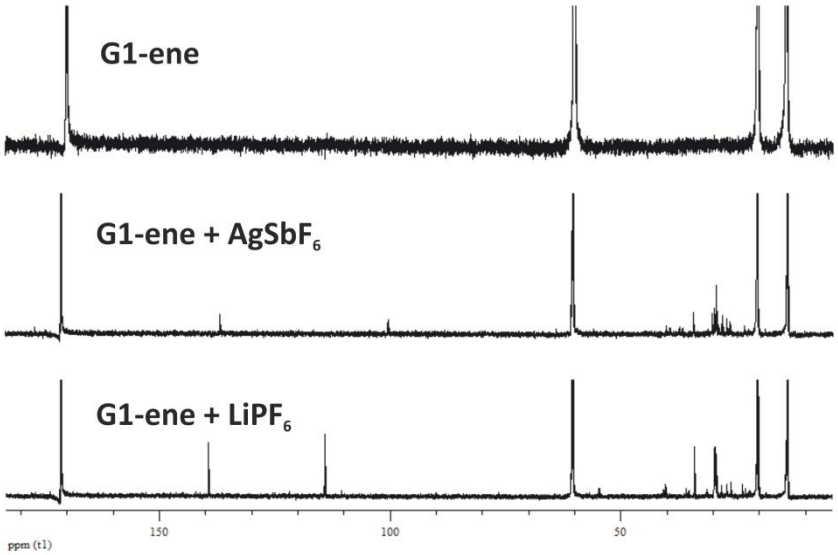

Figure 2.20. Spectra of **G1-ene** gel in EtOAc (top), solution after addition of $AgSbF_6$ (middle) and solution after addition of $LiPF_6$ (bottom).

2.3. Conclusions

In conclusion, it has been demonstrated that **G1-ene** can from gels in EtOAc that show a selective response to certain cations. The reasons behind this selective response have been investigated and it has been proven that the Ag^+-alkene interaction is essential for the

response of **G1-ene** to $AgSbF_6$, but the alkene group is not required for Li^+ to trigger breakdown. There is no response of the gel to larger, less charge dense group I metal ions such as Na^+ and K^+. It is proposed that the selectivity observed amongst the group I metals is mediated by the higher charge density of Li^+ which means it is a stronger binder to C=O than Na^+ or K^+.

The rapid response to Ag^+, seen in gels of **G1-ene**, may be due to repulsive electrostatic interactions of alkene-bound Ag^+ ions, although it cannot be ruled out that initial binding of Ag^+ to the alkenes disrupts the gel fibres, making the amide groups more accessible for binding, which then disrupts the hydrogen bonding which underpins the gel.

Chapter 3

Multi-Component Gels: Non-Chiral Amines

Chapter 3 – Multi-Component Gels: Non-Chiral Amines

3.1. Basic Multi-Component Gels

3.1.1. Gelation with Monoamines

Compound **L,L,L-G2Lys** has previously been exploited in the Smith group due to its ability to form gels in organic solvents when mixed with a selection of diamines.[194, 197-201, 243, 414] However, the need to use diamines limited the scope of these gels.

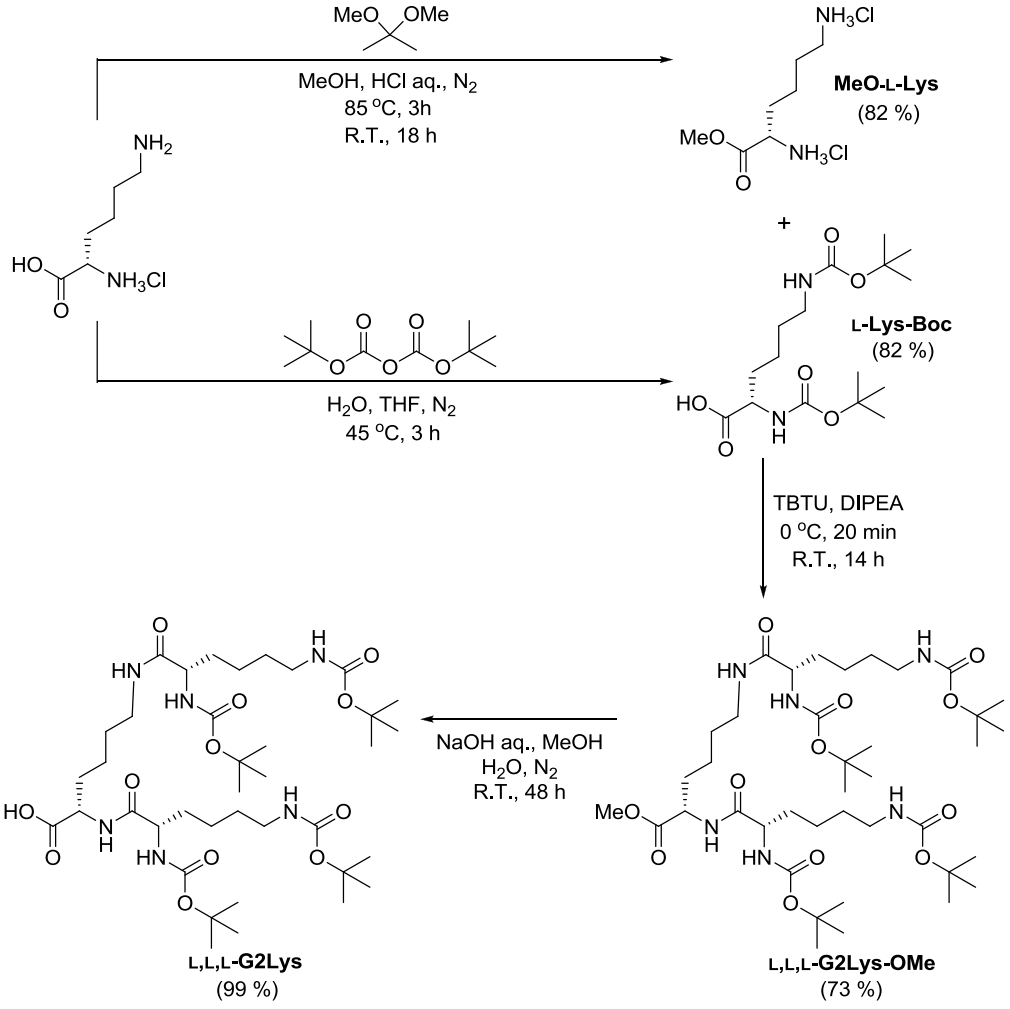

Scheme 3.1. Synthesis of **L,L,L-G2Lys**.

It was therefore decided to investigate whether monoamines could be used instead, dramatically increasing the tunability and of these systems. The first step was to synthesise **L,L,L-G2Lys**. This was carried out following published procedures as shown in Scheme 3.1.[415, 416]

in an overall yield of 59%. The ability of **L,L,L-G2Lys** to form gels with a range of monoamines was tested. It was initially assumed that each carboxylic acid on **L,L,L-G2Lys** would complex with one amine, so gel formation would be achieved with a 1:1 mixture of **L,L,L-G2Lys** and monoamine (previous work used a 2:1 mixture of **L,L,L-G2Lys** to diamine).[198] The amines tested are shown in Figure 3.1. divided as those that supported gelation or did not (formed solutions).

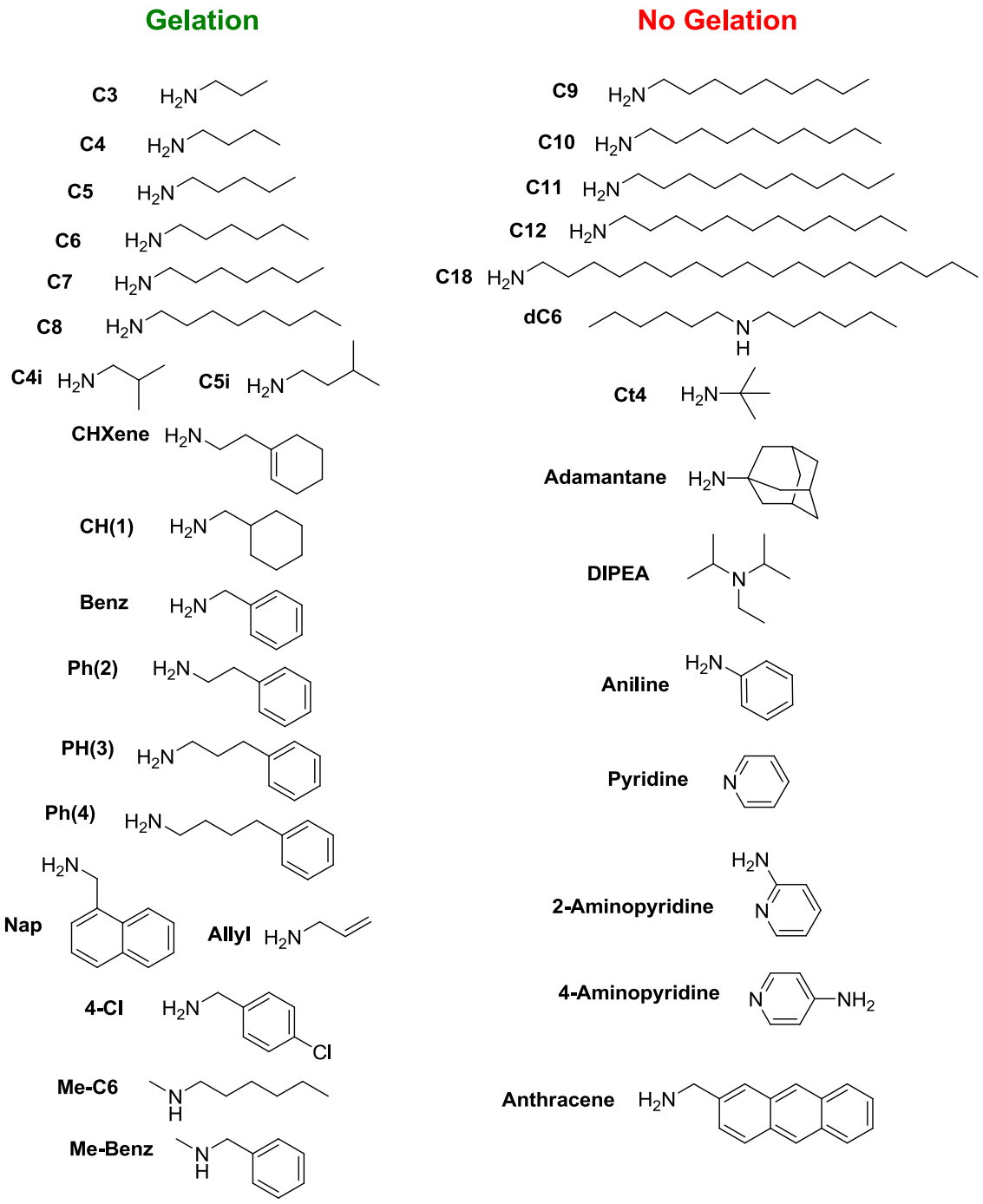

Figure 3.1. Amines that do and do not support gelation with **L,L,L-G2Lys** in toluene.

All of the tests were carried out by mixing 10 mM of **L,L,L-G2Lys** with 10 mM of amine in toluene (0.5 mL), the samples were heated to form a solution and left to cool overnight, before being checked to see if gelation had occurred. It was found that shorter unbranched alkyl amines were able to form gels with **L,L,L-G2Lys** (from **C3** to **C8**), whilst longer chain lengths (**C9** to **C18**) did not form gels, unless cooled to low temperature (-20°C). This is may be an entropic effect; as the alkyl chain becomes longer and able to adapt more conformations, the entropic loss upon fixing it in the gel network becomes higher. This results in it requiring lower temperatures to form a gel, due to the relationship shown in Equation 1.

$$\Delta G = \Delta H - T\Delta S \quad (1)$$

The branched alkyl, cyclic alkyl and allyl amines tested were all found to form gels with the exception of **Ct4** and **Adamantane**, probably due to the increased steric bulk of these amines stopping the intermolecular stacking of complexes required to form a gel. It was observed that aromatic amines could induce gelation, as long as the amine was not directly conjugated to the aromatic ring, or if **Anthracene** is used. Presumably this amine is too large and rigid to incorporate into the gel network. Secondary amines that were less sterically demanding (**Me-C6** and **Me-Benz**) were able to form gels whilst the more sterically hindered secondary (**dC6**) and tertiary amines (**DIPEA** and **Pyridine**) failed to induce gelation, as did pyridine containing primary amines (**2-Aminopyridine** and **4-Aminopyridine**). These amines produce a clear solution when mixed with **L,L,L-G2Lys** which is most likely due to steric bulk of the amine stopping effective self-assembly of the complexes formed. In summary however, many monoamines formed effective gels in 1:1 mixtures with **L,L,L-G2Lys**.

It was important to establish whether the stoichiometry of gel formation was indeed 1:1. This was initially tested by measuring the T_{gel} values of gels with different ratios of **L,L,L-G2Lys** to amine. The T_{gel} value is a measure of the thermal stability of a gel, it was determined by heating the gel at a rate no quicker than 1°C / 2 min in a thermostatted oil bath. As the temperature increases, the gel was checked to see that it was still stable to inversion (i.e. sample did not flow when turned upside down). The temperature at which the gel was no longer stable to inversion was taken as the T_{gel}. Therefore, the T_{gel} is a point of gel-sol transition, when the gelator network can no longer support the sample against the force of gravity.

In this experiment the concentration of **L,L,L-G2Lys** was held constant and the concentration of amine (in this case **C6**) was varied from 0.25 to 4 equivalents relative to **L,L,L-G2Lys**. The experiment was carried out with both a 2 mM and 10 mM concentration of **L,L,L-G2Lys**. The results are shown in Figure 3.2.

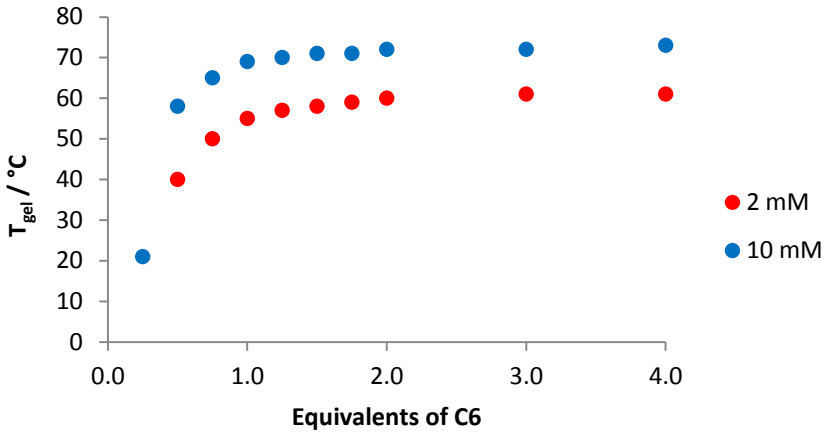

Figure 3.2. T_{gel} values of 2 mM and 10 mM **L,L,L-G2Lys** with varying equivalents of **C6** in toluene.

The T_{gel} values show that the thermal stability of the gels at both 2 mM and 10 mM increases rapidly up to a 1:1 ratio of **L,L,L-G2Lys** to **C6**. As the amount of amine increases further – to four equivalents – the thermal stability of the gels only increases very slightly. This suggests that a 1:1 mixture of **L,L,L-G2Lys** to **C6** is responsible for gelation. It may be that beyond 1 equivalent of amine, the equilibrium of complex formation between **L,L,L-G2Lys** and **C6** is pushed further towards complex formation, leading to this slight increase in T_{gel} value.

This finding was further verified by ^{1}H NMR spectroscopy. When gel samples are analysed by solution phase NMR, the solid-like gel network is silent and only molecules mobile in solution are "visible". The amount of material trapped in the network and free in solution can then be quantified if a mobile (solubilised) internal standard is used.

NMR tubes containing a 10 mM concentration of **L,L,L-G2Lys** and varying concentrations of **C6** were heated and allowed to cool. The integration of **L,L,L-G2Lys** and **C6** peaks in each case was measured and compared to an internal standard of a known concentration. The standard used was diphenylmethane (**DPM**), as it had a distinctive, sharp ^{1}H NMR peak and is chemically similar to the solvent, toluene-d_8, so should remain mobile in the liquid-like phase. The integration of **L,L,L-G2Lys** and **C6** in each sample is plotted in Figure 3.3.

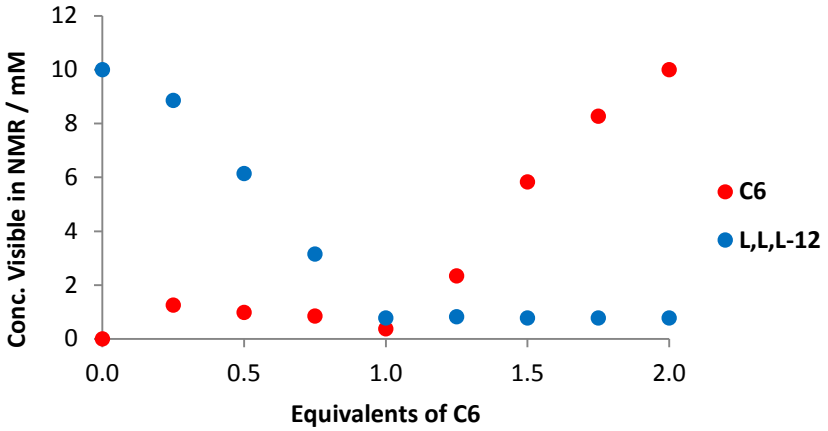

Figure 3.3. Amount of **L,L,L-G2Lys** and **C6** visible in ^{1}H NMR as amount of **C6** is varied.

At 0 equivalents of amine all of the **L,L,L-G2Lys** is mobile in solution . As amine is added, the amount of "mobile" **L,L,L-G2Lys** decreases proportionally. At a 1:1 ratio of **L,L,L-G2Lys** to **C6** (10 mM) both molecules are barely visible in the spectrum, meaning they form a 1:1 complex and become almost entirely fixed in the gel network. As an excess of amine is added it is "visible" in solution – indicating it is not incorporated into the gel network.

Finally, the ratio of **L,L,L-G2Lys** to amine required for gel formation was probed using FEG-SEM. Two gels were formed, both with 10 mM of **L,L,L-G2Lys**. One gel had one equivalent (10 mM) of **C6**, the other had 2 equivalents (20 mM). The gels were dried to form xerogels and the morphology of each examined (Figure 3.4.). The images from each gel were almost identical, suggesting the same species underpins gelation in each case.

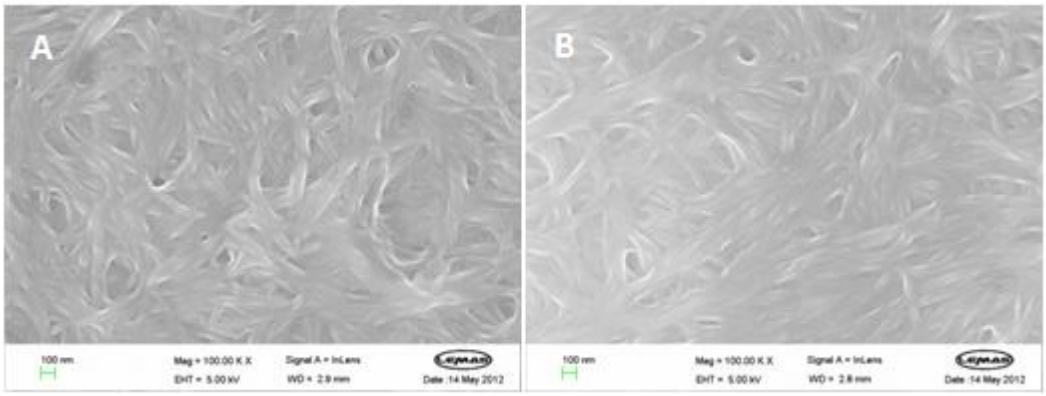

Figure 3.4. FEG-SEM images of xerogels formed from **L,L,L-G2Lys** and **C6**. A) 1 Equivalent of **C6**. B) 2 Equivalents of **C6**. Scale bars = 100 nm.

The combined T_{gel}, NMR and FEG-SEM experiments demonstrate unambiguously that the ratio of **L,L,L-G2Lys** to monoamine that forms the gelator network is 1:1.

It was important to examine the supramolecular interactions which underpin gel formation. Previously, mixtures of **L,L,L-G2Lys** and diamines had been found to be underpinned by an intermolecular network of hydrogen bonds involving the amide and carbamate groups of **L,L,L-G2Lys**.[201] To test if this would be the same with a monoamine, a gel formed from a 10 mM mixture of **L,L,L-G2Lys** and **C8** in toluene was investigated by ATR-FTIR and variable temperature NMR (VT-NMR).

The ATR-FTIR spectrum of a xerogel produced from this gel was assigned[417] and compared to the spectrum of powdered **L,L,L-G2Lys** that had been dissolved in toluene before the solvent was removed (both shown in Appendix B). The spectrum of the **L,L,L-G2Lys** powder shows a carbamate C=O stretch at 1690 cm^{-1}, amide C=O at 1658 cm^{-1} and an NH stretch at 3308 cm^{-1}. In the spectrum of the xerogel, the carbamate C=O stretch has shifted slightly to 1685 cm^{-1}, the amide C=O is shifted further to 1646 cm^{-1} and the NH stretch to 3320 cm^{-1}. This shows that both carbamate and amide groups are involved in intermolecular hydrogen bonding within the gel, with the amide more strongly involved. This is in agreement with previous work which demonstrated amide-amide hydrogen bonding is stronger than carbamate-carbamate[418]. Of course, this does not rule out amide-carbamate hydrogen bonds being formed but does show that amides are more strongly involved in hydrogen bonding. The NH shift just provides supporting evidence of amide and carbamate involvement in a hydrogen bond network.

It is interesting to consider the nature of the interaction between the acid and amine. Calculations carried out by Liljefors and Norrby[419] show that for a 1:1 acid-amine complex a solvent with a dielectric constant (ε) of at least 9 is required for full proton transfer from acid to amine to be favoured over a hydrogen bonded complex. The ε of toluene is 2.38 which is too low to favour proton transfer. Of course the pKa values of the lysine carboxylic acid (2.49) and **C6** (10.69) dictate that deprotonation should take place, but these are values that represent relative acidity in water, not in a relatively non-polar organic solvent. As it has already been established that the gel is formed by a strict 1:1 complex of acid to amine, the formation of 2:1 acid-amine complexes that are more likely to show deprotonation has been ruled out.[420] The lack of full deprotonation is sensible because a hydrogen bond has directionality, both components will have to align at a certain angle to one another to maximize the favourability of the bond, so a linear complex will form. This is likely to be

beneficial to gel formation, which requires complexes to stack together during the hierarchical process.

VT-NMR study of the gel showed the NH peaks of the amide and carbamate groups are barely visible at 25°C due to nearly all of the **L,L,L-G2Lys** molecules being "immobile" in the gel network. Despite this, their change in chemical shift as the temperature of the sample is increased can be monitored. The shifts of the NH protons are plotted in Figure 3.5. All of the NH protons exhibit an upfield shift upon heating, this shift can be explained by the breakdown of the complementary hydrogen bonding between these groups, which reduces the amount of electron density donated from the carbonyl oxygen of a neighbouring group to the NH proton, therefore leading to an upfield shift. One of the amide protons (NH2-Amide) overlaps the solvent peak at the highest temperatures, but both amide peaks show a larger total shift ($\Delta\delta_{NH1}$ = 0.469, $\Delta\delta_{NH2}$ = 0.405) than the carbamate resonance ($\Delta\delta_{NH3}$ = 0.302). This again suggests that the amide groups are more important to the hydrogen bonding network which underpins gelation than the carbamate groups. Both ATR-FTIR and VT-NMR experiments therefore demonstrate that the gel is held together by hydrogen bonding in which the amides form stronger interactions than the carbamate groups.

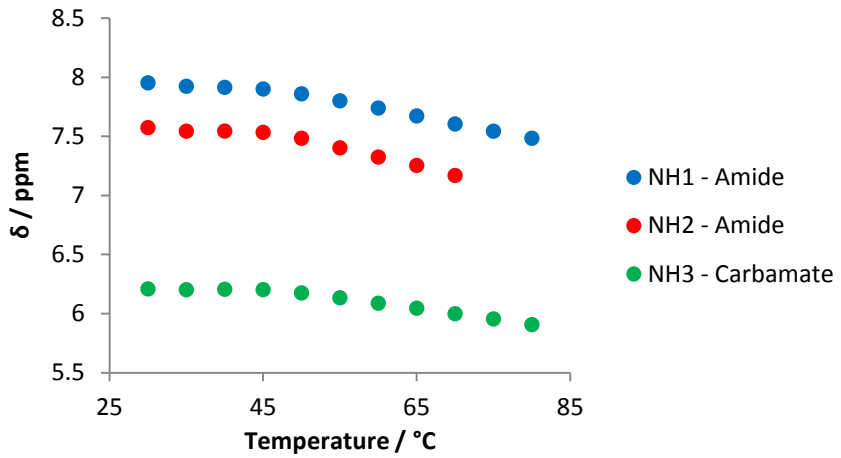

Figure 3.5. Chemical Shift of **L,L,L-G2Lys** NH protons in the gel with **C8**.

3.1.2. Effect of Solvent

When considering the structure of a supramolecular gel, the vast majority of the gel is solvent. As such it is of vital importance to understand the role played by solvent in controlling the assembly and properties of the gel.[421, 422] The influence of solvent on gelation ability has been investigated by a number of groups[75, 423-428] and has become increasingly well understood.

However, there is still no universal approach to different types of gelators or different types of solvents. The effect different solvents have on the assembly of a 1:1 mixture of **L,L,L-G2Lys** and **C6** (both 10 mM), and the thermal stability of any gels formed was investigated. Samples were made with a range of solvents, and the results recorded in Table 3.1. Also shown in Table 3.1. is a collection of parameters for each solvent.

Table 3.1. Results from samples made with different solvents, T_{gel} values of gels that were formed and solvent parameters of the solvents used. Solvent parameters are; ε = Dielectric constant[429, 430], E_T^N = Normalised Dimroth-Reichardt parameter[431], δ_0 = Hildebrand parameter[432], δ_d, δ_p, δ_h and δ_a = Hansen parameters[432], α, β and π^* = Kamlet-Taft parameters[433].

Solvent		T_{gel}	ε	E_T^N	δ_0	δ_d	δ_p	δ_h	δ_a	α	β	π^*
Decalin	TG	93	2.10	0.015	8.80	8.8	0	0	0	0	0.08	0.11
Methylcyclohexane	TG	89	2.10									
Cyclohexane	TG	87	2.10	0.006	8.18	8.18	0	0.1	0.10	0	0	0
1-Bromonaphthalene	OG	84	4.83		10.20	9.9	1.5	2.0	2.50			
Tetralin	CG	82	2.66	0.093	9.80	9.6	1.0	1.4	1.72			
Mesitylene	CG	78	2.27	0.068	8.80	8.8	0	0.3	0.30	0	0.13	0.41
Toluene	CG	71	2.38	0.099	8.90	8.8	0.7	1.0	1.22	0	0.11	0.54
1,2-Dichlorobenzene	CG	65	9.93	0.225	10.00	9.4	3.1	1.6	3.49	0	0.03	0.77
Bromobenzene	CG	61	5.40	0.182	10.60	10	2.7	2.0	3.36	0	0.06	0.77
Benzene	CG	60	2.27	0.111	9.10	9.0	0	1.0	1.00	0	0.10	0.59
Chlorobenzene	CG	59	5.53	0.188	9.57	9.28	9.1	1.0	2.33	0	0.07	0.71
EtOAc	OG	49	6.40	0.228	9.10	7.44	2.6	4.5	5.19	0	0.45	0.55
Acetonitrile	OG	42	3.88	0.460	11.90	7.5	8.8	3.0	9.30	0.19	0.40	0.75
Hexane	Ins		1.19	0.009	7.24	7.24	0	0	0	0	0	-0.4
THF	S		7.58	0.207	9.50	8.2	2.8	3.9	4.8	0	0.55	0.58
Tetraethylene glycol	S			0.664								
DCM	S		8.93	0.309	9.90	8.9	3.1	3.0	4.31	0.13	0.10	0.82
Chloroform	S		4.80	0.259	9.30	8.7	1.5	2.8	3.18	0.20	0.10	0.58
EtOH	S		25.7	0.654	12.92	7.73	4.3	9.5	10.45	0.86	0.75	0.54
MeOH	S		31.2	0.762	14.50	7.4	6.0	10.9	12.40	0.98	0.66	0.60
Acetone	S		21.5	0.355	9.77	7.58	5.1	3.4	6.13	0.08	0.43	0.71
DMF	S		26.6	0.386	12.14	8.52	6.7	5.5	8.69	0	0.69	0.88
DMSO	S			0.444	12.93	9.0	8.0	5.0	9.43	0	0.76	1.00

TG = Translucent Gel, OG = Opaque Gel, CG =Clear Gel, Ins = Insoluble, S = Solution

The results in Table 3.1. show that in general terms cyclic non-aromatic solvents form the most thermally stable gels, followed by the range of aromatic solvents, which all form strong, clear gels. Opaque gels are formed in EtOAc and acetonitrile. Hexane was tested and found to cause a precipitate to form. All of the other solvents, including; the hydroxyl containing solvents (MeOH, EtOH and tetraethylene glycol), chloroform and DCM, THF, DMF, acetone and DMSO fully solubilised the **L,L,L-G2Lys** and **C6** mixture. The solvent parameters shown in Table 3.1. were used to try to rationalise this behaviour. The parameters are values that describe one or more property of that solvent. To start with, parameters which measure the polarity of each solvent were used. The first ones to be tested were the dielectric constant (ε), which is a measure of the polarisability of a solvent, and the normalised Dimroth-Reichardt parameter (E_T^N), which is a measure of a solvents ionising power. Both of these parameters have previously been used to rationalise the behaviour of gelators with mixed success.[434-438] The T_{gel} values that could be measured were plotted against the ε and E_T^N values of the solvents in which they were formed (Figure 3.6.).

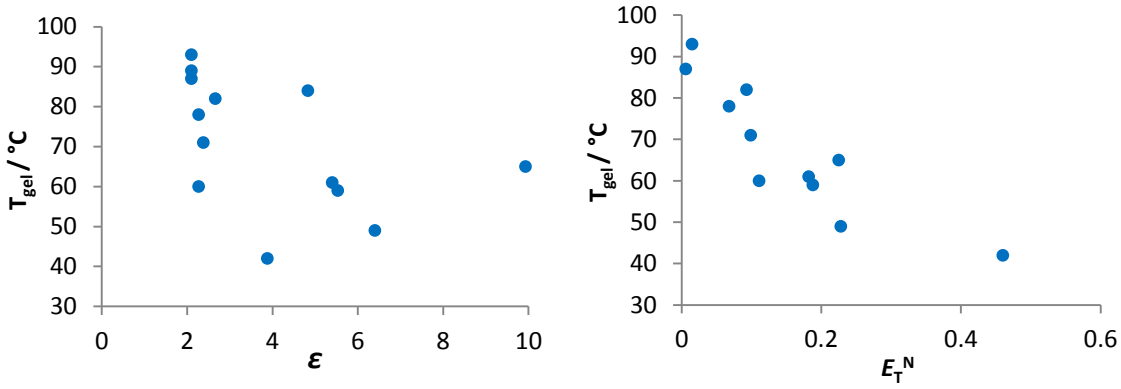

Figure 3.6. Change in T_{gel} values of 1:1 mixture of **L,L,L-G2Lys** and **C6** (both 10 mM) with changing ε and E_T^N values.

It is clear that changing ε of the solvent has little correlation to the change in T_{gel} value of the gel formed. A number of solvents have a ε value between 2.0-2.5 but the variation of T_{gel} values of gels formed in these solvents is large – over 30°C. The change in E_T^N values shows a greater correlation with the change in T_{gel} values. A general decrease in T_{gel} is observed with increasing E_T^N. The E_T^N values of solvents that can support gelation ranges from 0.006 (cyclohexane) to 0.460 (acetonitrile). This should mean, however, that hexane (0.009), THF (0.207), DCM (0.309) and chloroform (0.259) might be expected to support gelation, which

they do not. Increasing E_T^N value of the solvent has shown a good correlation with decreasing T_{gel} value but is still unable to determine whether a solvent will be able to support gelation.

As a gel is the result of the assembly of supramolecular polymers formed by small gelator molecules, the Hildebrand solubility parameter (δ_0) was the next solvent parameter investigated. This parameter is often used to explain and predict the behaviour of polymers in solution[439] and has also been used to rationalise gelator behaviour.[436, 437, 440] The value for each solvent is related to the amount of energy required to separate each molecule – in a mole of solvent – entirely from its neighbours (i.e. to form a perfect gas). Therefore, it is a value which represents the strength of the intermolecular forces between solvent molecules, some of which have to be overcome for dissolution to occur. The relationship between δ_0 and T_{gel} is shown in Figure 3.7.

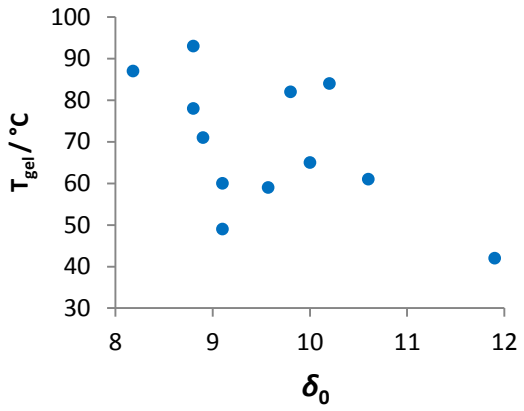

Figure 3.7. Change in T_{gel} values of 1:1 mixture of **L,L,L-G2Lys** and **C6** (both 10 mM) with changing δ_0.

The data shown in Figure 3.7. shows a very general decrease in T_{gel} with increasing δ_0 but the correlation is poor. Once again, solvents that might be expected to support gelation based on their δ_0 values do not. These non-gelling solvents are THF, DCM, chloroform and acetone, so δ_0 is of little use in predicting if a solvent will support gelation. It was noted that these non-conforming solvents are capable of dipole-dipole or hydrogen bonding interactions. The next logical step then was to try to rationalise the behaviour of our samples using the Hansen parameters. Again these parameters have also been used to rationalise gelator behaviour in solvents.[440-443] Importantly, this system of quantifying the properties of solvents distinguishes between different types of interaction. There are three individual Hansen parameters, each representing a different class of solvent – solvent interaction; δ_d = dispersion interactions, δ_p =

dipole-dipole interactions and δ_h = hydrogen bond interactions. Furthermore, the δ_p and δ_h values can be combined to give a polar parameter (δ_a). The relationship between the Hildebrand and Hansen parameters and the calculation of the polar Hansen parameter are shown in Equations (2) and (3).

$$\delta_0^2 = \delta_d^2 + \delta_p^2 + \delta_h^2 \quad (2)$$

$$\delta_a = \left(\delta_p^2 + \delta_h^2\right)^{1/2} \quad (3)$$

The T_{gel} values of the gels are plotted against the different Hansen parameters in Figure 3.8.

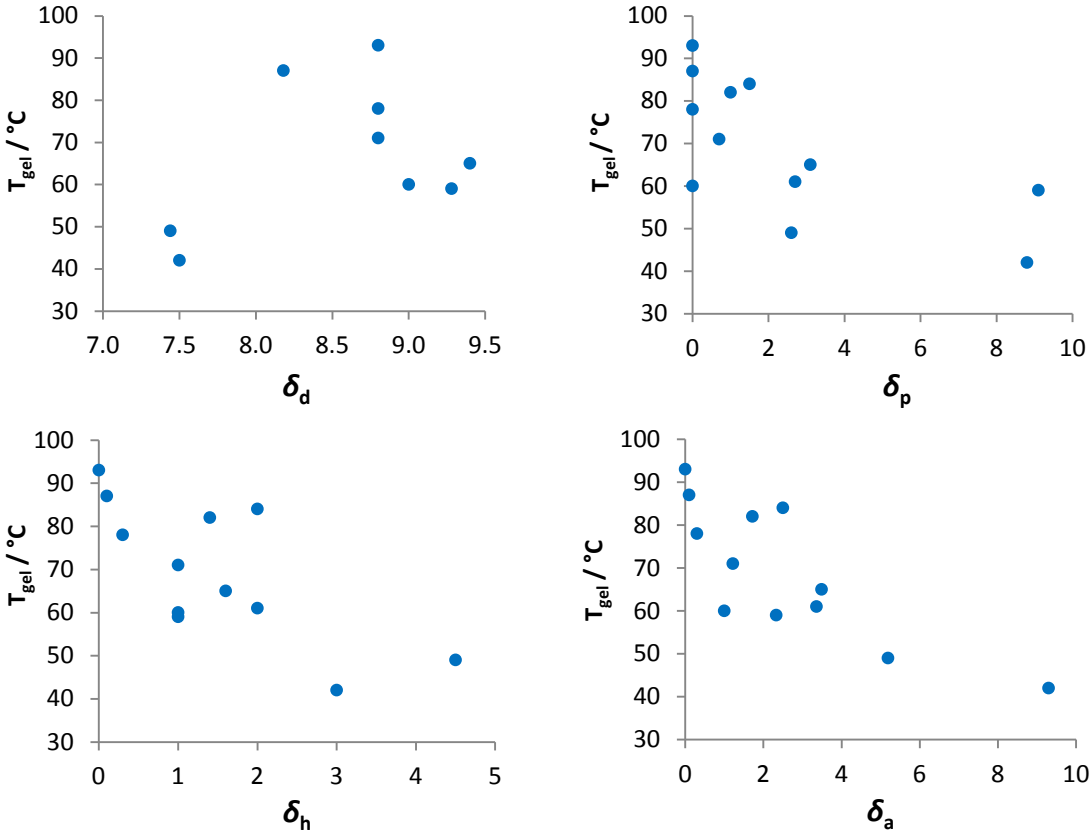

Figure 3.8. Change in T_{gel} values of 1:1 mixture of **L,L,L-G2Lys** and **C6** (both 10 mM) with changing δ_d, δ_p, δ_h and δ_a values.

The data in Figure 3.8. shows there is no correlation between the δ_d parameter of the solvent and T_{gel} value of the resulting gel. The δ_d values of solvents that can support gelation ranges from 7.44 (EtOAc) to 10.0 (1,2-dichlorobenzene). Every other solvent tested sits in this range, so they should all support gelation. This of course, is not the case. The data for the δ_p, δ_h and δ_a parameters are all very similar. There is a slight correlation between an increase in these

parameters and a decrease in T_{gel}, but it is quite poor and this cannot be stated reliably. Also, δ_p (like δ_d) predicts that all the solvents would support gelation. The parameters δ_h and δ_a predict that all of the solvents except MeOH, EtOH, DMF and DMSO would support gelation. All the parameters are wrong in this respect. It therefore seems that the Hansen solubility parameters cannot be used to rationalise or predict the gelation ability of the mixture of **L,L,L-G2Lys** and **C6** in different solvents.

One potential problem with the Hansen solubility parameters is that in presenting the – for example – hydrogen bonding interaction between identical solvent molecules as a single value (δ_h), a solvent that is a weak hydrogen bond acceptor and donor may have a higher value than a solvent that is only a strong acceptor or donor. This is a good description of solvent-solvent interactions but is less descriptive of solvent-solute interactions. Importantly, which solvents are more likely to disrupt the hydrogen bonding network that underpins gelation is due to solvent-solute interactions, not solvent-solvent interactions. In an attempt to solve this problem the Kamlet-Taft parameters were employed. These have also been used to rationalise the behaviour of gelators in different solvents with some success.[196, 414, 434, 442, 444-447] There are three of these parameters and they describe three different properties of a solvent; α = hydrogen bond donating ability, β = hydrogen bond accepting ability and π^* = polarisability. The T_{gel} values of the gels were plotted against the β and π^* values for each solvent (Figure 3.9.). The α values are not plotted as every solvent which supported gelation had α = 0 except for acetonitrile (α = 0.19).

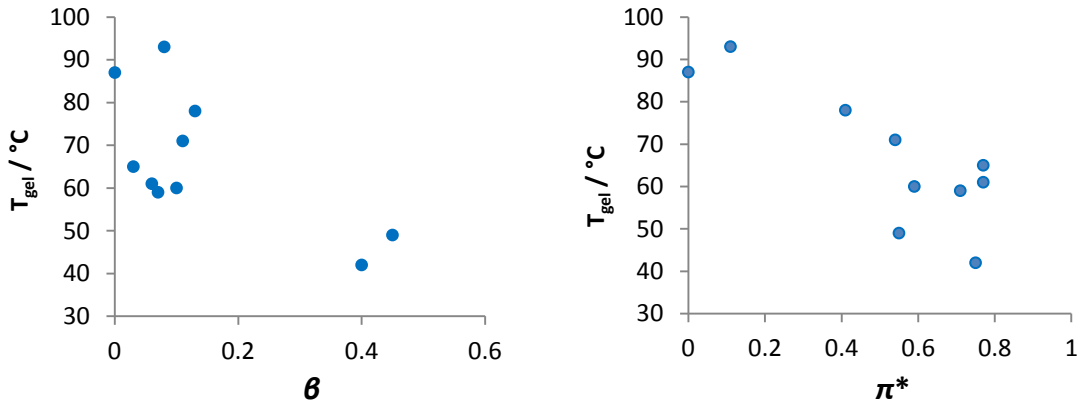

Figure 3.9. Change in T_{gel} values of 1:1 mixture of **L,L,L-G2Lys** and **C6** (both 10 mM) with changing β and π^* values.

It appears that the α value of the solvent is the most significant in determining whether a solvent will support gelation, as all but one solvent that supports gelation has no hydrogen bond donating ability. This is in agreement with previously published work.[414, 445, 447] It could be argued that acetonitrile (which supports gelation) has a very low α value (0.19), but then so do acetone (0.08), DCM (0.13) and chloroform (0.20). The *β* values plotted do not show any direct correlation with changing T_{gel} values, but in general terms, a lower *β* value is common in solvents that support gelation, the highest being 0.45 (EtOAc). However, again acetone (0.43), DCM (0.10) and chloroform (0.10) fall within this "gelling range". The *π** values plotted show little correlation to changing T_{gel}, perhaps there is an indication that a higher *π** value leads to a weaker gel but this is not distinct. There is also a wide spread of *π** values in the solvents that do support gelation, with only DMF and DMSO falling outside this range, and therefore using this parameter, the only solvents predicted not to support gelation.

It has previously been found that rationalising the behaviour of small molecule gelators using Kamlet-Taft parameters involved understanding the effect of all three parameters on the gelator, just using one of the parameters was not sufficient.[414, 445, 447] Likewise in this case, none of the Kamlet-Taft parameters individually can rationalise the behaviour of the **L,L,L-G2Lys** and **C6** mixture in a range of solvents, indeed all of them predict that acetone, chloroform and probably DCM (*π** is a little high) should form gels. However, it was noted that if the parameters were recombined (by simple addition) there was a correlation between changing Kamlet-Taft parameters and a change in T_{gel} (Figure 3.10.)

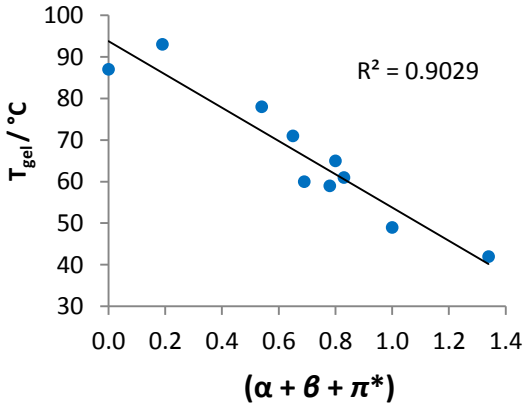

Figure 3.10. Change in T_{gel} values of 1:1 mixture of **L,L,L-G2Lys** and **C6** (both 10 mM) with changing (α + *β* + *π**).

A linear trend line produced for this data had an R^2 value of 0.9029. This can be improved by removing the cyclohexane data point from the data set. The T_{gel} value of the gel in this solvent (87°C) is above the solvent boiling point (80.7°C) and is therefore likely to be unreliable. With this point removed the R^2 value of the trend line increases to 0.9237. Acetonitrile is now the unusual solvent as it is the only one with an α value that is non-zero (α = 0.19). Interestingly, if we remove this point from the data set the R^2 value of the trend line barely changes to 0.9298, indicating no increase in the observed correlation. More of an improvement is seen if we retain this data point and only consider the β and π* parameters, discarding the α value (of course this only effects the value of the acetonitrile gel). By doing this the fit of the trend line to the data is slightly improved, the R^2 value increases to 0.9509. However, this relatively minor improvement in the correlation of the data plotted is based on changing a single data point and changing the analysis based on a single data point is not a reliable method for improvement. This analysis is similar to the kind of linear solvation energy relationships put forward by, for example, Kamlet, Abboud, Abraham and Taft[448]. These relationships are most commonly applied to the changing absorbance of compounds in different solvents[448, 449] and calculating the partition coefficient of solutes[450, 451]. They require that each relevant parameter is weighted by a coefficient. These coefficients can be found for our data by performing a linear regression analysis using Microsoft Excel. By analysing the T_{gel} values (still excluding the cyclohexane gel) in this way the importance of each parameter in describing the change of T_{gel} values can be found. The result of this analysis is shown in Equation (4).

$$T_{gel} = 103.88 + 4.8726\alpha - 57.768\beta - 52.935\pi^* \quad (4)$$

The value 103.88 (4.6% error) represents the intercept of the trend line on the Y-axis (thus, this is – coincidentally – the predicted T_{gel} for the gel formed in cyclohexane). The weighting of the α parameter 4.8726 (626% error) has far too much error to be reliable, a consequence of only having one data point with a non-zero α parameter. It is only worth noting then, that when this data point (acetonitrile gel) is not included in the analysis the other calculated values do not vary. The weighting given to β (-57.768, error 208%) and π^* (-52.935, error 13.8%) are both negative (the gradient of the graph is negative) and are very similar. This was an expected result as the change in T_{gel} values was already reasonably described by simple addition of both parameters. They appear to be of almost equal importance but this result must be viewed with suspicion as most of the solvents used fall into a very narrow range of β values and the large errors associated with both the calculated values.

Combination of the Kamlet-Taft parameters by addition has proven to give the best correlation with changing T_{gel} value with solvent. A method to calculate precisely how important each parameter is to T_{gel} value had failed to give convincing results or significantly increase our understanding. This is most likely due to the limited and largely similar collection of solvents that were gelled and therefore had a T_{gel} value to analyse. Using this addition of parameters to rationalise or predict which solvent will support gelation is also unreliable given that it again predicts that chloroform, DCM and acetone should all support gelation. Overall, the data indicates that the α parameter is the most important in determining whether a solvent will support gelation, only acetonitrile has a non-zero α value and can be gelated and all of the other solvents that support gelation have an α value of zero. This is simply because the gelator network is underpinned by gelator-gelator hydrogen bonding and hydrogen bond donating solvents are very good at disrupting this network formation, hydrogen bonding with the gelator so it remains in solution. The β parameter seems to be the next most important factor in determining whether a solvent will support gelation. Despite it appearing equally important to π^* in controlling the T_{gel} value of gels formed, only two gels are formed in solvents with a β value of over 0.13 and these are both opaque, rather than clear gels, indicating perhaps a different assembly of gelator complexes. This is likely due to the hydrogen bond accepting ability of a solvent having a similar, if less pronounced effect, as its hydrogen bond donating ability. The differing potency of these parameters had been observed in previous work[414, 445, 447]. The least important parameter in determining whether a gel could form in a solvent was π^*. Solvents with a wide range of π^* values were shown to support gelation and other with π^* values in the same range were incapable of supporting gelation. This is not surprising as the effect of solvent polarisability on gelation was always likely to be more subtle than the solvents hydrogen bonding ability, which more directly blocks network formation.

In conclusion, this analysis of solvent parameters has shown that all the types tested were poor at predicting which solvents would support gelation and which ones would not. The best correlations between changing solvent parameters and the T_{gel} of any gels formed was found with E_T^N and by combining all three Kamlet-Taft parameters ($\alpha + \beta + \pi^*$). This research shows that no solvent parameter tested was able to fully rationalise the behaviour of the **L,L,L-G2Lys** and **C6** mixture in a range of organic solvents.

3.1.3. Effect of Varying Amine

Alkyl amines ranging from **C3** to **C8** had been found to support gelation, whilst longer alkyl amines (**C9** to **C18**) had been found to support gelation only at low temperatures. The effect of alkyl chain length on gel stability and the reasons behind it were investigated. The first experiment was to find how the thermal stability of the gels that did form varied with amine alkyl chain length. Firstly, the T_{gel} values of gels made with **L,L,L-G2Lys** and amines **C3** to **C8** (1:1 mixture) were measured over a concentration range of 2-10 mM. The T_{gel} values were recorded and are shown in Figure 3.11., for ease of comparison, the T_{gel} values of only the 10 mM gels are compared in Figure 3.12.

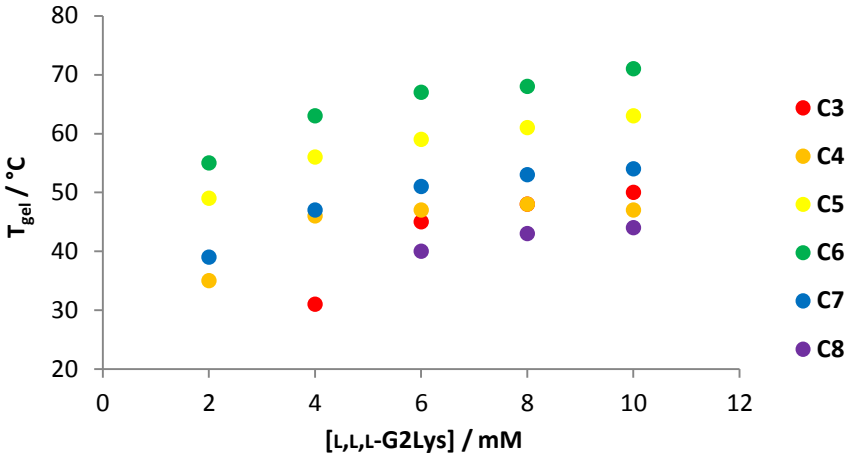

Figure 3.11. T_{gel} values of gels made with 1:1 mixture of **L,L,L-G2Lys** and alkyl amines. Toluene.

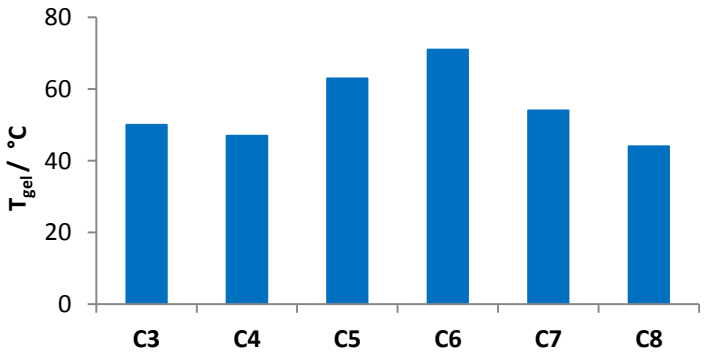

Figure 3.12. T_{gel} values of 10 mM gels with 1:1 mixture of **L,L,L-G2Lys** and alkyl amines. Toluene.

It is clear from the data that the thermal stability of the gels is roughly the same when **C3** or **C4** is used, it increases as the chain length grows to **C6** before decreasing as chain length increases to **C8**. The minimum gelation concentration (MGC) – minimum concentration of **L,L,L-G2Lys**

and amine required to immobilise 0.5 mL toluene – was also identified. These MGC values showed a similar but inverted pattern as smaller MGC values indicate more effective gelation (Figure 3.13). Both the T_{gel} and MGC values show that **C6** is the amine most suitable for gelation (highest T_{gel} and lowest MGC), followed by **C5**. **C3**, **C4** and **C7** are all similar and **C8** is the worst.

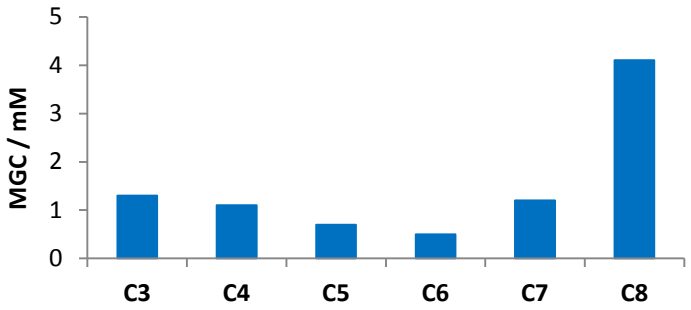

Figure 3.13. MGC values for gels made with 1:1 mixture of **L,L,L-G2Lys** and alkyl amines. Toluene.

The mechanism by which the alkyl chain length affects complex aggregation was investigated using circular dichroism (CD) spectroscopy. CD spectroscopy measures the difference in absorption of right and left handed circularly polarised light of a sample over a wavelength range. The CD signal is increased by the coupling of chromophores on different molecules in a supramolecular aggregate; often when the temperature is increased and the aggregate disassembles, no signal is observed. The CD spectrum acts as the chiral signature of the sample that is dependent on how the molecules are aggregated, especially the chirality of the aggregates. If the sample has no overall chirality there will be no difference in the absorbance of each type of circularly polarised light, so a non-chiral or racemic sample will give no CD spectrum.

It was hoped that the CD spectra of samples made with **L,L,L-G2Lys** and different amines would provide an insight into supramolecular polymer formation in each case. Due to the high sensitivity of the CD instrument, the solvent used must be very poorly absorbing in the wavelength range of interest. In our case this is around 200-220 nm where the amide groups of **L,L,L-G2Lys** absorb, ruling out the use of toluene. After testing a number of solvents it was found that a 95:5 mixture of methylcyclohexane to dioxane had low absorbance in the required range, and also produced clear samples with no precipitate. This was important so that the concentration of the sample is accurately known and also allows the passage of light

to the detector. Also important was that this solvent system was shown to support self-assembly and the T_{gel} values of gels (10 mM) formed in this solvent showed the same trend as those formed in toluene. It was also observed that when the samples were heated, the CD signal disappeared, proving that it was indeed due to aggregation, not absorbance of single molecules or complexes in solution. The spectra are shown in Figure 3.14.

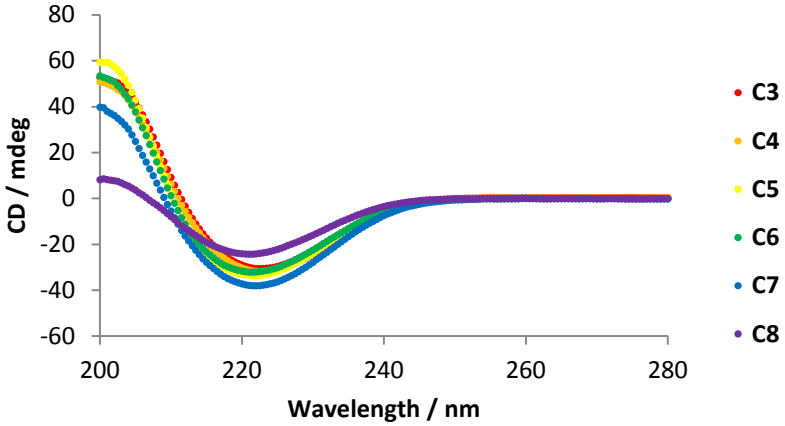

Figure 3.14. CD spectra of samples made with 1:1 mixture of **L,L,L-G2Lys** and alkyl amines. 0.625 mM. 95:5 Methylcyclohexane to Dioxane.

The CD spectra of samples made with **C3** to **C6** are almost identical, the spectrum of the sample with **C7** is only slightly different and the sample made with **C8** is more significantly different. This can be further demonstrated by plotting the CD signal at 200 nm for each sample (Figure 3.15.).

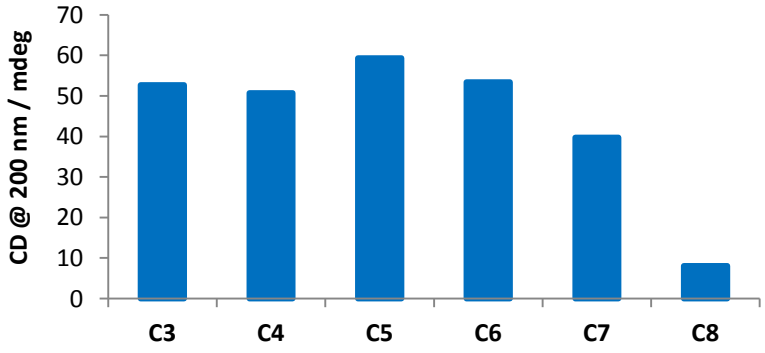

Figure 3.15. CD signal at 200 nm of samples made with 1:1 mixture of **L,L,L-G2Lys** and alkyl amines. 0.625 mM. 95:5 Methlycyclohexane to Dioxane.

The data clearly show that the CD spectra of **C3** to **C7** are largely similar whilst the **C8** spectrum is different, perhaps an indication that the aggregation of the complexes changes with this longer alkyl chain. This mixture also produces the lowest T_{gel} value and the highest MGC, and is the longest chain length at which gels can still form.

Xerogels were made from gels of **L,L,L-G2Lys** and amine **C3** to **C8** in toluene and analysed by FEG-SEM. The topography seen in these images shows the structure of the fibrous network of gelator, and even though the sample has been dried, can give us an insight or illustration of how molecular structure effects molecular organisation. A representative selection of these images, showing each sample is displayed in Figure 3.16.

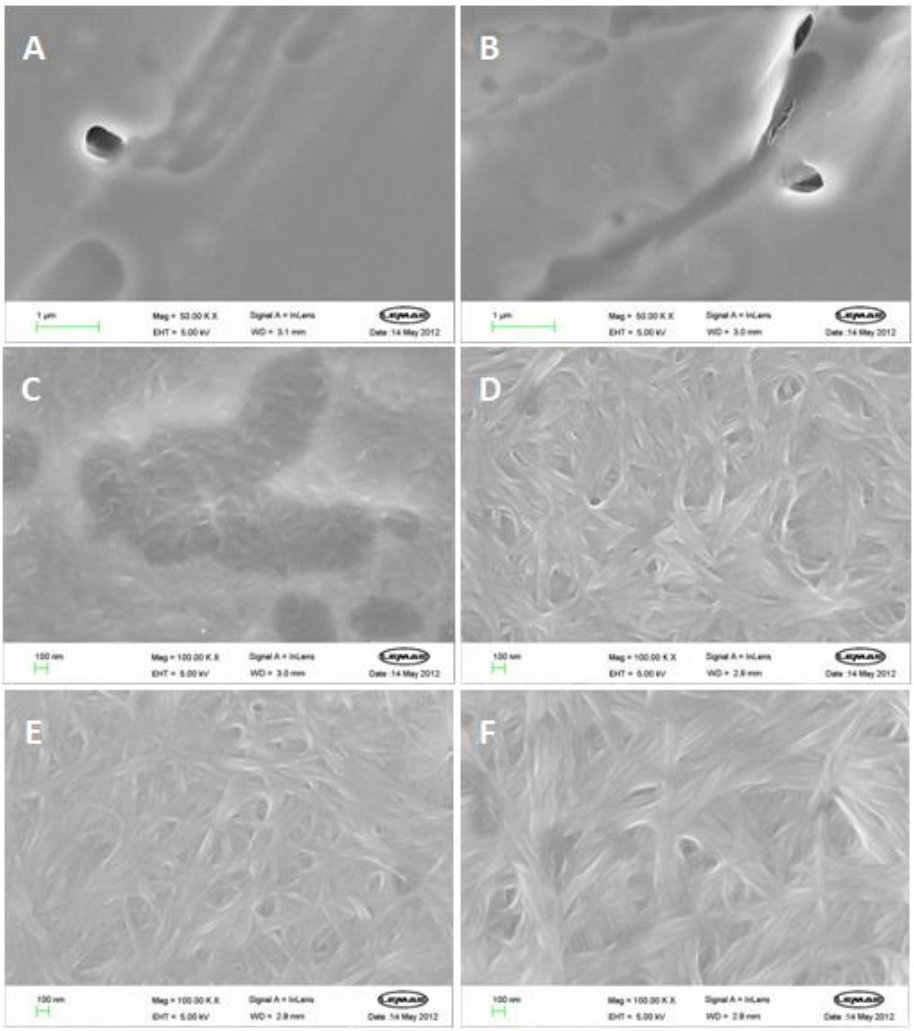

Figure 3.16. SEM images of xerogels formed from **L,L,L-G2Lys** and alkyl amines. A) with **C3**. B) with **C4**, Scale bars = 1 µm. C) with **C5**. D) with **C6**. E) with **C7**. F) with **C8**, Scale bars = 100 nm.

The samples made with **C3** and **C4** have a very flat topography. A small bundle of fibres is seen faintly in the image from the **C4** sample but otherwise both samples show no other fine detail, the holes seen in the images are holes in the stub the xerogel is spread over and were used to focus the microscope. Little insight is gained from these images. In the **C5** containing xerogel, more fibrous fine structure is visible. Fibres with a width of about 20 nm seem to be appearing out of the flat background. The **C6** sample is the first one to show a network that is more "typical" of a supramolecular gel. Well defined, thick bundles of fibres, around 100 nm wide form a continuous network. The **C7** sample shows a very similar network to this, while the **C8** sample shows a similar network but with thicker fibres (up to 200 nm). These images demonstrate that the alkyl chain length of the amine does influence the morphology of the gel. In general it is seen that as the amine chain length increases the bundles of fibres seen in the images become thicker, This could potentially be caused by favourable van der Waals forces generated by aggregation of larger alkyl chains encouraging more aggregation of fibres in these samples. It may also be that as the alkyl chain of the amines become larger they become less soluble in the aromatic solvent and this drives larger fibres to form. However, the results are not easily reconciled with the T_{gel} and CD data collected, as they suggest the gels could be split in to three groups; **C3** and **C4**, **C5** and **C6** to **C8** with their behaviour following this split. As we have already seen, this is not the case.

To gain further insight into the effect of increasing amine chain length on gel formation and stability, VT-NMR spectrometry was used. Gels of **L,L,L-G2Lys** and amines are formed in NMR tubes, with toluene-d_8. As previously stated, as the temperature increases the gel network breaks down. When this occurs, molecules fixed in the solid-like gelator network and NMR "invisible" are no longer trapped and become mobile in solution and NMR "visible". Using this change in observed concentration we can monitor the breakdown of the gel as temperature increases.[54, 435, 452-454] Obviously this involves simplifying the complex hierarchical process of gel formation to either single, "visible" complexes (or dimers, trimers, etc) and "invisible" gel network. However this approach has been used before, with notable success, to produce data that explains the behaviour of low molecular weight gelators.[54, 435, 454] An example of these experiments is shown in Figure 3.17.

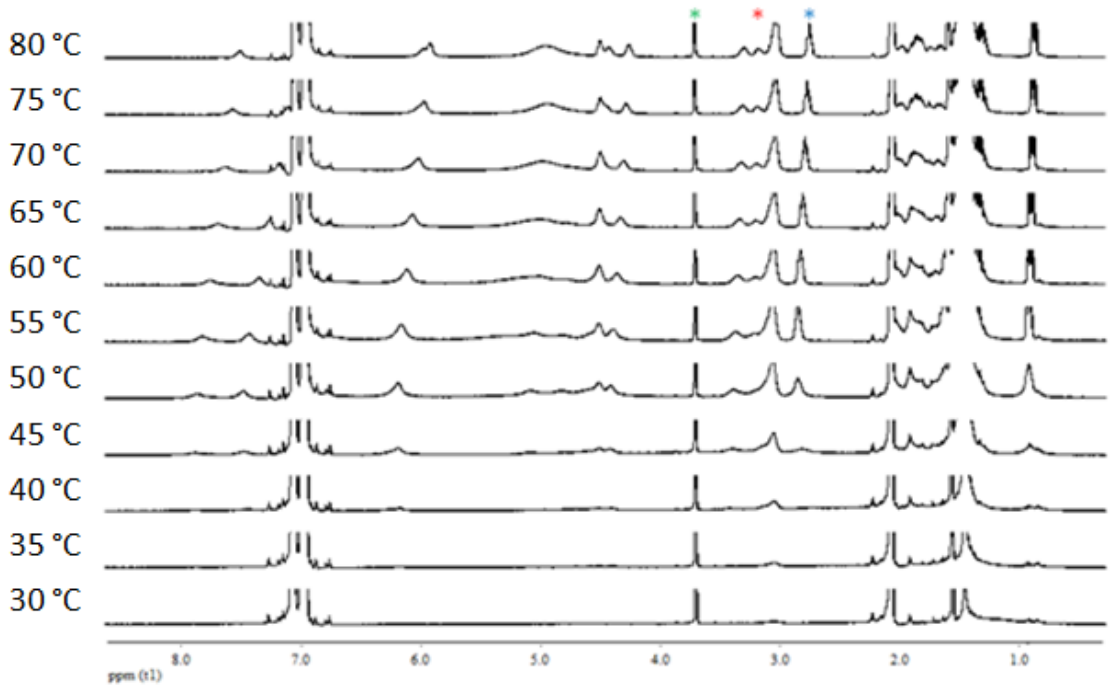

Figure 3.17. VT-NMR of 10 mM gel made with **L,L,L-G2Lys** (*) and **C4** (*). Internal standard (*) is 10 mM **DPM**.

Again the standard used was diphenylmethane (**DPM**) – selected for its similarity to the solvent (toluene-d_8) and the sharp, distinctive signal of the CH_2 at 3.7 ppm, shown marked with a (*) in Figure 3.17. The three CH_2NH groups of **L,L,L-G2Lys** are visible as a group of peaks ranging from 3.3-2.9 ppm and are marked with (*). The CH_2NH$_2$ of the alkyl amine is visible as a triplet at 2.7 ppm and is marked with (*). Plotting the integration of the **L,L,L-G2Lys** CH_2NH signals at each 5°C interval shows how the gel network breaks down and the gelator complex is solubilised with increasing temperature. This is shown for gels made with amine **C4 – C8** in Figure 3.18. The gel made with **C3** was not included in this study due to the higher volatility of this amine.

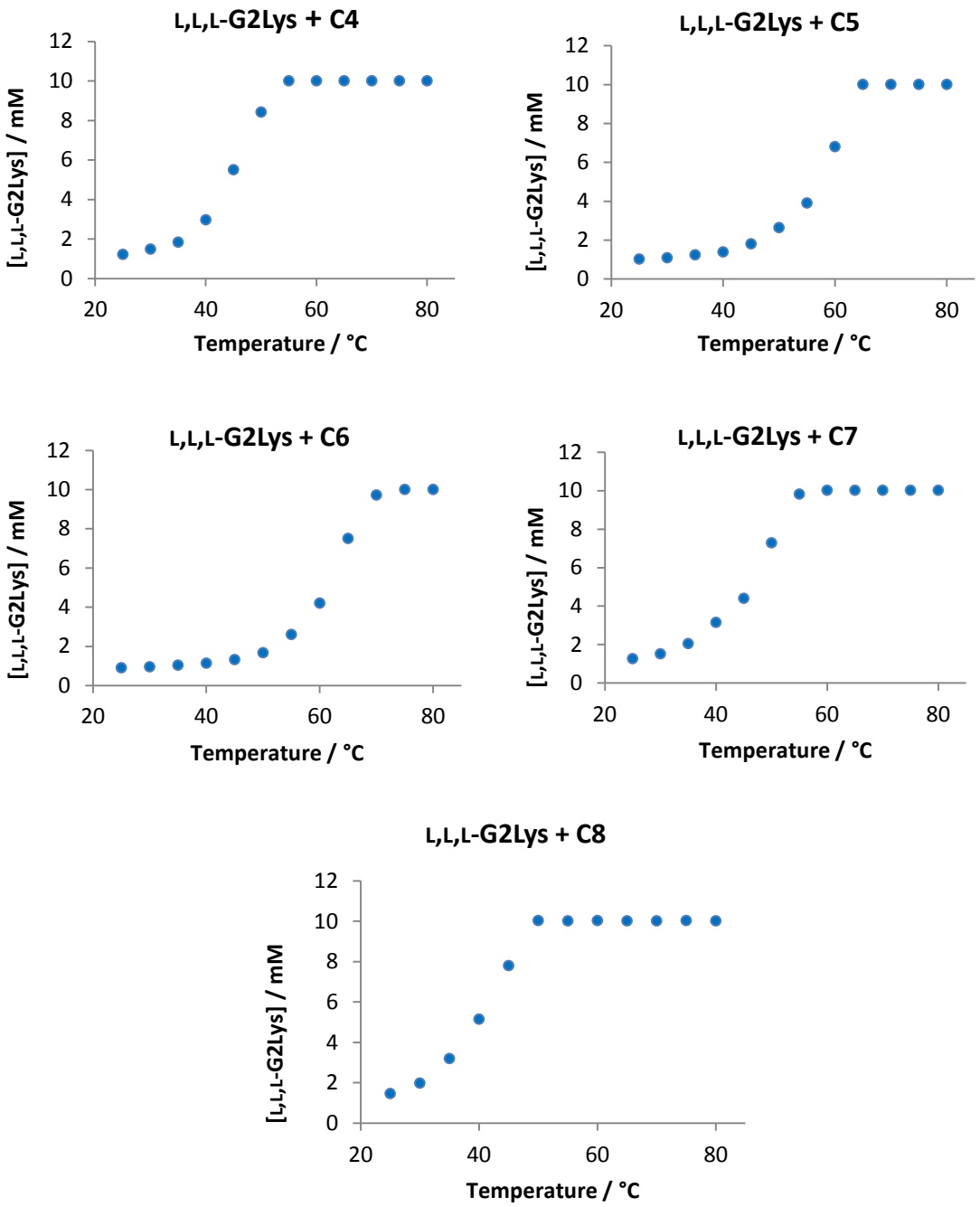

Figure 3.18. Concentration of **L,L,L-G2Lys** visible in gels of **L,L,L-G2Lys** and alkyl amines as temperature increases. Toluene-d_8.

From the plots shown in Figure 3.18 a number of parameters can be found. These include the temperature at which all the gelator network is broken down and all the **L,L,L-G2Lys** is "visible" in solution ($T_{100\%}$), and the percentage of the gelator complex still "invisible" (i.e. still fixed in the gel network) at the T_{gel} ([Insol]@T_{gel}). These can be compared to the T_{gel} and MGC values

for each sample. The comparison between $T_{100\%}$ and T_{gel} values are shown in Figure 3.19. In each case, both values are very similar and overall show the same trend – increasing from **C4** to **C6** and decreasing from **C6** to **C8**. The T_{gel} values are slightly lower than the corresponding $T_{100\%}$ values as they represent the point at which the gel network is no longer stable to inversion, i.e. the remaining gel network can no longer support itself against gravity, whereas the $T_{100\%}$ is the temperature at which the entire network is disassembled.

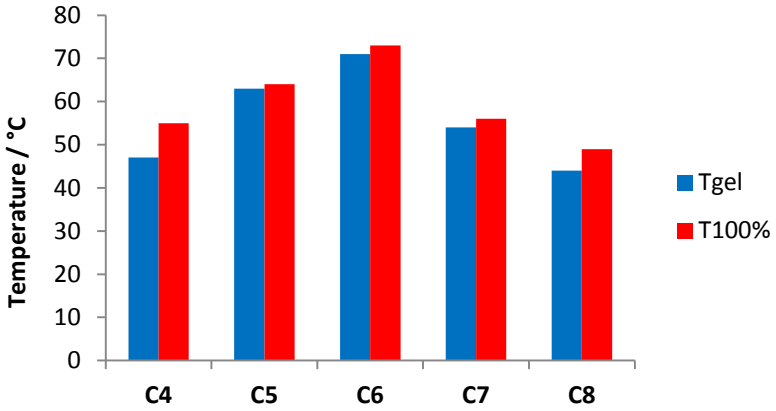

Figure 3.19. T_{gel} and $T_{100\%}$ values for gels made with 1:1 mixture of **L,L,L-G2Lys** and alkyl amines. Toluene.

The [Insol]@T_{gel} of each sample is compared to the MGC values in Figure 3.20. This value indicates how much of the network is intact (NMR "invisible") at the T_{gel}. As such it shows how much network is needed, in each case, to ensure the sample can support itself against gravity. This follows a pattern that is the inverse of the $T_{100\%}$ and T_{gel} measurements, as **C6** has the lowest value and it increases with both longer and shorter alkyl chains from this point – this is also the trend shown by the MGC measurements. Whilst the agreement between the two measurements is generally good, there is some difference between the exact values for each sample (especially for the gel made with **C8**). This apparent discrepancy is again because the two values are measuring subtly different things. The MGC is the minimum concentration of gelator in the whole sample required to form a gel that is stable to inversion (in a sample vial). The [Insol]@T_{gel} is the concentration of gelator "invisible" in the NMR of a sample, heated to its T_{gel} value. The two measurements are carried out in samples of different concentrations, at different temperatures and in different containers. Taking this into account the correlation between MGC and [Insol]@T_{gel} is acceptable, both values being a measure of the effectiveness of a gelating mixture.

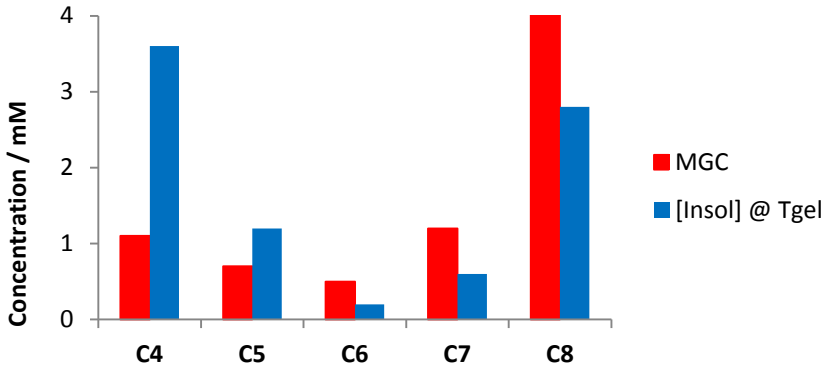

Figure 3.20. [Insol] @ T_{gel} values for gels made with 1:1 mixture of **L,L,L-G2Lys** and alkyl amines. Toluene.

All the VT-NMR data is in agreement with the measured T_{gel} values that the most thermally stable gel is formed when **L,L,L-G2Lys** is mixed with **C6**, and that thermal stability decreases with both increasing and decreasing alkyl chain length from this point. The same relationship has been found with the amount of gelator network required to form a gel with **L,L,L-G2Lys** and **C6** requiring the lowest concentration. It is clear that **C6** is the optimal amine in our series for gel formation with **L,L,L-G2Lys**, in toluene.

The VT-NMR data can provide further thermodynamic insight into the self-assembly process. The van 't Hoff equation (Equation 4) defines the relationship between an equilibrium constant of a process and the enthalpy and entropy change associated with the process.[455] The solubilisation of gel fibres, as monitored by VT-NMR experiments, is a process that has previously been analysed by using the van 't Hoff equation.[54, 435, 454] Solubility is an unusual case of equilibrium constant as it can be replaced in the this equation by the concentration of the soluble species, as the concentration of the insoluble species can be considered to equal 1 (Equations 5 and 6).

$$\ln K = \frac{-\Delta H_{diss}}{RT} + \frac{\Delta S_{diss}}{R} \quad (4)$$

$$K = \frac{[Sol]}{[Insol]} = \frac{[Sol]}{1} \quad (5)$$

$$\ln[Sol] = \frac{-\Delta H_{diss}}{RT} + \frac{\Delta S_{diss}}{R} \quad (6)$$

Where K = equilibrium constant of gel-sol transition (i.e. solubilisation of gel network), ΔH_{diss} = enthalpy change of dissolution, ΔS_{diss} = entropy change of dissolution, R = ideal gas constant, T = absolute temperature, [*Sol*] = concentration of gelator complex solubilised in solution and [*Insol*] = concentration of gelator in insoluble network.

As previously described, the solubilisation process is simplified into the transition between insoluble – and NMR "invisible" – gel fibres, and completely soluble – and NMR "visible" – complexes of **L,L,L-G2Lys** and amine. As the temperature increases, more gelator becomes visible in the NMR spectrum. As this change takes place the ln[*Sol*] can be plotted against $1/T$ to produce a plot that can be fitted to a straight line. The gradient of this line is equal to $-\Delta H_{diss}/R$ and the intercept is equal to $\Delta S_{diss}/R$. Plots like this were generated for each gel (Figure 3.21), and the ΔH_{diss} and ΔS_{diss} values found for each. These values are summarised in Table 3.2. along with the $T_{100\%}$ values for each gel, for ease of comparison.

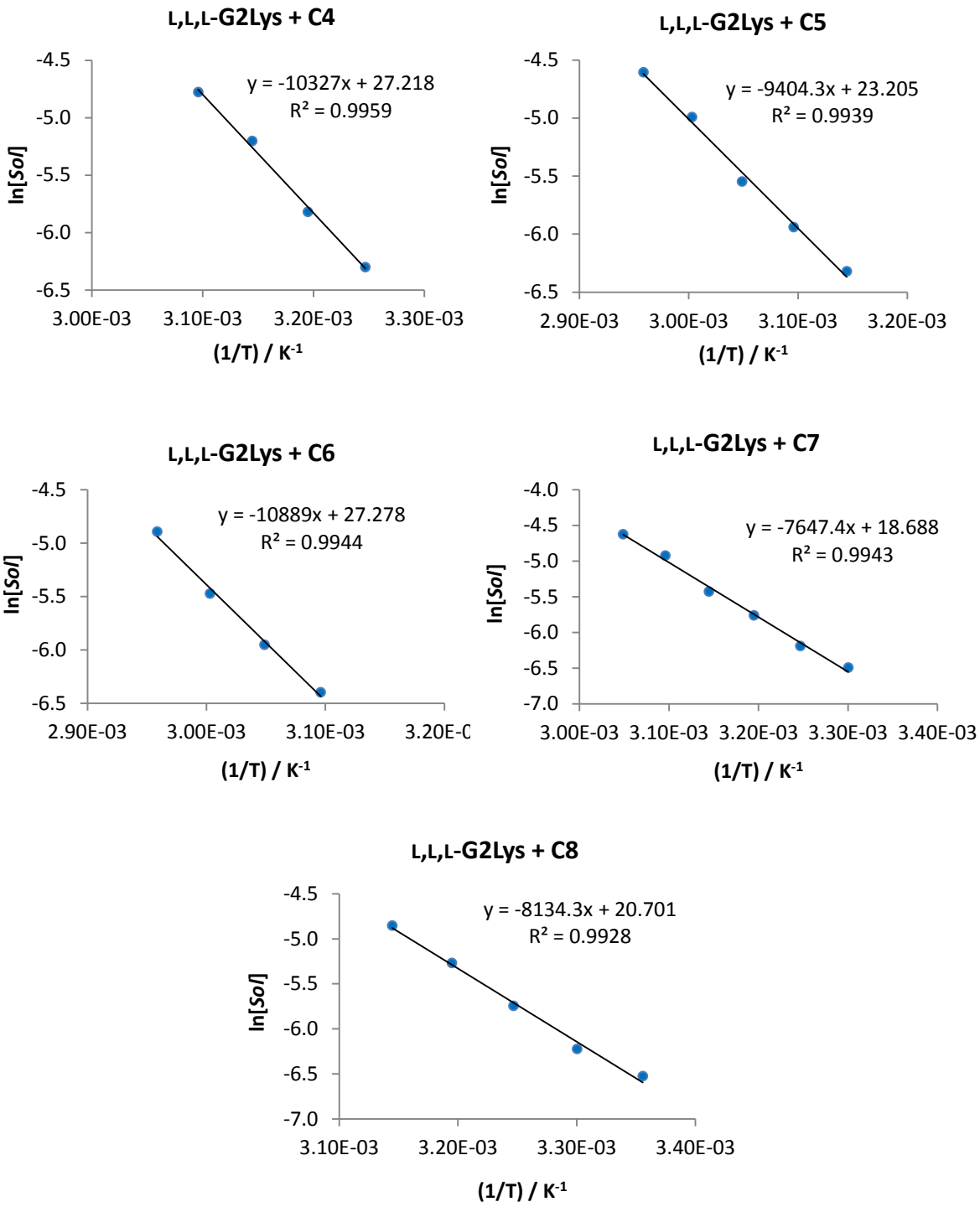

Figure 3.21. Van 't Hoff plots of alkyl amine gels. Toluene-d_8.

Table 3.2. Summary of data calculated from van 't Hoff plots.

Amine	ΔH_{diss} / KJ mol^{-1}	ΔS_{diss} / J K^{-1} mol^{-1}	$T_{100\%}$ / °C
C4	85.9	226	55
C5	78.2	192	64
C6	90.5	226	73
C7	63.6	155	56
C8	67.6	172	49

The values found in Table 3.2. show that the gel made with **L,L,L-G2Lys** and **C6**, which has the highest $T_{100\%}$ value also has the highest enthalpic and entropic gain upon dissolution. However, apart from this example there is no clear pattern between changes in $T_{100\%}$ and in either ΔH_{diss} or ΔS_{diss}. It appears that the change in thermal stability of the gels is due to a changing balance between both ΔH_{diss} and ΔS_{diss}. The gel made with **L,L,L-G2Lys** and **C6** is more enthalpically favoured which means the complexes are more tightly bound. In turn this makes the gel less entropically favoured. It is the balance between these two effects which determines the overall stability of the gel network to increases in temperature (reflected in Equation (1)). The changing thermal stabilities of the gels is due to a changing enthalpy-entropy balance, an idea which is related to enthalpy-entropy compensation,[456, 457] which is most commonly used in biology[54] but has application to supramolecular chemistry.[458, 459] To try to make sense of this data we can use the values found in Table 3.3. to calculate ΔG_{diss} values at room temperature (25°C) for each sample.

Table 3.3. Calculated Gibbs free energy values for sample made with each amine.

Amine	$\Delta G_{diss}^{25°C}$ / kJ mol^{-1}
C4	18.4
C5	20.7
C6	22.9
C7	17.3
C8	16.3

The complex of **L,L,L-G2Lys** and **C6**, which has been shown to be the best overall gelator, also has the highest $\Delta G_{diss}^{25°C}$ value – due to the balance between the enthalpy and entropy of dissolution – so the Gibbs free energy at room temperature is the most positive and therefore the dissolution of the network is furthest away from being spontaneous (when ΔG_{diss} becomes negative). From this point, the $\Delta G_{diss}^{25°C}$ value decreases with both increasing and decreasing chain length, the same pattern that is seen with T_{gel} and $T_{100\%}$ values and the inverse relationship seen with MGC and [Insol]@T_{gel}.

The accuracy of the ΔH_{diss} and ΔS_{diss} values calculated can be verified by using them to predict the concentration of **L,L,L-G2Lys**-amine complex in solution at any temperature. This can then be compared to the experimentally measured results. Close agreement between the experimental and calculated concentrations validate the method used to obtain the ΔH_{diss} and ΔS_{diss} values. This comparison is shown in Figure 3.22**.**

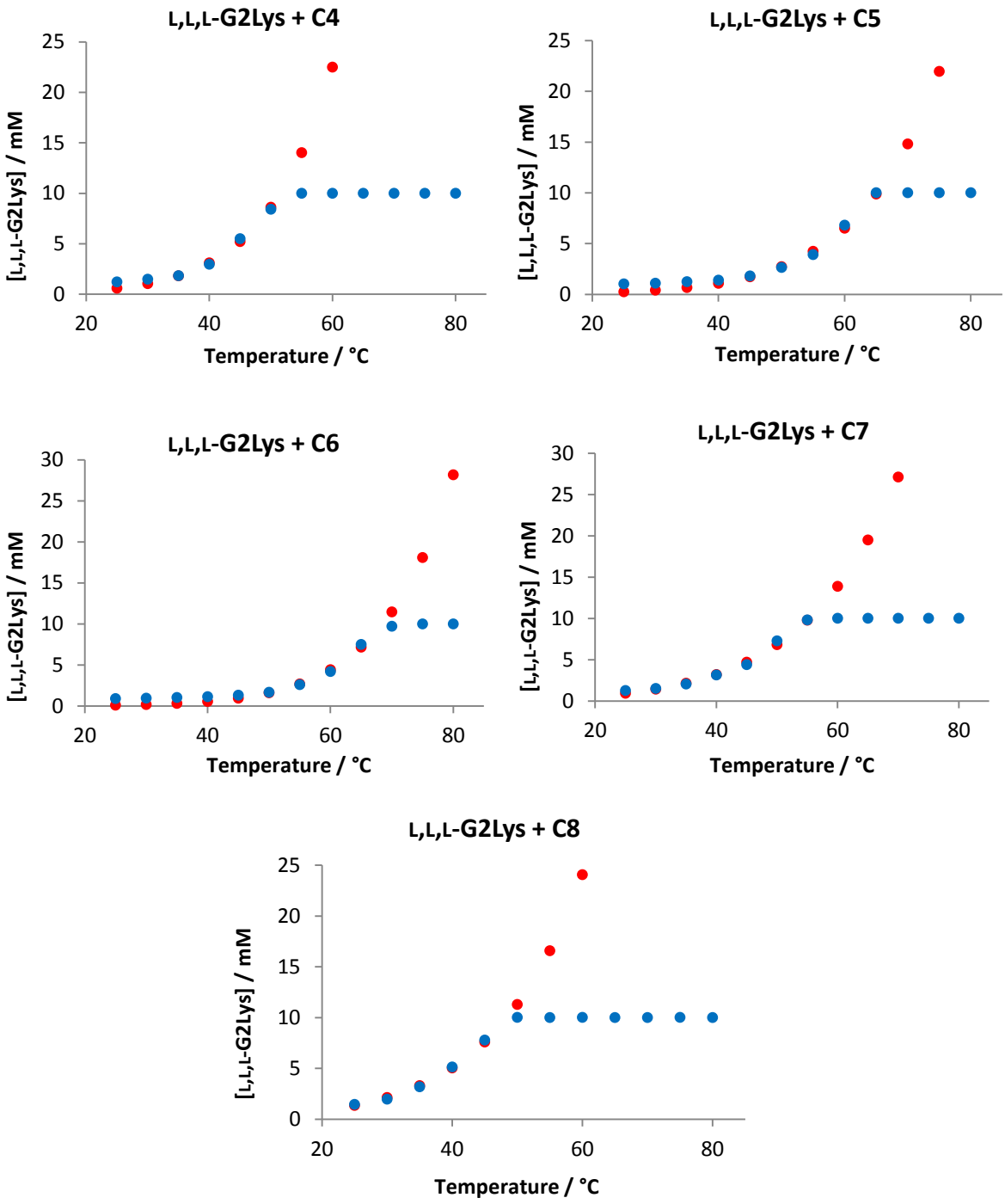

Figure 3.22. Plots showing experimental (blue) and calculated (red) concentration of solubilised gelator complex in each gel.

The plots show an excellent agreement between the experimentally observed data and the data generated using the calculated ΔH_{diss} and ΔS_{diss} values. At low temperature there is some divergence between the two sets of data. This is due to the fact that there is often no, or a

very small, peak visible for the gelator at these temperatures. This causes the measured concentration to be greatly affected (increased) by noise in the spectrum, so the integration (concentration) measured may be different to the actual concentration in solution. There is also an obvious divergence between the two data sets above 10 mM. The cause of this is that there is nothing the stop our calculated values predicting higher and higher concentrations as the temperature increases. Of course, in the NMR sample the total concentration of complex is 10 mM, so the concentration solubilised cannot exceed this. Overall, the plots validate the method used to find the ΔH_{diss} and ΔS_{diss} values .

In summary, gels of **L,L,L-G2Lys** and alkyl amines were greatly affected by the amine alkyl chain length. For amines **C9** and above, a gel was not formed. For amines **C3** to **C8** the thermal stability of the gel changes, with **C6** forming the most thermally stable gel with **L,L,L-G2Lys**. This mixture also forms a gel at a lower concentration than with other amines. CD spectroscopy and FEG-SEM have given an insight into changes in aggregation of complexes and the nature of the fibrous gel networks formed. Finally VT-NMR has been used to explore the thermodynamic differences between the different gel samples. The$T_{100\%}$ and [Insol]@T_{gel} values have been found for each gel and found to be in good agreement with measured T_{gel} and MGC measurements. The data from VT-NMR has been further exploited using the van 't Hoff equation to find the ΔH_{diss} and ΔS_{diss} for each gel. The results of this method were verified by using them to predict the dissolution of the gel network which matched excellently the experimentally observed results. The ΔH_{diss} and ΔS_{diss} of each gel have been used to calculate the ΔG_{diss} values at 25°C and at the $T_{100\%}$ of each sample, which have provided further insight into gel breakdown.

As the effect of varying the amine alkyl chain length of an amine on gel formation / stability had been investigated, it was interesting to consider whether a similar influence would be observed with aromatic amines. The four amines shown in Figure 3.23 had been previously mixed with **L,L,L-G2Lys** and shown to support gelation of toluene. The T_{gel} values of these toluene gels were measured over a short concentration range (Figure 3.24). The values for the 10 mM gels are collected for ease of comparison in Figure 3.25.

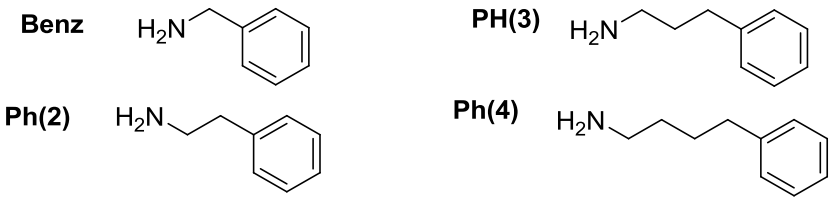

Figure 3.23. Structures of aromatic amines.

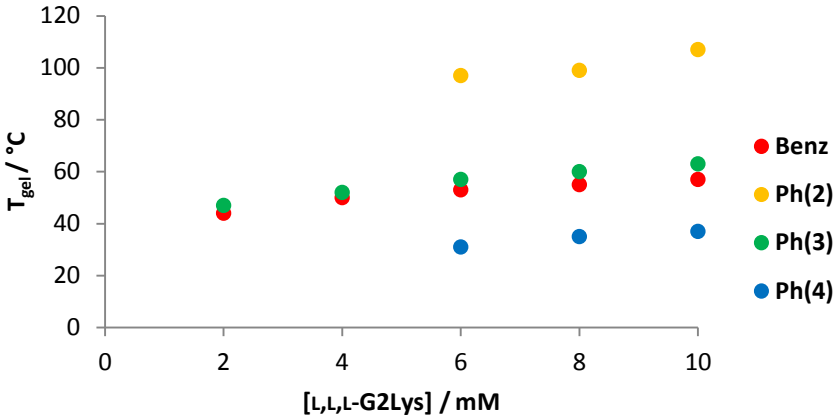

Figure 3.24. T_{gel} values of gels made with 1:1 mixture of **L,L,L-G2Lys** and aromatic amines. Toluene.

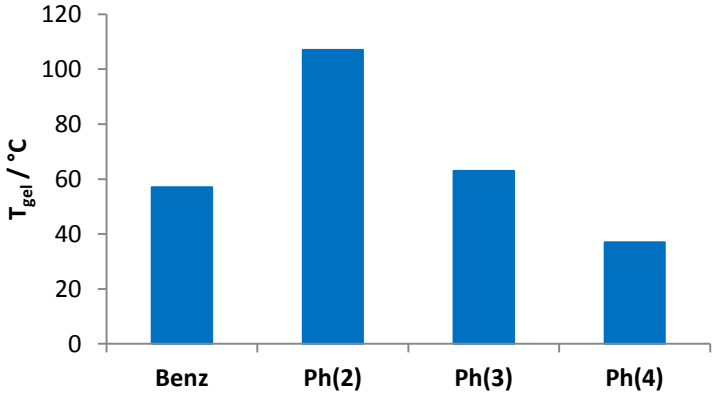

Figure 3.25. T_{gel} values of 10 mM gels made with 1:1 mixtures of **L,L,L-G2Lys** and alkyl amine. Toluene.

The gels made with **Benz** and **Ph(3)** – 1 and 3 methylene groups between amine and phenyl ring respectively – have practically the same stability. The gels formed with **Ph(2)** are much more stable and the gels formed with **Ph(4)** are less stable. Samples with mixtures of **L,L,L-**

G2Lys and **Ph(2)** or **Ph(4)** did could not induce gelation at 2 or 4 mM. The actual MGC values were found and are shown in Figure 3.26.

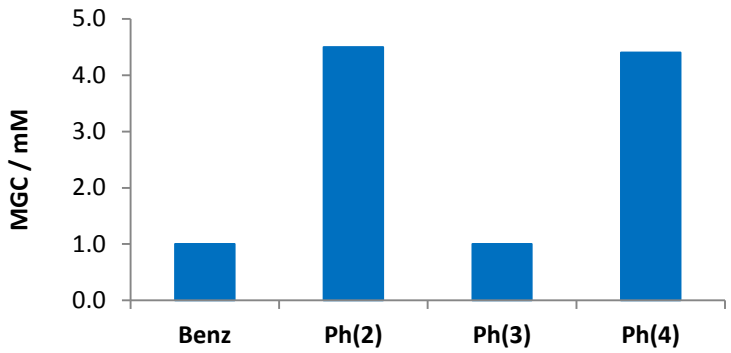

Figure 3.26. MGC values for gels made with 1:1 mixture of **L,L,L-G2Lys** and aromatic amines. Toluene.

There appears to be a strong odd-even effect on MGC, the MGC value rising when the amine has an even number of carbon atoms between the amine group and the phenyl ring and decreasing with an odd number. This means that despite **Ph(2)** forming the most thermally stable gels with **L,L,L-G2Lys** at higher concentrations, it, along with the **Ph(4)** sample, requires a higher concentration to form a gel initially. This again demonstrated the large effect a small change to molecular structure can have on gel properties. To gain further insight the same mixtures were analysed by CD spectroscopy. Again the solvent system used was 95:5 methylcyclohexane to dioxane and the resulting spectra are shown in Figure 3.27.

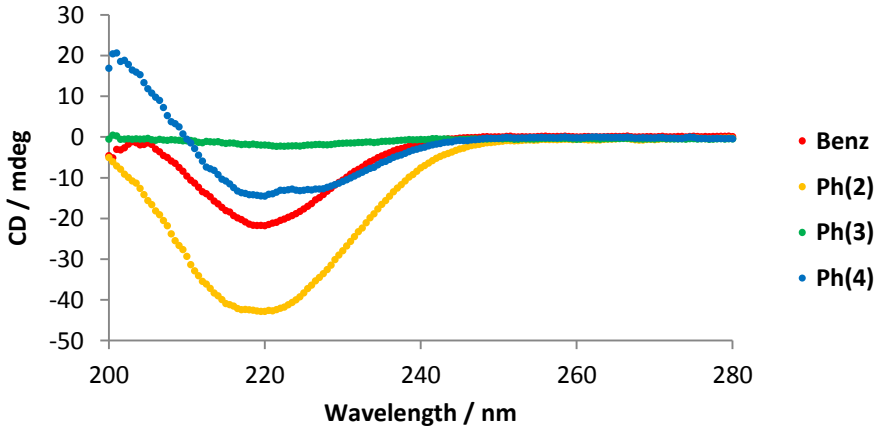

Figure 3.27. CD spectra of samples made with 1:1 mixture of **L,L,L-G2Lys** and aromatic amines. 0.625 mM. 95:5 Methylcyclohexane to Dioxane.

The spectra show complexes of **L,L,L-G2Lys** and each amine aggregate differently. All the amines show an absorbance band at around 220 nm (due to absorbance of organised amide and carbamate groups). None of the samples showed any other absorbance, even up to 400 nm. This means no π-π interactions were observed, so there appears to be no chirally organised π-π stacking in the aggregates. The intensity of the signal at 220 nm changes with each amine, **Ph(2)** showing the most pronounced signal, followed by **Ph(1)** and **Ph(4)** and finally a very weak signal from **Ph(3)**. This data is hard to correlate with the T_{gel} and MGC data already collected, other than saying the sample formed with **Ph(2)** – which forms the strongest gel – also has the largest CD signal.

To see how the aromatic amine used changed the morphology of the gels FEG-SEM was used to view the xerogels. A selection of representative images showing each sample are presented in Figure 3.28.

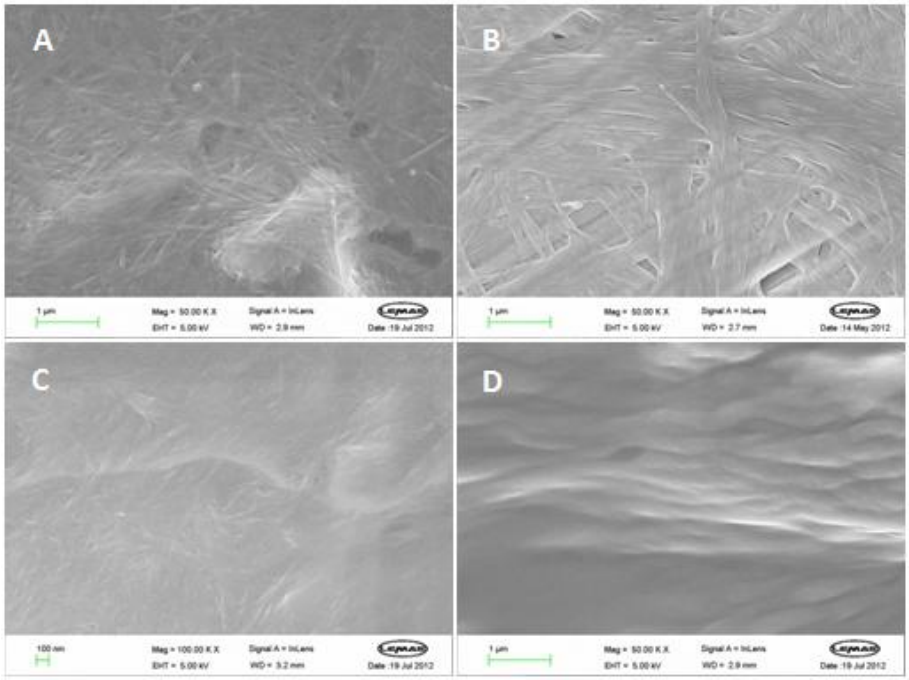

Figure 3.28. SEM images of xerogels formed from **L,L,L-G2Lys** and aromatic amines. A) with **Benz**, B) with **Ph(2)**, Scale bars = 1 µm. C) **Ph(3)**, Scale bar = 100 nm. D) with **Ph(4)**, Scale bar = 1 µm.

The xerogel formed with **L,L,L-G2Lys** and **Benz** has a network of thin (20-100 nm) fibres, typical of a supramolecular gel. It is interesting when compared to the xerogel formed with **Ph(2)** which also has some thin (20 nm) fibres visible but these aggregate into much thicker

structures (200-500 nm), which then form micron sized tapes travelling through the sample. Whilst drying may cause the formation of these larger objects the difference between this sample and the one formed with **Benz** is stark. It is surprising that a difference of one CH_2 group in such a large complex can, again, cause such a difference in morphology (and of course, T_{gel} and MGC values). The images for the xerogels formed with **L,L,L-G2Lys** and **Ph(3)** or **Ph(4)** are less striking. The **Ph(3)** containing xerogel is made up of thin fibres, similar to the **Benz** xerogel but even smaller and the sample as a whole has less well defined topography. The **Ph(4)** containing xerogel is made of barely visible fibres that aggregate (perhaps after drying) into poorly defined rope-like structures. Comparing this sample to the **Ph(2)** xerogel – the weakest and strongest gels – we see that whilst the **Ph(4)** has the most poorly defined, amorphous structure the **Ph(2)** xerogel has the most well-defined morphology, with highly organised aggregates forming the continuous gelator network. This is likely the cause of the difference in thermal stability. Unfortunately, the very high thermal stability of the gel made with **Ph(2)** means a meaningful NMR analysis of these gels could not be conducted, so the thermodynamics behind the extreme stability of gels with **L,L,L-G2Lys** and **Ph(2)**, compared to those formed with other amines could not be examined.

3.2. Component Selection

3.2.1. Component Selection in Simple Mixtures

It has been shown that when **L,L,L-G2Lys** forms gels with different amines, the gels formed have different nano-scale morphologies and different thermal stabilities. This led us to ask; if **L,L,L-G2Lys** was given a choice of different amines with which to form a gel, would one amine be included in the network over the others. This component selection would provide an opportunity to predictably generate a certain, ordered product from a complex starting mixture.

The first two amines that were studied were **C6** and **Benz**. Amine **C6** formed more stable gels with **L,L,L-G2Lys** (at 10 mM T_{gel} = 71°C) than **Benz** (at 10 mM T_{gel} = 57°C) and also has a higher pKa (10.69 for **C6** to 9.06 for **Benz**). These amines could also be distinguished in ^{1}H NMR by the different chemical shift of their CH_2NH$_2$ protons. Gels with a mixture of **L,L,L-G2Lys**, **C6** and **Benz** (1:1:1) were made with concentrations ranging from 2-10 mM and the T_{gel} values of these gels was measured. In these samples, **L,L,L-G2Lys** has a choice between the two different amines presented to it. These T_{gel} values were compared to those of **L,L,L-G2Lys** and either **C6** or **Benz**, rather than both (Figure 3.29.).

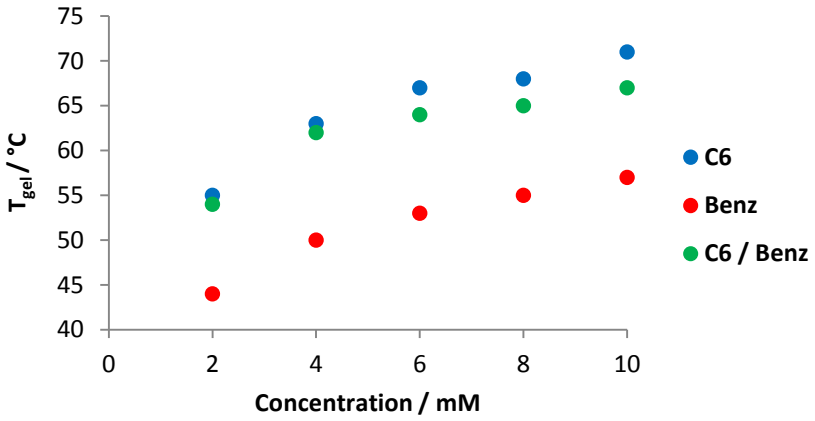

Figure 3.29. T_{gel} values of gels with **L,L,L-G2Lys** with either **C6**, **Benz** or a mixture of both. Toluene.

This initial experiment indicates that it is likely that far more **C6** than **Benz** is incorporated into the gel network, as the thermal stability of these gels is far closer to gels formed with **L,L,L-G2Lys** and **C6** only, than those formed with **Benz**. To gain a more accurate insight into the selective incorporation of **C6** over **Benz** VT-NMR was used. A gel with a 1:1:1 mixture of **L,L,L-G2Lys**, **C6** and **Benz** was formed in toluene-d_8 in an NMR tube. Any amine not incorporated into the gel will be visible at 25°C and the amine that is incorporated into the gelator network will only become visible at higher temperatures as the network is destroyed. This can be measured by comparing the integration of each amine to that of the internal standard **DPM**. The spectra recorded are shown in Figure 3.30. and the integration of each component with increasing temperature is plotted in Figure 3.31.

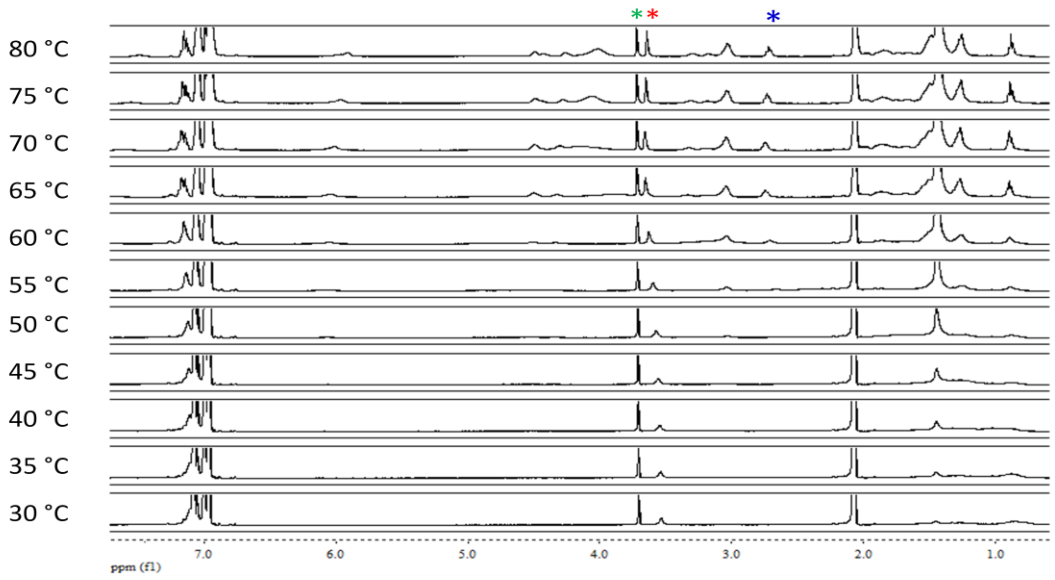

Figure 3.30. VT-NMR spectra of 10 mM gel containing **L,L,L-G2Lys**, **C6** (*), **Benz** (*) and **DPM** (*).

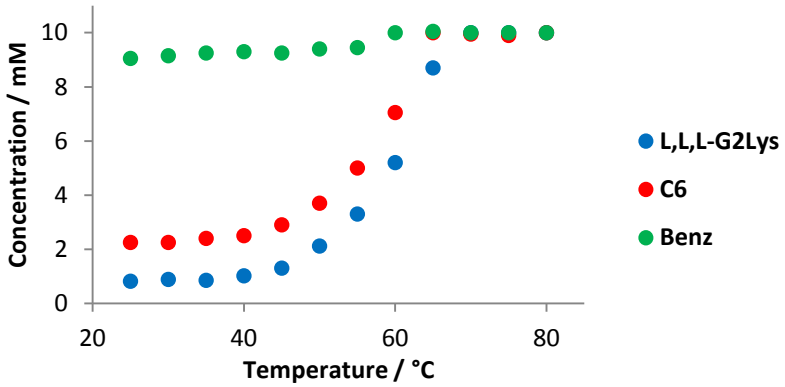

Figure 3.31. Concentration of components visible in ^{1}H NMR as temperature increases in gel with **L,L,L-G2Lys**, **C6** and **Benz**.

The spectra show that the majority of the **C6** amine is incorporated into the gel network, whilst the majority of the **Benz** amine is free in solution, demonstrating that **C6** is preferentially incorporated into the network with **L,L,L-G2Lys** over **Benz**. It is interesting to note that not all the **Benz** is visible in the spectrum at 25°C and its peak is broadened compared to its appearance at higher temperature. This indicates an amount of **Benz** is incorporated into the network and that some of the excess **Benz** in solution is in equilibrium with the amine in the network (the likely cause of peak broadening). Of the "missing" amine that is not visible at 25°C, is 89% is **C6** and 11% is **Benz**. This is the proportion of each amine immobilised in the gelator network.

Finally, a xerogel from a 10 mM gel made with a mix of **L,L,L-G2Lys**, **C6** and **Benz** was analysed by FEG-SEM and the morphology of this sample compared to that of xerogels made with **L,L,L-G2Lys** and either **C6** or **Benz** only (Figure 3.32.).

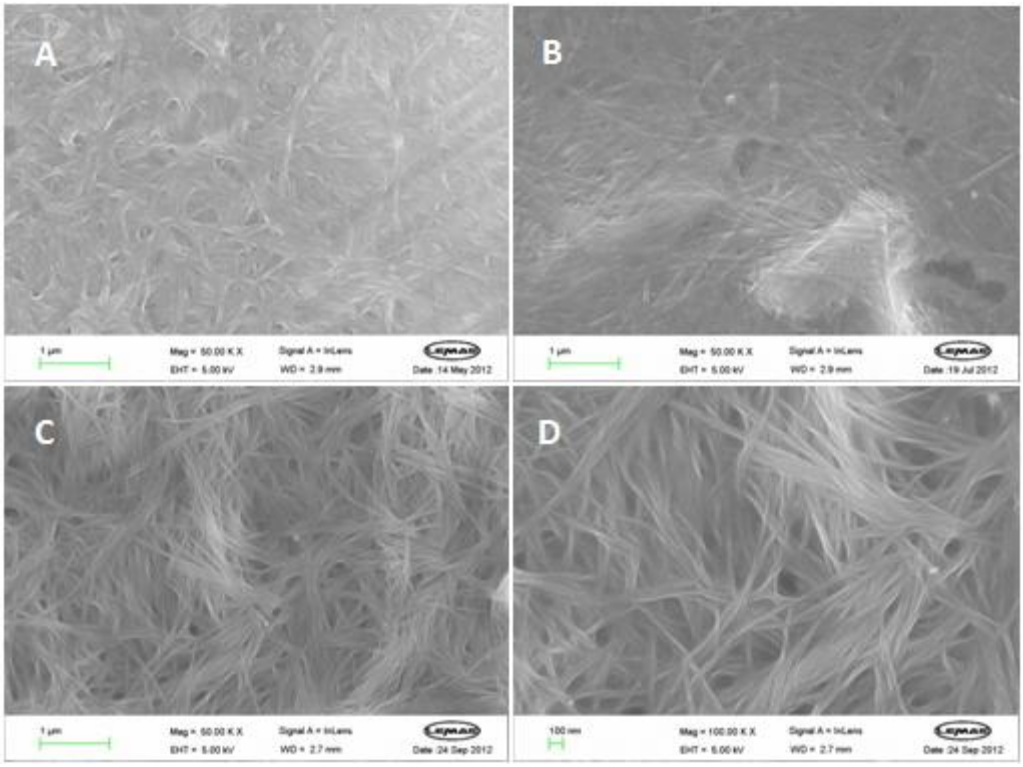

Figure 3.32. FEG-SEM images of xerogels formed from **L,L,L-G2Lys** and A) **C6**. B) **Benz**. C) **C6** and **Benz**, Scale bars = 1 µm. D) **C6** and **Benz**, Scale bar = 100 nm.

The morphology of the xerogel made with **C6** shows a network of fibres with a width of roughly 100 nm, whilst the xerogel made with **Benz** showed a network of thinner, straighter fibres. The images of the sample that was made with both amines is different to both, but shows some characteristics from each. The morphology is similar to that of the **C6** sample but the fibres are thinner and appear more straitened, both characteristic of the xerogel of made with **Benz**. This suggests that a co-assembly gel is formed with **L,L,L-G2Lys** and a mixture of amines. It has a morphology which is affected by both amines present, even if it is more effected by the amine that is present in the greater proportion (**C6**).

In summary, if **L,L,L-G2Lys** was given a choice of forming a gel with either **C6** or **Benz**, it was mostly **C6** that was incorporated, with a much smaller amount of **Benz**. This was a very impressive result, demonstrating the selective uptake of one amine over another into the gel network. The resulting gel had properties that were more similar to a gel formed with only

L,L,L-G2Lys and **C6** but was still influenced by the relatively small amount of **Benz** included. There are two possible reasons for this selective uptake of one amine over the other, as the formation of these multi-component gels is a hierarchical process (Figure 3.33.). The first step is the initial complex formation between **L,L,L-G2Lys** and the amine, despite there being no evidence of full deprotonation between acid and amine, it can be expected that the strength and favourability of this binding step will be determined by the pKa of the amine used. This is because the pKa will determine how attractive the each amine is to the acid hydrogen for hydrogen bonding. The subsequent steps will be the assembly of these complexes into a gel network. It is expected that the T_{gel} values of gels formed with each amine and **L,L,L-G2Lys** will be indicative of each amines ability to assemble into the gel network. This means we have two possible factors that may determine which amine is preferentially selected, the pKa which effects the initial complex formation and the T_{gel} which describes how well each amine is able to assemble into a stable gelator network. The next step was to investigate whether the difference in one or both of these values was responsible for the selective uptake of **C6** over **Benz**.

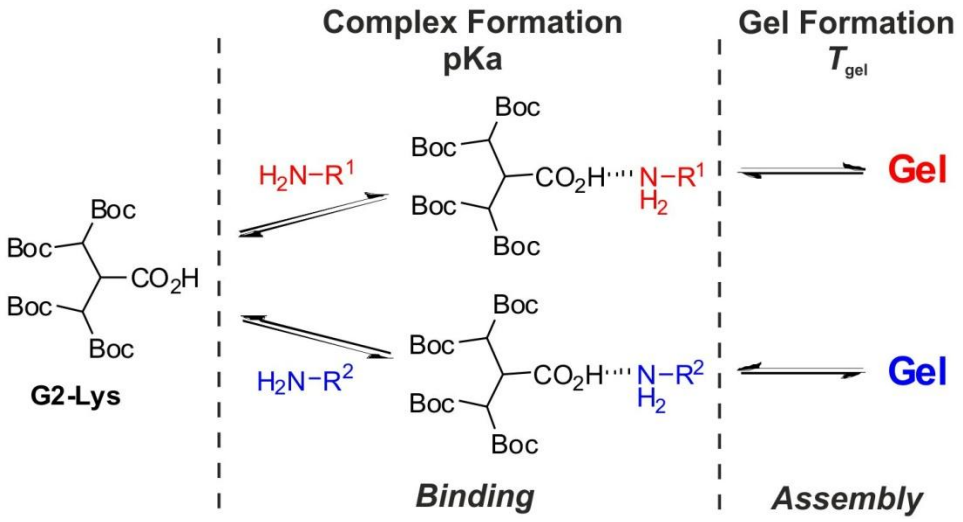

Figure 3.33. Representation of the two main steps in the formation of the multi-component gels. Binding – determined by the pKa of the amine and assembly – described by the T_{gel} value of the gel formed.

This was investigated by testing whether selective incorporation of **C6** in the presence of other amines with varying pKa and T_{gel} values would take place. The amines chosen were **4-Cl**, **CHXene** and **Nap** (Figure 3.34.) as these were distinguishable in ^{1}H NMR. The first thing to note is that pKa and T_{gel} values of the different amines do not correlate with each other (Table 3.4.).

For example, **CHXene** has the highest pKa but forms the weakest gel with **L,L,L-G2Lys**, conversely, **Nap** has a relatively low pKa value but forms the most thermally stable gels with **L,L,L-G2Lys**. The same T_{gel} and VT-NMR experiments were carried out on the mixtures of **L,L,L-G2Lys**, **C6** and each other amine. The T_{gel} values of the gels formed are shown in Figure 3.35., Figure 3.36. and Figure 3.37. The VT-NMR results are shown in Figure 3.38., Figure 3.39. and Figure 3.40.

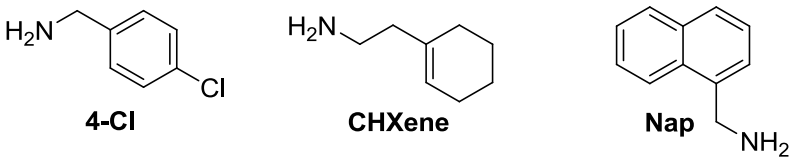

Figure 3.34. Structure of amines **4-Cl**, **CHXene** and **Nap.**

Table 3.4. pKa values of amines used (from SciFinder) and T_{gel} values of 10 mM gels with 1:1 mixture of each amine and **L,L,L-G2Lys**. Arranged in order of decreasing pKa value.

Amine	pKa	T_{gel} / °C
CHXene	10.94 (±0.1)	54
C6	10.69 (±0.1)	71
Benz	9.06 (±0.1)	57
Nap	9.06 (±0.3)	73
4-Cl	8.85 (±0.1)	61

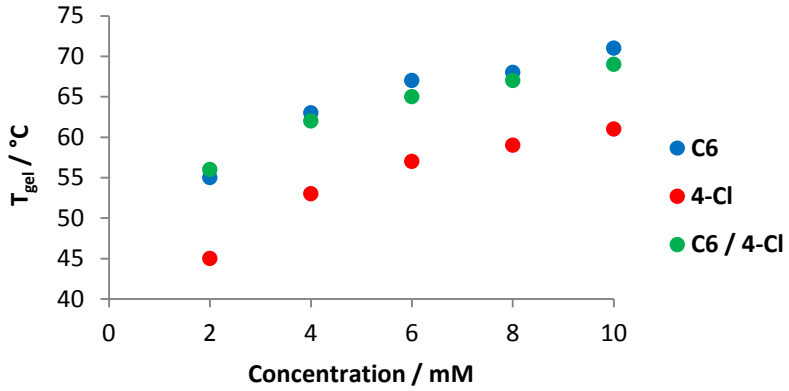

Figure 3.35. T_{gel} values of gels with **L,L,L-G2Lys** with either **C6**, **4-Cl** or a mixture of both. Toluene.

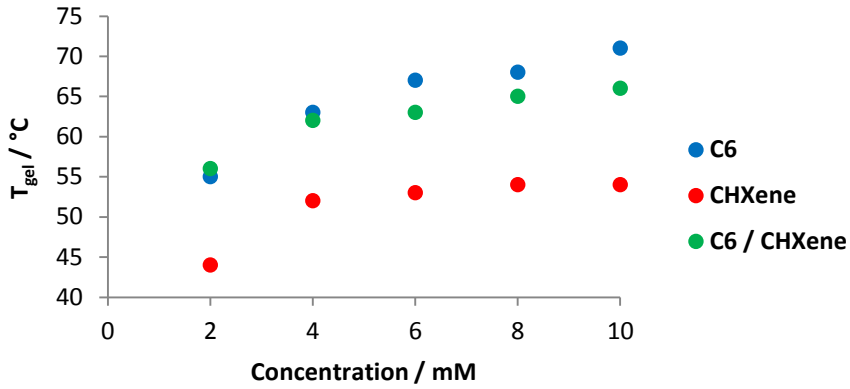

Figure 3.36. T_{gel} values of gels with **L,L,L-G2Lys** with either **C6**, **CHXene** or a mixture of both. Toluene.

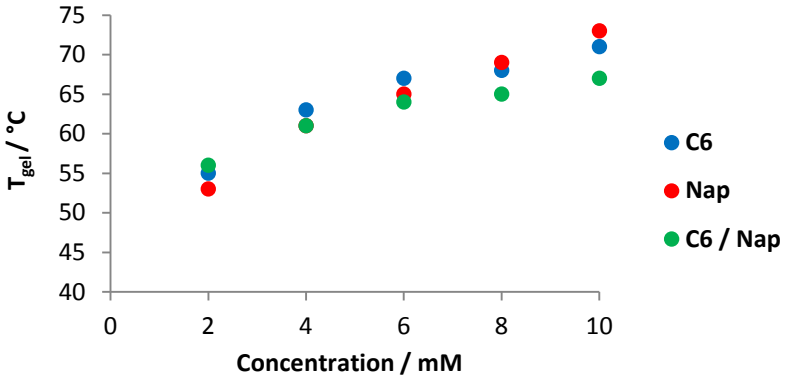

Figure 3.37. T_{gel} values of gels with **L,L,L-G2Lys** with either **C6**, **Nap** or a mixture of both. Toluene.

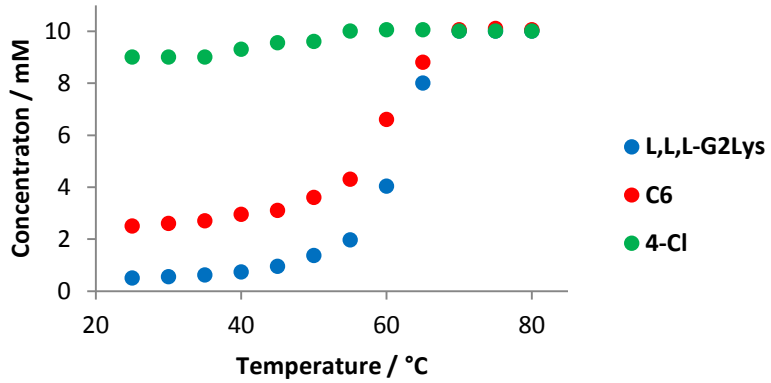

Figure 3.38. Concentration of components visible in ^{1}H NMR as temperature increases in gel with **L,L,L-G2Lys**, **C6** and **4-Cl**. Toluene-d_8.

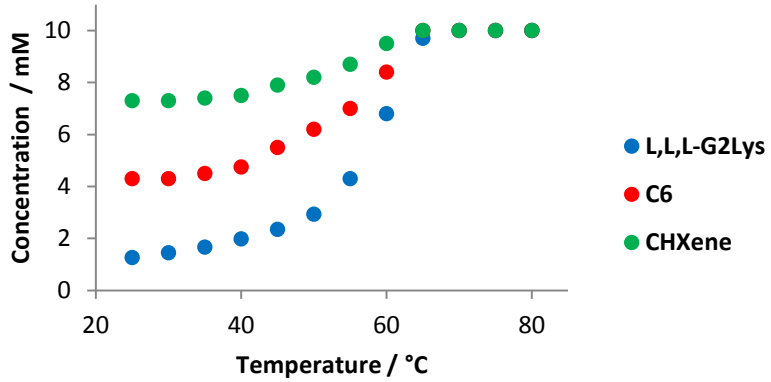

Figure 3.39. Concentration of components visible in ^{1}H NMR as temperature increases in gel with **L,L,L-G2Lys**, **C6** and **CHXene**. Toluene-d_8.

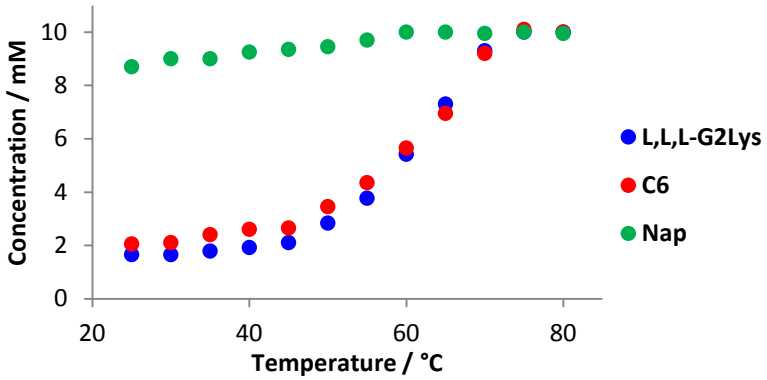

Figure 3.40. Concentration of components visible in ^{1}H NMR as temperature increases in gel with **L,L,L-G2Lys**, **C6** and **Nap**. Toluene-d_8.

These data indicate **C6** is incorporated over all the other amines into the gelator network. The T_{gel} values for mixed systems with **4-Cl** or **CHXene** are closer to those of the gels formed with **L,L,L-G2Lys** and **C6** only, rather than **L,L,L-G2Lys** and **4-Cl** or **CHXene** respectively. The VT-NMR shows that the sample containing **L,L,L-G2Lys**, **C6** and **4-Cl** behaves just like the previous mixture containing **Benz**, with **4-Cl** being overwhelmingly excluded from the gel network (which contains 88% **C6**, 12% **4-Cl**). This is unsurprising as both the pKa and T_{gel} values of this amine are lower than those of **C6**. In the sample containing both **C6** and **CHXene**, **C6** is again preferentially incorporated. This indicates that gel forming ability as predicted by T_{gel} can be used to control component selection. However the selectivity for **C6** in this last case is less pronounced, with more **CHXene** included than **Benz** or **4-Cl** in the other mixtures (gelator network is 68% **C6**, 32% **CHXene**). This is despite **CHXene** forming gels with **L,L,L-G2Lys** that have no better thermal stability than those formed with **Benz** or **4-Cl**. When the gels formed with **C6** and **Nap** were analysed, **C6** was again overwhelmingly incorporated into the gel network (86% **C6**, 14% **Nap**). This was due to the difference in pKa as they both form gels with similar Tgel values, with **C6** being more basic and being favoured at the complex formation step. This, along with the less pronounced selectivity for **C6** over **CHXene** indicates that pKa does have a role in directing component selection. The proportion of each amine that makes up the gelator network is summarised for each sample in Table 3.5.

Table 3.5. Percentage of each amine immobilised in gelator network.

Amines	% C6	% Benz	% 4-Cl	% CHXene	% Nap
C6 / Benz	89	11	-	-	-
C6 / 4-Cl	88	-	12	-	-
C6 / CHXene	68	-	-	32	-
C6 / Nap	86	-	-	-	14

The next step was to examine whether **Nap** could be selectively incorporated into a gel with **L,L,L-G2Lys** in the same way that **C6** had in the previous examples. **Nap** has hight T_{gel} and low pKa. The data for corresponding mixtures with **L,L,L-G2Lys**, **Nap** and either **Benz**, **4-Cl** or **CHXene** was collected and shown below. The T_{gel} values are shown in Figure 3.41., Figure 3.42. and Figure 3.43. The VT-NMR data is plotted in Figure 3.44. Figure 3.45. and Figure 3.46.

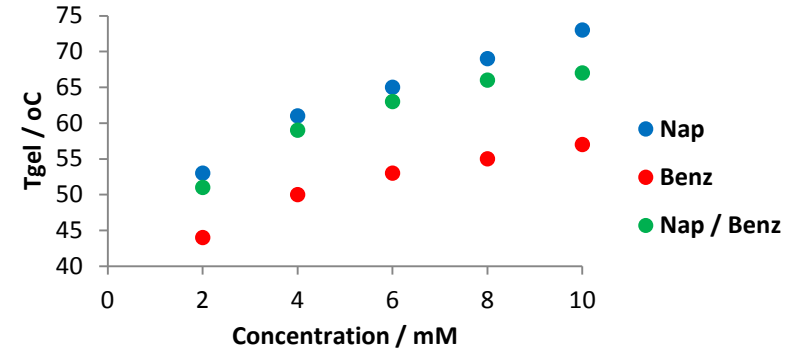

Figure 3.41. T_{gel} values of gels with **L,L,L-G2Lys** with either **Nap**, **Benz** or a mixture of both. Toluene.

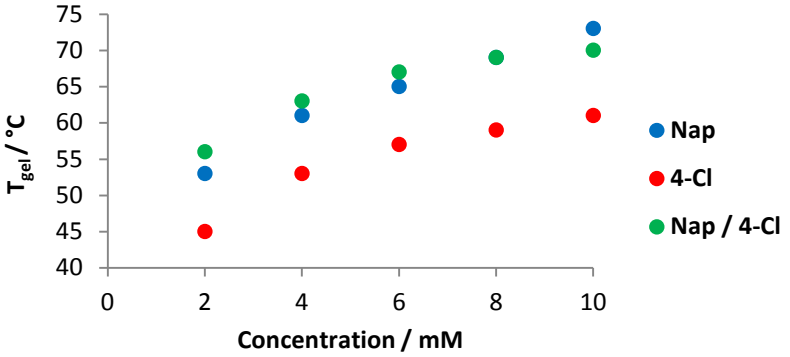

Figure 3.42. T_{gel} values of gels with **L,L,L-G2Lys** with either **Nap**, **4-Cl** or a mixture of both. Toluene.

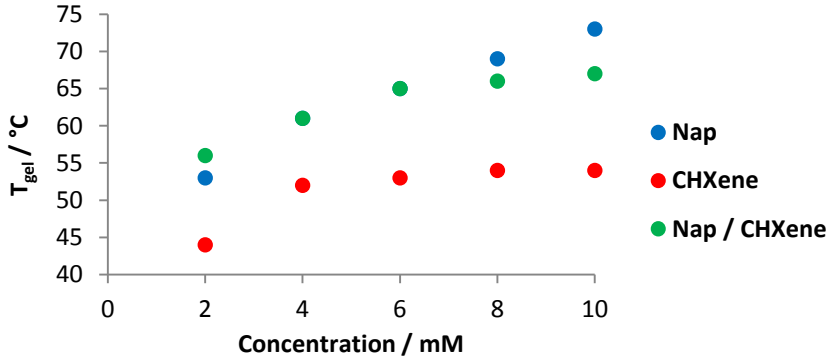

Figure 3.43. T_{gel} values of gels with **L,L,L-G2Lys** with either **Nap**, **CHXene** or a mixture of both. Toluene.

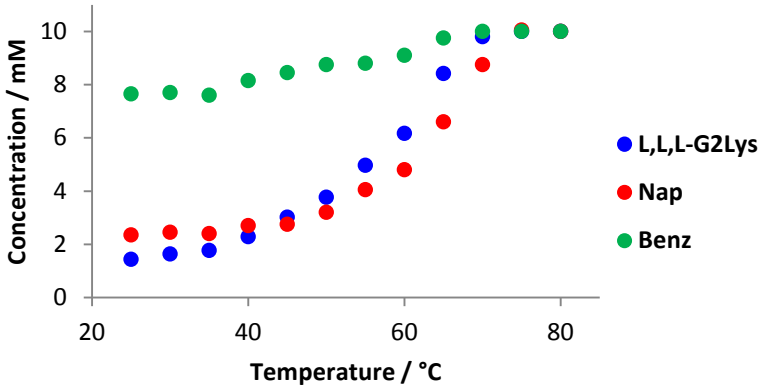

Figure 3.44. Concentration of components visible in ^{1}H NMR as temperature increases in gel with **L,L,L-G2Lys**, **Nap** and **Benz**. Toluene-d_8.

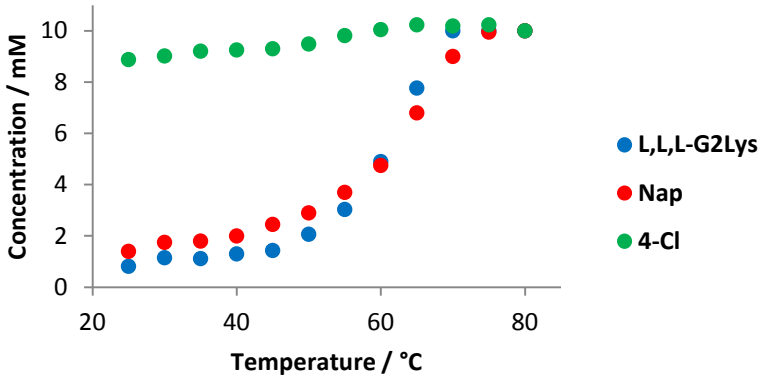

Figure 3.45. Concentration of components visible in ^{1}H NMR as temperature increases in gel with **L,L,L-G2Lys**, **Nap** and **4-Cl**. Toluene-d_8.

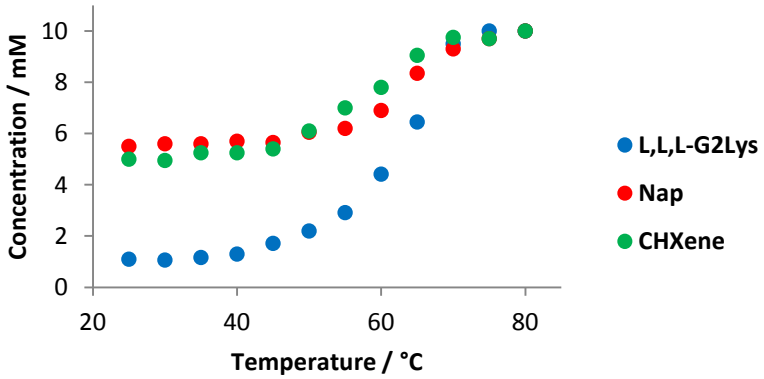

Figure 3.46. Concentration of components visible in ^{1}H NMR as temperature increases in gel with **L,L,L-G2Lys**, **Nap** and **CHXene**. Toluene-d_8.

The T_{gel} values of all the mixed amine samples are higher close to those of the gels formed from **L,L,L-G2Lys** and **Nap** only. This at first indicates that there may be selective incorporation of this amine in all the mixed samples. The VT-NMR data of the mixed gels made with **Benz** or **4-Cl** do show that **Nap** is taken is the main amine that forms the gelator network (77% and 88% respectively). This is not surprising as these amines have an equal or lower pKa value and form gels of lower thermal stability with **L,L,L-G2Lys**. This does provide more evidence though of gel forming ability (and therefore T_{gel}) controlling component selection. In contrast to this clear result, the VT-NMR data for the mixture of **L,L,L-G2Lys**, **Nap** and **CHXene** shows there is no preferential uptake of either amine, almost exactly the same amount of each is incorporated into the gelator fibres (47% **Nap**, 53% **CHXene**). This is occurs because despite **Nap** forming more stable gels with **L,L,L-G2Lys** than **CHXene**, it has a lower pKa. In this instance it appears that the two driving forces we have observed determining component selection both favour different amines. The result of this is that neither is preferentially incorporated and therefore we can state that neither step is completely dominant in determining the composition of the gel that is formed. The proportion of each amine that makes up the gelator network is summarised for each sample in Table 3.6.

Table 3.6. Percentage of each amine immobilised in gelator network.

Amines	% Nap	% Benz	% 4-Cl	% CHXene
Nap / Benz	77	23	-	-
Nap / 4-Cl	88	-	12	-
Nap / CHXene	47	-	-	53

3.2.2. Component Selection in Complex Mixtures

The selective incorporation of one amine over another into a gel network with **L,L,L-G2Lys** has been demonstrated with a range of different amines. It has been shown that the thermal stability of the gel formed with a certain amine – how good that amine is at forming a stable gel – and the pKa of the amines – how strong a complex it forms with **L,L,L-G2Lys** – were shown to be the driving factors. How this component selection would be effected if the samples had a more complex starting mixture of amines was then investigated.

First gels with an equal concentration of **L,L,L-G2Lys**, **Nap**, **Benz** and **4-Cl** were made (1:1:1:1 mixture). Whilst all of the amines have very similar pKa values, **Nap** forms more thermally stable gels with **L,L,L-G2Lys** and therefore is the best amine for forming a gel network. The T_{gel} values of these gels were compared to those of equivalent gels formed with **L,L,L-G2Lys** and each amine individually (Figure 3.47.)

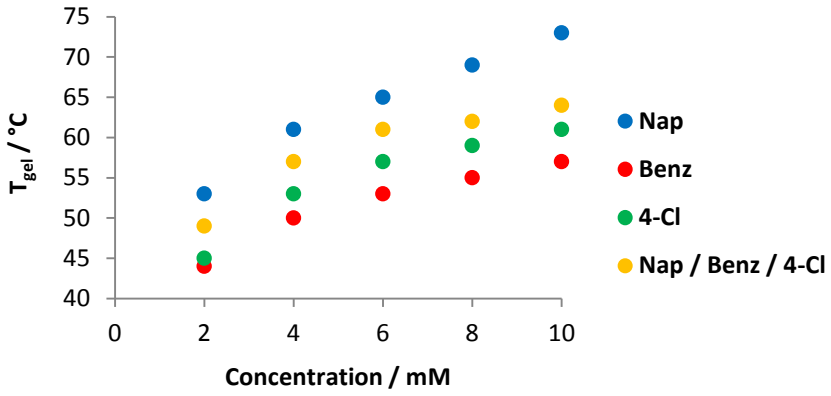

Figure 3.47. T_{gel} values of gels of **L,L,L-G2Lys** and either **Nap**, **Benz**, **4-Cl** or a mixture of all. Toluene.

These data indicate the T_{gel} values of the gel formed from the more complex mixture are depressed compared to those formed with **L,L,L-G2Lys** and **Nap** only but is still higher than those of gels with only **Benz** or **4-Cl**. The 10 mM gel formed from the complex mixture was then analysed by VT-NMR (Figure 3.48.).

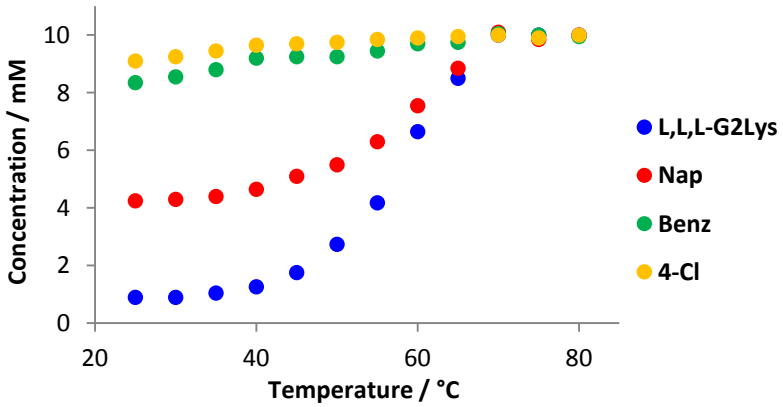

Figure 3.48. Concentration of components visible in ^{1}H NMR as temperature increases in gel with **L,L,L-G2Lys**, **Benz**, and **4-Cl**. Toluene-d_8.

These variable spectra show that at 25°C the amine "missing" from the spectra and therefore incorporated into the network is 69% **Nap**, 20% **Benz** and 11% **4-Cl**. This shows that **Nap** is preferentially included into the gelator network with **L,L,L-G2Lys** over **Benz** and **4-Cl** due to its greater ability to form a stable gel with **L,L,L-G2Lys**. However the selection of **Nap** into the fibrous network was less than when in competition with only one of **Benz** or **Nap**.

A more complex mixture with **Nap**, **Benz**, **4-Cl** and **CHXene** was then formed. This is of course the same as the previous sample but with **CHXene** added, an amine which forms relatively unstable gels with **L,L,L-G2Lys** but has a high pKa. When the T_{gel} values of these complex gels are measured they are also depressed to values below that of the gels formed from **L,L,L-G2Lys** and **Nap** only (Figure 3.49.).

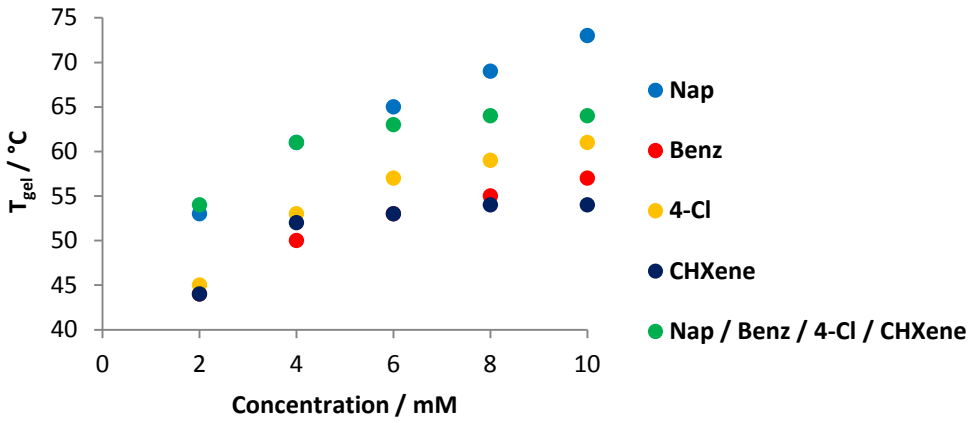

Figure 3.49. T_{gel} values of gels of **L,L,L-G2Lys** and either **Nap**, **Benz**, **4-Cl**, **CHXene** or a mixture of all. Toluene.

However, when the VT-NMR the 10 mM gel was recorded it showed that the amine in the gelator network was 48% **CHXene**, 23% **Nap**, 22% **Benz** and 7% **4-Cl**. **Nap** was no longer the majority amine in the gelator network, **CHXene** was now the most incorporated amine. Also, the selection of **Nap** over **Benz** was now removed with equal amounts of each being incorporated into the fibrous network. In a previous example, equal amounts of **CHXene** and **Nap** were taken into a gel network with **L,L,L-G2Lys** and the difference in pKa and T_{gel} values with the two amines cancel each other out. In this more complex sample, the amine with the higher pKa is most preferentially incorporated. This may be because with more amines being incorporated into the gel network, the T_{gel} value of the gel with **L,L,L-G2Lys** and a single amine is less relevant, where as the effect of pKa should be relatively unaffected and becomes the dominant factor. Comparing the FEG-SEM images of xerogels formed from **L,L,L-G2Lys** and

either **Benz** (Figure **3.28**.), **4-Cl**, **CHXene**, **Nap** or all of them (Figure 3.50.) shows that the sample with all the amines has an indistinct fibrous morphology, different to the samples with any of the amines alone, even **CHX-ene**. This further indicates that the gel formed from the complex mixture has morphology controlled by all of the amines incorporated, providing further evidence that the ability of each amine to assemble into a network is less relevant to directing component selection in this more complex mixtures.

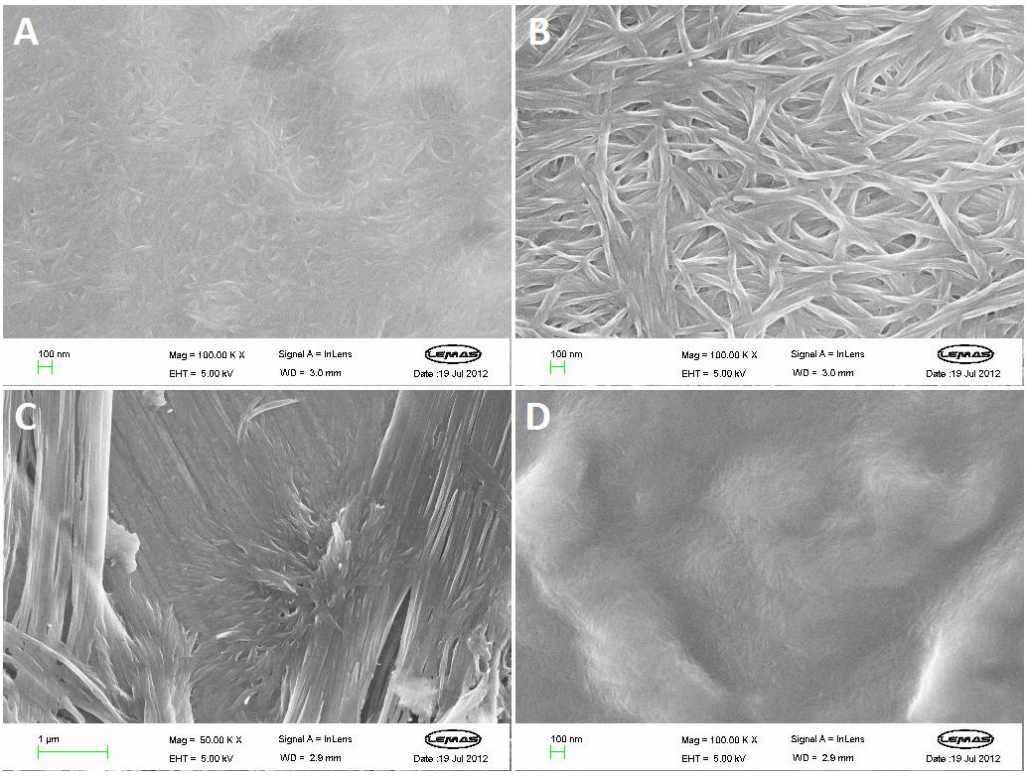

Figure 3.50. FEG-SEM images of xerogels formed from **L,L,L-G2Lys** and A) **4-Cl**. B) **CHXene**, Scale bars = 100 nm. C) **Nap**, Scale bar = 1 µm. D) **Nap**, **Benz**, **4-Cl** and **CHXene**, Scale bar = 100 nm.

To further investigate this more complex component selection, the gels were made with equal concentrations of **L,L,L-G2Lys**, **C6**, **Benz**, **4-Cl** and **CHXene** (1:1:1:1 mixture). This is the same as the previous sample investigated but **C6** has replaced **Nap**. The T_{gel} values of the gels formed form this complex mixture are below those of gels formed with **C6** as the sole amine and above those formed with the other amines individually (Figure 3.51.). When the VT-NMR of the 10 mM gel was analysed (Figure 3.52.) the composition of the gelator network was observed to be 50% **C6**, 32% **CHXene**, 10% **4-Cl** and 8% **Benz**, so **C6** was the amine preferentially incorporated into the network. This selectivity in preference to **Benz** and **4-Cl** is unsurprising due to **C6** having both a higher pKa and a greater ability to form a stable gel

network. **C6** is also selected in preference to **CHXene**, as it is in the sample with only these two amines, but to a lesser extent than in this simpler sample. The pKa of both amines is roughly the same, but the T_{gel} values of gels formed with **C6** are higher than those formed with **CHXene** and in the sample with only these two amines this leads to more **C6** being incorporated. In the more complicated sample the network contains amounts of four different amines and therefore the difference in T_{gel} of gels with individual amines is less important and is a less powerful driving force for component selection, resulting in the amount of **C6** being incorporated decreasing.

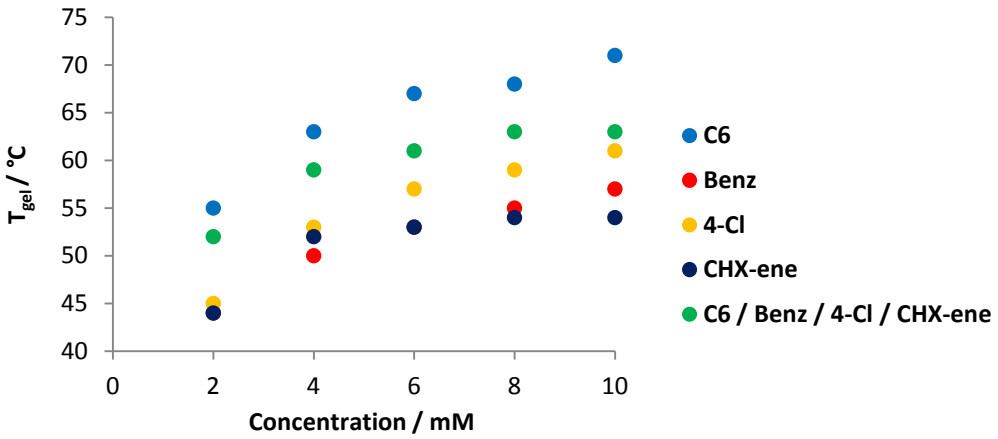

Figure 3.51. T_{gel} values of gels of **L,L,L-G2Lys** and either **C6**, **Benz**, **4-Cl** or **CHXene** or a mixture of all. Toluene.

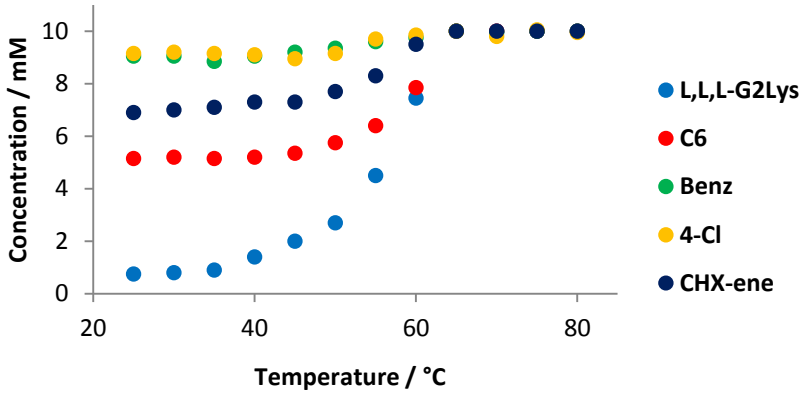

Figure 3.52. Concentration of components visible in ^{1}H NMR as temperature increases in gel with **L,L,L-G2Lys**, **C6**, **Benz**, **4-Cl** and **CHXene**. Toluene-d_8.

The xerogel network can be observed by FEG-SEM and shown an indistinct network that is not clearly similar to any of those formed from gels of **L,L,L-G2Lys** and each amine individually. Similarly this complex mixture can be analysed by CD as a 0.625 mM sample in 95:5

methylcyclohexane to dioxane. Except for the high CD signal of the sample with **C6** at 200 nm, the spectra are all similar. The spectrum for the complex mixture is non-identical to any of the others. This provides more evidence that the gel resulting from the more complex mixture appears to be a co-assembly of different amines with no amine dominating or solely directing the assembly of the complexes.

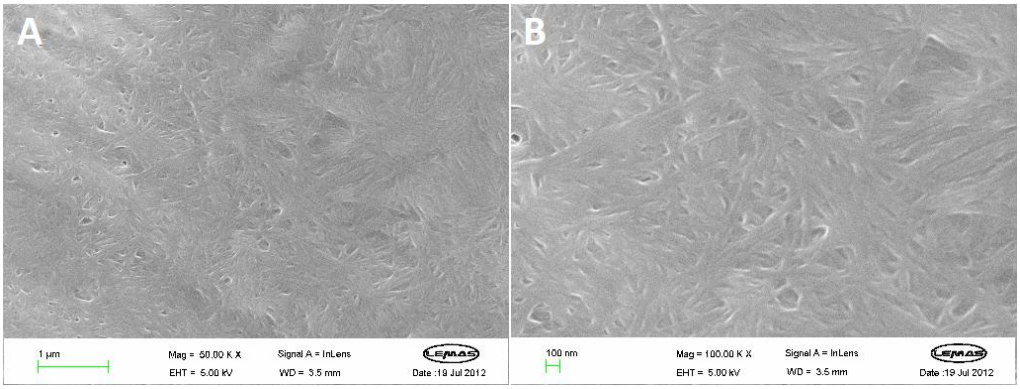

Figure 3.53. FEG-SEM images of xerogels formed from **L,L,L-G2Lys**, **C6**, **Benz**, **4-Cl** and **CHXene** A) Scale bar = 1 µm. B) Scale bar = 100 nm.

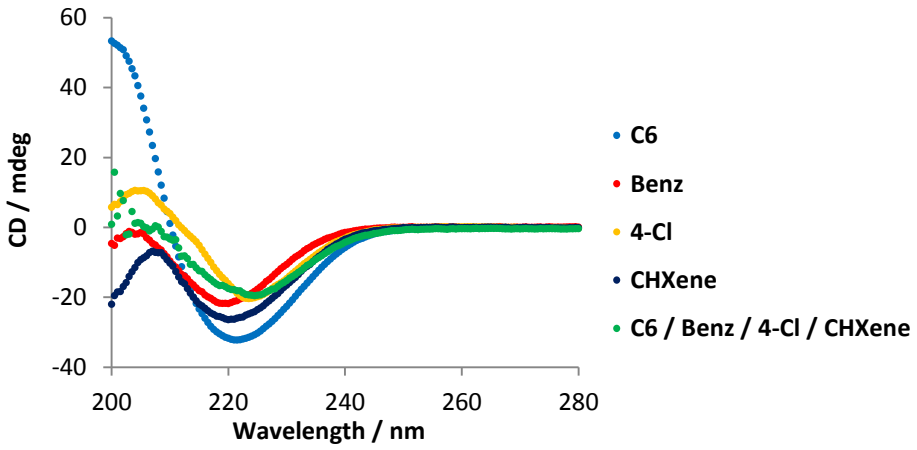

Figure 3.54. CD spectra of mixtures of **L,L,L-G2Lys** with either **C6**, **Benz**, **4-Cl**, **CHXene** or a combination of all. 95:5 Methylcyclohexane : Dioxane, 0.625 mM.

In summary, it has been shown that component selection can be achieved in these multi-component gels using either pKa, which indicates the favourability of complex formation between acid and amine, or the T_{gel} of a gel with **L,L,L-G2Lys** and an individual amine, which indicates its ability for form part of a stable gel network to rationalise the preference observed. This was initially observed with the selective incorporation of **C6** over **Benz** but

became clearer as a greater range of amines competed against each other to be incorporated. In the more complex mixtures pKa seemed to be more important in determining the final composition of the gelator network as it contained more amines – even if some were present in small quantities – and this made the T_{gel} of the gels formed with each amine individually less relevant.

3.2.3. Dynamic Component Selection

The final experiments performed on this system were to examine whether the selective formation of the most thermally stable network was based on a real preference for this network to form. The alternative argument is that as a sample cools it reaches the T_{gel} of the most thermally stable gel network – for instance **L,L,L-G2Lys** and **Nap** – and that this network forms. Then when the samples cools further and reaches the T_{gel} of the least thermally stable network – **L,L,L-G2Lys** and **Benz** for example – all of the **L,L,L-G2Lys** is already used and this network cannot form. This would generate a type of selectivity simply based on cooling rate and the kinetics of gelation, rather than thermodynamic stability.

Firstly, two samples were made in NMR tubes with a 10 mM concentration of **L,L,L-G2Lys**, **Nap** and **Benz**. One sample was formed from simple mixing of solutions of each component with no heating involved. This eliminates the effect of cooling on the formation of the networks. The second sample was made by heating the mixture as usual, but instead of leaving the sample to cool at room temperature, it was submerged in liquid nitrogen to ensure rapid cooling. If the cooling of the sample ensures the formation of one network before the other, this rapid cooling should at least reduce, if not eliminate, the selectivity observed. Unfortunately when each sample was analysed by ^{1}H NMR, the spectra produced were of very low quality. It proved impossible to analyse the spectra, most likely as the rapidly formed samples lacked the homogeneity of gels formed by slower cooling and produced very poor NMR spectra.

A second approach was taken to solve this problem. A gel was made in an NMR tube with a 10 mM concentration of **L,L,L-G2Lys** and **Benz**. A solution of an equal amount of **Nap** was pipetted on to the top of the gel, after it had formed, and the whole sample was left for 48 hours to ensure total diffusion of the **Nap** through the gel. The sample was then analysed by ^{1}H NMR to see whether exchange of amine components had taken place, indicative of thermodynamic control and reversibility. Of all the amine still incorporated into the gelator network 63% was now **Nap** and only 37% was **Benz**. The gel was left for a further five days and was analysed again by NMR. The percentage of the amine in the gelator network has changed slightly to 71%

Nap and 29% **Benz**. After this, a portion of **C6** was also pipetted on top of the gel and it was left for a further five days. When the resulting sample was analysed it showed that 67% of the gel network was **C6**, 27% was **Nap** and only 6% was **Benz**, proving that the amine favoured due to its pKa value could exchange with the others.

This experiment proves conclusively that the selectivity seen is due to a thermodynamic preference for one network which is able to express itself in the dynamic gel environment and clearly illustrates the dynamic and evolving nature of this class of materials.

3.3. Conclusions

It has been demonstrated that **L,L,L-G2Lys** can form a complex with certain monoamines and this complex is able to gelate a range of organic solvents. The amines that were compatible with gelation, the types of solvents that could be gelated and the forces that underpin this process have all been investigated. Furthermore it was seen that changing the amine affected the formation of the gel. This was investigated using CD, FEG-SEM and NMR methods, as well as simple T_{gel} and MGC measurement. The fact that both **L,L,L-G2Lys** and amine are soluble in the gelation solvent until mixed, and that gelation occurs upon simple mixing adds an interesting aspect to this system, and may be exploited towards practical applications in future work.

Furthermore, this work has shown that the selection of an amine, which is one component in a multi-component mixture, can be achieved. The driving forces behind this component selection have been investigated and the role of complex formation (pKa) and gel formation (T_{gel}) in this process have been probed. It has been found that both aspects can be used to drive component selection and, when favouring different results, can compete against and negate each other. This was particularly interesting, given not only the relatively small differences in pKa and T_{gel} that were studied. The driving forces of component selection were revealed and compared individually, as well as in more complex systems in which it was seen that pKa became more important and T_{gel} less important in determining the outcome of the experiment.

Finally, a thermodynamic equilibration experiment has been used to prove that component selection based on T_{gel} or pKa is due to the favourability of one product over another, and not simply due to the effects of cooling the sample leading to a kinetically chosen product.

Chapter 4

Multi-Component Gels: Chiral Amines

Chapter 4 – Multi-Component Gels: Chiral Amines

4.1. Effect of Amine Chirality on Gelation

4.1.1. Difference Between Enantiomeric Amines

In the previous chapter, it was shown that **L,L,L-G2Lys** formed a 1:1 complex with an amine and that these complexes further assembled to form a gel network. The identity of the amine mixed with **L,L,L-G2Lys** had a large effect on gel formation. As **L,L,L-G2Lys** is a chiral molecule – having three L (or *S*) chiral centres – if mixed with different enantiomers of a chiral amine, the complexes formed should be diastereomeric. This should mean that self-assembly and gel formation is different in each case.

Initially, to investigate whether this would be the case, two chiral amines, **C6R/S** and **C9R/S** were used (Figure 4.1.). Compound **L,L,L-G2Lys** was tested with each enantiomer of both amines individually as a 1:1 mixture of **L,L,L-G2Lys** and amine (both 10 mM) in toluene (0.5 mL). Both enantiomers of both amines were able to induce gelation when mixed with **L,L,L-G2Lys**. Interestingly, using different enantiomers of each amine produced gels with different T_{gel} values (Figure 4.1.).

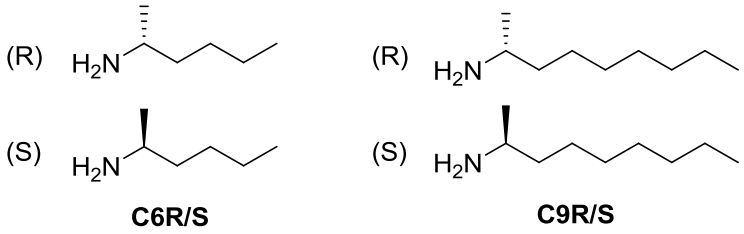

	R	S
2-Aminohexane	80°C	67°C
2-Aminononane	61°C	47°C

Figure 4.1. Chiral amines **C6R/S**, **C9R/S** and T_{gel} values of their 10 mM gels with **L,L,L-G2Lys**.

The gels formed with the *R* enantiomer of each amine were more thermally stable than those formed with the *S* enantiomer. This was a fascinating result, as it showed that in a complex

between **L,L,L-G2Lys** and an amine (mass of over 900 Da) which is effectively the orientation of a single methyl group has a pronounced effect on the stability of the gels that are formed. This is a significant impact of relatively low quality chiral information upon the assembly of these complexes.[279, 282, 461] As seen in the previous chapter, the amines with a six carbon chain produced gels with a higher thermal stability than those with a longer chain length.

These mixtures of **L,L,L-G2Lys** and each enantiomer were investigated using CD spectroscopy. As for the experiments in the previous chapter – analysing mixtures of **L,L,L-G2Lys** and non-chiral amines – a 95:5 mixture of methylcyclohexane to dioxane was chosen as solvent. The spectra produced by each sample are shown in Figure 4.2.

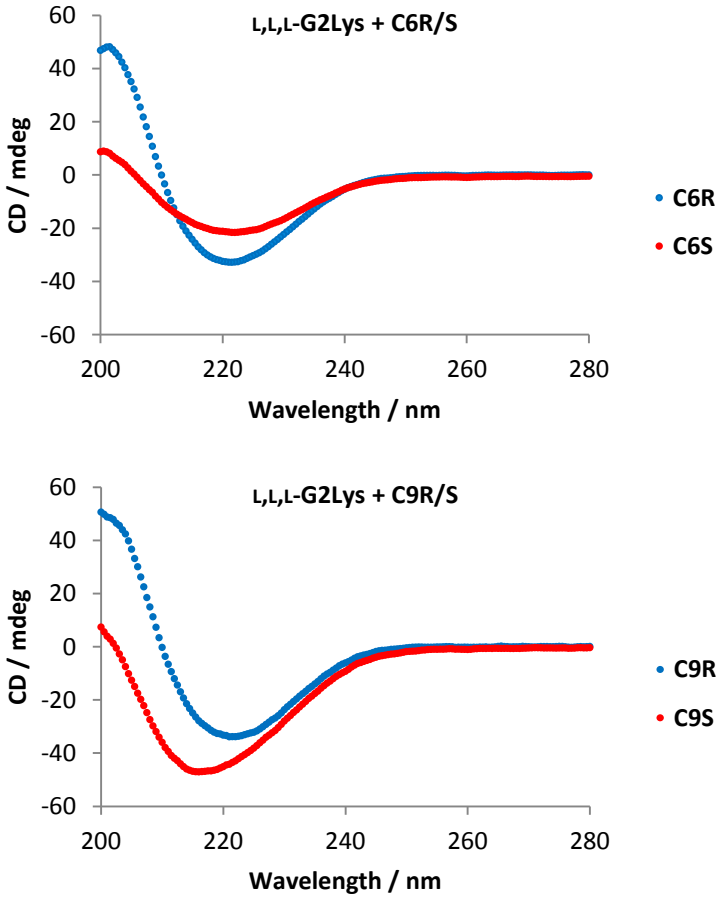

Figure 4.2. CD spectra of samples made with 1:1 mixture of **L,L,L-G2Lys** and **C6R**, **C6S**, **C9R** and **C9S**. 0.625 mM. 95:5 Methylcyclohexane to Dioxane.

In both cases the spectra produced with the different enantiomers are different. The spectra produced by the sample with **L,L,L-G2Lys** and **C6R** shows a negative Cotton effect band. The

band is not observable below 200 nm as solvent absorbance becomes too high. The sample made with **C6S** produces different spectrum with a simpler, broad CD band. This illustrates that the chiral organisation of the aggregates made using each enantiomer is different. The same is true for the samples made with **L,L,L-G2Lys** and either **C9R** or **C9S**. Despite CD being used to identify the structure of proteins, it is hard to extract any more information from our systems, other than that the spectra are different when each enantiomer is used. This is because there are no equivalent, known samples to which our systems can be compared, unlike the many biological samples that have been analysed using this technique, where protein/peptide secondary structures can be assigned.[462, 463]

To gain further insight into the structure of the gels formed with different amine enantiomers, the xerogels were formed and analysed by FEG-SEM. Xerogels were formed from 10 mM gels of **L,L,L-G2Lys** and either **C6R** or **C6S** in toluene. The images produced by these xerogels are shown in Figure 4.3.

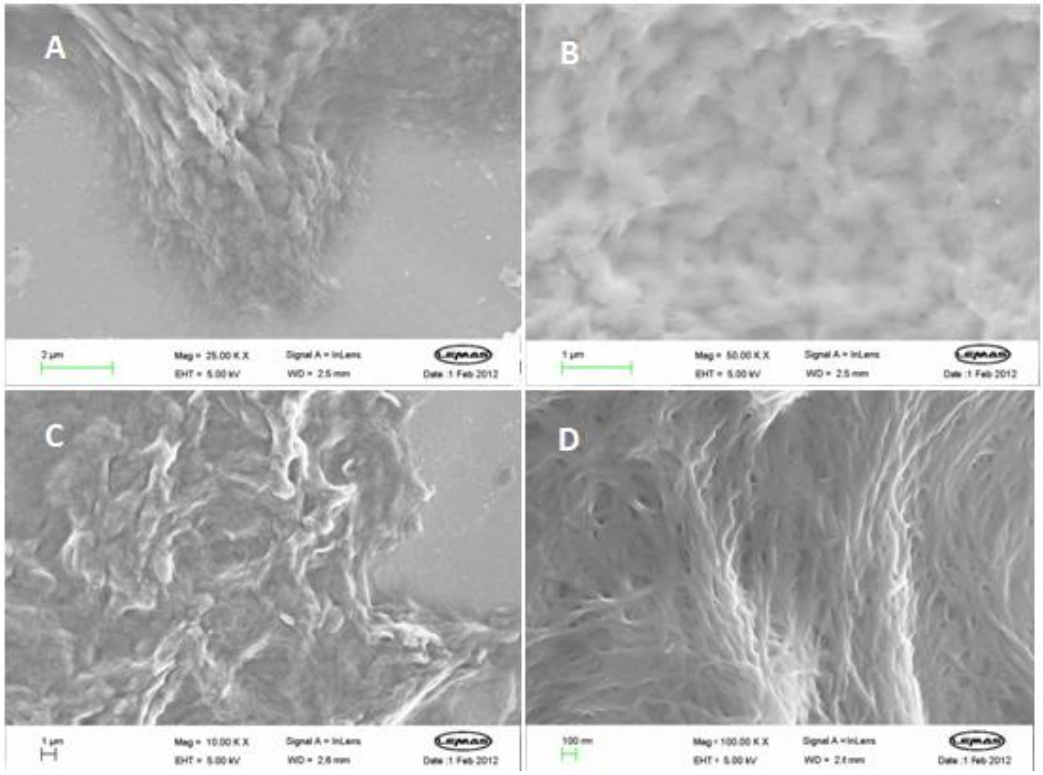

Figure 4.3. FEG-SEM images of xerogels formed from **L,L,L-G2Lys** and chiral amine A) with **C6R**, Scale bar = 2 µm. B) with **C6R**, Scale bar = 1 µm. C) with **C6S**, Scale bar = 1µm. D) with **C6S**, Scale bar = 100 nm.

The images show very different morphologies in each sample. The xerogel made with **L,L,L-G2Lys** and **C6R** appears to be made of very small fibres that are barely visible even at high magnification. These fibres run together to form an ill defined, bumpy topography. In the lower magnification image we can see larger rope like aggregates (potentially a consequence of drying). In contrast to this, the sample made with **L,L,L-G2Lys** and **C6S** shows a network of much more defined, thicker fibres that crosslink to form the gel network. The higher magnification image shows these fibres further aggregating to form larger structures; however, this may also be an artefact of drying.

The xerogels were also studied under TEM (Figure 4.4.). The sample preparation is slightly different with very small amounts of the gels transferred onto copper grids, allowed to dry and stained with uranyl acetate before viewing.

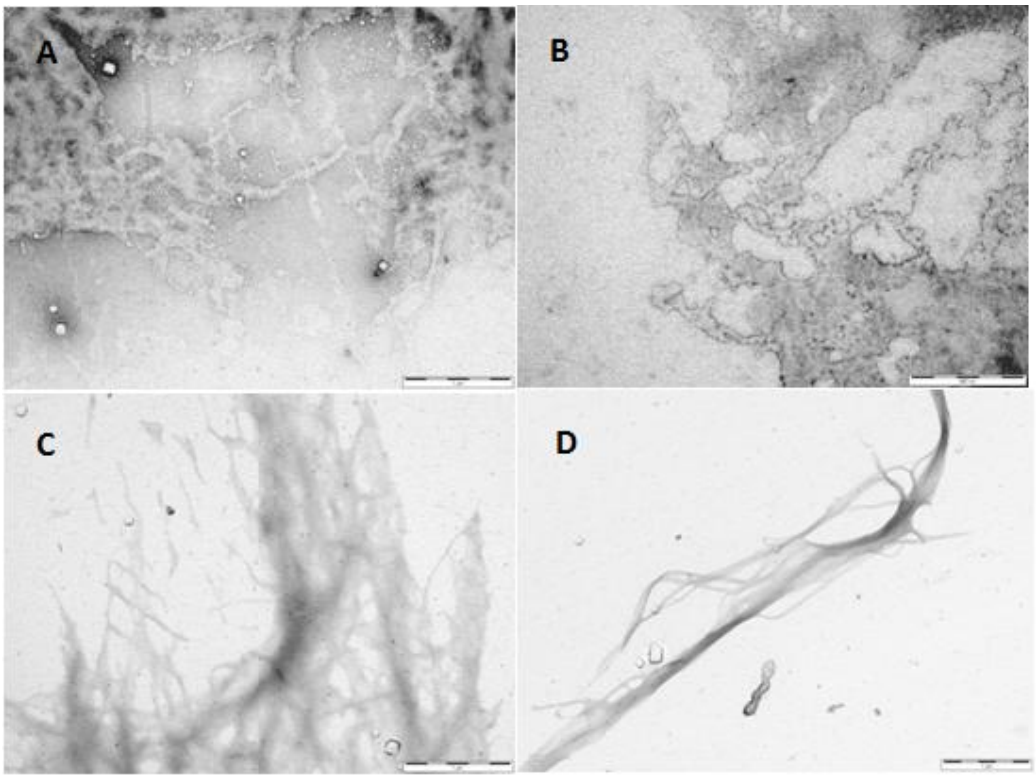

Figure 4.4. TEM images of xerogels formed from **L,L,L-G2Lys** and chiral amines A) with **C6R**, Scale bar = 1 µm. B) with **C6R**, Scale bar = 500 nm. C) with **C6S**. D) with **C6S**, Scale bars = 1 µm.

The sample made with **C6R** again produces a very poorly defined xerogel. Sample is visible on the grid but no detailed structure or individual fibres are distinguishable. In contrast, the gel made with the *S* enantiomer exhibits a network consisting of well defined fibrous aggregates. The images produced by TEM concur with the images produced by FEG-SEM. Both techniques

show that the gel made with **C6R** has a network of very small fibres. The gel made with **C6S** has a much more well-defined network of thicker fibres. This is unusual as it would be expected that the gel with a more defined and perhaps more ordered network would be more stable however, in general, their fibres, such as those formed with **C6R** can comprise a network with a large number of contact points and a greater degree of entanglement. Crucially however the two samples exhibit distinctly different morphologies, which must be result of differing amine chirality leading to diastereomeric gelating complexes.

In summary, gels made with **L,L,L-G2Lys** and either **C6R** or **C6S** had different thermal stabilities (T_{gel}), were aggregated differently in solution (CD) and had different morphologies under electron microscopy (FEG-SEM and TEM). The next question was to explore how gels made with mixtures of each enantiomer would behave, and how the ratio of *R* to *S* enantiomer would control this behaviour. This would demonstrate how tuneable the system is. A series of gels with a 1:1 mix of **L,L,L-G2Lys** (10 mM) and **C6R/S** (10 mM in total) were formed. The ratio of **C6R** to **C6S** in each sample was varied and the T_{gel} value of each of these gels was measured. The results are shown in Figure 4.5. and plotted as T_{gel} versus increasing percentage of **C6S** used.

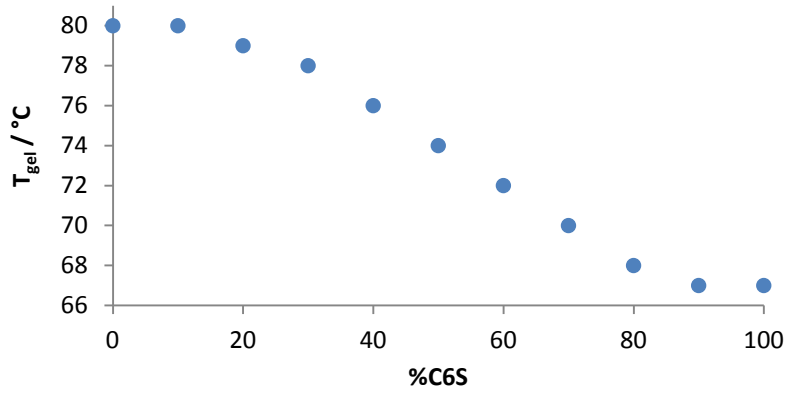

Figure 4.5. T_{gel} values of 10 mM gels made **L,L,L-G2Lys** and varying ratio of **C6R** to **C6S**. Toluene.

Overall the T_{gel} values in Figure 4.5. show how the thermal stability of the gels decreases when an increasing amount of **C6S** is incorporated into the network with **L,L,L-G2Lys**. However, the shape of the curve produced by the T_{gel} values is very interesting. It appears that it takes ca. 20% of **C6S** to be incorporated into the network until it is significantly disrupted and the stability of the gel decreases, and that similarly it takes ca. 20% of **C6R** being incorporated into the gel network before it is significantly changed to increase the thermal stability of the gel.

This curve is similar to what is called a "majority rules" curve, seen occasionally when studying supramolecular polymers made from mixtures of enantiomers.[286, 296-301, 303, 307, 312, 313, 337-339, 376, 378] It appears that until roughly 20% of the network is made of the minority diastereomeric complex (**L,L,L-G2Lys** and either **C6R** or **C6S**) the complex that is in the majority can control the gelator network and the stability of the gel formed, in this way the majority enantiomeric amine can impose its chiral preference on the minority.

To investigate whether this change in thermal stability was linked to a change in chiral organisation, the same mixtures of **L,L,L-G2Lys** with varying ratios of **C6R** and **C6S** were analysed by CD spectroscopy (Figure 4.6.). Again the solvent used was a 95:5 mixture of methylcyclohexane to dioxane. The spectra are again labelled as the percentage of total amine that is **C6S** in the sample, i.e. 0% **C6S** could equally be labelled 100% **C6R**.

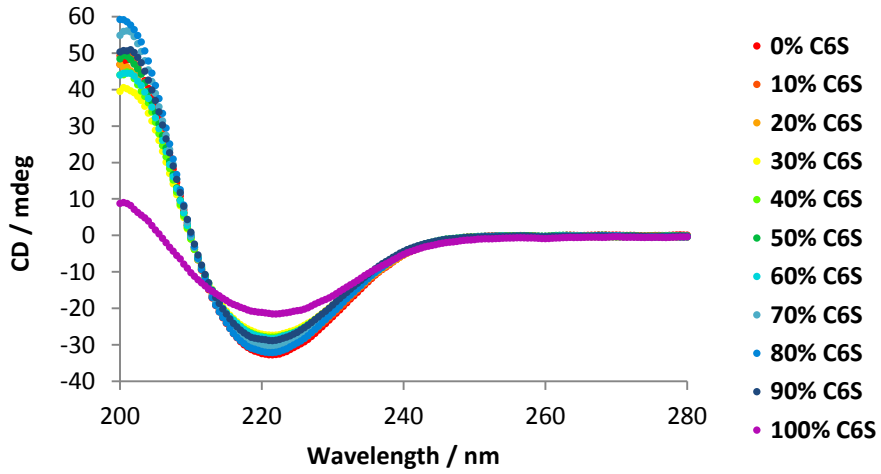

Figure 4.6. CD signal for samples of **L,L,L-G2Lys**.and a varying ratio of **C6R** and **C6S**. 95:5 Methylcyclohexane to Dioxane, 0.625 mM.

The spectra recorded show that, surprisingly, the spectra from samples with from 0% to 90% **C6S** produce virtually identical spectra. Only when the sample is made with entirely **C6S** do we see a significant change in the CD spectrum. This is more clearly observed if the CD signal at 202 nm (wavelength of maximum positive elipcicity for most samples) and to a lesser extent 220 nm (wavelength of maximum negative elipcicity) is plotted for each mixture (Figure 4.7.).

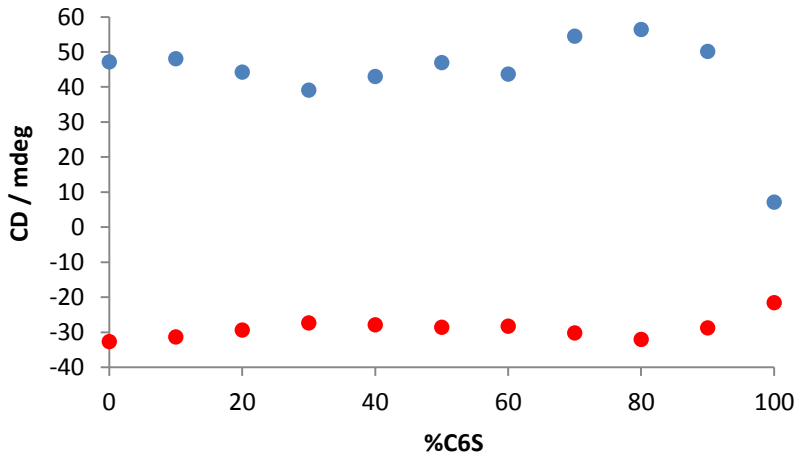

Figure 4.7. CD signal for each sample.

This CD data is reminiscent of a sergeants and soldiers[291-295, 297, 298, 302-304, 306, 308-311, 315, 316, 335, 341, 342, 344, 464-467] experiment, in which a small amount of one enantiomer is able to impose its preference, in terms of nanoscale chirality, onto a non-chiral molecule. In this case **C6R** would be the sergeant. The T_{gel} values of the equivalent gels in 95:5 methylcyclohexane to dioxane follow a similar trend to those in toluene but the CD spectra do not show a clear relationship with either. Fascinatingly, this would suggest that nanoscale chirality responds in a sergeant and soldiers-like manner but that this is not translated through to the macroscopic scale which shows a majority rules response. Intriguingly, this hints that chiral information may be expressed differently at different length scales within these hierarchical materials. An apparent discrepancy between macroscopic and chiroptical properties has been observed previously by Maitra and co-workers.[340]

In the light of these results, it was important to confirm that the mixtures produced one network – a co-assembly – made with **L,L,L-G2Lys**, **C6R** and **C6S**, and not two separate networks, each made from a different diastereomeric complex. The formation of a co-assembly was first probed using differential scanning calorimetry (DSC). This technique allows the enthalpy change of a transition to be monitored giving both the temperature at which the transition occurs and the enthalpy change of the transition. In self-sorting gels, where two separate networks are formed, two separate thermal transitions can sometimes be observed.[268] Toluene gels at a concentration of 10 mM were placed in a DSC pan and analysed. Unfortunately, the gels gave either a very small signal or no signal at all, as most of the sample is solvent the enthalpy change is small. The concentration of the gels was increased to 50 mM but this also increased T_{gel}, making the temperature of the gel-sol transition closer to the

boiling point of toluene. This was unacceptable as the sample pan may burst, potentially damaging the instrument, or producing unreliable results. To remedy this problem 1,2,3,4-tetrahydronaphthalene was used as a solvent, as it is chemically very similar to toluene but with a much higher boiling point. Gels with a concentration of 50 mM could now be analysed. These samples did indeed produce more easily detectable enthalpy changes (Appendix C). Unfortunately as our samples were mostly solvent, even the small amount of evaporation that occurred meant the measured enthalpy change of each transition was unreliable. The first heat-cool cycle of a sample was ignored as this represents the lump of gel added using a spatula melting and reforming in the pan for the first time and is inherently different to the subsequent cycles. After this first heat-cool the temperature of each transition remained consistent for each sample. Three samples were measured, all 50 mM gels with **L,L,L-G2Lys** and either **C6R**, **C6S** or a mixture of both. As expected, the gel formed with **C6R** had transitions at higher temperatures than the gel formed with **C6S**. When the gel with a 1:0.5:0.5 mixture of **L,L,L-G2Lys**, **C6R** and **C6S** was analysed, it showed a single transition, clearly suggesting that a single, co-assembly network is formed, containing both enantiomers of the amine. Pleasingly, this transition occurs at temperatures in between those for the gels formed with **C6R** or **C6S** individually. Also, neither the endothermic nor exothermic peaks of this mixed sample were any broader than those of the other samples, further supporting the conclusion that only one network is formed.

Table 4.1. Temperature of enthalpic changes relating to gel-sol (endotherm) and sol-gel (exotherm) transitions in gels formed with **C6R** and **C6S**.

%C6R	%C6S	Endotherm	Exotherm
100	0	104°C	93°C
50	50	95°C	81°C
0	100	85°C	65°C

Further examination of gels formed was conducted using VT-NMR experiments. Three 10 mM gels were formed in NMR tubes using toluene-d_8, one with a mixture of **L,L,L-G2Lys** and **C6R**, one with **L,L,L-G2Lys** and **C6S** and one with a mixture of **L,L,L-G2Lys**, **C6R** and **C6S** (1:0.5:0.5 equivalents). All of these samples also contained a 10 mM concentration of **DPM** as an internal standard. The temperature of the sample was increased and the ^{1}H NMR spectra recorded at

5°C intervals. The concentration of mobile **L,L,L-G2Lys** at each temperature was plotted to follow the dissolution of the gel network (Figure 4.8.).

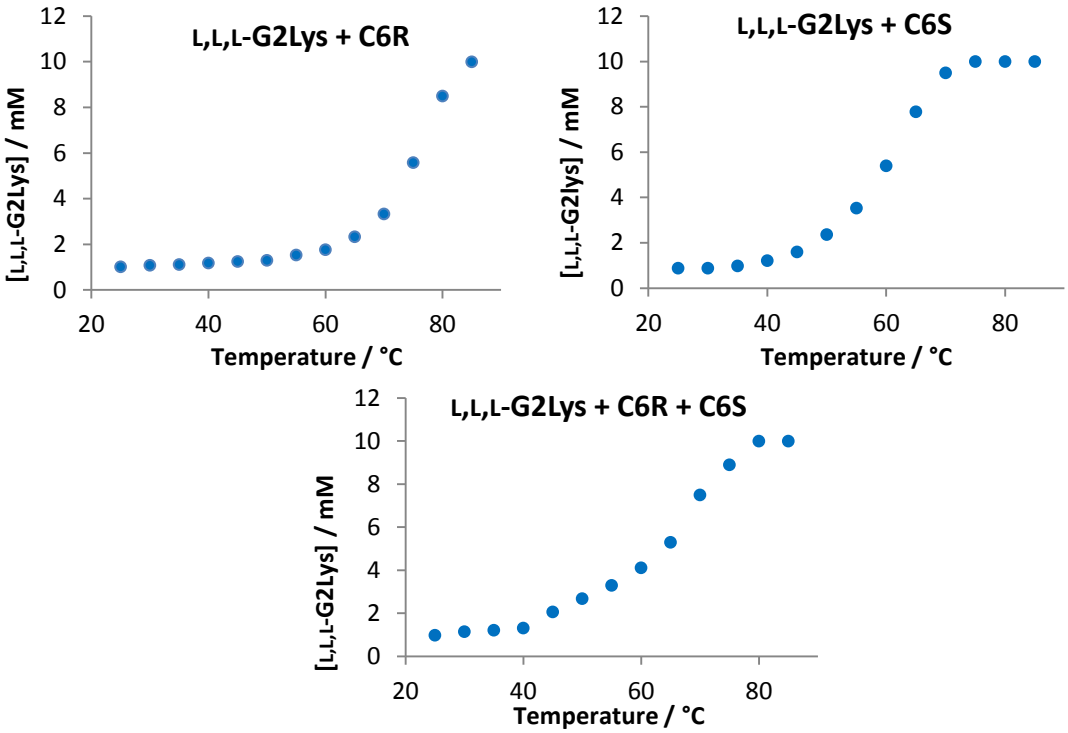

Figure 4.8. Concentration of **L,L,L-G2Lys** visible in gels of **L,L,L-G2Lys** and **C6R/S** as temperature increases. Toluene-d_8.

The graphs are similar to those shown for the samples with **L,L,L-G2Lys** and non-chiral amines in the previous chapter. As with these previous samples, the $T_{100\%}$ – the temperature at which all the gelator is dissolved and "visible" in the ^{1}H NMR – and the [Insol]@T_{gel} – the concentration of gelator that is "invisible" and still part of the gelator network at the T_{gel} – can be found for each gel. These values are recorded in Table 4.2.

Table 4.2. Comparison of molecular ($T_{100\%}$ and [Insol]@T_{gel}) and materials properties (T_{gel} and MGC) for gels formed with enantiomeric amines **C6R/S**.

%C6R	%C6S	$T_{100\%}$	T_{gel}	[Insol]@T_{gel}	MGC
100	0	83°C	80°C	1.8 mM	0.5 mM
50	50	77°C	74°C	1.6 mM	1.0 mM
0	100	69°C	67°C	1.4 mM	1.5 mM

The $T_{100\%}$ and T_{gel} values are similar for each sample, with the $T_{100\%}$ values slightly higher in each case as this represents the point at which the gelator network is completely disbanded, where as the T_{gel} is the point at which the network can no longer support itself against the force of gravity. When comparing the MGC values to the [Insol]@T_{gel} values they clearly have opposite trends. The MGC values indicated that the gelator complex made with **L,L,L-G2Lys** and **C6R** is the most effective gelating species and the complex made with **C6S** the least effective, the sample with a mixture of these enantiomers is between the two. The [Insol]@T_{gel} values on the other hand appear to show that all of the samples require a roughly equivalent concentration of formed network but be stable to inversion. The values of [Insol]@T_{gel} are generally higher than the MGC values. However, as proposed in the previous chapter, some discrepancy between these two properties can be expected given that they are measured using such different methods.

The ΔH_{diss} and ΔS_{diss} values for each gel can be found using the method explained in the previous chapter. The plots of ln[*Sol*] against 1/T are shown in Figure 4.9. and the ΔH_{diss} and ΔS_{diss} values calculated from these plots are collected in Table 4.3.

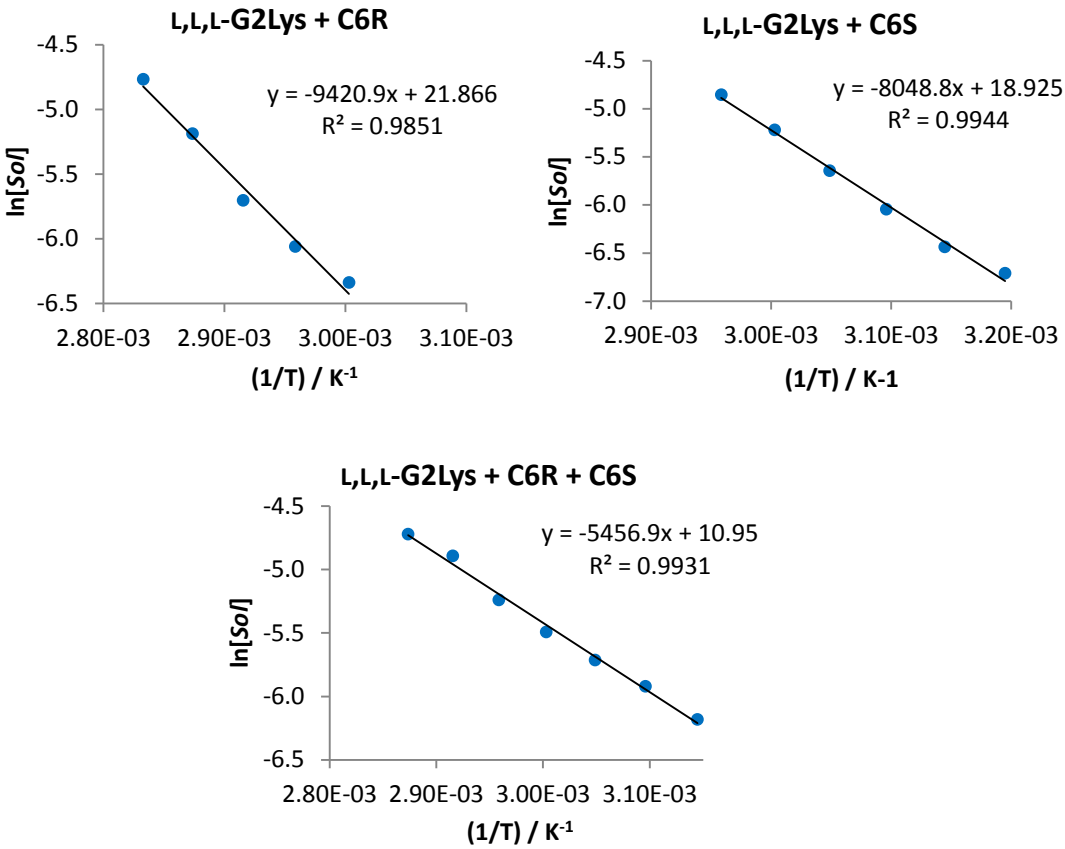

Figure 4.9. Van 't Hoff plots of gels formed form **L,L,L-G2Lys** and **C6R/S**.

Table 4.3. Summary of data calculated from van 't Hoff plots.

Amine	ΔH_{diss} / KJ mol^{-1}	ΔS_{diss} / J K^{-1} mol^{-1}
C6R	78.3	181
C6S	66.9	157
C6R + C6S	45.4	91.0

The values of ΔH_{diss} and ΔS_{diss} produced by the plots are very revealing and indicate a similar enthropy-enthalpy compensation type effect to that observed in the previous chapter. The values for the sample made with **C6R** are higher than those for the gel made with **C6S**. This would suggest that the **L,L,L-G2Lys** and **C6R** gel, with a larger entropic gain upon dissolution is likely a highly organised, more rigid, potentially more closely packed structure. The larger endothermic change upon dissolution of this network indicates that it is better able to take

advantage of favourable hydrogen bonding interactions in the gel phase, perhaps again indicative of a more closely packed structure. The fact these values are lower for the **C6S** sample indicates that this sample is less well organised and as a result is unable to take advantage of hydrogen bonding to the same extent. The most surprising result is that the gel produced with both **C6R** and **C6S** has ΔH_{diss} and ΔS_{diss} values that are much lower than for the other gels. This indicates that complexes in the network are far less tightly bound, making dissolution less entropically favourable and less able to take advantage of the intermolecular hydrogen bonding. This would also make the fibres more disordered and gelation less entropically unfavoured. This is possibly due to the network having to accommodate both **C6R** and **C6S** into the fibres and the diastereomeric complexes formed not packing into supramolecular aggregates together efficiently. These results are indicative of a balance between enthalpic and entropic factors, as for the more disordered mixed fibres the reduction in entropic cost more than compensates for the loss of enthalpic favourability compared to **C6S**. This is indicative of a co-assembly with **L,L,L-G2Lys** and both enantiomers of the amine forming the gel network. This can be observed by looking at the FEG-SEM images of the xerogel formed from this mixed gel (Figure 4.10.) which shows a single network that is similar to both the xerogels made with **C6R** or **C6S**.

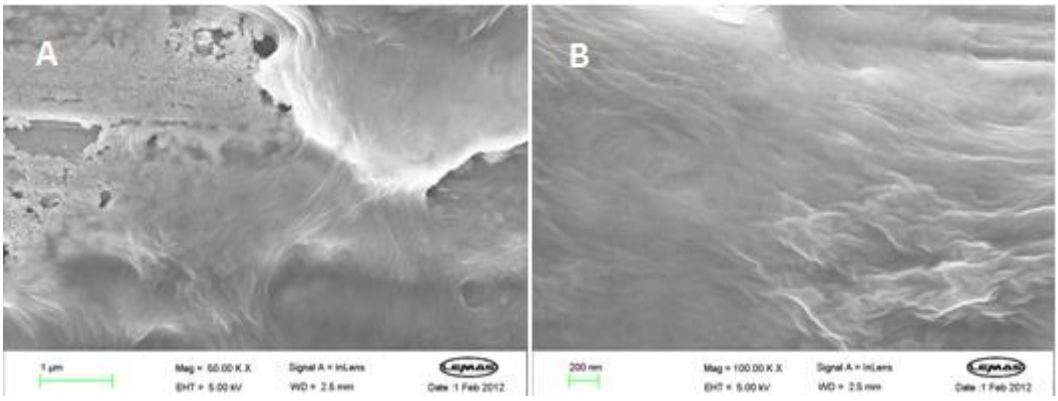

Figure 4.10. FEG-SEM images of xerogels formed from **L,L,L-G2Lys**, **C6R** and **C6S** A) Scale bar = 1 µm, B) Scale bar = 200 nm.

The fact that the T_{gel} of this gel is exactly between that of the gels formed with either **C6R** or **C6S** is down to the balance between ΔH_{diss} and ΔS_{diss}, which are both individually well below the values for the gels made with only one enantiomer. The formation of the gel made with **C6R** is driven by its high enthalpic favourability which offsets the fact it is highly entropically unfavourable. The formation of the gel formed with both **C6R** and **C6S** occurs because of its

low entropic cost, which compensates for its low enthalpic gain. The gel formed with **C6S** has the worst balance of enthalpy and entropy and as a result is the least stable gel. The ΔH_{diss} and ΔS_{diss} generated by this analysis can, as in the previous chapter, be used to predict the concentration of **L,L,L-G2Lys** visible in the ^{1}H NMR as the temperature increases. This can be compared to the experimentally observed results to validate this model (Figure 4.11.).

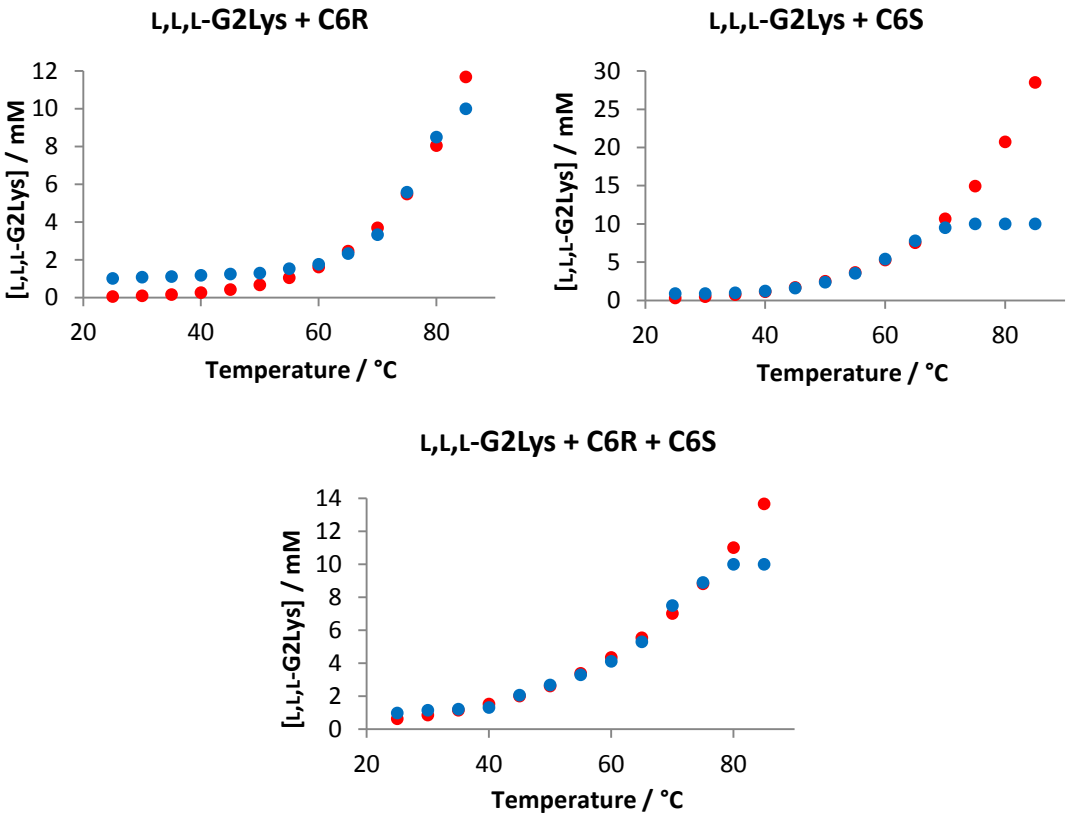

Figure 4.11. Plots showing experimental (blue) and calculated (red) concentration of solubilised gelator complex in each gel. Toluene-d_8.

The predicted data maps well onto the experimentally recorded data in all cases (Figure 4.11), only diverging at very low concentration where integration of the base line gives an artificially high concentration and above 10 mM, where there is no limit on how much soluble complex the calculated results can predict, even in samples with a total concentration of 10 mM.

4.1.2. Using Different Chiral Amines

Now that the effect of forming gels with **L,L,L-G2Lys** and mixtures of **C6R** and **C6S** had been investigated, it was still to be seen whether using a range of different chiral amines would have

the same consequences. A variety of commercially available chiral amines (Figure 4.12.) were tested for their ability to gelate toluene when mixed with **L,L,L-G2Lys**. Then the thermal stabilities of gels with different ratios of both enantiomers of each amine were measured in the same way that gels formed with mixtures of **L,L,L-G2Lys**, **C6R** and **C6S** were tested. The results produced by each amine should provide an insight into how the structure of the amine mediates the effect of chirality.

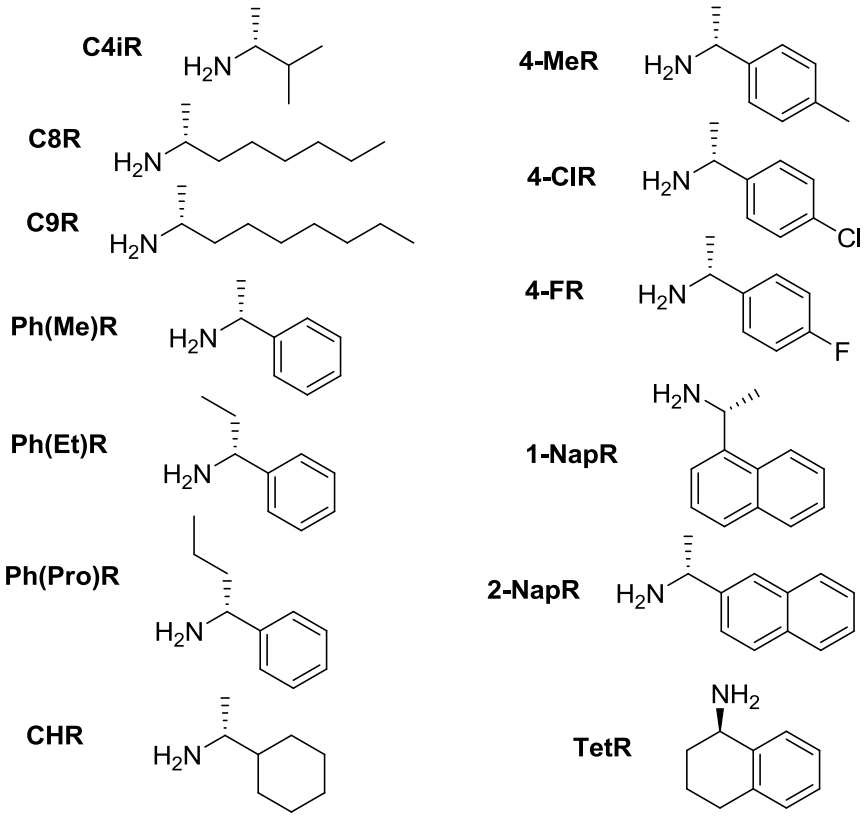

Figure 4.12. Chiral amines chosen for screening, only *R* enantiomers are shown.

The first amines tested were chiral alkyl amines **C4iR/S**, **C8R/S**, **C9R/S** and **CHR/S**. As shown previously in Figure 4.5. this data for **C6R/S** showed a curve similar to the majority rules type curves commonly seen for mixtures of enantiomers. We can see this is not the same for gels made with **L,L,L-G2Lys** and **C8R/S** or **C9R/S**, comparable amines with a longer alkyl chain length (Figure 4.13.). The graphs for gels made with **C8R/S** or **C9R/S** show less symmetrical line shapes than the graph of gels made with **C6R/S**. In the region where there is a large majority of **C8S** or **C9S** present the T_{gel} values do not begin to really increase until ca. 30% of **C8R** or **C9R** is added respectively. However in the region where the *R* enantiomer is in excess, the decrease in T_{gel} value seems to begin as soon as any *S* enantiomer is added. In both these instances the *S*

enantiomer appears to be more disruptive than the *R* enantiomer is. The temperature range over which the different T_{gel} values are spread is roughly the same in each case. For 2-aminohexylamine gels the different between the 100% *R* and 100% *S* gels is 13°C, where as for **C8R/S** and **C9R/S** this value is 16°C.

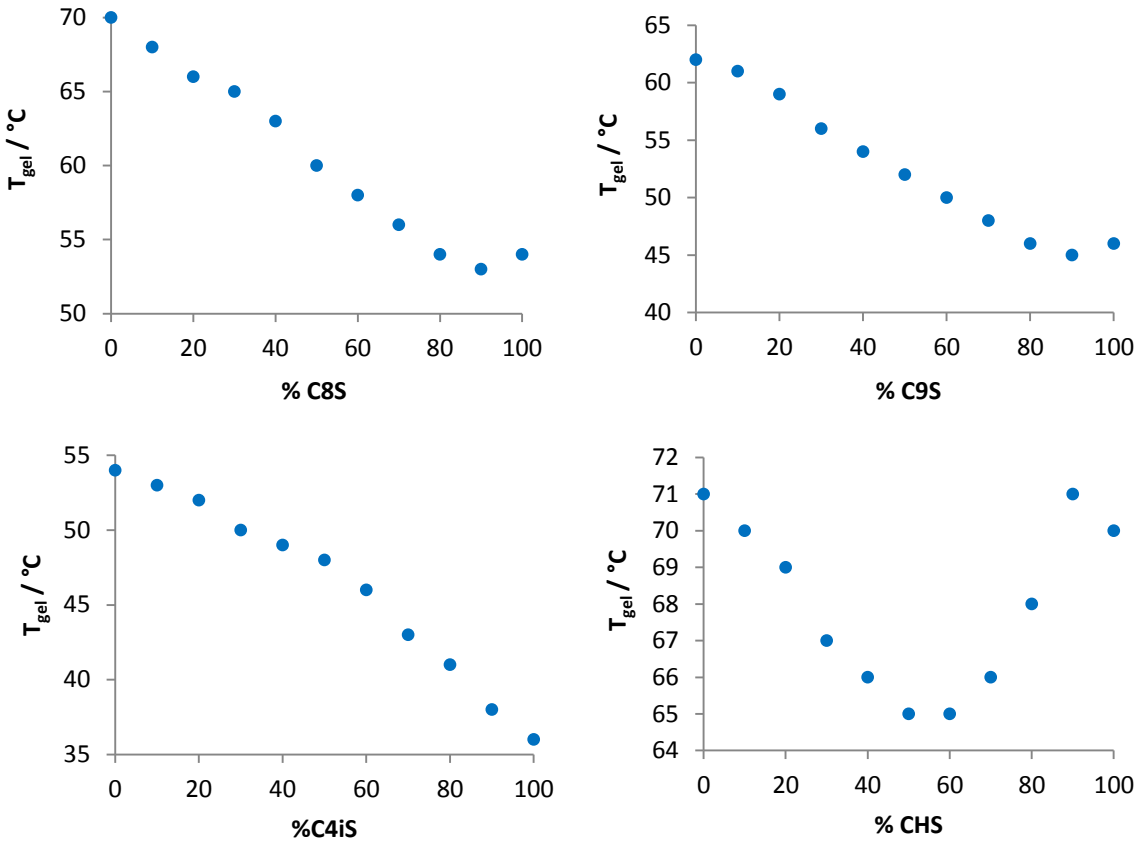

Figure 4.13. T_{gel} values of gels with **L,L,L-G2Lys** and a varying ratio of either **C8R** and **C8S**, **C9R** and **C9S**, **C4iR** and **C4iS** or **CHR** and **CHS**. Toluene.

The data for gels made with **C4iR/S** produce a slightly different graph. Mixing the enantiomers of this short, branched amine produces a graph with little curvature. There is a slight curve which makes all the points sit above where a straight line would lie, however with the ±1°C error associated with each point, this could in fact be a straight line. When this is compared to the other amines it is seen that the larger amines **C8R/S** and **C9R/S** show the *S* enantiomer having more disruptive effect, with **C6R/S** both enantiomers seen to have an equal effect (symmetrical line shape) and with **C4iR/S** the *R* enantiomer seems to be dominant. With the gels formed with **CHR/S** the thermal stability of the gels decreases when the two enantiomers are mixed together. This graph is, incidentally, very similar to what is often observed when two

enantiomeric gelators are mixed together and the mixed chirality systems form less stable gels.[326]

The graphs for gels made with aromatic amines **Ph(Me)R/S**, **4-MeR/S**, **4-ClR/S** and **4-FR/S** are shown in Figure 4.14. Aromatic amines **Ph(Et)R/S** and **Ph(Pro)R/S** did not induce gelation in toluene when mixed with **L,L,L-G2Lys**. This is likely due to the increased steric bulk of the amines resulting in complexes that are too bulky to pack into the supramolecular fibres required for gelation. Interestingly, **Ph(Et)R/S** was better at inducing viscosity or forming partial gels than **Ph(Pro)R/S**, providing more evidence that their poor gelation ability is down to the increasing steric bulk around the chiral centre. This is a finding almost as surprising as the effect chirality has, as the change in steric bulk is just one or two CH_2 groups being added to a complex with a mass of over 900 Da – this suggests that there must be close packing around the chiral centres consistent with the significant effects of chirality on gel stability.

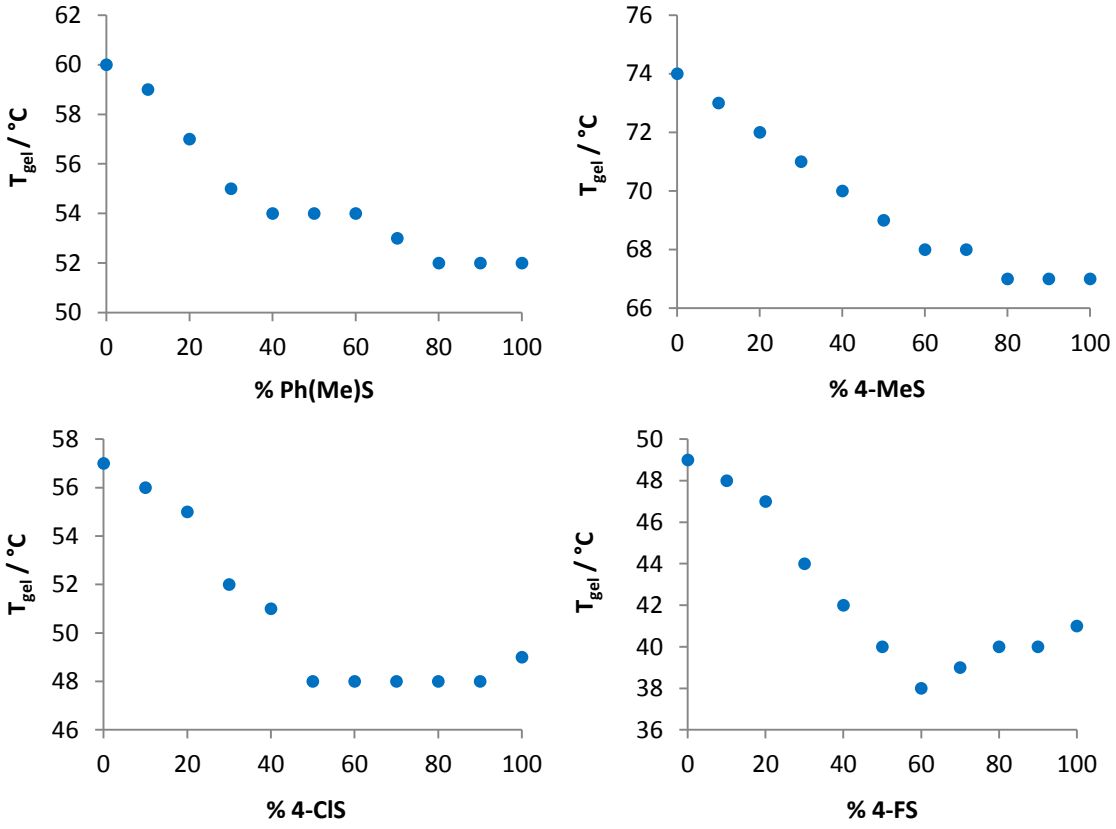

Figure 4.14. T_{gel} values of gels with **L,L,L-G2Lys** and a varying ratio of either **Ph(Me)R** and **Ph(Me)S**, **4-MeR** and **4-MeS**, **4-ClR** and **4-ClS** or **4-FR** and **4-FS**. Toluene.

In all the graphs, the difference in T_{gel} between the gel made with entirely the *R* or *S* enantiomer is constant at 7-8°C. The graphs made produced from gels made with mixtures of **Ph(Me)R/S**, **4-MeR/S** and **4-ClR/S** are all very similar, especially the first two. The *S* enantiomers seem to be much more disruptive than the *R*, with even a small amount of *S* amine causing the thermal stability of the gels to drop noticeably. It takes a much higher percentage of *R* amine to cause the stability of the mixed gels to increase. The gels made with **4-ClR/S** show the *S* enantiomer possibly having a more disruptive effect than in the other samples, but not greatly. The gels made with **4-FR/S** are a little different, with some that are made from a mixture of both enantiomers being less stable than gels made with either entirely **4-FR** or **4-FS**. The differences between these amines are not likely to be due to electronic effects as there were no π-π interactions observed in the CD spectra of closely related samples made with non-chiral amines (previous chapter). Therefore, this difference in behaviour is more likely due to steric effects, arising from having to accommodate a different group at the *para* position of the aromatic ring. This chapter and the previous one highlight the difference even a slight change in steric constraints can make to gel network formation. It is interesting to compare the gels formed with **Ph(Me)R/S** to those formed with **CHR/S** which formed the weakest gels with mixing **CHR** and **CHS**, with the only chemical difference between the two being the lack of aromaticity of the amine. This may be due to the effect of loss of planarity on the molecular packing when aromaticity of the amine is lost, preventing the effective co-assembly of the different amine enantiomers.

Linked to this comparison are the results from gels made of mixtures of **L,L,L-G2Lys** and **1-NapR/S** or **2-NapR/S** (Figure 4.15.). Of course, both can be seen as being related to **Ph(Me)R/S**, but with a larger, more bulky aromatic system. Despite this, neither graph is similar to that produced by gels containing **Ph(Me)R/S**. Gels produced with mixtures of **L,L,L-G2Lys** and **1-NapR/S** show a very clear trend in T_{gel} values, where **1-NapR** has a larger effect on the T_{gel} values than **1-NapS**. After 20% of **1-NapS** is incorporated the T_{gel} values drop a small amount (7°C). The T_{gel} values to not decrease further until ca. 70% of **1-NapS** is incorporated into the network. The difference between the T_{gel} values of the gel made with **L,L,L-G2Lys** and **1-NapR** and the gel made with **L,L,L-G2Lys** and **1-NapS** is 26°C, a very large difference when compared to the other amines tested. In contrast to this, the T_{gel} values produced by samples made with **2-NapR/S** are spread over 4°C. Being separated by such a short range and with an error of ±1°C on each measurement, there is no trend to be seen. It is striking that despite the huge difference in the behaviour of gels made with these two amines they differ only by the

position of substitution on the aromatic system. This offers further evidence that very small differences in molecular shape alters the molecular packing of the complexes in the gel network, which in turn has a large effect on gel formation.

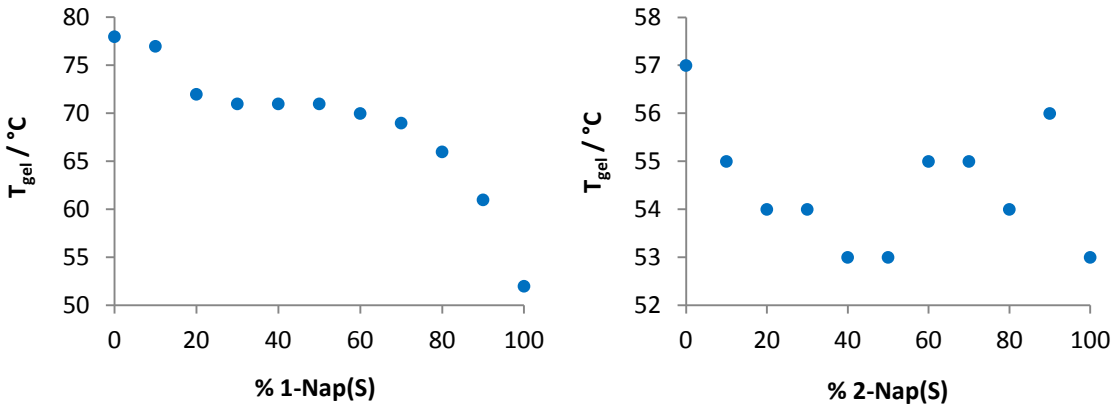

Figure 4.15. T_{gel} values of gels with **L,L,L-G2Lys** and a varying ratio of **1-NapR** and **1-NapS**. Toluene.

The final chiral amine tested was **TetR/S**. This amine differed from the others because there was no methyl group attached to the chiral centre (or ethyl / propyl in the case of the unsuccessful **Ph(Et)R/S** and **Ph(Pro)R/S** containing samples). In this case the chiral centre was part of a cyclic ring system. The T_{gel} values of these gels span a range of 18°C with the largest change in T_{gel} occurring in the region between ca. 30% of *R* or *S* enantiomer has been added. There is nothing radically different shown in these values compared to what is shown by the other amines.

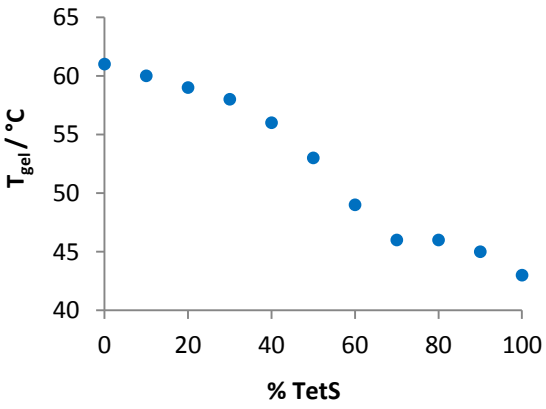

Figure 4.16. T_{gel} values of gels with **L,L,L-G2Lys** and a varying ratio of **TetR** and **TetS**. Toluene.

In summary, it appears that the chirality of the amine mixed with **L,L,L-G2Lys** has a large effect on the assembly of the resulting complexes and in turn, a pronounced effect on the gel that is produced. The difference between the gel formed with **L,L,L-G2Lys** and either **C6R** or **C6S** has been probed in detail using a range of techniques and it has been seen that the chirality of the amine profoundly affected the assembly of complexes in solution (CD), the morphology of fibrous network formed (FEG-SEM and TEM) and ultimately the stability of the material produced (T_{gel} and NMR). Furthermore, it has been found that when a gel is formed from a mixture of **L,L,L-G2Lys** and **C6R/S** with varying ratios of *R* to *S* enantiomer, a co-assembled network is formed. This new co-assembly has properties that are controlled by the presence of both enantiomers of the amine and can be changed by adjusting to ratio of one enantiomer to the other. This shows the remarkable tunability of these systems. Finally, the way the structure of the rest of the amine altered the effect of chirality has been investigated by studying a range of different chiral amines. This study has not been conclusive in producing predictive rules but does reveal the sensitivity (and therefore tunability) of these systems. This is best demonstrated by contrasting the results for gels made with **1-NapR/S** which differ in thermal stability by 26°C while gels made with **2-NapR/S** only differ by 4°C.

4.2. Component Selection with Chiral Amines

4.2.1. Testing Whether Component Selection Can Be Achieved

Gels made with a 1:1 mixture of **L,L,L-G2Lys** and either the *R* or *S* enantiomer of an amine have different thermal stabilities in most of the cases tested. It was demonstrated in the previous chapter, that when different amines form gels of different thermal stabilities with **L,L,L-G2Lys**, one can be selectively incorporated into the gel network over another. The next step was to discover whether this work could be repeated using different enantiomers of an amine, i.e. could enantioselective uptake of one enantiomer over another into the gel network be achieved due to the different stabilities of the diastereomeric gels formed with **L,L,L-G2Lys**?

Gels were made with **L,L,L-G2Lys** and either **C6R** or **C6S** in toluene, over the concentration range of 2-10 mM and the T_{gel} values of these gels were measured. Then gels with a 1:1:1 mixture of **L,L,L-G2Lys**, **C6R** and **C6S** were made. In this mixture, the **L,L,L-G2Lys** can form a network with entirely **C6R** or **C6S**, or any mixture of both. In effect, rather than being complexed to both amines, as in the previous experiments, **L,L,L-G2Lys** has a choice of enantiomer with which to form a gel. The T_{gel} values of these more complex gels were

measured and compared to those of the gels formed with **L,L,L-G2Lys** and **C6R** or **C6S** only (Figure 4.17.).

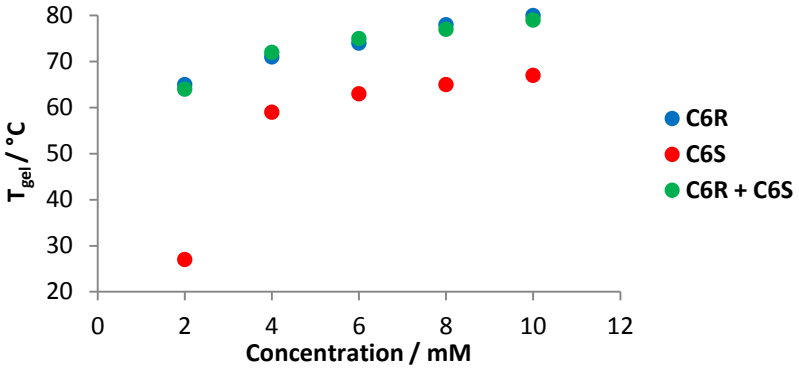

Figure 4.17. T_{gel} values of gels with **L,L,L-G2Lys** and either **C6R**, **C6S** or a mixture both.

Unsurprisingly, the T_{gel} values of the gels made with **L,L,L-G2Lys** and **C6R** are higher at all concentrations than those for gels made with **L,L,L-G2Lys** and **C6S**. The most impressive result is that the T_{gel} values of the gel made from a complex mixture of both enantiomers overlap almost completely with those formed with only the **C6R** enantiomer. This gives a very strong indication that the gel network is formed overwhelmingly with **L,L,L-G2Lys** and **C6R**, whilst the **C6S** remains in solution. In fact, comparing the T_{gel} value of the 10 mM gel formed with the mixture of **C6R** and **C6S** with the data in Figure 4.5. it seems to indicate that <20 % of the gelator network is made with **C6S**. The 1:1:1 mixture of **L,L,L-G2Lys**, **C6R** and **C6S** could be further analysed by CD and the spectrum compared to that of the samples made with **L,L,L-G2Lys** and **C6R** or **C6S**. The spectra of all three samples are shown in Figure 4.18.

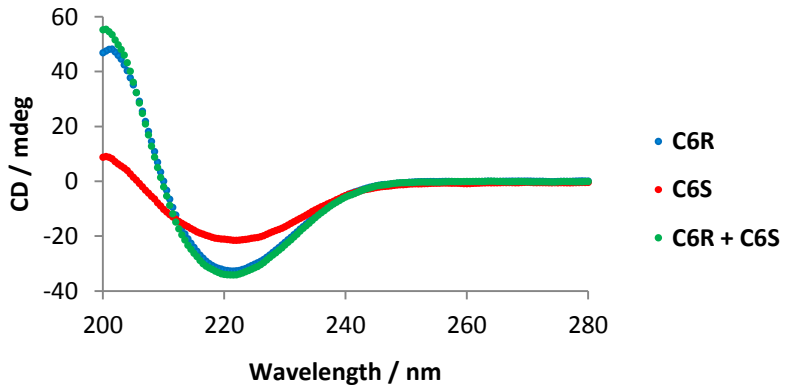

Figure 4.18. CD spectra of samples made with **L,L,L-G2Lys** and either **C6R**, **C6S** or a mixture both. 0.625 mM. 95:5 Methylcyclohexane to Dioxane.

The spectrum for the sample where **L,L,L-G2Lys** can form a network with either **C6R** or **C6S** is almost identical to the spectrum produced by the sample made with only **L,L,L-G2Lys** and **C6R**. This could be taken as another strong indicator of selective uptake of **C6R** into the self-assembled aggregates with **L,L,L-G2Lys**. However, the CD spectra shown in Figure 4.6. showed that the CD spectrum is basically invariant with the changing proportion of **C6R** to **C6S** incorporated into the network, until 90-100 % of the amine used was **C6S**.

The xerogel produced from the mixture of **L,L,L-G2Lys**, **C6R** and **C6S** was imaged by FEG-SEM (Figure 4.19.). The images show a sample with a very ill-defined morphology. There are no distinct fibres visible. When these images are compared to the samples made with only **L,L,L-G2Lys** and **C6R** or **C6S** (Figure 4.3.) it becomes clear the morphology of this sample is far more similar to that made with **C6R** than that made with **C6S**. This again suggests that the network formed is mostly **L,L,L-G2Lys** and **C6R**.

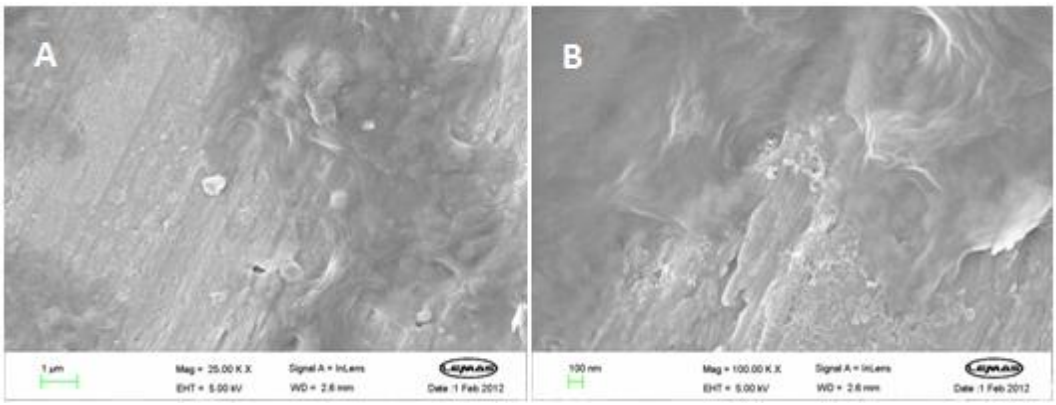

Figure 4.19. FEG-SEM images of xerogels formed from **L,L,L-G2Lys**, **C6R** and **C6S**. A) Scale bar = 1 µm. B) Scale bar = 100 nm.

Further analysis of the gel made with a 1:1:1 mixture of **L,L,L-G2Lys**, **C6R** and **C6S** was performed using VT-NMR, in the same way as for the other gels. The gel made with both enantiomers (10 mM) was made in an NMR tube with toluene-d_8. The sample was heated and spectra recorded at 5°C intervals form 25 to 80°C. The concentration of **L,L,L-G2Lys** mobile in solution at each point can be found by comparison with an internal standard (**DPM**). This data was then taken and used to produce a van 't Hoff plot from which the ΔH_{diss} and ΔS_{diss} of the gel can be found. These values can again be tested by using them to predict how much **L,L,L-G2Lys** will become soluble as the temperature increases and comparing that to the experimentally observed results. The plots showing the van 't Hoff plot and the experimental and calculated solubility of **L,L,L-G2Lys** is shown in Figure 4.20.

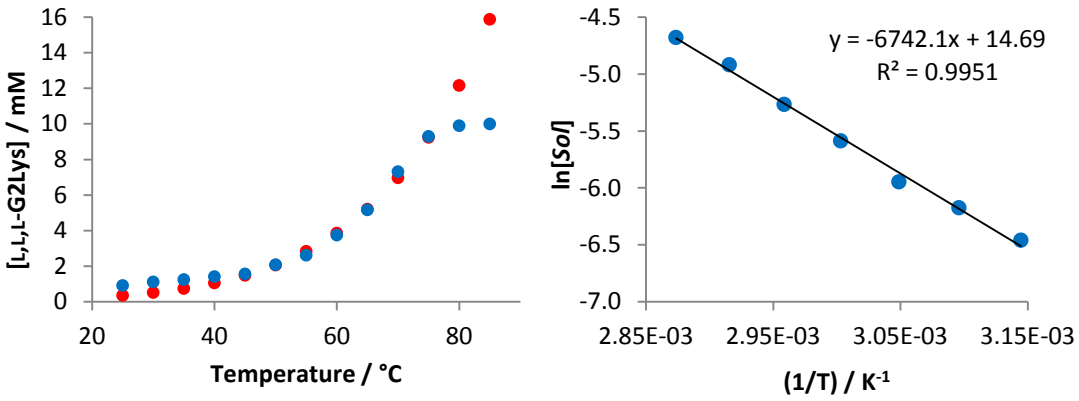

Figure 4.20. Plots showing experimental (blue) and calculated (red) concentration of **L,L,L-G2Lys** as temperature increases and the van 't Hoff plot.

The gel produces a ΔH_{diss} value of 56.0 kJ mol^{-1} and a ΔS_{diss} value of 122 J mol^{-1}. The change in solubility predicted by these values as the temperature increases is very close to the experimentally observed results. When they are compared to those of gels made with **L,L,L-G2Lys** and either **C6R** or **C6S**, or a 1:0.5:0.5 mixture of each component (Table 4.3.), these values are lower than those for either gel made with **L,L,L-G2Lys** and a single enantiomer. This indicates that the gel is not made with entirely **C6R** or **C6S** incorporated into the gelator network with **L,L,L-G2Lys** but suggests that there might be some exchange lowering the entropy. Comparison between the gels made with a 1:1:1 and a 1:0.5:0.5 mixture of **L,L,L-G2Lys**, **C6R** and **C6S** show that the ΔH_{diss} and ΔS_{diss} values of the 1:1:1 mixture are higher than those formed with a 1:0.5:0.5 mixture. This indicates that the amount of **C6R** and **C6S** incorporated into the network is not equal in the 1:1:1 sample. Based on the previous results, it is therefore likely more *R* enantiomer is included into the network, rather than more **C6S**. Therefore, when combined with the other experiments carried out, this provides more evidence that **C6R** is preferentially taken into the gelator network with **L,L,L-G2Lys,** over **C6S**.

Given the limitations of FEG-SEM, to further investigate the different morphologies between the gels made with either **C6R** or **C6S** or mixtures of both, small and wide angle x-ray scattering experiments (SAXS and WAXS) were conducted by the group of Professor Ian Hamley (Department of Chemistry, University of Reading) (raw data shown in Appendix C). Scattering experiments were carried out on both solvated gels and xerogels made with **L,L,L-G2Lys** and either **C6R** or **C6S**, a 1:0.5:0.5 mixture or a 1:1:1 mixture where **L,L,L-G2Lys** can select one enantiomer or the other. The data are summarised in Table 4.4.

The SAXS data for the solvated gels showed the gels made with **C6R** and **C6S** had different cylinder form factors of 4 and 3 nm respectively. The gel with 0.5 equivalent of each had a cylinder form factor of 3 nm – the same as the gel made with only **C6S**. The gel made with 1 equivalent of both **C6R** and **C6S**, where **L,L,L-G2Lys** can form a network with either had a cylinder form factor of 4 nm – the same as the gel made with only **C6R**. The WAXS data for these samples showed they were well ordered but all samples showed the same peaks at 2.40, 2.08 and 1.53 Å. The SAXS data for the xerogels showed a number of defined Bragg peaks. The sample made with **L,L,L-G2Lys** and **C6R** showed peaks at 2.50 and 1.55 nm. Again this was very similar to the sample made with **L,L,L-G2Lys** and 1 equivalent of both **C6R** and **C6S**. The peaks for this sample were seen at 2.45 and 1.55 nm. Also like the data for the solvated gels, the xerogels made with **L,L,L-G2Lys** and either **C6S** or 0.5 equivalents of **C6R** and **C6S** showed very similar results, both samples showing Bragg peaks at 2.30 and 1.55 nm. The WAXS data for the xerogel samples was poorly defined showing some broad peaks which are shown in Table 4.4. In summary, the scattering data gives further insight into the difference between the networks formed with only **C6R** or **C6S**, samples which give different Bragg peaks (xerogels) and cylinder form factors (gels). Surprisingly, the samples made with 0.5 equivalents of both **C6R** and **C6S** show data very similar to that of the gel formed with only **C6S**. The previous experiments conducted on this mixture indicated it showed a mixed character, having properties of each amine present. More predictably was that the samples formed with 1 equivalent of both **C6R** and **C6S** were very similar to the sample formed with only **C6R** providing further evidence that this amine is selectively incorporated into the gelator network over **C6S**.

Table 4.4. Summary of SAXS and WAXS data form gel and xerogel samples. CFF = Cylindrical form factor.

	Gel		Xerogel	
Sample	**SAXS**	**WAXS**	**SAXS**	**WAXS**
L,L,L-G2Lys:C6R	CFF = 4 nm	2.40, 2.08, 1.53 Å	d = 2.50, 1.55 nm	7.30, 4.50, 4.07 Å
L,L,L-G2Lys:C6S	CFF = 3 nm	2.40, 2.08, 1.53 Å	d = 2.30, 1.55 nm	7.30, 4.50, 4.07 Å
L,L,L-G2Lys:C6R:C6S 1:0.5:0.5	CFF = 3 nm	2.40, 2.08, 1.53 Å	d = 2.30, 1.55 nm	7.30, 4.50, 4.07 Å
L,L,L-G2Lys:C6R:C6S 1:1:1	CFF = 4 nm	2.40, 2.08, 1.53 Å	d = 2.45, 1.55 nm	7.30, 4.50, 4.07 Å

The use of a chiral shift reagent to try to quantify the amount of *R* or *S* enantiomer of **C6R/S** that is excluded from the gel network was investigated. The first such reagent tested was chiral europium complex $Eu(hfc)_3$ (Figure 4.21.). Unfortunately, when this reagent was added to an equimolar mixture of **C6R** and **C6S** it was unable to separate the peaks belonging to the two enantiomers. The NMR peaks of the CH_3CH resonace of **C6R/S** with increasing amounts of $Eu(hfc)_3$ is shown in Figure 4.21.

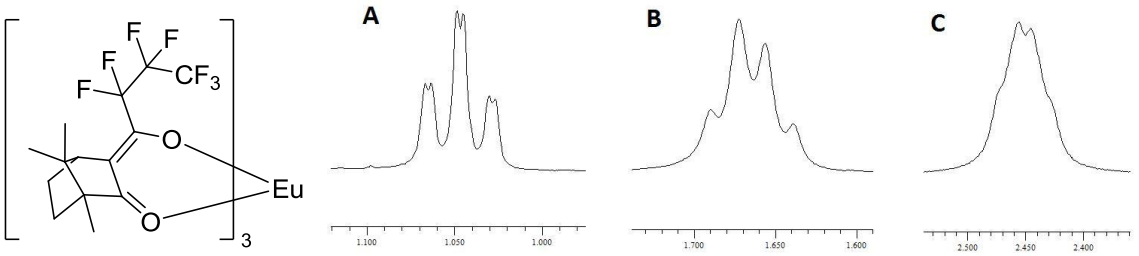

Figure 4.21. Structure of chiral shift reagent $Eu(hfc)_3$ and ^{1}H NMR spectra of CH_3CH peak with increasing amounts of $Eu(hfc)_3$ added. A) 0.1 Eq. of $Eu(hfc)_3$, B) 0.5 Eq. of $Eu(hfc)_3$ and C) 1.0 Eq. of $Eu(hfc)_3$.

The peaks shown in Figure 4.21. indicate that $Eu(hfc)_3$ could separate the peaks of each enantiomer to some extent, but not enough for each peak to be independently resolved. To try and improve this result a different chiral shift reagent was used. The compound Boc-Phe-

OH (Figure **4.22**.) was mixed with both **C6R** and **C6S** in different NMR samples. The chemical shift of the C*H*$_3$CH peak was different for each enantiomer (Δδ = 0.013 ppm). When Boc-Phe-OH was added to an equimolar mixture of **C6R/S** the doublets produced by each C*H*$_3$CH peak overlap to form an apparent triplet as shown in Figure **4.22**. It was considered that the outer peaks of the triplet could be integrated to give the relative amount of **C6R** or **C6S** in a sample. Unfortunately, with a gel formed with an excess of **C6R/S** the signal produced by C*H*$_3$CH groups of each enantiomer were unable to be resolved. A possible explanation for this is that small amounts of **L,L,L-G2Lys** that may be present in the solution phase can also form a reversible interaction with the amines through a similar carboxylic acid group. This competing process could have reduced the effectiveness of Boc-Phe-OH as a chiral shift reagent, even if present in low concentration.

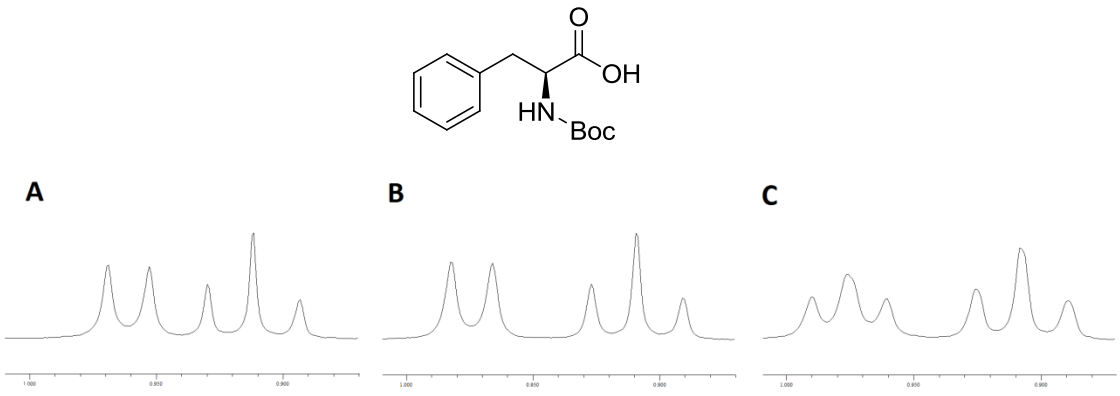

Figure 4.22. Structure of chiral shift reagent Boc-Phe-OH and ^{1}H NMR spectra of C*H*$_3$ peaks of A) **C6R**, B) **C6S** and C) **C6R/S**.

A different NMR experiment was attempted with gels formed with a 1:1:1 mixture of **L,L,L-G2Lys**, **C6R** and **C6S** in toluene (0.5 mL). After the gels had formed a further amount of toluene (0.5 mL) was gently pipetted on top of the gels and the samples were left for 24 hours. This was to allow the amine that was not included in the gel network to diffuse into the excess toluene. This solvent was then removed using a pipette and placed in a round bottom flask. The mixture was stirred at room temperature and an excess of (*S*)-methylbenzyl isocyanate was added to derivatise all of the chiral amine that had diffused into the toluene solutions. This turned the enantiomers of the amine into two different diastereomers (Scheme 4.1.), which, it was hoped, could be distinguished and quantified by ^{1}H NMR. The toluene was removed to leave a white solid. That the desired reaction had taken place was confirmed using NMR and MS.

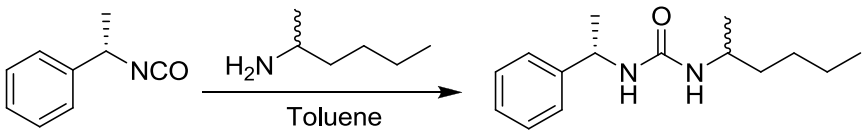

Scheme 4.1. Reaction of (*S*)-methylbenzyl isocyanate with **C6R/S**.

The solid was redissolved in $CDCl_3$, analysed by ^1H NMR and compared to samples prepared using the same method but with either **C6R** or **C6S** alone. In these simpler systems the difference in chemical shift between the peaks of the CH_3CH groups (that were originally on the amine) of each diastereomer was 0.085 ppm, a far larger difference than that achieved by Boc-Phe-OH (0.013 ppm), consistent with covalent bond formation rather than non-covalent acid-base interaction. Surprisingly there was also a large difference in the chemical shift of the peak of the terminal CH_3CH_2 group of each diastereomer (Δδ = 0.072 ppm). When the product from gels formed with both **C6R** and **C6S** was analysed the peaks of both diastereomers were easily resolved and the amount of each could be easily quantified from the CH_3CH_2 peaks of each (Figure 4.23.). Of all the urea in the sample, 20% was formed from **C6R** and 80% was formed from **C6S**. Therefore we propose that the gelator network is formed from the inverse composition (80% **C6R** and 20% **C6S**), demonstrating unambiguously that there is pronounced selective uptake of the enantiomer that forms the most stable gel network with **L,L,L-G2Lys** and providing quantitative analysis of this uptake. As such we suggest that gels of this type maybe of interest for applications in chiral resolution and enantioselective reaction pathways.

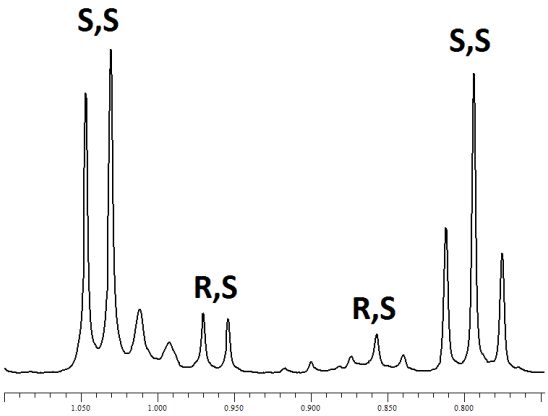

Figure 4.23. ^1H NMR of urea mixture produced from the supernatant taken from gel formed with **C6R** and **C6S**. $CDCl_3$.

It was important to determine whether the apparent selectivity for the *R* amine was due to a difference in the thermal stability of the gels formed with each enantiomer and not due to a difference in acid-base formation and complex assembly. Of course each enantiomer has the same pKa but the complexes formed with chiral **L,L,L-G2Lys** are diastereomeric, which can sometimes have different stability constants. If this were true for these complexes, than it would provide another explanation for the observed selectivity. To examine whether the formation of each diastereomeric complex was different, titration experiments were carried out. The concentration of either **C6R** or **C6S** remained constant while the concentration of **L,L,L-G2Lys** was varied. This titration had to be carried out in a solvent which did not support self-assembly of the complexes. If assembly were to take place, the formation of each complex may be changed, being differently stabilised by gel formation. As such, the experiment was carried out in $CDCl_3$. The change in chemical shift of the CH peak of **C6R** or **C6S** as the concentration of **L,L,L-G2Lys** increases is shown in Figure 4.24.

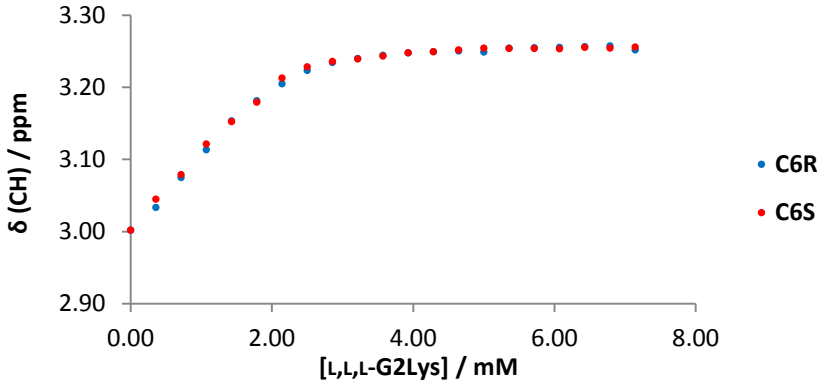

Figure 4.24. Change in chemical shift of C*H* peak of **C6R** and **C6S** with increasing concentration of **L,L,L-G2Lys**. $CDCl_3$.

The change in chemical shift of each enantiomer appears to be roughly equal. To quantify binding in each case, stability constants were fitted using WinEQNMR2.[413] In each case, constants were found using a 1:1 binding model. With **C6R** *log*K = 4.30, with **C6S** *log*K = 4.37. Both constants have around a 15% error. The experimentally measured values of the sample with **C6R** overlaid with the fit predicted using the calculated *log*K value is shown in Figure 4.25. This experiment shows quantifiably that in each case, the stability constant of the complex formed is the same – acid-base complex formation is not influencing the selective uptake of one amine enantiomer over the other.

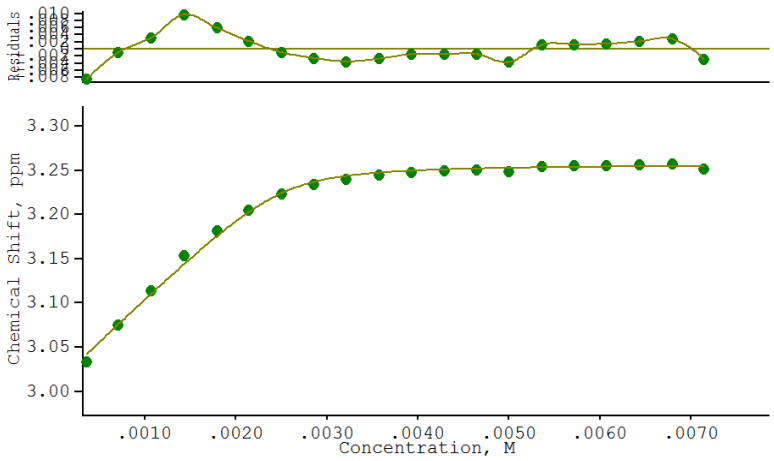

Figure 4.25. Plot showing measured shift of C*H* group of **C6R** with increasing amount of **L,L,L-G2Lys** (points) compared to theoretical data using calculated binding constant (line). Plot above shows residual error for each point.

This experiment indicated that gel formation was indeed the cause of selective incorporation of **C6R** in to the gel network, but as in the previous chapter it needed to be confirmed that this was a thermodynamic preference, not the result of a kinetically trapped gel forming when cooling the sample. This would occur if, as the sample was cooled, the network with **L,L,L-G2Lys** and **C6R** formed first simply because it has the highest T_{gel}. On reaching the temperature at which the network with **C6S** could form, all of the **L,L,L-G2Lys** would already be "used" in forming the network with **C6R**, resulting in selective uptake but controlled by kinetics. A gel with **L,L,L-G2Lys** and **C6S** was formed and then **C6R** was allowed to diffuse through the sample for 5 days (to ensure equilibration). The proportion of each amine in the network was then calculated by derivatising the excess solution phase amine with (*S*)-methyl isocyanate as already described (Figure 4.26.).

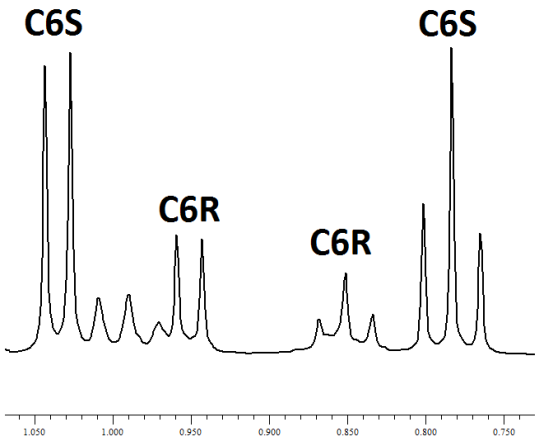

Figure 4.26. ^{1}H NMR of urea mixture produced from the supernatant taken from gel formed with **C6S** followed by diffusion of **C6R** through sample. $CDCl_3$.

The spectrum clearly shows an excess of **C6S** in solution that has clearly been displaced from the gel network by **C6R**. In the solution phase, 33% of the amine is **C6R** and 67% is **C6S**. Therefore the gelator network is 67% **C6R** and 33% **C6S**, a remarkable result which demonstrates unambiguously that the preference for **C6R** was a thermodynamic preference. This demonstrated how these gels are responsive and tuneable to different components being added, and can adapt and evolve their compositions in response to chemical stimulus. The selective uptake of **C6R** in this example is only slightly lower than that observed for the gel formed with a heat – cool cycle (80% **C6R**, 20% **C6S**). It is not surprising that the gel allowed to equilibrate over time at room temperature shows less selective incorporation of *R* amine as the network would need to be completely re-ordered to accommodate this amine, as opposed to just forming with the *R* amine instantly.

4.2.2. Component Selection With Different Amines

In summary, it has been demonstrated that when a 1:1:1 mixture of **L,L,L-G2Lys**, **C6R** and **C6S** is used to form a gel, the resulting gelator network is overwhelmingly composed of **L,L,L-G2Lys** and **C6R** whilst most of the **C6S** is left unincorporated in solution. The most conclusive experiments which unambiguously showed this were the T_{gel} values (when compared to those made with different proportions of each enantiomer) and the derivitisation of amines excluded from the gelator network with (*S*)-methylbenzyl isocyanate. We then decided to apply these techniques to similar mixtures of other chiral amines. This would allow the ability

of **L,L,L-G2Lys** to choose between different enantiomeric amines to be studied and perhaps rationalised.

The T_{gel} values of gels made with **L,L,L-G2Lys** and either **C4iR**, **C4iS** or a 1:1:1 mixture with both were compared (Figure 4.27.). The values for the gels made with a 1:1:1 mixture, where **L,L,L-G2Lys** can form a network with either amine are far closer to the values of the gels formed **C4iR** than those using **C4iS**. This gives us a qualitative indication that **C4iR** is preferentially incorporated into the gelator network with **L,L,L-G2Lys**. Once again, the T_{gel} values of the samples made with changing proportions of **C4iR** and **C4iS** (Figure 4.13.) can be used as a rough calibration curve, and the T_{gel} value of the 10 mM gel made with a 1:1:1 mixture can be used to find a predicted composition. In this case, taking into account the ±1°C error on the T_{gel} values, the predicted composition is somewhere between 20-40% **C4iS** incorporated in the gelator network. This provides us with a semi-quantitative prediction of the amount of each enantiomer present in the gel network. This result is only semi-quantitative mainly due to the relatively small differences in T_{gel} that result from the gradual change in amine composition. The amine which is excluded from the network – not selected by **L,L,L-G2Lys** – may also affect the thermal stability of the gel to some, albeit small extent due to dymanic exchange with occurs with amine fixed in the gelator network. To further quantify the uptake of each amine, the experiment using (*S*)-methylbenzyl isocyanate to derivatise the excess, non incorporated chiral amine was carried out. This experiment indicated that 32% of the amine left in solution after the gel has formed was **C4iR** and 68% of the amine was **C4iS** (Figure 4.28.). Obviously, the gel network should be the mirror image of these values, the amine incorporated into it being 68% **C4iR** and 32% **C4iS**. This shows conclusively that the selectivity shown in mixtures of **C6R** and **C6S** can also be shown for **C4iR** and **C4iS**.

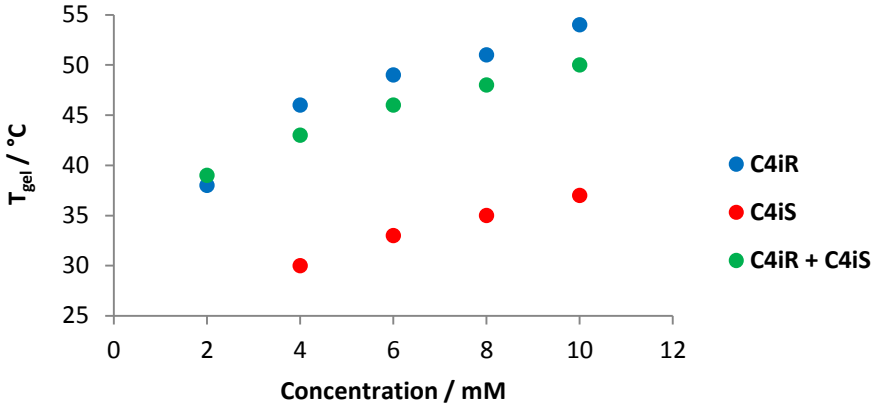

Figure 4.27. T_{gel} values of gels with **L,L,L-G2Lys** and either **C4iR**, **C4iS** or a mixture both. Toluene.

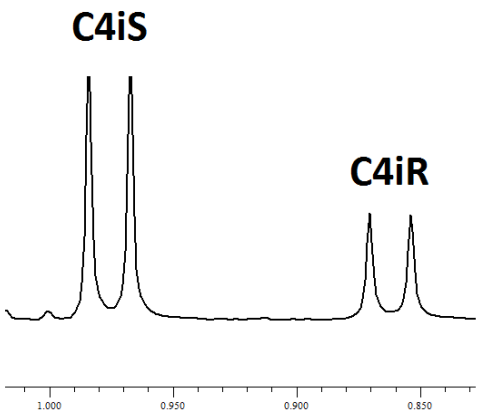

Figure 4.28. ^{1}H NMR of urea mixture produced from the supernatant taken from gel formed with **C4iR** and **C4iS**. $CDCl_3$.

The T_{gel} values of the gels made with a 1:1:1 mixture of **L,L,L-G2Lys**, **C8R** and **C8S** suggested that the *R* enantiomer was selectively incorporated into the gel network over the *S* enantiomer (Figure 4.29.). When the 10 mM gel was compared to the T_{gel} values of gels made with an overall amine concentration of 10 mM but a changing ratio of **C8R** to **C8S** (Figure 4.13.) it suggested that the gelator network is composed of between 20-40% **C8S**. When the excess amine was derivatised with (*S*)-methylbenzyl isocyanate it showed that 83% of the amine in solution was **C8S** and 17 % was **C8R** (Figure 4.30.). The composition of the gel network should be the mirror image of this (83% **C8R**, 17% **C6S**), again showing strong selective uptake of the *R* enantiomer – which forms a more stable gel network – over the *S* enantiomer – which forms a less stable gel network. The apparent selectivity here may be slightly artificially inflated by the

C*H*$_3$CH peak of the urea formed with the *S* enantiomer overlapping with another peak in the ^{1}H NMR spectrum, but this certainly does not account for all the selectivity observed between *R* and *S* amine.

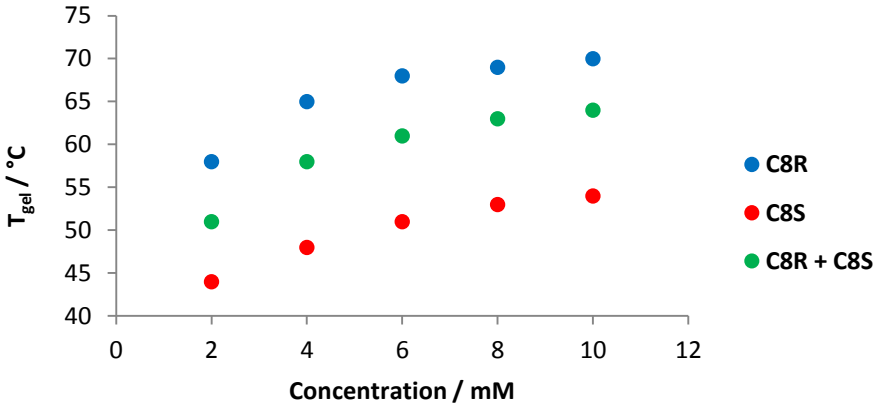

Figure 4.29. T_{gel} values of gels with **L,L,L-G2Lys** and either **C8R**, **C8S** or a mixture both. Toluene.

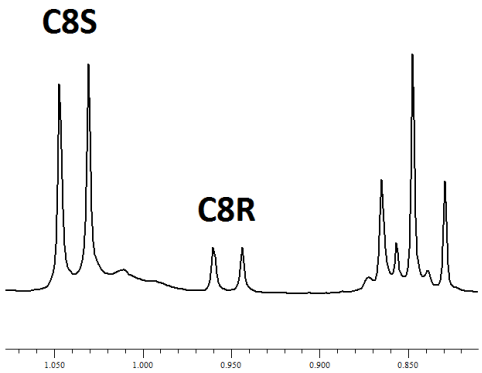

Figure 4.30. ^{1}H NMR of urea mixture produced from the supernatant taken from gel formed with **C8R** and **C8S**. $CDCl_3$.

A very similar result was seen when gels with **C9R** and **C9S** were tested. The T_{gel} values of gels formed from a 1:1:1 mixture with both **C9R** and **C9S** appear to be almost exactly in-between those made with either **C9R** or **C9S** (Figure 4.31.). However, using Figure 4.13. as a rough calibration curve for the 10 mM gel suggests that 30-50% of the gelator network is **C9S**, indicating semi-qualitatively a likely selective uptake of the *R* enantiomer of this amine similar to the other samples tested so far. When the excess amine was derivitised and the resulting diastereomers analysed by ^{1}H NMR it becomes clear that there is a selective uptake of **C9R** into the gelator network as most of the amine left in solution is **C9S** (Figure 4.32.). Integrating each

C*H*$_3$CH peak suggests that 21% of the amine in solution is **C9R** and 79% is **C9S** but this may again be affected by some overlap between the peak of the **C9S** derived diastereomer and another small peak.

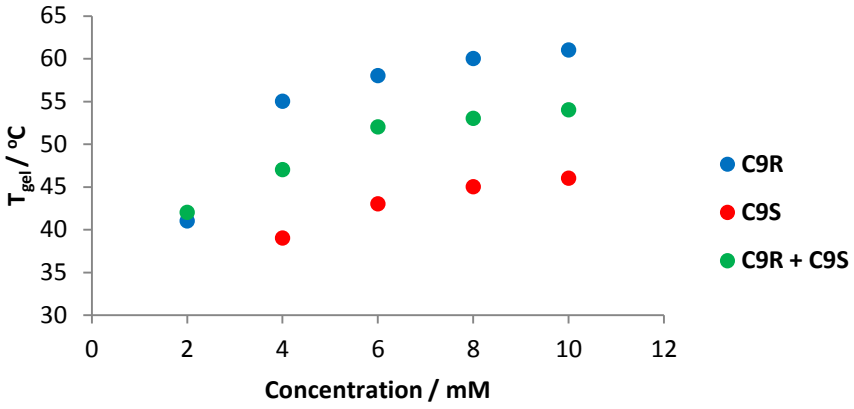

Figure 4.31. T_{gel} values of gels with **L,L,L-G2Lys** and either **C9R**, **C9S** or a mixture both. Toluene.

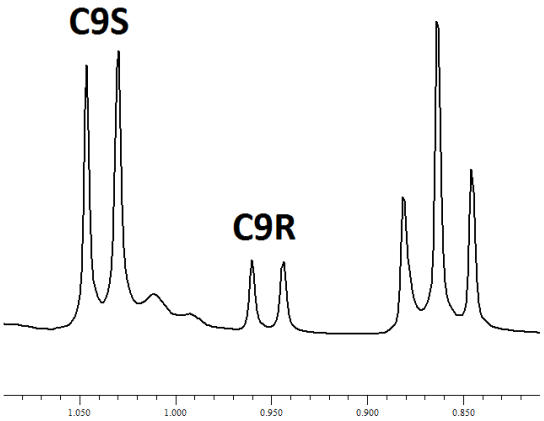

Figure 4.32. ^{1}H NMR of urea mixture produced from the supernatant taken from gel formed with **C9R** and **C9S**. $CDCl_3$.

Whether a chiral cyclic alkyl amine could be separated in this way was then tested using **CHR** and **CHS**. The T_{gel} values of gels formed with a 1:1:1 mixture containing both enantiomers were below those formed with either **CHR** or **CHS** individually (Figure 4.33.). This may have seemed unusual but as Figure 4.13. illustrates, with these amines, gels formed with **CHR** or **CHS** have very similar T_{gel} values and gels formed form a mixture of both show a drop in T_{gel} value. Using Figure 4.13. as a calibration curve suggested that the composition of the network in the 10 mM gel formed form a 1:1:1 mixture with both enantiomers was somewhere between 20-80% **CHS** – a very broad range. When the excess amine was derivatised and analysed by ^{1}H NMR, it

indicated that in contrast to the other samples analysed, most of the amine present in the solution was the *R* enantiomer (Figure 4.34.). The peaks were not completely resolvable but integration of the "outer" peaks of each doublet indicated ca. 23% of the amine in solution was **CHS**. This could be due to real selectivity for **CHS** into the gel network but is more likely due to the fact that the diastereomer made from **CHS** was very poorly soluble, which was clearly seen when it was analysed individually by NMR, meaning its concentration in the NMR sample is artificially lowered.

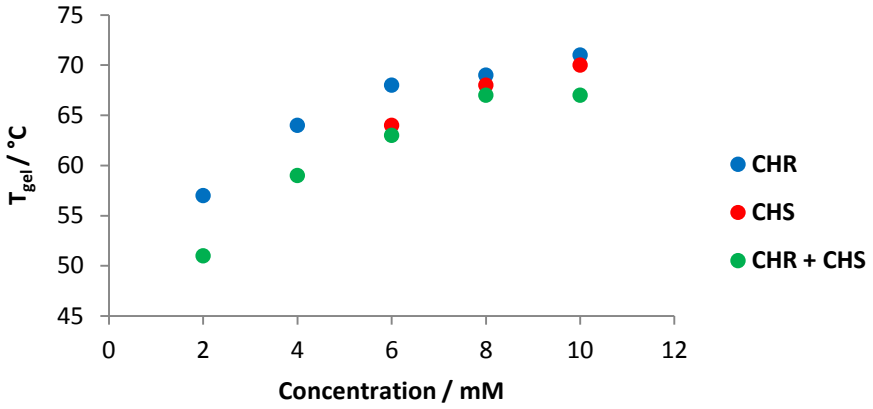

Figure 4.33. T_{gel} values of gels with **L,L,L-G2Lys** and either **CHR**, **CHS** or a mixture both. Toluene.

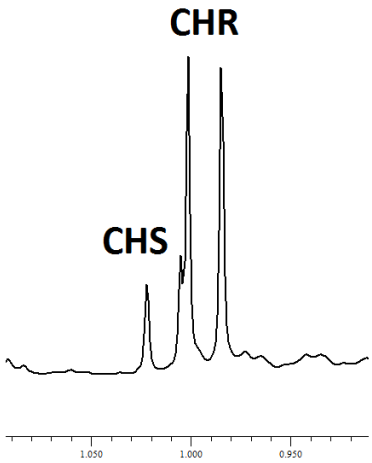

Figure 4.34. ^{1}H NMR of urea mixture produced from the supernatant taken from gel formed with **CHR** and **CHS**. MeOH-d_8.

The selective incorporation of one enantiomer of an amine over the other into a gel network with **L,L,L-G2Lys** has thus far been investigated using alkyl amines. Whether aromatic amines would show different results was then studied. The T_{gel} values of gels made with a 1:1:1

mixture of **L,L,L-G2Lys**, **Ph(Me)R** and **Ph(Me)S** overlap almost completely with those made with only **Ph(Me)R** (Figure 4.35.). Using Figure 4.14. as a rough calibration curve indicates that it is likely 0-20% of the gelator network is **Ph(Me)S**. Unfortunately this could not be confirmed by NMR analysis of the derivatised excess amine. The amine was too structurally similar to (*S*)-methylbenzyl isocyanate for its peaks to be easily resolved in ^{1}H NMR. Another complication was that one of the pathways by which the highly reactive isocyanate degrades is to react with water, this can form **Ph(Me)S**, as shown in Figure **4.36**., which would produce an artificially high amount of **Ph(Me)S** in this experiment.

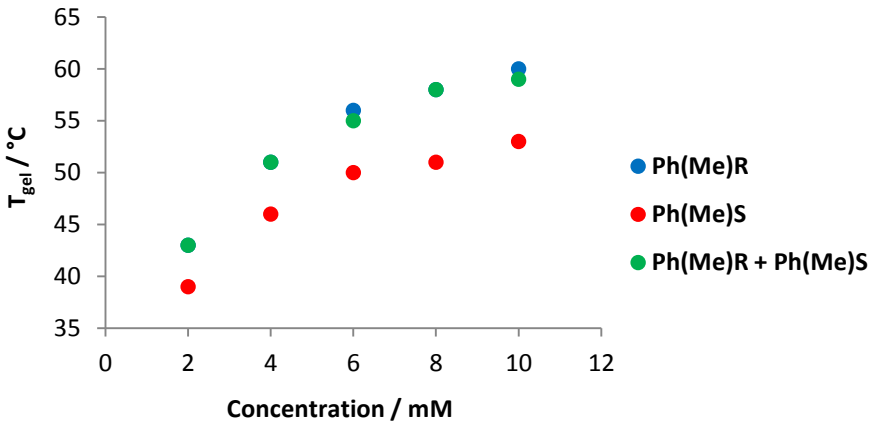

Figure 4.35. T_{gel} values of gels with **L,L,L-G2Lys** and either **Ph(Me)R**, **Ph(Me)S** or a mixture both. Toluene.

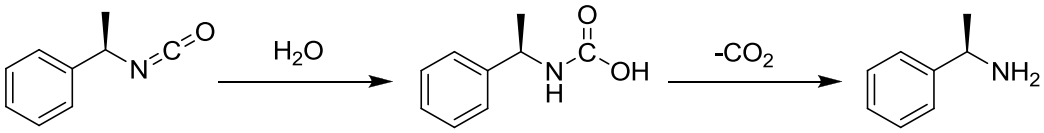

Figure 4.36. Reaction of (*S*)-methylbenzyl isocyanate with water to produce **Ph(Me)S**.

For the gels made with a 1:1:1 mixture of **L,L,L-G2Lys**, **4-ClR** and **4-ClS**, the T_{gel} results also suggest there is selective uptake of **4-ClR** (Figure 4.37.). The T_{gel} values of these gels lie closer to those made with **4-ClS** than those made with **4-ClR**. However, when is used as a rough calibration curve the values suggest that only 20-40% of the amine in the network is **4-ClS**. When the excess amine was derivatised and analysed by NMR the peaks of each diastereomer could not be resolved from each other, as the peaks of the amine derived moiety of the ureas overlapped with the isocyanate derived part of the molecule.

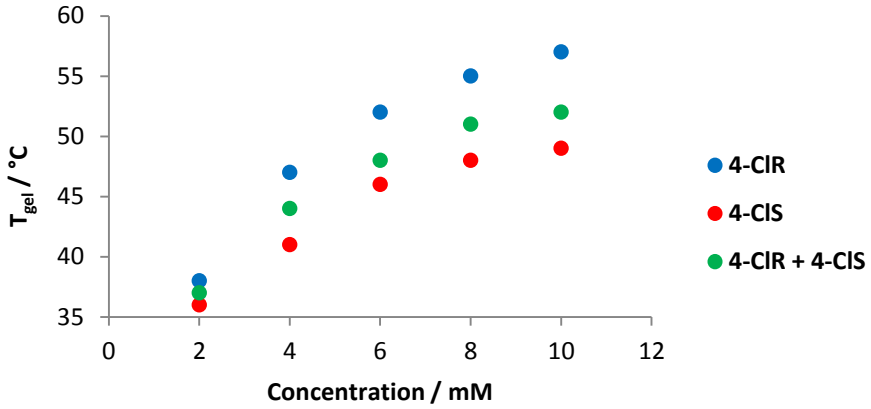

Figure 4.37. T_{gel} values of gels with **L,L,L-G2Lys** and either **4-ClR**, **4-ClS** or a mixture both. Toluene.

The T_{gel} values of gels made with 1:1:1 mixtures of **L,L,L-G2Lys**, **4-FR** and **4-FS** showed an unusual trend, being very close to those of gels made with **4-FR** at low concentrations – when the samples made with **4-FS** are partial or weak gels – and then becoming closer to the values of gels made with **4-FS** as these form more stable gels at higher concentration (Figure 4.38.). The values of gels at 10 mM, when compared to Figure 4.14. indicate that between 30-50% of the network of the mixed gel is **4-FS**, indicating that there is likely some selective uptake of **4-FR** into the gel network. This could not be confirmed by NMR analysis of the derivatised excess amine as once again different peaks of each diastereomer overlapped and could not be resolved.

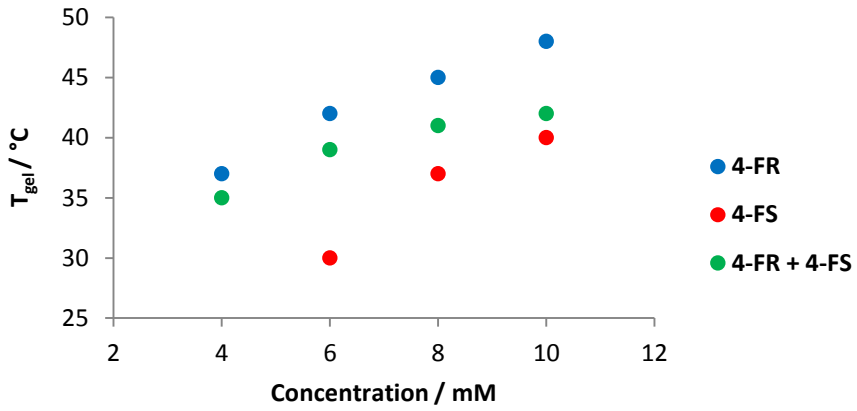

Figure 4.38. T_{gel} values of gels with **L,L,L-G2Lys** and either **4-FR**, **4-FS** or a mixture both. Toluene.

The final example of gels formed with amines containing a *para* substituted phenyl ring were those formed from a 1:1:1 mixture of **L,L,L-G2Lys**, **4-MeR** and **4-MeS**. The T_{gel} values of these gels were very similar to those formed with only **L,L,L-G2Lys** and **4-MeR** (Figure 4.39.). This implied a high degree of selectivity, especially when compared to Figure 4.14. which indicated 0-30% of the mixed gel network being **4-MeS**. Thankfully, when the excess amine was derivatised with (*S*)-methylbenzyl isocyanate and analysed by ^{1}H NMR, the CH_3 group in the *para* position of the phenyl ring of each diastereomer could be distinguished (Figure 4.40.). This indicated that of the amine in solution, 32% was **4-MeR** and 68% was **4-MeS**, so therefore the gel network contains 68% **4-MeR** and 32% **4-MeS** confirming that the T_{gel} measurements of macroscopic performance do correlate with the chiral composition on the molecular level.

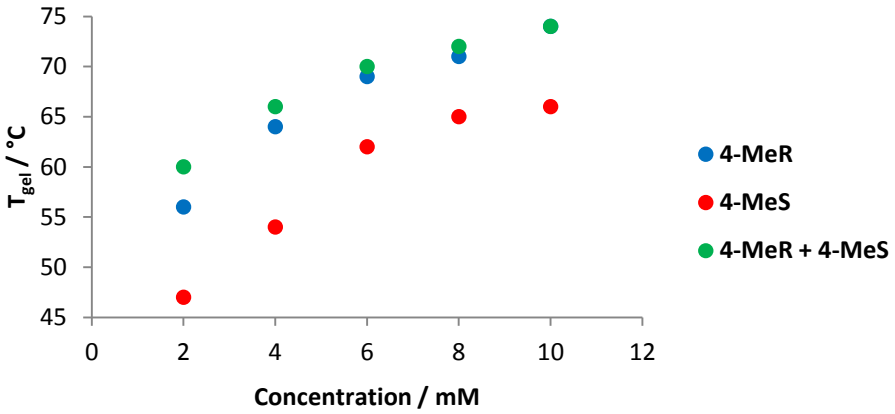

Figure 4.39. T_{gel} values of gels with **L,L,L-G2Lys** and either **4-MeR**, **4-MeS** or a mixture both. Toluene.

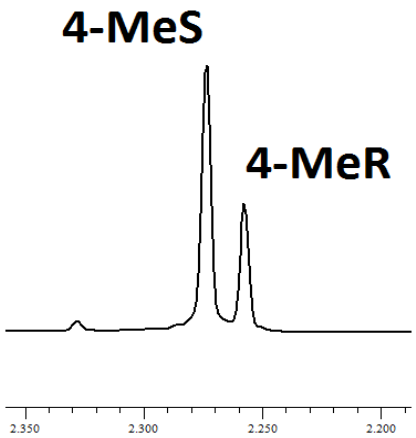

Figure 4.40. ^{1}H NMR of urea mixture produced from the supernatant taken from gel formed with **4-MeR** and **4-MeS**. MeOH-d_8.

When naphthyl-based amine enantiomers **1-NapR** or **1-NapS** were used to form gels with **L,L,L-G2Lys** the thermal stabilities of the gels varied considerably, the difference in T_{gel} of the 10 mM gels being 26°C (Figure 4.15.). The T_{gel} values of gels made with an equimolar mixture of **L,L,L-G2Lys**, **1-NapR** and **1-NapS** are shown in Figure 4.41. and are very similar to those seen for gels made with only **L,L,L-G2Lys** and **1-NapR**. When Figure 4.15. was used to estimate the composition of the gelator network in the 10 mM gel formed with a 1:1:1 mixture it suggested that between 10-30% of the amine in the network was **1-NapS** and therefore that the *R* enantiomer was selectively incorporated into the gelator network. When the excess amine that is excluded for the gelator network was removed, derivatised and analysed by ^{1}H NMR the C*H*$_3$CH peaks from the resulting diastereomers could be partially resolved in the spectrum (Figure 4.42.). Integration of the "outer" peaks of each doublet gave the composition of the solution as 38% **1-NapR** and 62% **1-NapS** (so the gel would be 62% **1-NapR** and 38% **1-NapS**). However, the peak of the **1-NapR** derived diastereomer was overlapping with another smaller peak which will artificially increase its apparent integration. Also, only integrating half of each doublet is not ideal as effects such as "roofing" can cause each individual peak in a doublet to have a different integration. Whilst it is clear in the spectrum that the **1-NapR** derived diastereomer peak has a lower integration than that of the **1-NapS** derived diastereomer, the quantification of the relative amounts should only be considered approximate. Nevertheless, it demonstrates that the *R* enantiomer is selectively incorporated into the gel network.

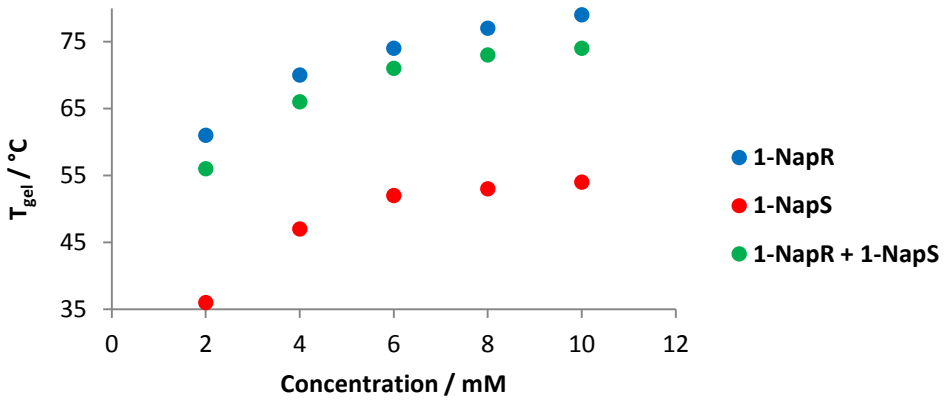

Figure 4.41. T_{gel} values of gels with **L,L,L-G2Lys** and either **1-NapR**, **1-NapS** or a mixture both. Toluene.

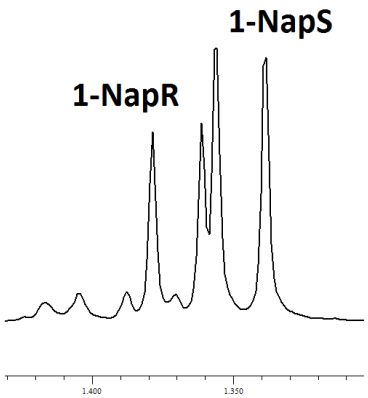

Figure 4.42. ^{1}H NMR of urea mixture produced from the supernatant taken from gel formed with **1-NapR** and **1-NapS**. MeOH-d_8.

The enantiomers **2-NapR** and **2-NapS** are structurally very similar to **1-NapR** and **1-NapS** but when forming gels with **L,L,L-G2Lys** behave very differently (Figure 4.15.). There was only a very small difference between the thermal stabilities of gels formed using either amine (4°C for 10 mM gels). It was unsurprising to find that the T_{gel} values of the gels formed with either compared to the gels formed from a 1:1:1 mixture including both, were of little value in determining how much of each amine enantiomer is incorporated in the gel network Figure **4.43**.). The T_{gel} values of the gels formed from a 1:1:1 mixture are more similar to those formed with **2-NapR** than those formed with **2-NapS**, but when the ±1°C error is considered it is not a significant difference. When the excess amine was derivatised and analysed by ^{1}H NMR it appeared to show there was 46% **2-NapR** derived diastereomer and 54% **2-NapS** diastereomer, indicating, of course, that the composition of the gel network will be the opposite of this. As such, it appears that this system exhibits less chiral discrimination – this would agree with the relatively small impact of chiral mixing on macroscopic gel thermal stability. However, once again this result must be treated with caution as both peaks overlap smaller peaks in the spectrum which means the integrations are approximate (Figure 4.44.).

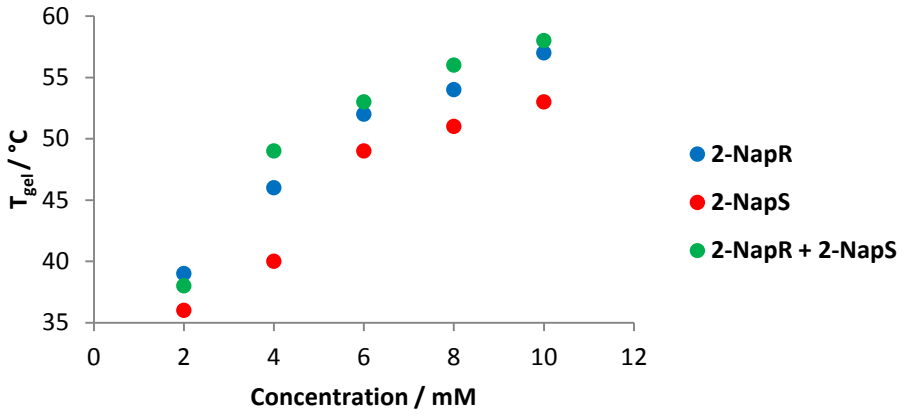

Figure 4.43. T_{gel} values of gels with **L,L,L-G2Lys** and either **2-NapR**, 2-Nap**S** or a mixture both. Toluene.

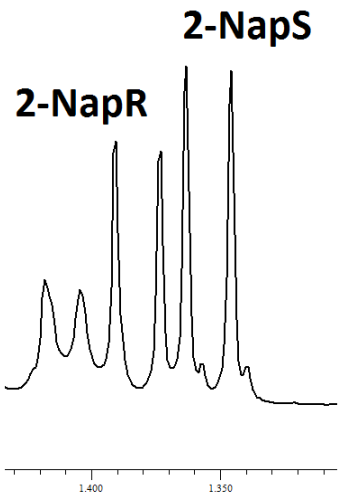

Figure 4.44. ^{1}H NMR of urea mixture produced from the supernatant taken from gel formed with **2-NapR** and **2-NapS**. MeOH-d_8.

The final enantiomeric amines to be tested in this way were **TetR** and **TetS**. These amines were different to the others tested as the chiral centre on each did not have a methyl group attached to it, but gained their chirality from a ring system. Despite this, when changing the ratio of *R* to *S* incorporated into a gel with **L,L,L-G2Lys** they showed a similar change with *R* to *S* ratio to a number of other amines. When the T_{gel} values of gels with a 1:1:1 mixture of **L,L,L-G2Lys**, **TetR** and **TetS** were compared to those containing either one enantiomer or the other (Figure **4.45**.) they were far closer to those formed with **TetR** than **TetS**. Comparing to the data in Figure 4.16. seemed to indicate that 30-50% of the amine in solution was **TetS** so the gelator

network is likely composed of more **TetR** than **TetS**. Unfortunately, when the excess amine was derivitised and analysed by ^{1}H NMR, no diastereotopic protons could be resolved in the spectrum. This meant that the amount of each amine taken in to the gel network with **L,L,L-G2Lys** could not be quantified.

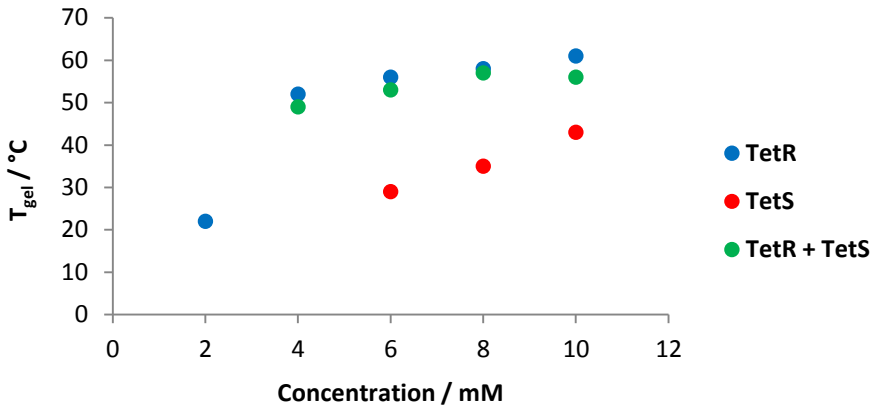

Figure 4.45. T_{gel} values of gels with **L,L,L-G2Lys** and either **TetR**, **TetS** or a mixture both. Toluene.

Testing a number of different chiral amines for preferential uptake of one enantiomer over the other in gels with **L,L,L-G2Lys** has shown that it does take place in most cases, but that like the behaviour of gels formed with changing proportions of *R* to *S* enantiomer, there seems to be few clear trends to rationalise or predict how the wider structure of the amine will mediate or enhance the effect of chirality. Strong preferential incorporation of the *R* enantiomer – which forms the more stable gel network with **L,L,L-G2Lys –** has been shown using **C6R/S**, **C4iR/S**, **C8R/S** and **C9R/S**. The gels made with **CHR/S** indicate the opposite preference – for preferential inclusion of the *S* enantiomer – but this suspect result is likely due to the very poor solubility of the urea formed with the *S* enantiomer. For aromatic amines **Ph(Me)R/S**, **4-ClR/S** and **4-FR/S** the T_{gel} values of the 1:1:1 mixture indicate there was some degree of preferential incorporation of the *R* enantiomer into the gel network but this could not be confirmed using ^{1}H NMR methods. Fortunately, for the **4-MeR/S** system the preference for gel formation with the *R* enantiomer could be confirmed by NMR. The T_{gel} values of gels formed from **1-NapR/S** suggest there is some selective uptake of the *R* enantiomer but this is not absolutely clear in the NMR experiment. The T_{gel} values for the gels made with **2-NapR/S** are not useful but the result of the NMR experiment indicates a relative lack of enantiodiscrimination. Finally T_{gel} values of the gels made from **TetR/S** suggest there is some preferential incorporation of the *R* enantiomer but there is no separation of the diastereomers formed in the ^{1}H NMR spectrum.

4.3. Conclusion

In conclusion, the work in this chapter has proved that the chirality of the amine used to form a gel with **L,L,L-G2Lys** has a very large bearing on the assembly of the complexes into self-assembled networks and the gels that are formed. This has been investigated most thoroughly using **C6R/S** but has also been observed using a range of other amines, all with what would otherwise be regarded as poor quality chiral centres. Furthermore it has been shown that the properties of the gel material formed can be changed gradually by varying the ratio of *R* to *S* present in the gel network, demonstrating the tunability of the systems studied. This demonstrates the remarkable effect of chirality on gelation of these systems.

The selective incorporation of one enantiomer of an amine over the other into the gel network has also been demonstrated, most thoroughly by studying **C6R/S**, but has also been shown to occur with a number of other chiral amines studied. This shows that the kind of component selection achieved in the previous chapter could be repeated using enantiomeric amines. As in the previous chapter it is the amine that forms the most stable gel network that is primarily incorporated into it. This has been proved by forming a gel with **C6S** and then allowing **C6R** to diffuse through the sample and displace it, proving it is a real thermodynamic preference and not a kinetic effect, showing that these gels can endure and adapt to chemical stimuli to which they are exposed.

Chapter 5

Multi-Component Gels: Dendron Chirality

Chapter 5 – Multi-Component Gels: Dendron Chirality

5.1. Enantiomeric Dendrons

5.1.1. Mixing with Non-Chiral Amines

In the previous chapter, the effect of changing amine chirality on gelation was investigated. It seemed a logical extension of this work to investigate how changing the chirality of the **L,L,L-G2Lys** molecule would affect assembly and gel formation. The first step was to synthesise the enantiomeric form of the dendron, **D,D,D-G2Lys**, using D-lysine as shown in Scheme 5.1.

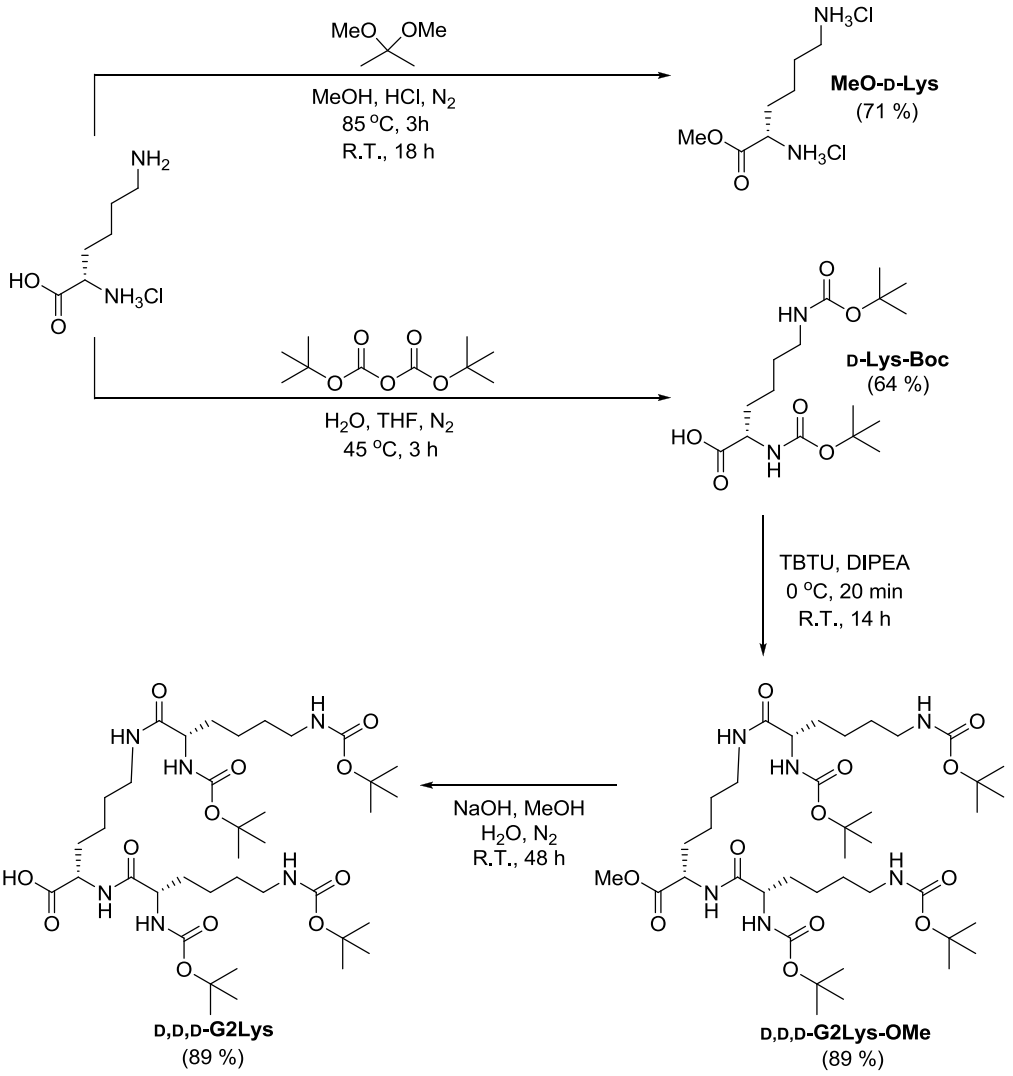

Scheme 5.1. Synthesis of **D,D,D-G2Lys**

This would be particularly interesting as it would allow the study of both enantiomeric gels – using non-chiral amines – and diastereomeric gels – using chiral amines. Once **D,D,D-G2Lys** was synthesised, its ability to form gels with non-chiral aliphatic amines could be was tested and it was of course found to be equal to **L,L,L-G2Lys** as these gels have an enantiomeric relationship. Once this had been established the effect of mixing both enantiomers on gel formation could be investigated. The T_{gel} values of gels formed with 10 mM of aliphatic amine and an overall 10 mM concentration of lysine dendron – which is composed of a varying ratio of **L,L,L-G2Lys** to **D,D,D-G2Lys** – were measured. These values were collected for gels formed with amines **C4**-**C8** and are shown in Figure 5.1. The graphs for all the gels have the same scale on the y-axis for ease of comparison and the x-axis is reported as % **D,D,D-G2Lys** included in the mixture.

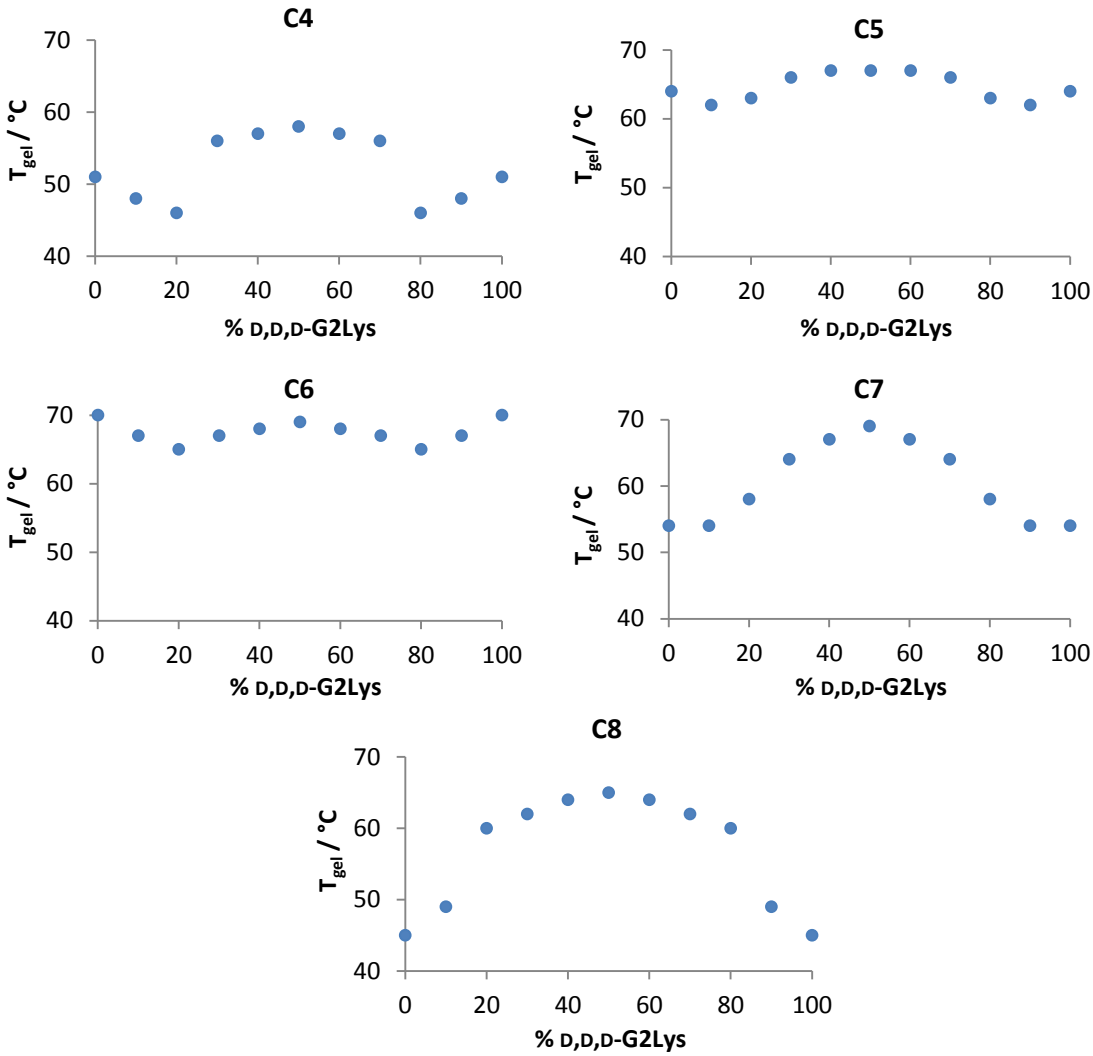

Figure 5.1. T_{gel} values of gels with **C4**, **C5**, **C6**, **C7** or **C8** with a varying ratio of **L,L,L-G2Lys** and **D,D,D-G2Lys**. Toluene.

The first observation is that all the graphs are symmetrical, reflected around 50% **D,D,D-G2Lys** (the racemic gel). This is because of course, the two different complexes created are enantiomers, so 100% **L,L,L-G2Lys** (i.e. 0% **D,D,D-G2Lys**) and 100% **D,D,D-G2Lys**, or the 90% **L,L,L-G2Lys** and 90% **D,D,D-G2Lys** gels, should have the same T_{gel} values. Shown in Figure 5.1. are the results of varying amounts of each enantiomer of lysine dendron on gels formed with the amine with the shortest alkyl chain, **C4**. This graph shows that the gels made with only one enantiomer of lysine dendron have T_{gel} values of ca. 51°C, and as up to 20% of the other enantiomer is included the T_{gel} values decrease. When 30% of the other enantiomer is included, however, the T_{gel} values increase markedly. As more of the other enantiomer is added the T_{gel} values continue to increase until the racemic mixture is formed which produced the maximum T_{gel} value. A similar but less pronounced trend is observed with both **C5** and **C6** (Figure 5.1.), with the T_{gel} values of the **C6** gels being generally higher than those with **C5** which, in turn, are higher than those with **C4**. The results for the gels made with **C7** show a slightly different trend (Figure 5.1.), with no change in T_{gel} values when 10% of the minority enantiomer is added. However, as more is added there is a steady increase in T_{gel} value until the racemic gel is formed which, again, has the maximum T_{gel} value. The gels formed with **C8** show a similar pattern to this (Figure 5.1.) but show an instant increase in T_{gel} with only 10% of the minority enantiomer in the mixture, whilst the maximum T_{gel} value is still the racemic gel. Gels which increase in stability on enantiomeric mixing are very rare and only a small number have been reported in the literature, to the best of our knowledge, all discovered by the Žinić group.[327-330, 468, 469]

The T_{gel} values of the gels made with **C6** (Figure 5.1.) can be compared with gels made from **L,L,L-G2Lys**, **D,D,D-G2Lys** and 1,12-diaminododecane reported in previous work by Smith and co-workers.[326] In these systems (also in toluene), 15 mM of lysine dendron was mixed with 7.5 mM of the diamine (still a 1:1 ratio of acid:amine). Interestingly, in this system the most stable gels were formed with 100% **L,L,L-G2Lys** or 100% **D,D,D-G2Lys** and as the enantiomers were mixed the thermal stability of the gels decreased, the exact opposite of what happens in this equivalent system with monoamines.

To further understand how the ratio of **L,L,L-G2Lys** to **D,D,D-G2Lys** affected self-assembly with aliphatic amines, CD spectroscopy was used. Samples were made with a 0.625 mM total concentration of lysine dendron – with a varying ratio of each enantiomer – and a 0.625 mM concentration of **C8** – chosen due to the large range of T_{gel} values seen with these gels. All the samples were made in a 95:5 mixture of methylcyclohexane to dioxane which produced

optically transparent samples with a total absorbance at the wavelengths of interest (200-250 nm) that was not unacceptably high. The resulting spectra are shown in Figure 5.2., they are labelled according to increasing amount of **D,D,D-G2Lys** in the sample.

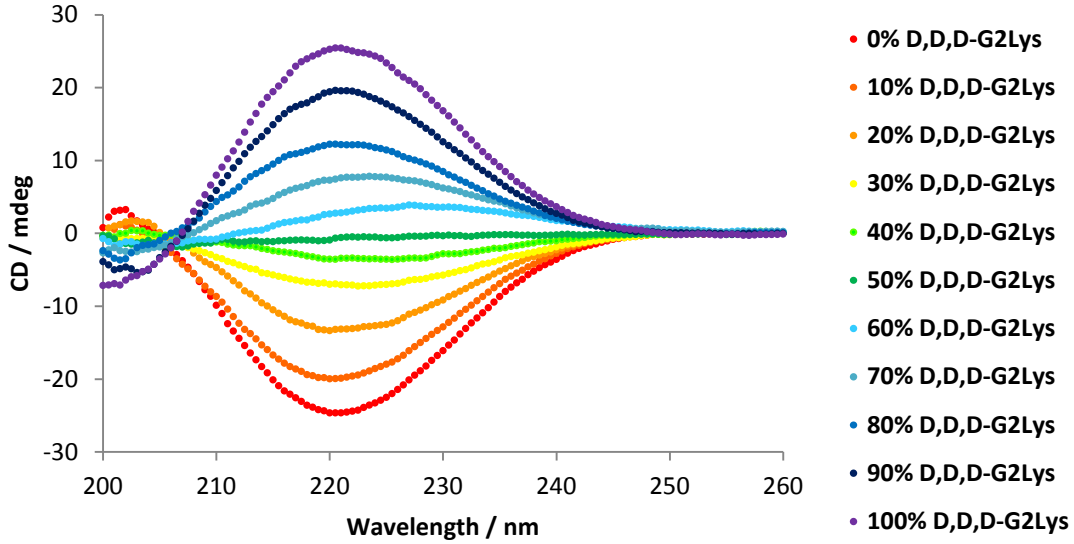

Figure 5.2. CD signal for samples of **C8** and a varying ratio of **L,L,L-G2Lys** and **D,D,D-G2Lys**. 0.625 mM, 95:5 Methylcyclohexane to Dioxane.

Pleasingly, the CD spectra produce a symmetrical set of curves with each pair of enantiomeric gels producing equal and opposite spectra. This clearly shows that the changing amounts of **L,L,L-G2Lys** and **D,D,D-G2Lys** included in the sample are affecting the chiral organisation of the aggregates. This change can be seen more clearly by plotting the CD value of each sample at 220 nm (the λ_{max} of the CD for most samples) which is shown in Figure 5.3.

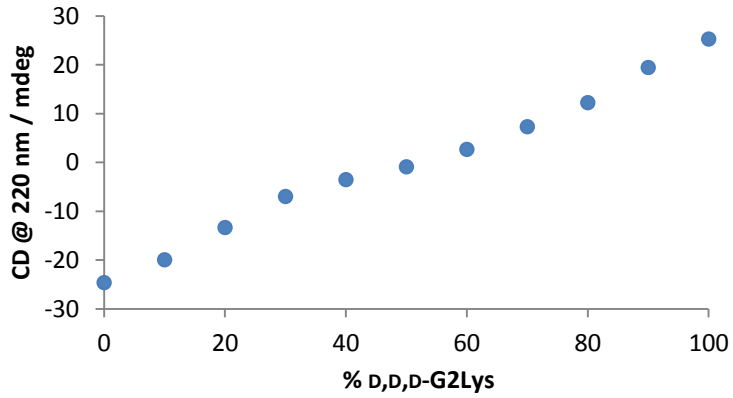

Figure 5.3. CD signal at 220 nm for each sample.

This graph shows that in this system, there is no majority rules effect[296-301, 303, 307, 312, 313, 337-339, 376, 378] where the enantiomer present in excess enforces its mode of organisation on the entire system. In fact the only slight deviation from linearity appears to be due to the minority enantiomer causing slightly disproportionate disruption between 20-80% **D,D,D-G2Lys**, with the racemic sample exhibiting no overall CD signal. This experiment clearly shows that the amount of each enantiomer of lysine dendron included in the sample strongly influences the chiral organisation of the aggregates formed. The gradual change in the CD spectra is different to that seen in the T_{gel} values, where changing proportions of each enantiomer a steep rise between 10-20% of one enantiomer included. This is another example of macroscopic properties being mismatched with chiroptical observations.[340]

To further characterise the gels formed with either **L,L,L-G2Lys**, **D,D,D-G2Lys** or both, 10 mM gels with **C8** in toluene-d_8 were probed using VT-NMR spectroscopy. A 10 mM concentration of **DPM** was included as an internal standard. The gels were heated from 25-80°C with spectra being recorded at each 5°C interval and the concentration of lysine dendron recorded. The results for the gel made with a 5 mM concentration of both **L,L,L-G2Lys** and **D,D,D-G2Lys** are shown in Figure 5.4. The gel made with **L,L,L-G2Lys** and **C8** was already analysed in Chapter 3, so it is not shown here. Neither is the gel made with **D,D,D-G2Lys** and **C8** as this was almost identical to its enantiomeric gel.

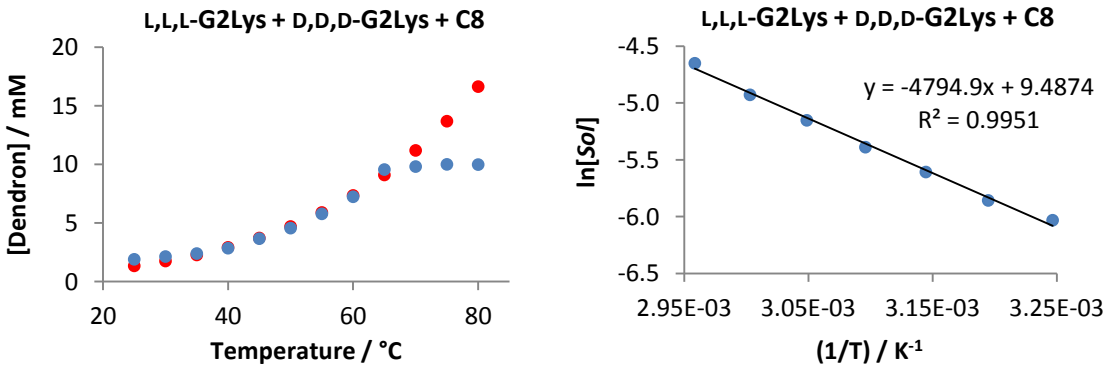

Figure 5.4. Plots showing experimental (blue) and calculated (red) concentration of lysine dendron in the racemic gel as temperature increases and the van 't Hoff plot.

From this data, the $T_{100\%}$ and [Insol]@T_{gel} values could be calculated for the racemic gel, which were 67°C and 0.5 mM. This $T_{100\%}$ value was slightly higher than the measured T_{gel} value (65°C), as was seen in the enantiopure gels, due to the $T_{100\%}$ value representing the complete dissolution of the gelator network. The [Insol]@T_{gel} is lower than the measured MGC value (2.8

mM) but this had also been seen for previous samples as both values measure slightly different things under different conditions. The $T_{100\%}$, [Insol]@T_{gel} and MGC values of this gel can be compared to those of the enantiopure gel analysed in Chapter 3 and all show that the network of the racemic gel is more thermally stable and requires a lower concentration to form a gel than the enantiopure mixture (Table 5.1.). Also shown in Figure 5.4. is the van 't Hoff plot for the racemic gel, which produced ΔH_{diss} and ΔS_{diss} values which are shown in Table 5.1. and compared to the values of the enantiopure gel made with **L,L,L-G2Lys** (the values of the enantiopure gel with **D,D,D-G2Lys** were almost identical). These values are verified by using them to predict the changing solubility with increasing temperature and comparing these to the experimentally results (Figure 5.4.), in this case show a very good correlation.

Table 5.1. Summary of data calculated from van 't Hoff plots.

Dendron	**$T_{100\%}$ / °C**	**[Insol]@T_{gel} / mM**	**ΔH_{diss} / KJ mol^{-1}**	**ΔS_{diss} / J K^{-1} mol^{-1}**
L,L,L-G2Lys	49	2.8	67.6	172
L,L,L-G2Lys and **D,D,D-G2Lys**	67	0.5	39.9	78.9

The values for the racemic gel are very different to the enantiopure system. The ΔH_{diss} for the racemic gel is lower than the enantiopure gels, as is the ΔS_{diss} value. This indicates a gelator network which is less highly organised than the enantiopure samples, which may, therefore, be less able to take advantage of hydrogen bonding interactions between gelating complexes (lower ΔH_{diss}). However, this gel is still more thermally stable because this loss of enthalpic benefit on forming a gel is offset by formation being less entropically disfavoured. This is likely to be indicative of a more disordered network formed with both enantiomers.

Both the enantiomeric gels and the racemic gel were dried to form xerogels, which were analysed by FEG-SEM. The images collected from the three samples are shown in Figure 5.5.

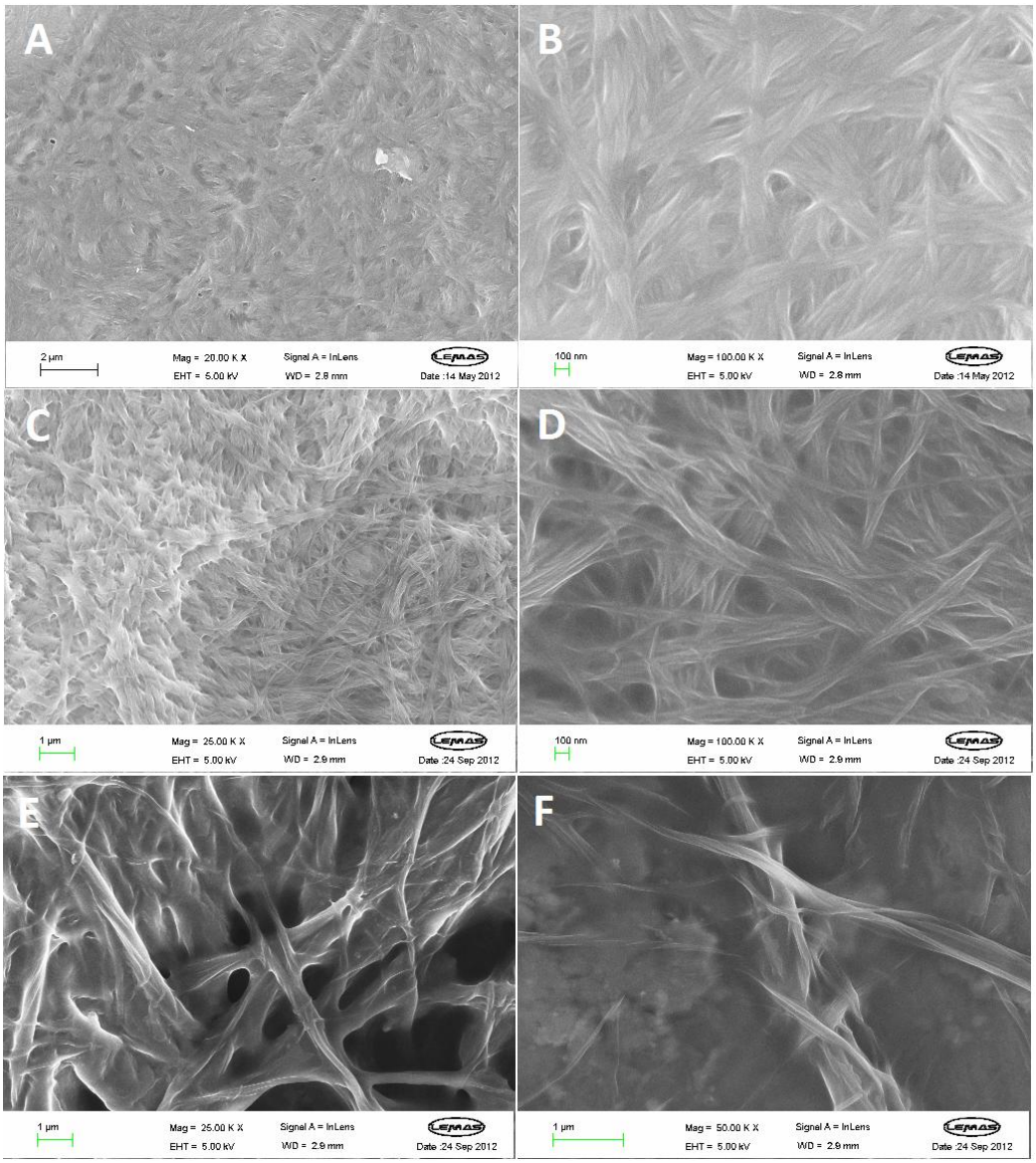

Figure 5.5. FEG-SEM images of xerogels formed from **C8** and A) and B) **L,L,L-G2Lys**, Scale bars = 2 µm and 100nm. C) and D) **D,D,D-G2Lys,** E , Scale bars = 1 µm and 100 nm. E) and F) **L,L,L-G2Lys** and **D,D,D-G2Lys** , Scale bars = 1 µm.

The FEG-SEM images both enantiopure gels made are almost identical. They may appear slightly different due to the slightly different contrast in each image. Both xerogels are formed of small fibres of ca. 20 nm width which aggregate further to form a continuous network that looks matted and highly interwoven in the lower magnification images. The racemic xerogel,

on the other hand, has a network made of slightly thicker fibres (ca. 50 nm), which then aggregate to form thicker, smoother fibres which are part of the continuous network. This is in agreement with previous work conducted on the same system but using 1,12-diaminododecane as the amine.[326] The importance of this result is that it confirms – as expected – that the gel formed from both enantiomers is underpinned by a single mixed network, and that two separate networks of resolved, self-sorted complexes do not appear. However, in the contrast to the previous study[326] this morphology forms a more stable gel rather than a less stable one. There are two possible explanations for this arrangement. The first is that the complexes of both enantiomers co-assemble into mixed chirality supramolecular polymers (tape formation) at the initial stages of gel formation. These tapes then further assemble to form the continuous gel network. The other possible explanation is that the two enantiomers form separate supramolecular polymers which then aggregate together to form thicker mixed chirality fibres, similar to the mechanism proposed by Žinić and co-workers[328] which is based on Fuhrhop's "chiral bilayer effect"[470] which describes the higher propensity for a racemic mixture of amphiphile hydrogelators to crystallise, compared to the gel forming enantiopure compounds. However both of these reports claim that the racemic network was either more densely packed or constructed of smaller, thinner fibres which, based on the VT-NMR and FEG-SEM results, is not the case in our system.

In summary, a family of racemic gels were more stable than their enantiopure counterparts have been described.

5.1.2. Changing Chirality of Dendron with Chiral Amines

The next logical step was to use chiral amines to investigate how varying the chirality of the dendron would affect the formation and thermal stability of diastereomeric gels. This would be a similar study to that conducted in the previous chapter where the gel is made of two diastereomeric complexes. In this experiment, each sample has a 10 mM concentration of *R* chiral amine and a 10 mM total concentration of lysine dendron, with a varying ratio of **L,L,L-G2Lys** to **D,D,D-G2Lys**. The first amine tested was **C8R** given its similarity to the most interesting amine studied in enantiomeric gels, **C8**. The T_{gel} values of the gels produced when **C8R** is used are shown in Figure 5.6.

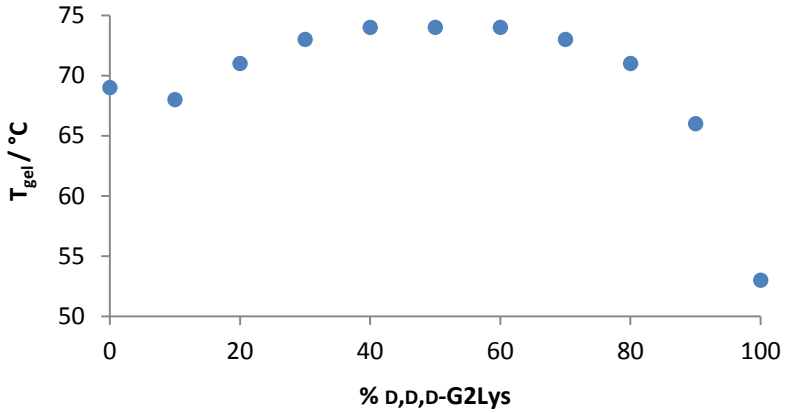

Figure 5.6. T_{gel} values of gels with **C8R** and a varying ratio of **L,L,L-G2Lys** and **D,D,D-G2Lys**. Toluene.

The gel formed from **L,L,L-G2Lys** and **C8R** was also studied in the previous chapter and therefore the T_{gel} value was already known. The gel formed from **D,D,D-G2Lys** and **C8R** has an enantiomeric relationship with the gel formed from **L,L,L-G2Lys** and **C8S** which was studied in the previous chapter – therefore these gels also have the same T_{gel} value. It may be expected then, that mixing **C8R** with varying ratios of **L,L,L-G2Lys** and **D,D,D-G2Lys** will produce the same, or similar data as mixing **L,L,L-G2Lys**, with a varying ratio of **C8R** and **C8S** (Figure 4.13.). However this is not the case, as the complexes formed by **L,L,L-G2Lys** with **C8S** and **D,D,D-G2Lys** with **C8R** are, despite being enantiomers, are both different diastereomers of **L,L,L-G2Lys** and **C8R** and will interact and behave differently to each other when mixed with this complex. In this case (Figure 5.6.), there is a small decrease in T_{gel} when 10% **D,D,D-G2Lys** is included before the T_{gel} value increases with increasing amount of **D,D,D-G2Lys** incorporated. The highest T_{gel} values are centred on the gel with equal amounts of **L,L,L-G2Lys** and **D,D,D-G2Lys**, as is the case for the gels made with non-chiral aliphatic amine **C8**. As even more **D,D,D-G2Lys** is added, the T_{gel} values decrease dramatically to the lowest value, of the gel formed with entirely **D,D,D-G2Lys** and **C8R**.

We can further investigate the mixing of **L,L,L-G2Lys** and **D,D,D-G2Lys** with **C8R** using CD spectroscopy. Samples were made with a 0.625 mM concentration of **C8R** and a 0.625 mM total concentration of lysine dendron, with a varying ratios of **L,L,L-G2Lys** to **D,D,D-G2Lys**. Again the solvent used was 95:5 methylcyclohexane to dioxane as it supported self-assembly and produced optically transparent samples. The spectra recorded at shown in Figure 5.7.

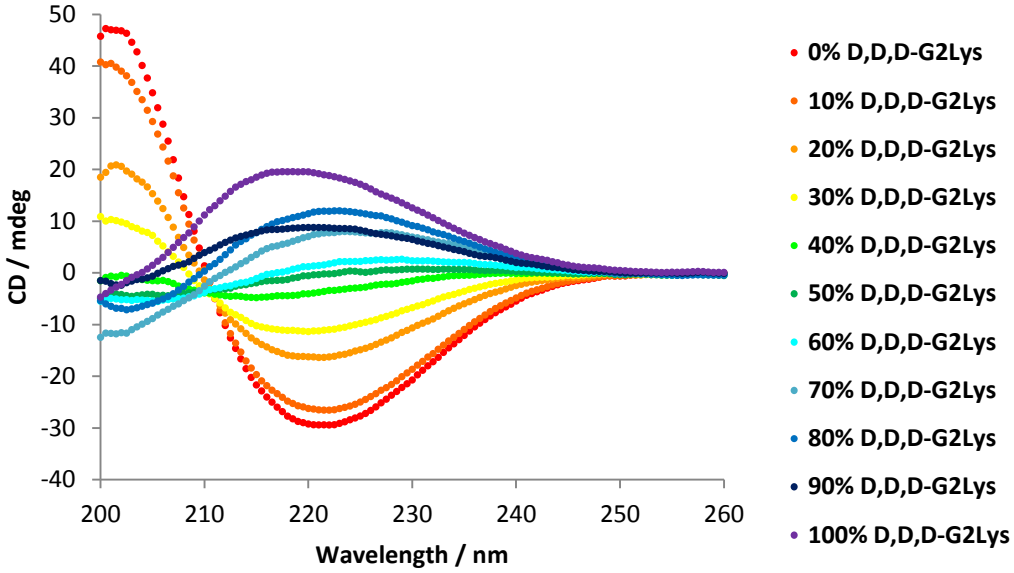

Figure 5.7. CD signal for samples of **C8R** and a varying ratio of **L,L,L-G2Lys** and **D,D,D-G2Lys**. 0.625 mM, Methylcyclohexane to Dioxane.

As the samples were made with increasing amounts of **D,D,D-G2Lys**, there is a definite change in the CD spectrum. Of course the change in the spectra with increasing amounts of **L,L,L-G2Lys** or **D,D,D-G2Lys** is not equal, i.e. the overlay of the spectra is not symmetrical as shown in Figure 5.2., as the two complexes are now diastereomers, not enantiomers. The CD signal from each sample at a set wavelength was not plotted for each sample as the λ_{max} changes significantly as the composition of the samples changes. However it does appear that the largest change in spectra occurs in the range of small amounts of **L,L,L-G2Lys** being included. This would suggest that small amounts of **L,L,L-G2Lys** can induce its own behaviour onto the co-assembly and do so more strongly than its enantiomer. This matches the behaviour seen in the T_{gel} graph (Figure 5.6.) were the largest change in T_{gel} values is seen in the samples with small amounts of **L,L,L-G2Lys** (80-100% **D,D,D-G2Lys**)

To gain further insight into the assembly of these gels, VT-NMR spectroscopy was used again. Gels with a 10 mM concentration of **C8R**, 10 mM concentration of **DPM** (internal standard) and either 10 mM **L,L,L-G2Lys**, 10 mM **D,D,D-G2Lys** or 5 mM of each enantiomer were made in toluene-d_8. These gels were heated and the ^{1}H NMR spectra was recorded at each 5°C interval. The plots showing increasing concentration of lysine dendron "visible" in the solution phase as the temperature increases is shown for each gel in Figure 5.8.

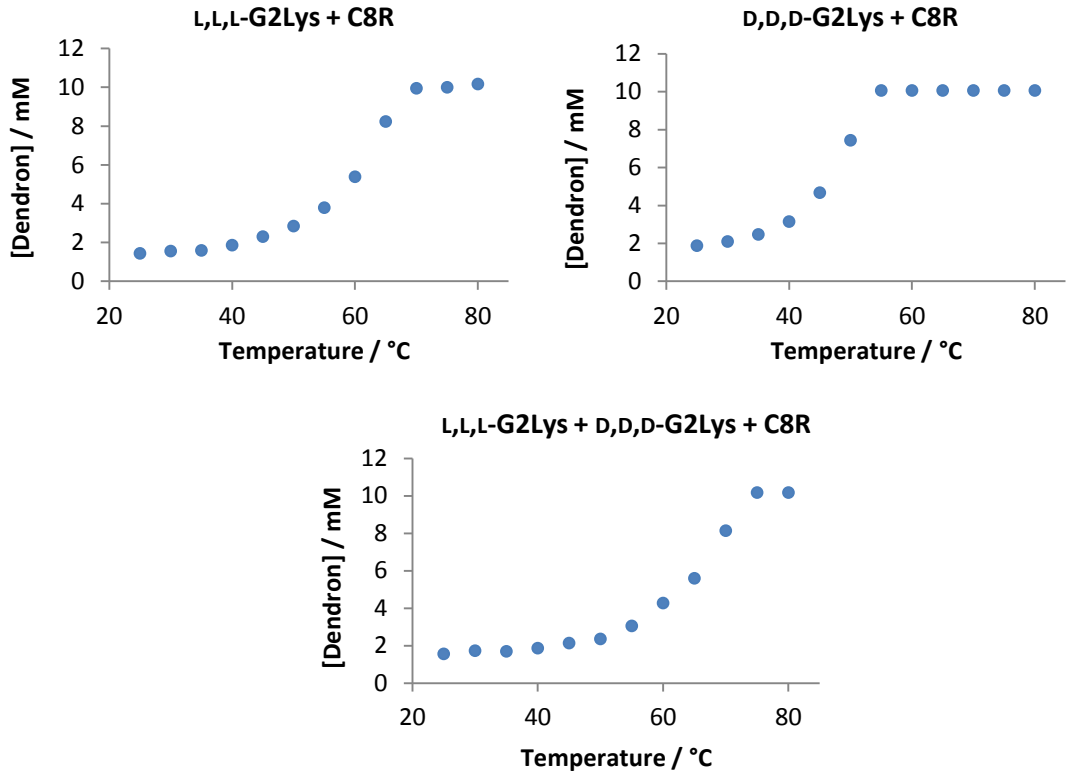

Figure 5.8. Concentration of lysine dendron visible in gels of **L,L,L-G2Lys, D,D,D-G2Lys** and **C8R** as temperature increases. Toluene-d_8.

The graphs show the now familiar increase in soluble gelating complex as the temperature of the sample increases. The $T_{100\%}$ and [Insol]@T_{gel} were found for each gel and can be compared to the related macroscopic T_{gel} and MGC values (Table 5.2.).

Table 5.2. Comparison of molecular ($T_{100\%}$ and [Insol]@T_{gel}) and materials properties (T_{gel} and MGC) for gels formed with **L,L,L-G2Lys, D,D,D-G2Lys** and **C8R**.

Dendron	$T_{100\%}$	T_{gel}	[Insol]@T_{gel}	MGC
L,L,L-G2Lys	72°C	69°C	0.5 mM	0.6 mM
L,L,L-G2Lys + D,D,D-G2Lys	75°C	74°C	1.2 mM	1.4 mM
D,D,D-G2Lys	55°C	53°C	1.3 mM	1.6 mM

As seen for other gels analysed in this manner, there is a clear relationship between $T_{100\%}$ and T_{gel}, with the $T_{100\%}$ values being slightly higher than the T_{gel} values as this represents complete

dissolution of the gel network. This again shows that the gel formed with a mixture of **L,L,L-G2Lys** and **D,D,D-G2Lys** is the most thermally stable, closely followed by the sample made with only **L,L,L-G2Lys** with the sample made with **D,D,D-G2Lys** significantly less stable. The [Insol]@T_{gel} values in this case match the MGC values very well, not only showing the same trend but very similar concentrations. Using plots of ln[*Sol*] against 1/T, the ΔH_{diss} and ΔS_{diss} of the gelator network can be found for each sample. The plots used to find these values are shown in Figure 5.9. The thermodynamic parameters derived from this treatment are collected in Figure 5.9.

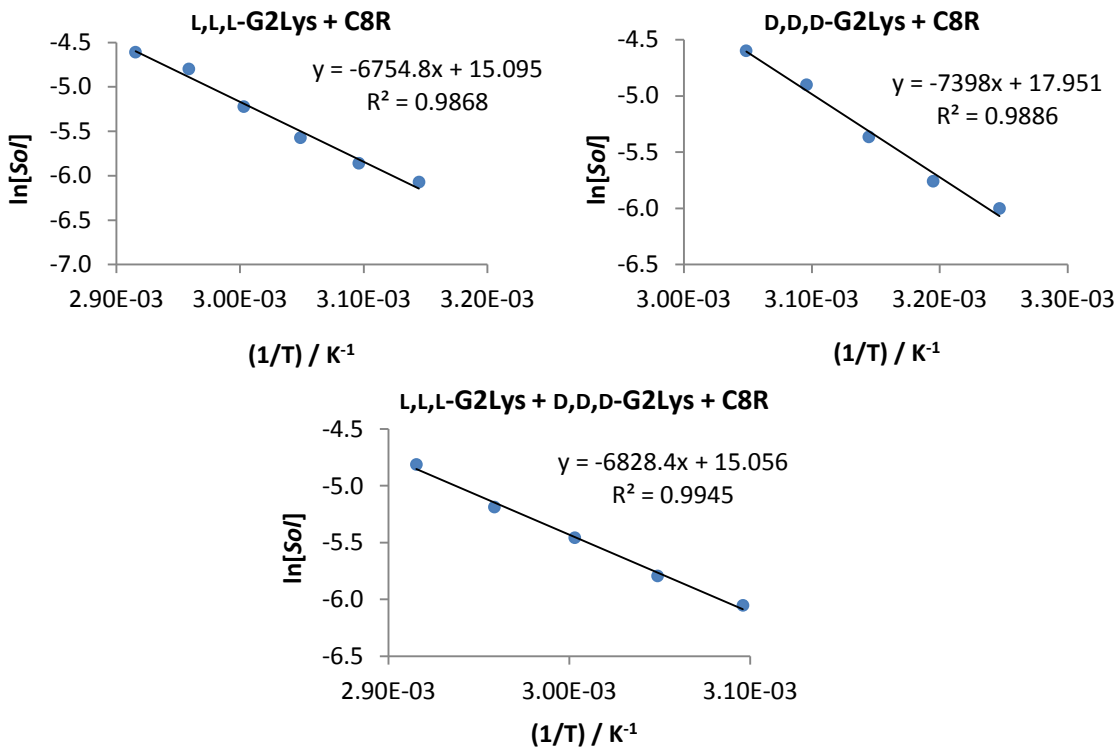

Figure 5.9. Van 't Hoff plots of gels formed from **L,L,L-G2Lys, D,D,D-G2Lys** or **L,L,L-G2Lys** and **D,D,D-G2Lys** with **C8R.**

Table 5.3. Summary of data calculated from van 't Hoff plots.

Dendron	ΔH_{diss} / KJ mol^{-1}	ΔS_{diss} / J K^{-1} mol^{-1}
L,L,L-G2Lys	56.2	125
L,L,L-G2Lys + D,D,D-G2Lys	56.8	125
D,D,D-G2Lys	61.5	149

Both the ΔH_{diss} and ΔS_{diss} values of the gel formed from **D,D,D-G2Lys** and **C8R** are higher than those of the gel formed form **L,L,L-G2Lys** and **C8R**. This likely indicates a more organised gel network that is more able to take advantage of hydrogen bonding between gelator complexes. This makes dissolution less enthalpically favourable, but more entropically favourable. With the gels studied in the previous chapter this led to a more thermally stable gel, with the benefit of the hydrogen bonding compensating for the gain of entropy upon dissolution until high temperatures (Table 4.3.). In this instance however, this is not the case. What appears as the more highly organised network is actually less thermally stable, as the enthalpic gain from hydrogen bonding cannot compensate for the loss of entropy upon network formation at higher temperatures. The gel formed with both **L,L,L-G2Lys** and **D,D,D-G2Lys** has almost identical values to that formed with just **L,L,L-G2Lys** (and **C8R**). This explains why the two samples have very similar T_{gel} and $T_{100\%}$ values, with the entropic favourability of dissolution overcoming the enthalpic disadvantage of dissolution at roughly the same temperature. This also provides more evidence of the **L,L,L-G2Lys** and **C8R** complex directing the aggregation of the co-assembly. The values found by this analysis and the model used to find them can be verified by using them to predict the changing solubility of each sample and comparing this to the experimentally measured results (Figure 5.10.). In these instances, the calculated values give a good description of the experimentally observed change.

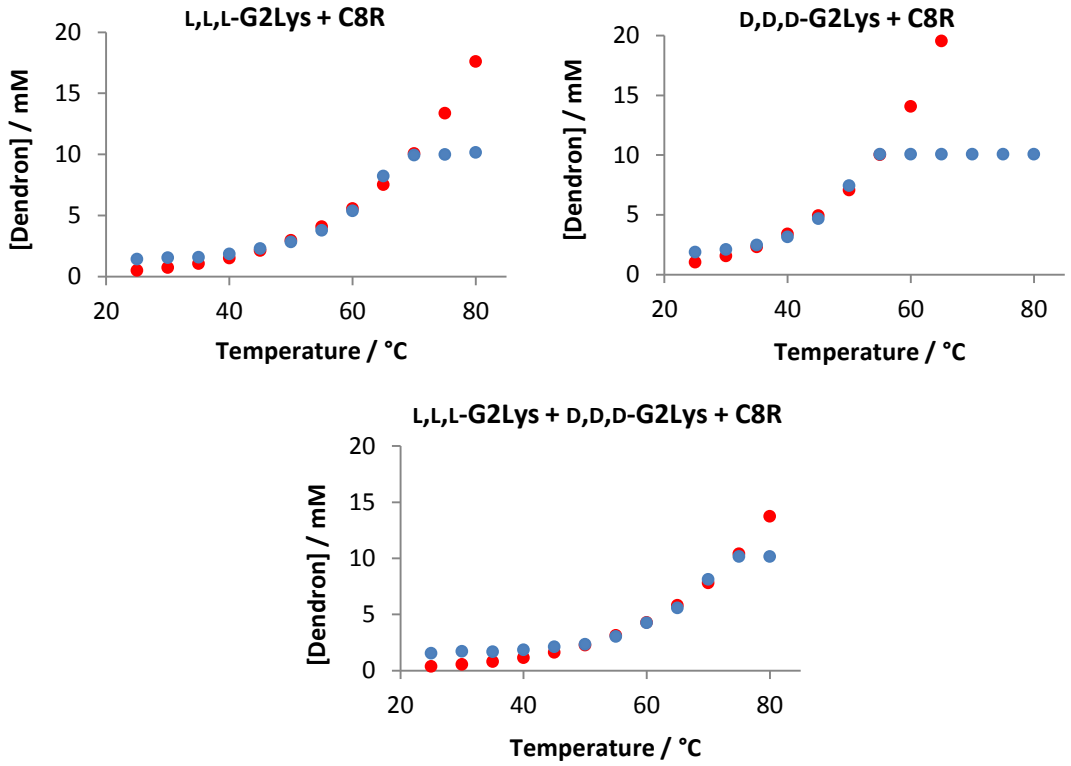

Figure 5.10. Plots showing experimental (blue) and calculated (red) concentration of solubilised gelator complex in each gel.

These gels were investigated further by drying them to form xerogels which were imaged using FEG-SEM (Figure 5.11.). The images of the xerogel formed from **L,L,L-G2Lys** and **C8R** are very similar to those of the gel formed with **L,L,L-G2Lys** and **C6R** (Figure 4.3.). The network consists of very thin fibres (ca. 10-15 nm), barely visible even under high magnification. In contrast to this, the corresponding sample made with **D,D,D-G2Lys** much thicker fibres (ca. 200 nm) are observed, the difference between the two samples is marked. Between these two extremes is the sample formed with both **L,L,L-G2Lys** and **D,D,D-G2Lys**, which consists of fibres of ca. 50-100 nm. It was interesting to note how this seems to indicate that the combination of **L,L,L-G2Lys** and **D,D,D-G2Lys** imparts properties of both gelating complexes and indicate that a co-assembled gel network is formed.

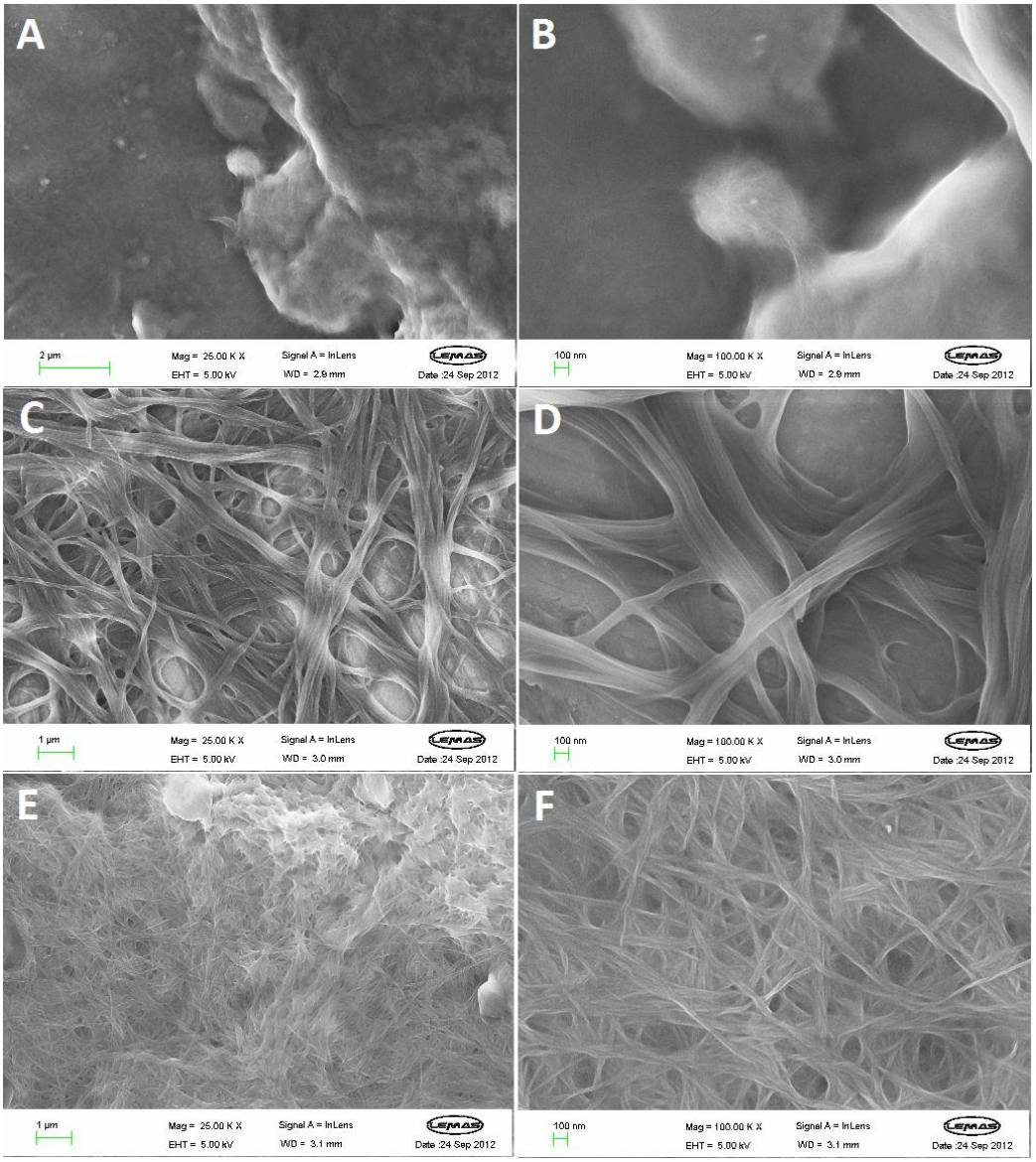

Figure 5.11. FEG-SEM images of xerogels of with **C8R** and A) and B) **L,L,L-G2Lys,** C ,Scale bars = 2 µm and 100 nm. C) and D) **D,D,D-G2Lys**, Scale bars = 1 µm and 100 nm. E) and F) **L,L,L-G2Lys** and **D,D,D-G2Lys**, Scale bars = 1 µm and 100 nm.

In summary, gels formed from either **L,L,L-G2Lys** or **D,D,D-G2Lys** with **C8R** have different thermal stabilities, CD spectra, different ΔH_{diss} and ΔS_{diss} and form networks of radically different morphologies as viewed by FEG-SEM. It appears that the gel formed by an equal mixture of **L,L,L-G2Lys** and **D,D,D-G2Lys** with **C8R** has a similar T_{gel} value and NMR data to the gel formed with only **L,L,L-G2Lys** and **C8R** but this may be coincidental, as the morphology of the fibres formed and chiral organisation of the sample are affected by the presence of both **L,L,L-G2Lys** and **D,D,D-G2Lys**.

The next question was how different ratios of **L,L,L-G2Lys** to **D,D,D-G2Lys** would control the thermal stability of gels formed with other chiral amines. The *R* enantiomers of the other chiral amines were used to test this by forming gels with a 10 mM concentration of amine and a 10 mM concentration of total lysine dendron with a varying ratio of **L,L,L-G2Lys** to **D,D,D-G2Lys**. The first amines tested were the non-aromatic **C4iR**, **C6R**, **C9R** and **CHR**. The T_{gel} values of the gels produced with these amines are shown in Figure 5.12.

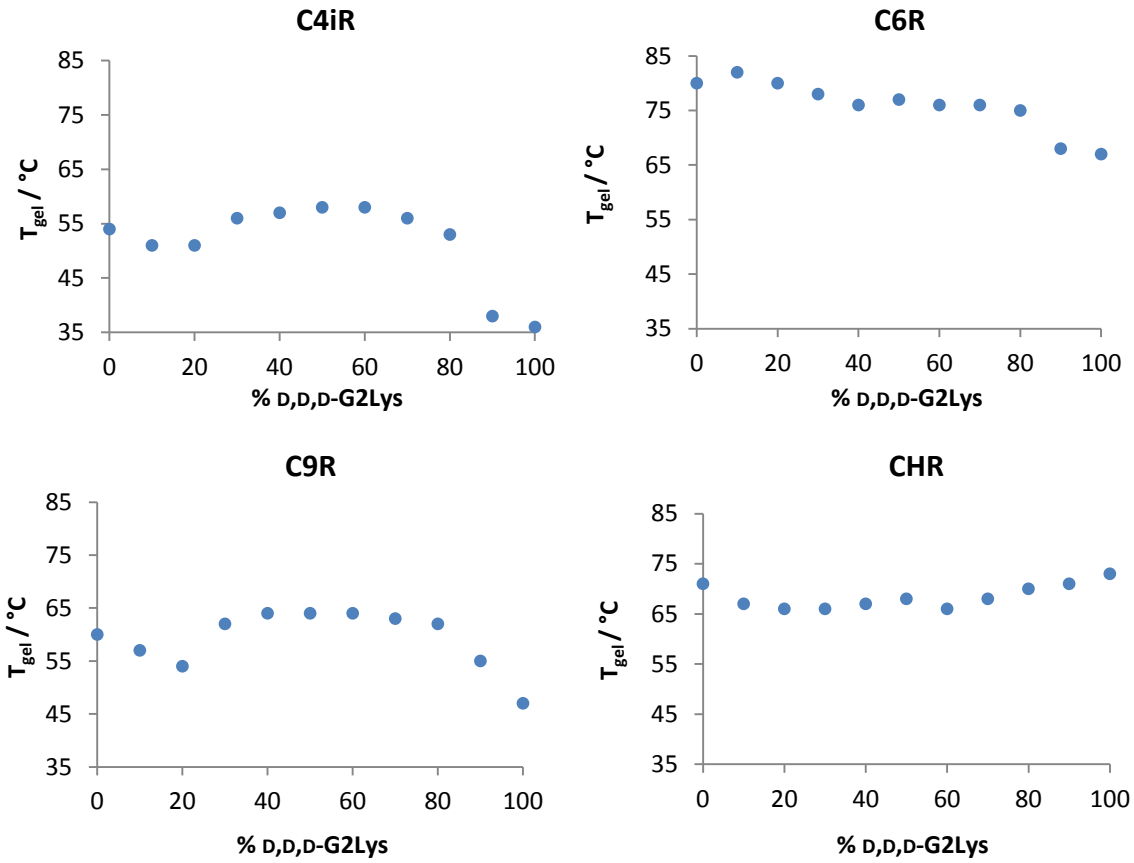

Figure 5.12. T_{gel} values of gels with a varying ratio of **L,L,L-G2Lys** and **D,D,D-G2Lys** and either **C4iR**, **C6R**, **C9R** or **CHR**. Toluene.

The first point to make about all the graphs is that the gel formed with 100% **D,D,D-G2Lys** and *R* amine has, in each case, the same T_{gel} value as the equivalent enantiomeric gel formed with **L,L,L-G2Lys** and *S* amine – shown in the previous chapter (Figure 4.13.). In all the graphs, however, the trend between these gels and those formed with only **L,L,L-G2Lys** and *R*/*S* amine is completely different. The gels formed from either **C4iR** or **C9R** demonstrate a very similar trend to those formed with **C8R** (Figure 5.6). These all show an initial decrease in T_{gel} until ca. 20% of **D,D,D-G2Lys** is included in the sample, followed by an increase in T_{gel} to a maximum value when around 50% of the gel network is made of complexes containing **D,D,D-G2Lys**. As

more of this enantiomer is added the thermal stability of the gel drops dramatically, reaching a minimum value at 100% **D,D,D-G2Lys**. The gels made with **C6R**, a very similar amine are surprisingly, very different. These gels show a slight increase in T_{gel} upon inclusion of ca. 10% of **D,D,D-G2Lys** before a linear drop in T_{gel} with increasing **D,D,D-G2Lys** until ca. 40% is incorporated. The T_{gel} values then plateau to ca. 80% **D,D,D-G2Lys** before dropping sharply as more is added, reaching a minimum at 100% **D,D,D-G2Lys**. The gels made with **CHR** show decreasing T_{gel} with increasing **D,D,D-G2Lys** to roughly 30% before rising slightly to the gel made with 50% **D,D,D-G2Lys**. This decreases again when 60% **D,D,D-G2Lys** is included before an almost linear increase in T_{gel} until the gel made with entirely **D,D,D-G2Lys** and **CHR**. The trend seen in this series occur over a very small temperature range (7°C), so there is not a large difference in the thermal stabilities of the two diastereomeric gels and those formed from mixing both dendrons. The next amines tested were the aromatic amines **Ph(Me)R**, **4-MeR**, **4-ClR** and **4-FR**. The T_{gel} values of these gels are shown in Figure 5.13.

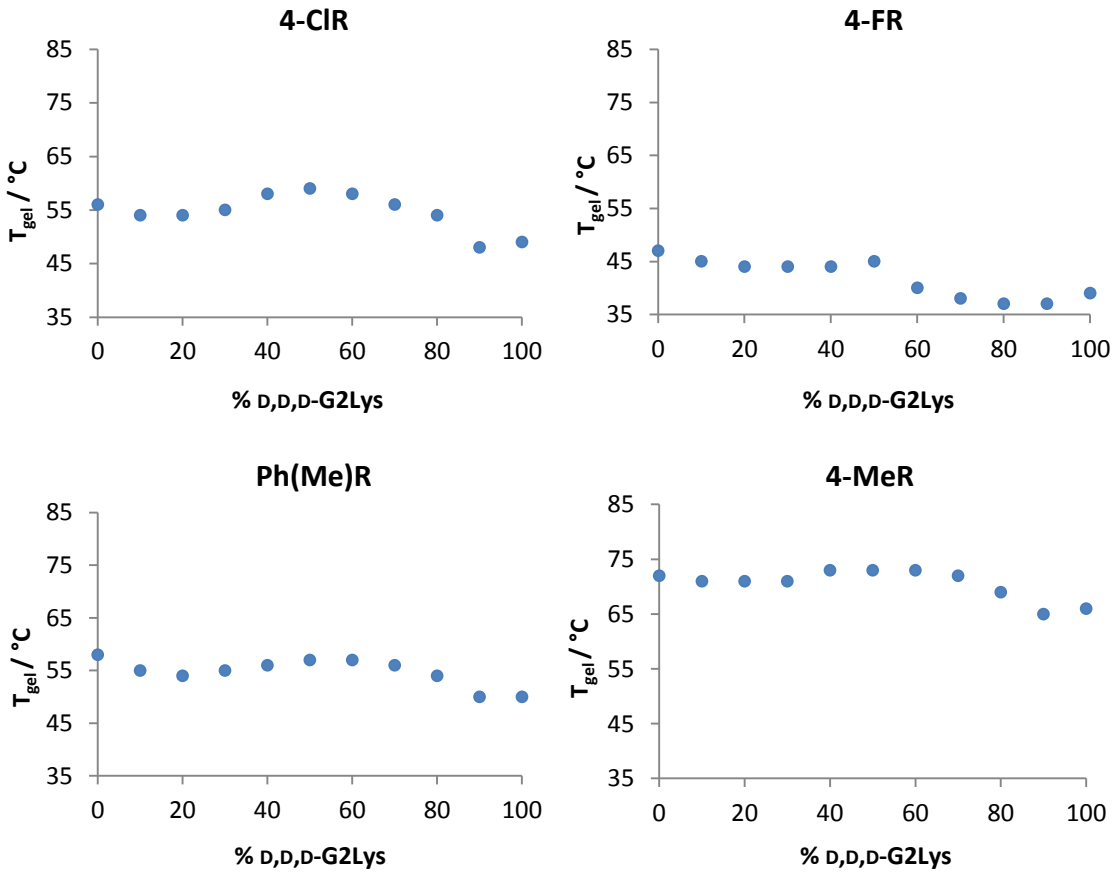

Figure 5.13. T_{gel} values of gels with a varying ratio of **L,L,L-G2Lys** and **D,D,D-G2Lys**.and either **Ph(Me)R**, **4-MeR**, **4-ClR** or **4-FR**. Toluene.

Again, in all of these spectra the T_{gel} values of the gels formed with only **D,D,D-G2Lys** and the *R* amine is identical to its enantiomer formed with **L,L,L-G2Lys** and the *S* amine (Figure 4.14.). The trend observed when varying the chirality of the dendron was different to that observed when varying the chirality of the amine in the previous chapter (Figure 4.14.). The graphs for samples formed with amines **Ph(Me)R**, **4-MeR** and **4-ClR** are all very similar, showing a decrease in T_{gel} value until ca. 20-30% **D,D,D-G2Lys**, increasing T_{gel} with 40-60% **D,D,D-G2Lys** and decreasing T_{gel} as more **D,D,D-G2Lys** is used to a minimum T_{gel} at 90-100% **D,D,D-G2Lys**. Of these three graphs the **Ph(Me)R** and **4-ClR** gels are spread over the same temperature range whilst the **4-MeR** T_{gel} values are roughly 15°C higher. The gels made with **4-FR** behave slightly differently. These are the weakest set of gels and show a similar trend to that observed in the other samples but the increase in T_{gel} at ca. 50% **D,D,D-G2Lys** occurs over a much smaller range of % **D,D,D-G2Lys** and the thermal stability of the gels drops dramatically with increasing **D,D,D-G2Lys** content from this mid-point. The final set of amines tested were the naphthylmethylamine based **1-NapR** and **2-NapR** and **TetR** which as discussed in the previous chapter has a very different chiral centre to the other amines tested.

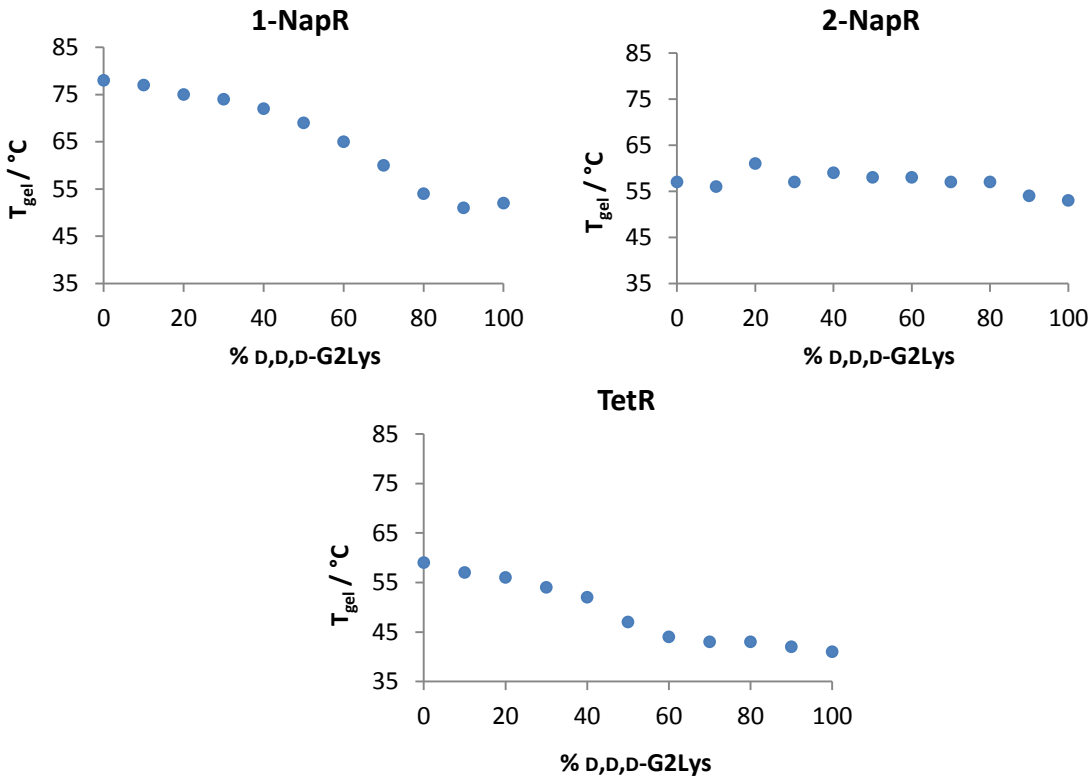

Figure 5.14. T_{gel} values of gels with a varying ratio of **L,L,L-G2Lys** and **D,D,D-G2Lys**.and either **1-NapR**, **2-NapR** or **TetR**. Toluene.

Reassuringly, the T_{gel} values of the **D,D,D-G2Lys** and *R* amine gels were again the same as their enantiomeric **L,L,L-G2Lys** and *S* amine gels in all cases (Figure 4.15.). The gels made with these amines were surprisingly similar to their equivalent gels made by varying *R* to *S* amine with **L,L,L-G2Lys** (Figure 4.15.). In this instance, the gels formed with **1-NapR** show a more gradual decrease in T_{gel} with increasing amounts of **D,D,D-G2Lys** than the corresponding gels formed with increasing amounts of **1-NapS** seen in the previous chapter with the large plateau visible in that experiment replaced by a more gentle curve in this experiment – but the similarities between the two are striking. The same is true for the gels formed with **2-NapR** but only in that the T_{gel} values are spread over such a small range that the graph is fairly useless, and the ±1 °C error on each value means trying to see any gradual change becomes impossible. The gels formed with **TetR** are the most striking as the trend observed with increasing amount of **D,D,D-G2Lys** is exactly the same as that observed in the previous chapter with increasing amounts of **TetS** (Figure 4.15.).

In summary, changing the chiral amine has had a pronounced effect on how the varying chirality of the lysine dendron controls gel formation. This has once again shown how tuneable these two-component gels are and the fascinating effects of mixing diastereomers on assembly and gel formation. In every case, the **L,L,L-G2Lys** gel has a higher T_{gel} than the 100% **D,D,D-G2Lys** gel. This was expected as the **D,D,D-G2Lys** and *R* amine gel was the enantiomer of the **L,L,L-G2Lys** and *S* amine gels formed in the previous chapter, which also had lower T_{gel} values than the **L,L,L-G2Lys** and *R* amine gels. However, between these two extreme points, the effect of gradually varying dendron chirality is different to that observed when varying the chirality of the amine.

5.2. Component Selection with Chiral Dendrons

5.2.1. Testing Whether Component Selection Can Be Achieved

In the previous chapters, it was described how amines which form more stable gels can be selectively incorporated into the gel network in preference to amines that form less stable gels. In this case it can be determined whether the reverse is true, i.e. if the enantiomer of the dendron which formed the more stable gel with an *R* amine could be selectively incorporated into the gel network in preference to the other dendron enantiomer. The first amine for which this was tested was **C8R**. Gels were made with this amine and an equivalent of either **L,L,L-G2Lys**, or **D,D,D-G2Lys**, or an equivalent of each, (a 1:1:1 mixture) over a concentration range of 2-10 mM. In these mixed samples, the amine can form a gel network with either enantiomer

of the lysine dendron or a mixture of both. The T_{gel} values produced by these gels are shown in Figure 5.15.

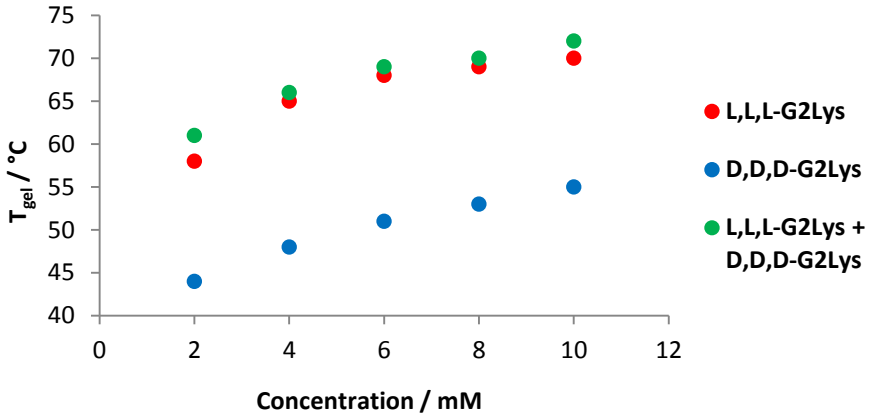

Figure 5.15. T_{gel} values of gels with **C8R** and either **L,L,L-G2Lys**, **D,D,D-G2Lys** or a mixture both. Toluene.

The samples made with **C8R** and **D,D,D-G2Lys** are roughly 15-20°C less thermally stable than the gels formed from **C8R** and **L,L,L-G2Lys** at all concentrations. However, the T_{gel} values of the gels formed from a mixture of **C8R**, **L,L,L-G2Lys** and **D,D,D-G2Lys** are, within error, the same as those for the gels of only **C8R** and **L,L,L-G2Lys**. By comparing the T_{gel} of the 10 mM gel made from the 1:1:1 mixture to the T_{gel} values in Figure 5.6. it becomes clear that this may be the result of preferential inclusion of **L,L,L-G2Lys**, or something close to equal inclusion of **L,L,L-G2Lys** and **D,D,D-G2Lys** into the gel network. The only result this experiment rules out is the preferential inclusion of **D,D,D-G2Lys**, which in any case, was not a likely outcome. A sample made with 0.625 mM **C8R** and an equivalent of both enantiomers of dendron in 95:5 methylcyclohexane to dioxane and was then analysed by CD spectroscopy. Unfortunately the excess, uncomplexed dendron formed a precipitate in the sample. The technique usually requires an optically transparent sample and the amount of light blocked / scattered by the precipitate in the mixture meant a reliable and meaningful spectrum could not be recorded.

The gel made from a 1:1:1 mixture of **C8R**, **L,L,L-G2Lys** and **D,D,D-G2Lys** was analysed further using VT-NMR. The same experiment which has been applied to the other gels where the sample is heated gradually, with a ^{1}H NMR spectrum being recorded at 5°C intervals to find the concentration of gelating complex "visible" in solution as the temperature increases. The increase in concentration of **C8R** with increasing temperature is shown in Figure 5.16. In this case the integration of amine is used as there is obviously a 10 mM excess of lysine dendron

which is in solution, even at low temperature. This data was then used to produce a van 't Hoff plot from which the parameters ΔH_{diss} and ΔS_{diss} can be calculated. These can be verified, as before, by using them to predict the amount of gelator complex soluble at each temperature and comparing this to the experimentally observed data Figure 5.16.

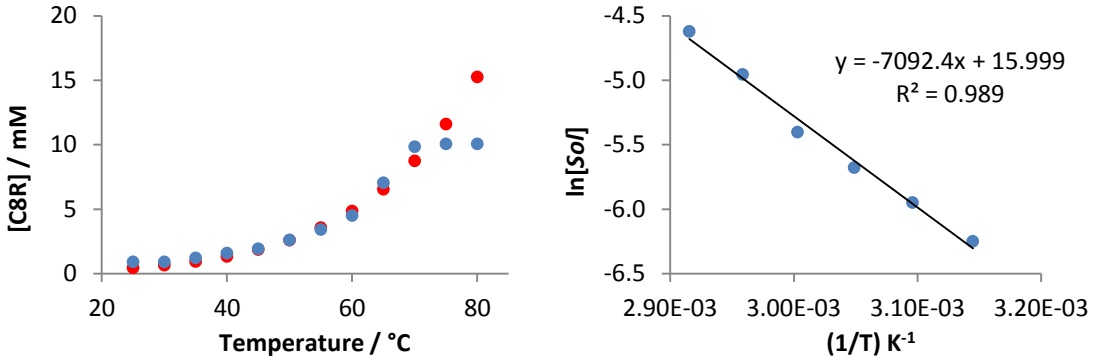

Figure 5.16. Plots showing experimental (blue) and calculated (red) concentration of **C8R** as temperature increases and the van 't Hoff plot.

It is important to note that at 25°C a 10 mM concentration of lysine dendron is seen in the spectrum of the sample and therefore not included in the gel network. The ΔH_{diss} and ΔS_{diss} values calculated from this data are 59.0 kJ mol^{-1} and 133 J K^{-1} mol^{-1} respectively. Both of these values are slightly higher than those calculated for the samples made with **C8R** and **L,L,L-G2Lys** (56.2 kJ mol^{-1} and 125 J K^{-1} mol^{-1}) or 0.5 equivalents of **L,L,L-G2Lys** and **D,D,D-G2Lys** (56.8 kJ mol^{-1} and 125 J K^{-1} mol^{-1}). The fact gels have such similar values means the values for the gel with a 1:1:1 mixture of **C8R**, **L,L,L-G2Lys** and **D,D,D-G2Lys** are difficult to interpret and does not aid the analysis of how much of each enantiomer of dendron is incorporated into the gel network.

The next experiment to probe this proposed selectivity was to analyse the xerogel from a gel formed with the 1:1:1 mixture using FEG-SEM. Representative images of this sample are shown in Figure 5.17. The morphology of the network of this xerogel is very similar to that of the sample formed with **C8R** and **L,L,L-G2Lys** only (Figure 5.11.), with very thin (ca. 10-15 nm) fibres forming the collapsed network. In contrast, the network appears to be very different to that formed by **C8R** and **D,D,D-G2Lys** or 0.5 equivalents of **L,L,L-G2Lys** and **D,D,D-G2Lys** (Figure 5.11.). The images therefore suggest that the network is predominantly assemble from **L,L,L-G2Lys** and **C8R**.

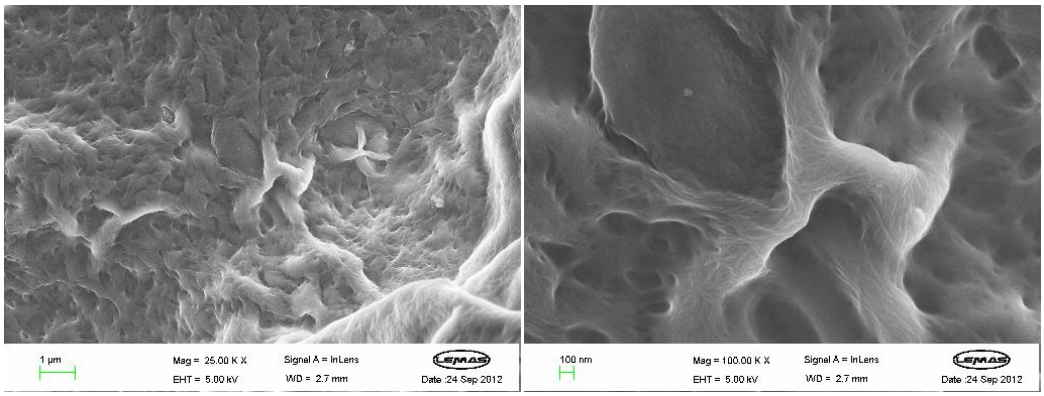

Figure 5.17. FEG-SEM images of xerogels made with a 1:1:1 mixture of **C8R**, **L,L,L-G2Lys** and **D,D,D-G2Lys**, Scale bars = 1 µm and 100 nm.

Quantification of the proportion of **L,L,L-G2Lys** and **D,D,D-G2Lys** taken into the gelator network was attempted using the commercially available chiral shift reagent $Eu(hfc)_3$. Spectra of **L,L,L-G2Lys** or **D,D,D-G2Lys** with 0.5, 1.0 and 2.0 equivalents of $Eu(hfc)_3$ were recorded. Unfortunately, this compound was unable to induce a different change in the spectra of each enantiomer and therefore separate them from one another. A different approach was then attempted, using the chiral amine **Ph(Pro)R** as a chiral shift reagent. This is a chiral compound that has been shown to form a non-assembling complex with the lysine dendrons in the previous chapter. However, this chiral compound was also unable to induce a difference in the spectra of each enantiomer of dendron, nor could each enantiomer of the dendron induce a different change on the resonances of **Ph(Pro)R**. Neither chiral shift reagent was able to separate the two enantiomers **L,L,L-G2Lys** and **D,D,D-G2Lys** in ^{1}H NMR spectroscopy and therefore neither were useful for quantifying the amount of each taken into the gelator network. The approach taken in the previous chapter was to remove an amount of the excess component and derivitise this with a chiral reagent. This was readily feasible with the amine that was reacted with a chiral isocyanate and coupled both chiral centres in close proximity through a planar urea group. This resulted in two diastereomers, one where the methyl group on the chiral centre (which has a sharp and easily visible ^{1}H NMR resonance) is in close proximity to the aromatic ring on the other side of the urea, the other where the methyl group is further away from the aromatic ring. Due to the electron density of the aromatic system the methyl groups in the two diastereomers will experience different environments and will appear differently shifted in the ^{1}H NMR. This was always unlikely with the lysine dendrons as the proton resonances of the lysine side chain are indistinct and overlap with other peaks. The approach used in the last chapter to covalently derivatise the excess components and analyse

their chirality was unsuited to the carboxylic acid containing dendrons as, aside from the problem of clearly seeing proton resonances discussed above, they are less able to undergo instantaneous reaction with a mild reagent, under mild conditions (e.g. without base which can cause racemisation of the peptide). For these reasons, the quantification of the selective uptake of **L,L,L-G2Lys** or **D,D,D-G2Lys** into a gel network with **C8R** was discontinued and work focussed on how mixtures of other *R* amines with an excess of **L,L,L-G2Lys** and **D,D,D-G2Lys** would behave.

5.2.2. Component Selection With Different Amines

Again, gels with a 1:1:1 mixture of *R* amine, **L,L,L-G2Lys** and **D,D,D-G2Lys** were made in toluene and their T_{gel} values analysed. These were then compared to the T_{gel} values of gels made with a 1:1 mixture of amine and either **L,L,L-G2Lys** or **D,D,D-G2Lys**. Gels formed using alkyl amines **C4i**, **C6R**, **C9R** and **CHR** were the first gels to be tested (Figure 5.18.).

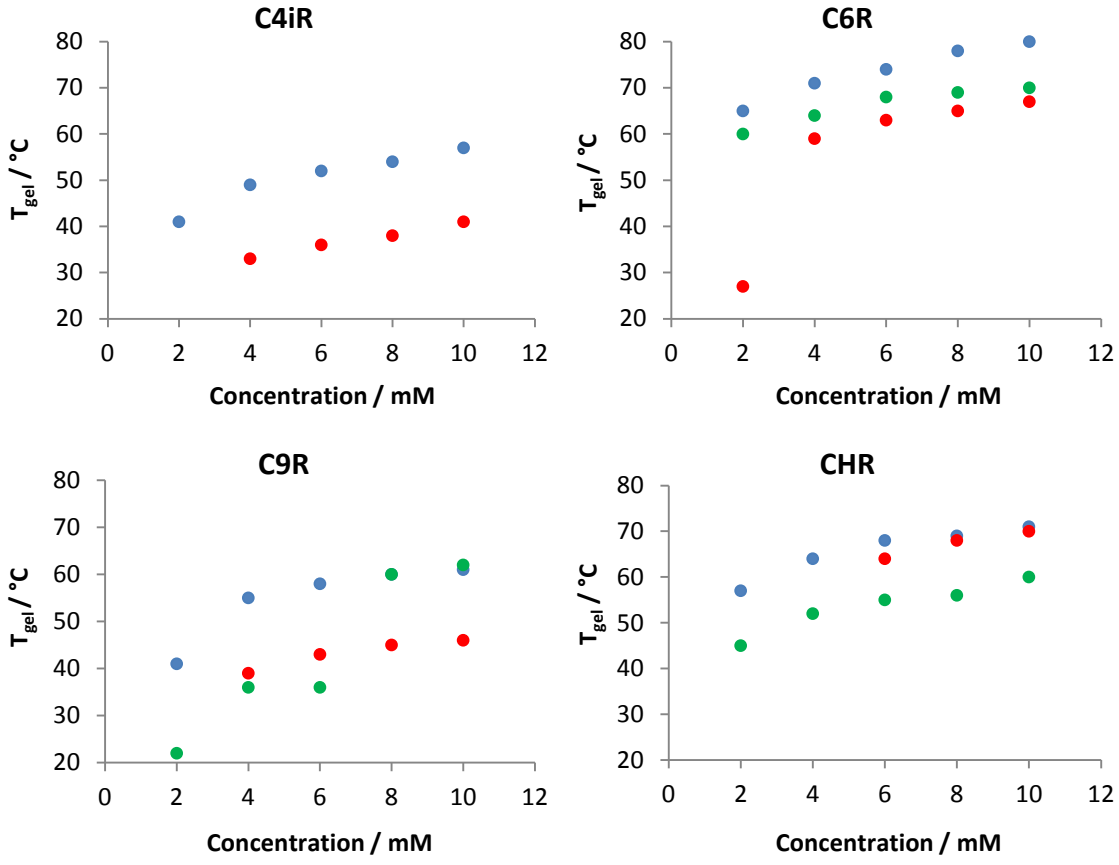

Figure 5.18. T_{gel} values of gels with **C4iR**, **C6R**, **C9R** or **CHR** and either **L,L,L-G2Lys** (blue), **D,D,D-G2Lys** (red) or **L,L,L-G2Lys** and **D,D,D-G2Lys** (green). Toluene.

The most striking thing about the results is that the samples made with **C4iR**, **L,L,L-G2Lys** and **D,D,D-G2Lys** do not have any T_{gel} values recorded on the graph. This is because the samples were only capable of forming partial gels, despite the equivalent samples made with either **L,L,L-G2Lys** or **D,D,D-G2Lys** both forming stable, measurable samples at all but the lowest concentration. At first, it was thought that this may be an anomalous result but the gels made with **CHR** also show the gelating ability of the mixture of **L,L,L-G2Lys** and **D,D,D-G2Lys** to be far less than that of either enantiomer alone with this chiral amine. Those formed with **C6R**, **L,L,L-G2Lys** and **D,D,D-G2Lys** tend to be between the values of those formed with either enantiomer alone with **C6R**. The gels formed with **C9R**, **L,L,L-G2Lys** and **D,D,D-G2Lys** show a very unexpected trend, being less stable than the other gels at low concentration, before being as stable as the gels formed with **C9R** and only **L,L,L-G2Lys** in the most concentrated samples. These were surprising results and were hard to understand and rationalise based on the model of inclusion of different components put forward in the previous chapters. To try to gain more information to aid in the understanding of this process, gels formed with aromatic chiral amines **Ph(Me)R**, **4-MeR**, **4-ClR** and **4-FR** with either **L,L,L-G2Lys**, **D,D,D-G2Lys** or both were analysed (Figure 5.19.)

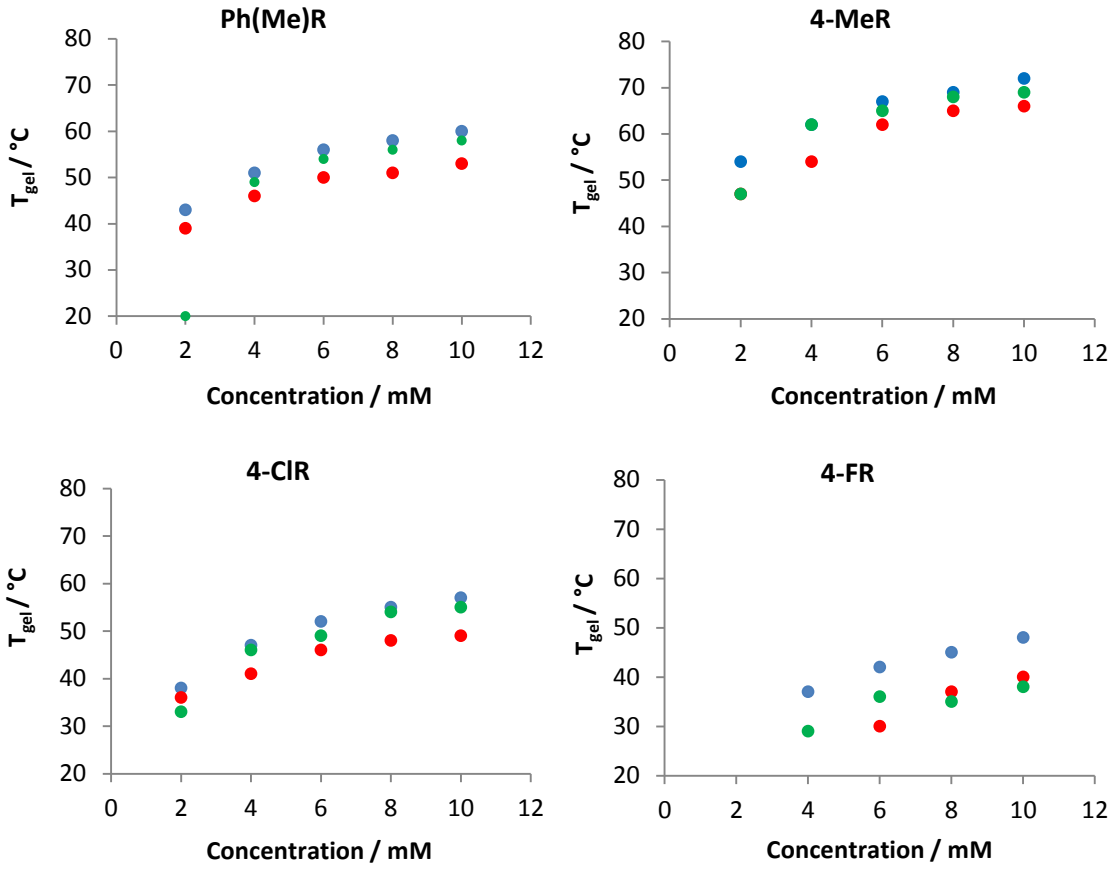

Figure 5.19. T_{gel} values of gels with **Ph(Me)R**, **4-MeR**, **4-ClR** or **4-FR** and either **L,L,L-G2Lys** (blue), **D,D,D-G2Lys** (red) or **L,L,L-G2Lys** and **D,D,D-G2Lys** (green). Toluene.

The results of these samples are less striking than those in the alkyl amine samples. The results for the gels formed with **Ph(Me)R**, **4-MeR**, and **4-ClR** were all very similar, with the T_{gel} values of the gels formed with **L,L,L-G2Lys** and **D,D,D-G2Lys** in between those of the gels formed with either **L,L,L-G2Lys** or **D,D,D-G2Lys**. However, in each case the 2 mM gel dendron enantiomers has an unexpectedly low T_{gel}. The gels formed with **4-FR** show a slightly different trend with no gels being formed at 2 mM and the thermal stabilities of the gels formed with both enantiomers becoming more similar to those of gels formed with only **D,D,D-G2Lys** and **4-FR** as the concentration of the samples increases. Due to the small difference in thermal stability between 10 mM gels formed with **L,L,L-G2Lys** or **D,D,D-G2Lys** in all cases (ca. 8-9°C) and the varying change in thermal stability of gels with increasing incorporation of **D,D,D-G2Lys** (Figure 5.13.) it is hard to state whether any selective uptake of one enantiomer of the dendron into the gel network occurs. Finally, gels with other aromatic amines **1-NapR**, **2-NapR** and **TetR** were made and tested in this manner. The resulting T_{gel} values are shown in Figure 5.20.

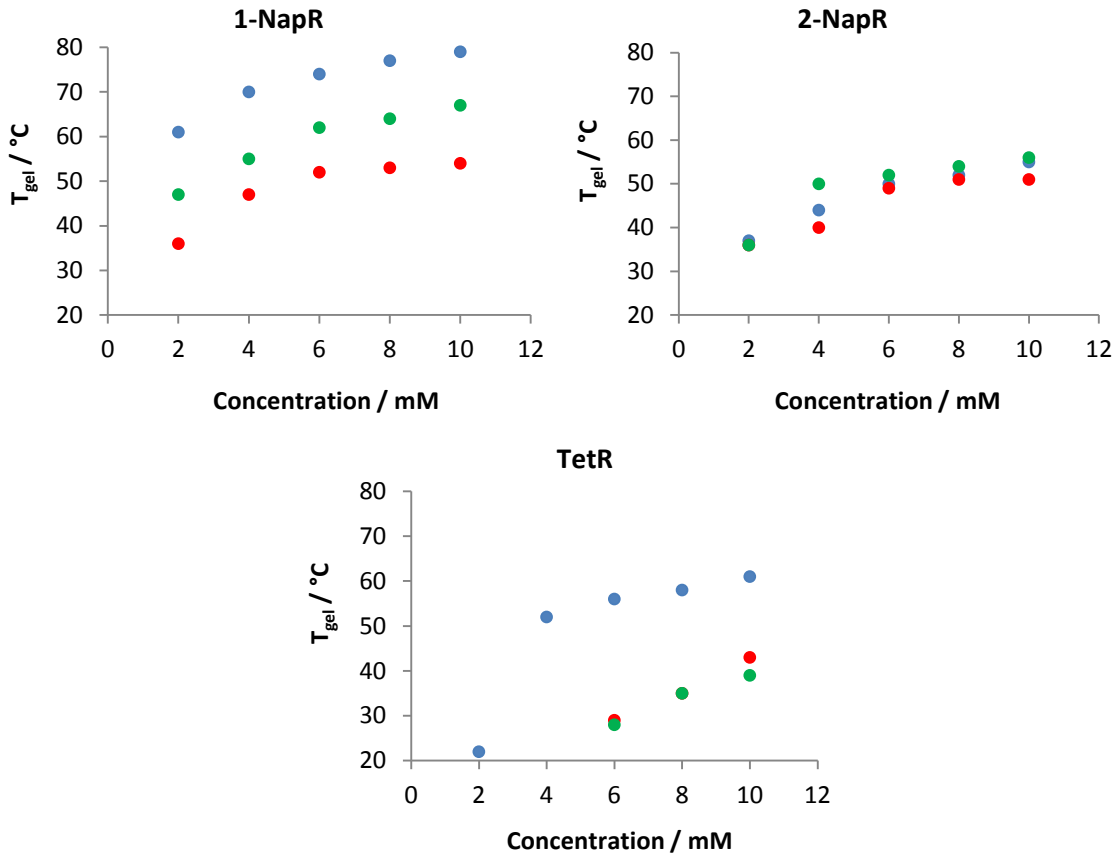

Figure 5.20. T_{gel} values of gels with **1-NapR**, **2-NapR**, or **TetR** and either **L,L,L-G2Lys** (blue), **D,D,D-G2Lys** (red) or **L,L,L-G2Lys** and **D,D,D-G2Lys** (green). Toluene.

The T_{gel} values of gels formed with **1-NapR**, **L,L,L-G2Lys** and **D,D,D-G2Lys** were almost exactly midway between the values of the equivalent gels formed with only **L,L,L-G2Lys** or **D,D,D-G2Lys**. When compared against the graph for T_{gel} against increasing percentage of **D,D,D-G2Lys** in the gelator network (Figure 5.14.) this indicated a roughly 50 / 50 mixture of **L,L,L-G2Lys** and **D,D,D-G2Lys** in the gelator network of the 10 mM sample. The gels made with **2-NapR**, **L,L,L-G2Lys** and **D,D,D-G2Lys** appear to have T_{gel} values between those of the gels formed with **2-NapR** and only **L,L,L-G2Lys** or **D,D,D-G2Lys**. However, because of the very small difference between the gels formed with **L,L,L-G2Lys** or **D,D,D-G2Lys**, and the very unpredictable change in T_{gel} with increasing amount of **D,D,D-G2Lys** in the gelator network (Figure 5.14.), it is hard to draw a meaningful conclusion from this data. Finally, the T_{gel} values produced by gels formed from **TetR**, **L,L,L-G2Lys** and **D,D,D-G2Lys** do not form at 2 and 4 mM, when gels of **TetR** and **D,D,D-G2Lys** do not form either. At higher concentration, gels of this mixture are formed they have T_{gel} values which are the same as those of the weaker **TetR** and **D,D,D-G2Lys** mixture. Compared to the values in Figure 5.14. this seems to indicate that more **D,D,D-G2Lys** is

incorporated into the gelator network than **L,L,L-G2Lys**. This is contrary to the findings the previous chapters as there is no reason for this selective incorporation to occur. These Tgel values have provided information that is difficult to rationalise given what we have discovered and proven about component selection in these multi-component supramolecular gels so far.

However, when the gels where **L,L,L-G2Lys** has been mixed with more than one equivalent of an amine have been viewed by ^{1}H NMR the peak of the amine free in solution has appeared to be broadened. This was attributed to most likely be due to the amine in solution being in exchange with the amine trapped in the gelator network. In these gels, the amine is part of the gelating complex but is not involved in intermolecular interactions between complexes other than van der Waals forces, changing packing of the complexes, or in some cases changing the interactions between the complex and the solvent. A similar broadening has been observed in the spectra of gels with more than one equivalent of lysine dendron, in this case it is the dendron resonances that are broadened and most likely signify some or all of the dendron is in equilibrium with dendron in the gelator network. The dendrons are the primary molecule in the gelating complex involved in fibre formation as they contain the amide and carbamate groups which partake in the intermolecular hydrogen bonding which underpins the gel network. It is therefore reasonable to expect that the exchange of lysine dendrons will have a larger impact on the stability of the gelator network than the swapping of amines back and forth from solution, especially if the dendrons can have different chirality. One way to investigate this was to produce gels made with a 2:1 ratio of **L,L,L-G2Lys** to amine. Comparing these results to those of the gels made with a 1:1 ratio of these molecules would probe the disruptive effect caused by excess dendron, without the added influence of chirality. The gels were made using the amine **C4iR** as the samples made with this amine appeared to be most affected by having one equivalent of both **L,L,L-G2Lys** and **D,D,D-G2Lys** (Figure 5.18.). As can be seen (Figure 5.21.), the presence of excess amine does indeed somewhat decrease thermal stability. As such, it is proposed that this exchange mechanism, exacerbated by changing the chirality of the dendron is behind some of the results seen in this section. If true this seems to have more effect with some acid-amine complexes than it does with others, again demonstrating how tuneable – even if undesirably – these systems are.

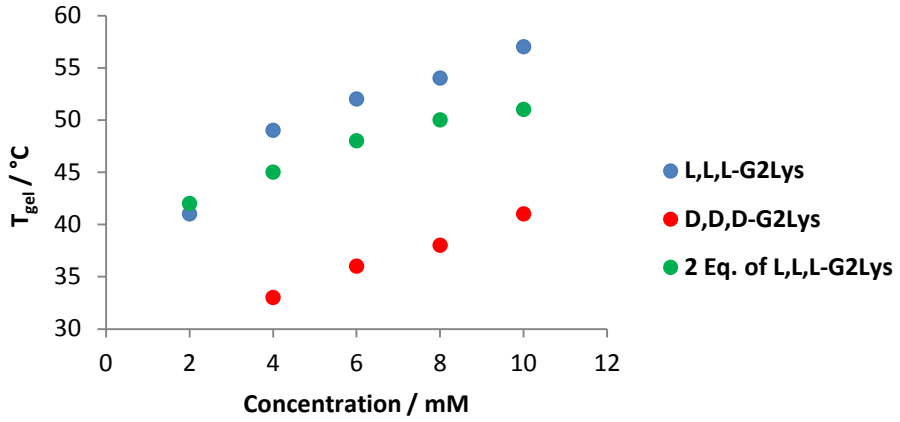

Figure 5.21. T_{gel} values of gels with **C4iR** and either **L,L,L-G2Lys** (blue), **D,D,D-G2Lys** (red) or 2 equivalents of **L,L,L-G2Lys** (green). Toluene.

In conclusion, varying the ratio of **L,L,L-G2Lys** to **D,D,D-G2Lys** in a gel network has been shown to have a profound effect on the assembly of the gelating complexes, the nanoscale morphology of the networks formed and the thermal stability of the gels produced. This has been shown not just with non-chiral amines (especially **C8**) but also with a range of chiral amines (especially **C8R**). The question of whether one enantiomer of the lysine dendron is selectively incorporated into a gel network with an enantiomer of achiral amine has been investigated and the results have been inconclusive. The most compelling result has been found through FEG-SEM which shown a striking similarity between the network formed between a 1:1 mixture of **C8R** and **L,L,L-G2Lys**, and that formed from a 1:1:1 mixture of **C8R**, **L,L,L-G2Lys** and **D,D,D-G2Lys**.

5.3. Mixed Chirality Dendrons

Given the dramatic changes observed when varying dendron chirality from **L,L,L-G2Lys** to **D,D,D-G2Lys**, a pair of dendrons which were diastereomeric to these enantiomers – **L,D,D-G2Lys** and **D,L,L-G2Lys** (Figure 5.22) – which have been previously studied by Smith and co-workers[326] were synthesised using the same methodology used to synthesise **L,L,L-G2Lys** and **D,D,D-G2Lys**.

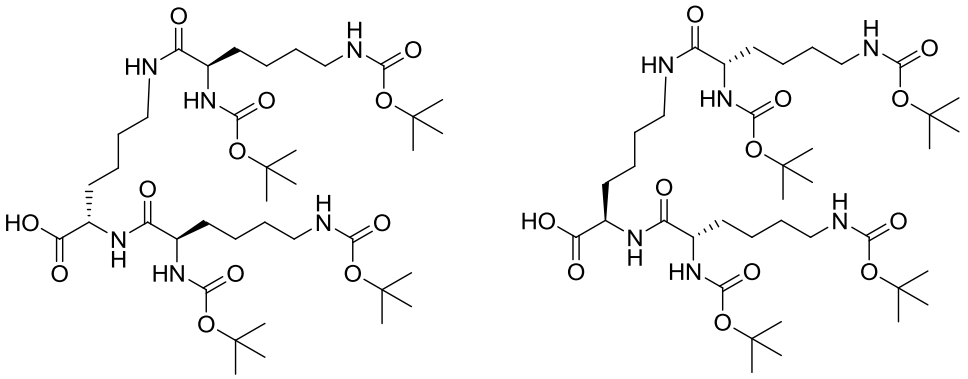

Figure 5.22. Structure of enantiomeric lysine dendron molecules **L,D,D-G2Lys** and **D,L,L-G2Lys**

These dendrons are enantiomers of each other but are diastereomers of **L,L,L-G2Lys** and **D,D,D-G2Lys**. They were synthesised so observe the effect of changing the chirality of the chiral centre closest to the acid would have on the gelation ability of the complexes formed. The first experiment conducted with them was to form gels with non-chiral aliphatic amines (**C4**-**C8**) with a varying ratio of **L,D,D-G2Lys** and **D,L,L-G2Lys** and observe the change in T_{gel} with changing composition in each case. The results are shown in Figure **5.23** and plotted as T_{gel} against % **D,L,L-G2Lys** used.

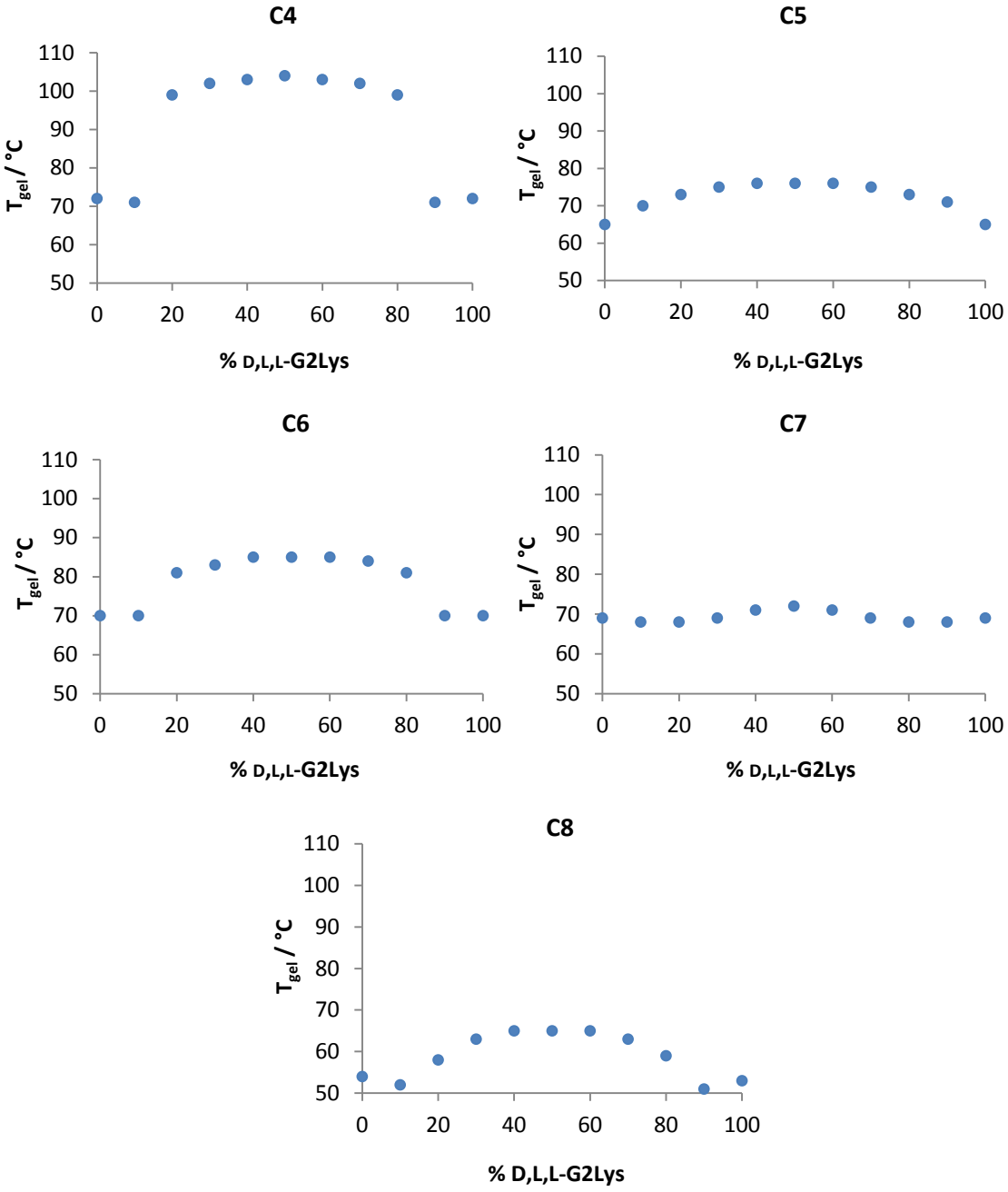

Figure 5.23. T_{gel} values of gels with a varying ratio of **L,L,L-G2Lys** and **D,D,D-G2Lys**.and either **C4**, **C5**, **C6**, **C7** or **C8**. Toluene.

Again, as both gelating complexes formed are enantiomers of each other **L,D,D-G2Lys** with amine, and **D,L,L-G2Lys** with amine, all the curves are symmetrical. The first gels tested, those made with **C4**, show the most dramatic change in T_{gel} with changing ratio of **L,D,D-G2Lys** to **D,L,L-G2Lys** in the gelator network. There is initially no change in thermal stability when ca. 10% of the minority enantiomer of lysine dendron is added but then as ca. 20% is included the

thermal stability increases by roughly 30°C, there is then a plateau based around a high point at 50% **L,D,D-G2Lys** which represents the maximum T_{gel} of these gels (104°C), before this decreases as more **D,L,L-G2Lys** is included. These gels show the largest increase in T_{gel} value upon mixing of both enantiomers, the T_{gel} values being spread over a range of 32°C. These values were higher than those obtained for equivalent gels made from **C4**, **L,L,L-G2Lys** and **D,D,D-G2Lys**. The trend shown by gels formed with **C5** is slightly different, as the T_{gel} begins to increase immediately when only ca. 10% of the minority enantiomer is included. This results in a more gradual curve shape to the T_{gel} graph and there are no dramatic increases in T_{gel} following a small change in composition. Also, these gels occur over a narrower range of T_{gel} values (11°C) and are generally less thermally stable across the composition range than those made with **C4**. They are roughly equally stable to equivalent gels made with **C5**, **L,L,L-G2Lys** and **D,D,D-G2Lys** (Figure 5.1.). The gels formed with **C6** are more similar to those formed with **C4** as adding 10% of the minority enantiomer leads to no change in T_{gel} but addition of 20% leads to a large increase, however, the total increase from mixing the enantiomers is smaller (15°C) than when **C4** is used. These gels are more stable than their **L,L,L-G2Lys** and **D,D,D-G2Lys** equivalents (Figure 5.1.). The most unusual gels tested were those made with **C7** which showed a much smaller total change in T_{gel} value when the enantiomers of lysine dendron were mixed. Many of these values are the same within error, but it is clear that once again the most thermally stable gel is formed with 50% **D,L,L-G2Lys**. All these gels have similar stability as the most stable gels formed with **C7**, **L,L,L-G2Lys** and **D,D,D-G2Lys**. The gels formed with **C8**, showed a gradual change in T_{gel} as more minority enantiomer was incorporated centred around a the maximum T_{gel} at 50% **D,L,L-G2Lys** (65°C). These gels were roughly equally stable to those formed with **C8**, **L,L,L-G2Lys** and **D,D,D-G2Lys**. In summary these data show that the thermal stability increases when both enantiomer of the lysine dendron are mixed together, with the maximum T_{gel} values occurring for the racemic gels. The results differ to those obtained from equivalent gels formed from **L,L,L-G2Lys** and **D,D,D-G2Lys** (Figure 5.1.) as in those systems **C8** was the most effective amine for accentuating the difference in thermal stability between enantiopure and mixed chirality gels, whereas in this case **C4** is clearly the most effective amine. It is unusual that enantiomeric mixtures should form enhanced gels and this may suggest that interactions between opposite enantiomers (heterochiral) are favoured over interactions between the same enantiomers (homochiral)

To further assess the effect of mixing **L,D,D-G2Lys** and **D,L,L-G2Lys** with a non-chiral amine on the assembly of the complexes, CD was used. Samples with a varying ratio of **L,D,D-G2Lys** to

D,L,L-G2Lys were formed with all the amines tested in 95:5 methylcyclohexane to dioxane. Unfortunately, all of the series had a number of samples that formed a precipitate instead of a homogeneous, optically transparent sample. This meant the CD spectra of the entire series could not be recorded. Samples were made using increasing amounts of dioxane in the solvent but many mixtures formed a precipitate in this solvent too. When very high proportions of dioxane (up to 50%) was used, precipitates were no longer formed but no CD signal was observed, as this solvent mixture would not support self-assembly of the complexes. As a series of samples could not be accurately analysed, only the results of the mixtures of **C4** with either **L,D,D-G2Lys**, **D,L,L-G2Lys** or a racemic mixture of both (1:0.5:0.5) are shown in Figure 5.24. These spectra clearly show that the samples formed with **L,D,D-G2Lys** or **D,L,L-G2Lys** have equal and opposite CD spectra and the sample made with both has a CD spectrum that is almost zero across the entire wavelength range.

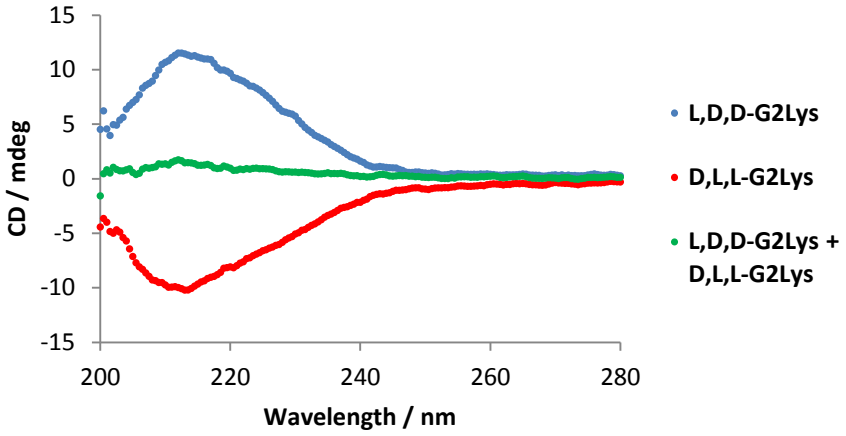

Figure 5.24. CD spectra of samples made with **C4** and either **L,D,D-G2Lys**, **D,L,L-G2Lys** or a mixture both. 0.625 mM. 95:5 Methylcyclohexane to Dioxane.

The gels formed by **L,D,D-G2Lys** and **D,L,L-G2Lys** were further characterised using VT-NMR experiments. The obvious choice would be to analyse the gels made with **C4** as these showed the largest change in thermal stability with changing ratio of **L,D,D-G2Lys** to **D,L,L-G2Lys**. Unfortunately, the T_{gel} of the 10 mM gel made with both **L,D,D-G2Lys** and **D,L,L-G2Lys** with **C4** is 104°C which is too high to be analysed in toluene-d_8 using the NMR spectrometer. This meant the gels formed with **L,D,D-G2Lys** and **D,L,L-G2Lys** with **C5** were analysed instead. These gels also show a maximum T_{gel} for the racemic gel but the difference between this and the enantiopure gels is only 11°C. The plots showing the increase in concentration of lysine dendron visible as the temperature increases are shown in Figure 5.25. Only the plots for the

gels with **L,D,D-G2Lys** with **C5** and **L,D,D-G2Lys** and **D,L,L-G2Lys** with **C5** are shown as the plot for the gel made with only **D,L,L-G2Lys** was almost identical to its enantiomer.

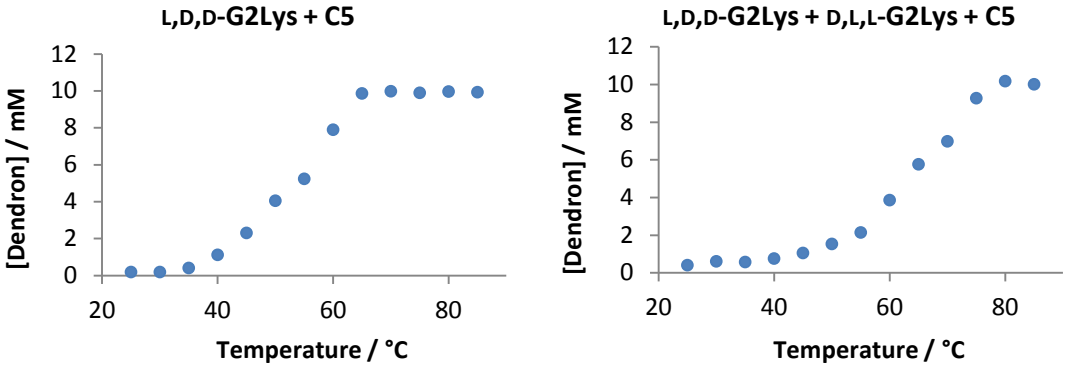

Figure 5.25. Concentration of lysine dendron visible in gels of **L,D,D-G2Lys,** or **L,D,D-G2Lys** and **D,L,L-G2Lys** with **C5** as temperature increases. Toluene-d_8.

The graphs clearly show that the gel network made with a single enantiomer of lysine dendron is disbanded at a lower temperature than the one made with both enantiomers, supporting the macroscopic T_{gel} results. This is reflected in the $T_{100\%}$ values for both gels – 66°C for the enantiopure gel and 77°C for the racemic gel. This fits well with the T_{gel} values for each gel with are 65°C and 75°C respectively. That the mixed chirality system is a more effective gelation mixture is also supported by the MGC values which are 6.0 mM for the enantiopure gel and 1.0 mM for the racemic gel. These are very different to the [Insol]@T_{gel} values which are 0.4 mM for the enantiopure gel and 0.7 mM for the racemic gel. However, as has already been discussed MGC and [Insol]@T_{gel} measure subtly different things, and will not match in all cases. Again we can use this data to find the ΔH_{diss} and ΔS_{diss} values for each gel by producing van 't Hoff plots. The plots produced are shown in Figure 5.26. and the data calculated from them is shown in Table 5.4. The plot for the gel formed from **D,L,L-G2Lys** and **C5** is not shown as it is almost identical to its enantiomer.

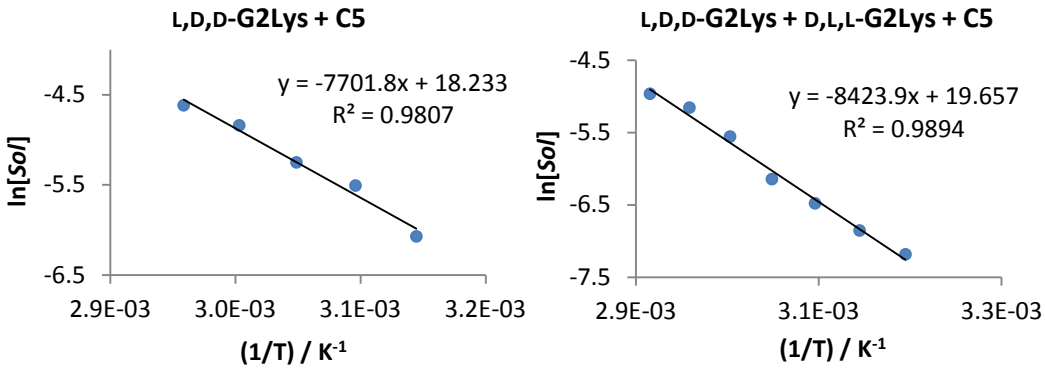

Figure 5.26. Van 't Hoff plots of gels formed from **L,D,D-G2Lys** or **L,L,L-G2Lys** and **D,D,D-G2Lys** with **C5.**

Table 5.4. Summary of data calculated from van 't Hoff plots.

Dendron	ΔH_{diss} / KJ mol^{-1}	ΔS_{diss} / J K^{-1} mol^{-1}
L,D,D-G2Lys	64.0	152
L,D,D-G2Lys + D,L,L-G2Lys	70.0	163
D,L,L-G2Lys	63.9	153

It is expected that the enantiomeric gels exhibit the same ΔH_{diss} and ΔS_{diss} values and reassuringly they do. The values of the racemic gel are different to both of these gels, showing higher ΔH_{diss} and ΔS_{diss} values, which suggests a more highly organised gelator network in this case. This is the opposite of what is seen in the gel formed form equal amounts of **L,L,L-G2Lys** and **D,D,D-G2Lys** with **C8** (Table 5.1.) where the racemic gel had lower ΔH_{diss} and ΔS_{diss} values than the enantiopure gels. Despite this being different to what has been observed before, it could be verified by being used to accurately predict the solubilisation of the gelator networks with increasing temperature (Figure 5.27.).

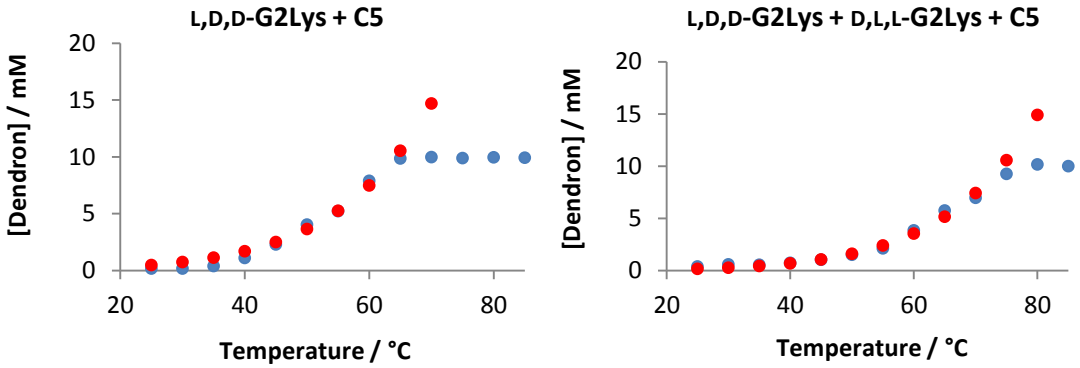

Figure 5.27. Plots showing experimental (blue) and calculated (red) concentration of lysine dendron as temperature increases and the van 't Hoff plot.

To try to gain further insight into the formation of gels with **L,D,D-G2Lys** and **D,L,L-G2Lys** FEG-SEM was used. The gels formed from **C4** and either **L,D,D-G2Lys**, **D,L,L-G2Lys** or both were dried to form xerogels which were imaged using FEG-SEM (Figure 5.28.). The images produced by the enantiopure xerogels showed little fine detail, with a network of very thin fibres being just visible on what otherwise appears to be a surface with a very flat topography. In contrast to this, the racemic xerogel showed a much more clearly visible network of thin fibres (ca. 20 nm) which aggregate to form thicker fibres (ca.100 nm). Despite the enantiopure gels providing poor images this proves that the gel formed with both dendrons had a very different morphology than either enantiopure sample and that this network was indeed a co-assembly formed with both enantiomers and that they did not resolve into two different networks.

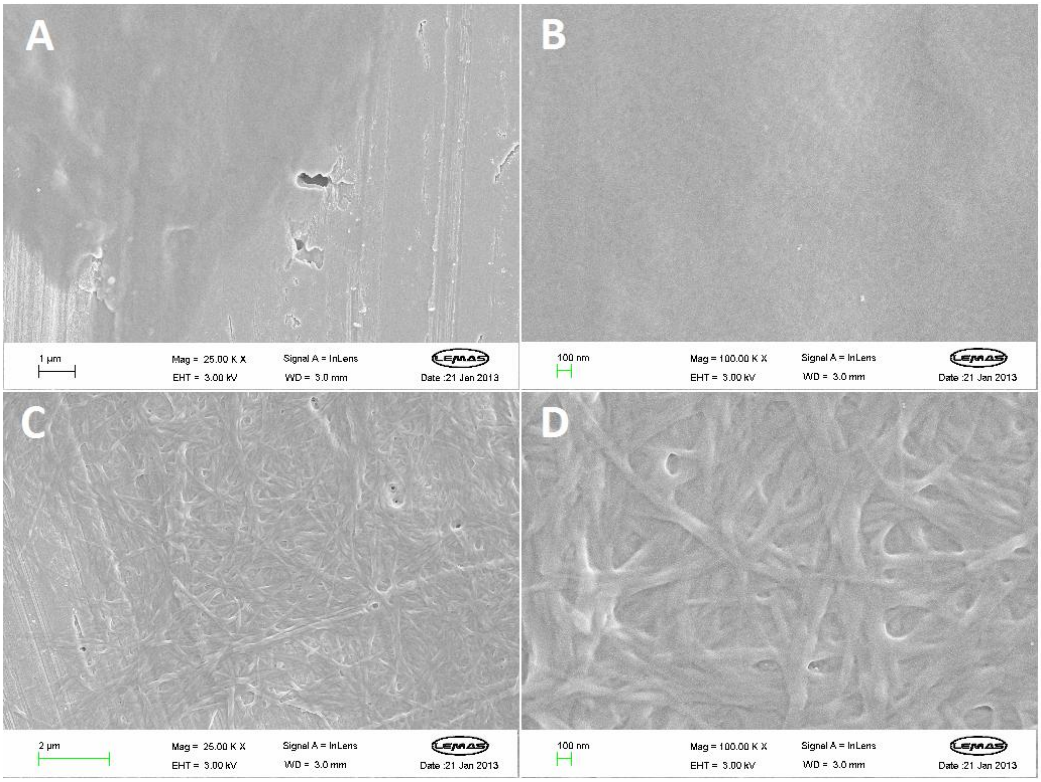

Figure 5.28. FEG-SEM images of xerogels of with **C4** and A) and B) **L,D,D-G2Lys** ,Scale bars = 1 µm and 100 nm. C) and D) **L,D,D-G2Lys** and **D,L,L-G2Lys** ,Scale bars = 2 µm and 100 nm.

In summary it has been shown that forming a gel with different proportions of **L,D,D-G2Lys** and **D,L,L-G2Lys** with non-chiral alkyl amines can have a profound effect on the T_{gel} values of the gels formed. Similar to mixtures of **L,L,L-G2Lys** and **D,D,D-G2Lys** the maximum T_{gel} in most cases was when equal amounts of **L,D,D-G2Lys** and **D,L,L-G2Lys** were included, with the enantiopure gels representing or being near to the minimum thermal stabilities observed. However, the effect on gels with each amine was different with **L,D,D-G2Lys** and **D,L,L-G2Lys** – which showed the widest range of T_{gel} values with **C4** – than **L,L,L-G2Lys** or **D,D,D-G2Lys** – which showed the widest spread of T_{gel} values with **C8**. The CD spectroscopy that was attempted with **L,D,D-G2Lys** or **D,L,L-G2Lys** was less informative than that with **L,L,L-G2Lys** or **D,D,D-G2Lys** as many of the samples began to precipitate which meant obtaining reliable spectra became impossible. The few spectra recorded though, are equal and opposite for the aggregates formed with each enantiomer, with the mixed chirality sample showing no overall signal. The VT-NMR analysis of these gels showed that the stronger gels formed with both **L,D,D-G2Lys** and **D,L,L-G2Lys** had higher ΔH_{diss} and ΔS_{diss} values than the enantiopure gels, interestingly this was not the case with the equivalent gels formed from **L,L,L-G2Lys** or **D,D,D-G2Lys** where although the gels did

become more thermally stable they did so with a less enthalpically favoured gelation event. This demonstrates the dramatic effects that varying a single chiral centre can have on the reversible self-assembly process. The FEG-SEM images of the enantiopure gels showed a very different morphology for the enantiopure and racemic gels and demonstrated that the gel made with both enantiomers of dendron was indeed single network of both gelators.

5.4. Conclusion

In conclusion it has been shown that the mixing of either **L,L,L-G2Lys** with its enantiomer **D,D,D-G2Lys** or **L,D,D-G2Lys** with its enantiomer **D,L,L-G2Lys** with non-chiral aliphatic amines produces very thermally stable gels. Generally, the gels made with a mixture of enantiomers were more thermally stable than their enantiopure counterparts, a rare result and in contrast to studies on similar systems.[326] It has been seen that this stability, the morphology and chiroptical properties can be tuned by varying the ratio of each enantiomer. In this example therefore the assembly of mixed chirality systems is favoured over enantiopure aggregation due to a changing balance between the enthalpic benefit and entropic cost of gelation with changing chirality of the molecules.

It has also been shown that gels formed from either **L,L,L-G2Lys** or **D,D,D-G2Lys** with a chiral amine have a diastereomeric relationship, the same as gels of **L,L,L-G2Lys** and *R* or *S* amines did in the previous chapter. Again the properties of the gel could be tuned by varying the ratio of one enantiomer of dendron to the other. The same component selection experiments documented in the previous two chapters were attempted here but failed to provided conclusive evidence of selection of one enantiomer, most likely due to excess dendron in exchange with that in the gel fibre being highly disruptive.

Chapter 6

Conclusions and Future Work

Chapter 6 – Conclusion and Future Work

The first part of this project investigated a stimuli responsive gel that showed a gel-sol transition in the presence of certain cations. It was shown that the response to Ag^+ was due to the silver(I)-alkene interaction. This was proven both by observing this interaction in a small molecule analogue of the gelator and the lack of any response in a similar gelator with no alkene groups. The gel also showed a gel-sol transition upon addition of Li^+ which was due to its high charge density allowing it to disrupt the gel fibres by binding to the amide groups which otherwise partake in intermolecular hydrogen bonding that underpins gel formation. Alkene groups were not necessary for the gelator to exhibit this response. The gel showed no response to Na^+ or K^+ as these ions were less charge dense and therefore unable to disrupt the intermolecular hydrogen bonding of the gelator molecules. As such this gelator was an example of a responsive system operating through two different mechanisms.

A series of two-component organogelators composed of a lysine dendron and different monoamines were then studied. A simple type of this gel was characterised along with the effect of forming this gel with different solvents and then the effect of changing the amine. Crucially it was shown that using different amines led to the formation of very different gels with different thermal stabilities. Component selection was then investigated in this system with the lysine dendron being challenged with different amines with which it could form a gel. It was shown that either the amine which formed the most stable gel or the amine with the highest pKa was preferentially included into the gel network. If one amine was favoured by both factors its selective incorporation would be more pronounced and if both factors favoured different amines neither would be preferentially selected. Importantly it was shown that when a pre-formed gel was challenged with an amine that was preferential for gel formation, exchange took place – over time, at room temperature – and the superior amine was included into the gel network at the expense of the other, demonstrating the dynamic and responsive evolving nature of gel-phase soft materials.

The chirality of these systems was then probed. It was shown that different enantiomers of the same amine would form very different diastereomeric gels with the lysine dendron, which was itself chiral. Different percentages of each enantiomer of amine were mixed and the thermal stability of the gel changed depending on the ratio of enantiomers. This demonstrates the easy tunability of these systems. The same component selection studies were carried out for these

chiral systems and it was shown via derivatisation of the excess amine that there was indeed preferential uptake of the more effective gel-forming enantiomer into the gel network in most cases. The chirality of the dendron was then changed. First, mixing different ratios of enantiomeric dendrons with non-chiral amines again demonstrated the tunability of these gels and also provided a rare example of a racemic gel being more thermally stable than its enantiomeric equivalents. Then the dendrons were mixed with a single enantiomer of chiral amine. The same tunability was observed but this time component selection was harder to prove, despite some evidence that it was occurring as in the other examples.

This work has provided a deeper understanding of component selection process in dynamic supramolecular gels and has shown that chirality, as well as general structure can be used to drive this phenomenon. These are useful fundamental lessons for designing "smart" responsive materials that are able to change their composition when a new component is added. This could be used to generate more interesting materials if the amines used have some functionality, for example a conductive or catalytic group attached. This function could be switched off by adding a better gel forming amine, which would act as a type of inhibitor. If this inhibitor amine were itself switchable (for example undergoing a photoisomerisation) the whole system and therefore its properties would be easily switchable too. This is just one proposal for using component-selective gels to generate useful supramolecular gels.

It may also be possible to use these systems to examine interpenetrating gelator networks. When an amine has been excluded from the gelator network – i.e. not selected – it could be further reacted with, for example, an isocyanate. This would provide an instantaneously formed second urea based gelator network around the already formed multi-component gel network. How the first network would affect the formation of the second and how the two would interact would be a very interesting study. A different approach to this type of experiment would be to form a gel with lysine dendron and an amine and then layer a second gel with lysine dendron and a different amine on top of it – instant gelation upon mixing should make this strait forward. It could then be investigated whether the networks begin to grow into each other or indeed whether the amines would eventually mix throughout both gelator networks. Related to this study would be the formation of self-healing materials, something made possible by the fact some of the gels studied in this thesis exhibit thixotropic behaviour, something not studied in this project but certainly very useful for further study and the development of novel applications.

Chapter 7

Experimental

Chapter 7 – Experimental

7.1. General Experimental

All solvents and reagents were used as supplied from commercial suppliers. Unless stated otherwise, the solutions used in the preparation of compounds had the following concentrations: Brine (saturated), $NaHCO_3$ (saturated), $NaHSO_4$ (1.33 mol dm^{-3}), HCl (1 mol dm^{-3}) and NaOH (mol dm^{-3}). Silica gel column chromatography was carried out on silica gel provided by Fluka (60 Å, 35-70 µL). Thin layer chromatography was carried out on commercially available Merck aluminium-backed TLC plates (60, F_{254}) with stains visualised by either UV light, CeMo stain, Ninhydrin stain or $KMnO_4$ stain. Gels were formed in screw top glass vials with a 2 mL volume and i.d. = 5 mm. For compound characterisation, a Jeol ECX spectrometer (^{1}H 400 MHz, ^{13}C 100 MHz) was used. All chemical shifts (δ) are quoted to ppm and referenced to a residual solvent peak. Coupling constant values (*J*) are reported in Hz. ^{1}H and ^{13}C spectra were assigned with the assistance of COSY and HSQC spectra. The appearance of peaks is reported using the following notation: s – singlet, d – doublet, t – triplet, qr – quartet, qn – quintet, m – multiplet and br – broadened. ATR-FTIR was carried out using a Jasco FT/IR 4100 instrument fitted with a Pike MIRacle ATR sampling accessory. Absorbance bands are reported as the wavenumber of maximum absorbance (in cm^{-1}) and labelled as *s* – strong, *m* – medium or *w* – weak. Positive ion electrospray mass spectra were recorded on a Finnigan LCQ mass spectrometer. Melting points were measured on a Stuart SMP3 apparatus using soda glass capillary tubes. Melting points are recorded as ranges and are uncorrected. Optical rotation ($[\alpha]_D$) was measured on a Jasco DIP-370 digital polarimeter with a sodium bulb and 589 nm filter using a cell with a 2 mL volume and 100 mm path length. ^{13}C NMR titration and Job plot experiments were carried out on a Bruker AMX 300 spectrometer (^{1}H 300 MHz, ^{13}C 75 MHz) and referenced to TMS (internal standard). Circular dichroism (CD) was measured with a Jasco J810 circular dichromator fitted with a Peltier temperature control unit using a quartz cell with a path length of 1 mm using the following settings: Data Pitch – 0.5 nm, Scanning Mode – Continuous, Scanning Speed – 100 nm min^{-1}, Response – 1 s, Bandwidth – 2 nm, Accumulation – 5. All CD data are presented as elipticity and recorded in mdeg. The DSC experiment was carried out on a Perkin Elmer DSC 7 with a TAC 7/DX thermal analysis instrument controller. The samples were analysed in 40 µm aluminium sample pans, at a rate of 10°C / min and referenced to an Iridium standard. The samples for scanning electron

microscopy were prepared by being spread over an aluminium stub and dried. They were then coated with a 5 nm layer of Pt/Pd using an Agar High Resolution Sputter Coater and were imaged with a LEO 1530 Gemini FEGSEM fitted with an Oxford Instruments 80mm X-Max SDD detector. The images were collected by John Harrington at Leeds Electron Microscopy and Spectroscopy Centre, University of Leeds. Transition electron microscopy was performed on copper backed TEM grids using a FEI Tecnai G^2 fitted with a CCD camera. Samples were stained with a 1% aqueous uranyl acetate solution. Images were collected by Meg Stark at Biology Technology Faculty, University of York.

7.2. Procedures

7.2.1. Gel Formation – Single Component Gelators

A known amount of gelator was weighed into a 2 mL sample vial. Solvent (0.5 mL) was added using a Gilson pipette. The sample was sonicated in a water bath for 30 minutes, removed, and heated with a heat gun until a homogenous, clear solution was formed. The sample was then left at room temperature overnight to cool, over which time the sample gelates.

7.2.2. Gel Formation – Multi-Component Gelators

Stock solutions of the lysine dendron and the amine were made. Amounts of these stock solutions were added to a 2 mL sample vial with any excess toluene if required using a Gilson pipette. Often a gel is formed instantly upon mixing. This sample was then heated with a heat gun until a homogeneous, clear solution was formed. The sample was then left at room temperature overnight to cool, over which time the sample gelates. This process was undertaken to ensure the gels formed were homogeneous.

When mixtures of amines or dendrons were used in a gel, these stock solutions were mixed first, before the other component was added. This was to ensure mixing with each enantiomer or different amine occurred at the same time.

7.2.3. T_{gel} Measurements

Gel samples were placed in a thermostatted oil bath and heated at a rate no faster than 0.5 °C per minute. As the temperature was increased, the gel was removed from the oil bath and turned upside down. The temperature at which the gel can no longer support itself against

gravity – when the entire gel falls from the top of the inverted vile – is taken as the T_{gel} of the sample. All T_{gel} values were repeated at least once. The error on each T_{gel} value is ±1°C .

7.2.4. Minimum Gelation Concentration (MGC)

Gels of different concentrations were formed in the usual way. They were then tested to see if they were stable to inversion – if the gel could support itself against gravity. The lowest concentration at which this occurred was taken as the MGC value. If the sample exhibited no flow under inversion it was taken as a gel.

7.2.5. Addition of Metal Salts to Gels

A known mass of salt was weighed into a 2 mL sample vial (internal diameter of 8 mm) and dissolved in EtOAc (0.5 mL), added using a Gilson pipette. Then this was carefully pipetted on to the top of the gel – as to not disturb the surface – using a Pasteur pipette. The mixture of gel and salt solution was then left on the bench for 24 hours so any change caused by the salt could take place. After this point the sample was checked by eye and the result recorded.

7.2.6. Field Emission Gun Scanning Electron Microscopy (FEG-SEM)

The gels were formed in the usual way. Once they had set, a small amount was removed with a spatula and spread thinly onto an aluminium SEM stub. This was allowed to air dry in a dessicator to leave the xerogel. This xerogel was then coated with a layer of Pt/Pd and viewed under the microscope.

7.2.7. Transmission Electron Microscopy (TEM)

The gels were formed in the usual way. Once they had set, a small amount was removed with a spatula and brought – very briefly – into contact with a copper backed TEM grid. The small amount of material that had transferred to the grid was allowed to air dry for at least ten minutes before being stained and allowed to dry for a further ten minutes. The sample was then viewed under the microscope. Samples were then stained with a drop of 1% aqueous solution of uranyl acetate, which was allowed to dry before being re-imaged..

7.2.8. Attenuated Internal Reflection Fourier Transform Infra Red (ATR-FTIR)

The gels were formed in the usual way. If required, addition of metal salts was also carried out. These samples were then dried under vacuum until all the solvent had been removed. The resulting xerogel was then analysed as a solid under ATR-FTIR.

7.2.9. Circular Dichroism (CD)

An amount of methylcyclohexane (spectrophotometric grade) was pipetted into a 2 mL sample vial. An amount of amine stock solution (in methylcyclohexane) was then added. This was followed by addition of lysine dendrimer stock solution (in dioxane).This sample was then heated until a clear homogeneous solution was formed. This was left to cool overnight so any molecular aggregation can take place. For analysis the samples are carefully pipetted into the CD cuvette and analysed in the spectrometer. Samples were checked for the absence of linear birefringence effects by taking equivalent measurements of the same sample with the cuvette turned to different angles relative to the incident beam. Linear birefringence effects were not observed for the samples recorded.

7.3. Compounds

7.3.1. L-Lys-Boc[471]

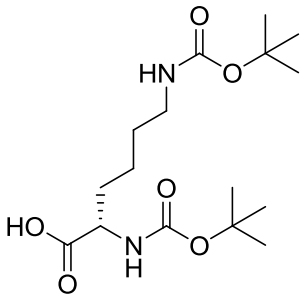

L-Lysine monohydrochloride (10.0 g, 54.8 mmol) and NaOH (4.40 g, 110 mmol) were dissolved in water (100 mL). Di-*tert*-butyl dicarbonate (25.0 g, 114.6 mmol) in THF (100 mL) was added dropwise and the reaction left to stir under nitrogen for 3 hours at 45°C. The volatiles were removed under vacuum and the remaining residue was diluted with water (500 mL) and washed with cyclohexane. The aqueous solution was acidified to pH 3 with 1.33 M $NaHSO_4$ solution and the product extracted with EtOAc. The organic phase was washed with brine and water before being dried over $MgSO_4$. The solution was filtered and the solvent removed

under vacuum. The residue was diluted with DCM which was then removed under vacuum to produce a hygroscopic white solid foam. Yield 15.5 g (44.7 mmol, 82%). R_f = 0.14 (9:1 DCM:MeOH, Nihydrin stain). M.P. = 137-138°C (Lit. = 134-136°C)[471]. $[\alpha]_D^{589}$ = +9.85 (*c* = 1, $CHCl_3$). ^{1}H NMR (400 MHz, $CDCl_3$) δ 5.31 (1H, d, *J*=8.0, CHN*H*), 4.74 (1H, br s, CH_2N*H*), 4.28 (1H, m, C*H*), 3.10 (2H, m, CH_2NH), 1.92-1.61 (2H, m CHCH_2), 1.58-1.26 (22H, m, CH_2, CH_3). ^{13}C NMR (100 MHz, $CDCl_3$) δ 176.30 (*C*O_2H), 156.27 (*C*ONH), 79.93, 79.31 (both *C*$(CH_3)_3$), 53.17 (*C*H), 40.05 (*C*H_2NH), 31.99 (*C*H_2CH), 29.45 (*C*H_2CH_2NH), 28.37, 28.30 (both *C*H_3), 22.38 (*C*H_2CH_2CH). ν_{max} 2913*m* (O-H), 1697*s* (C=O), 1512*m* (N-H), 1362*m* (O-H), 1243*m* (C=O), 1161*s* (C=O). ESI MS $C_{16}H_{30}N_2O_6$ m/z calculated $[M+H]^+$ 347.2177, found 347.2169 (12%), calculated $[M+Na]^+$ 369.1996, found 369.1986 (100%).

7.3.2. C_{12}-(Lys-Boc)$_2$[201]

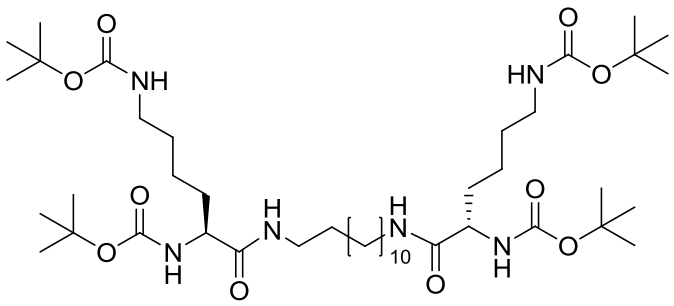

Compound **L-Lys-Boc** (16.7 g, 48.2 mmol) was dissolved in DCM 500 mL and cooled to 0°C. TBTU (15.5 g, 48.2 mmol) was added, followed by DIPEA (16.4 mL, 12.2 g, 94.1 mmol). The mixture was stirred at 0°C for 10 minutes before finely powdered 1,12-diaminododecane was added. The reaction was stirred at 0°C for a further 20 minutes before being allowed to stir at room temperature for 24 hours. The reaction mixture was washed with sat. $NaHCO_3$, 1.33 M $NaHSO_3$, sat. $NaHCO_3$, sat. brine and water. The organic phase was dried over $MgSO_4$ and filtered, before the volatiles were removed under vacuum. This crude product was further purified by flash chromatography (silica, 7:3 cyclohexane:EtOAc) to produce a white solid foam. Yield 16.5 g (19.3 mmol, 84%). R_f = 0.38 (9:1 DCM:MeOH, Ninhydrin stain). M.P. = 102-103°C (Lit. = 104-105°C)[201]. $[\alpha]_D^{589}$ = -10.1 (*c* = 1, MeOH). ^{1}H NMR (400 MHz, $CDCl_3$) δ 6.19 (2H, br s, CHCON*H*), 5.16 (2H, br s, CHN*H*COO), 4.62 (2H, br s, CH_2N*H*COO), 4.00 (2H, br s, C*H*), 3.22 (4H, m, CH_2NHCOCH), 3.09 (4H, m, CH_2NHCOO), 1.88-1.55 (4H, m, CHCH_2), 1.53-1.19 (64H, m, CH_2, CH_3). ^{13}C NMR (100 MHz, $CDCl_3$) δ 172.04 (*C*=O), 156.27 (*C*=O), 80.05, 79.43 (both *C*$(CH_3)_3$), 54.44 (*C*H), 39.99 (*C*H_2NHCO), 39.57 (*C*H_2NHCOO), 32.12, 29.78, 29.56, 29.45, 29.25 (all *C*H_2), 28.53, 28.42 (both *C*H_3), 26.88, 22.74 (*C*H_2). ν_{max} 3296*m* (N-H), 2926*m* (C-H), 2856*m* (C-H),

1690*s* (C=O), 1652*s* (C=O), 1516*s* (N-H), 1364*m*, 1247*m*, 1165*m*, 1043*m*, 861*m*. ESI MS $C_{44}H_{85}N_6O_{10}$ m/z calculated $[M+H]^+$ 857.6322, found 857.6323 (100%), calculated $[M+Na]^+$ 879.6141, found 879.6137 (96%).

7.3.3. *p*-NP-ene[472, 473]

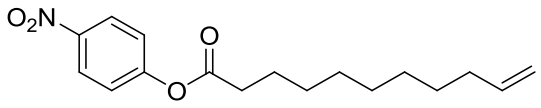

p-Nitrophenol (3.37 g, 24.2 mmol) was dissolved in toluene (20 mL) and pyridine (1.80 mL, 22.3 mmol). 10-Undecenoyl chloride (4.30 mL, 20.0 mmol) was added and the reaction was refluxed at 120°C for 2 hours. After being allowed to cool to room temperature, the reaction mixture was neutralised with sat. $NaHCO_3$ solution. The aqueous layer was removed and the organic layer washed with water, 5% NaOH and 0.1 M HCl. The organic layer was then dried over $MgSO_4$, filtered and the volatiles removed under vacuum to leave an orange oil. Yield 5.03 g (16.5 mmol, 83%). R_f = 0.67 (9:1 DCM:MeOH, UV light, CeMo stain). ^{1}H NMR (400 MHz, $CDCl_3$) δ 8.22 (2H, d, *J*=9.2, C*H*CNO_2), 7.24 (2H, d, *J*=9.2, C*H*CO), 5.78 (1H, ddt (overlapped), *J*=17.2, 10.4, 6.8, C*H*=CH_2), 4.96 (1H, ddt, *J*=17.2, 1.6, 1.2 CH=C*H*H *cis*), 4.89 (1H, ddt (overlapped), *J*=10.4, 1.6, 1.0, CH=CH*H trans*), 2.57 (2H, t, *J*=7.6, COCH_2), 2.01 (2H, qr, J=6.8, CH_2CH=CH_2), 1.72 (2H, qn, *J*=7.6, $COCH_2CH_2$), 1.42 – 1.25 (10H, m, CH_2). ^{13}C NMR (100 MHz, $CDCl_3$) δ 171.19 (*C*=O), 155.63 (Ar*C*O), 145.20 (Ar*C*NO_2), 139.07 (*C*H=CH_2), 125.12 (O_2NCCH), 122.50 (OC*C*H), 114.25 (CH=*C*H_2), 34.26 (CO*C*H_2), 33.85 (*C*H_2CH=CH_2), 29.35, 29.26, 29.12, 29.03, 28.94 (all *C*H_2), 24.75 (*C*H_2CH_2CO). ν_{max} 3277*m* (ArC-H), 2923*m* (C-H), 2853*m* (C-H), 1633*s* (C=O), 1524*s* (NO_2), 1345*m* (NO_2), 1208*s* (C-O), 1161*m* (C-O), 1095*s*, 910*m*, 865*m*, 612*s*. ESI MS $C_{17}H_{23}NO_2$ m/z calculated $[M+H]^+$ 306.1700, found 306.1694 (29%), calculated $[M+Na]^+$ 328.1519, found 328.1508 (100%).

7.3.4. G1-ene[472, 474]

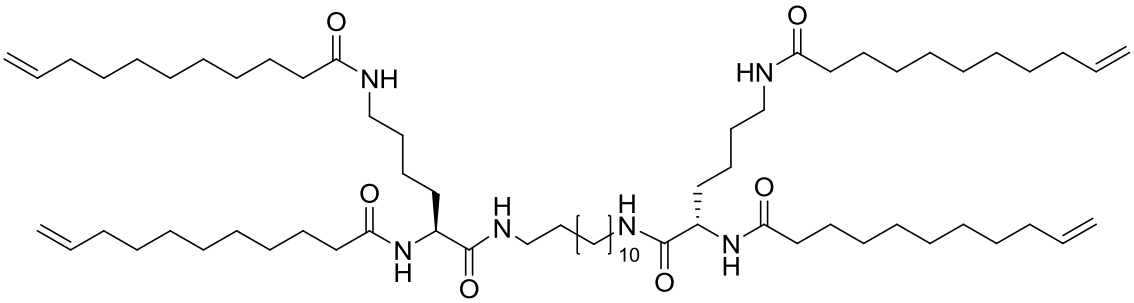

Compound **2** (2.00 g, 2.33 mmol) was dissolved in MeOH (50 mL). $HCl_{(g)}$ was bubbled through the solution for roughly 10 seconds and it was left stirring until all starting material had reacted (monitored by TLC). The volatiles were removed under vacuum and the solid redissolved in DCM (100 mL). TEA (1.95 mL, 13.98 mmol) was added, followed by dropwise addition of **3** (1.78 g, 5.81 mmol). The reaction was refluxed at 45°C for 48 hours before being allowed to cool to room temperature. The product was removed by filtration and washed with 1 M NaOH, 1 M HCl and water, then recrystalised from acetonitrile (twice) to leave a white solid which was dried for 24 hours in vacuum oven. Yield 1.22 g (1.88 mmol, 81%). R_f = 0.42 (9:1 DCM:MeOH, CeMo stain). M.P. = 171-172°C (Lit. = 173-174°C)[472]. ^{1}H NMR (400 MHz, $CDCl_3$) δ 6.60 (2H, br t, CHCON*H*), 6.53 (2H, d, *J*=7.6, CHN*H*CO), 5.90 (2H, br t, CH_2N*H*CO), 5.79 (4H, ddt (overlapped), *J*=17.2, 10.4, 6.8, C*H*=CH_2), 4.98 (4H, ddt, *J*=17.2, 2.0, 1.6, CH=C*H*H *cis*), 4.92 (4H, ddt (overlapped), *J*=10.4, 1.6, 1.0, CH=CH*H trans*), 4.36 (2H, m, C*H*), 3.21 (8H, m, NHCH_2), 2.21 (4H, t, *J*=7.6, COCH_2), 2.15 (4H, t, *J*=7.6, COCH_2), 2.02 (8H, qr, *J*=6.8 CH_2CH=CH_2), 1.88-1.18 (80H, m, CH_2). ^{13}C NMR (100 MHz, $CDCl_3$) δ 173.43 (*C*=O), 171.71 (*C*=O), 139.14 (*C*H=CH_2), 114.18 (CH=*C*H_2), 52.95 (*C*H), 39.64 (*C*H_2NH) 38.72 (*C*H_2NH), 36.89 (*C*H_2CO), 36.64 (*C*H_2CO), 33.78 (*C*H_2CH=CH_2), 29.73, 29.38, 29.25, 29.12, 28.97, 26.76, 25.84, 25.74, 22.59 (all *C*H_2). ν_{max} 3287*m* (N-H), 2919*m* (C-H), 2850*m* (C-H), 1634*s* (C=O), 1554*s* (N-H), 1463*m*, 1236*w*, 991*w*, 912*m*, 720*m*. ESI MS $C_{68}H_{124}N_6O_6$ m/z calculated $[M+H]^+$ 1121.9655, found 1121.9648 (59%), calculated $[M+Na]^+$ 1143.9475, found 1143.9452 (100%).

7.3.5. MeO-L-Lys[475]

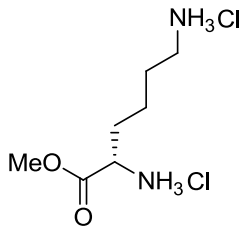

L-Lysine hydrochloride (7.50 g, 46.9 mmol) was added to a mixture of 2,2-dimethoxypropane (55 mL, 0.447 mol) and MeOH (85 mL, 2.1 mol). Conc. HCl (13.6 mL) was then added and the reaction refluxed at 85°C under nitrogen for 3 hours, then stirred at room temperature for 18 hours. The solvent was removed under vacuum and the crude product recrystalised (twice) from MeOH and EtO_2 to leave a white solid. Yield 8.91 g (38.2 mmol, 82%). R_f = 0.77 (5:5 NH_4OH:MeOH, Ninhydrin stain). M.P. 194-196°C (Lit. = 200-201°C). $[\alpha]_D^{589}$ = +21.0 (*c* = 1,

MeOH). ^{1}H NMR (400 MHz, D_2O) δ 4.13 (1H, t, *J*=6.4, C*H*), 3.81 (3H, s, OCH_3), 2.97 (2H, t, *J*=7.6, CH_2NH$_2$), 2.04-1.85 (2H, m, NH$_2$CHCH_2), 1.68 (2H, qn, *J*=7.6, CH_2CH$_2$NH$_2$), 1.56-1.38 (2H, m, CHCH$_2$CH_2). ^{13}C NMR (100 MHz, D_2O) δ 170.63 (*C*=O), 53.69 (*C*H), 52.71 (*C*H$_3$O), 39.20 (*C*H$_2$NH$_2$), 29.47 (CH*C*H$_2$), 26.33 (*C*H$_2$CH$_2$NH$_2$), 21.55 (CHCH$_2$*C*H$_2$). ν_{max} 2943*s* (N-H), 1739*s* (C=O), 1602*m*, 1505*m*, 1450*m*, 1228*m*, 1196*m*, 1160*m*, 1142*m*, 1038*m*, 1004*m*, 952*m*, 928*m*, 856*m*, 740*m*. ESI MS $C_7H_{16}N_2O_2$ m/z calculated $[M+H]^+$ 161.1285, found 161.1279 (100%).

7.3.6. MeO-Lys-ene[471, 475]

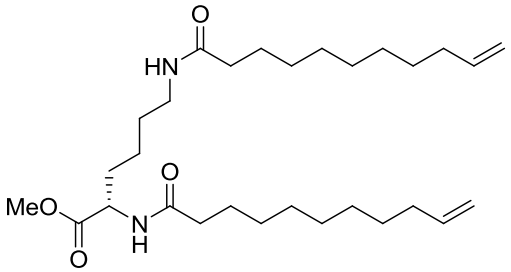

Undecylenic acid (332 mg, 1.80 mmol) was dissolved in DCM (50 mL) and the solution was cooled to 0 °C. TBTU (606 mg, 1.89 mmol) was added and the reaction mixture stirred at 0°C for 20 minutes at which point finely powdered **MeO-L-Lys** (200 mg, 0.858 mmol) was added. The reaction was stirred for a further 10 minutes before DIPEA (0.90 mL, 5.15 mmol) was added dropwise. The reaction was stirred at 0°C for 20 minutes before being allowed to warm to room temperature and stirred for a further 21 hours. The organic reaction mixture was washed with sat. $NaHCO_3$, 1.33 M $NaHSO_4$, sat. brine and water. The organic phase was dried over $MgSO_4$, filtered and the volatiles were removed under vacuum to leave the crude product. This was further purified by flash chromatography (silica, 98:2 DCM:MeOH) to produce a white waxy solid. Yield 300 mg (0.609 mmol, 71%). R_f = 0.42 (9:1 DCM:MeOH, CeMo stain). M.P. = 70-72°C (Lit. = 71-72°C)[471]. $[\alpha]_D^{589}$ = +4.61 (*c* = 1, $CHCl_3$). ^{1}H NMR (400 MHz, $CDCl_3$) δ 6.14 (1H, d, *J*=8.0, CHN*H*), 5.80 (2H, ddt (overlapped), *J*=17.2, 10.4, 6.8, C*H*=CH$_2$), 5.62 (1H, br t, CH$_2$N*H*), 4.98 (2H, ddt, *J*=17.2, 1.8, 1.6, CH=C*H*H *cis*), 4.92 (2H, ddt (overlapped), *J*=10.4, 1.6, 1.0, CH=CH*H trans*), 4.57 (1H, m, C*H*), 3.73(3H, s, CH_3O), 3.23 (2H, m, NHCH_2), 2.20 (2H, t, CH_2CO), 2.15 (2H, t, CH_2CO), 2.02 (4H, qr, *J*=6.8, CH_2CH=CH$_2$), 1.89 – 1.23 (30H, m, CH_2). ^{13}C NMR (100 MHz, $CDCl_3$) δ 173.62, 173.40, 173.18 (all *C*=O), 139.24 (*C*H=CH$_2$), 114.24 (CH=*C*H$_2$), 52.47 (*C*H$_3$), 51.71 (*C*H), 38.76 (*C*H$_2$NH), 36.89, 36.59 (both CO*C*H$_2$), 33.87 (*C*H$_2$CH=CH$_2$), 32.06, 29.42, 29.34, 29.24, 29.17, 28.97, 28.93, 28.93, 25.91 (all *C*H$_2$). δ ν_{max} 3305*m* (N-H), 2921*m* (C-H), 2850*m* (C-H), 1729*m* (C=O), 1637*s* (C=O), 1541*m* (N-H), 1348*m*, 1240*m*, 1214*m*, 1126*m*,

993*m*, 908*m*. ESI MS $C_{29}H_{52}N_2O_4$ m/z calculated $[M+H]^+$ 493.4000, found 493.3995 (100%), , calculated $[M+Na]^+$ 515.3819, found 515.3808 (50%).

7.3.7. Lys-ene[471, 475]

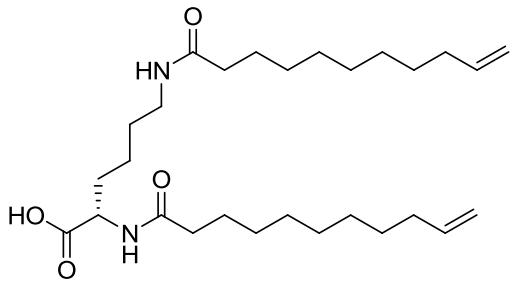

Compound **MeO-Lys-ene** (394 mg, 0.80 mmol) was dissolved in a mixture of MeOH (10 mL) and 1 M NaOH (10 mL). This mixture was refluxed at 80°C overnight. The solvent was removed under vacuum and the resulting residue diluted with water (10 mL). This aqueous solution was acidified to pH 3 with 1.33 M $NaHSO_4$ solution, and the product was extracted with DCM. These organic phases were combined and washed with brine and water. The organic layer was dried over $MgSO_4$, filtered and the volatiles removed under vacuum. The crude product was recrystalised from cyclohexane to leave white solid. Yield 253 mg (0.529 mmol, 66%). R_f = 0.10 (9:1 DCM:MeOH, CeMo stain). M.P. = 88-90°C (Lit. = 90-91°C)[471]. $[\alpha]_D^{589}$ = +2.69 (*c* = 1, $CHCl_3$). ^{1}H NMR (400 MHz, $CDCl_3$) δ 6.93 (1H, d, *J*=7.2, CHN*H*), 5.80 (2H, ddt (overlapped), *J*=17.2, 10.4, 6.8, C*H*=CH_2), 5.69 (1H, br t, CH_2N*H*), 4.99 (2H, ddt, *J*=17.2, 1.8, 1.6, CH=C*H*H *cis*), 4.93 (2H, ddt (overlapped), *J*=10.4, 1.6, 1.0, CH=CH*H trans*), 4.42 (1H, m, C*H*), 3.29 (2H, br d, NHCH_2), 2.30 (2H, t, *J*=7.6, CH_2CO), 2.20 (2H, t, *J*=7.6, CH_2CO), 2.02 (4H, qr, *J*=6.8, CH_2CH=CH_2), 1.96-1.71 (2H, br d, CHCH_2), 1.70-1.10 (28H, m, CH_2). ^{13}C NMR (100 MHz, $CDCl_3$) δ 174.58, 174.52 (both *C*=O), 139.24 (*C*H=CH_2), 114.27 (CH=*C*H_2), 52.23 (*C*H), 38.76 (*C*H_2NH), 36.87, 36.49 (*C*H_2C=O), 33.88 (*C*H_2CH=CH_2), 31.16, 29.43, 29.38, 29.17, 29.00, 25.87, 25.76, 22.02 (all CH_2). δ ν_{max} 3308*m* (N-H), 2120*m* (C-H), 2850*m* (C-H), 1723*m* (C=O), 1637*s* (C=O), 1586*m*, 1541*s* (N-H), 1416*w*, 1208*m*, 1139*m*, 991*m*, 908*m*. ESI MS $C_{29}H_{52}N_2O_4$ m/z calculated $[M+H]^+$ 479.3843, found 4793854 (100%).

7.3.8. C_4-Lys-ene

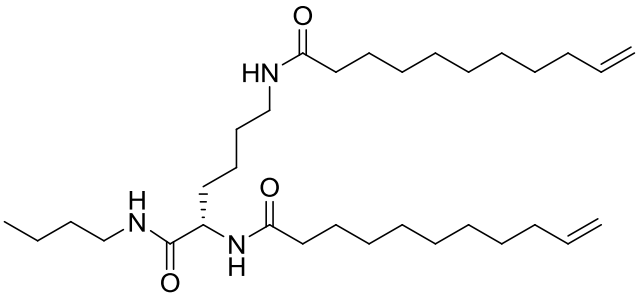

Compound **Lys-ene** (2.30 g, 4.81 mmol) was dissolved in DCM (250 mL) and cooled to 0 °C. TBTU (1.70 g, 5.29 mmol) was added, followed by dropwise addition of DIPEA (0.84 mL,0.93 g, 7.21 mmol).This mixture was left to stir at 0°C for 10 minutes before *n*-butylamine (0.52 mL, 0.39 g, 5.29 mmol) was added and left to stir at 0°C for a further 20 minutes. The reaction was then left to stir for 16 hours at room temperature. The reaction mixture was washed with sat. $NaHCO_3$, 1.33 M $NaHSO_4$, sat. $NaHCO_3$, sat. brine and water. The organic phase was dried over $MgSO_4$ which was then removed by filtration. The volatiles were removed under vacuum to leave a crude product that was purified by recrystalisation form MeOH and Et_2O (twice) to leave an off-white solid. Yield 1.80 g (3.37 mmol, 70%). R_f = 0.26 (9:1 DCM:MeOH, CeMo stain). M.P. = 135-137°C. $[\alpha]_D^{589}$ = -12.4 (*c* = 1, MeOH). ^{1}H NMR (400 MHz, $CDCl_3$) δ 7.37 (1H, t, *J*=5.2, N*H*COCH), 7.12 (1H, d, *J*=7.6, CHN*H*), 6.54 (1H, t, *J*=4.8 $CH_2NHCOCH_2$), 5.75 (2H, ddt (overlapped), *J*=17.2, 10.4, 6.4, C*H*=CH_2), 4.94 (2H, ddt, *J*=17.2, 2.0, 1.6, CH=C*H*H *cis*), 4.87 (2H, ddt (overlapped), *J*=10.4, 1.6, 1.2, CH=CH*H trans*), 4.52 (1H, qr, *J*=7.6, C*H*), 3.16 (4H, m, NHCH_2), 2.19 (2H, t, *J*=8, CH_2CO), 2.13 (2H, t, *J*=8.0, CH_2CO), 1.99 (4H, qr, *J*=7.6, CH_2CH=CH_2), 1.82-1.152 (34H, m, CH_2), 0.87 (3H, t, *J*=7.6, CH_3). ^{13}C NMR (100 MHz, $CDCl_3$) δ 173.68 (*C*=O), 172.00 (*C*=O), 139.16 (*C*H=CH_2), 114.25 (CH=*C*H_2), 52.86 (C*H*), 39.31 (*C*H_2NH) 39.09 (*C*H_2NH), 36.79 (*C*H_2CO), 36.46 (*C*H_2CO), 33.86 (*C*H_2CH=CH_2), 32.51 (*C*H_2CH), 31.56, 29.47, 29.18, 28.97, 25.98, 25.87, 22.90, 20.18 (all *C*H_2), 13.85 (*C*H_3). ν_{max} 3288*m* (N-H), 3081*w*, 2919*m* (C-H), 2850*m* (C-H), 1634*m* (C=O), 1554*s* (C=O), 993*m*, 909*m*. ESI MS $C_{32}H_{59}N_3O_3$ m/z calculated $[M+H]^+$ 534.4629, found 534.4629 (100%), calculated $[M+Na]^+$ 556.4449, found 556.4454 (76%).

7.3.9. A-ene[476]

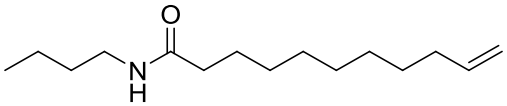

Butylamine (1.35 mL, 13.67 mmol) was added to TEA (2.10 mL, 15.04 mmol) in DCM (50 mL). The reaction was cooled to 0°C and 10-undecenoyl chloride (3.23 mL, 15.04 mmol) was added dropwise. The reaction was allowed to warm to room temperature and left stirring overnight. The reaction mixture was washed with sat. $NaHCO_3$, sat. brine, 1.33 M $NaHSO_3$ and water. The organic phase was dried over $MgSO_4$, filtered and the volatiles removed under vacuum. The crude product was then further purified by flash chromatography (silica, 7:3 cyclohexane:EtOAc) to produce a white waxy low melting point solid. Yield 2.81 g (11.70 mmol, 78%). R_f = 0.55 (9:1 DCM:MeOH, CeMo). M.P. = 34-35°C (Lit. = 35°C)[476]. ^{1}H NMR (400 MHz, $CDCl_3$) δ 5.80 (1H, ddt (overlapped), *J*=17.2, 10.4, 6.4, C*H*=CH_2), 5.40 (1H, br s, N*H*), 4.98 (1H, ddt, *J*=17.2, 2.0, 1.6, CH=C*H*H *cis*), 4.92 (1H, ddt (overlapped), *J*=10.4, 2.0, 1.6, CH=CH*H trans*), 3.24 (2H, dt (overlapped), *J*=6.0, 7.2, CH_2NH), 2.14 (2H, t, *J*=7.6, CH_2CO), 2.03 (2H, m, CH_2CH=CH_2), 1.61 (2H, m, CH_2CH_2CH=CH_2), 1.47 (2H, m, CH_2CH_2NH), 1.41-1.22 (12H, m, CH_2), 0.92 (3H, t, *J*=7.4, CH_3). ^{13}C NMR (100 MHz, $CDCl_3$) δ 173.07 (*C*=O), 139.11 (*C*H), 114.07 (=*C*H_2), 39.26 (*C*H_2NH), 36.98 (*C*H_2CO), 33.86 (*C*H_2CH=CH_2), 31.83 (NHCH_2*C*H_2), 29.39, 29.14, 28.96 (all *C*H_2), 25.92 (*C*H_2CH_2CO), 20.15 (*C*H_2), 13.84 (*C*H_3). ν_{max} 3291*m* (N-H), 3077*w* (=C-H), 2917*m* (C-H), 2850*m* (C-H), 1635*s* (C=O), 1549*s* (N-H), 1436*w*, 1367*w*, 991*w*, 913*m*. ESI MS $C_{15}H_{29}NO$ m/z calculated $[M+H]^+$ 240.2322, found 240.2328 (100%).

7.3.10. A-ane[477]

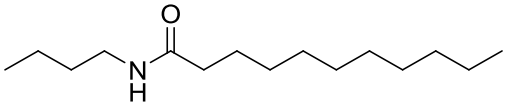

Butylamine (1.35 mL, 13.67 mmol) was added to TEA (2.10 mL, 15.04 mmol) in DCM (50 mL). The reaction was cooled to 0°C and undecanoyl chloride (3.31 mL, 15.04 mmol) was added dropwise. The reaction was allowed to warm to room temperature and left stirring overnight. The reaction mixture was washed with sat. $NaHCO_3$, sat. brine, 1.33 M $NaHSO_3$ and sat. brine. The organic phase was dried over $MgSO_4$, filtered and the volatiles removed under vacuum. The crude product was then further purified by flash chromatography (silica, 7:3

EtOAc:cyclohexane) to produce a white waxy solid. Yield = 2.91 g (12.03 mmol, 88%). R_f = 0.67 (9:1 DCM and MeOH, CeMo stain). M.P. 46.2-46.9°C (Lit. = 47.0-47.2°C)[477]. ^{1}H NMR (400 MHz, $CDCl_3$) δ 5.38 (1H, br s, N*H*), 3.24 (2H, dt, *J*=6, 7.2, CH_2NH), 2.15 (2H, t, *J*=7.6, CH_2CO), 1.61 (2H, m, COCH$_2$CH_2), 1.47 (2H, m, NHCH$_2$CH_2), 1.39 – 1.18 (16H, m, CH_2), 0.92 (3H, t, *J*=7.2, CH_3), 0.87 (3H, t, *J*=7.2, CH_3). ^{13}C NMR (100 MHz, $CDCl_3$) δ 173.15 (*C*=O), 39.27 (NH*C*H$_2$), 37.04 (CO*C*H$_2$), 31.97 (NHCH$_2$*C*H$_2$), 31.85 (*C*H$_2$), 29.64, 29.58, 29.44, 29.39 (all *C*H$_2$), 25.93 (*C*OCH$_2$*C*H$_2$), 22.76, 20.15 (both *C*H$_2$), 14.19, 13.84 (both *C*H$_3$). ν_{max} 3316*m* (N-H), 2914*s* (C-H), 2848*m* (C-H), 1633*s* (C=O), 1543*s* (N-H), 1469*m*, 1425*w*, 1224*w*, 714*w*, 666*w*. ESI MS $C_{15}H_{31}NO$ m/z calculated $[M+H]^+$ 242.2478, found 242.2476 (100%), calculated $[M+Na]^+$ 264.2298, found 264.2293 (46%).

7.3.11. *p*-NP-ane

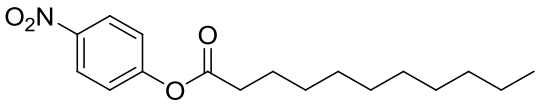

p-Nitrophenol (3.37 g, 24.2 mmol) was dissolved in toluene (20 mL) and pyridine (1.80 mL, 22.3 mmol). Undecanoyl chloride (4.31 mL, 20.0 mmol) was added and the reaction was refluxed at 120^{o}C for 5 hours. After being allowed to cool to room temperature, the reaction was neutralised with sat. $NaHCO_3$ solution. The aqueous layer was removed and the organic layer washed with water, 5% NaOH and 0.1 M HCl. The organic phase was then dried over $MgSO_4$, filtered and the volatiles removed under vacuum to leave an off-white low melting point solid. Yield 4.85 g (15.8 mmol, 79%). R_f = 0.88 (9:1 DCM:MeOH, CeMo stain). M.P. = 35-36°C. ^{1}H NMR (400 MHz, $CDCl_3$) δ 8.25 (2H, d, *J*=9.2, O_2NCC*H*), 7.26 (2H, d, *J*=9.2, OCC*H*), 2.59 (2H, t, *J*=7.6, COCH_2), 1.75 (2H, qn, *J*=7.6, COCH$_2$CH_2), 1.45 – 1.18 (14H, m, CH_2), 0.87 (3H, t, *J*=6.8, CH_3). ^{13}C NMR (100 MHz, $CDCl_3$) δ 171.43 (*C*=O), 155.61 (Ar*C*O), 145.32 (Ar*C*NO$_2$), 125.28 (NO$_2$*C*CH), 122.53 (OC*C*H), 34.43 (CO*C*H$_2$), 31.98, 29.63, 29.52, 29.39, 29.31, 29.14 (all *C*H$_2$), 24.83 (COCH$_2$*C*H$_2$), 22.77 (*C*H$_2$), 14.21 (*C*H$_3$). ν_{max} 2916*m* (C-H), 2849*s* (C-H), 1755*s* (C=O), 1522*s* (NO$_2$), 1346*m* (NO$_2$), 1212*m* (C-O), 1139*s* (C-O), 1104*m*, 926*m*, 853*m*, 717*m*.

7.3.12. G1-ane

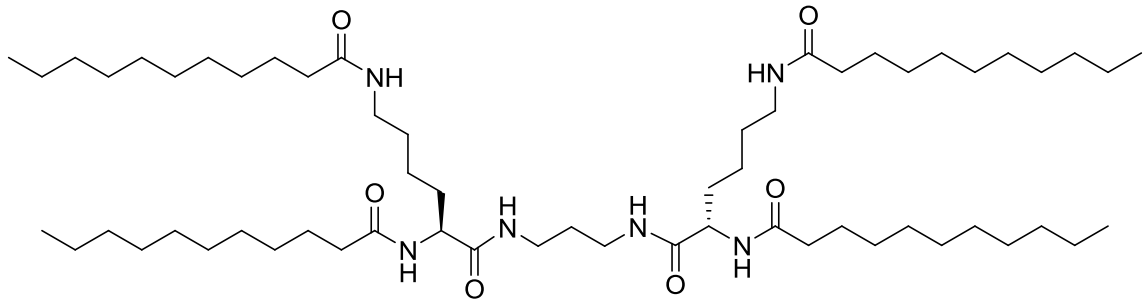

Compound **C_{12}-(L-Lys-Boc)$_2$** (1.00 g, 1.17 mmol) dissolved in MeOH (25 mL). $HCl_{(g)}$ was bubbled through solution for roughly 10 seconds and it was left stirring until all starting material had reacted (monitored by TLC). The volatiles were removed under vacuum and the solid redissolved in DCM (150 mL). TEA (1.30 mL, 9.34 mmol) added, followed by dropwise addition of ***p*-NP-ane** (2.15 g, 7.00 mmol) as a solution in DCM (10 mL). The reaction was refluxed at 50°C for 7 days before being allowed to cool to room temperature. The product was removed by filtration and washed with 1 M NaOH, 1 M HCl and water then recrystalised from MeOH to leave white solid which was dried for 24 hours in vacuum oven. Yield 0.80 g (0.71 mmol, 60%). R_f = 0.33 (9:1 DCM:MeOH, CeMo stain). M.P. 178-181 °C. ^{1}H NMR (400 MHz, $CDCl_3$) δ 6.44 (2H, t, *J*=5.2, N*H*COCH), 6.34 (2H, d, *J*=8.0, CHN*H*CO), 5.72 (2H, t, *J*=5.6 $CH_2NHCOCH_2$), 4.36 (2H, m, C*H*), 3.23 (8H, m, NHCH_2), 2.21 (4H, t, *J*=7.6 CH_2CO), 2.16 (4H, t, *J*=7.6, CH_2CO), 1.90 – 1.17 (92H, m, CH_2), 0.89 (12H, t, *J*=6.8, CH_3). ^{13}C NMR (100MHz, $CDCl_3$) δ 173.59 (*C*=O), 173.43 (*C*=O), 171.72 (*C*=O), 52.95 (*C*H), 39.63 (*C*H_2NH), 38.73 (*C*H_2NH), 36.90 (*C*H_2CO), 36.65 (*C*H_2CO), 31.92, 31.74, 29.61, 28.55, 29.42, 29.39, 29.37, 29.32, 29.26, 29.17, 29.15, 29.00, 26.76, 25.86, 25.76, 22.76, 22.60 (all *C*H_2), 14.04 (*C*H_3). ν_{max} 3305*m* (N-H), 2917*m* (C-H), 2849*m* (C-H), 1635*s* (C=O), 1561*m* (N-H), 1462*w*, 1274*w*, 1214*w*, 717*m*. ESI MS $C_{68}H_{132}N_6O_6$ m/z calculated $[M+H]^+$ 1130.0281, found 1130.0272 (46%), calculated $[M+Na]^+$ 1152.0101, found 1152.0057 (41%).

7.3.13. L,L,L-G2Lys-OMe[416]

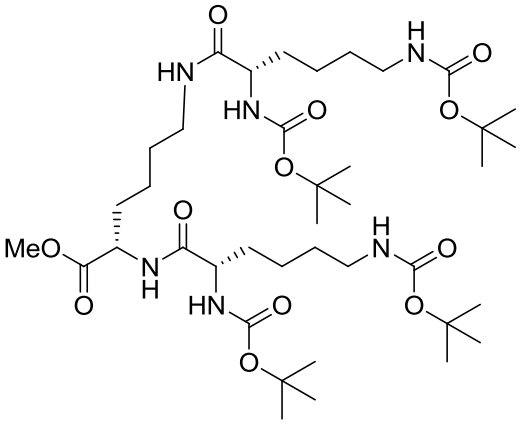

Compound **L-Lys-Boc** (29.4 g, 84.9 mmol) was dissolved in DCM (500 mL) and cooled to 0°C. TBTU was added (27.3 g, 84.9 mmol) and the reaction was stirred at 0°C for 20 minutes. Finely ground **MeO-L-Lys** (9.00 g, 38.6 mmol) was added followed by dropwise addition of DIPEA (44 mL, 0.255 mol). The reaction was stirred at 0°C for 30 minutes before being stirred overnight at room temperature. The volatiles were then removed under vacuum and the residue was redissolved in EtOAc (500 mL). This was then washed with sat. $NaHCO_3$, water, 1.33 M $NaHSO_4$, sat. $NaHCO_3$, sat. brine and water before being dried over $MgSO_4$. This was removed by filtration and the solvent was removed under vacuum. The crude product was purified using flash chromatography (silica, 7:3 EtOAc:cyclohexane). The product was redissolved in DCM and the solvent was removed under vacuum, this was repeated two more times to leave a white solid foam. Yield = 25.9 g (69.6 mmol, 82%). R_f = 0.32 (9:1 DCM:MeOH, CeMo stain). M.P. = 75-80°C (Lit. = 75-80°C)[416]. $[\alpha]_D^{589}$ = -17.6 (*c* = 1, MeOH). ^{1}H NMR (400 MHz, CD_3COCD_3) δ 7.65 (1H, d, *J*=6.4, CH_3O_2CCHNH), 7.43 (1H, br s, $CH_2NHCOCH$), 6.23 (1H, d, *J*=7.4, NHCOCHN*H*), 6.16 (1H, d, *J*=7.4, NHCOCHN*H*), 5.97 (2H, br s, CH_2NHCOO), 4.35 (1H, br s, CH_3O_2CCH), 4.28 (1H, m, C*H*NHCOO), 4.09 (1H, m, C*H*NHCOO), 3.68 (3H, s, CH_3O), 3.38-2.98 (6H, m, CH_2NH), 1.88-1.60 (6H, m, $CHCH_2$), 1.58-1.28 (48H, m, CH_2, CH_3). ^{13}C NMR (100 MHz, CD_3COCD_3) δ 174.49 (CO_2CH_3), 174.26 (NH*C*OCH), 157.67 (NH*C*OO), 80.42, 80.32, 79.31 (all $C(CH_3)_3$), 56.46, 55.90 (both *C*HNHCOO), 53.95 (CH_3O_2CCH), 53.27 (CH_3O), 41.79 (CH_2NHCOO × 2), 39.81 ($CH_2NHCOCH$), 34.25, 33.92, 32.66 (all CH_2CH), 31.48, 31.41, 30.65 (all CH_2), 29.68 (CH_3 × 12), 24.71, 24.45, 24.17 (all CH_2). ν_{max} 3300*m* (N-H), 2976*m* (C-H), 2932*m* (C-H), 2865*m* (C-H), 1683*s* (C=O), 1652*s* (C=O), 1515*s* (N-H), 1455*m*, 1391*m*, 1365*s*, 1247*s*, 1164*s*. ESI MS $C_{39}H_{72}N_6O_{12}$ m/z calculated $[M+H]^+$ 817.5281, found 817.5254 (57%), calculated $[M+Na]^+$ 839.5100, found 839.5058 (100%).

7.3.14. L,L,L-G2Lys[416]

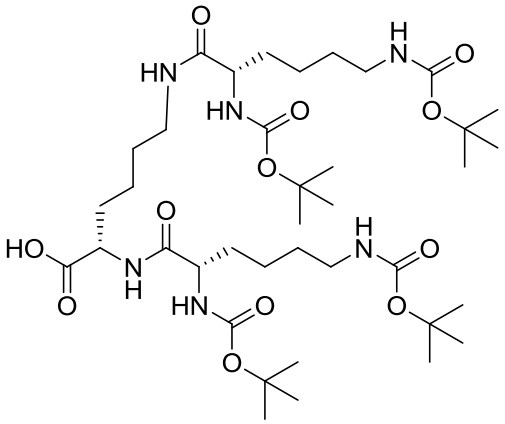

Compound **L,L,L-G2Lys-OMe** (3.40 g, 4.16 mmol) was dissolved in MeOH (175 mL) and the mixture was cooled to 0°C and put under a nitrogen atmosphere. 1 M NaOH (13 mL) was added and the mixture stirred at 0°C for a further 20 minutes. The reaction was allowed to warm to room temperature and stirred for a further 24 hours. The volatiles were removed under vacuum and the residue was dissolved in water (200 mL). This solution was acidified to pH 3 with addition of 1.33 M $NaHSO_4$ solution and the product was extracted with EtOAc. The organic phases were combined and washed with water and brine before being dried over $MgSO_4$. This was removed by filtration and the volatiles were removed under vacuum. The residue was redissolved in DCM which was then removed under vacuum, this process was repeated twice more to leave a white solid foam which was finely ground and dried in a vacuum oven for 24 hours. Yield = 2.71 g (3.37 mmol, 81%). R_f = 0.08 (9:1 DCM:MeOH, CeMo stain). M.P. = 87-98°C (Lit. 90-100°C)[416]. $[\alpha]_D^{589}$ = -10.9 (*c* = 1, MeOH) . ^{1}H NMR (400 MHz, CD_3COCD_3) δ 7.69 (1H, d, *J*=6.8, HO_2CCHNH), 7.58 (1H, br s, $CH_2NHCOCH$), 6.30 (2H, 2 × d (overlapped), *J*=7.4, NHCOCHN*H*), 6.06 (2H, 2 × t (overlapped), *J*=4.8, CH_2NHCOO), 4.37 (1H, m, HO_2CCH), 4.29 (1H, m, C*H*NHCOO), 4.13 (1H, m, C*H*NHCOO), 3.22 (2H, m, $CHCONHCH_2$), 3.05 (4H, m, CH_2NHCOO), 1.93-1.58 (6H, m, $CHCH_2$), 1.57-1.27 (48H, m, CH_2, CH_3). ^{13}C NMR (100 MHz, CD_3COCD_3) δ 174.81 (CO_2H), 174.64, 174.56 (both *C*ONH), 157.80, 157.74, 157.69, 157.63 (all $COOC(CH_3)_3$), 80.43, 80.34, 79.44, 79.37 (all $C(CH_3)_3$), 56.34, 55.96 (both *C*HNHCOO), 53.79 (HO_2CCH), 40.04 (CH_2NHCOO × 2), 38.33 ($CHCONHCH_2$), 32.41, 32.28, 31.08 (all $CHCH_2$), 29.67, 28.89 (both CH_2), 27.95 (CH_3 × 12), 22.95, 22.82, 22.54 (all CH_2). ν_{max} 3308*m* (N-H), 2976*m* (C-H), 2932*m* (C-H), 2865*m* (C-H), 1690*s* (C=O), 1658*s* (C=O), 1518*s* (N-H), 1453*m*, 1391*m*, 1365*s*, 1248*s*, 1166*s*. ESI MS $C_{38}H_{70}N_6O_{12}$ m/z calculated $[M+H]^+$ 803.5124, found 803.5116 (100%), calculated $[M+Na]^+$ 825.4944, found 825.4930 (75%).

7.3.15. D-Lys-Boc[326]

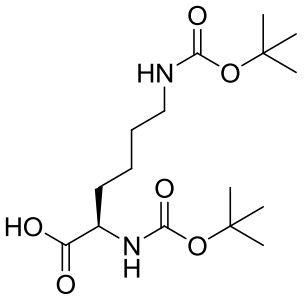

D-Lys-Boc was synthesised using the same method used for **L-Lys-Boc** (Section 7.3.1.) using D-Lysine monohydrochloride (3.70 g, 20.28 mmol), NaOH (1.63 g, 40.75 mmol), Di-*tert*-butyl dicarbonate (9.25 g, 42.40 mmol), water (50 mL) and THF (50 mL). Yield 4.49 g (12.98 mmol, 64%). R_f = 0.14 (9:1 DCM:MeOH, Nihydrin stain). M.P. = 136-138°C. $[\alpha]_D^{589}$ = -11.3 (*c* = 1, $CHCl_3$). ^{1}H NMR (400 MHz, $CDCl_3$) δ 5.33 (1H, d, *J*=8.0, CHN*H*), 4.76 (1H, br s, CH_2N*H*), 4.27 (1H, m, C*H*), 3.09 (2H, m, CH_2NH), 1.91-1.60 (2H, m CHCH_2), 1.57-1.25 (22H, m, CH_2, CH_3). ^{13}C NMR (100 MHz, $CDCl_3$) δ 176.36 (*C*O_2H), 156.25 (*C*ONH), 79.89, 79.27 (both *C*$(CH_3)_3$), 53.13 (*C*H), 40.03 (*C*H_2NH), 32.01 (*C*H_2CH), 29.40 (*C*H_2CH_2NH), 28.35, 28.28 (both *C*H_3), 22.36 (*C*H_2CH_2CH). ν_{max} 3330*m* (N-H), 2977*m* (C-H), 2933*m* (C-H), 2868*m* (C-H), 1694*s* (C=O), 1516*s* (N-H), 1366*s*, 1249*s*, 1159*s*. ESI MS $C_{16}H_{30}N_2O_6$ m/z calculated $[M+H]^+$ 347.2177, found 347.2169 (33%), calculated $[M+Na]^+$ 369.1996, found 369.1985 (100%).

7.3.16. MeO-D-Lys[326]

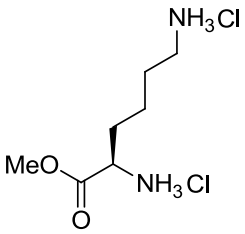

MeO-D-Lys was synthesised using the same method for **MeO-L-Lys** (Section 7.3.5.) but was recrystalised three times instead of twice. The reaction used L-Lysine hydrochloride (2.48 g, 13.6 mmol), 2,2-dimethoxypropane (18 mL, 15.2 g, 0.148 mol), MeOH (28 mL, 0.7 mol) and Conc. HCl (4.5 mL). Yield 1.55 g (9.68 mmol, 71%). R_f = 0.77 (5:5 NH_4OH:MeOH, Ninhydrin stain). M.P. = 202-204 °C. $[\alpha]_D^{589}$ = -21.6 (*c* = 1, MeOH). ^{1}H NMR (400 MHz, D_2O) δ 4.17 (1H, t, *J*=6.4, C*H*), 3.84 (3H, s, OCH_3), 3.01 (2H, t, *J*=7.6, CH_2NH_2), 2.09-1.88 (2H, m, NH_2CHCH_2), 1.72

(2H, qn, *J*=7.6, C*H*$_2$CH$_2$NH$_2$), 1.61-1.41 (2H, m, CHCH$_2$C*H*$_2$). ^{13}C NMR (100 MHz, D$_2$O) δ 170.62 (*C*=O), 53.67 (*C*H), 52.70 (*C*H$_3$O), 39.09 (*C*H$_2$NH$_2$), 29.30 (CH*C*H$_2$), 26.32 (*C*H$_2$CH$_2$NH$_2$), 21.54 (CHCH$_2$*C*H$_2$). ν_{max} 2944*s* (N-H), 1740*s* (C=O), 1603*m*, 1505*m*, 1450*m*, 1228*m*, 1197*m*, 1161*w*, 1143*w*, 1038*w*, 1003*w*, 956*w*, 928*m*. ESI MS $C_7H_{16}N_2O_2$ m/z calculated $[M+H]^+$ 161.1285, found 161.1289 (100%).

7.3.17. D,D,D-G2Lys-OMe[326]

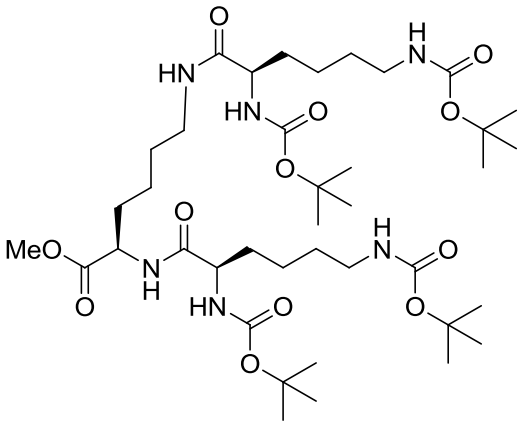

D,D,D-G2Lys-OMe was synthesised using the same method used for **L,L,L-G2Lys-OMe** (Section 7.3.13.) using **D-Lys-Boc** (2.50 g, 7.22 mmol), TBTU (2.43 g, 7.56 mmol), **MeO-D-Lys** (0.80 g, 3.44 mmol), DIPEA (3.6 mL, 20.6 mmol) and DCM (100 mL). Yield = 2.50 g (3.06 mmol, 89%). R_f = 0.32 (9:1 DCM:MeOH, CeMo stain). M.P. = 74-80 °C. $[\alpha]_D^{589}$ = +15.5 (*c* = 1, MeOH). ^{1}H NMR (400 MHz, CD$_3$COCD$_3$) δ 7.63 (1H, d, *J*=6.4, CH$_3$O$_2$CCHN*H*), 7.41 (1H, br s, CH$_2$N*H*COCH), 6.21 (1H, d, *J*=7.4, NHCOCHN*H*), 6.16 (1H, d, *J*=7.4, NHCOCHN*H*), 5.97 (2H, br s, CH$_2$N*H*COO), 4.35 (1H, br s, CH$_3$O$_2$CC*H*), 4.27 (1H, m, C*H*NHCOO), 4.08 (1H, m, C*H*NHCOO), 3.68 (3H, s, C*H*$_3$O), 3.39-3.01 (6H, m, C*H*$_2$NH), 1.90-1.60 (6H, m, CHC*H*$_2$), 1.58-1.30 (48H, m, C*H*$_2$, C*H*$_3$). ^{13}C NMR (100 MHz, CD$_3$COCD$_3$) δ 174.47 (*C*O$_2$CH$_3$), 174.27 (NH*C*OCH), 157.69 (NH*C*OO), 80.42, 80.31, 79.32 (all *C*(CH$_3$)$_3$), 56.48, 55.91 (both *C*HNHCOO), 53.94 (CH$_3$O$_2$C*C*H), 53.26 (*C*H$_3$O), 41.79 (*C*H$_2$NHCOO × 2), 39.78 (*C*H$_2$NHCOCH), 34.25, 33.89, 32.65 (all *C*H$_2$CH), 31.49, 31.42, 30.65 (all *C*H$_2$), 29.69 (*C*H$_3$ × 12), 24.71, 24.46, 24.14 (all *C*H$_2$). ν_{max} 3309*m* (N-H), 2976*m* (C-H), 2933*m* (C-H), 2865*m* (C-H), 1689*s* (C=O), 1652*s* (C=O), 1515*s* (N-H), 1455*m*, 1391*m*, 1365*s*, 1247*s*, 1164*s*. ESI MS $C_{39}H_{72}N_6O_{12}$ m/z calculated $[M+H]^+$ 817.5281, found 817.5258 (60%), calculated $[M+Na]^+$ 839.5100, found 839.5060 (100%).

7.3.18. D,D,D-G2Lys[326]

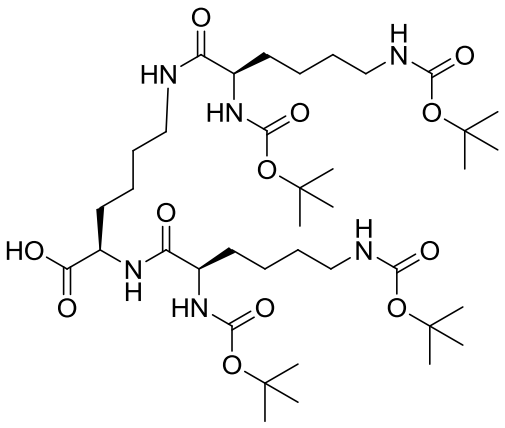

D,D,D-G2Lys was synthesised using the same method used for **L,L,L-G2Lys** (Section 7.3.14.) using **D,D,D-G2Lys-OMe** (2.40 g, 2.94 mmol), 1 M NaOH (9 mL) and MeOH (100 mL). Yield = 2.10 g (2.62 mmol, 89%). R_f = 0.08 (9:1 DCM:MeOH, CeMo stain). M.P. = 86-98°C (Lit. = 95°C)[326]. $[\alpha]_D^{589}$ = +9.83 (*c* = 1, MeOH). ^{1}H NMR (400 MHz, CD_3COCD_3) δ 7.63 (1H, d, *J*=6.4, HO_2CCHNH), 7.50 (1H, br s, CH_2NH), 6.24 (2H, 2 × d (overlapped), *J*=7.4, NHCOCHN*H*), 6.01 (2H, 2 × t (overlapped), *J*=4.8, CH_2NHCOO), 4.39 (1H, m, HO_2CCH), 4.27 (1H, m, C*H*NHCOO), 4.12 (1H, m, C*H*NHCOO), 3.22 (2H, m, CHCONHCH_2), 3.05 (4H, m, CH_2NHCOO), 1.92-1.60 (6H, m, CHCH_2), 1.58-1.29 (48H, m, CH_2, CH_3). ^{13}C NMR (100 MHz, CD_3COCD_3) δ 174.75 (*C*O_2H), 174.47, 174.40 (both *C*ONH), 157.83, 157.78, 157.75, 157.71 (all *C*OOC$(CH_3)_3$), 80.44, 80.34, 79.46, 79.38 (all *C*$(CH_3)_3$), 56.36, 55.95 (both *C*HNHCOO), 53.77 (HO_2CCH), 41.68 (*C*H_2NHCOO × 2), 40.06 (CHCONH*C*H_2), 34.09, 34.00, 32.81 (all *C*H_2CH), 31.40, 30.63 (both *C*H_2), 29.69 (*C*H_3 × 12), 24.69, 24.56, 24.28 (all *C*H_2). ν_{max} 3314*m* (N-H), 2976*m* (C-H), 2933*m* (C-H), 2868*m* (C-H), 1693*s* (C=O), 1659*s* (C=O), 1515*s* (N-H), 1455*m*, 1392*m*, 1366*s*, 1248*s*, 1164*s*. ESI MS $C_{38}H_{70}N_6O_{12}$ m/z calculated $[M+H]^+$ 803.5124, found 803.5145 (34%), calculated $[M+Na]^+$ 825.4944, found 825.4928 (100%).

7.3.19. L,D,D-G2Lys-OMe[326]

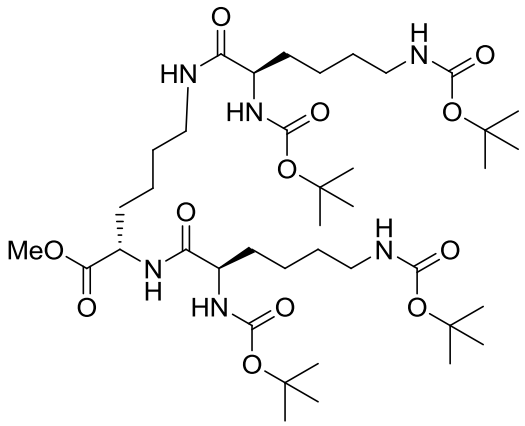

L,D,D-G2Lys-OMe was synthesised using the same method used for **L,L,L-G2Lys-OMe** (Section 7.3.13.) using **D-Lys-Boc** (2.50 g, 7.22 mmol), TBTU was added (2.43 g, 7.56 mmol), **MeO-L-Lys** (0.80 g, 3.44 mmol) and DCM. Yield = 2.11 g (2.58 mmol, 75%). R_f = 0.32 (9:1 DCM:MeOH, CeMo stain). M.P. = 66-70°C. $[\alpha]_D^{589}$ = +3.59 (*c* = 1, MeOH). ^{1}H NMR (400 MHz, CD_3COCD_3) δ 7.53 (1H, d, *J*=8.0, $CH_3O_2CCHN\mathit{H}$), 7.33 (1H, br s, $CH_2N\mathit{H}COCH$), 6.16-5.92 (4H, m, N*H*COO), 4.40 (1H, dt (overlapped), *J*=4.8, 8.0, $CH_3O_2CC\mathit{H}$), 4.13 (1H, m, C*H*NHCOO), 4.04 (1H, m, C*H*NHCOO), 3.67 (3H, s, $C\mathit{H}_3O$), 3.20 (2H, m, $C\mathit{H}_2NHCOCH$), 3.06 (4H, m, $C\mathit{H}_2NHCOO$), 1.89-1.58 (6H, m, $CHC\mathit{H}_2$), 1.57-1.30 (48H, m, $C\mathit{H}_2$, $C\mathit{H}_3$). ^{13}C NMR (100 MHz, CD_3COCD_3) δ 174.19 ($\mathit{C}O_2CH_3$), 173.98 (NH*C*OCH), 157.75, 157.71, 157.37 (all NH*C*OO), 80.30, 80.15, 79.35, 79.32 (all $\mathit{C}(CH_3)_3$), 56.41, 56.35 (both *C*HNHCOO), 53.77 ($CH_3O_2C\mathit{C}H$), 53.77 ($\mathit{C}H_3O$), 41.76, 41.72 (both $\mathit{C}H_2NHCOO$), 40.24 ($\mathit{C}H_2NHCOCH$), 34.17, 33.98, 32.98 (all $\mathit{C}H_2CH$), 31.50, 30.85 (both $\mathit{C}H_2$), 29.69, 29.60 ($\mathit{C}H_3$ × 12), 24.66, 224.53, 24.34 (all $\mathit{C}H_2$). ν_{max} 3316*m* (N-H), 2976*m* (C-H), 2933*m* (C-H), 2866*m* (C-H), 1693*s* (C=O), 1660*s* (C=O), 1515*s* (N-H), 1455*m*, 1391*m*, 1365*s*, 1247*s*, 1164*s*. ESI MS $C_{39}H_{72}N_6O_{12}$ m/z calculated $[M+H]^+$ 817.5281, found 817.5295 (7%), calculated $[M+Na]^+$ 839.5100, found 839.5084 (100%).

7.3.20. L,D,D-G2Lys[326]

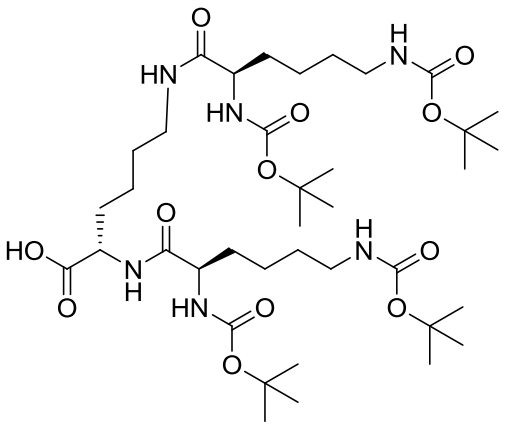

L,D,D-G2Lys was synthesised using the same method used for **L,L,L-G2Lys** (Section 7.3.14.) using **L,D,D-G2Lys-OMe** (2.10 g, 2.57 mmol), 1 M NaOH (8 mL) and MeOH (100 mL). Yield = 1.69 g (2.11 mmol, 82%). R_f = 0.09 (9:1 DCM:MeOH, CeMo stain). M.P. = 84-94°C (Lit. = 86°C)[326]. $[\alpha]_D^{589}$ = +9.19 (*c* = 1, MeOH). ^{1}H NMR (400 MHz, CD_3COCD_3) δ 7.50 (1H, d, *J*=7.6, $HO_2CCHN\mathit{H}$), 7.37 (1H, br s, $CH_2N\mathit{H}COCH$), 6.23-5.96 (4H, N*H*COO), 4.44 (1H, m, $HO_2CC\mathit{H}$), 4.14 (1H, m, C*H*NHCOO), 4.04 (1H, m, C*H*NHCOO), 3.22 (2H, br s, $C\mathit{H}_2NHCOCH$), 3.05 (4H, m, $C\mathit{H}_2NHCOO$), 1.95-1.59 (6H, m, $CHC\mathit{H}_2$), 1.57-1.28 (48H, m, $C\mathit{H}_2$, $C\mathit{H}_3$). ^{13}C NMR (100 MHz, CD_3COCD_3) δ 174.63 ($\mathit{C}O_2H$), 174.14, 174.08 (both NHC*O*CH), 157.78, 157.44, 157.36 (all NH*C*OO), 80.37, 80.20, 79.45, 79.39 (all $\mathit{C}(CH_3)_3$), 56.42, 56.35 (both *C*HNHCOO), 53.66 ($HO_2C\mathit{C}H$), 41.79, 41.67 (both $\mathit{C}H_2NHCOO$), 40.40 ($\mathit{C}H_2NHCOCH$), 34.17, 33.89, 33.04 (all $\mathit{C}H_2CH$), 31.50, 30.85 (both $\mathit{C}H_2$), 29.703, 29.608 ($\mathit{C}H_3$ × 12), 24.65, 24.60, 24.34 (all $\mathit{C}H_2$). ν_{max} 3314*m* (N-H), 2976*m* (C-H), 2933*m* (C-H), 2868*m* (C-H), 1693*s* (C=O), 1660*s* (C=O), 1515*s* (N-H), 1455*m*, 1392*m*, 1366*s*, 1248*s*, 1163*s*. ESI MS $C_{38}H_{70}N_6O_{12}$ m/z calculated $[M+H]^+$ 803.5124, found 803.5113 (63%), calculated $[M+Na]^+$ 825.4944, found 825.4916 (100%).

7.3.21. D,L,L-G2Lys-OMe[326]

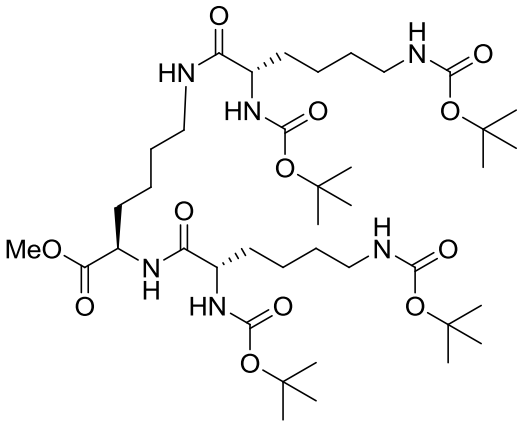

D,L,L-G2Lys-OMe was synthesised using the same method used for **L,L,L-G2Lys-OMe** (Section 7.3.13.) using **L-Lys-Boc** (2.5 g, 7.22 mmol), TBTU was added (2.43 g, 7.56 mmol), **MeO-D-Lys** (0.8 g, 3.44 mol) and DCM (100 mL). Yield = 1.71 g (2.10 mmol, 61%). R_f = 0.32 (9:1 DCM:MeOH, CeMo stain). M.P. = 66-70°C. $[\alpha]_D^{589}$ = -5.83 (*c* = 1, MeOH). ^{1}H NMR (400 MHz, CD_3COCD_3) δ 7.53 (1H, d, *J*=7.6, CH_3O_2CCHNH), 7.33 (1H, br s, $CH_2NHCOCH$), 6.16-5.92 (4H, m, NHCOO), 4.40 (1H, dt (overlapped), *J*=4.8, 8.0, CH_3O_2CCH), 4.13 (1H, m, CHNHCOO), 4.04 (1H, m, CHNHCOO), 3.67 (3H, s, CH_3O), 3.20 (2H, m, $CH_2NHCOCH$), 3.06 (4H, m, CH_2NHCOO), 1.89-1.58 (6H, m, $CHCH_2$), 1.57-1.30 (48H, m, CH_2, CH_3). ^{13}C NMR (100 MHz, CD_3COCD_3) δ 174.19 (CO_2CH_3), 173.97 (NHCOCH), 157.75, 157.71, 157.37 (all NHCOO), 80.30, 80.15, 79.35, 79.32 (all $C(CH_3)_3$), 56.42, 56.36 (both CHNHCOO), 53.78 (CH_3O_2CCH), 53.27 (CH_3O), 41.76, 41.73 (both CH_2NHCOO), 40.24 ($CH_2NHCOCH$), 34.17, 33.98, 32.98 (all CH_2CH), 31.49, 30.85 (both CH_2), 29.69, 29.59 (CH_3 × 12), 24.65, 24.53, 24.33 (all CH_2). ν_{max} 3315*m* (N-H), 2976*m* (C-H), 2932*m* (C-H), 2865*m* (C-H), 1693*s* (C=O), 1660*s* (C=O), 1515*s* (N-H), 1455*m*, 1391*m*, 1365*s*, 1247*s*, 1164*s*. ESI MS $C_{39}H_{72}N_6O_{12}$ m/z calculated $[M+H]^+$ 817.5281, found 817.5301 (8%), calculated $[M+Na]^+$ 839.5100, found 839.5083 (100%).

7.3.22. D,L,L-G2Lys[326]

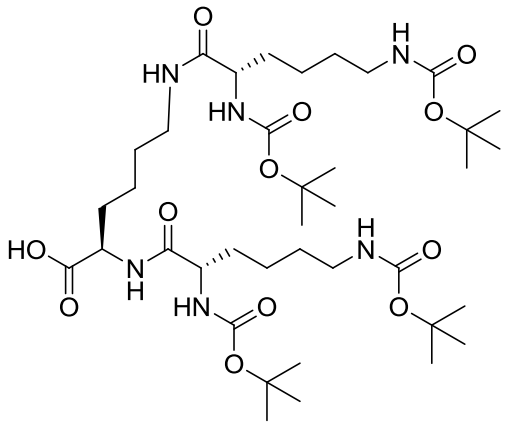

D,L,L-G2Lys was synthesised using the same method used for **L,L,L-G2Lys** (Section 7.3.14.) using **D,L,L-G2Lys-OMe** (1.70 g, 2.08 mmol), 1 M NaOH (7 mL) and MeOH (100 mL). Yield = 1.30 g (1.62 mmol, 78%). R_f = 0.09 (9:1 DCM:MeOH, CeMo stain). M.P. = 84-94°C (Lit. = 84°C)[326]. $[\alpha]_D^{589}$ = -11.7 (*c* = 1, MeOH). ^{1}H NMR (400 MHz, CD_3COCD_3) δ 7.52 (1H, d, *J*=7.6, HO_2CCHNH), 7.40 (1H, br s, $CH_2NHCOCH$), 6.24-5.95 (4H, $NHCOO$), 4.43 (1H, m, HO_2CCH), 4.14 (1H, m, $CHNHCOO$), 4.05 (1H, m, $CHNHCOO$), 3.21 (2H, br s, $CH_2NHCOCH$), 3.05 (4H, m, CH_2NHCOO), 1.94-1.59 (6H, m, $CHCH_2$), 1.57-1.30 (48H, m, CH_2, CH_3). ^{13}C NMR (100 MHz, CD_3COCD_3) δ 174.65 (CO_2H), 174.13, 174.08 (both $NHCOCH$), 157.78, 157.44, 157.35 (all $NHCOO$), 80.37, 80.20, 79.45, 79.39 (all $C(CH_3)_3$), 56.42, 56.34 (both $CHNHCOO$), 53.65 (HO_2CCH), 41.77, 41.40 (both CH_2NHCOO), 40.42 ($CH_2NHCOCH$), 34.16, 33.87, 33.03 (all CH_2CH), 31.46, 30.83 (both CH_2), 29.71, 29.61 (CH_3 × 12), 24.65, 24.60, 24.34 (all CH_2). ν_{max} 3314*m* (N-H), 2977*m* (C-H), 2933*m* (C-H), 2868*m* (C-H), 1693*s* (C=O), 1660*s* (C=O), 1515*s* (N-H), 1455*m*, 1392*m*, 1366*s*, 1248*s*, 1163*s*. ESI MS $C_{38}H_{70}N_6O_{12}$ m/z calculated $[M+H]^+$ 803.5124, found 803.5131 (65%), calculated $[M+Na]^+$ 825.4944, found 825.4927 (100%).

Appendices

Appendix A

A.1. Attenuated Total Reflectance-Fourier Transform Infra Red Data

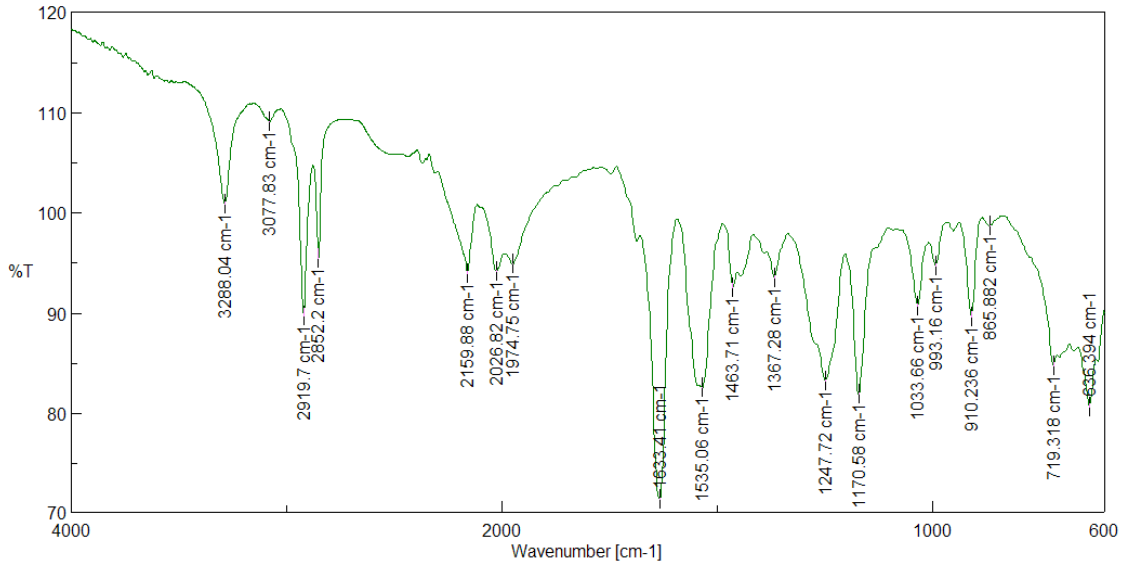

Figure A.1.1. ATR-FTIR of **G1-ene** xerogel.

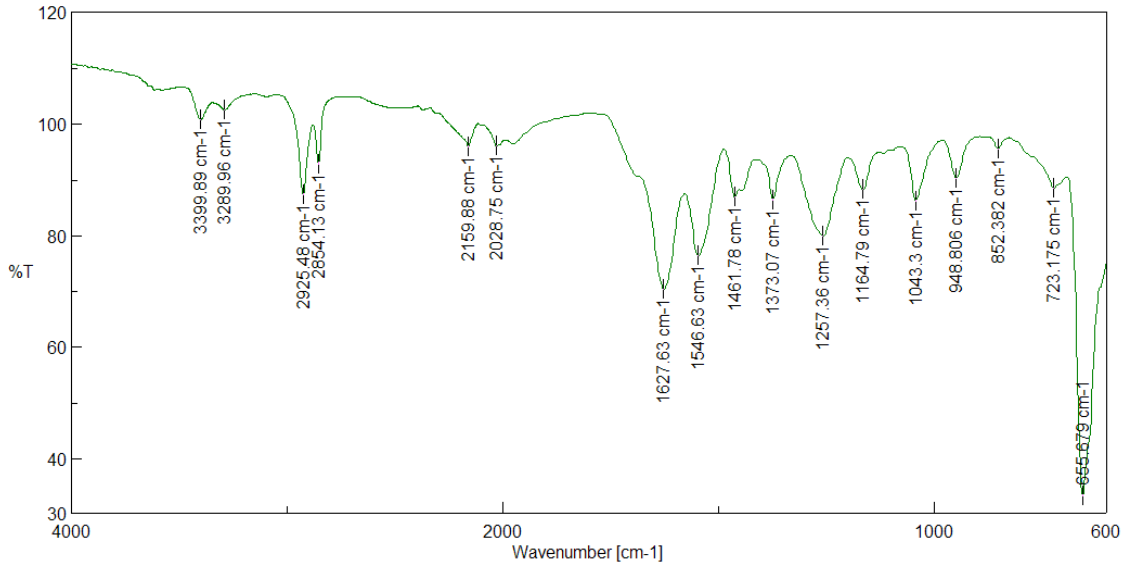

Figure A.1.2. ATR-FTIR of **G1-ene**/$AgSbF_6$ xerogel.

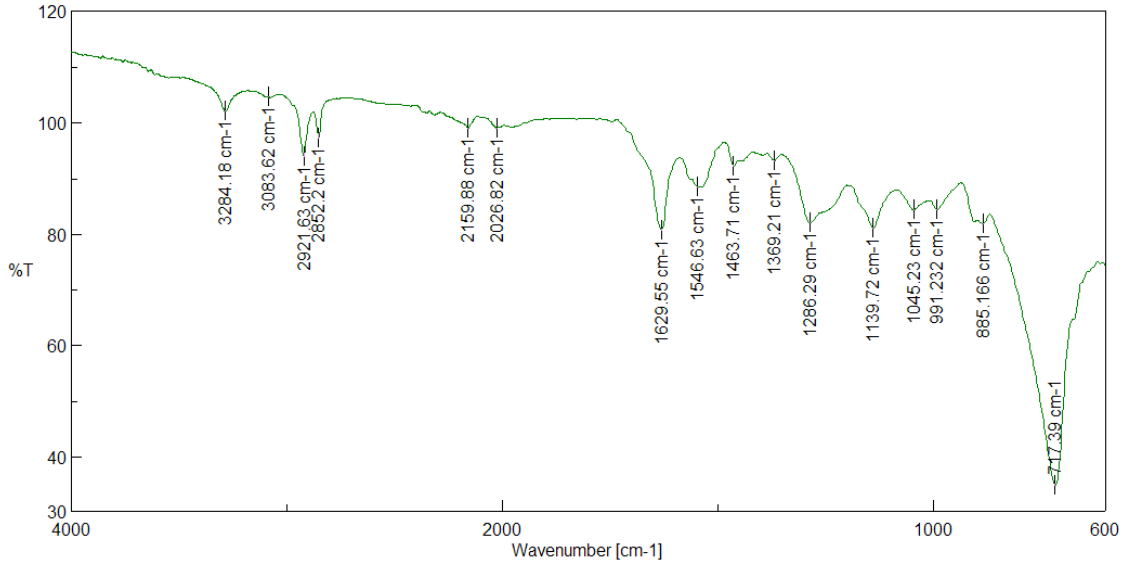

Figure A.1.3. ATR-FTIR of **G1-ene**/$LiPF_6$ xerogel.

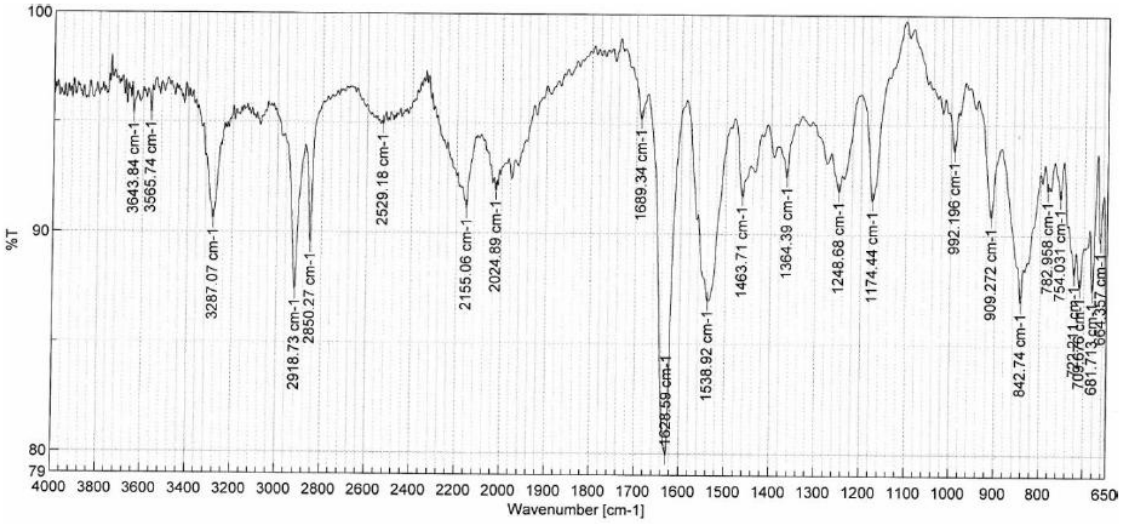

Figure A.1.4. ATR-FTIR of **G1-ene**/$NaPF_6$ xerogel.

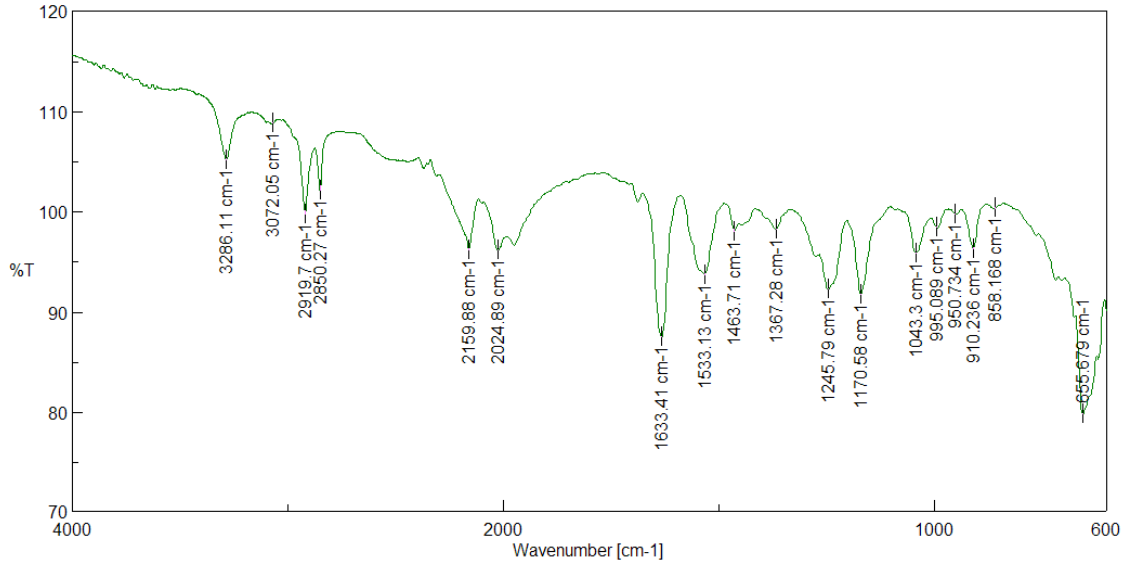

Figure A.1.5. ATR-FTIR of **G1-ene**/$KSbF_6$ xerogel.

Appendix B

B.1. Attenuated Total Reflectance-Fourier Transform Infra Red Data

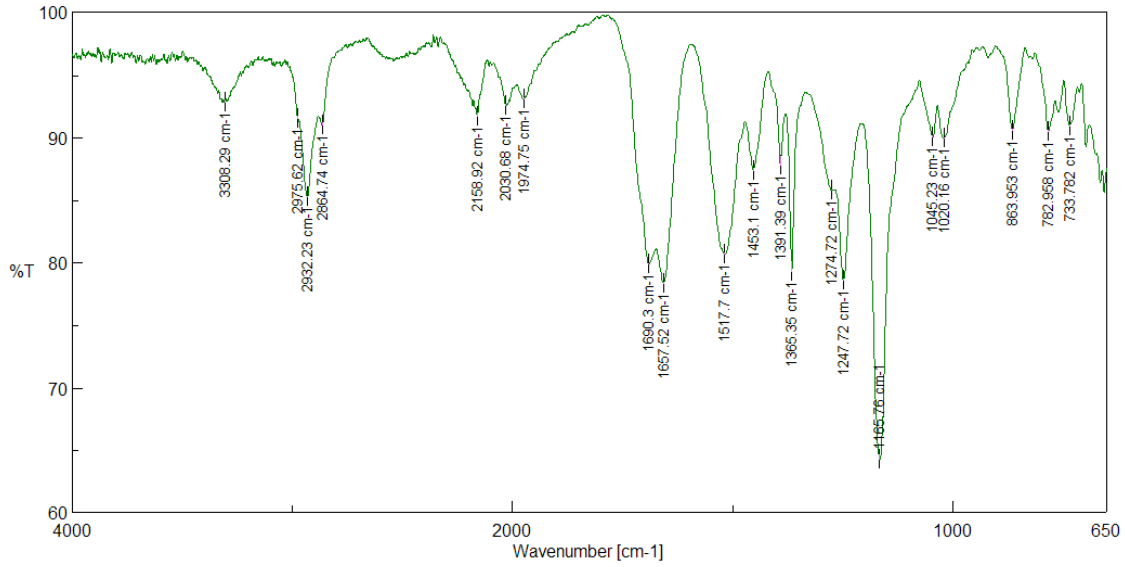

Figure B.1.1. ATR-FTIR of **L,L,L-G2Lys** solid dried from toluene.

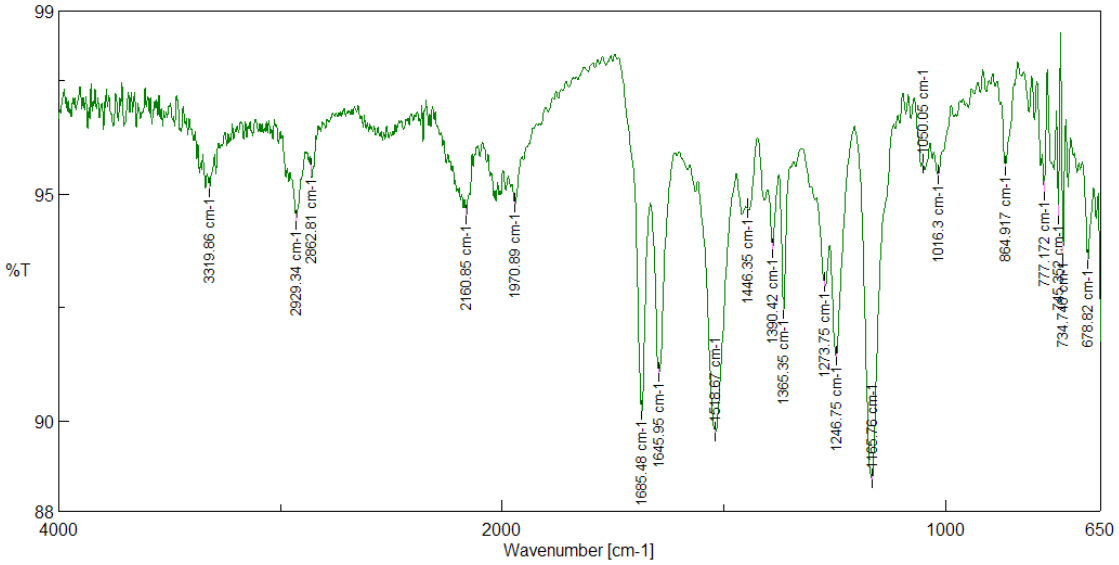

Figure B.1.2. ATR-FTIR of **L,L,L-G2Lys** and **C8** xerogel.

Appendix C

C.1. Differential Scanning Calorimetry Data

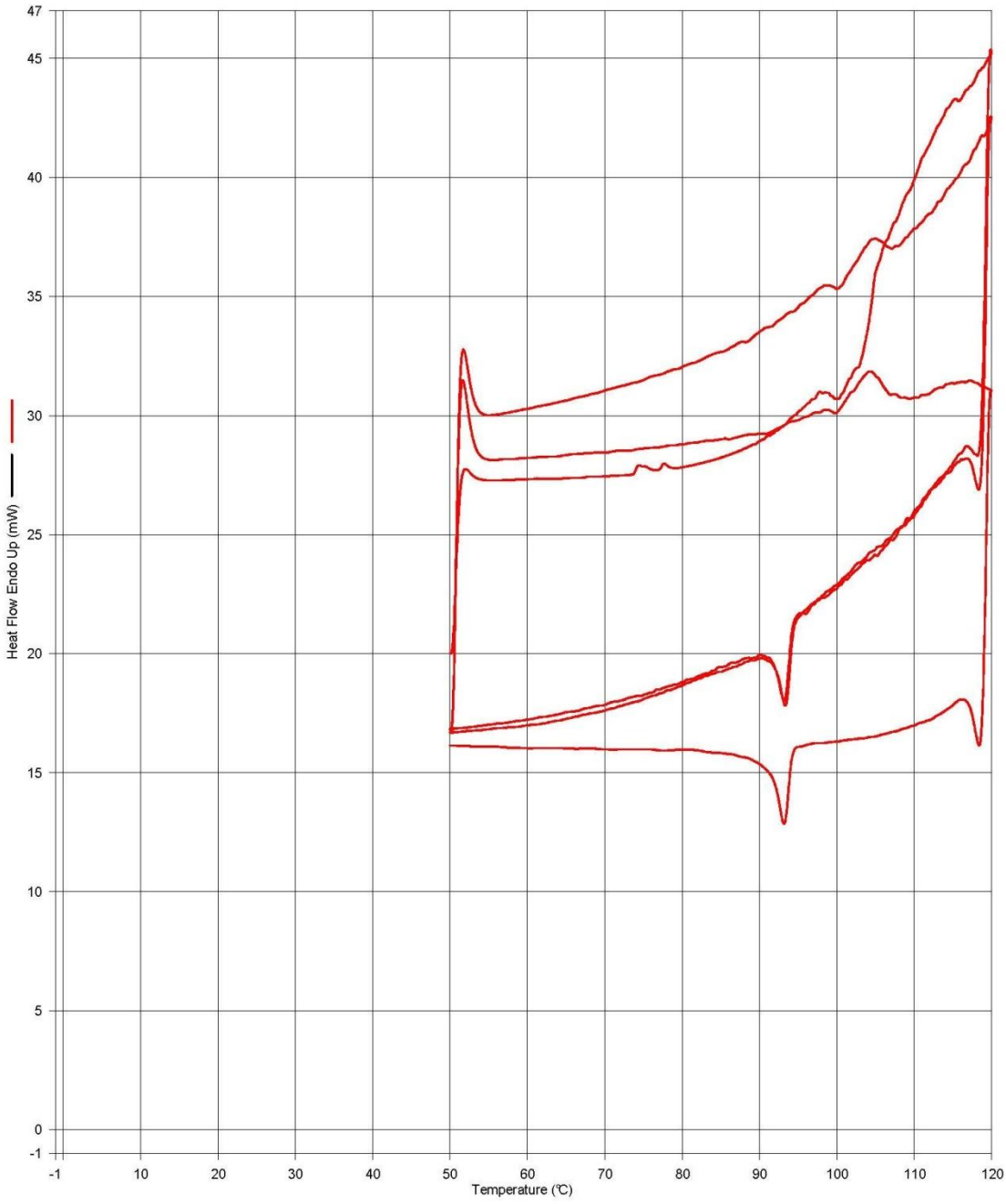

Figure C.1.1. DSC trace of 50 mM Tetralin **L,L,L-G2Lys** and **C6R** gel.

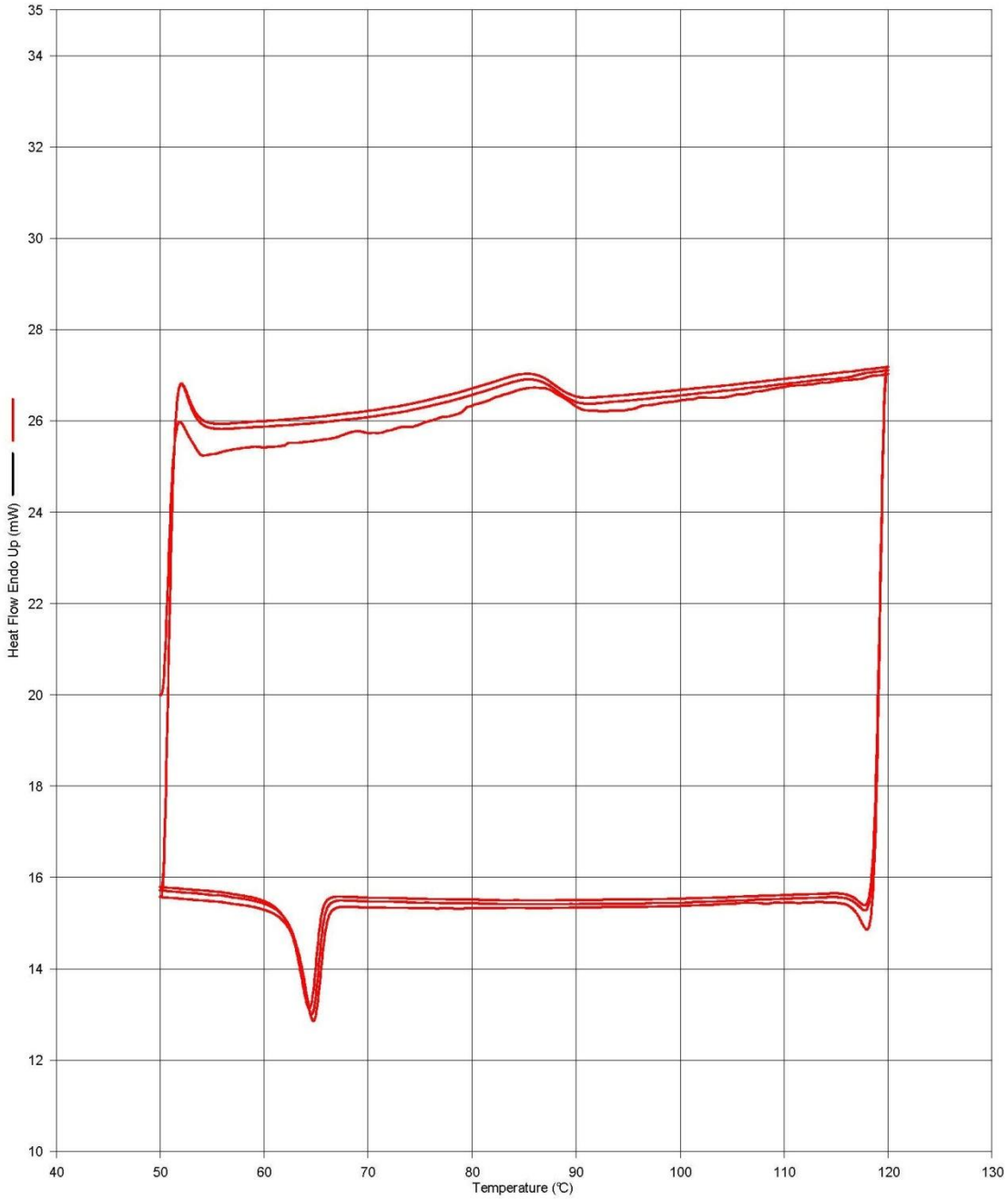

Figure C.1.2. DSC trace of 50 mM Tetralin **L,L,L-G2Lys** and **C6S** gel.

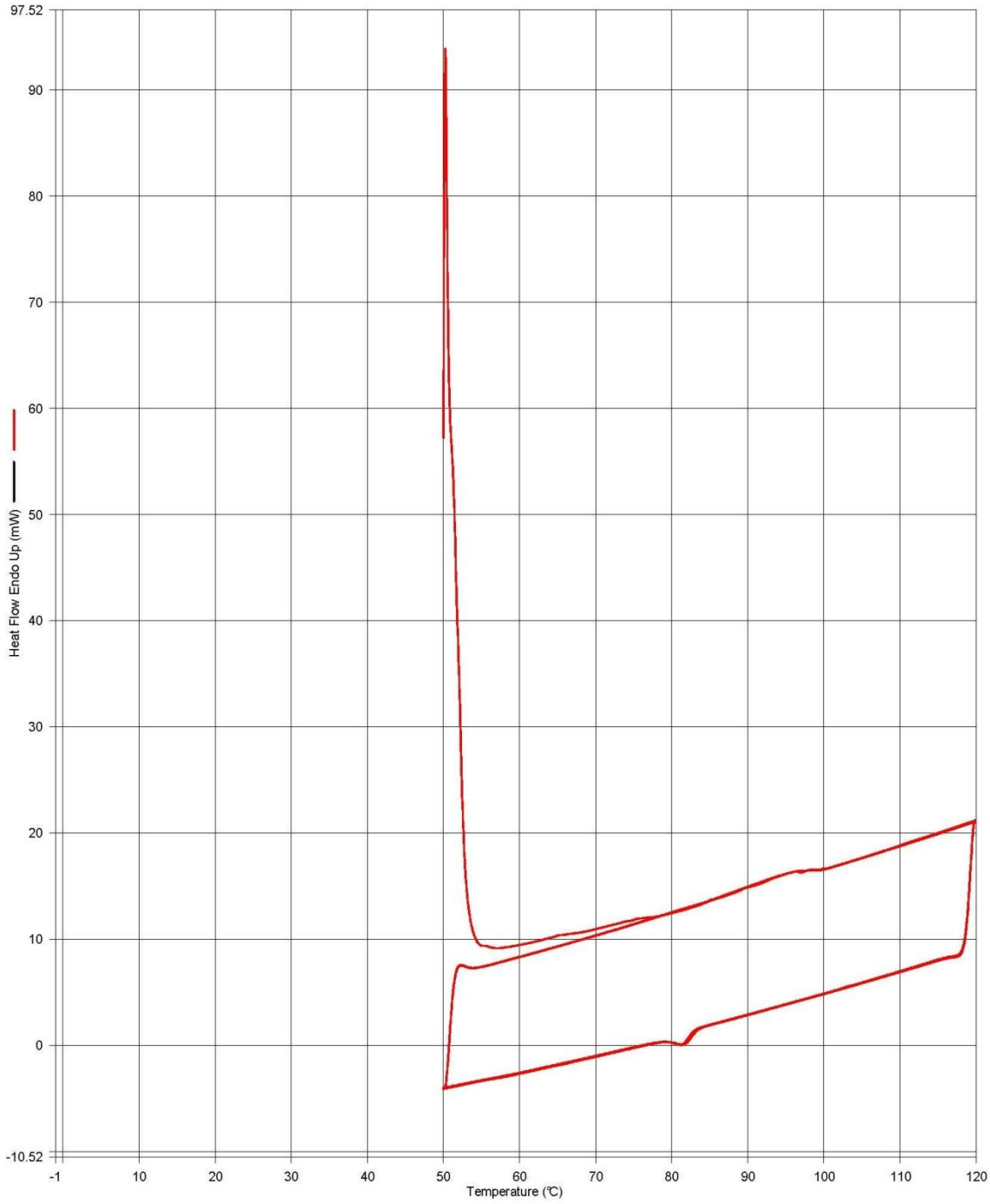

Figure C.1.3. DSC trace of 50 mM Tetralin **L,L,L-G2Lys**, **C6R** and **C6S** gel.

C.2. Small and Wide Angle X-ray Scattering Data

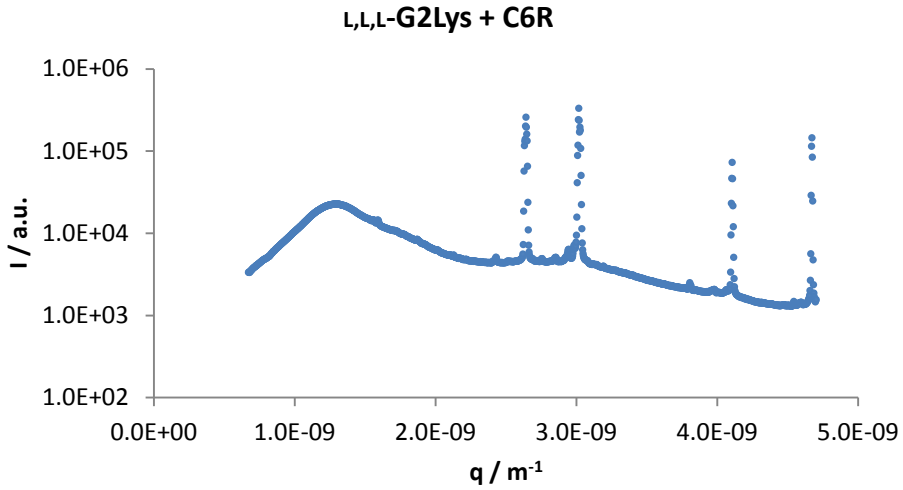

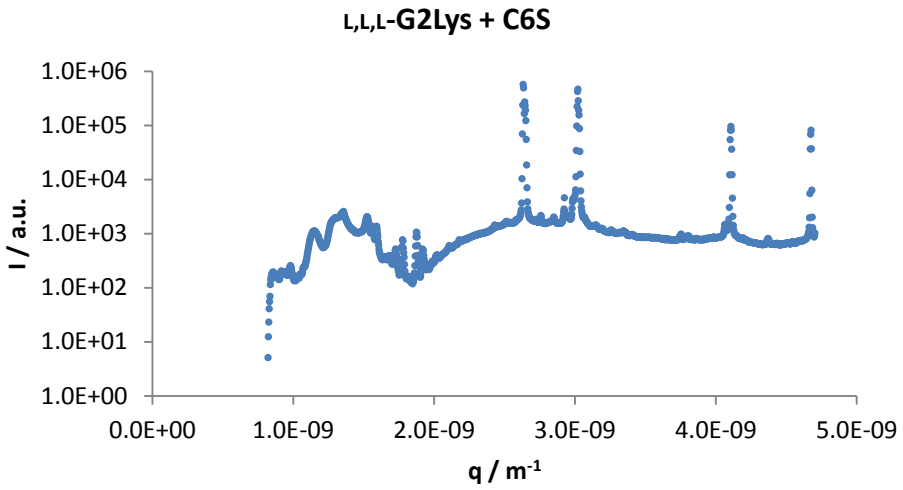

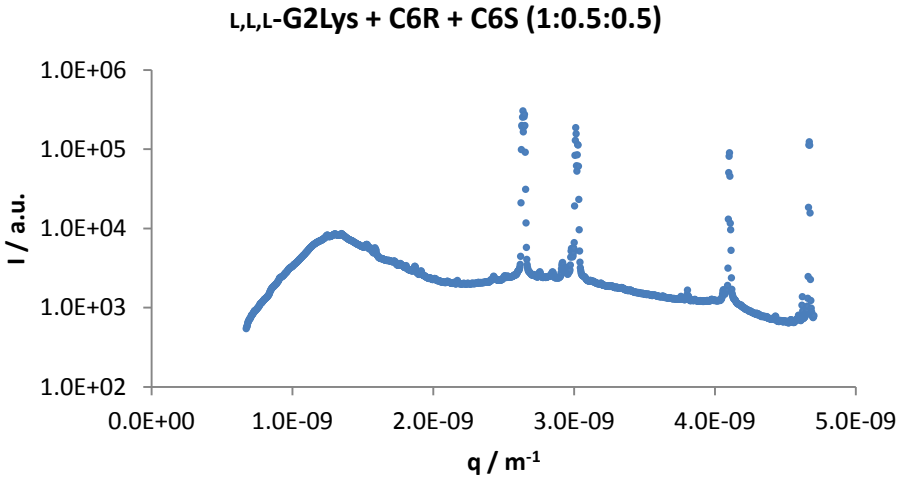

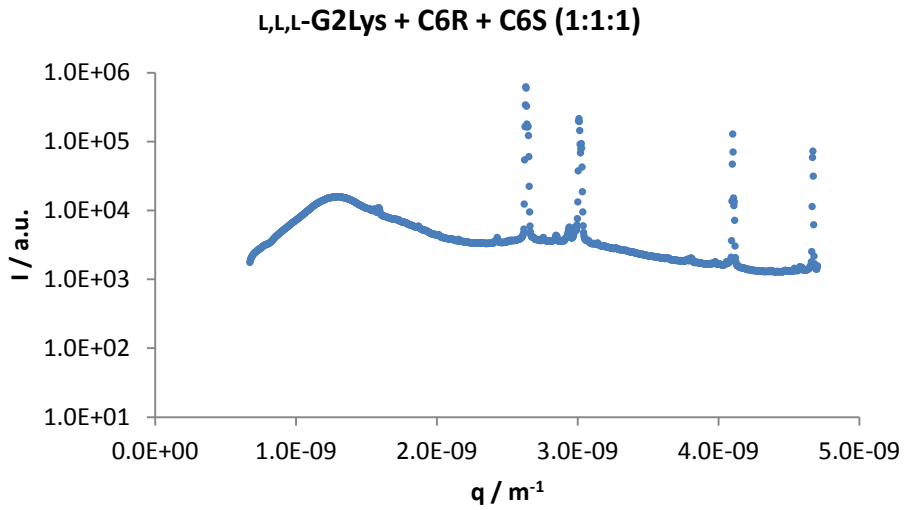

Figure C.2.1. Wide Angle X-ray Scattering (WAXS) data for toluene gels with 10 mM **L,L,L-G2Lys** and **C6R/S**.

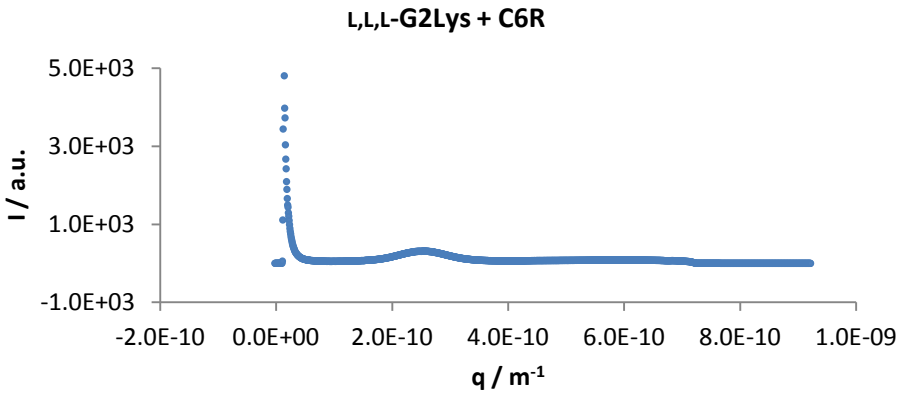

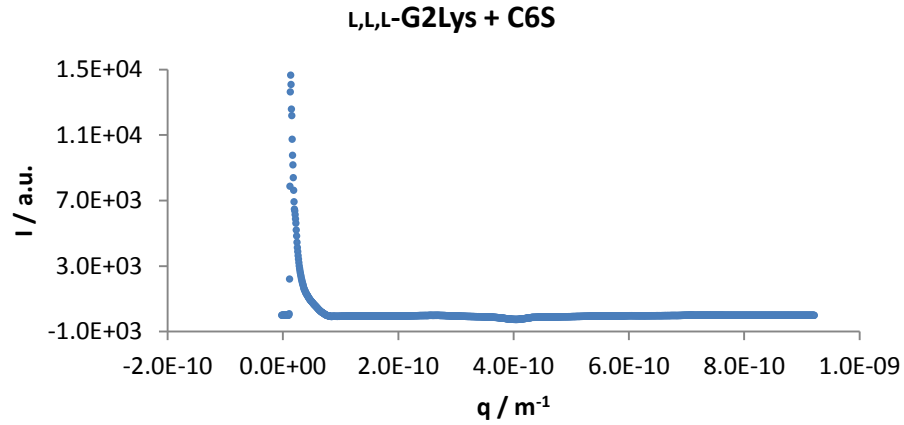

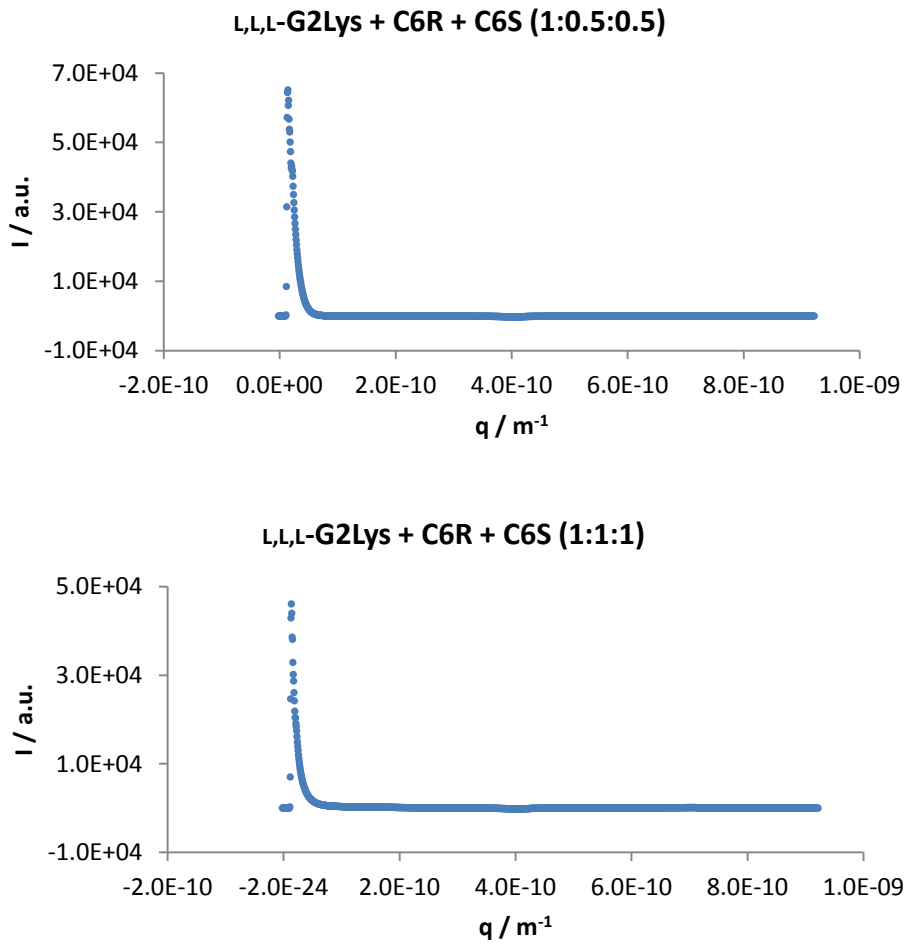

Figure C.2.2. Small Angle X-ray Scattering (SAXS) data for toluene gels with 10 mM **L,L,L-G2Lys** and **C6R/S**.

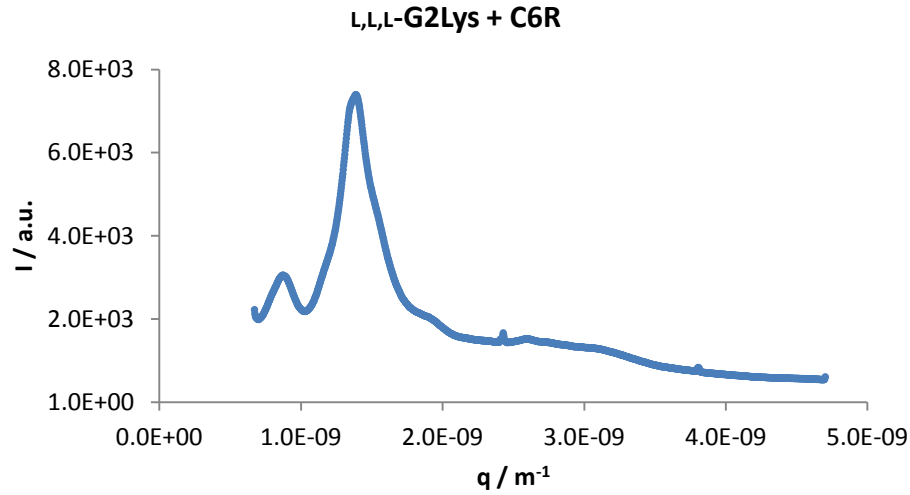

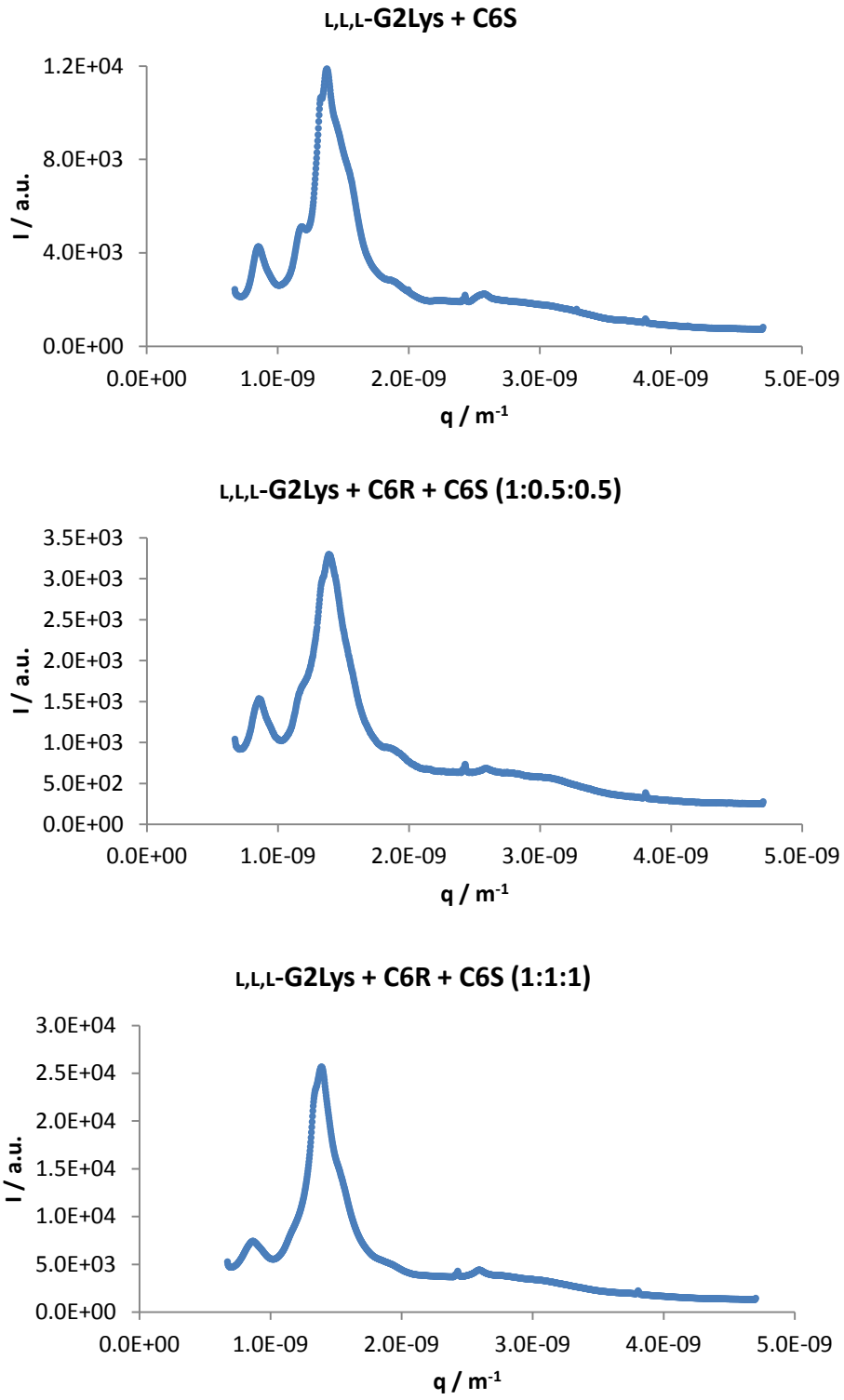

Figure C.2.3. Wide Angle X-ray Scattering (WAXS) data for xerogels formed from toluene gels with 10 mM **L,L,L-G2Lys** and **C6R/S**.

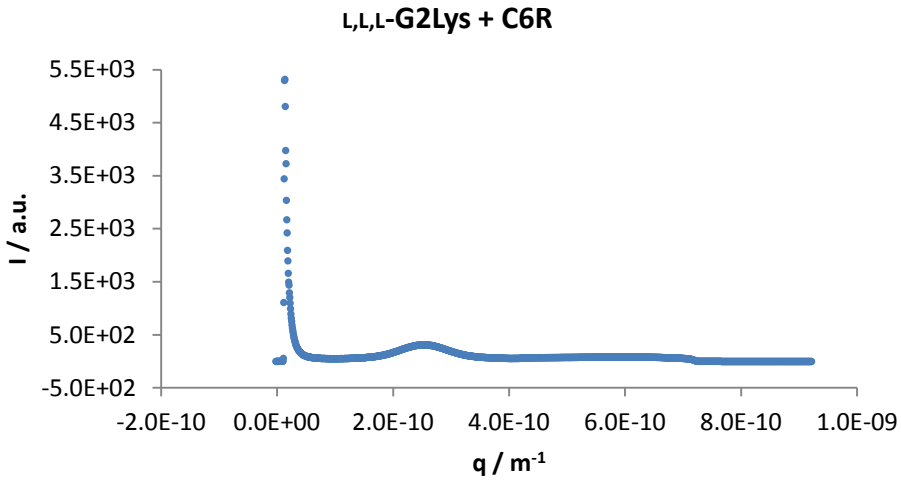
L,L,L-G2Lys + C6R
5.5E+03
4.5E+03
3.5E+03
2.5E+03
1.5E+03
5.0E+02
-5.0E+02
I / a.u.
-2.0E-10
0.0E+00
2.0E-10
4.0E-10
6.0E-10
8.0E-10
1.0E-09
q / m-1

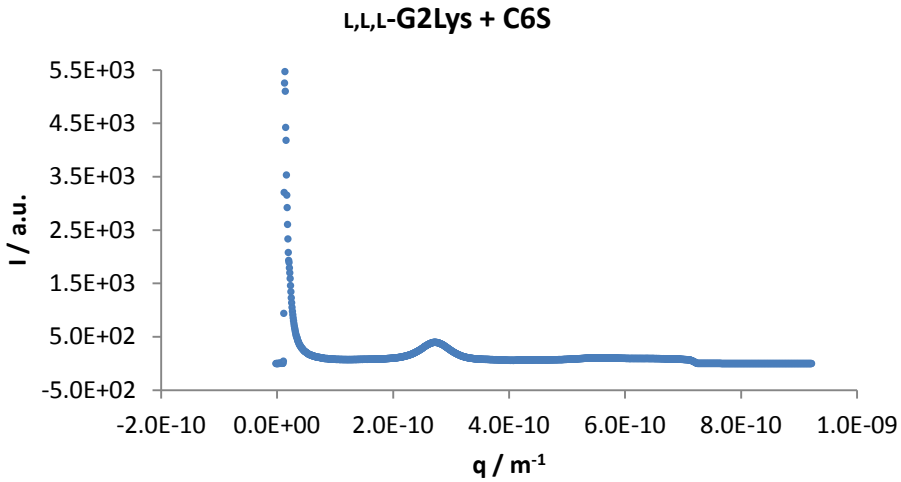
L,L,L-G2Lys + C6S
5.5E+03
4.5E+03
3.5E+03
2.5E+03
1.5E+03
5.0E+02
-5.0E+02
I / a.u.
-2.0E-10
0.0E+00
2.0E-10
4.0E-10
6.0E-10
8.0E-10
1.0E-09
q / m-1

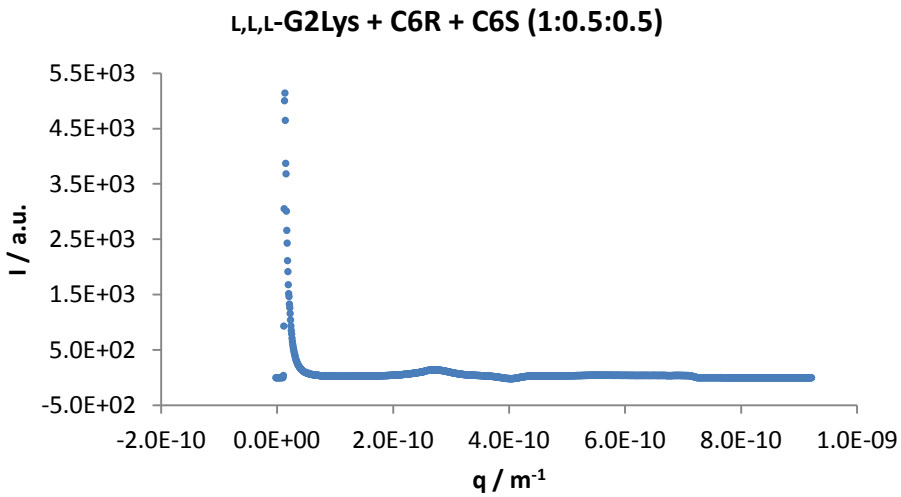
L,L,L-G2Lys + C6R + C6S (1:0.5:0.5)
5.5E+03
4.5E+03
3.5E+03
2.5E+03
1.5E+03
5.0E+02
-5.0E+02
I / a.u.
-2.0E-10
0.0E+00
2.0E-10
4.0E-10
6.0E-10
8.0E-10
1.0E-09
q / m-1

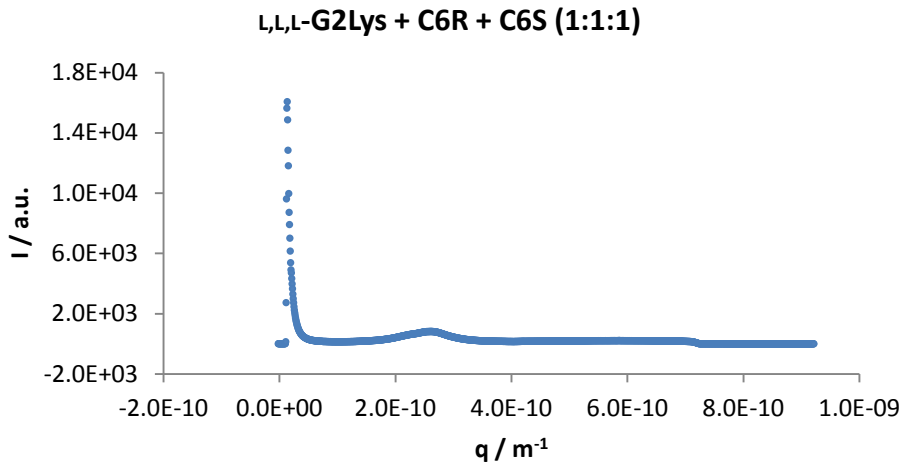

Figure C.2.4. Small Angle X-ray Scattering (SAXS) data for xerogels formed from toluene gels with 10 mM L,L,L-**G2Lys** and **C6R/S**.

Abbreviations

AFM	Atomic Force Microscopy
ATR-FTIR	Attenuated Total Reflectance Fourier Transform Infra-Red Spectroscopy
br	Broadened
CD	Circular Dichroism
[Insol]@T_{gel}	Concentration of gelator soluble at the T_{gel} value
CFF	Cylinder Form Factor
Boc	Di-*tert*-butyl dicarbonate
DIPEA	Diisopropyl ethylamine
DMF	Dimethylformamide
DMSO	Dimethylsulfoxide
de	Diastereomeric Excess
DCM	Dichloromethane
Et_2O	Diethyl ether
DSC	Differential Scanning Calorimetry
ddt	Double Double Triplet
dd	Double Doublet
dt	Double Triplet
d	Doublet
ee	Enantiomeric Excess
EtOAc	Ethyl acetate
FEG-SEM	Field Emission Gun Scanning Electron Microscopy

Fmoc	Fluorenylmethyloxycarbonyl chloride
LCST	Lower Critical Solution Temperature
MS	Mass Spectrometry
m	Medium signal
M.P.	Melting Point
m	meta
MeOH	Methanol
Me	Methyl group (CH_3)
µm	Micrometer
MGC	Minimum Gelation Concentration
m	Multiplet
nm	Nanometer
NMR	Nuclear Magnetic Resonance
TBTU	*o*-(Benzotriazol-1-yl)-N,N,N',N'-tetramethyluronium tetrafluoroborate
o	ortho
p	para
ppm	Parts per million
qr	Quartet
qn	Quintet
Sat.	Saturated
s	Singlet
SAXS	Small Angle X-ray Scattering
s	Strong signal

$\mathbf{T_{100\%}}$	Temperature at which all of gelator is solubilised
$\mathbf{T_{gel}}$	Temperature of gel-sol transition
THF	Tetrahydrofuran
TLC	Thin Layer Chromatography
TEM	Transition Electron Microscopy
TEA	Triethylamine
OTf	Trifluoromethanesulfonate
t	Triplet
UV	Ultraviolet
VT-NMR	Variable Temperature Nuclear Magnetic Resonance
w	Weak signal
WAXS	Wide Angle X-ray Scattering

References

1. J. M. Lehn, *Angew. Chem. Int. Ed. Engl.*, 1990, **29**, 1304-1319.
2. G. V. Oshovsky, D. N. Reinhoudt and W. Verboom, *Angew. Chem. Int. Ed.*, 2007, **46**, 2366-2393.
3. F. Diederich, *Angew. Chem. Int. Ed.*, 2007, **46**, 68-69.
4. J. M. Lehn, *Chem. Soc. Rev.*, 2007, **36**, 151-160.
5. G. R. Desiraju, *Nature*, 2001, **412**, 397-400.
6. J. W. Steed and J. L. Atwood, *Supramolecular Chemistry*, John Wiley & Sons Ltd, 2009.
7. A. S. C. Lawrence, *Trans. Faraday Soc.*, 1935, **31**, 0189-0194.
8. J. D. Watson and F. H. C. Crick, *Cold Spring Harb. Sym.*, 1953, **18**, 123-131.
9. D. J. Cram, *Angew. Chem. Int. Ed. Engl.*, 1988, **27**, 1009-1020.
10. J. M. Lehn, *Angew. Chem. Int. Ed. Engl.*, 1988, **27**, 89-112.
11. C. J. Pedersen, *Angew. Chem. Int. Ed. Engl.*, 1988, **27**, 1021-1027.
12. F. Hof, S. L. Craig, C. Nuckolls and J. Rebek, *Angew. Chem. Int. Edit.*, 2002, **41**, 1488-1508.
13. C. J. Pedersen, *J. Am. Chem. Soc.*, 1967, **89**, 2495-2496.
14. P. D. Beer and P. A. Gale, *Angew. Chem. Int. Ed.*, 2001, **40**, 486-516.
15. F. P. Schmidtchen and M. Berger, *Chem. Rev.*, 1997, **97**, 1609-1646.
16. J. M. Lehn, *Pure Appl. Chem*, 1994, **66**, 1961-1966.
17. E. A. Meyer, R. K. Castellano and F. Diederich, *Angew. Chem. Int. Ed.*, 2003, **42**, 1210-1250.
18. G. M. Whitesides, J. P. Mathias and C. T. Seto, *Science*, 1991, **254**, 1312-1319.
19. G. M. Whitesides and B. Grzybowski, *Science*, 2002, **295**, 2418-2421.
20. D. Philp and J. F. Stoddart, *Angew. Chem. Int. Ed.*, 1996, **35**, 1155-1196.
21. D. N. Reinhoudt and M. Crego-Calama, *Science*, 2002, **295**, 2403-2407.
22. J. M. Lehn, *Proc. Natl. Acad. Sci. USA* , 2002, **99**, 4763-4768.
23. J. M. Lehn, *Science*, 2002, **295**, 2400-2403.
24. B. A. Grzybowski, C. E. Wilmer, J. Kim, K. P. Browne and K. J. M. Bishop, *Soft Matter*, 2009, **5**, 1110-1128.
25. M. Fialkowski, K. J. M. Bishop, R. Klajn, S. K. Smoukov, C. J. Campbell and B. A. Grzybowski, *J Phys. Chem. B*, 2006, **110**, 2482-2496.
26. K. J. M. Bishop, C. E. Wilmer, S. Soh and B. A. Grzybowski, *Small*, 2009, **5**, 1600-1630.

27. L. J. Prins and P. Scrimin, *Angew. Chem. Int. Ed.*, 2009, **48**, 2288-2306.
28. M. D. Ward and P. R. Raithby, *Chem. Soc. Rev.*, 2013, **42**, 1619-1636.
29. M. Shimomura and T. Sawadaishi, *Curr. Opin. Colloid Interface Sci.*, 2001, **6**, 11-16.
30. S. Zhang, *Nat. Biotech.*, 2003, **21**, 1171-1178.
31. L. J. Prins, D. N. Reinhoudt and P. Timmerman, *Angew. Chem. Int. Ed.*, 2001, **40**, 2382-2426.
32. T. Graham, *Phil. Trans. R. Soc. Lon.*, 1861, **151**, 183-224.
33. W. B. Hardy, *Proc. R. Soc. Lon. A*, 1912, **87**, 29-37.
34. J. B. McNair, *J. Phys. Chem. US*, 1916, **20**, 633-639.
35. D. Jordon Lloyd, in *Colloid Chemistry*, ed. J. Alexander, The Chemical Catalog Co., New York, 1926, vol. 1, p. 767.
36. P. J. Flory, *Faraday Discussions of the Chemical Society*, 1974, **57**, 7-18.
37. Y. Osada and J. P. Gong, *Adv. Mater.*, 1998, **10**, 827-837.
38. M. Suzuki and K. Hanabusa, *Chem. Soc. Rev.*, 2010, **39**, 455-463.
39. P. Terech and R. G. Weiss, *Chem. Rev.*, 1997, **97**, 3133-3159.
40. D. K. Smith, *Tetrahedron*, 2007, **63**, 7283-7284.
41. J. H. van Esch, *Langmuir*, 2009, **25**, 8392-8394.
42. M. de Loos, B. L. Feringa and J. H. van Esch, *Eur. J. Org. Chem.*, 2005, 3615-3631.
43. P. Dastidar, *Chem. Soc. Rev.*, 2008, **37**, 2699-2715.
44. A. Aggeli, I. A. Nyrkova, M. Bell, R. Harding, L. Carrick, T. C. B. McLeish, A. N. Semenov and N. Boden, *Proc. Natl. Acad. Sci. USA*, 2001, **98**, 11857-11862.
45. T. F. A. De Greef, M. M. J. Smulders, M. Wolffs, A. P. H. J. Schenning, R. P. Sijbesma and E. W. Meijer, *Chem. Rev.*, 2009, **109**, 5687-5754.
46. M. M. J. Smulders, M. M. L. Nieuwenhuizen, T. F. A. de Greef, P. van der Schoot, A. Schenning and E. W. Meijer, *Chem. Eur. J.*, 2010, **16**, 362-367.
47. P. Jonkheijm, P. van der Schoot, A. P. H. J. Schenning and E. W. Meijer, *Science*, 2006, **313**, 80-83.
48. M. de Loos, J. van Esch, R. M. Kellogg and B. L. Feringa, *Angew. Chem. Int. Ed.*, 2001, **40**, 613-616.
49. A. Arnaud and L. Bouteiller, *Langmuir*, 2004, **20**, 6858-6863.
50. J. E. A. Webb, M. J. Crossley, P. Turner and P. Thordarson, *J. Am. Chem. Soc.*, 2007, **129**, 7155-7162.
51. M. Lescanne, A. Colin, O. Mondain-Monval, F. Fages and J. L. Pozzo, *Langmuir*, 2003, **19**, 2013-2020.

52. M. Lescanne, P. Grondin, A. d'Aléo, F. Fages, J. L. Pozzo, O. M. Monval, P. Reinheimer and A. Colin, *Langmuir*, 2004, **20**, 3032-3041.
53. V. Simic, L. Bouteiller and M. Jalabert, *J. Am. Chem. Soc.*, 2003, **125**, 13148-13154.
54. A. R. Hirst, I. A. Coates, T. R. Boucheteau, J. F. Miravet, B. Escuder, V. Castelletto, I. W. Hamley and D. K. Smith, *J. Am. Chem. Soc.*, 2008, **130**, 9113-9121.
55. F. Aparicio, F. García and L. Sánchez, *Chem. Eur. J.*, 2013, **19**, 3239-3248.
56. J. F. Douglas, *Langmuir*, 2009, **25**, 8386-8391.
57. S. R. Raghavan and J. F. Douglas, *Soft Matter*, 2012, **8**, 8539-8546.
58. Y. J. Wang, L. M. Tang and J. Yu, *Cryst. Growth Des.*, 2008, **8**, 884-889.
59. K. M. Anderson, G. M. Day, M. J. Paterson, P. Byrne, N. Clarke and J. W. Steed, *Angew. Chem. Int. Ed.*, 2008, **47**, 1058-1062.
60. D. J. Adams, K. Morris, L. Chen, L. C. Serpell, J. Bacsa and G. M. Day, *Soft Matter*, 2010, **6**, 4144-4156.
61. K. A. Houton, K. L. Morris, L. Chen, M. Schmidtmann, J. T. A. Jones, L. C. Serpell, G. O. Lloyd and D. J. Adams, *Langmuir*, 2012, **28**, 9797-9806.
62. Y. Xu, C. Q. Kang, Y. Chen, Z. Bian, X. P. Qiu, L. X. Gao and Q. X. Meng, *Chem. Eur. J.*, 2012, **18**, 16955-16961.
63. J. X. Cui, Z. H. Shen and X. H. Wan, *Langmuir*, 2010, **26**, 97-103.
64. P. Terech, N. M. Sangeetha and U. Maitra, *J. Phys. Chem. B*, 2006, **110**, 15224-15233.
65. F. M. Menger and K. L. Caran, *J. Am. Chem. Soc.*, 2000, **122**, 11679-11691.
66. J. R. Moffat and D. K. Smith, *Chem. Commun.*, 2008, 2248-2250.
67. Nonappa, M. Lahtinen, B. Behera, E. Kolehmainen and U. Maitra, *Soft Matter*, 2010, **6**, 1748-1757.
68. G. O. Lloyd, M. O. M. Piepenbrock, J. A. Foster, N. Clarke and J. W. Steed, *Soft Matter*, 2012, **8**, 204-216.
69. V. A. Mallia, P. D. Butler, B. Sarkar, K. T. Holman and R. G. Weiss, *J. Am. Chem. Soc.*, 2011, **133**, 15045-15054.
70. D. J. Abdallah and R. G. Weiss, *Adv. Mater.*, 2000, **12**, 1237-1247.
71. M. George and R. G. Weiss, *Acc. Chem. Res.*, 2006, **39**, 489-497.
72. L. A. Estroff and A. D. Hamilton, *Chem. Rev.*, 2004, **104**, 1201-1217.
73. J. Le Bideau, L. Viau and A. Vioux, *Chem. Soc. Rev.*, 2011, **40**, 907-925.
74. K. Hanabusa, H. Fukui, M. Suzuki and H. Shirai, *Langmuir*, 2005, **21**, 10383-10390.
75. N. Minakuchi, K. Hoe, D. Yamaki, S. Ten-no, K. Nakashima, M. Goto, M. Mizuhata and T. Maruyama, *Langmuir*, 2012, **28**, 9259-9266.

76. T. Kato, Y. Hirai, S. Nakaso and M. Moriyama, *Chem. Soc. Rev.*, 2007, **36**, 1857-1867.
77. F. Placin, J. P. Desvergne and F. Cansell, *J. Mater. Chem.*, 2000, **10**, 2147-2149.
78. C. Shi, Z. Huang, S. Kilic, J. Xu, R. M. Enick, E. J. Beckman, A. J. Carr, R. E. Melendez and A. D. Hamilton, *Science*, 1999, **286**, 1540-1543.
79. A. C. Pierre and G. M. Pajonk, *Chem. Rev.*, 2002, **102**, 4243-4265.
80. N. Husing and U. Schubert, *Angew. Chem. Int. Ed.*, 1998, **37**, 23-45.
81. M. Yemloul, E. Steiner, A. Robert, S. Bouguet-Bonnet, F. Allix, B. Jamart-Gregoire and D. Canet, *J. Phys. Chem. B*, 2011, **115**, 2511-2517.
82. J. Tritt-Goc, M. Bielejewski and R. Luboradzki, *Tetrahedron*, 2011, **67**, 8170-8176.
83. J. Tritt-Goc and J. Kowalczuk, *Langmuir*, 2012, **28**, 14039-14044.
84. Y. Jeong, K. Hanabusa, H. Masunaga, I. Akiba, K. Miyoshi, S. Sakurai and K. Sakurai, *Langmuir*, 2005, **21**, 586-594.
85. T. Pinault, B. Isare and L. Bouteiller, *ChemPhysChem*, 2006, **7**, 816-819.
86. Y. Nakano, T. Hirose, P. J. M. Stals, E. W. Meijer and A. R. A. Palmans, *Chem. Sci.*, 2012, **3**, 148-155.
87. H. Q. Xu, J. Song, T. Tian and R. X. Feng, *Soft Matter*, 2012, **8**, 3478-3486.
88. P. Jonkheijm, P. van der Schoot, A. Schenning and E. W. Meijer, *Science*, 2006, **313**, 80-83.
89. S. Cantekin, Y. Nakano, J. C. Everts, P. van der Schoot, E. W. Meijer and A. R. A. Palmans, *Chem. Commun.*, 2012, **48**, 3803-3805.
90. J. W. Steed, *Nat. Chem.*, 2011, **3**, 9-10.
91. K. Hanabusa, M. Yamada, M. Kimura and H. Shirai, *Angew. Chem. Int. Ed. Eng.*, 1996, **35**, 1949-1951.
92. J. vanEsch, S. DeFeyter, R. M. Kellogg, F. DeSchryver and B. L. Feringa, *Chem. Eur. J.*, 1997, **3**, 1238-1243.
93. J. vanEsch, R. M. Kellogg and B. L. Feringa, *Tetrahedron Lett.*, 1997, **38**, 281-284.
94. J. van Esch, F. Schoonbeek, M. de Loos, H. Kooijman, A. L. Spek, R. M. Kellogg and B. L. Feringa, *Chem. Eur. J.*, 1999, **5**, 937-950.
95. J. Brinksma, B. L. Feringa, R. M. Kellogg, R. Vreeker and J. van Esch, *Langmuir*, 2000, **16**, 9249-9255.
96. N. Zweep, A. Hopkinson, A. Meetsma, W. R. Browne, B. L. Feringa and J. H. van Esch, *Langmuir*, 2009, **25**, 8802-8809.
97. M. Suzuki, Y. Nakajima, M. Yumoto, M. Kimura, H. Shirai and K. Hanabusa, *Langmuir*, 2003, **19**, 8622-8624.

98. M. Suzuki, M. Yumoto, M. Kimura, H. Shirai and K. Hanabusa, *Chem. Eur. J.*, 2003, **9**, 348-354.
99. M. Suzuki and K. Hanabusa, *Chem. Soc. Rev.*, 2009, **38**, 967-975.
100. D. J. Adams, *Macromol. Biosci.*, 2011, **11**, 160-173.
101. E. K. Johnson, D. J. Adams and P. J. Cameron, *J. Mater. Chem.*, 2011, **21**, 2024-2027.
102. A. M. Smith, R. J. Williams, C. Tang, P. Coppo, R. F. Collins, M. L. Turner, A. Saiani and R. V. Ulijn, *Adv. Mater.*, 2008, **20**, 37-41.
103. S. Cantekin, T. F. A. de Greef and A. R. A. Palmans, *Chem. Soc. Rev.*, 2012, **41**, 6125-6137.
104. R. C. T. Howe, A. P. Smalley, A. P. M. Guttenplan, M. W. R. Doggett, M. D. Eddleston, J. C. Tan and G. O. Lloyd, *Chem. Commun.*, 2013, **49**, 4268-4270.
105. A. Ajayaghosh and V. K. Praveen, *Acc. Chem. Res.*, 2007, **40**, 644-656.
106. M. Zinic, F. Vogtle and F. Fages, in *Top Curr Chem*, ed. F. Fages, Springer-Verlag Berlin, Berlin, 2005, vol. 256, pp. 39-76.
107. H. Svobodova, V. Noponen, E. Kolehmainen and E. Sievanen, *Rsc. Adv.*, 2012, **2**, 4985-5007.
108. O. Gronwald and S. Shinkai, *Chem. Eur. J.*, 2001, **7**, 4328-4334.
109. K. Yoza, Y. Ono, K. Yoshihara, T. Akao, H. Shinmori, M. Takeuchi, S. Shinkai and D. N. Reinhoudt, *Chem. Commun.*, 1998, 907-908.
110. D. J. Abdallah and R. G. Weiss, *Langmuir*, 2000, **16**, 352-355.
111. G. Cravotto and P. Cintas, *Chem. Soc. Rev.*, 2009, **38**, 2684-2697.
112. A. Kotal, T. K. Paira, S. Banerjee and T. K. Mandal, *Langmuir*, 2009, **26**, 6576-6582.
113. T. Naota and H. Koori, *J. Am. Chem. Soc.*, 2005, **127**, 9324-9325.
114. D. Bardelang, F. Camerel, J. C. Margeson, D. M. Leek, M. Schmutz, M. B. Zaman, K. Yu, D. V. Soldatov, R. Ziessel, C. I. Ratcliffe and J. A. Ripmeester, *J. Am. Chem. Soc.*, 2008, **130**, 3313-3315.
115. T. W. C. o. N. A. Research Division, *Gelling Crude Oil to Reduce Marine Pollution from Tanker Oil Spills, Project No. 15080 DJN*, 1971.
116. S. Bhattacharya and Y. Krishnan-Ghosh, *Chem. Commun.*, 2001, 185-186.
117. S. R. Jadhav, P. K. Vemula, R. Kumar, S. R. Raghavan and G. John, *Angew. Chem. Int. Ed.*, 2010, **49**, 7695-7698.
118. S. Basak, J. Nanda and A. Banerjee, *J. Mater. Chem.*, 2012, **22**, 11658-11664.
119. A. Prathap and K. M. Sureshan, *Chem. Commun.*, 2012, **48**, 5250-5252.

120. M. Suzuki, Y. Nakajima, M. Yumoto, M. Kimura, H. Shirai and K. Hanabusa, *Org. Biomol. Chem.*, 2004, **2**, 1155-1159.
121. M. Suzuki, H. Saito, H. Shirai and K. Hanabusa, *New. J. Chem.*, 2007, **31**, 1654-1660.
122. D. R. Trivedi and P. Dastidar, *Chem. Mater.*, 2006, **18**, 1470-1478.
123. U. K. Das, D. R. Trivedi, N. N. Adarsh and P. Dastidar, *J. Org. Chem.*, 2009, **74**, 7111-7121.
124. H. Cao, P. Duan, X. Zhu, J. Jiang and M. Liu, *Chem. Eur. J.*, 2012, **18**, 5546-5550.
125. C. E. Stanley, N. Clarke, K. M. Anderson, J. A. Elder, J. T. Lenthall and J. W. Steed, *Chem. Commun.*, 2006, 3199-3201.
126. X. Yang, G. Zhang and D. Zhang, *J. Mater. Chem.*, 2012, **22**, 38-50.
127. V. Jayawarna, M. Ali, T. A. Jowitt, A. F. Miller, A. Saiani, J. E. Gough and R. V. Ulijn, *Adv. Mater.*, 2006, **18**, 611-614.
128. D. J. Adams, M. F. Butler, W. J. Frith, M. Kirkland, L. Mullen and P. Sanderson, *Soft Matter*, 2009, **5**, 1856-1862.
129. R. V. Ulijn, *J. Mater. Chem.*, 2006, **16**, 2217-2225.
130. Z. Yang, G. Liang and B. Xu, *Acc. Chem. Res.*, 2008, **41**, 315-326.
131. Z. Yang, H. Gu, D. Fu, P. Gao, J. K. Lam and B. Xu, *Adv. Mater.*, 2004, **16**, 1440-1444.
132. Z. Yang and B. Xu, *Chem. Commun.*, 2004, 2424-2425.
133. J. A. Saez, B. Escuder and J. F. Miravet, *Chem. Commun.*, 2010, **46**, 7996-7998.
134. P. Deindorfer, A. Eremin, R. Stannarius, R. Davis and R. Zentel, *Soft Matter*, 2006, **2**, 693-698.
135. S. Matsumoto, S. Yamaguchi, S. Ueno, H. Komatsu, M. Ikeda, K. Ishizuka, Y. Iko, K. V. Tabata, H. Aoki, S. Ito, H. Noji and I. Hamachi, *Chem. Eur. J.*, 2008, **14**, 3977-3986.
136. S. Matsumoto, S. Yamaguchi, A. Wada, T. Matsui, M. Ikeda and I. Hamachi, *Chem. Commun.*, 2008, 1545-1547.
137. K. Murata, M. Aoki, T. Nishi, A. Ikeda and S. Shinkai, *J. Chem. Soc. Chem. Commun.*, 1991, 1715-1718.
138. L. Milanesi, C. A. Hunter, N. Tzokova, J. P. Waltho and S. Tomas, *Chem. Eur. J.*, 2011, **17**, 9753-9761.
139. S. A. Ahmed, X. Sallenave, F. Fages, G. Mieden-Gundert, W. M. Müller, U. Müller, F. Vögtle and J.-L. Pozzo, *Langmuir*, 2002, **18**, 7096-7101.
140. N. M. Sangeetha and U. Maitra, *Chem. Soc. Rev.*, 2005, **34**, 821-836.
141. S. Banerjee, R. K. Das and U. Maitra, *J. Mater. Chem.*, 2009, **19**, 6649-6687.

142. A. R. Hirst, B. Escuder, J. F. Miravet and D. K. Smith, *Angew. Chem. Int. Ed.*, 2008, **47**, 8002-8018.
143. I. W. Hamley, *Angew. Chem. Int. Ed.*, 2003, **42**, 1692-1712.
144. D. D. Diaz, D. Kuhbeck and R. J. Koopmans, *Chem. Soc. Rev.*, 2011, **40**, 427-448.
145. B. Escuder, F. Rodriguez-Llansola and J. F. Miravet, *New. J. Chem.*, 2010, **34**, 1044-1054.
146. F. Rodriguez-Llansola, B. Escuder and J. F. Miravet, *J. Am. Chem. Soc.*, 2009, **131**, 11478-11484.
147. J. F. Miravet and B. Escuder, *Org. Lett.*, 2005, **7**, 4791-4794.
148. F. Rodriguez-Llansola, J. F. Miravet and B. Escuder, *Chem. Commun.*, 2009, 7303-7305.
149. F. Rodriguez-Llansola, B. Escuder and J. F. Miravet, *Org. Biomol. Chem.*, 2009, **7**, 3091-3094.
150. J. D. Hartgerink, *Curr. Opin. Chem. Biol.*, 2004, **8**, 604-609.
151. K. J. C. van Bommel, A. Friggeri and S. Shinkai, *Angew. Chem. Int. Ed.*, 2003, **42**, 980-999.
152. J. R. Moffat, I. A. Coates, F. J. Leng and D. K. Smith, *Langmuir*, 2009, **25**, 8786-8793.
153. C. S. Love, V. Chechik, D. K. Smith, I. Ashworth and C. Brennan, *Chem. Commun.*, 2005, 5647-5649.
154. I. A. Coates and D. K. Smith, *Chem. Eur. J.*, 2009, **15**, 6340-6344.
155. D. D. Diaz, J. J. Cid, P. Vazquez and T. Torres, *Chem. Eur. J.*, 2008, **14**, 9261-9273.
156. D. D. Diaz, K. Rajagopal, E. Strable, J. Schneider and M. G. Finn, *J. Am. Chem. Soc.*, 2006, **128**, 6056-6057.
157. C. Kim, S. J. Lee, I. H. Lee and K. T. Kim, *Chem. Mater.*, 2003, **15**, 3638-3642.
158. M. George and R. G. Weiss, *Chem. Mater.*, 2003, **15**, 2879-2888.
159. L. Hsu, G. L. Cvetanovich and S. I. Stupp, *J. Am. Chem. Soc.*, 2008, **130**, 3892-3899.
160. B. Xu, *Langmuir*, 2009, **25**, 8375-8377.
161. R. V. Ulijn, N. Bibi, V. Jayawarna, P. D. Thornton, S. J. Todd, R. J. Mart, A. M. Smith and J. E. Gough, *Mater. Today*, 2007, **10**, 40-48.
162. S. G. Zhang, *Nat. Biotechnol.*, 2003, **21**, 1171-1178.
163. R. G. Ellis-Behnke, Y. X. Liang, S. W. You, D. K. C. Tay, S. G. Zhang, K. F. So and G. E. Schneider, *Proc. Natl. Acad. Sci. USA* , 2006, **103**, 5054-5059.
164. T. C. Holmes, S. de Lacalle, X. Su, G. S. Liu, A. Rich and S. G. Zhang, *Proc. Natl. Acad. Sci. USA*, 2000, **97**, 6728-6733.

165. Z. M. Yang, G. L. Liang, M. L. Ma, A. S. Abbah, W. W. Lu and B. Xu, *Chem. Commun.*, 2007, 843-845.
166. A. Vintiloiu and J. C. Leroux, *J. Control. Release*, 2008, **125**, 179-192.
167. K. J. C. van Bommel, M. C. A. Stuart, B. L. Feringa and J. van Esch, *Org. Biomol. Chem.*, 2005, **3**, 2917-2920.
168. P. K. Vemula, G. A. Cruikshank, J. M. Karp and G. John, *Biomaterials*, 2009, **30**, 383-393.
169. D. B. Amabilino and J. Puigmarti-Luis, *Soft Matter*, 2010, **6**, 1605-1612.
170. J. Puigmarti-Luis, V. Laukhin, A. P. del Pino, J. Vidal-Gancedo, C. Rovira, E. Laukhina and D. B. Amabilino, *Angew. Chem. Int. Ed.*, 2007, **46**, 238-241.
171. A. Schenning and E. W. Meijer, *Chem. Commun.*, 2005, 3245-3258.
172. S. S. Babu, S. Prasanthkumar and A. Ajayaghosh, *Angew. Chem. Int. Ed.*, 2012, **51**, 1766-1776.
173. L. J. Pan, G. H. Yu, D. Y. Zhai, H. R. Lee, W. T. Zhao, N. Liu, H. L. Wang, B. C. K. Tee, Y. Shi, Y. Cui and Z. N. Bao, *Proc. Natl. Acad. Sci. USA* , 2012, **109**, 9287-9292.
174. W. S. Li, M. J. Teng, X. R. Jia and Y. Wei, *Tetrahedron Lett.*, 2010, **51**, 5336-5340.
175. J. Chen, W. W. Wu and A. J. McNeil, *Chem. Commun.*, 2012, **48**, 7310-7312.
176. F. Rodriguez-Llansola, J. F. Miravet and B. Escuder, *Chem. Commun.*, 2011, **47**, 4706-4708.
177. G. John, S. R. Jadhav, V. M. Menon and V. T. John, *Angew. Chem. Int. Ed.*, 2012, **51**, 1760-1762.
178. L. E. Buerkle and S. J. Rowan, *Chem. Soc. Rev.*, 2012, **41**, 6089-6102.
179. A. R. Hirst and D. K. Smith, *Chem. Eur. J.*, 2005, **11**, 5496-5508.
180. K. Hanabusa, T. Miki, Y. Taguchi, T. Koyama and H. Shirai, *J. Chem. Soc. Chem. Comm.*, 1993, 1382-1384.
181. S. Yagai, M. Higashi, T. Karatsu and A. Kitamura, *Chem. Mater.*, 2004, **16**, 3582-3585.
182. S. Manna, A. Saha and A. K. Nandi, *Chem. Commun.*, 2006, 4285-4287.
183. A. Saha, S. Manna and A. K. Nandi, *Langmuir*, 2007, **23**, 13126-13135.
184. S. W. Jeong and S. Shinkai, *Nanotechnology*, 1997, **8**, 179-185.
185. K. Inoue, Y. Ono, Y. Kanekiyo, T. Ishi-i, K. Yoshihara and S. Shinkai, *J. Org. Chem.*, 1999, **64**, 2933-2937.
186. H. Basit, A. Pal, S. Sen and S. Bhattacharya, *Chem. Eur. J.*, 2008, **14**, 6534-6545.
187. A. Pal, H. Basit, S. Sen, V. K. Aswal and S. Bhattacharya, *J. Mater. Chem.*, 2009, **19**, 4325-4334.
188. M. Suzuki, H. Saito and K. Hanabusa, *Langmuir*, 2009, **25**, 8579-8585.

189. A. Ballabh, D. R. Trivedi and P. Dastidar, *Chem. Mater.*, 2003, **15**, 2136-2140.
190. D. R. Trivedi, A. Ballabh and P. Dastidar, *Chem Mater*, 2003, **15**, 3971-3973.
191. H. Y. Lee, S. R. Nam and J. I. Hong, *J. Am. Chem. Soc.*, 2007, **129**, 1040-1041.
192. S. R. Nam, H. Y. Lee and J. I. Hong, *Tetrahedron*, 2008, **64**, 10531-10537.
193. M. Ayabe, T. Kishida, N. Fujita, K. Sada and S. Shinkai, *Org. Biomol. Chem.*, 2003, **1**, 2744-2747.
194. J. G. Hardy, A. R. Hirst and D. K. Smith, *Soft Matter*, 2012, **8**, 3399-3406.
195. J. G. Hardy, A. R. Hirst, D. K. Smith, C. Brennan and I. Ashworth, *Chem. Commun.*, 2005, 385-387.
196. K. S. Partridge, D. K. Smith, G. M. Dykes and P. T. McGrail, *Chem. Commun.*, 2001, 319-320.
197. A. R. Hirst, D. K. Smith and J. P. Harrington, *Chem. Eur. J.*, 2005, **11**, 6552-6559.
198. A. R. Hirst, D. K. Smith, M. C. Feiters, H. P. M. Geurts and A. C. Wright, *J. Am. Chem. Soc.*, 2003, **125**, 9010-9011.
199. A. R. Hirst, D. K. Smith, M. C. Feiters and H. P. M. Geurts, *Langmuir*, 2004, **20**, 7070-7077.
200. A. R. Hirst and D. K. Smith, *Org. Biomol. Chem.*, 2004, **2**, 2965-2971.
201. B. Q. Huang, A. R. Hirst, D. K. Smith, V. Castelletto and I. W. Hamley, *J. Am. Chem. Soc.*, 2005, **127**, 7130-7139.
202. T. Ishi-i, R. Iguchi, E. Snip, M. Ikeda and S. Shinkai, *Langmuir*, 2001, **17**, 5825-5833.
203. D. Rizkov, J. Gun, O. Lev, R. Sicsic and A. Melman, *Langmuir*, 2005, **21**, 12130-12138.
204. T. M. Shu, J. C. Wu, M. Lu, L. Q. Chen, T. Yi, F. Y. Li and C. H. Huang, *J. Mater. Chem.*, 2008, **18**, 886-893.
205. K. V. Rao, K. Jayaramulu, T. K. Maji and S. J. George, *Angew. Chem. Int. Ed.*, 2010, **49**, 4218-4222.
206. P. Bairi, B. Roy, P. Routh, K. Sen and A. K. Nandi, *Soft Matter*, 2012, **8**, 7436-7445.
207. Y. L. Liu, Y. Yu, J. A. Gao, Z. Q. Wang and X. Zhang, *Angew. Chem. Int. Ed.*, 2010, **49**, 6576-6579.
208. B. G. Bag, G. C. Maity and S. K. Dinda, *Org. Lett.*, 2006, **8**, 5457-5460.
209. U. Maitra, P. V. Kumar, N. Chandra, L. J. D'Souza, M. D. Prasanna and A. R. Raju, *Chem. Commun.*, 1999, 595-596.
210. P. Babu, N. M. Sangeetha, P. Vijaykumar, U. Maitra, K. Rissanen and A. R. Raju, *Chem. Eur. J.*, 2003, **9**, 1922-1932.
211. Y. Wang, L. Tang and J. Yu, *Cryst. Growth Des.*, 2008, **8**, 884-889.

212. B. A. Simmons, C. E. Taylor, F. A. Landis, V. T. John, G. L. McPherson, D. K. Schwartz and R. Moore, *J. Am. Chem. Soc.*, 2001, **123**, 2414-2421.

213. M. Tata, V. T. John, Y. Y. Waguespack and G. L. McPherson, *J. Am. Chem. Soc.*, 1994, **116**, 9464-9470.

214. M. Tata, V. T. John, Y. Y. Waguespack and G. L. McPherson, *J Phys. Chem. US*, 1994, **98**, 3809-3817.

215. X. D. Xu, M. Ayyagari, M. Tata, V. T. John and G. L. McPherson, *J. Phys. Chem. US*, 1993, **97**, 11350-11353.

216. S. H. Tung, Y. E. Huang and S. R. Raghavan, *Soft Matter*, 2008, **4**, 1086-1093.

217. T. Taira, Y. Suzaki and K. Osakada, *Chem. Eur. J.*, 2010, **16**, 6518-6529.

218. H. Danjo, K. Hirata, S. Yoshigai, I. Azumaya and K. Yamaguchi, *J. Am. Chem. Soc.*, 2009, **131**, 1638-1639.

219. M. O. M. Piepenbrock, G. O. Lloyd, N. Clarke and J. W. Steed, *Chem. Rev.*, 2010, **110**, 1960-2004.

220. A. Y. Y. Tam and V. W. W. Yam, *Chem. Soc. Rev.*, 2013, **42**, 1540-1567.

221. T. Vermonden, W. M. de Vos, A. T. M. Marcelis and E. J. R. Sudholter, *Eur. J. Inorg. Chem.*, 2004, 2847-2852.

222. T. Vermonden, M. J. van Steenbergen, N. A. M. Besseling, A. T. M. Marcelis, W. E. Hennink, E. J. R. Sudholter and M. A. C. Stuart, *J. Am. Chem. Soc.*, 2004, **126**, 15802-15808.

223. W. G. Weng, J. B. Beck, A. M. Jamieson and S. J. Rowan, *J. Am. Chem. Soc.*, 2006, **128**, 11663-11672.

224. J. B. Beck and S. J. Rowan, *J. Am. Chem. Soc.*, 2003, **125**, 13922-13923.

225. J. Gao, H. M. Wang, L. Wang, J. Y. Wang, D. L. Kong and Z. M. Yang, *J. Am. Chem. Soc.*, 2009, **131**, 11286-11287.

226. C. B. Minkenberg, W. E. Hendriksen, F. Li, E. Mendes, R. Eelkema and J. H. van Esch, *Chem. Commun.*, 2012, **48**, 9837-9839.

227. Q. Wang, J. L. Mynar, M. Yoshida, E. Lee, M. Lee, K. Okuro, K. Kinbara and T. Aida, *Nature*, 2010, **463**, 339-343.

228. P. T. Corbett, J. Leclaire, L. Vial, K. R. West, J. L. Wietor, J. K. M. Sanders and S. Otto, *Chem. Rev.*, 2006, **106**, 3652-3711.

229. E. Moulin, G. Cormos and N. Giuseppone, *Chem. Soc. Rev.*, 2012, **41**, 1031-1049.

230. R. A. R. Hunta and S. Otto, *Chem. Commun.*, 2011, **47**, 847-858.

231. R. Nguyen, L. Allouche, E. Buhler and N. Giuseppone, *Angew. Chem. Int. Ed.*, 2009, **48**, 1093-1096.
232. R. Nguyen, E. Buhler and N. Giuseppone, *Macromolecules*, 2009, **42**, 5913-5915.
233. J. Leclaire, G. Husson, N. Devaux, V. Delorme, L. Charles, F. Ziarelli, P. Desbois, A. Chaumonnot, M. Jacquin, F. Fotiadu and G. Buono, *J. Am. Chem. Soc.*, 2010, **132**, 3582-3593.
234. J. F. Folmer-Andersen and J. M. Lehn, *Angew. Chem. Int. Ed.*, 2009, **48**, 7664-7667.
235. N. Giuseppone, G. Fuks and J. M. Lehn, *Chem. Eur. J.*, 2006, **12**, 1723-1735.
236. N. Giuseppone and J. M. Lehn, *J. Am. Chem. Soc.*, 2004, **126**, 11448-11449.
237. L. L. Lao, J. L. Schmitt and J. M. Lehn, *Chem. Eur. J.*, 2010, **16**, 4903-4910.
238. N. Sreenivasachary and J. M. Lehn, *Proc. Natl. Acad. Sci. USA* , 2005, **102**, 5938-5943.
239. E. Buhler, N. Sreenivasachary, S. J. Candau and J. M. Lehn, *J. Am. Chem. Soc.*, 2007, **129**, 10058-10059.
240. G. T. Wang, J. B. Lin, X. K. Jiang and Z. T. Li, *Langmuir*, 2009, **25**, 8414-8418.
241. R. J. Williams, A. M. Smith, R. Collins, N. Hodson, A. K. Das and R. V. Ulijn, *Nat. Nanotechnol.*, 2009, **4**, 19-24.
242. A. K. Das, A. R. Hirst and R. V. Ulijn, *Faraday Discuss.*, 2009, **143**, 293-303.
243. A. R. Hirst, J. E. Miravet, B. Escuder, L. Noirez, V. Castelletto, I. W. Hamley and D. K. Smith, *Chem. Eur. J.*, 2009, **15**, 372-379.
244. M. M. Smith, W. Edwards and D. K. Smith, *Chem. Sci.*, 2013, **4**, 671-676.
245. M. J. Mayoral, C. Rest, J. Schellheimer, V. Stepanenko and G. Fernandez, *Chem. Eur. J.*, 2012, **18**, 15607-15611.
246. P. N. Taylor and H. L. Anderson, *J. Am. Chem. Soc.*, 1999, **121**, 11538-11545.
247. A. Friggeri, O. Gronwald, K. J. C. van Bommel, S. Shinkai and D. N. Reinhoudt, *J. Am. Chem. Soc.*, 2002, **124**, 10754-10758.
248. R. Luboradzki and Z. Pakulski, *Supramol. Chem.*, 2009, **21**, 379-383.
249. B. Escuder, S. Marti and J. F. Miravet, *Langmuir*, 2005, **21**, 6776-6787.
250. S. Khanna, M. K. Khan and P. Sundararajan, *Langmuir*, 2009, **25**, 13183-13193.
251. M. Suzuki, M. Yumoto, H. Shirai and K. Hanabusa, *Chem. Eur. J.*, 2008, **14**, 2133-2144.
252. L. Bouteiller, O. Colombani, F. Lortie and P. Terech, *J. Am. Chem. Soc.*, 2005, **127**, 8893-8898.
253. B. Isare, L. Bouteiller, G. Ducouret and F. Lequeux, *Supramol. Chem.*, 2009, **21**, 416-421.
254. H. A. Behanna, K. Rajangam and S. I. Stupp, *J. Am. Chem. Soc.*, 2007, **129**, 321-327.

255. D. M. Ryan, T. M. Doran and B. L. Nilsson, *Chem. Commun.*, 2011, **47**, 475-477.
256. S. Banerjee, R. K. Das, P. Terech, A. de Geyer, C. Aymonier, A. Loppinet-Serani, G. Raffy, U. Maitra, A. Del Guerzo and J.-P. Desvergne, *J. Mat. Chem. C*, 2013.
257. S. L. Zhou, S. Matsumoto, H. D. Tian, H. Yamane, A. Ojida, S. Kiyonaka and I. Hamachi, *Chem. Eur. J.*, 2005, **11**, 1130-1136.
258. M. Ikeda, Y. Shimizu, S. Matsumoto, H. Komatsu, S. Tamaru, T. Takigawa and I. Hamachi, *Macromol. Biosci.*, 2008, **8**, 1019-1025.
259. D. D. Diaz, E. Morin, E. M. Schon, G. Budin, A. Wagner and J. S. Remy, *J. Mater. Chem.*, 2011, **21**, 641-644.
260. B. Bilgicer, X. Xing and K. Kumar, *J. Am. Chem. Soc.*, 2001, **123**, 11815-11816.
261. R. Kramer, J. M. Lehn and A. Marquisrigault, *Proc. Natl. Acad. Sci. USA* , 1993, **90**, 5394-5398.
262. S. J. Rowan, D. G. Hamilton, P. A. Brady and J. K. M. Sanders, *J. Am. Chem. Soc.*, 1997, **119**, 2578-2579.
263. A. X. Wu and L. Isaacs, *J. Am. Chem. Soc.*, 2003, **125**, 4831-4835.
264. N. A. Schnarr and A. J. Kennan, *J. Am. Chem. Soc.*, 2003, **125**, 667-671.
265. I. W. Hwang, T. Kamada, T. K. Ahn, D. M. Ko, T. Nakamura, A. Tsuda, A. Osuka and D. Kim, *J. Am. Chem. Soc.*, 2004, **126**, 16187-16198.
266. A. R. Hirst, B. Q. Huang, V. Castelletto, I. W. Hamley and D. K. Smith, *Chem. Eur. J.*, 2007, **13**, 2180-2188.
267. J. R. Moffat and D. K. Smith, *Chem. Commun.*, 2009, 316-318.
268. M. M. Smith and D. K. Smith, *Soft Matter*, 2011, **7**, 4856-4860.
269. K. Sugiyasu, S. I. Kawano, N. Fujita and S. Shinkai, *Chem. Mater.*, 2008, **20**, 2863-2865.
270. A. Das and S. Ghosh, *Chem. Commun.*, 2011, **47**, 8922-8924.
271. K. L. Morris, L. Chen, J. Raeburn, O. R. Sellick, P. Cotanda, A. Paul, P. C. Griffiths, S. M. King, R. K. O'Reilly, L. C. Serpell and D. J. Adams, *Nat. Commun.*, 2013, **4**, 1480.
272. D. G. Velazquez and R. Luque, *Chem. Eur. J.*, 2011, **17**, 3847-3849.
273. A. Brizard, M. Stuart, K. van Bommel, A. Friggeri, M. de Jong and J. van Esch, *Angew. Chem. Int. Ed.*, 2008, **47**, 2063-2066.
274. X. Y. Liu, P. D. Sawant, W. B. Tan, I. B. M. Noor, C. Pramesti and B. H. Chen, *J. Am. Chem. Soc.*, 2002, **124**, 15055-15063.
275. J. L. Li, X. Y. Liu, C. S. Strom and J. Y. Xiong, *Adv. Mater.*, 2006, **18**, 2574-2578.
276. S. K. Tang, X. Y. Liu and C. S. Strom, *Adv. Funct. Mater.*, 2009, **19**, 2252-2259.
277. L. E. Buerkle, R. Galleguillos and S. J. Rowan, *Soft Matter*, 2011, **7**, 6984-6990.

278. G. A. Hembury, V. V. Borovkov and Y. Inoue, *Chem. Rev.*, 2008, **108**, 1-73.

279. J. Cornelissen, A. E. Rowan, R. J. M. Nolte and N. Sommerdijk, *Chem. Rev.*, 2001, **101**, 4039-4070.

280. P. Cintas, *Angew. Chem. Int. Ed.*, 2002, **41**, 1139-1145.

281. D. G. Blackmond and M. Klussmann, *Chem. Commun.*, 2007, 3990-3996.

282. D. K. Smith, *Chem. Soc. Rev.*, 2009, **38**, 684-694.

283. M. M. Green, M. P. Reidy, R. J. Johnson, G. Darling, D. J. Oleary and G. Willson, *J. Am. Chem. Soc.*, 1989, **111**, 6452-6454.

284. A. J. Bur and L. J. Fetters, *Chem. Rev.*, 1976, **76**, 727-746.

285. M. M. Green, B. A. Garetz, B. Munoz, H. P. Chang, S. Hoke and R. G. Cooks, *J. Am. Chem. Soc.*, 1995, **117**, 4181-4182.

286. S. K. Jha, K. S. Cheon, M. M. Green and J. V. Selinger, *J. Am. Chem. Soc.*, 1999, **121**, 1665-1673.

287. M. M. Green, N. C. Peterson, T. Sato, A. Teramoto, R. Cook and S. Lifson, *Science*, 1995, **268**, 1860-1866.

288. K. Tang, M. M. Green, K. S. Cheon, J. V. Selinger and B. A. Garetz, *J. Am. Chem. Soc.*, 2003, **125**, 7313-7323.

289. C. C. Lee, C. Grenier, E. W. Meijer and A. Schenning, *Chem. Soc. Rev.*, 2009, **38**, 671-683.

290. A. R. A. Palmans and E. W. Meijer, *Angew. Chem. Int. Ed.*, 2007, **46**, 8948-8968.

291. A. R. A. Palmans, J. A. J. M. Vekemans, E. E. Havinga and E. W. Meijer, *Angew. Chem. Int. Ed.*, 1997, **36**, 2648-2651.

292. M. M. J. Smulders, A. Schenning and E. W. Meijer, *J. Am. Chem. Soc.*, 2008, **130**, 606-611.

293. A. Schenning, A. F. M. Kilbinger, F. Biscarini, M. Cavallini, H. J. Cooper, P. J. Derrick, W. J. Feast, R. Lazzaroni, P. Leclere, L. A. McDonell, E. W. Meijer and S. C. J. Meskers, *J. Am. Chem. Soc.*, 2002, **124**, 1269-1275.

294. L. Brunsveld, B. G. G. Lohmeijer, J. Vekemans and E. W. Meijer, *Chem. Commun.*, 2000, 2305-2306.

295. L. Brunsveld, J. Vekemans, J. Hirschberg, R. P. Sijbesma and E. W. Meijer, *Proc. Natl. Acad. Sci. USA*, 2002, **99**, 4977-4982.

296. J. van Gestel, A. R. A. Palmans, B. Titulaer, J. A. J. M. Vekemans and E. W. Meijer, *J. Am. Chem. Soc.*, 2005, **127**, 5490-5494.

297. A. J. Wilson, J. van Gestel, R. P. Sijbesma and E. W. Meijer, *Chem. Commun.*, 2006, 4404-4406.

298. M. M. J. Smulders, I. A. W. Filot, J. M. A. Leenders, P. van der Schoot, A. R. A. Palmans, A. Schenning and E. W. Meijer, *J. Am. Chem. Soc.*, 2010, **132**, 611-619.

299. P. J. M. Stals, J. C. Everts, R. de Bruijn, I. A. W. Filot, M. M. J. Smulders, R. Martin-Rapun, E. A. Pidko, T. F. A. de Greef, A. R. A. Palmans and E. W. Meijer, *Chem. Eur. J.*, 2010, **16**, 810-821.

300. S. J. George, Z. Tomovic, M. M. J. Smulders, T. F. A. de Greef, P. Leclere, E. W. Meijer and A. Schenning, *Angew. Chem. Int. Ed.*, 2007, **46**, 8206-8211.

301. S. Cantekin, H. M. M. ten Eikelder, A. J. Markvoort, M. A. J. Veld, P. A. Korevaar, M. M. Green, A. R. A. Palmans and E. W. Meijer, *Angew. Chem. Int. Ed.*, 2012, **51**, 6426-6431.

302. S. Cantekin, D. W. R. Balkenende, M. M. J. Smulders, A. R. A. Palmans and E. W. Meijer, *Nat. Chem.*, 2011, **3**, 42-46.

303. F. Helmich, M. M. J. Smulders, C. C. Lee, A. Schenning and E. W. Meijer, *J. Am. Chem. Soc.*, 2011, **133**, 12238-12246.

304. F. Helmich, C. C. Lee, A. Schenning and E. W. Meijer, *J. Am. Chem. Soc.*, 2010, **132**, 16753-16755.

305. J. van Gestel, P. van der Schoot and M. A. J. Michels, *Macromolecules*, 2003, **36**, 6668-6673.

306. J. van Gestel, P. van der Schoot and M. A. J. Michels, *J. Chem. Phys.*, 2004, **120**, 8253-8261.

307. J. van Gestel, *J. Phys. Chem. B*, 2006, **110**, 4365-4370.

308. F. Garcia, J. Buendia and L. Sanchez, *J. Org. Chem.*, 2011, **76**, 6271-6276.

309. T. E. Kaiser, V. Stepanenko and F. Wurthner, *J. Am. Chem. Soc.*, 2009, **131**, 6719-6732.

310. A. Lohr and F. Wurthner, *Chem. Commun.*, 2008, 2227-2229.

311. A. L. Nussbaumer, D. Studer, V. L. Malinovskii and R. Haner, *Angew. Chem. Int. Ed.*, 2011, **50**, 5490-5494.

312. H. M. M. ten Eikelder, A. J. Markvoort, T. F. A. de Greef and P. A. J. Hilbers, *J. Phys. Chem. B*, 2012, **116**, 5291-5301.

313. A. Lohr and F. Wurthner, *Angew. Chem. Int. Ed.*, 2008, **47**, 1232-1236.

314. T. Ishi-i, M. Crego-Calama, P. Timmerman, D. N. Reinhoudt and S. Shinkai, *J. Am. Chem. Soc.*, 2002, **124**, 14631-14641.

315. L. J. Prins, P. Timmerman and D. N. Reinhoudt, *J. Am. Chem. Soc.*, 2001, **123**, 10153-10163.

316. M. A. Mateos-Timoneda, M. Crego-Calama and D. N. Reinhoudt, *Chem. Eur. J.*, 2006, **12**, 2630-2638.
317. H. Fenniri, B.-L. Deng and A. E. Ribbe, *J. Am. Chem. Soc.*, 2002, **124**, 11064-11072.
318. Tachiban.T and H. Kambara, *J. Am. Chem. Soc.*, 1965, **87**, 3015-3016.
319. A. Pal, T. Patra and J. Dey, *Chem. Phys. Lett.*, 2013, **556**, 245-250.
320. S. Bhattacharya, S. N. G. Acharya and A. R. Raju, *Chem. Commun.*, 1996, 2101-2102.
321. K. Hanabusa, M. Yamada, M. Kimura and H. Shirai, *Angew. Chem. Int. Ed. Engl.*, 1996, **35**, 1949-1951.
322. K. Hanabusa, K. Okui, K. Karaki, M. Kimura and H. Shirai, *J. Colloid Interf. Sci.*, 1997, **195**, 86-93.
323. K. Hanabusa, H. Kobayashi, M. Suzuki, M. Kimura and H. Shirai, *Colloid Polym. Sci.*, 1998, **276**, 252-259.
324. X. Luo, B. Liu and Y. Liang, *Chem. Commun.*, 2001, 1556-1557.
325. J. U. Kim, D. Schollmeyer, M. Brehmer and R. Zentel, *J. Colloid Interf. Sci.*, 2011, **357**, 428-433.
326. A. R. Hirst, D. K. Smith, M. C. Feiters and H. P. M. Geurts, *Chem. Eur. J.*, 2004, **10**, 5901-5910.
327. L. Frkanec and M. Zinic, *Chem. Commun.*, 2010, **46**, 522-537.
328. J. Makarevic, M. Jokic, Z. Raza, Z. Stefanic, B. Kojic-Prodic and M. Zinic, *Chem. Eur. J.*, 2003, **9**, 5567-5580.
329. V. Caplar, L. Frkanec, N. S. Vujicic and M. Zinic, *Chem. Eur. J.*, 2010, **16**, 3066-3082.
330. V. Caplar, M. Zinic, J. L. Pozzo, F. Fages, G. Mieden-Gundert and F. Vogtle, *Eur. J. Org. Chem.*, 2004, 4048-4059.
331. Z. Dzolic, K. Wolsperger and M. Zinic, *New. J. Chem.*, 2006, **30**, 1411-1419.
332. A. Friggeri, C. van der pol, K. J. C. van Bommel, A. Heeres, M. C. A. Stuart, B. L. Feringa and J. van Esch, *Chem. Eur. J.*, 2005, **11**, 5353-5361.
333. K. J. Nagy, M. C. Giano, A. Jin, D. J. Pochan and J. P. Schneider, *J. Am. Chem. Soc.*, 2011, **133**, 14975-14977.
334. P. Iavicoli, H. Xu, L. N. Feldborg, M. Linares, M. Paradinas, S. Stafstrom, C. Ocal, B. L. Nieto-Ortega, J. Casado, J. T. L. Navarrete, R. Lazzaroni, S. De Feyter and D. B. Amabilino, *J. Am. Chem. Soc.*, 2010, **132**, 9350-9362.
335. T. Ishi-i, R. Kuwahara, A. Takata, Y. Jeong, K. Sakurai and S. Mataka, *Chem. Eur. J.*, 2006, **12**, 763-776.

336. K. Sada, M. Takeuchi, N. Fujita, M. Numata and S. Shinkai, *Chem. Soc. Rev.*, 2007, **36**, 415-435.

337. M. Tanaka, T. Ikeda, J. Mack, N. Kobayashi and T. Haino, *J. Org. Chem.*, 2011, **76**, 5082-5091.

338. W. Jin, T. Fukushima, M. Niki, A. Kosaka, N. Ishii and T. Aida, *Proc. Natl. Acad. Sci. USA* , 2005, **102**, 10801-10806.

339. T. Seki, A. Asano, S. Seki, Y. Kikkawa, H. Murayama, T. Karatsu, A. Kitamura and S. Yagai, *Chem. Eur. J.*, 2011, **17**, 3598-3608.

340. R. K. Das, R. Kandanelli, J. Linnanto, K. Bose and U. Maitra, *Langmuir*, 2010, **26**, 16141-16149.

341. C. H. Li, K. C. Chang, C. C. Tsou, Y. K. Lan, H. C. Yang and S. S. Sun, *J. Org. Chem.*, 2011, **76**, 5524-5530.

342. A. Ajayaghosh, R. Varghese, S. Mahesh and V. K. Praveen, *Angew. Chem. Int. Ed.*, 2006, **45**, 7729-7732.

343. A. Ajayaghosh, R. Varghese, S. J. George and C. Vijayakumar, *Angew. Chem. Int. Ed.*, 2006, **45**, 1141-1144.

344. W. Cai, G. T. Wang, P. Du, R. X. Wang, X. K. Jiang and Z. T. Li, *J. Am. Chem. Soc.*, 2008, **130**, 13450-13459.

345. A. A. Sobczuk, Y. Tsuchiya, T. Shiraki, S. Tamaru and S. Shinkai, *Chem. Eur. J.*, 2012, **18**, 2832-2838.

346. X. F. Wang, P. F. Duan and M. H. Liu, *Chem. Commun.*, 2012, **48**, 7501-7503.

347. H. Ihara, T. Sakurai, T. Yamada, T. Hashimoto, M. Takafuji, T. Sagawa and H. Hachisako, *Langmuir*, 2002, **18**, 7120-7123.

348. X. F. Zhu, P. F. Duan, L. Zhang and M. H. Liu, *Chem. Eur. J.*, 2011, **17**, 3429-3437.

349. B. W. Messmore, P. A. Sukerkar and S. I. Stupp, *J. Am. Chem. Soc.*, 2005, **127**, 7992-7993.

350. B. Adhikari, J. Nanda and A. Banerjee, *Soft Matter*, 2011, **7**, 8913-8922.

351. S. Cicchi, G. Ghini, L. Lascialfari, A. Brandi, F. Betti, D. Berti, P. Baglioni, L. Di Bari, G. Pescitelli, M. Mannini and A. Caneschi, *Soft Matter*, 2010, **6**, 1655-1661.

352. T. Tu, W. W. Fang, X. L. Bao, X. B. Li and K. H. Dotz, *Angew. Chem. Int. Ed.*, 2011, **50**, 6601-6605.

353. X. Chen, Z. Huang, S. Y. Chen, K. Li, X. Q. Yu and L. Pu, *J. Am. Chem. Soc.*, 2010, **132**, 7297-7299.

354. Y. Zhang, H. W. Gu, Z. M. Yang and B. Xu, *J. Am. Chem. Soc.*, 2003, **125**, 13680-13681.

355. Q. X. Jin, L. Zhang, X. F. Zhu, P. F. Duan and M. H. Liu, *Chem. Eur. J.*, 2012, **18**, 4916-4922.

356. J. J. D. de Jong, L. N. Lucas, R. M. Kellogg, J. H. van Esch and B. L. Feringa, *Science*, 2004, **304**, 278-281.

357. J. J. D. de Jong, T. D. Tiemersma-Wegman, J. H. van Esch and B. L. Feringa, *J. Am. Chem. Soc.*, 2005, **127**, 13804-13805.

358. A. Dawn, N. Fujita, S. Haraguchi, K. Sada, S. Tamaru and S. Shinkai, *Org. Biomol. Chem.*, 2009, **7**, 4378-4385.

359. A. Dawn, T. Shiraki, S. Haraguchi, H. Sato, K. Sada and S. Shinkai, *Chem. Eur. J.*, 2010, **16**, 3676-3689.

360. R. Iwaura and T. Shimizu, *Angew. Chem. Int. Ed.*, 2006, **45**, 4601-4604.

361. K. Okano, M. Taguchi, M. Fujiki and T. Yamashita, *Angew. Chem. Int. Ed.*, 2011, **50**, 12474-12477.

362. K. Okano, O. Arteaga, J. M. Ribo and T. Yamashita, *Chem. Eur. J.*, 2011, **17**, 9288-9292.

363. H. Unsal and N. Aydogan, *J. Colloid Interf. Sci.*, 2013, **394**, 301-311.

364. S. T. Wu, Y. R. Wu, Q. Q. Kang, H. Zhang, L. S. Long, Z. P. Zheng, R. B. Huang and L. S. Zheng, *Angew. Chem. Int. Ed.*, 2007, **46**, 8475-8479.

365. J. Yuan and M. H. Liu, *J. Am. Chem. Soc.*, 2003, **125**, 5051-5056.

366. U. DeRossi, S. Dahne, S. C. J. Meskers and H. Dekkers, *Angew. Chem. Int. Ed. Engl.*, 1996, **35**, 760-763.

367. S. Y. Zhang, S. Y. Yang, J. B. Lan, S. J. Yang and J. S. You, *Chem. Commun.*, 2008, 6170-6172.

368. T. Ezuhara, K. Endo and Y. Aoyama, *J. Am. Chem. Soc.*, 1999, **121**, 3279-3283.

369. S. Azeroual, J. Surprenant, T. D. Lazzara, M. Kocun, Y. Tao, L. A. Cuccia and J. M. Lehn, *Chem. Commun.*, 2012, **48**, 2292-2294.

370. J. M. Ribo, J. Crusats, F. Sagues, J. Claret and R. Rubires, *Science*, 2001, **292**, 2063-2066.

371. B. Bosnich, *J. Am. Chem. Soc.*, 1967, **89**, 6143-6148.

372. M. M. Green, C. Khatri and N. C. Peterson, *J. Am. Chem. Soc.*, 1993, **115**, 4941-4942.

373. C. A. Khatri, Y. Pavlova, M. M. Green and H. Morawetz, *J. Am. Chem. Soc.*, 1997, **119**, 6991-6995.

374. A. R. A. Palmans, J. Vekemans, E. E. Havinga and E. W. Meijer, *Angew. Chem. Int. Ed.*, 1997, **36**, 2648-2651.

375. S. J. George, Z. Tomovic, A. Schenning and E. W. Meijer, *Chem. Commun.*, 2011, **47**, 3451-3453.

376. M. Wolffs, J. L. J. van Velthoven, X. W. Lou, R. A. A. Bovee, M. Pouderoijen, J. L. J. van Dongen, A. Schenning and E. W. Meijer, *Chem. Eur. J.*, 2012, **18**, 15057-15064.
377. H. von Berlepsch, S. Kirstein and C. Bottcher, *J. Phys. Chem. B*, 2003, **107**, 9646-9654.
378. B. Isare, M. Linares, L. Zargarian, S. Fermandjian, M. Miura, S. Motohashi, N. Vanthuyne, R. Lazzaroni and L. Bouteiller, *Chem. Eur. J.*, 2010, **16**, 173-177.
379. Y. Kawagoe, M. Fujiki and Y. Nakano, *New. J. Chem.*, 2010, **34**, 637-647.
380. M. Mukai, H. Minamikawa, M. Aoyagi, M. Asakawa, T. Shimizu and M. Kogiso, *Soft Matter*, 2012, **8**, 11979-11981.
381. S. Ghosh, X. Q. Li, V. Stepanenko and F. Würthner, *Chem. Eur. J.*, 2008, **14**, 11343-11357.
382. S. I. Kawano, N. Fujita, K. J. C. van Bommel and S. Shinkai, *Chem. Lett.*, 2003, **32**, 12-13.
383. H. J. Kim, J. H. Lee and M. Lee, *Angew. Chem. Int. Ed.*, 2005, **44**, 5810-5814.
384. H. J. Kim, W. C. Zin and M. Lee, *J. Am. Chem. Soc.*, 2004, **126**, 7009-7014.
385. Y. B. He, Z. Bian, C. Q. Kang and L. X. Gao, *Chem. Commun.*, 2010, **46**, 5695-5697.
386. Y. B. He, Z. Bian, C. Q. Kang and L. X. Gao, *Chem. Commun.*, 2011, **47**, 1589-1591.
387. A. Westcott, C. J. Sumby, R. D. Walshaw and M. J. Hardie, *New. J. Chem.*, 2009, **33**, 902-912.
388. L. Applegarth, N. Clark, A. C. Richardson, A. D. M. Parker, I. Radosavljevic-Evans, A. E. Goeta, J. A. K. Howard and J. W. Steed, *Chem. Commun.*, 2005, 5423-5425.
389. M. O. M. Piepenbrock, N. Clarke and J. W. Steed, *Soft Matter*, 2011, **7**, 2412-2418.
390. S. Dutta, A. Shome, S. Debnath and P. K. Das, *Soft Matter*, 2009, **5**, 1607-1620.
391. J. Seo, J. W. Chung, I. Cho and S. Y. Park, *Soft Matter*, 2012, **8**, 7617-7622.
392. J. S. Shen, D. H. Li, Q. G. Cai and Y. B. Jiang, *J. Mater. Chem.*, 2009, **19**, 6219-6224.
393. P. Bairi, B. Roy and A. K. Nandi, *J. Mater. Chem.*, 2011, **21**, 11747-11749.
394. K. Chen, L. M. Tang, Y. Xia and Y. J. Wang, *Langmuir*, 2008, **24**, 13838-13841.
395. Q. T. Liu, Y. L. Wang, W. Li and L. X. Wu, *Langmuir*, 2007, **23**, 8217-8223.
396. W. Deng and D. H. Thompson, *Soft Matter*, 2010, **6**, 1884-1887.
397. A. N. Khlobystov, A. J. Blake, N. R. Champness, D. A. Lemenovskii, A. G. Majouga, N. V. Zyk and M. Schroder, *Coordin. Chem. Rev.*, 2001, **222**, 155-192.
398. M. J. Manard, P. R. Kemper and M. T. Bowers, *Int. J. Mass Spectrom.*, 2005, **241**, 109-117.
399. Beverwij.Cd, Vanderke.Gj, A. J. Leusink and J. G. Noltes, *Organomet. Chem. Rev. A*, 1970, **5**, 215-280.
400. S. Winstein and H. J. Lucas, *J. Am. Chem. Soc.*, 1938, **60**, 836-847.

401. C. M. Williams and L. N. Mander, *Tetrahedron*, 2001, **57**, 425-447.
402. T. J. Wenzel and R. E. Sievers, *Anal. Chem.*, 1981, **53**, 393-399.
403. T. J. Wenzel and R. E. Sievers, *J. Am. Chem. Soc.*, 1982, **104**, 382-388.
404. J. D. C. M. van Dongen and C. D. M. Beverwijk, *J. Organomet. Chem.*, 1973, **51**, C36-C38.
405. C. D.M. Beverwijk and J. P. C. M. van Dongen, *Tetrahedron Lett.*, 1972, 4291-4294.
406. J. Burgess and P. J. Steel, *Coordin. Chem. Rev.*, 2011, **255**, 2094-2103.
407. J. R. A. Cottam and P. J. Steel, *J. Organomet. Chem.*, 2006, **691**, 2286-2290.
408. J. Burgess, J. R. A. Cottam and P. J. Steel, *Aust. J. Chem.*, 2006, **59**, 295-297.
409. S. T. Lam and V. W. W. Yam, *Chem. Eur. J.*, 2010, **16**, 11588-11593.
410. G. H. Penner and X. L. Liu, *Prog. Nucl. Mag. Res. Spec.*, 2006, **49**, 151-167.
411. A. Kishimura, T. Yamashita and T. Aida, *J. Am. Chem. Soc.*, 2005, **127**, 179-183.
412. D. Stacchiola, G. Wu, M. Kaltchev and W. T. Tysoe, *Surf. Sci.*, 2001, **486**, 9-23.
413. M. J. Hynes, *J. Chem. Soc. Dalton Trans.*, 1993, 311-312.
414. A. R. Hirst and D. K. Smith, *Langmuir*, 2004, **20**, 10851-10857.
415. M. Driffield, D. M. Goodall and D. K. Smith, *Org. Biomol. Chem.*, 2003, **1**, 2612-2620.
416. G. M. Dykes, L. J. Brierley, D. K. Smith, P. T. McGrail and G. J. Seeley, *Chem. Eur. J.*, 2001, **7**, 4730-4739.
417. C. N. R. Rao, *Chemical Applications of Infrared Septroscopy*, Academic Press Inc., New York-London, 1963.
418. J. G. Hardy, A. R. Hirst, I. Ashworth, C. Brennan and D. K. Smith, *Tetrahedron*, 2007, **63**, 7397-7406.
419. T. Liljefors and P. O. Norrby, *J. Am. Chem. Soc.*, 1997, **119**, 1052-1058.
420. M. Szafran, *J. Mol. Struct.*, 1996, **381**, 39-64.
421. M. L. Muro-Small, J. Chen and A. J. McNeil, *Langmuir*, 2011, **27**, 13248-13253.
422. J. H. van Esch, *Langmuir*, 2009, **25**, 8392-8394.
423. J. Puigmarti-Luis, A. P. del Pino, V. Laukhin, L. N. Feldborg, C. Rovira, E. Laukhina and D. B. Amabilino, *J. Mater. Chem.*, 2010, **20**, 466-474.
424. S. Bhattacharya and A. Pal, *J. Phys. Chem. B*, 2008, **112**, 4918-4927.
425. D. K. Kumar, D. A. Jose, A. Das and P. Dastidar, *Chem. Commun.*, 2005, 4059-4061.
426. P. C. Xue, Y. Zhang, J. H. Jia, D. F. Xu, X. F. Zhang, X. L. Liu, H. P. Zhou, P. Zhang, R. Lu, M. Takafuji and H. Ihara, *Soft Matter*, 2011, **7**, 8296-8304.
427. D. Dasgupta, A. Thierry, C. Rochas, A. Ajayaghosh and J. M. Guenet, *Soft Matter*, 2012, **8**, 8714-8721.

428. P. C. Xue, R. Lu, X. C. Yang, L. Zhao, D. F. Xu, Y. Liu, H. Zhang, H. Nomoto, M. Takafuji and H. Ihara, *Chem. Eur. J.*, 2009, **15**, 9824-9835.

429. C. Marsden and S. Mann, *Solvents Guide*, 2nd edn., Cleaver-Hume Press, Ltd., London, 1963.

430. J. A. Riddick, W. B. Bunger and T. K. Sakano, *Organic Solvents: Physical Properties and Methods of Purification*, 4th edn., John Wiley & Sons, New York, 1986.

431. C. Reichardt, *Solvents and Solvent Effects in Organic Chemistry*, 2nd edn., VCH, Weinheim, 1988.

432. C. M. Hansen, *J. Paint Techn.*, 1967, **39**, 104-117.

433. Y. Marcus, *Chem. Soc. Rev.*, 1993, **22**, 409-416.

434. A. Aggeli, M. Bell, N. Boden, J. N. Keen, P. F. Knowles, T. C. B. McLeish, M. Pitkeathly and S. E. Radford, *Nature*, 1997, **386**, 259-262.

435. J. Makarevic, M. Jokic, B. Peric, V. Tomisic, B. Kojic-Prodic and M. Zinic, *Chem. Eur. J.*, 2001, **7**, 3328-3341.

436. G. Y. Zhu and J. S. Dordick, *Chem. Mater.*, 2006, **18**, 5988-5995.

437. M. Bielejewski, A. Lapinski, R. Luboradzki and J. Tritt-Goc, *Langmuir*, 2009, **25**, 8274-8279.

438. J. Kaszynska, A. Lapinski, M. Bielejewski, R. Luboradzki and J. Tritt-Goc, *Tetrahedron*, 2012, **68**, 3803-3810.

439. B. A. Miller-Chou and J. L. Koenig, *Prog. Polym. Sci.*, 2003, **28**, 1223-1270.

440. P. Curcio, F. Allix, G. Pickaert and B. Jamart-Gregoire, *Chem. Eur. J.*, 2011, **17**, 13603-13612.

441. M. Raynal and L. Bouteiller, *Chem. Commun.*, 2011, **47**, 8271-8273.

442. K. Hanabusa, M. Matsumoto, M. Kimura, A. Kakehi and H. Shirai, *J. Colloid Interf. Sci.*, 2000, **224**, 231-244.

443. Y. P. Wu, S. Wu, G. Zou and Q. J. Zhang, *Soft Matter*, 2011, **7**, 9177-9183.

444. M. Bielejewski, A. Lapinski, R. Luboradzki and J. Tritt-Goc, *Tetrahedron*, 2011, **67**, 7222-7230.

445. A. Mallick, E. M. Schon, T. Panda, K. Sreenivas, D. D. Diaz and R. Banerjee, *J. Mater. Chem.*, 2012, **22**, 14951-14963.

446. M. Lofman, J. Koivukorpi, V. Noponen, H. Salo and E. Sievanen, *J. Colloid Interf. Sci.*, 2011, **360**, 633-644.

447. W. Edwards, C. A. Lagadec and D. K. Smith, *Soft Matter*, 2011, **7**, 110-117.

448. M. J. Kamlet, J. L. M. Abboud, M. H. Abraham and R. W. Taft, *J. Org. Chem.*, 1983, **48**, 2877-2887.

449. K. M. Solntsev, D. Huppert and N. Agmon, *J. Phys. Chem. A*, 1998, **102**, 9599-9606.

450. M. J. Kamlet, R. M. Doherty, M. H. Abraham, Y. Marcus and R. W. Taft, *J. Phys. Chem. US*, 1988, **92**, 5244-5255.

451. A. J. Leo, *Chem. Rev.*, 1993, **93**, 1281-1306.

452. D. C. Duncan and D. G. Whitten, *Langmuir*, 2000, **16**, 6445-6452.

453. B. Escuder, M. LLusar and J. F. Miravet, *J. Org. Chem.*, 2006, **71**, 7747-7752.

454. V. J. Nebot, J. Armengol, J. Smets, S. F. Prieto, B. Escuder and J. F. Miravet, *Chem. Eur. J.*, 2012, **18**, 4063-4072.

455. P. W. Atkins and J. De Paula, *Atkins' Physical Chemistry*, 9th edn., Oxford University Press, Oxford, 2010.

456. A. Cornish-Bowden, *J. Biosciences*, 2002, **27**, 121-126.

457. K. Sharp, *Protein Sci.*, 2001, **10**, 661-667.

458. D. H. Leung, R. G. Bergman and K. N. Raymond, *J. Am. Chem. Soc.*, 2008, **130**, 2798-2805.

459. C. Piguet, *Dalton Trans.*, 2011, **40**, 8059-8071.

460. M. Boiani, A. Baschieri, C. Cesari, R. Mazzoni, S. Stagni, S. Zacchini and L. Sambri, *New. J. Chem.*, 2012, **36**, 1469-1478.

461. M. A. Mateos-Timoneda, M. Crego-Calama and D. N. Reinhoudt, *Chem. Soc. Rev.*, 2004, **33**, 363-372.

462. S. M. Kelly, T. J. Jess and N. C. Price, *Biophys. Biochem. Acta*, 2005, **1751**, 119-139.

463. G. Gottarelli, S. Lena, S. Masiero, S. Pieraccini and G. P. Spada, *Chirality*, 2008, **20**, 471-485.

464. A. Lohr and F. Wurthner, *Isr. J. Chem.*, 2011, **51**, 1052-1066.

465. T. W. Anderson, G. D. Pantos and J. K. M. Sanders, *Org. Biomol. Chem.*, 2011, **9**, 7547-7553.

466. T. W. Anderson, J. K. M. Sanders and G. D. Pantos, *Org. Biomol. Chem.*, 2010, **8**, 4274-4280.

467. J. J. van Gorp, J. Vekemans and E. W. Meijer, *J. Am. Chem. Soc.*, 2002, **124**, 14759-14769.

468. A. D'Aleo, J. L. Pozzo, F. Fages, M. Schmutz, G. Mieden-Gundert, F. Vogtle, V. Caplar and M. Zinic, *Chem. Commun.*, 2004, 190-191.

469. J. Makarevic, M. Jokic, L. Frkanec, V. Caplar, N. S. Vujicic and M. Zinic, *Beilstein. J. Org. Chem.*, 2010, **6**, 945-959.

470. J. H. Fuhrhop, P. Schnieder, J. Rosenberg and E. Boekema, *J. Am. Chem. Soc.*, 1987, **109**, 3387-3390.

471. C. S. Love, PhD Thesis, University of York, 2004.

472. I. A. Coates, PhD Thesis, University of York, 2008.

473. L. R. Romsted and E. H. Cordes, *J. Am. Chem. Soc.*, 1968, **90**, 4404-4409.

474. J. R. Moffat, G. J. Seeley, J. T. Carter, A. Burgess and D. K. Smith, *Chem. Commun.*, 2008, 4601-4603.

475. J. R. Moffat, PhD Thesis, University of York, 2007.

476. D. J. Bergmann, E. M. Campi, W. R. Jackson, A. F. Patti and D. Saylik, *Aust. J. Chem.*, 2000, **53**, 835-844.

477. S. S. Hecht and E. S. Rothman, *J. Org. Chem.*, 1973, **38**, 3733-3737.